TU/e EINDHOVEN UNIVERSITY OF TECHNOLOGY

Resource-aware and resilient control

Citation for published version (APA):
Dolk, V. S. (2017). *Resource-aware and resilient control: with applications to cooperative driving*. [Phd Thesis 1 (Research TU/e / Graduation TU/e), Mechanical Engineering]. Technische Universiteit Eindhoven.

Document status and date:
Published: 06/11/2017

Document Version:
Publisher's PDF, also known as Version of Record (includes final page, issue and volume numbers)

Please check the document version of this publication:

• A submitted manuscript is the version of the article upon submission and before peer-review. There can be important differences between the submitted version and the official published version of record. People interested in the research are advised to contact the author for the final version of the publication, or visit the DOI to the publisher's website.
• The final author version and the galley proof are versions of the publication after peer review.
• The final published version features the final layout of the paper including the volume, issue and page numbers.

Link to publication

General rights
Copyright and moral rights for the publications made accessible in the public portal are retained by the authors and/or other copyright owners and it is a condition of accessing publications that users recognise and abide by the legal requirements associated with these rights.

• Users may download and print one copy of any publication from the public portal for the purpose of private study or research.
• You may not further distribute the material or use it for any profit-making activity or commercial gain
• You may freely distribute the URL identifying the publication in the public portal.

If the publication is distributed under the terms of Article 25fa of the Dutch Copyright Act, indicated by the "Taverne" license above, please follow below link for the End User Agreement:

www.tue.nl/taverne

Take down policy
If you believe that this document breaches copyright please contact us at:

openaccess@tue.nl

providing details and we will investigate your claim.

Download date: 16. Nov. 2023

Resource-aware and Resilient Control

with Applications to Cooperative Driving

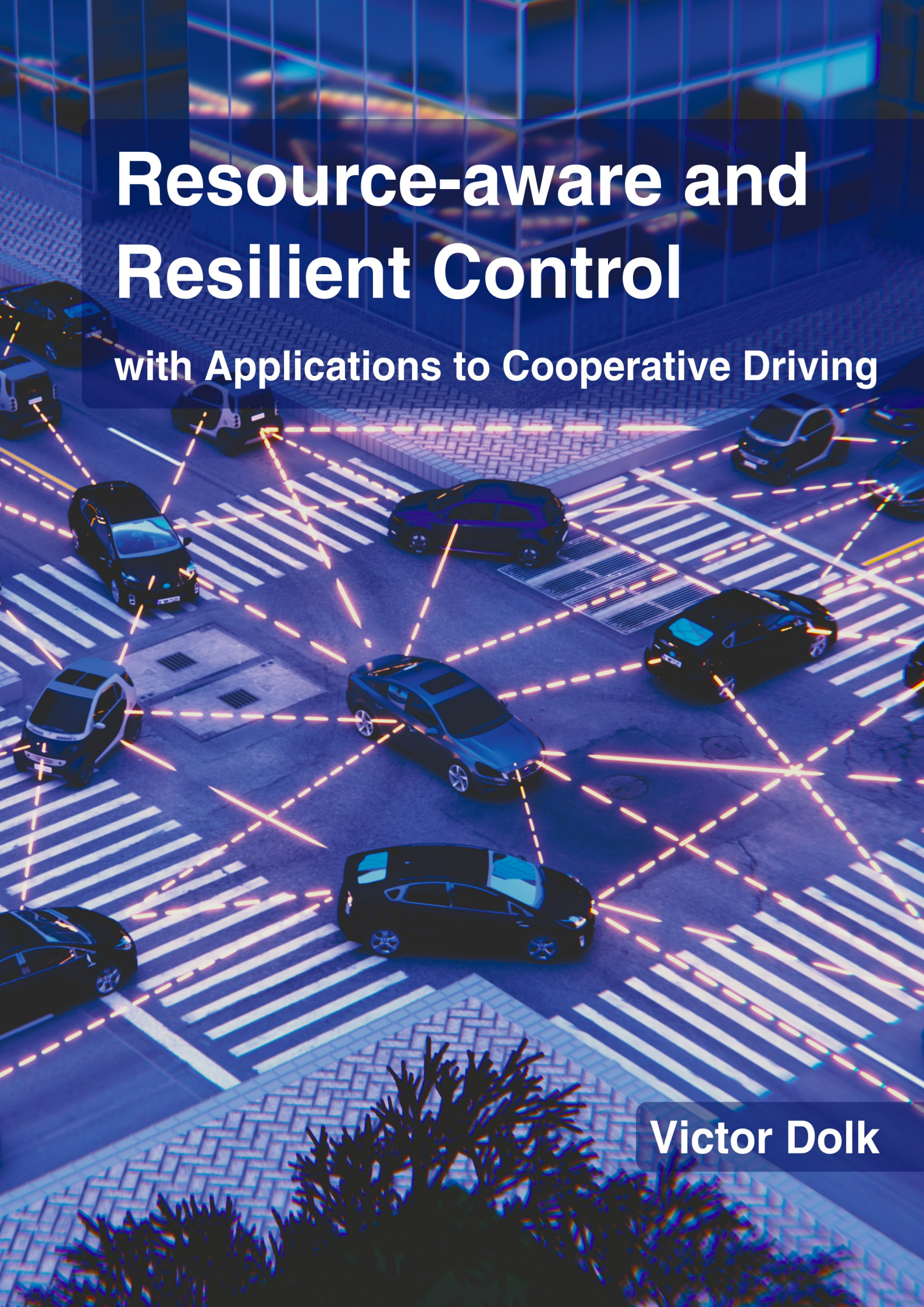

Victor Dolk

Resource-aware and Resilient Control with Applications to Cooperative Driving

Victor Dolk

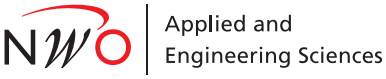

The researched reported in this thesis is part of the research programme "Integrated design approach for safety-critical real-time automotive systems" with project number 12698, which is (partly) financed by the Netherlands Organisation for Scientific Research (NWO).

A catalogue record is available from the Eindhoven University of Technology Library.
ISBN: 978-90-386-4377-9

Reproduction: Ipskamp Drukkers B.V.

©2017 by V.S. Dolk. All rights reserved.

Resource-aware and Resilient Control with Applications to Cooperative Driving

PROEFSCHRIFT

ter verkrijging van de graad van doctor aan de
Technische Universiteit Eindhoven, op gezag van de
rector magnificus, prof.dr.ir. F.P.T. Baaijens, voor een
commissie aangewezen door het College voor
Promoties, in het openbaar te verdedigen
op maandag 6 november 2017 om 16.00 uur

door

Victor Sebastiaan Dolk

geboren te Breda

Dit proefschrift is goedgekeurd door de promotoren en de samenstelling van de promotiecommissie is als volgt:

voorzitter:	prof.dr. L.P.H. de Goey
promotor:	prof.dr.ir. W.P.M.H. Heemels
copromotoren:	dr.ir. J. Ploeg
	dr. P. Tesi (Rijksuniversiteit Groningen)
leden:	prof.dr.ir. K.H. Johansson (KTH)
	prof.dr.ir. B. De Schutter (TU Delft)
	prof.dr.ir. N. van de Wouw
	prof.dr.ir. S. Weiland

Het onderzoek dat in dit proefschrift wordt beschreven is uitgevoerd in overeenstemming met de TU/e Gedragscode Wetenschapsbeoefening.

Societal Summary

The number of connected devices is growing at a rapid pace. Due to this growth, the use of networked systems has become a versatile technology, which is expected to have a crucial role in making transportation systems, power grids, buildings and industry more efficient and more sustainable. In particular, wireless communication networks have enabled many novel promising applications including intelligent transport systems (ITS), remote surgery and smart farming systems. In many of these applications, the network is not only used to facilitate data exchange but also to manipulate the physical environment via connected actuators. The resulting systems are also known as cyber-physical systems. It is generally known that the design of these cyber-physical systems is complex, as it requires novel integrated design approaches among multiple disciplines. In addition, a major concern of cyber-physical systems is their vulnerability to malicious attacks.

Given the benefits and challenges described above, cyber-physical systems have drawn significant attention in the field of control theory. In particular, the design of control systems in which the sensor and/or actuator data is transmitted over a shared (possibly wireless) communication network, has become a prominent topic within the control community. Networked communication introduces inevitable network-induced imperfections such as packet losses and communication delays, which in general affect the behavior of the closed-loop system significantly. The more packets are being transmitted over the wireless medium, the more severe these network-induced phenomena become. Hence, there is a strong need for resource-aware control strategies that aim to only utilize the communication resources when actually needed to maintain the desired closed-loop behavior while being robust to packet losses, communication delays and potential malicious attacks.

In this thesis, a novel design framework for resource-aware and resilient control systems is presented. In particular, we study event-triggered control (ETC) systems in which, in contrast to most conventional digital control setups, the

transmission of sensor and actuation is determined on the basis of current output measurements. As such, ETC allows to better balance between control performance and utilization of communication resources. The proposed framework has been experimentally validated on a platoon of cars equipped with Cooperative Adaptive Cruise Control (CACC), which is a promising ITS that allows to reduce fuel consumption and to improve safety and traffic throughput.

Summary

Resource-aware and Resilient Control with Applications to Cooperative Driving

In the near future, intelligent transportation systems (ITS) equipped with vehicle-to-vehicle (V2V) and vehicle-to-infrastructure (V2I) communication will be used to optimize traffic flows with respect to throughput, safety and fuel consumption. One promising example of ITS technology is Cooperative Adaptive Cruise Control (CACC), a driver assistance system, which exploits V2V communication to enable the formation of vehicle platoons with small inter-vehicle distances while avoiding amplifications of disturbances along the vehicle string that result in so-called ghost traffic jams. The design of these and many other safety-critical networked cyber-physical systems is, however, challenging due to the inherent imperfections of the (wireless) communication including limited bandwidth, time-varying transmission delays, quantization effects, and packet losses. The more packets are being transmitted over the wireless medium, the more severe the network-induced phenomena become. This calls for communication strategies that make careful use of the communication resources. Moreover, one of the main concerns in networked cyber-physical systems is that they are vulnerable to malicious attacks. For these reasons, there is a strong need for integrated design approaches that result in resource-aware and resilient control systems guaranteeing safe, secure and high-performance operation of (wireless) networked control systems (NCSs).

To address the problem of robust resource-aware control design, in this thesis, the use of event-triggered control (ETC) is examined as opposed to the conventional time-triggered control (TTC) schemes. In time-triggered control and communication, the sampling/transmission instants are scheduled at fixed times that are often equidistantly distributed in time. In the context of (wireless) NCSs, these TTC schemes typically result in many redundant transmissions since transmissions are scheduled regardless of the state of the system. As an

alternative, it seems more natural to let the transmission instants depend on the available sensor information to make sure that communication resources are only used when needed to maintain desired closed-loop properties. In ETC schemes, the sampling instants are determined on-line by means of well-designed triggering conditions that depend on output measurements of the system. In this way, event-triggered control schemes have the potential to better balance (communication) resource utilization and control performance than time-triggered approaches.

As existing ETC schemes do not satisfy the requirements for cooperative driving in a platoon including properties such as string stability (attenuation of disturbances along the vehicle string), a positive lower bound on the inter-sampling times (Zeno-freeness), robustness to time-varying delays and large average inter-transmission intervals, in this thesis a novel ETC approach is proposed with such properties. The approach enables to design ETC schemes for a class of nonlinear systems that result in control performance guarantees and Zeno-freeness on the other hand despite the presence of disturbances. Moreover, robustness to time-varying delays in terms of a maximum allowable delay is guaranteed by design as well. Key to obtaining all these beneficial properties is the unique combination of dynamic event-triggering conditions and time regularization. Interestingly, under the same performance and robustness criteria, the positive lower bound on the inter-sampling times obtained with the proposed ETC strategy is close to or equal to the maximum allowable transmission intervals of TTC schemes. However, simulations show that the average transmission intervals generated by the proposed ETC strategy can be much larger due to the event-based triggering and thereby leading to less utilization of the communication medium and thus less congestion of the network. The ideas presented above are extended towards general multi-agent systems exploiting time-triggered and event-triggered communication with non-uniform delays and addressing consensus, input-to-output stability and output regulation problems.

ETC strategies that rely on time-regularization often require continuous availability of output measurements. Therefore, we also present a Riccati-based approach tailored to linear systems that allows to design novel classes ETC strategies including dynamic periodic ETC strategies. The benefit of periodic ETC strategies is that they only need to monitor the outputs of the plant at discrete instants in time. Therefore, periodic ETC strategies are more easy to implement in practice. In addition, by exploiting the Riccati-based approach, much less conservative results can be obtained for linear systems in comparison with the previous ETC approach.

To demonstrate the potential benefits of the ETC on real-life systems, the proposed framework is implemented on a platoon of cars equipped with CACC. The experimental test results confirmed the practical applicability of the ETC scheme and its potential to reduce the utilization of communication resources significantly without sacrificing the string stability properties. In fact, the results

have a high degree of predictability as the experiments match the numerical simulations closely.

As mentioned before, wireless communication links are often subject to packet losses, quantization effects and possibly malicious attacks. To deal with packet losses, we present two types of ETC schemes that, under the assumption that the number of successive packet losses is bounded, can still realize the desired closed-loop properties. The first type relies on the presence of acknowledgement signals that allow to identify whether or not a transmitted packet has been dropped. The second type does not require acknowledgement signals.

The use of quantization is typically required in NCSs as well because the bit rate of (wireless) communication channels is often limited. In this thesis, we show that the proposed ETC design can be enhanced with dynamic quantizers. Interestingly, the theoretical results reveal the intuitive trade-off between size of the data packages per transmission and the number of transmission per time unit.

At last, (cyber-)security is an important issue in NCSs. As such, it is of importance that besides the resource-aware requirement, the control strategy is resilient to malicious attacks. A common type of attack to networked systems is the so-called denial-of-service (DoS). Attacks of this type are intended to interfere with the communication channel causing periods in time at which transmission of data is not possible. We propose an ETC scheme that still leads to the desired control performance despite the presence of these DoS attacks under the natural assumption that the attackers resources are limited in the sense that the frequency and the duration of the DoS attacks are bounded.

All results described above form important steps forward to realize resilient and resource-aware cyber-physical systems including ITSs such as CACC-based vehicle platooning.

Contents

Societal Summary **i**

Summary **iii**

1 Introduction **1**
1.1 Historical background 2
1.2 Today's opportunities and challenges 3
1.3 Event-triggered control systems 9
1.4 Objectives and contributions 16
1.5 List of publications 19

2 Output-based and Decentralized Dynamic Event-triggered Control with Guaranteed $\mathcal{L}_p$-gain Performance and Zeno-freeness **23**
2.1 Introduction 23
2.2 NCS setup and problem statement 29
2.3 Mathematical Model of the Event-triggered Control Setup 31
2.4 ETM design conditions with stability and $\mathcal{L}_p$-gain guarantees . . 36
2.5 Design of event generators 40
2.6 Numerical example 46
2.7 Conclusions 54

3 Riccati-Based Design of Event-Triggered Controllers for Linear Systems with Delays **55**
3.1 Introduction 56
3.2 Control setup 58
3.3 Main results for the CETC case 59
3.4 Main results for the PETC case 67
3.5 Reduced conservatism using state-space partitioning 71
3.6 Numerical examples 75
3.7 Conclusions 78

4 Input-to-state Stabilizing Event-triggered Control for Linear Systems with Distributed and Quantized Output Measurements 81
4.1 Introduction . . . 82
4.2 Preliminaries . . . 85
4.3 Problem formulation . . . 87
4.4 Hybrid model . . . 91
4.5 Main result . . . 94
4.6 Illustrative example . . . 100
4.7 Conclusions . . . 103

5 Event-triggered Control Systems under Packet Losses 107
5.1 Introduction . . . 107
5.2 Definitions and preliminaries . . . 109
5.3 NCS model and problem statement . . . 111
5.4 Hybrid model of the ETC scheme with acknowledgements . . . 116
5.5 ETM design with acknowledgments of packet losses . . . 118
5.6 ETM design conditions without acknowledgments of packet losses 121
5.7 Numerical example . . . 124
5.8 Conclusions . . . 128

6 Event-triggered Control Systems under Denial-of-Service Attacks 131
6.1 Introduction . . . 131
6.2 Definitions and preliminaries . . . 133
6.3 NCS model and problem statement . . . 134
6.4 Mathematical formulation of the ETC setup . . . 138
6.5 Design conditions and stability guarantees . . . 142
6.6 Case study on cooperative adaptive cruise control . . . 146
6.7 Conclusions . . . 148

7 Event-triggered Control of Nonlinear Multi-agent systems subject to Non-uniform Time-Varying Delays 151
7.1 Introduction . . . 151
7.2 Definitions and preliminaries . . . 154
7.3 Multi-agent control setup and problem statement . . . 155
7.4 Mathematical formulation of the event-triggered multi-agent system . . . 160
7.5 Design conditions and main result . . . 165
7.6 Packet losses and Denial-of-Service attacks . . . 170
7.7 Conclusions . . . 174

8 Event-triggered Control for String-Stable Vehicle Platooning 175
8.1 Introduction 176
8.2 Definitions and preliminaries 179
8.3 Model description, control objectives and problem formulation . 181
8.4 Tuning of the network-free CACC system 185
8.5 Wireless and event-triggered communication 186
8.6 ETM Design with string stability guarantees 192
8.7 Experimental validation 196
8.8 Conclusions 200

9 Conclusions, Recommendations and Final Thoughts 201
9.1 Concluding remarks 201
9.2 Recommendations 205
9.3 Final thoughts 208

A Proofs of Chapter 2 209

B Proofs of Chapter 3 213

C Proofs of Chapter 4 219

D Proofs of Chapter 5 227

E Proofs of Chapter 6 235

F Proofs of Chapter 7 243

G Proofs of Chapter 8 253

Bibliography 257

Dankwoord 281

Curriculum vitae 285

Chapter 1

Introduction

Over the last decades, the number of connected devices has grown at a rapid pace. It is expected that this growth continues with predictions ranging from 20.8 billion to 1 trillion connected devices in 2020 [177]. Although these numbers are nothing more than speculation, many studies reveal the potential benefits of interconnected/networked systems. For example, in [252], it is shown that information and communication technology (ICT) can play a crucial role in increasing the efficiency of transport systems, power grids, buildings and industry, to name a few. In fact, the study in [252] predicts that ICT enables a 15% reduction of carbon dioxide emissions without the need of major changes in the current architecture of systems. Besides the environmental benefits, networked systems offer greater flexibility, lower installation costs and better maintenance than systems with dedicated point-to-point (wired) links. In particular, the use of wireless communication is promising due to its ability to overcome the physical limitations of wired connections.

The growing number of communication and sensor networks and their possibilities did not go unnoticed by the field of control theory. Control theory is concerned about the analysis and design of control systems, which are defined in [169] as follows:

> *"At its simplest, a control system is a device in which a sensed quantity is used to modify the behavior of a system through computation and actuation."*

The rise of communication and sensor networks enables many novel control applications with significant societal impacts, see, *e.g.*, [21, 136, 169]. In fact, due to the growing complexity of interconnected systems, it is expected that the field of control theory will be inevitable in the successful operation of large interconnected systems. However, control systems operating over possibly shared and

wireless communication channels, often referred to as networked control systems (NCSs), also introduce many challenges that are far from being fully understood, see also [32, 125, 261] for recent overviews on NCSs. For this reason, there is a strong need for novel analysis and synthesis tools in control theory to guarantee safe, secure and well-functioning operation of (wireless) NCSs.

Before elaborating on the specific contributions of this thesis, we first provide a brief historical overview of important developments that gave rise to the increasing interest in NCSs.

1.1 Historical background

The technology that initiated the trend of (wired and wireless) networked systems is packet switching, which was introduced in the mid 60's [26, 61, 62], see also Figure 1.1. In essence, packet switching is a communication method in which data to be transmitted is broken up into small blocks referred to as packets. By transmitting independent packets instead of a continuous stream of data via dedicated point-to-point connections as, for example, in the public switched telephone network, the medium over which the packets are transmitted can be shared by other users/devices. Moreover, packet switching enhances the efficiency and robustness of the network in comparison with communication methods that rely on dedicated point-to-point connections. The concept of packet switching was adopted by the Pentagon's Advanced Research Projects Agency Network (ARPANET) program of the United States Department of Defense to establish the first computer network [197]. The main purpose of the ARPANET program was to create a network that enables the sharing of computation resources among institutions. Even though the initial idea of ARPANET never became a success due to the quick rise of affordable personal computers, it did form the basis for the internet protocol suite (TCP/IP) [53], which constitutes a key ingredient for what we know today as the internet.

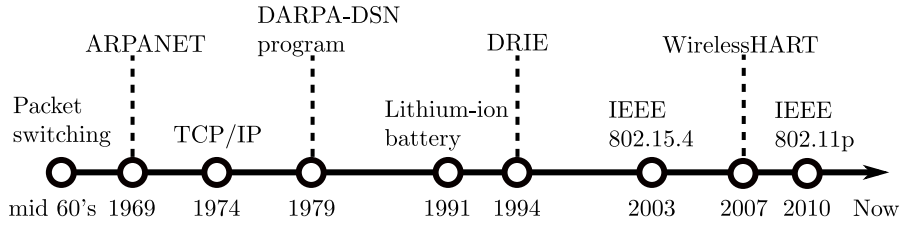

Fig. 1.1. Important developments that gave rise to the increasing interest in networked control systems

In the beginning of the internet era, distributed (computer) networks were primarily used as information infrastructure. However, researchers already en-

visioned the potential benefits of large networks that consist of small interconnected sensors. For this reason, the United States Defense Advanced Research Projects Agency (DARPA) initiated the Distributed Sensor Network (DSN) program in 1979 to identify and tackle the challenges in implementing distributed/wireless sensor networks (WSN) [57]. Although there was a strong market demand for WSNs, it was not until twenty years later that the first commercially available WSNs emerged [57]. This long timespan is explained by the fact that many challenges in sensor technology, network protocols and energy storage had to be overcome before production of small and inexpensive sensors on a large scale was possible. Important milestones that led to affordable WSNs include the first commercially available lithium-ion batteries by Sony in 1991, see also [1], which, due to their high energy density, are useful for portable devices, deep reactive ion-etching (DRIE) invented at Robert Bosch GmbH in 1994, see also [135], which enabled the production of inexpensive micro-electric-mechanical systems, and the release of the IEEE 802.15.4 international standard for low-rate personal area networks in 2003, which focuses on energy efficient inexpensive wireless connections and formed the basis for industrial protocols such as ZigBee, WirelessHART, ISA100.11a and MiWi. Among these protocols, WirelessHART was the first open wireless protocol designed for industry, which was released in 2007 [215].

Initially, WSNs were used for monitoring purposes such as wildfire monitoring [79], air pollution monitoring [257] and structural monitoring [256]. A promising trend today is to not only use these WSNs for monitoring purposes, but also for manipulating the physical environment connected to the network. This interaction between networked and physical systems induces many new challenges in the design of the overall system, see, *e.g.*, [137, 169]. In fact, the design of these so-called cyber-physical systems (CPSs) requires an integrated design approach, involving multiple disciplines due to its complexity and the presence of many uncertainties see, *e.g.*, [16]. Hence, current established paradigms and fundamental theories in each of these individual disciplines do not suffice to harvest all the potential benefits of (wireless) networked systems and cyber-physical systems. As mentioned before, control theory has an important role in the design of CPSs. However, as we will discuss later on, the design of control systems in which sensor and/or actuation signals are sent over communication channels that are shared and/or wireless is far from trivial. For these reasons, the field of NCSs has received a vast amount of attention from the control community over the last few decades, see, [30, 32, 118, 125, 261] and the references therein, and even led to new journals [182].

1.2 Today's opportunities and challenges

NCSs have a wide range of applications including remote surgery [157], process industry [216, 255], water management [172], smart power grids [14, 237] and

intelligent transport systems [27,210]. See also [21,136,169] for recent overviews of high-impact applications of NCSs. In the sequel, we discuss the applications in smart power grids and intelligent transport systems in more detail and address some of the challenges that arise in the control design due to the presence of networked communication.

1.2.1 Opportunities and challenges

Smart power grids

To realize reliable operation of power grids, it is important that the total power generation is in balance with the demand and losses. An imbalance causes frequency deviations, which are not desirable as it effects the efficiency of the grid and might even lead to power outages. For this reason, it is important to make sure that the frequency remains close to its nominal value. The traditional approach to achieve this, is to employ local control algorithms in the sense that the local power generation is only adjusted according to changes in the local demand, see, for instance, [35, 127]. Due to the increasing number of local energy storages such as electric vehicles and renewable energy sources, which cause larger fluctuations in the power demand and supply, in the near future, this traditional approach will no longer be suitable for maintaining an efficient and reliable power grid. For this reason, there is a great interest in developing novel control architectures that lead to robust and efficient power grids. A promising direction in solving this problem is the use of distributed control architectures, which are designed from a multi-agent systems (MAS) perspective and exploit the communication among control areas, see Figure 1.2 and, *e.g.*, [14,201,237].

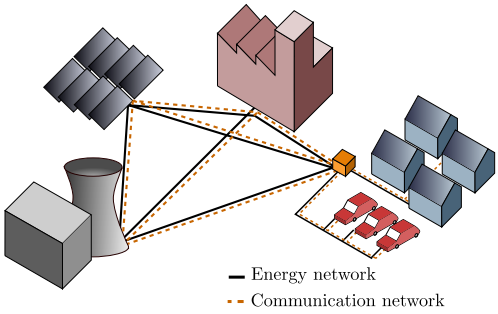

Fig. 1.2. Smart power grid.

The introduction of communication in power grids, however, also raises novel concerns. Due to the increasing dependency on networked communication and the number of interconnected devices, malicious cyber attacks have become a serious thread to power grids. In fact, the first example of a power outage caused by cyber attacks was the power outage in Ukraine, December 2015, which caused

hundreds of thousands of households to be without electricity [142]. Roughly speaking, three type of attacks can be distinguished: attacks targeting the availability of networks, also referred to as denial-of-service (DoS) attacks, attacks targeting the integrity of data sent over a network, also known as deception attacks, and attacks targeting the confidentiality of data [246]. From a control perspective, it is therefore of importance to develop control algorithms that are resilient and able to detect the presence of these attacks.

Intelligent transportation systems

The worldwide demand for mobility is increasing rapidly. In the mean while, there is a strong need for a traffic infrastructure that is cleaner, cheaper, more efficient and safer. Complying with all these necessities is a challenging problem, as accommodating one of the aspects often comes at the cost of the others. For example, the expansion of the current infrastructure to accommodate a higher throughput is in general costly, has a negative impact on the environment and does not necessarily enhance safety. For this reason, it is of great interest to develop solutions that are capable of tackling all of the aforementioned aspects simultaneously. Automated and cooperative (or connected) driving via *dedicated short range communication* (DSRC) communication are promising technologies in this regard since these technologies enable to improve traffic throughput, fuel consumption and safety without the need for expanding current (road) infrastructure, see, *e.g.*, [85,108,139,212,213,223,240]. In particular, the combination of these two technologies, *i.e.*, *cooperative automated driving*, is expected to be an adequate approach for realizing a more efficient a traffic infrastructure. For this reason, the IEEE 802.11p standard was released in 2012 which is used as basis for the Wireless Access in Vehicular Environment (WAVE) standard in the United States and the ITS-G5 standard in Europe for low-latency inter-vehicular communication [86].

A well-known example of a cooperative automated driving system is cooperative adaptive cruise control (CACC), see Figure 1.3. The main goal of CACC systems is to establish vehicle platoons with small inter-vehicle distances while avoiding the propagation of disturbances along the vehicle string, see also [34, 129, 171, 180, 181, 187, 202, 204, 223, 240]. The latter property is also referred to as *string stability* and is important in order to avoid the formation of phantom traffic jams. Small inter-vehicle distances are desired as they lead to a larger road capacity and less fuel consumption due to the reduction in aerodynamic drag. The latter is in particular interesting for heavy-duty vehicles, see also [12, 13, 38, 107, 238]. A key ingredient to realize small inter-vehicle distances and achieve string stability simultaneously is the use of vehicle-to-vehicle (V2V) communication.

The first work that studied the potential impact of V2V communication on traffic flow and capacity already dates back to the mid '60 [139]. The first

successful demonstration of CACC was in 1997 [95, 211]. These experiments merely focused on showing the practical feasibility of vehicle platooning. In [171,187], the string stability properties of vehicle platoons equipped with CACC were experimentally validated. Moreover, it was shown that indeed CACC is outperforms conventional adaptive cruise control (ACC) systems in attenuating disturbances along the vehicle string while realizing small time gaps in between the vehicles. Interestingly, the principle of CACC can also be exploited in the automation of traffic at intersections, see also Figure 1.3 and [159, 263]. The latter has successfully been demonstrated during the Grand Cooperative Driving Challenge (GCDC) 2016. In short, CACC is a proven technology that, due to V2V communication, enables the formation of vehicle platoons with small inter-vehicle distances while avoiding amplifications of disturbances along the vehicle string.

Fig. 1.3. (left) Platoon of vehicle equipped with DSRC and CACC. (right) Automated intersection crossing based on CACC. These scenarios were demonstrated during the Grand Cooperative Driving Challenge (GCDC) 2016 ©[2016] i-GAME

The use of wireless communication also has drawbacks as it comes with inevitable network-induced imperfections caused by the digital nature of the communication network. To be more concrete, the rate at which data-packages can be transmitted is limited and the communication channel is subject to communication delays. In case the transmission rate is too small and/or the communication delays too large, string stability and other performance properties might no longer be guaranteed for a given time gap, see, for instance, [67, 85, 90, 130, 151, 180, 181, 187, 203]. On the other hand, high communication rates degrade the reliability of the DSRC channel and increase the transmission delays as reported in [28,134,152], which might also put restrictions on the minimum time gap that can be achieved safely in dense traffic, see also [187]. Hence, excessive utilization of communication resources might impede the benefits of CACC with respect to traffic throughput and fuel consumption. In other words, in order to exploit the full potential of CACC systems, it is important that the communication resources are only utilized when actually needed to establish a string-stable platoon and thus to avoid redundant transmissions.

To deal with the aforementioned issue, Decentralized Congestion Control (DCC) mechanisms have been proposed for V2V communication in the ETSI TS 102 687 standard [82]. These mechanisms include transmit power control, transmit access control and transmit rate control. In particular, the transmit rate control is expected to be an adequate mechanism to avoid congestion of the communication channels, see, *e.g.*, [25, 234]. However, standardization regarding CACC systems and the exact employment of the DCC mechanisms is still an ongoing process and far from conclusive, see also [86] for a recent overview of standards for cooperative intelligent transport systems. For this reason, it is of interest to develop CACC systems with mechanisms that aim to reduce the utilization of communication resources while guaranteeing the reliability (in terms of packet losses) and the quality of the network (in terms of communication delays), and the desired control performance (in terms of string stability).

1.2.2 Challenges for control design

As already highlighted in the previous subsection, the introduction of (wireless) networked communication also has drawbacks due to the inevitable network-induced imperfections. In general, these imperfections can be divided into the following five categories:

i) **Sampled data**: Due to the digital nature of the communication channel, the communication in NCSs is inherently packet-based. As a consequence, sensor and actuation data can only be transmitted at discrete instants in time.

ii) **Packet losses**: Packet losses often occur due to packet collisions, which are typically caused by excessive use of the communication channel. Especially in wireless networks, transmissions might also fail due to physical imperfections of the communication channel leading to corrupted data.

iii) **Quantization**: Due to the digital nature of communication channels in NCSs, only a finite number of bits can be transmitted per time unit. For this reason, it is necessary to quantize the signals sent over the network.

iv) **Time-varying transmission delays**: Given the fact that communication and computation resources are limited and often shared with other users/tasks, a data package can never be sent and instantaneously be received and processed. Moreover, due to uncertainties in the communication channel and the fact local clocks are typically not synchronized, the sizes of these delays typically vary in time. As such, time-varying transmissions delays are inherent to networked communication.

v) **Communication constraints**: In NCSs, it is in general not possible to exchange all sensor and actuation data simultaneously. To cope with the

latter, scheduling protocols are often introduced to coordinate which node is granted access to the communication medium.

Additionally to these network-induced imperfections, one of the major concerns in NCSs is cyber-security since the use of (wireless) communication also introduces vulnerabilities with respect to malicious deception and denial-of-service (DoS) attacks. As already mentioned, deception attacks intend to tamper transmitted data packages by injecting false information, see for more details, *e.g.*, [183], and DoS attacks intend to interfere with the communication channel, which typically causes periods in time in which communication is not possible, see, for instance, [253]. Let us remark that DoS attacks are closely related to the occurrence of packet losses (see category i)). However, as we will discuss in the next section, the characterization and treatment of packet losses due to malicious attacks are substantially different from those of packet losses caused by the natural phenomena mentioned in category ii) above.

Obviously, network-induced imperfections and the presence of malicious attacks affect the behavior of the closed-loop system. It is therefore important to take these imperfections and vulnerabilities into account in the control design. However, one of the difficulties in doing so is to incorporate both the continuous behavior of the physical system (also referred to as the physical part of the system) and the discrete/digital behavior of the communication channel (also referred to as the cyber part of the system). This combination of continuous and discrete behavior results in mathematical models called hybrid system [98, 154], for which it is in general difficult to assess the stability and performance of the closed-loop system. Although significant advances have been made in hybrid system theory over the last two decades, see, for example, [98, 106, 113, 119, 154] and the references therein, providing tight stability and performance bounds for hybrid systems, thereby quantifying the effect of the aforementioned phenomena, is far from trivial and far from being fully understood.

Besides having a thorough understanding of the influence of network-induced imperfections, it is also important to consider the fact that the control architecture itself affects the quality and the reliability of the network. In particular, the scheduling of transmission instants can have a significant influence on the number of packet losses, sizes of the transmission delays and the resilience of the system. Hence, in NCSs, there is a strong interaction between the cyber and the physical part of the system. As a consequence, the control design and the design of the ICT infrastructure of NCS can typically not be regarded as separate issues without compromising the performance and/or reliability of the overall system. Hence, the design of high performance and reliable NCSs require novel *integrated* design approaches that bridge the gap between the control and the ICT community.

This thesis addresses the design of *resource-aware* and *resilient* control schemes for safety-critical systems. Resource-aware control schemes are control schemes that aim to minimize the utilization of communication resources while achie-

ving desired stability and performance criteria despite the presence of the aforementioned network-induced imperfections. Resilient control schemes are control schemes that, despite the vulnerabilities to malicious attacks, lead to desired stability and performance properties. To be more specific, we address the design, analysis and validation of ETC schemes that are applicable to output-based feedback systems, take into account the presence of disturbances and network-induced imperfections, and that are resilient to malicious DoS attacks.

In the remainder of this chapter, we discuss these topics in more detail and provide a brief literature review. Moreover, we highlight the obtained contributions followed together with an outline of the remainder of thesis.

1.3 Event-triggered control systems

1.3.1 General overview

In most traditional (digital) control setups, the instants at which the system's outputs are sampled and transmitted are determined purely based on time, often according to a fixed sampling rate. In general, such a time-triggered control (TTC) scheme is predictable in the sense that the transmission instants are known in advance and easy to implement. For these reasons, a significant part of the literature on NCSs aims at finding time-based specifications such that the closed-loop system meets the desired stability and performance criteria, see, *e.g.*, [29, 51, 58, 120, 125, 173, 245]. Since in time-triggered control schemes, the sampling behavior does not depend on the actual state of the system, these time-based specifications should hold for all situations (all states) the system can attain and are therefore typically determined via worst-case estimates. As a result, time-triggered control schemes often result in redundant transmissions in the sense that more transmissions are generated than actually needed to achieve the desired stability and/or performance criteria. Since excessive use of communication resources affect the quality and reliability of the communication channel, the latter is typically not desired in the context of NCSs.

In NCSs, where communication resources are often shared with other devices/users, it seems more natural to let the transmission intervals depend on output measurements of the system with the aim to utilize the communication resources more efficiently than time-triggered control schemes. Examples of such resource-aware control strategies include *self-triggered control* (STC), see, *e.g.*, [15, 101, 158, 244, 249, 250], and *event-triggered control* (ETC), see, *e.g.*, [18, 20, 37, 117, 155, 224, 258] for some early approaches, and [114] for a recent overview. In ETC schemes, the transmissions instants are driven by an event-generator, also referred to as the *event-triggering mechanism* (ETM), whose events are determined via conditions that depend on current (and possibly previous) output measurements, see also Figure 1.4. As an example, an event could be generated whenever the norm of the difference between the most

recently transmitted output measurement and the current output measurements exceeds a certain, not necessarily constant, threshold. In STC schemes, the next

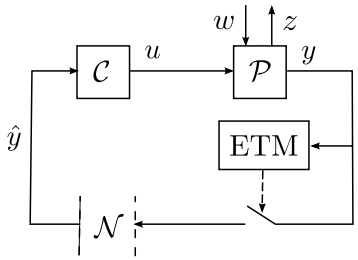

Fig. 1.4. Schematic representation of an event-triggered control (ETC) scheme, where $\mathcal{P}$ denotes the plant, $\mathcal{C}$ the controller, $\mathcal{N}$ the communication channel, y the output measurement, $\hat{y}$ the most recently transmitted output measurement, u the control input, w the disturbance and z the performance output.

transmission instant is also determined on the basis of output measurements but already in advance at the current transmission instant. Consequently, STC schemes do not require the acquisition of measurements in between two consecutive transmissions and do not need to continuously evaluate the triggering condition. For this reason, STC schemes are in general more suitable for battery-powered processes than ETC schemes. Moreover, since in STC schemes, the transmission instants are already known in advance, tasks triggered by STC schemes are in general easier to schedule than tasks triggered by ETC schemes. ETC schemes on the other hand, are in particular of interest for wireless safety-critical systems with unpredictable behavior in which network congestion should be avoided such as a platoon of vehicle equipped with CACC. In fact, the focus of this thesis will be on the design of ETC schemes for such safety-critical applications.

Roughly speaking, literature on ETC can be divided into two categories, namely, optimization based approaches and Lyapunov-based approaches. In the first category, the ETC design problem is formulated as an optimization problem in which the performance of the system, similarly as in well-known LQR and LQG problems, is expressed in terms of for example a quadratic cost, see, *e.g.*, [17, 19, 37, 54, 164, 165, 195, 236, 236, 258]. In the second category, which will be considered in this thesis, the ETC systems are typically described in terms of an impulsive system, see, *e.g.*, [40, 112], a hybrid system, see, *e.g.*, [72, 191], or a time-delay system where the delay is described by some piecewise linear function, see, *e.g.*, [184, 205] and the control objectives are expressed in terms of asymptotic stability, $\mathcal{L}_p$-stability or input-to-state (ISS) stability.

One of the main difficulties of Lyapunov-based ETC schemes is to design the *event-triggering mechanism* in such a way that desired performance and stability criteria are guaranteed together with a positive *minimum inter-event*

time (MIET). This positive MIET is an essential property in order to exclude the occurrence of an infinite number of events in finite time, (also known as Zeno behavior), and to enable the practical implementation of the ETC system. Especially for output-based and decentralized control configurations and/or situations where disturbances are present, guaranteeing a (global) positive MIET is not trivial. In fact, it has been shown recently in [41] that many ETMs proposed in literature do not lead to systems that have a positive MIET that is robust to disturbances, or do not guarantee the desired stability and performance properties. For example, the approaches in [251, 259] do consider input-to-output stability properties but do not provide a strictly positive MIET for the case disturbances are present. For output-based and decentralized control configurations, the inter-event times of many ETMs even converge to zero in the absence of disturbances [41, 78].

To deal with the issue described above, recent works on ETC often employ time regularization [5,7,44,54,87,117,218,219,225–228], in the sense that the triggering of an event is only allowed after a specific time duration τ_{miet} has elapsed since the most recent transmission. Hence, in this situation, the MIET is lower-bounded by τ_{miet} regardless of whether disturbances are present or not. An alternative for enforcing a strictly positive MIET is to use of so-called periodic event-triggered control (PETC) schemes [40, 43, 54, 112, 113, 117, 126, 184, 243, 247, 260], in which the triggering condition is checked at fixed periodic sampling time instants with sampling period h. In this case, the MIET is lower-bounded by the sampling period h. Of course, the time-constants τ_{miet} and h cannot be chosen arbitrarily and should be chosen (together with other parameters in the controller) such that the desired stability and performance criteria can still be met. Only a few works in literature provide design conditions for these time-constants in combination with output-based ETC schemes under the presence of disturbances. These include [9, 40, 44, 72] for ETC schemes with time-regularization and [40, 43, 112, 113, 243, 247] for PETC schemes.

The majority of the aforementioned works on ETC consider *static* ETMs. In these ETMs, the triggering condition is described by an algebraic function that explicitly depends on the current output measurement and the output measurement that is available at the controller side. Recently, it was shown in [96] that *dynamic* ETMs, *i.e.*, ETMs that rely on a dynamic variable instead of a static expression, can significantly prolong the inter-event times without having to comprise the performance and stability guarantees with respect to their static counter part. The concept of dynamic ETMs was introduced in [189] in which triggering rules for a class of nonlinear systems were presented.

1.3.2 Quantization

Besides reducing the amount of transmissions, it is also of importance to limit the size of the packages that are transmitted over the network. For this rea-

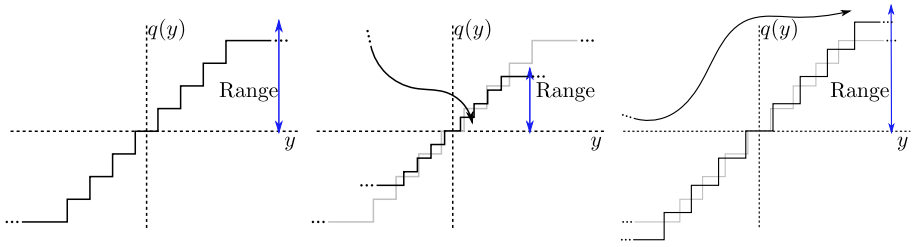

Fig. 1.5. Dynamic quantizer.

son, quantization forms an essential part of NCSs, see, *e.g.*, [116, 167, 175]. In essence, a quantizer is a device that maps a real-valued signal into a piece-wise constant signal that can only attain a finite number of values, see also Figure 1.5. Each value that the quantized signal can attain corresponds to a quantization region. As such, by means of quantization, a real-valued measurement can be encoded into a digital packet consisting of a finite number of bits. As shown, for example, in [144], desired closed-loop stability properties may no longer be guaranteed when the control system relies on quantized measurements due to two reasons. The first reason is that if the measured signal is outside the range of the quantizer, which is determined by the union of all quantization regions, then typically the quantization error is large. As a consequence, the system might exhibit unstable behavior. The second reason is that the accuracy of the quantized measurement near the equilibrium might be insufficient for the desired convergence properties. The majority of the literature on quantization for NCSs considers static quantizers in which the quantization regions are fixed in advance. To ensure that the feedback information remains within range of the static quantizer, the quantizer range is typically chosen relatively large with respect to the sizes of the individual quantizer regions. Hence, in static quantizers, the number of quantization regions is typically large, which implies large packet sizes and/or multiple packets. In fact, it is often even assumed that the quantizer range is infinite [242]. However, this requirement is impractical due to limited bandwidth of the communication channel.

To overcome this requirement, the authors of [48] proposed so-called dynamic quantizers in which the quantizer regions can be dynamically scaled according to the available feedback information, see also Figure 1.5. To scale the quantizer region, a zoom variable is employed to either enlarge the quantizer regions to avoid saturation (referred to as the zoom-out stage) or to reduce them in order to extract more precise information (referred to as the zoom-in stage). As such, dynamic quantizers allow to avoid saturation with only a small number of quantization regions (and thus a small number of bits that need to be communicated). Hence, in the context of NCS, dynamic quantizers offer a better balance between the desired control performance, the minimum and average inter-transmission

intervals and the size of the packages that are transmitted over the network than static quantizers. However, the use of dynamic quantizers also introduces new challenges in the stability analysis and practical implementation. For example, similar as in event-triggered control systems as discussed in Section 1.3.1, Zeno-behavior, *i.e.*, the accumulation of zoom instants and/or the chattering behavior between the zoom-in and the zoom-out stages, should be excluded. In addition, the zoom variable should remain bounded, see also, e.g., [145].

Despite the practical importance of synthesizing both event-triggered controllers and dynamic quantizers for NCS, only a few works in literature have addressed this problem, see, [141,150,221,229,231]. In [141,150,221,229] availability of full state measurements is assumed. To the best of our knowledge, only [231] considers the case of output-based feedback control, however, without the presence of external disturbances.

1.3.3 Packet losses and Denial-of-Service attacks

As mentioned in Section 1.2.2, the presence of packet losses in NCSs is in general unavoidable. For this reason, a significant portion of works on time-triggered NCSs consider the presence of packet losses, see, for instance, [125, 173, 204] and the references therein. The portion of works on event-triggered NCSs that consider packet losses is, however, still relatively small.

The presence of packet losses can either be characterized with stochastic dropout models or deterministic dropout models. Examples of ETC strategies that consider stochastic dropout models include [37, 132, 156, 164, 165] in which optimal control approaches for discrete-time systems are adopted. Except for [132], a key assumption in these works is the presence of an acknowledgment scheme as, *e.g.*, in transmission control protocols (TCP). By using acknowledgment signals, it is known whether a transmitted package has been successfully received or not.

In [103, 104, 138, 184, 251], ETC schemes for continuous-time systems with deterministic dropout models are considered. To be more precise, it is assumed that the number of successive packet dropouts is upper-bounded. This upper-bound is often referred to as the maximum allowable number of successive packet drops (MANSD). To deal with the presence of packet losses, the authors of [103, 104, 138, 259] proposed to combine time-triggered and event-triggered solutions in the sense that transmissions are only scheduled in an event-based fashion if the previous transmission has been successful. Otherwise, the transmissions are scheduled according to a fixed sampling rate. Clearly, this approach relies on an acknowledgment scheme as well. In [251] it was shown that the design of a triggering rule of the form as in [224] can be adapted such that the MANSD can be tolerated without the need for an acknowledgment scheme, which is, *e.g.*, the case in the user datagram protocol (UDP). To avoid Zeno-behavior in the presence of disturbances, [184] considers a periodic event-triggered control

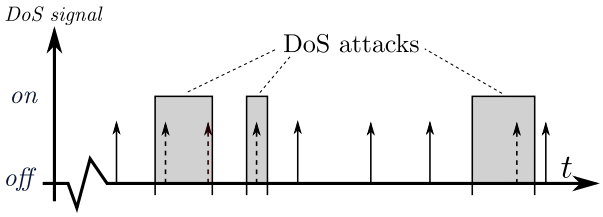

Fig. 1.6. Schematic representation of a sequence of DoS attacks. The solid arrows indicate successful transmissions and the dashed arrows transmissions that are blocked by the attacker. The gray areas indicate the presence of a DoS attack.

(PETC) scheme. In a similar manner as in [251], it was shown that the design of such a PETC rule can be adapted to tolerate a MANSD without the need for an acknowledgment scheme. A significant drawback of the aforementioned approaches is that they rely on the availability of full state information which is often not the case in practice.

As mentioned in Section 1.6, packet losses might be caused by *denial-of-service* (DoS) attacks, see also Figure 1.6. To cope with this type of malicious attacks, it is important that no assumptions regarding the underlying jamming strategy of the attacker are made as, in practice, this strategy is often not known. In the context of event-triggered control systems, stochastic packet dropout models are not suitable for characterizing the presence of DoS attacks since they impose a certain structure on the sequence of DoS attacks and thereby only capture a class of jamming strategies. However, it is reasonable to assume that the resources of the attacker are not infinite and that several provisions can be taken to mitigate these DoS attacks. For this reason, the authors of [63, 64] proposed to characterize the presence of DoS attacks in terms of the frequency and the duration of the attacker's actions. This characterization allows to capture a wide class of DoS attacks including *trivial*, *periodic*, *random* and *protocol-aware* jamming attacks [65, 253]. The approaches presented in [63, 64] are restricted to the case of static state feedback as well. Results on deterministic packet dropout models that rely on a MANSD bound might also be exploited to deal with the presence of DoS attacks. However, this approach typically leads to conservative results.

1.3.4 Multi-agent systems

The decentralized coordination of multi-agent systems (MAS) is an extensively studied control problem due to its wide variety of applications. Especially in the last few decades, there is a growing interest in MAS due to the emerging field of NCSs which enable cooperative control solutions in *ad hoc* networks with re-

latively inexpensive hardware. These cooperative control solutions are relevant for, *e.g.*, intelligent transportation systems, power grids, smart farms with unmanned air vehicles (UAVs) (see Figure 1.7), building automation and aerospace applications. In multi-agent control problems, agents have to cooperate in order to achieve a certain common objective as each individual agent typically employs a local control law and does not have access to the full states of all the agents.

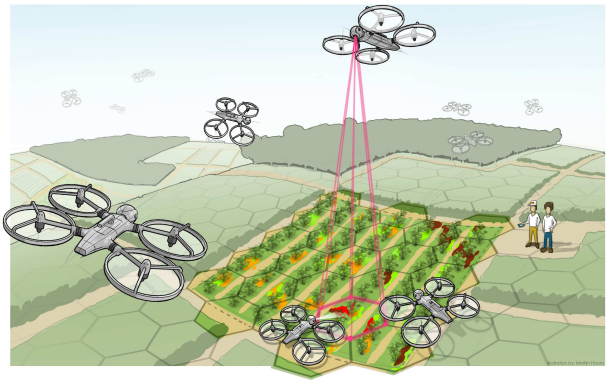

Fig. 1.7. Smart farming with unmanned air vehicles (UAVs) ©[2017] Avular B.V.

It is obvious that communication among agents is crucial for achieving the common control objective. Despite the latter fact, the majority of the literature on MAS considers often only a subset of the network-induced imperfections discussed in Section 1.2.2. For example, in [67, 146, 222, 230], non-uniform time-varying delays are considered, but the communication is assumed to be continuous. As such, the sampled-data nature of the communication links is not taken into account. In contrast, [69, 93, 94, 104, 105, 133, 140, 148, 160, 185, 206, 251, 262] proposed event-triggered control (ETC) strategies for MAS that aim to reduce the utilization of communication resources and thereby do take into account the packet-based nature of the communication channel. However, the ETC approaches presented in [69, 93, 105, 133, 140, 148, 160, 185] do not consider delays and the approaches in [206, 262] assume that the delays are uniform and constant. Notable exceptions include [94, 104, 251]. As pointed out in [104, 251], one of the main issues in MAS is dealing with inconsistent information among agents. In [94], this issue is avoided by compensating for the effect of the delay upon arrival of new information. This approach requires that the internal clocks of all agents are perfectly synchronized. In [104, 251], transmission protocols that rely on acknowledgment and permission signals have been proposed in order to avoid state inconsistencies. To be more specific, by means of these acknowledgment

and permission signals, the information available at each individual agent is updated simultaneously. However, the latter approach might put a burden on the communication channel. For this reason, [104] also considered the case without permission signals in which state inconsistencies are present.

Hence, from the discussions in this sections, it is clear that several important problems are open and require attention before the implementation of NCSs in many applications, which need formal stability, performance and safety guarantees.

1.4 Objectives and contributions

Based on the observations above, the general objective of this thesis can be stated as

> *Develop tools for the design of resource-aware and resilient control strategies for safety-critical networked control systems and provide proof-of-concepts in real-life applications.*

As advocated in Section 1.3.1, ETC is an adequate method to avoid excessive use of communication resources in safety-critical NCSs. However, as pointed out in the concise literature review provided above, design and analysis tools for ETC schemes that are applicable to output-based feedback systems that take into account the presence of disturbances and network-induced imperfections and that are resilient to malicious attacks, are lacking. Hence, we can refine the general objective in terms of the following research objectives:

(i) To develop novel design frameworks for event-triggered control algorithms for output-based feedback systems that aim to reduce the utilization of communication resources and take into account the inevitable network-induced imperfections. (Chapter 2-5)

(ii) To develop resilient event-triggered control algorithms for output-based feedback systems that, in addition to the resource-aware requirement, realize desired closed-loop behavior despite the presence of malicious denial-of-service attacks. (Chapter 6)

(iii) To develop event-triggered control algorithms for multi-agent systems. (Chapter 7)

(iv) To experimental validate of the proposed resource-aware control strategy on a relevant safety-critical system. (Chapter 7)

Next, we discuss the contribution of each chapter in addressing these objectives.

1.4.1 Contributions of the individual chapters

Chapter 2 presents a novel ETC strategy, which results in guaranteed finite $\mathcal{L}_p$-gains and a strictly positive lower bounds on the inter-event times. To be more specific, the presented ETC approach is suitable for a class of nonlinear feedback systems, can be synthesized in an output-based and/or decentralized form, takes the specific medium access protocols into account, and is robust to (variable) transmission delays by design. Interestingly, in contrast with the majority of existing event-generators that only use static conditions, the newly proposed event-triggering conditions are based on dynamic elements, which have several advantages including larger average inter-event times (for the same stability and/or performance guarantees). The developed theory leads to families of event-triggered controllers that correspond to different trade-offs between (minimum and average) inter-event times, maximum allowable delays and $\mathcal{L}_p$-gains. In addition, it is shown that for linear systems, the provided design conditions can be verified systematically based on Linear Matrix Inequalities (LMIs).

Chapter 3 proposes new static and dynamic continuous event-generators (which require continuous measuring of the plant output) and periodic event-generators (which only require periodic sampling of the plant output) for linear control systems with communication delays. All event-generators we propose lead to closed-loop systems which are globally exponentially stable with a guaranteed decay rate, $\mathcal{L}_2$-stable with a guaranteed $\mathcal{L}_2$-gain, and have a guaranteed positive minimum inter-event time. By using new Riccati-based analysis tools tailored to linear systems, the conservatism in our decay rate and $\mathcal{L}_2$-gain estimates is small. The dynamic event-generators even further reduce this conservatism, and as a result typically generate significantly fewer events than their static counterparts, while guaranteeing the same control performance.

Chapter 4 presents event-triggering and dynamic quantization mechanisms for linear control systems that ensure an input-to-state stability (ISS) property of a set around the origin with respect to the external disturbances. The proposed approach prevents the occurrence of Zeno behavior in the transmission instants and the quantization updates. An additional feature of the proposed scheme is that transmission instants can only be generated when the sampling error becomes larger than the quantizer error bound, which helps in avoiding redundant usage of the network. Interestingly, the proposed design strategy reveals the intuitive trade-off between the amount of transmissions and the number of quantization regions (and thereby the size of each transmitted data package).

Chapter 5 considers ETC systems in the presence of packet losses. Despite the existence of techniques to mitigate packet collisions, the presence of packet losses in wireless communication networks is in general unavoidable. For this reason, it is of importance that also in the presence of packet losses, ETC strategies are able to reduce the utilization of communication resources while guaranteeing desired stability and performance criteria and a strictly positive lower bound on the inter-event times. In *Chapter 5*, we propose ETC strategies

for a class on nonlinear systems that take into account presence of potential packet losses. To be more specific, we consider two types of control configurations, namely, configurations with an acknowledgment scheme (as, *e.g.*, in the transmission control protocol (TCP)) and configurations without an acknowledgment scheme (as, *e.g.*, in the user datagram protocol (UDP)).

Chapter 6 presents a systematic design framework for dynamic event-triggered control (ETC) strategies applicable to a class of nonlinear output-based feedback systems under Denial-of-Service (DoS) attacks. These malicious DoS attacks are intended to interfere with the communication channel causing periods in time at which transmission of measurement data is impossible. We show that the proposed ETC scheme, if well designed, can tolerate a class of DoS signals characterized by frequency and duration properties without jeopardizing the stability, performance and Zeno-freeness of the ETC system. In fact, the design procedure of the ETC condition allows trade-offs between performance, robustness to DoS attacks and utilization of communication resources.

Chapter 7 considers a class of nonlinear multi-agent systems (MAS) subject to disturbances and the inevitable imperfections induced by packet-based networked communication. These imperfections include non-uniform time-varying transmission delays, limited communication resources and communication constraints. To reduce the utilization of communication resources, we propose a dynamic event-triggered control scheme resulting in aperiodic transmission of information. Under suitable conditions, the designed event-triggered controllers leads to a broad range of performance and stability properties (which are expressed in terms of dissipativity conditions [241, 254]), strictly positive lower bounds on the inter-event times and robustness for non-uniform time-varying delays in terms of maximum allowable delays. Moreover, the framework allows for the consideration of destination protocols that are shown to connect to network scheduling protocols. Interestingly, the same concept is applicable in the context of packet losses and denial-of-service attacks

In **Chapter 8**, we experimentally validate the benefits of using ETC by means of a platoon of three passenger vehicles equipped with Cooperative Adaptive Cruise Control (CACC) systems. We indeed show that CACC systems based on Dedicated Short Range Communication (DSRC) enable the formation of vehicle platoons with small inter-vehicle distances while avoiding amplifications of disturbances along the vehicle string. By means of ETC, excessive utilization of communication resources, which jeopardizes the reliability of the DSRC channel, is avoided while (string-)stability properties are still guaranteed.

In addition to these main chapters, we provide the main conclusions of thesis and recommendations in Chapter 9 and all mathematical proofs are included in the appendix.

1.5 List of publications

Each chapter is based on a research paper and is self-contained. As such, each chapter can be read independently.
Chapter 2 is based on

- V.S. Dolk, D.P. Borgers and W.P.M.H. Heemels, *Output-based and Decentralized Dynamic Event-triggered Control with Guaranteed Lp-gain Performance and Zeno-freeness*, IEEE Transactions on Automatic Control, 2017, vol. 62, no. 1, pp. 34-49, Jan. 2017, [72],

of which a preliminary version appeared as

- V.S. Dolk, D.P. Borgers, W.P.M.H. Heemels, *Dynamic event-triggered control: Tradeoffs between transmission intervals and performance*, IEEE Conference on Decision and Control (CDC), Los Angeles, USA, 2014, pp. 2764-2769, [71].

Chapter 3 is based on

- D.P. Borgers, V.S. Dolk and W.P.M.H. Heemels, *Riccati-Based Design of Event-Triggered Controllers for Linear Systems with Delays*, IEEE Transactions on Automatic Control, 2017, *Accepted for publication*, [40].

of which preliminary versions appeared as

- D.P. Borgers, V.S. Dolk and W.P.M.H. Heemels, *Dynamic Periodic Event-Triggered Control for Linear Systems*, 20th ACM International Conference on Hybrid Systems: Computation and Control (HSCC), Pittsburgh, USA, 2017, [45],

- D.P. Borgers, V.S. Dolk and W.P.M.H. Heemels, *Dynamic Event-Triggered Control with Time Regularization for Linear Systems*, IEEE Conference on Decision and Control (CDC), Las Vegas, USA, 2016, pp. 1352-1357, [44].

Chapter 4 is based on

- M.M.O. Abdelrahim, V.S. Dolk and W.P.M.H. Heemels, *Input-to-state Stabilizing Event-triggered Control for Linear Systems with Distributed and Quantized Output Measurements*, IEEE Transactions on Automatic Control, 2017, *Under review*, [2],

of which a preliminary version appeared as

- M.M.O Abdelrahim, V.S. Dolk, W.P.M.H. Heemels, *Input-to-state Stabilizing Event-triggered Control for Linear Systems with Output Quantization*, IEEE Conference on Decision and Control (CDC), Las Vegas, USA, 2016, pp. 483-488, [3].

Chapter 5 is based on

- V.S. Dolk and W.P.M.H. Heemels, *Event-triggered Control under Packet Losses*, Automatica, 2017, vol. 80, pp. 143-155, Jun. 2017, [74],

of which a preliminary version appeared as

- V.S. Dolk, W.P.M.H. Heemels, *Dynamic Event-triggered Control under Packet Losses: The Case with Acknowledgements*, First International Conference on Event-based Control, Communications & Signal Processing (EBCCSP), Krakow, Poland, 2015, pp. 1-7, [73].

Chapter 6 is based on

- V.S. Dolk, P. Tesi, C. De Persis and W.P.M.H. Heemels, *Event-triggered Control Systems under Denial-of-Service Attacks*, IEEE Transactions on Control of Network Systems (Special Issue on Secure Control of Cyber Physical Systems), 2017, vol. 4, no. 1, pp. 93-105, Mar. 2017, [77],

of which a preliminary version appeared as

- V.S. Dolk, P. Tesi, C. De Persis and W.P.M.H. Heemels, *Output-based Event-triggered Control Systems under Denial-of-Service Attacks*, IEEE Conference on Decision and Control (CDC), Osaka, Japan, 2015, pp. 4824-4829, [76].

Chapter 7 is based on

- V.S. Dolk, M.M.O. Abdelrahim, R. Postoyan and W.P.M.H. Heemels, *Event-triggered Multi-agent systems under Non-uniform Time-Varying Delays*, 2017, *Under review*, [239].

of which a preliminary version appeared as

- V.S. Dolk, M.M.O. Abdelrahim and W.P.M.H. Heemels, *Event-triggered Consensus Seeking under Non-uniform Time-Varying Delays*, IFAC World Congress 2017, [70].

Chapter 8 is based on

- V.S. Dolk, J. Ploeg and W.P.M.H. Heemels, *Event-triggered Control for String-Stable Vehicle Platooning*, IEEE Transactions on Intelligent Transport Systems, 2017, *Accepted for publication*, [75].

Besides the above mentioned works, the research presented in this thesis also led to the following publications:

- V.S. Dolk, J. Den Ouden, S. Steeghs, J. Gideon Devanesan, I. Badshah, A. Sudhakaran, K. Elferink and D. Chakraborty, *Cooperative Automated Driving for Various Traffic Scenarios: Experimental Validation in the GCDC 2016*, IEEE Transactions on Intelligent Transport Systems, 2017, *Accepted for publication*

- T. Korssen, V.S. Dolk, J.M. van de Mortel-Fronczak, M.A. Reniers and W.P.M.H. Heemels, *Systematic Model-Based Design and Implementation of Supervisors for Advanced Driver Assistance Systems*, IEEE Transactions on Intelligent Transport Systems, 2017, *Accepted for publication*

- S.H.J. Heijmans, V.S. Dolk, D.P. Borgers, W.P.M.H. Heemels, *Stability Analysis of Spatially Invariant Systems with Event-Triggered Communication*, International Conference on Event-Based Control, Communication and Signal Processing (EBCCSP), 2016, pp. 1-8, [123].

- W.P.M.H. Heemels, D.P. Borgers, V.S. Dolk, R. Geiselhart, S.H.J. Heijmans, *Constructions of Lyapunov Functions for Large-scale Networked Control Systems with Packet-based Communication*, European Control Conference (ECC), 2016, pp. 936-938, [109].

Chapter 2

Output-based and Decentralized Dynamic Event-triggered Control with Guaranteed $\mathcal{L}_p$-gain Performance and Zeno-freeness

Abstract – Networked control systems are often subject to limited communication resources. By only communicating output measurements when needed, event-triggered control is an adequate method to reduce the usage of communication resources while retaining desired closed-loop performance. In this chapter, a novel event-triggered control (ETC) strategy for a class of nonlinear feedback systems is proposed that can simultaneously guarantee a finite $\mathcal{L}_p$-gain and a strictly positive lower bound on the inter-event times. The new ETC scheme can be synthesized in an output-based and/or decentralized form, takes the specific medium access protocols into account, and is robust to (variable) transmission delays by design. Interestingly, in contrast with the majority of existing event-generators that only use static conditions the newly proposed event-triggering conditions are based on dynamic elements, which has several advantages including larger average inter-event times. The developed theory leads to families of event-triggered controllers that correspond to different trade-offs between (minimum and average) inter-event times, maximum allowable delays and $\mathcal{L}_p$-gains. A linear and a nonlinear numerical example will illustrate all the benefits of this new dynamic ETC scheme.

2.1 Introduction

Networked control systems (NCSs) are distributed systems consisting of plants and controllers of which sensor and actuation data is transmitted over shared

This chapter is based on [71, 72].

(wired or wireless) communication networks. These NCSs offer many advantages compared to conventional control systems in which sensor and actuation data is transmitted over dedicated point-to-point (wired) links. In particular, NCSs offer reduced installation costs, greater flexibility and better maintainability. Additionally, wireless communication is able to overcome the physical limitations of employing wired links. However, the usage of wireless communication also comes with inevitable network-induced imperfections. Indeed, since networked communication is inherently digital (packet-based), sensor and actuation data need to be quantized and cannot be transmitted continuously, but only at discrete time instants. Because the communication medium is often shared by multiple sensor, controller and actuator nodes, communication constraints are obviously also present. For this reason, there is a need for a medium access protocol, which governs the access of the nodes to the network, in order to prevent package dropouts, see, *e.g.*, [120,125,173,245]. Furthermore, NCSs are typically subject to variable transmission delays which are in some cases further amplified by high occupation rates of the network.

In traditional (networked) control setups, the transmission instants are determined purely based on time. In fact, in standard digital sampled-data control the transmissions are often triggered periodically in time, possibly with some jitter and delays in the communication. This time-triggered communication approach is predictable and easy to implement. For these reasons, a large portion of the NCS literature aims at finding time-based specifications such that the closed-loop system meets the desired stability and performance criteria, see, *e.g.*, [29, 51, 120, 125, 173, 245]. However, a time-triggered approach often results in redundant transmissions, as many transmissions will occur at times when this is not actually needed to achieve the desired stability and performance properties. This is due to the fact that time-based specifications are typically determined via worst-case estimates and should hold for all situations (all states) the system can attain.

As an alternative, it seems more natural to let the transmission intervals depend on the state of the system, thereby determining the actual need of having to use the communication resources. This resource-aware control view seems more appealing to deal with the scarcity of communication resources, especially when the control systems share the communication network with other devices and users. Examples of resource-aware control strategies include self-triggered control, see [15, 101, 158, 244, 249, 250], and event-triggered control, see [18, 20, 54, 117, 155, 224] for some early approaches, and see [114] for a recent overview.

In an event-triggered control approach, the transmission times are determined on-line, using well-designed event conditions based on, *e.g.*, output measurements of the system. As such, event-triggered control (ETC) is much better equipped than time-triggered control to balance resource utilization and control performance. One of the main difficulties of ETC is to design the *event-triggering mechanism* (ETM) in such a way that global asymptotic stability (GAS) (in

absence of disturbances) and/or finite $\mathcal{L}_p$-stability (for $p \in [1, \infty)$) are guaranteed together with a positive *minimum inter-event time* (MIET), especially for output-based and decentralized control configurations and the situation where disturbances are present [41,78]. This positive MIET is an essential property in order to exclude Zeno behavior (the occurrence of an infinite number of events in finite time), and to enable practical implementation of the ETC system. As such, an important problem is the construction of ETMs satisfying the following properties:

(i) Zeno-freeness in the sense of the existence of strictly positive MIETs, even in the presence of disturbances.

(ii) GAS in absence of disturbances and guaranteed $\mathcal{L}_p$-stability with finite $\mathcal{L}_p$-gains (for $p \in [1, \infty)$) with respect to a disturbance w and a certain performance output z.

Achieving these two requirements simultaneously is not trivial, as it has been shown recently in [41] that many ETMs do not lead to systems that have a positive MIET that is robust to disturbances, or do not guarantee GAS or $\mathcal{L}_p$-stability with finite $\mathcal{L}_p$-gains (where $p \in [1, \infty)$). For example, the approaches in [251, 259] consider $\mathcal{L}_p$-gains, however they do not provide a strictly positive MIET for the case that $w \neq 0$.

Even in the absence of disturbances, inter-event times of many ETMs converge to zero in case of output-based and decentralized control configurations [41, 78]. For this reason, recent works on ETC employ either time regularization [5, 7, 54, 87, 117, 218, 219, 225–228], in the sense that the triggering condition is only checked after a specific time duration δ since the last transmission has elapsed, or periodic event-triggered control (PETC) [54,112,117,126,164,184], in the sense that the triggering condition is checked at fixed periodic sampling time instants with sampling period h, such that the MIET is larger than or equal to δ or h, respectively. However, only a few of these works provide $\mathcal{L}_p$-stability analyses in case of output-based and decentralized event-triggered control. These include [112, 126] and [184], all using PETC schemes.

In this chapter, building upon the work of [51, 120], and extending our preliminary work [71] that focussed on the centralized state-feedback case only, a novel time-regularized *event-triggered control* strategy is introduced that does satisfy the above mentioned criteria. Our new method uses the unique combination of *dynamic* event-triggering conditions [96, 191] and time regularization [5,7,87,112,117,225–228]. Unlike [96,191], which consider the state-feedback case where neither delays nor disturbances are present, here we consider the output-based and/or decentralized case with delays and disturbances. The use of dynamic ETMs is a key ingredient, as *static* ETMs (which are studied in the majority of the ETC literature) in combination with time-regularization, often reduce to approximately time-triggered periodic communication, in presence of

disturbances when the state is close to the origin which typically leads to redundant transmission instants, see, *e.g.*, Example 3 in [41] or the numerical example in [71]. Under the same stability and performance properties, our dynamic ETC scheme does not exhibit this undesirable behavior and satisfies next to (i)-(ii), also the following properties:

(iii) When the system is close to the desired equilibrium, the transmission instants do not unnecessarily become (almost) equidistantly distributed in time with inter-transmission intervals close to the enforced lower bounds δ or h, as mentioned before.

(iv) Robust performance in the sense that the guarantees on GAS and/or the $\mathcal{L}_p$-gains also hold in the presence of (variable) transmission delays (within certain bounds).

(v) Output-based and/or decentralized (asynchronous and multi-network) form (in the sense that multiple networks can be present in the system).

A starting point of our results is the work [120], which leads in the context of NCSs to *time-based* specifications in terms of a so-called *maximum allowable transmission interval* (MATI) and a *maximum allowable delay* (MAD). The resulting trade-off curves in [120] specify that as long as the transmission intervals are smaller than the MATI and the delays are smaller than the (corresponding) MAD, specific upper bounds on the $\mathcal{L}_p$-gains are guaranteed. Hence, the MATI and the MAD are bounds used to express the timing specifications. Interestingly, for a given $\mathcal{L}_p$-gain, the MIET and the MAD of the ETC strategy proposed here are close to or equal to the MATI and MAD in [51, 120] corresponding to the same $\mathcal{L}_p$-gain. However, simulations show that the *average* transmission interval of the proposed strategy is much larger due to the event-based triggering. Hence, the ETC method also achieves the following property, which is a general requirement for any ETC scheme:

(vi) Effectively achieve the same control performance, but significantly reduce the number of transmissions compared to control strategies using time-based specifications, with the MIET close to the available MATI bounds but the *average* inter-event times much larger.

Although we do not prove this analytically in the present chapter, we show through numerical examples that the proposed dynamic ETC scheme indeed displays this property in situations where the conventional (static) ETC schemes fail. In fact, the newly proposed ETC scheme satisfies all the six criteria (i)-(vi), which is, to the best of our knowledge, the first time that this has been accomplished. Moreover, the corresponding event-triggering conditions can be constructed via a systematic procedure allowing trade-offs among performance in terms of $\mathcal{L}_p$-gains, robustness in terms of MADs, and network utilization, which will be demonstrated by means of two numerical examples.

The remainder of this chapter is organized as follows. After presenting the necessary preliminaries and notational conventions in Section 2.1.1, we introduce the decentralized networked control setup and the problem statement in Section 2.2, which are formalized in Section 2.3 by deriving a complete mathematical model of the closed-loop system. In Section 2.4 we derive conditions for the proposed event-triggering strategy such that stability or $\mathcal{L}_p$-gain properties can be guaranteed. Section 2.5 shows how an ETM can be designed systematically and implemented. Finally, we illustrate the presented theory with two numerical examples in Section 2.6, and provide conclusions in Section 2.7.

2.1.1 Definitions and Preliminaries

The following notational conventions are used in this chapter. $\mathbb{N}$ denotes the set of all non-negative integers, $\mathbb{N}_{>0}$ denotes the set of all positive integers, $\mathbb{R}$ denotes the field of all real numbers and $\mathbb{R}_{\geqslant 0}$ denotes the set of all non-negative reals. For $N \in \mathbb{N}$, we write the set $\{1, 2, \ldots, N\}$ as $\bar{N}$. For N vectors $x_i \in \mathbb{R}^{n_i}, i \in \bar{N}$, we denote the vector obtained by stacking all vectors in one (column) vector $x \in \mathbb{R}^n$ with $n = \sum_{i=1}^{N} n_i$ by $(x_1, x_2, \ldots, x_N)$, *i.e.*, $(x_1, x_2, \ldots, x_N) = \begin{bmatrix} x_1^\top & x_2^\top & \cdots & x_N^\top \end{bmatrix}^\top$. The vectors in $\mathbb{R}^N$ consisting of all ones and zeros are denoted by $\mathbf{1}_N$ and $\mathbf{0}_N$, respectively. By $|\cdot|$ and $\langle \cdot, \cdot \rangle$ we denote the Euclidean norm and the usual inner product of real vectors, respectively. With $\bar{e}_i$ we denote the compound vector of all e_j, $j \in \bar{N} \,/\{i\}$, *i.e.*, $\bar{e}_i = (e_1, \ldots, e_{i-1}, e_{i+1}, \ldots, e_N)$. For a real symmetric matrix A, $\lambda_{\max}(A)$ denotes the largest eigenvalue of A. I_N denotes the identity matrix of dimension $N \times N$ and, if N is clear for the context, we write I. $0_{N \times M}$ denotes an $N \times M$ matrix with all entries equal to zero. The expression $\operatorname{diag}(A_1, A_2, \ldots, A_N)$ with matrices $A_i \in \mathbb{R}^{n_i \times m_i}$ denotes a block-diagonal matrix. A function $\alpha : \mathbb{R}_{\geqslant 0} \to \mathbb{R}_{\geqslant 0}$ is said to be of class $\mathcal{K}$ if it is continuous, strictly increasing and $\alpha(0) = 0$. It is said to be of class $\mathcal{K}_\infty$ if it is of class $\mathcal{K}$ and it is unbounded. A continuous function $\beta : \mathbb{R}_{\geqslant 0} \times \mathbb{R}_{\geqslant 0} \to \mathbb{R}_{\geqslant 0}$ is said to be of class $\mathcal{KL}$ if, for each fixed s, the mapping $r \mapsto \beta(r, s)$ belongs to class $\mathcal{K}$ and for each fixed r, the mapping $s \to \beta(r, s)$ is decreasing and $\beta(r, s) \to 0$ as $s \to \infty$. A continuous function $\gamma : \mathbb{R}_{\geqslant 0} \times \mathbb{R}_{\geqslant 0} \times \mathbb{R}_{\geqslant 0} \to \mathbb{R}_{\geqslant 0}$ is said to be of class $\mathcal{KLL}$ if, for each $r \geqslant 0$, both $\gamma(\cdot, \cdot, r)$ and $\gamma(\cdot, r, \cdot)$ belong to class $\mathcal{KL}$. A function $f : \mathbb{R}^n \to \mathbb{R}^n$ is said to be locally Lipschitz continuous if for each $x_0 \in \mathbb{R}^n$ there exist constants $\delta > 0$ and $L > 0$ such that for all $x \in \mathbb{R}^n$ we have that $|x - x_0| \leqslant \delta \Rightarrow |f(x) - f(x_0)| \leqslant L|x - x_0|$. A function $f : \mathbb{R}^n \to \mathbb{R}^n$ is said to be linearly bounded if there exists a constant $L > 0$ such that for all $x \in \mathbb{R}^n$, we have that $|f(x)| \leqslant L|x|$. A set-valued mapping from a set X to a set Y, associates, with every point $x \in X$, a subset of Y. The notation $F : X \rightrightarrows Y$, indicates that F is a set-valued mapping from X to Y with $M(x) \subset Y$ for all $x \in X$.

In this chapter, we will model network control systems (NCSs) as a hybrid

system $\mathcal{H}$ of the form

$$\dot{\xi} = F(\xi, w), \text{ when } \xi \in C, \tag{2.1a}$$

$$\xi^+ \in G(\xi), \quad \text{when } \xi \in D, \tag{2.1b}$$

where F describes the flow dynamics, G the jump dynamics, C the flow set and D the jump set. We now recall some definitions given in [98] on the solutions of such hybrid system.

Definition 2.1. *A* compact hybrid time domain *is a set* $\mathcal{D} = \bigcup_{j=0}^{J-1} [t_j, t_{j+1}] \times \{j\} \subset \mathbb{R}_{\geqslant 0} \times \mathbb{N}$ *with* $J \in \mathbb{N}_{>0}$ *and* $0 = t_0 \leqslant t_1 \ldots \leqslant t_J$. *A* hybrid time domain *is a set* $\mathcal{D} \subset \mathbb{R}_{\geqslant 0} \times \mathbb{N}$ *such that* $\mathcal{D} \cap ([0, T] \times \{0, 1, \ldots, J\})$ *is a compact hybrid time domain for each* $(T, J) \in \mathcal{D}$.

Definition 2.2. *A* hybrid trajectory *is a pair* $(dom\,\xi, \xi)$ *consisting of a hybrid time domain* $dom\,\xi$ *and a function* ξ *defined on* $dom\,\xi$ *that is absolutely continuous in* t *on* $(dom\,\xi) \cap (\mathbb{R}_{\geqslant 0} \times \{j\})$ *for each* $j \in \mathbb{N}$.

Definition 2.3. *For the hybrid system* $\mathcal{H}$ *given by the state space* $\mathbb{R}^n$, *the (disturbance) input space* $\mathbb{R}^{n_w}$ *and the data* (F, G, C, D), *where the flow map* $F : \mathbb{R}^n \times \mathbb{R}^{n_w} \to \mathbb{R}^n$, *the jump map* $G : \mathbb{R}^n \rightrightarrows \mathbb{R}^n$, *and the flow set* C *and the jump set* D *are subsets of* $\mathbb{R}^n$, *a hybrid trajectory* $(dom\,\xi, \xi)$ *with* $\xi : \ dom\,\xi \to \mathbb{R}^n$ *is a* solution to $\mathcal{H}$ *for a locally integrable input function* $w : \mathbb{R}_{\geqslant 0} \to \mathbb{R}^{n_w}$, *if*

1) for all $j \in \mathbb{N}$ *and for almost all* $t \in I_j := \{t \in \mathbb{R}_{\geqslant 0} \mid (t, j) \in dom\,\xi\}$, *we have* $\xi(t, j) \in C$ *and* $\dot{\xi}(t, j) = F(\xi(t, j), w(t))$.

2) for all $(t, j) \in dom\,\xi$ *such that* $(t, j + 1) \in dom\,\xi$, *we have* $\xi(t, j) \in D$ *and* $\xi(t, j + 1) \in G(\xi(t, j))$.

For the motivation and more details on these definitions, the interested reader is referred to [98]. We will often not mention $\mathrm{dom}\,\xi$ explicitly, and understand that with each hybrid trajectory ξ comes a hybrid time domain $\mathrm{dom}\,\xi$.

In addition, for $p \in \mathbb{R}_{\geqslant 1}$, we introduce the $\mathcal{L}_p$-norm of a function ξ defined on a hybrid time domain $\mathrm{dom}\,\xi = \bigcup_{j=0}^{J-1} [t_j, t_{j+1}] \times \{j\}$ with J possibly ∞ and/or $t_J = \infty$ by

$$\|\xi\|_{\mathcal{L}_p} = \left(\sum_{j=0}^{J-1} \int_{t_j}^{t_{j+1}} |\xi(t, j)|^p dt \right)^{1/p} \tag{2.2}$$

provided the right-hand side is well-defined and finite. In case $\|\xi\|_{\mathcal{L}_p}$ is finite, we say that $\xi \in \mathcal{L}_p$. Note that this definition is essentially identical to the usual $\mathcal{L}_p$-norm in case a function is defined on a subset of $\mathbb{R}_{\geqslant 0}$.

Lemma 2.1. *Consider* $a, b \in \mathbb{R}$ *and some constant* $\varepsilon > 0$, *then it holds that* $2ab \leqslant (1/\varepsilon)\, a^2 + \varepsilon b^2$.

2.2 NCS setup and problem statement

In this section, we introduce the (decentralized) event-triggered NCS with communication constraints caused by network limitations and network-induced imperfections such as varying transmission delays. Based on this description, we also provide the problem statement considered in this chapter.

2.2.1 Networked control configuration

In this chapter, we consider the networked control configuration shown in Figure 2.1 which consists of a continuous-time nonlinear plant $\mathcal{P}$ and a controller $\mathcal{C}$ which are connected via N independent communication networks. In an NCS, in contrast to conventional control setups that rely on dedicated point-to-point links, the sensor and/or actuator data is communicated over (wireless) networks in a package-based manner. The plant $\mathcal{P}$ is given by

$$\mathcal{P}: \begin{cases} \dot{x}_p &= f_p(x_p, \hat{u}, w) \\ y &= g_p(x_p), \end{cases} \tag{2.3}$$

where $x_p \in \mathbb{R}^{n_p}$ denotes the plant state, $w \in \mathbb{R}^{n_w}$ is a disturbance input, $\hat{u} \in \mathbb{R}^{n_u}$ represents a vector of the most recently received control signals and $y \in \mathbb{R}^{n_y}$ is the output of $\mathcal{P}$. The controller $\mathcal{C}$ is given by

$$\mathcal{C}: \begin{cases} \dot{x}_c &= f_c(x_c, \hat{y}) \\ u &= g_c(x_c), \end{cases} \tag{2.4}$$

where $x_c \in \mathbb{R}^{n_c}$ denotes the controller state, $\hat{y} \in \mathbb{R}^{n_y}$ represents a vector of most recently received sensor data and $u \in \mathbb{R}^{n_u}$ represents a vector of control signals. The functions f_p and f_c are assumed to be continuous and the functions g_p and g_c are assumed to be continuously differentiable.

The communication of sensor and actuator data between $\mathcal{P}$ and $\mathcal{C}$ is (possibly) performed via multiple networks $\mathcal{N}_1, \mathcal{N}_2, \ldots, \mathcal{N}_N$ that operate asynchronously and independently. To facilitate the description and analysis of the decentralized event-triggered control setup, we define $v := (y, u) \in \mathbb{R}^{n_v}$ and $\hat{v} := (\hat{y}, \hat{u}) \in \mathbb{R}^{n_v}$ with $n_v := n_y + n_u$. For simplicity of exposition, we assume (possibly after reordering) that $v = (v_1, v_2, \ldots, v_N)$ and $\hat{v} = (\hat{v}_1, \hat{v}_2, \ldots, \hat{v}_N)$ and that $v_i,\ i \in \bar{N}$, is communicated over the network $\mathcal{N}_i,\ i \in \bar{N}$.

2.2.2 Communication networks and protocols

In the networked control configuration of Figure 2.1, output v_i is sampled and transmitted over the network $\mathcal{N}_i,\ i \in \bar{N}$, to the plant $\mathcal{P}$ or controller $\mathcal{C}$, at transmission times $t_j^i, j \in \mathbb{N}$, satisfying $0 \leqslant t_0^i < t_1^i < t_2^i < \ldots$. The update of $\hat{v}_i$

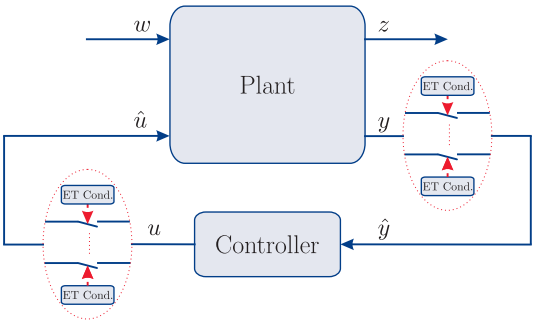

Fig. 2.1. Networked control setup consisting of a plant $\mathcal{P}$ and a controller $\mathcal{C}$, connected via N independent communication networks $\mathcal{N}_i$, $i \in \bar{N}$.

corresponding to transmission time t_j^i occurs after a communication delay of τ_j^i time units. See [120] for a more detailed discussion on communication delays.

In this chapter, we consider the so-called small-delay case, meaning that reception of new information occurs before the next transmission is due. In fact, we assume that the communication delays in each network $\mathcal{N}_i$, $i \in \bar{N}$, are upper-bounded by a *maximum allowable delay* (MAD). To be more precise, we adopt the following standing assumption.

Assumption 2.1. *The transmission delays in network* $\mathcal{N}_i$, $i \in \bar{N}$, *satisfy* $0 \leqslant \tau_j^i \leqslant \tau_{mad}^i \leqslant \tau_{miet}^i$, *for all* $j \in \mathbb{N}$, *where* τ_{mad}^i *denotes the* maximum allowable delay *of network* $\mathcal{N}_i$ *and where* τ_{miet}^i *denotes a lower-bound on the* minimum inter-event time *of network* $\mathcal{N}_i$, i.e., $\tau_{miet}^i \leqslant \inf_{j\in\mathbb{N}}(t_{j+1}^i - t_j^i)$.

An update of $\hat{v}_i$ at $t_j^i + \tau_j^i$ for some $i \in \bar{N}$ and $j \in \mathbb{N}$, can be described as

$$\hat{v}_i((t_j^i + \tau_j^i)^+) = v_i(t_j^i) + h_i(j, e_i(t_j^i)), \tag{2.5}$$

where $e_i \in \mathbb{R}^{n_{v,i}}$ denotes the network-induced error $e_i := \hat{v}_i - v_i$ and where $e := \hat{v} - v = (e_1, e_2, \ldots, e_N)$. The functions h_i, $i \in \bar{N}$, can be used to model medium access protocols as described in [51, 120, 173]. These medium access protocols are typically employed in case network $\mathcal{N}_i$ is shared by multiple (sensor or actuator) nodes where each of these nodes correspond to a subset of the entries of $v_i/\hat{v}_i$, $i \in \bar{N}$.

Remark 2.1. In the ETC literature, the standard case that is typically considered is that each network updates asynchronously according to $\hat{v}_i((t_j^i+\tau_j^i)^+) = v_i(t_j^i)$, which corresponds to $h_i(j, e_i) = 0$, for all $i \in \bar{N}$, $j \in \mathbb{N}$ and all $e_i \in \mathbb{R}^{n_{v,i}}$. However, by building upon [51, 120, 173], a framework can be obtained that allows us to study next to this standard sampled-data ETC setup, also other access protocols including the Round-Robin (RR) and the Try-Once-Discard

(TOD) protocols in one framework without additional burden. Therefore, we decided to present the work at this level of generality. We envision that the combination of ETC and medium access protocols could be valuable in future extensions and particular applications.

Remark 2.2. For simplicity of exposition, we focus here on the control configuration as in Figure 2.1. However, the ETC method presented in this work also applies to other configurations such as the case of static state feedback control and the case where either $\hat{u} = u$ or $\hat{y} = y$, meaning that the corresponding signals are not transmitted over a (shared) network, but are continuously available. These configurations can all be captured in the same hybrid model as presented in Section 2.3.2 on which our ETC design is based. To illustrate this flexibility, we will consider two numerical examples in which $\hat{u} = u$ in Section 2.6.

2.2.3 Problem statement

As motivated in the introduction, in most NCSs it is desirable to reduce the usage of communication resources as much as possible (while still guaranteeing the required stability and performance properties). Therefore, we consider event-triggered communication as illustrated in Figure 2.1.

The problem considered in this work is to derive a systematic methodology for the design of triggering conditions such that the criteria (i)-(vi) discussed in the introduction are met. A more rigorous problem formulation is provided in the next section, based on a complete mathematical model for the event-triggered closed-loop NCS.

2.3 Mathematical Model of the Event-triggered Control Setup

2.3.1 Event-triggering mechanism

In this work, for each network $\mathcal{N}_i$, $i \in \bar{N}$, the proposed event-triggering mechanism takes the form

$$t_0^i = 0,\ t_{j+1}^i := \inf\left\{t > t_j^i + \tau_{miet}^i \mid \eta_i(t) \leqslant 0\right\}, \tag{2.6}$$

for $i \in \bar{N}$ and for all $j \in \mathbb{N}$, where $\tau_{miet}^i \in \mathbb{R}_{>0}$ is a lower bound on the MIET (see also Standing Assumption 2.1) and $\eta_i \in \mathbb{R}_{\geqslant 0}$ is an auxiliary variable. The variable η_i will evolve according to

$$\dot{\eta}_i = \Psi_i(o_i), \tag{2.7}$$

for $i \in \bar{N}$, for some well-designed function Ψ_i, which we will specify in Section 2.4. Let us already remark that the argument o_i represents locally available information only, such as v_i, e_i and some other local variables, which are introduced

in Section 2.3.2. In this manner, the event generators will have a decentralized and output-based structure and thereby enable satisfaction of property (v) mentioned in the introduction. Note that the state variables η_i, $i \in \bar{N}$, evolve independently of each other and thus the transmissions for the networks $\mathcal{N}_i$, $i \in \bar{N}$, are indeed triggered asynchronously and independently. Observe that by taking $\tau^i_{miet} \in \mathbb{R}_{>0}, i \in \bar{N}$, the adopted time regularization imposes that the next event can only take place after at least a fixed amount of time $\tau^i_{miet} > 0$ has elapsed, *i.e.*, $t^i_{j+1} - t^i_j \geqslant \tau^i_{miet}$, for each $j \in \mathbb{N}$. In this way, so-called Zeno behavior is excluded from the ETC system and property (i) mentioned in the introduction is satisfied. Moreover, observe that Standing Assumption 2.1 is indeed valid for the event-triggered system if τ^i_{miet} is designed such that $\tau^i_{miet} \geqslant \tau^i_{mad}$, for all $i \in \bar{N}$. As we will show in Section 2.4, the time τ^i_{miet} can be taken close to or, under some conditions, equal to the MATI bounds as derived in [51,120,173,245]. As such, the smallest inter-transmission times (lower bounded by the MIET) in the ETC scheme are always close to or equal to the largest inter-transmission times (MATI) in time-based triggering with the consequence that the resource utilization of the ETC scheme will never be worse than the triggering based on time-based specifications (MATI), as in [51, 120, 173, 245]. In addition, we will show that the average inter-transmission times are typically much larger in the novel ETC schemes that we will propose. This corresponds to property (vi) mentioned in the introduction. Finally, notice that a *dynamic event-triggering mechanism* (2.6)-(2.7) is employed which, as we will discuss in Remark 2.4 and show in the numerical examples, is important in realizing property (iii) mentioned in the introduction. The satisfaction of properties (ii) and (iv) follow from the analysis in Section 2.4.

2.3.2 Hybrid model

In order to analyze asymptotic stability and $\mathcal{L}_p$-stability in the next section, we model the NCS employing event-triggered communication by means of the hybrid system framework as developed in [98, 100], which was also employed in [5, 7, 51, 110, 120, 173, 191] in the context of NCSs.

To provide this hybrid model, we assume that the value of $\hat{v}_i$ evolves according to a zero-order hold model, meaning that $\hat{v}_i$ is kept constant between the update times $t^i_j + \tau^i_j$ and $t^i_{j+1} + \tau^i_{j+1}$ for all $j \in \mathbb{N}$, *i.e.*,

$$\dot{\hat{v}}_i(t) = 0, \quad t \in (t^i_j + \tau^i_j, t^i_{j+1} + \tau^i_{j+1}]. \tag{2.8}$$

By means of (2.5), following [120], we can write the jump dynamics of e_i at an

update event as follows

$$\begin{aligned} e_i((t_j^i+\tau_j^i)^+) &= \hat{v}_i((t_j^i+\tau_j^i)^+) - v_i(t_j^i+\tau_j^i) \\ &= h_i(j, e_i(t_j^i)) + v_i(t_j^i) - \hat{v}_i(t_j^i) \\ &\quad - v_i(t_j^i+\tau_j^i) + \hat{v}_i(t_j^i+\tau_j^i) \\ &= h_i(j, e_i(t_j^i)) - e_i(t_j^i) + e_i(t_j^i+\tau_j^i). \end{aligned} \tag{2.9}$$

Notice that we used the fact that $\hat{v}_i(t_j^i) = \hat{v}_i(t_j^i+\tau_j^i)$, for each $j \in \mathbb{N}$, due to the zero-order hold assumption and Standing Assumption 2.1. Here we consider $\hat{v}_i$ and e_i as left-continuous signals in the sense that for all $t>0$, $\hat{v}_i(t) = \lim_{s\uparrow t} \hat{v}_i(s)$.

In order to formulate the dynamics of the event-triggered NCS in terms of flow and jump equations as in [98, 100], we will introduce as in [120] additional states $l_i \in \{0,1\}$, $s_i \in \mathbb{R}^{n_i}$, $\kappa_i, \in \mathbb{N}$ and $\tau_i \in \mathbb{R}_{\geqslant 0}$, $i \in \bar{N}$. The variable l_i is a boolean, which keeps track of whether the next event in network $\mathcal{N}_i$ is a transmission event or an update event, indicated by $l_i = 0$ and $l_i = 1$, respectively. The variable s_i serves as a memory variable to store the value $h_i(j, e_i(t_j^i)) - e_i(t_j^i)$ (present in (2.9)) at the moment of a transmission at time t_j^i and is used to model the update event at time $t_j^i + \tau_j^i$. The integer variable κ_i is used to keep track of the total amount of transmissions in network $\mathcal{N}_i$ over time and the timer variable τ_i, $i \in \bar{N}$, is adopted to capture the time elapsed since the last transmissions and to assure that Standing Assumption 2.1 remains valid. Consider the state vector $\xi := (x, e, \tau, \kappa, s, l, \eta) \in \mathbb{X}$ with $\mathbb{X} := \{(x, e, \tau, \kappa, s, l, \eta) \in \mathbb{R}^{n_x} \times \mathbb{R}^{n_v} \times \mathbb{R}^N_{\geqslant 0} \times \mathbb{N}^N \times \mathbb{R}^{n_v} \times \{0,1\}^N \times \mathbb{R}^N_{\geqslant 0}\}$, and the vectors $\tau := (\tau_1, \tau_2, \ldots, \tau_N) \in \mathbb{R}^N_{\geqslant 0}$, $\kappa := (\kappa_1, \kappa_2, \ldots, \kappa_N) \in \mathbb{N}^N$, $s := (s_1, s_2, \ldots, s_N) \in \mathbb{R}^{n_v}$, $l := (l_1, l_2, \ldots, l_N) \in \{0,1\}^N$ and $\eta := (\eta_1, \eta_2, \ldots, \eta_N) \in \mathbb{R}^N_{\geqslant 0}$. By combining these new state variables with (2.3), (2.4) and (2.7), the flow dynamics of the interconnection $(\mathcal{P}, \mathcal{C}, \mathcal{N}_1, \ldots, \mathcal{N}_N)$ is given by

$$F(\xi, w) := \big(f(x,e,w), g(x,e,w), \mathbf{1}_N, \mathbf{0}_N, \mathbf{0}_N, \mathbf{0}_N, \Psi(v, e, \tau, \kappa, s, l, \eta)\big), \tag{2.10}$$

where $\Psi(v, e, \tau, \kappa, s, l, \eta) = (\Psi_1(o_1), \Psi_2(o_2), \ldots, \Psi_N(o_N))$ with $o_i = \big(v_i, e_i, \tau_i, \kappa_i, s_i, l_i, \eta_i\big) \in \mathbb{O}_i := \mathbb{R}^{n_{v,i}} \times \{0,1\} \times \mathbb{R}^{n_{v,i}} \times \mathbb{R}^{n_{v,i}} \times \mathbb{R}_{\geqslant 0} \times \mathbb{R}_{\geqslant 0}$, and where $f(x,e,w)$ is given by

$$f(x,e,w) = \begin{bmatrix} f_p(x_p, g_c(x_c) + \Gamma_u e, w) \\ f_c(x_c, g_p(x_p) + \Gamma_y e) \end{bmatrix}, \tag{2.11}$$

where $\Gamma_y := \begin{bmatrix} I_{n_y} & 0_{n_y \times n_u} \end{bmatrix}$ and $\Gamma_u := \begin{bmatrix} 0_{n_u \times n_y} & I_{n_u} \end{bmatrix}$. To obtain the expression for $g(x,e,w)$, observe that due to (2.8) we have that $\dot{e} = -\dot{v}$. By combining this fact with (2.3) and (2.4), we obtain that

$$g(x,e,w) = \begin{bmatrix} -\frac{\partial g_p}{\partial x_p}(x_p) f_p(x_p, g_c(x_c) + \Gamma_u e, w) \\ -\frac{\partial g_c}{\partial x_c}(x_c) f_c(x_c, g_p(x_p) + \Gamma_y e) \end{bmatrix}. \tag{2.12}$$

The corresponding flow set is given by

$$C := \bigcap_{i \in \bar{N}} C_i \tag{2.13}$$

with

$$C_i := \big\{\xi \in \mathbb{X} \mid \big((\tau_i \leqslant \tau^i_{miet} \vee \eta_i \geqslant 0) \wedge l_i = 0\big) \\ \vee \big(0 \leqslant \tau_i \leqslant \tau^i_{mad} \wedge l_i = 1\big)\big\}, \tag{2.14}$$

for $i \in \bar{N}$.

To define the jump map, we introduce the notation $\Gamma_i \in \mathbb{R}^{N\times N}$, representing a matrix of which the ii-th (diagonal) entry is equal to one and all other entries are zero, and $\bar{\Gamma}_i \in \mathbb{R}^{n_v \times n_v}$ is a diagonal matrix consisting of diagonal elements being zero for the indices corresponding to the networks $\mathcal{N}_1, \ldots, \mathcal{N}_{i-1}$, $\mathcal{N}_{i+1}, \ldots, \mathcal{N}_N$ and one for the network $\mathcal{N}_i$. In particular,

$$\big(\bar{\Gamma}_i\big)_{jj} = \begin{cases} 1, & \sum_{l=1}^{i-1} n_{v,l} < j \leqslant \sum_{l=1}^{i} n_{v,l}, \\ 0, & \text{otherwise.} \end{cases}$$

The jump dynamics is given by $\xi^+ \in G(\xi)$ with jump map $G(\xi) = \bigcup_{i=1}^N G_i(\xi)$, where

$$G_i(\xi) := \begin{cases} \{G_{0,i}(\xi)\}, & \text{when } \xi \in D_i \wedge l_i = 0 \\ \{G_{1,i}(\xi)\}, & \text{when } \xi \in D_i \wedge l_i = 1 \\ \emptyset, & \text{when } \xi \notin D_i \end{cases} \tag{2.15}$$

and

$$G_{0,i}(\xi) := \begin{pmatrix} x \\ e \\ (I_N - \Gamma_i)\tau \\ \kappa + \Gamma_i \mathbf{1}_N \\ \bar{\Gamma}_i(h(\kappa, e) - e) + (I_{n_v} - \bar{\Gamma}_i)s \\ l + \Gamma_i \mathbf{1}_N \\ \eta \end{pmatrix}, \tag{2.16}$$

$$G_{1,i}(\xi) := \big(x, \bar{\Gamma}_i s + e, \tau, \kappa, (I_{n_v} - \bar{\Gamma}_i)s, l - \Gamma_i \mathbf{1}_N, \eta\big), \tag{2.17}$$

where $h(\kappa, e) = (h_1(\kappa_1, e_1), h_2(\kappa_2, e_2), \ldots, h_N(\kappa_N, e_N))$. The function $G_{0,i}$ describes how the entire state ξ jumps when network $\mathcal{N}_i$ grants access to one of its nodes to transmit. Note that the memory state s_i is assigned the value $h_i(\kappa_i, e_i) - e_i$, which corresponds to the term $h_i(j, e_i(t^i_j)) - e_i(t^i_j)$ in (2.9), while the transmission error e_i remains the same. Furthermore, observe that l_i jumps to the value 1, which ensures that the next event in network $\mathcal{N}_i$ can only be an update event (thereby guaranteeing the small-delay assumption as described in Standing Assumption 1). The function $G_{1,i}$ describes how ξ jumps when in $\mathcal{N}_i$

an update event occurs. Observe that the reset of e_i as described by this part of the jump map corresponds to (2.9) and that l_i toggles back to 0, enforcing a transmission event as the next event in network $\mathcal{N}_i$. Also important to note is that the jump for s_i when $l_i = 1$ can be chosen arbitrarily from a modeling point of view since no information needs to be stored at the moment of an update event. We arbitrate here the update $s_i^+ = 0$. The corresponding jump set is given by

$$D := \bigcup_{i \in \bar{N}} D_i, \tag{2.18}$$

where

$$D_i := \left\{ \xi \in \mathbb{X} \mid \left(\tau_i \geqslant \tau_{miet}^i \wedge \eta_i \leqslant 0 \wedge l_i = 0 \right) \vee (l_i = 1) \right\}. \tag{2.19}$$

By means of definitions (2.10)-(2.19) presented above, we can now obtain the hybrid model $\mathcal{H} = (F, G, C, D)$ as in (2.1) representing the entire decentralized ETC setup as illustrated in Figure 2.1.

Definition 2.4. *For the hybrid system $\mathcal{H}$ with $w = 0$, the set given by $\mathcal{E} := \{\xi \in \mathbb{X} \mid x = \mathbf{0}_{n_x}, e = s = \mathbf{0}_{n_v}, \eta = \mathbf{0}_N\}$ is said to be* uniformly globally asymptotically stable *(UGAS) if there exists a function $\beta \in \mathcal{KLL}$ such that, for any initial condition $\xi(0,0) \in \mathbb{X}_0$ with $\mathbb{X}_0 = \{\xi \in \mathbb{X} \mid \ l = \mathbf{0}_N\}$, all corresponding solutions ξ as in Definition 2.3 satisfy*

$$|\, (x(t,j), e(t,j), s(t,j), \eta(t,j)) \,| \leqslant \beta \left(|\, (x(0,0), e(0,0), s(0,0), \eta(0,0)) \,|, t, j \right)$$

for all $(t,j) \in dom\, \xi$. The set $\mathcal{E}$ is said to be uniformly globally exponentially stable *(UGES) if β can be taken of the form $\beta(r,t,k) = Mr \exp(-\varrho(t+k))$ for some $M \geqslant 0$ and $\varrho > 0$ in the inequality above.*

In case of the disturbance w being present, the performance of the hybrid system $\mathcal{H}$ might be defined as the level of disturbance attenuation with respect to some output variable

$$z = q(x, w). \tag{2.20}$$

Definition 2.5. *The hybrid system $\mathcal{H}$ is said to be $\mathcal{L}_p$-stable from input w to output z with an $\mathcal{L}_p$-gain less than or equal to θ, if there exists a $\mathcal{K}_\infty$-function β such that for any exogenous input $w \in \mathcal{L}_p$, and any initial condition $\xi(0,0) \in \mathbb{X}_0$ with $\mathbb{X}_0 = \{\xi \in \mathbb{X} \mid l = \mathbf{0}_N\}$, each corresponding solution to $\mathcal{H}$ satisfies*

$$\|z\|_{\mathcal{L}_p} \leqslant \beta(|\, (x(0,0), e(0,0), s(0,0), \eta(0,0)) \,|) + \theta \|w\|_{\mathcal{L}_p}. \tag{2.21}$$

The problem that we loosely formulated at the end of Section 2.2 can now be formally given as follows.

Problem 2.1. *Given a controller (2.4) for the plant (2.3) and a desired $\mathcal{L}_p$-gain $\theta \in \mathbb{R}_{\geqslant 0}$ in case disturbances are present, determine the values of $\tau_{miet}^i \in \mathbb{R}_{>0}$,*

the function Ψ^i in the event generator given by (2.6) and (2.7), and values of the maximum allowable delays τ^i_{mad}, for each network $\mathcal{N}_i, i \in \bar{N}$, such that the system $\mathcal{H}$ is UGAS (and sometimes even UGES) in case $w = 0$ and/or, in the presence of disturbances, $\mathcal{L}_p$-stable with an $\mathcal{L}_p$-gain less than or equal to θ, with a strictly positive τ^i_{miet} to assure Zeno-freeness and with large (average) inter-event times $t^i_{j+1} - t^i_j$, $j \in \mathbb{N}$.

2.4 ETM design conditions with stability and $\mathcal{L}_p$-gain guarantees

In Sections 2.4.1 and 2.4.2, conditions are presented such that the ETM given by (2.6) and (2.7) ensures UGAS (and sometimes even UGES) in case $w = 0$ and $\mathcal{L}_p$-stability with a desired $\mathcal{L}_p$-gain in case disturbances are present for the system $\mathcal{H}$. In both cases, in order to specify suitable τ^i_{miet}, τ^i_{mad} and Ψ_i, for all $i \in \bar{N}$, for the ETM given by (2.6)-(2.7), we need to consider the following condition.

Condition 2.1. *([120]) For each $i \in \bar{N}$, there exist a function $\tilde{W}_i : \mathbb{N} \times \{0,1\} \times \mathbb{R}^{n_{v,i}} \times \mathbb{R}^{n_{v,i}} \to \mathbb{R}_{\geqslant 0}$ with $\tilde{W}_i(\kappa_i, l_i, \cdot, \cdot)$ locally Lipschitz for all fixed $\kappa_i \in \mathbb{N}$ and $l_i \in \{0,1\}$, $\mathcal{K}_\infty$-functions $\underline{\beta}_{W,i}$ and $\bar{\beta}_{W,i}$, and $0 < \lambda_i < 1$ such that for all $\kappa_i \in \mathbb{N}$, $l_i \in \{0,1\}$, $s_i \in \mathbb{R}^{n_{v,i}}$ and all $e_i \in \mathbb{R}^{n_{v,i}}$, it holds that*

$$\tilde{W}_i(\kappa_i + 1, 1, e_i, h_i(\kappa_i, e_i) - e_i) \leqslant \lambda_i \tilde{W}_i(\kappa_i, 0, e_i, s_i), \tag{2.22}$$

$$\tilde{W}_i(\kappa_i, 0, s_i + e_i, 0) \leqslant \tilde{W}_i(\kappa_i, 1, e_i, s_i), \tag{2.23}$$

and

$$\underline{\beta}_{\tilde{W},i}(|(e_i, s_i)|) \leqslant \tilde{W}_i(\kappa_i, l_i, e_i, s_i) \leqslant \bar{\beta}_{\tilde{W},i}(|(e_i, s_i)|), \tag{2.24}$$

The construction of the functions and constants mentioned in Condition 2.1 depends on which local medium access protocols are employed and can be done systematically. More details on this construction are provided in Section 2.5.2, see also [120].

2.4.1 Stability analysis

In order to guarantee UGAS or UGES, consider the following addition to Condition 2.1. For the sake of brevity, we sometimes omit the arguments of $\tilde{W}_i(\kappa_i, l_i, e_i, s_i)$.

Condition 2.2. *For each $i \in \bar{N}$, there exist continuous functions $H_{l_i,i} : \mathbb{R}^{n_x} \times \mathbb{R}^{(n_v - n_{v,i})} \to \mathbb{R}$ and constants $L_{l_i,i} \geqslant 0$, for $l_i \in \{0,1\}$, such that for all $\kappa_i \in \mathbb{N}$, $l_i \in \{0,1\}$, $s_i \in \mathbb{R}^{n_{v,i}}$, $x \in \mathbb{R}^{n_x}$, and almost all $e_i \in \mathbb{R}^{n_{v,i}}$ it holds that*

$$\left\langle \frac{\partial \tilde{W}_i}{\partial e_i}, g_i(x, e_i, 0) \right\rangle \leqslant L_{l_i,i} \tilde{W}_i + H_{l_i,i}(x, \bar{e}_i). \tag{2.25}$$

Furthermore, there exists a locally Lipschitz function $\tilde{V} : \mathbb{R}^{n_x} \to \mathbb{R}_{\geqslant 0}$, $\mathcal{K}_\infty$-*functions* $\underline{\beta}_{\tilde{V}}$ *and* $\bar{\beta}_{\tilde{V}}$, *positive definite functions* $\tilde{\rho} : \mathbb{R}_{\geqslant 0} \to \mathbb{R}_{\geqslant 0}$ *and* $\sigma_{l_i,i} : \mathbb{R}_{\geqslant 0} \to \mathbb{R}_{\geqslant 0}$, *positive semi-definite functions* $\tilde{\varrho}_i : \mathbb{R}^{n_{v,i}} \to \mathbb{R}_{\geqslant 0}$ *and constants* $\gamma_{l_i,i} > 0$, $l_i \in \{0,1\}$, $i \in \bar{N}$, *such that for all* $\kappa \in \mathbb{N}^N$, $l \in \{0,1\}^N$, $s, e \in \mathbb{R}^{n_v}$, *and almost all* $x \in \mathbb{R}^{n_x}$, *it holds that*

$$\Big\langle \nabla \tilde{V}(x), f(x,e,0) \Big\rangle \leqslant -\tilde{\rho}(|x|) + \sum_{i=1}^{N} \Big(-\tilde{\varrho}_i(v_i) - H_{l_i,i}^2(x,e) - \sigma_{l_i,i}(\tilde{W}_i) + \gamma_{l_i,i}^2 \tilde{W}_i^2 \Big), \quad (2.26)$$

and for all $x \in \mathbb{R}^{n_x}$

$$\underline{\beta}_{\tilde{V}}(|x|) \leqslant \tilde{V}(x) \leqslant \bar{\beta}_{\tilde{V}}(|x|). \quad (2.27)$$

The condition (2.26) is essentially a scaled $\mathcal{L}_2$-gain condition from $(\tilde{W}_1, \tilde{W}_2, \ldots, \tilde{W}_N)$ to $(H_{l_1,1}, H_{l_2,2}, \ldots, H_{l_N,N})$, which in the special case of a centralized control configuration, *i.e.*, when taking $N = 1$, is similar to the conditions used in [51,120,173]. In fact, the inequalities (2.25)-(2.26) recover the conditions used in [120] for $N = 1$ and form a generalization for the decentralized multi-network case ($N > 1$). Consider now functions $\phi_{l_i,i} : \mathbb{R}_{\geqslant 0} \to \mathbb{R}_{\geqslant 0}$, with $i \in \bar{N}$ and $l_i \in \{0,1\}$, which evolve according to

$$\frac{d}{d\tau_i}\phi_{l_i,i} = \begin{cases} -2L_{l_i,i}\phi_{l_i,i} - \gamma_{l_i,i}(\phi_{l_i,i}^2 + 1), & \text{for } \tau_i \in [0, \tau_{miet}^i] \\ 0, & \text{for } \tau_i > \tau_{miet}^i, \end{cases} \quad (2.28)$$

where $L_{l_i,i}$ and $\gamma_{l_i,i}$ are constants given in Condition 2.2 and the initial conditions $\phi_{l_i,i}(0)$ are still to be specified.

Theorem 2.2. *Consider the system* $\mathcal{H}$ *that satisfies Condition 2.1 and Condition 2.2. Suppose the following statements hold for each* $i \in \bar{N}$*:*

(i) There exist positive real constants τ_{miet}^i *and* τ_{mad}^i *with* $\tau_{miet}^i \geqslant \tau_{mad}^i$ *satisfying*

$$\gamma_{0,i}\phi_{0,i}(\tau_{miet}^i) \geqslant \lambda_i^2 \gamma_{1,i}\phi_{1,i}(0), \quad (2.29)$$

$$\gamma_{1,i}\phi_{1,i}(\tau_i) \geqslant \gamma_{0,i}\phi_{0,i}(\tau_i), \text{ for all } \tau_i \in [0, \tau_{mad}^i], \quad (2.30)$$

where $\phi_{0,i}$ *and* $\phi_{1,i}$ *evolve according to* (2.28) *for some fixed initial conditions* $\phi_{l_i,i}(0)$ *that satisfy* $\gamma_{1,i}\phi_{1,i}(0) \geqslant \gamma_{0,i}\phi_{0,i}(0) > \lambda_i^2 \gamma_{1,i}\phi_{1,i}(0) > 0$, *and with* λ_i *as in* (2.22).

(ii) There exist a function $\Psi_i : \mathbb{R}^{n_{v,i}} \times \mathbb{R}^{n_{v,i}} \times \mathbb{R}_{\geqslant 0} \times \mathbb{N} \times \mathbb{R}^{n_{v,i}} \times \{0,1\} \times \mathbb{R}_{\geqslant 0} \to \mathbb{R}$ *with* $\Psi_i(\cdot,\cdot,\cdot,\cdot,\cdot,\cdot,\eta_i)$ *locally Lipschitz for all* $\eta_i \in \mathbb{R}_{\geqslant 0}$ *and a locally Lipschitz* $\mathcal{K}_\infty$ *function* $\delta_{\eta_i} : \mathbb{R}_{\geqslant 0} \to \mathbb{R}_{\geqslant 0}$, *such that for all* $\xi \in \mathbb{X}$

$$\Psi_i(o_i) \leqslant M_i(\xi) - \delta_{\eta_i}(|\eta_i|), \quad (2.31)$$

and for all $\xi \in \mathbb{X}$ *with* $0 \leqslant \tau_i \leqslant \tau^i_{miet}$

$$\Psi_i(o_i) + \delta_{\eta_i}(\eta_i) \geqslant 0, \tag{2.32}$$

where $o_i = (v_i, e_i, \tau_i, \kappa_i, s_i, l_i, \eta_i)$ *and where*

$$M_i(\xi) = \begin{cases} M_{1,i}(\xi), & \text{for } \tau_i \in [0, \tau^i_{miet}] \\ M_{2,i}(\xi), & \text{for } \tau_i > \tau_i > \tau^i_{miet} \end{cases} \tag{2.33}$$

with

$$M_{1,i}(\xi) := \tilde{\varrho}_i(v_i) + \left(H_{l_i,i}(x, \bar{e}_i) - \gamma_{l_i,i}\phi_{l_i,i}\tilde{W}_i\right)^2, \tag{2.34}$$

$$\begin{aligned} M_{2,i}(\xi) := {} & \tilde{\varrho}_i(v_i) + H^2_{0,i}(x, \bar{e}_i) - 2\gamma_{0,i}\phi_{0,i}\tilde{W}_i H_{0,i}(x, \bar{e}_i) \\ & - \left(\gamma^2_{0,i} + 2\gamma_{0,i}\phi_{0,i}L_{0,i}\right)\tilde{W}_i^2. \end{aligned} \tag{2.35}$$

Then the event generator given by (2.6) and (2.7) assures that for the hybrid system $\mathcal{H}$*, described by (2.1) and (2.10)-(2.18), the set* $\mathcal{E}$*, as defined in Definition 2.4, is UGAS. If, in addition, for each* $i \in \bar{N}$ *there exist strictly positive numbers* $b_{1,i}$*,* $b_{2,i}$*,* c_1*,* c_2*,* $c_{4,i}$ *and* $c_{5,i}$ *such that for all* $r \in \mathbb{R}_{\geqslant 0}$*,* $\underline{\beta}_{\tilde{W},i}(r) = b_{1,i}r$*,* $\bar{\beta}_{\tilde{W},i}(r) = b_{2,i}r$*,* $\underline{\beta}_{\tilde{V}}(r) = c_1 r^2$*,* $\bar{\beta}_{\tilde{V}}(r) = c_2 r^2$*,* $\tilde{\rho}(r) \geqslant c_3 r^2$*,* $\delta_{\eta_i}(r) \geqslant c_{4,i}r$ *and* $\sigma_{l_i}(r) \geqslant c_{5,i}r^2$*,* $l_i = 0, 1$*, then the set* $\mathcal{E}$ *is UGES.*

The proof is given in the appendix. Observe that the functions Ψ_i only depend on the local (state) variables $o_i \in \mathbb{O}_i$ and not on the entire state ξ according to (2.31). This is needed to warrant output-based decentralized implementation of the event generators.

2.4.2 $\mathcal{L}_p$-gain performance Analysis

A convenient way to analyze the $\mathcal{L}_p$-gain of a control system is by constructing a so-called *storage function* S, which is positive semi-definite, and satisfies the dissipation inequality $\dot{S} \leqslant \theta^p|w|^p - |q(x,w)|^p$ during flow and $S^+ \leqslant S$ at jumps, where $\theta^p|w|^p - |q(x,w)|^p$ is the supply rate, θ an upper bound for the $\mathcal{L}_p$-gain and $q(x,w)$ as in (2.20) [241]. In order to construct such a storage function, we first consider the following conditions.

Condition 2.3. *([51, 120]) For each* $i \in \bar{N}$*, there exist continuous functions* $H_{l_i,i} : \mathbb{R}^{n_x} \times \mathbb{R}^{(n_v - n_{v,i})} \times \mathbb{R}^{n_w} \to \mathbb{R}$ *and constants* $L_{l_i,i} \geqslant 0$*, for* $l_i \in \{0,1\}$*, such that for all* $\kappa_i \in \mathbb{N}$*,* $l_i \in \{0,1\}$*,* $s_i \in \mathbb{R}^{n_{v,i}}$*,* $x \in \mathbb{R}^{n_x}$*, and almost all* $e_i \in \mathbb{R}^{n_{v,i}}$ *it holds that*

$$\left\langle \frac{\partial \tilde{W}_i}{\partial e_i}, g_i(x, e_i, w) \right\rangle \leqslant L_{l_i,i}\tilde{W}_i + H_{l_i,i}(x, \bar{e}_i, w). \tag{2.36}$$

Furthermore, there exist a locally Lipschitz function $\tilde{V} : \mathbb{R}^{n_x} \to \mathbb{R}_{\geqslant 0}$*,* $\mathcal{K}_\infty$*-functions* $\underline{\beta}_{\tilde{V}}$ *and* $\bar{\beta}_{\tilde{V}}$*, positive semi-definite functions* $\tilde{\varrho}_i : \mathbb{R}^{n_{v,i}} \to \mathbb{R}_{\geqslant 0}$*,* $i \in \bar{N}$*,*

and constants $\alpha_i, \gamma_{l_i,i} > 0$, $l_i \in \{0,1\}$, $i \in \bar{N}$, *such that for all* $\kappa \in \mathbb{N}$, $s, e \in \mathbb{R}^{n_v}$, $w \in \mathbb{R}^{n_w}$, $l \in \{0,1\}^N$ *and almost all* $x \in \mathbb{R}^{n_x}$, *it holds that*

$$\Big\langle \nabla \tilde{V}(x), f(x,e,w) \Big\rangle \leqslant \sum_{i=1}^{N} \Big(-\tilde{\varrho}_i(v_i) - H_{l_i,i}^2(x, \bar{e}_i, w) + \gamma_{l_i,i}^2 \tilde{W}_i^2 \Big) + \tilde{\mu}(\theta^p |w|^p - |q(x,w)|^p), \quad (2.37)$$

for some constants $\tilde{\mu} > 0$ *and* $\theta \geqslant 0$, *and for all* $x \in \mathbb{R}^{n_x}$ *it holds that*

$$\underline{\beta}_{\tilde{V}}(|x|) \leqslant \tilde{V}(x) \leqslant \bar{\beta}_{\tilde{V}}(|x|). \quad (2.38)$$

Theorem 2.3. *Consider the system* $\mathcal{H}$ *that satisfies Condition 2.1, Condition 2.3 and condition (i) of Theorem 2.2. Suppose there exists a function* $\Psi_i : \mathbb{R}^{n_{v,i}} \times \mathbb{R}^{n_{v,i}} \times \mathbb{R}_{\geqslant 0} \times \mathbb{N} \times \mathbb{R}^{n_{v,i}} \times \{0,1\} \times \mathbb{R}_{\geqslant 0} \to \mathbb{R} \times \mathbb{R}_{\geqslant 0} \to \mathbb{R}$ *with* $\Psi_i(\cdot,\cdot,\cdot,\cdot,\cdot,\cdot,\cdot,\eta_i)$ *locally Lipschitz for all* $\eta_i \in \mathbb{R}_{\geqslant 0}$ *for each* $i \in \bar{N}$ *that satisfies for all* $\xi \in \mathbb{X}$

$$\Psi_i(o_i) \leqslant M_i(\xi, w) \quad (2.39)$$

and

$$\Psi_i(o_i) \geqslant 0, \ \textit{when } 0 \leqslant \tau_i \leqslant \tau_{miet}^i, \quad (2.40)$$

where $o_i = (v_i, e_i, \tau_i, \kappa_i, s_i, l_i, \eta_i)$ *and where*

$$M_i(\xi, w) = \begin{cases} M_{1,i}(\xi, w), & \textit{for } 0 \leqslant \tau_i \leqslant \tau_{miet}^i \\ M_{2,i}(\xi, w), & \textit{for } \tau_i > \tau_{miet}^i \end{cases}$$

with

$$M_{1,i}(\xi, w) := \tilde{\varrho}_i(v_i) + \Big(H_{l_i,i}(x, \bar{e}_i, w) - \gamma_{l_i,i} \phi_{l_i,i} \tilde{W}_i \Big)^2, \quad (2.41)$$

$$M_{2,i}(\xi, w) := \tilde{\varrho}_i(v_i) + H_{0,i}^2(x, \bar{e}_i, w) - 2\gamma_{0,i}\phi_{0,i}\tilde{W}_i H_{0,i}(x, \bar{e}_i, w) - \left(\gamma_{0,i}^2 + 2\gamma_{0,i}\phi_{0,i}L_{0,i}\right)\tilde{W}_i^2. \quad (2.42)$$

Then the event-generator given by (2.6) and (2.7) guarantees that the system $\mathcal{H}$, *described by (2.1) and (2.10)-(2.18), is* $\mathcal{L}_p$*-stable with respect to input* w *and output* z *according to (2.20) with an* $\mathcal{L}_p$*-gain less than or equal to* θ.

The proof is given in the appendix.

Remark 2.3. The conditions presented in this section can also be used to determine time-based stability and $\mathcal{L}_p$-gain conditions for decentralized (multiple-networks) time-triggered NCSs in terms of τ_{mati}^i and τ_{mad}^i. Indeed, by taking $\tilde{\varrho}_i(y_i, u_i) = 0$, for all $i \in \bar{N}$, and $\tau_{mati}^i = \tau_{miet}^i$, where τ_{miet}^i and τ_{mad}^i follow from (2.29) and (2.30), respectively, for each $\mathcal{N}_i$ $(\tau_{mati}^i, \tau_{mad}^i)$-conditions are obtained guaranteeing UGAS/UGES of $\mathcal{E}$ and an $\mathcal{L}_p$-gain less than or equal to θ. If we consider the centralized (single-network) time-triggered case, *i.e.*, $N = 1$, we recover the results presented in [120].

2.5 Design of event generators

In this section we will demonstrate how to construct the event generator as in (2.6)-(2.7) through the definition of the functions $\Psi_i : \mathbb{O}_i \to \mathbb{R}$, $i \in \bar{N}$, satisfying (2.31) and (2.32) in case we can assume that $w = 0$ and the control objective is to guarantee UGAS of $\mathcal{E}$, or satisfying (2.39) and (2.40) in case $w \neq 0$ and the control objective is to guarantee $\mathcal{L}_p$ stability.

2.5.1 General design considerations

As already mentioned, due to the decentralized control setup, only local information $o_i \in \mathbb{O}_i$ is available at each ETM. Hence, the functions Ψ_i, $i \in \bar{N}$, have to be constructed such that they only depend on locally available variables. To do so, we first need to derive lower-bounds for the functions $M_{1,i}$ and $M_{2,i}$, as given in (2.34) and (2.35), respectively, which only depend on these local variables. A lower bound for the function $M_{1,i}$ can easily be obtained from (2.34), namely

$$M_{1,i}(\xi) \geqslant \tilde{\varrho}_i(v_i). \tag{2.43}$$

By employing Lemma 2.1, we can derive a lower bound for $M_{2,i}$ in (2.35) as

$$\begin{aligned} M_{2,i}(\xi) \geqslant & \tilde{\varrho}_i + H_{0,i}^2 - H_{0,i}^2 - \left(\gamma_{0,i}\phi_{0,i}\tilde{W}_i\right)^2 - (\gamma_{0,i}^2 + 2\gamma_{0,i}\phi_{0,i}L_{0,i})\tilde{W}_i^2 \\ \geqslant & \tilde{\varrho}_i - \gamma_{0,i}\left(2\phi_{0,i}L_{0,i} + \gamma_{0,i}(1+\phi_{0,i}^2)\right)\tilde{W}_i^2. \end{aligned} \tag{2.44}$$

By combining (2.32), (2.43) and (2.44), we can now define the functions Ψ_i, $i \in \bar{N}$, which satisfy (2.31), as

$$\Psi_i(o_i) = \tilde{\varrho}_i(v_i) - \delta_{\eta_i}(\eta_i) - (1 - \omega_i(\tau_i))\bar{\gamma}_i\tilde{W}_i^2, \tag{2.45}$$

where

$$\omega_i(\tau_i) := \begin{cases} 1, & \text{for } 0 \leqslant \tau_i \leqslant \tau_{miet}^i \\ 0, & \text{for } \tau_i > \tau_{miet}^i, \end{cases} \tag{2.46}$$

and where $\bar{\gamma}_i = \gamma_{0,i}\left(2\phi_{0,i}L_{0,i} + \gamma_{0,i}(1+\phi_{0,i}^2)\right)$, which is, given (2.28), a constant for $\tau_i \geqslant \tau_{miet}^i$. Due to (2.45) and (2.46), the flow map F as given in (2.10) is discontinuous in τ_i. However, since $\dot{\tau}_i = 1$, this does not cause any problems in the existence of solutions.

For the $\mathcal{L}_p$-stability case, we can define Ψ_i similar to (2.45), namely, by taking $\delta_{\eta_i}(\eta_i) = 0$.

Remark 2.4. The functions $\tilde{\varrho}_i$, $i \in \bar{N}$, can be arbitrary semi-positive definite functions. From (2.31), (2.34) and (2.35) for the UGAS case and from (2.39), (2.41) and (2.42) for the $\mathcal{L}_p$-stability case, we can see that if $\tilde{\varrho}_i$, $i \in \bar{N}$, is chosen positive definite, the bound on Ψ_i becomes less stringent than the case where $\tilde{\varrho}_i = 0$, $i \in \bar{N}$, in the sense that Ψ_i can be chosen larger with respect to the

arguments u_i and y_i. From (2.7), we can see that if Ψ_i is larger, it will in general take longer before η_i in (2.6) becomes non-positive. The drawback is that the bound on the derivative of V given by (2.26) becomes more stringent as well. As a consequence, $\gamma_{l_i,i}$, for $i \in \bar{N}$ and $l_i \in \{0,1\}$, have to increase which implies that τ^i_{miet} and τ^i_{mad} will decrease. Note, however, that only for the situation that y_i and u_i are relatively small for $0 \leqslant \tau_i \leqslant \tau^i_{miet}$ and $\Psi_i < 0$ for $\tau_i > \tau^i_{miet}$, inter-event times close to τ^i_{miet} can be expected. Typically, this situation corresponds to the case that the disturbance is close to zero for $0 \leqslant \tau_i \leqslant \tau^i_{miet}$ and is large for $\tau_i > \tau^i_{miet}$. Due to this dependency on τ_i, this worst-case disturbance is unlikely to occur in a practical setting. Thus, by choosing $\tilde{\varrho}_i$ larger, we can derive a triggering condition which in general yields larger inter-event times on average (up to a certain point). Hence, this discussion already reveals that there is a trade-off between the guaranteed minimum inter-event times, robustness in terms of MADs and the expected average inter-event times.

Remark 2.5. The conditions given by (2.32) and (2.40) assure that $\eta_i(t) \geqslant 0$ when $0 \leqslant \tau_i \leqslant \tau^i_{miet}$. Hence, the dynamic triggering mechanism given by (2.6) and (2.7) can be modified to a static triggering mechanism as follows,

$$t^i_0 = 0,\, t^i_{j+1} := \inf\left\{t \geqslant t^i_j + \tau^i_{miet} \mid \Psi_i(o_i) \leqslant 0\right\}, \tag{2.47}$$

where Ψ_i as in (2.45) with $\delta_{\eta_i}(\eta_i) = 0$. Observe that according to this triggering condition, a transmission event takes place in network $\mathcal{N}_i$, each time $\eta_i(t)$ starts decreasing in contrast to the dynamic triggering mechanism given by (2.6) and (2.7). Hence, the dynamic triggering condition outperforms its static alternative in any case with respect to the inter-event times.

Remark 2.6. In the specific case where *no* delays and *no* disturbances are present, where only *one* network with *one* node is considered, and where we employ the static triggering condition given by (2.47), we recover the design in [5].

2.5.2 Construction of Lyapunov and storage Functions

To construct the Lyapunov and storage functions $\tilde{V}$ and $\tilde{W}_i$, and the constants as presented in Condition 2.1-2.3, we are inspired by the results in [110, 120]. The starting points are based on well known conditions, as used in [51, 173, 245] for the delay-free case.

Condition 2.4. *All protocols are UGES, in the sense that for each $i \in \bar{N}$ there exists a function $W_i : \mathbb{N} \times \mathbb{R}^{n_{v,i}} \to \mathbb{R}_{\geqslant 0}$ that is locally Lipschitz in its second argument such that for all $\kappa_i \in \mathbb{N}$ and all $e_i \in \mathbb{R}^{n_{v,i}}$ it holds that*

$$\underline{\alpha}_{W,i}|e_i| \leqslant W_i(\kappa_i, e_i) \leqslant \bar{\alpha}_{W,i}|e_i| \tag{2.48a}$$

$$W_i(\kappa_i + 1, h_i(\kappa_i, e_i)) \leqslant \lambda_i W_i(\kappa_i, e_i) \tag{2.48b}$$

for constants $0 < \underline{\alpha}_{W,i} \leqslant \bar{\alpha}_{W,i}$ and $0 < \lambda_i < 1$.

For the standard sampled-data (SD) systems where $h_i(\kappa_i, e_i) = 0$ for all $\kappa_i \in \mathbb{N}$, $e_i \in \mathbb{R}^{n_{v,i}}$, we can take $W_i(\kappa_i, e_i) = |e_i|$ and $\lambda_i > 0$ arbitrary small. The Try-Once-Discard protocol (TOD), the Round-Robin protocol (RR) and many more are also known to satisfy the above mentioned conditions, see [120, 173] for details on how to construct the corresponding functions W_i. Additional to Condition 2.4, we require that for all $\kappa_i \in \mathbb{N}$, $e_i \in \mathbb{R}^{n_{v,i}}$

$$W_i(\kappa_i + 1, e_i) \leqslant \lambda_{W,i} W_i(\kappa_i, e_i) \tag{2.49}$$

for some constant $\lambda_{W,i} \geqslant 1$, and that for almost all $e_i \in \mathbb{R}^{n_{v,i}}$ and all $\kappa_i \in \mathbb{N}$

$$\left| \frac{\partial W_i}{\partial e_i}(\kappa_i, e_i) \right| \leqslant c_i \tag{2.50}$$

for some constant $c_i \in \mathbb{R}_{>0}$. Moreover, in case $w = 0$ and thus if we aim to find a *Lyapunov function* to guarantee UGAS (and sometimes even UGES), we assume that the growth of e_i is bounded according to

$$|g_i(x, e_i, 0)| \leqslant c_i^{-1} \left(H_{x,i}(x, \bar{e}_i) + M_{e,i}|e_i| \right), \tag{2.51}$$

where $H_{x,i} : \mathbb{R}^{n_{x,i}} \times \mathbb{R}^{(n_v - n_{v,i})} \to \mathbb{R}_{\geqslant 0}$, and, in case $w \neq 0$ and thus if we aim to find a *storage function* to guarantee $\mathcal{L}_p$-stability, we assume that

$$|g_i(x, e_i, w)| \leqslant c_i^{-1} \left(H_i(x, \bar{e}_i, w) + M_{e,i}|e_i| \right), \tag{2.52}$$

where $H_i : \mathbb{R}^{n_x} \times \mathbb{R}^{(n_v - n_{v,i})} \times \mathbb{R}^{n_w} \to \mathbb{R}_{\geqslant 0}$. In both cases $M_{e,i} \geqslant 0$ is a constant. Similar to Condition 2.2, we establish a scaled $\mathcal{L}_2$-gain from $(W_1, W_2, \ldots, W_N)$ to $(H_{x,1}, H_{x,2}, \ldots, H_{x,N})$, by assuming the existence of a locally Lipschitz continuous function $V : \mathbb{R}^{n_x} \to \mathbb{R}_{\geqslant 0}$, which is radially unbounded, *i.e.*, for all $x \in \mathbb{R}^{n_x}$

$$\underline{\alpha}_V(|x|) \leqslant V(x) \leqslant \bar{\alpha}_V(|x|) \tag{2.53}$$

for some $\mathcal{K}_\infty$-functions $\underline{\alpha}_V$ and $\bar{\alpha}_V$, and

$$\begin{aligned} \langle \nabla V(x), f(x, e, 0) \rangle \leqslant -\rho(|x|) - \sum_{i=1}^{N} \left(H_{x,i}^2(x, \bar{e}_i) + \varrho_i(v_i) \right) \\ + \sum_{i=1}^{N} (\gamma_i^2 - \varepsilon) W_i^2(\kappa_i, e_i) \end{aligned} \tag{2.54}$$

for almost all $x \in \mathbb{R}^{n_x}$ and all $e \in \mathbb{R}^{n_v}$ with $\rho : \mathbb{R}_{\geqslant 0} \to \mathbb{R}_{\geqslant 0}$ positive definite and some semi-positive definite functions $\varrho_i : \mathbb{R}^{n_{v,i}} \to \mathbb{R}_{\geqslant 0}$ and where the constants ε, γ_i satisfy $0 < \varepsilon < \min\{\gamma_i^2, 1\}$, where ε is typically taken small. A similar condition can be obtained to construct a storage function V for $\mathcal{L}_p$-stability,

namely,

$$\langle \nabla V(x), f(x,e,w)\rangle \leqslant -\sum_{i=1}^{N}\left(H_i^2(x,\bar{e}_i,w)+\varrho_i(v_i)\right) + \sum_{i=1}^{N}\gamma_i^2 W_i^2(\kappa_i,e_i)+\mu\left(\theta^p|w|^p-|q(x,w)|^p\right), \quad (2.55)$$

for almost all $x\in\mathbb{R}^{n_x}$, all $e\in\mathbb{R}^{n_v}$ and all $w\in\mathbb{R}^{n_w}$.

Based on the above mentioned conditions, which correspond to the delay-free case, see [120], the constants and functions satisfying Conditions 2.1-2.3, which are imposed in case variable transmission delays are present, can now be obtained.

Proposition 2.4. *Consider system $\mathcal{H}$. If Condition 2.4 and inequalities (2.49)-(2.51), (2.53) and (2.54) hold (in case $w=0$) or Condition 2.4 and inequalities (2.49)-(2.50), (2.52), (2.53) and (2.55) hold (in case $w\neq 0$), then the functions $\tilde{V}$ and $\tilde{W}_i$ given by*

$$\begin{aligned}\tilde{W}_i(\kappa_i,0,e_i,s_i)&=\max\{W_i(\kappa_i,e_i),W_i(\kappa_i,e_i+s_i)\}\\ \tilde{W}_i(\kappa_i,1,e_i,s_i)&=\max\left\{\frac{\lambda_i}{\lambda_{W,i}}W_i(\kappa_i,e_i),W_i(\kappa_i,e_i+s_i)\right\}\\ \tilde{V}(x)&=V(x),\end{aligned}$$

satisfy Condition 2.1 and Condition 2.2, and Condition 2.1 and Condition 2.3, respectively, with $\underline{\beta}_{\tilde{W},i}(r)=\underline{\beta}_{\tilde{W},i}r$, $\bar{\beta}_{\tilde{W},i}(r)=\bar{\beta}_{\tilde{W},i}r$, $\underline{\beta}_{\tilde{V}}=\underline{\alpha}_V$, $\bar{\beta}_{\tilde{V}}=\bar{\alpha}_V$, $\sigma_{0,i}(r)=\varepsilon r^2$, $\sigma_{1,i}(r)=\varepsilon\lambda_{W,i}^2/\lambda_i^2 r^2$, $\tilde{\rho}(r)=\rho(r)$, $\tilde{\varrho}_i(v_i)=\varrho(v_i)$, $H_{l_i,i}(x,\bar{e}_i)=H_{x,i}(x,\bar{e}_i)$, $H_{l_i,i}(x,\bar{e}_i,w)=H_i(x,\bar{e}_i,w)$, $\tilde{\mu}=\mu$, and

$$L_{0,i}=\frac{M_{e,i}}{\underline{\alpha}_{W,i}},\qquad L_{1,i}=\frac{M_{e,i}\lambda_{W,i}}{\lambda_i\underline{\alpha}_{W,i}} \quad (2.56)$$

$$\gamma_{0,i}=\gamma_i,\qquad \gamma_{1,i}=\frac{\gamma_i\lambda_{W,i}}{\lambda_i}, \quad (2.57)$$

where $\underline{\beta}_{\tilde{W},i}$ and $\bar{\beta}_{\tilde{W},i}$.

The proof is based on [120], and is omitted here for space reasons.

The following lemma can be used to implement (2.45) in practice, where the mode l_i might not be available to the event generator, *i.e.*, in case the delays are unknown the update times (and thus the modes l_i) are also unknown.

Lemma 2.5. *Consider system $\mathcal{H}$ and suppose there exists a function W_i that satisfies Condition 2.4,* (2.49) *and* (2.50)*, then*

$$(1-\omega_i(\tau_i))\bar{\gamma}_i\tilde{W}_i^2=(1-\omega_i(\tau_i))\bar{\gamma}_i W_i^2 \quad (2.58)$$

with $\tilde{W}_i$ as given in Proposition 2.4 and ω_i as given in (2.46)*.*

Remark 2.7. Note that the conditions presented above put some restrictions on the class of nonlinear systems that can be considered. Indeed, observe that the inequalities (2.51) and (2.52) require that $g_i(x, e_i, w)$ is linearly bounded with respect to e_i. In case the nonlinear terms in $f_i(x, e_i, w)$ and $g_i(x, e_i, w)$ are linearly bounded with respect to all arguments (*e.g.*, in case f_i and g_i are globally Lipschitz maps), one can essentially apply the results for linear systems presented in Section 2.5.3 mutatis mutandis. However, the presented framework is not restricted to this class of linearly bounded systems as we demonstrate by an example in Section 2.6.2.

2.5.3 The linear case

In this section, we will discuss how to systematically construct the functions and constants satisfying the conditions presented in Section 2.5.2, when $f(x, e, w)$ as in (2.10) can be written as

$$\dot{x} = A_{11}x + A_{12}e + A_{13}w \tag{2.59}$$

with $v_i = C_i x$ and where the performance output (2.20) is given by

$$z = C_z x + D_z w. \tag{2.60}$$

Based on (2.59), we find that the dynamics of the transmission errors $e_i,\ i \in \bar{N}$, are given by

$$\dot{e}_i = A_{21,i}x + A_{22,i}e + A_{23,i}w, \tag{2.61}$$

where $A_{21,i} = -C_i A_{11}$, $A_{22,i} = -C_i A_{12}$ and $A_{23,i} = -C_i A_{13}$, $i \in \bar{N}$. By employing the notation

$$A_{21} = \begin{bmatrix} A_{21,1} \\ \vdots \\ A_{21,N} \end{bmatrix}, A_{22} = \begin{bmatrix} A_{22,1} \\ \vdots \\ A_{22,N} \end{bmatrix}, A_{23} = \begin{bmatrix} A_{23,1} \\ \vdots \\ A_{23,N} \end{bmatrix},$$

we can write the dynamics of the transmission errors compactly as

$$\dot{e} = A_{21}x + A_{22}e + A_{23}w. \tag{2.62}$$

For the sake of brevity, we will only consider the $\mathcal{L}_2$-gain analysis.

In order to construct the functions Ψ_i for each network $\mathcal{N}_i$, $i \in \bar{N}$, that satisfy (2.39) and (2.40), we first have to find the functions W_i and the constants c_i, λ_i, $\lambda_{W,i}$, $\underline{\alpha}_{W,i}$ and $\bar{\alpha}_{W,i}$ such that Condition 2.4 and inequalities (2.49) and (2.50) hold. For the SD protocol, we can take $W_{i,\mathrm{SD}}(\kappa_i, e_i) = |e_i|$, $\underline{\alpha}_{W,i,\mathrm{SD}} = \bar{\alpha}_{W,i,\mathrm{SD}} = 1$, $c_{i,\mathrm{SD}} = 1$ and $\lambda_{W,i,\mathrm{SD}} = 1$ in (2.48)-(2.50). Furthermore, $0 < \lambda_{i,\mathrm{SD}} < 1$, can be chosen arbitrarily. See [173] for more details on how to construct the functions W_i and the constants c_i, λ_i, $\lambda_{W,i}$, $\underline{\alpha}_{W,i}$ and $\bar{\alpha}_{W,i}$ for other protocols including the RR and TOD protocol.

To construct a function V satisfying (2.55), we introduce $\Gamma := \text{diag}(\gamma_1 I_{n_{e,1}}, \gamma_2 I_{n_{e,2}}, \ldots, \gamma_N I_{n_{e,N}})$, to obtain

$$\sum_{i=1}^{N} \gamma_i^2 W_{i,SD}^2(\kappa_i, e_i) = e^\top \Gamma^2 e. \tag{2.63}$$

In order to find the function $H_i(x, \bar{e}_i, w)$ (needed in (2.55)) and constant $M_{e,i}$ satisfying (2.52), consider that (2.61) implies

$$|\dot{e}_i| \leqslant \left| A_{21,i} x + \tilde{A}_{22,i} e + A_{23,i} w \right| + \left| A_{22,i} \bar{\Gamma}_i e \right|, \tag{2.64}$$

where $\tilde{A}_{22,i} := A_{22,i}(I_{n_v} - \bar{\Gamma}_i)$. Note that the term $\tilde{A}_{22,i} e$ is independent of e_i.

Based on (2.64), (2.52) can be satisfied by defining $M_{e,i}$ and $H_i(x, \bar{e}_i, w)$ as

$$M_{e,i} := c_i \sqrt{\lambda_{max}({\bar{\Gamma}_i}^\top A_{22,i}^\top A_{22,i} \bar{\Gamma}_i)} \tag{2.65}$$

$$H_i(x, \bar{e}_i, w) := c_i |A_{21,i} x + \tilde{A}_{22,i} e + A_{23,i} w|, \tag{2.66}$$

where c_i is a constant satisfying (2.50), as just specified for the SD protocol. By introducing $\bar{C} := \text{diag}\left(c_1 I_{n_{e,1}}, c_2 I_{n_{e,2}}, \ldots, c_N I_{n_{e,N}}\right)$, we obtain

$$\sum_{i=1}^{N} H_i^2(x, w) = \left| \bar{C} \left(A_{21} x + \tilde{A}_{22} e + A_{23} w \right) \right|^2. \tag{2.67}$$

As already mentioned, the function ϱ_i in (2.55) is an arbitrary positive semi-definite function. Hence, we can take ϱ_i in the quadratic form

$$\varrho_i(v_i) = v_i^\top Q_i v_i, \tag{2.68}$$

where Q_i is an arbitrary positive semi-definite matrix. Since $v_i = C_i x_i$, we have that

$$\sum_{i=1}^{N} \rho_i(v_i) = x^\top C^\top Q C x, \tag{2.69}$$

where $C := \left[C_1^\top \;\; C_2^\top \;\; \cdots \;\; C_N^\top \right]^\top$ and $Q := \text{diag}\big(Q_1, Q_2, \ldots, Q_N\big)$.

Now consider the quadratic candidate storage function $V(x) = x^T P x$. By using (2.60), (2.59), (2.63), (2.67), and (2.69), the inequality given in (2.55) can be formulated in terms of the linear matrix inequality (LMI) given by

$$\begin{pmatrix} R_{11} & R_{12} & R_{13} \\ \star & R_{22} & R_{23} \\ \star & \star & R_{33} \end{pmatrix} \preceq 0, \; P = P^\top \succeq 0, \tag{2.70}$$

where

$$
\begin{aligned}
R_{11} &:= A_{11}^\top P + P A_{11} + A_{21}^\top \bar{C}^2 A_{21} + \mu C_z^\top C_z + C^\top Q C,\\
R_{12} &:= P A_{12} + A_{21}^\top \bar{C}^2 \tilde{A}_{22},\\
R_{13} &:= P A_{13} + A_{21}^\top \bar{C}^2 A_{23} + \mu C_z^\top D_z,\\
R_{22} &:= -\Gamma^2 + \tilde{A}_{22}^\top \bar{C}^2 \tilde{A}_{22},\\
R_{23} &:= \tilde{A}_{22}^\top \bar{C}^2 A_{23},\\
R_{33} &:= \mu D_z^T D_z + A_{23}^\top \bar{C}^2 A_{23} - \mu\theta^2 I.
\end{aligned}
$$

From (2.28) and (2.57), we can conclude that smaller values of γ_i yield, in general, larger minimum inter-event times. Hence, matrix P and constant μ can be computed by minimizing a weighted sum $\sum_{i=1}^{N} \alpha_i \gamma_i^2$ where $\alpha_i \in \mathbb{R}_{>0}$, $i \in \bar{N}$ subject to the LMI given in (2.70) for a fixed $\mathcal{L}_2$-gain θ. Note that different combinations of $(\alpha_1, \alpha_2, \ldots, \alpha_N)$ lead to different $(\gamma_1, \gamma_2, \ldots, \gamma_N)$ and thus different trade-offs in resource utilization among different networks.

Hence, following the above procedure with the LMI (2.70) satisfied, gives in view of (2.45) and Lemma 2.5, that the hybrid system $\mathcal{H}$ has an $\mathcal{L}_2$-gain smaller than or equal to θ, if the functions Ψ_i in the ETMs (2.6)-(2.7) are selected as

$$
\Psi_i(o_i) = \begin{bmatrix} y_i \\ u_i \end{bmatrix}^\top Q_i \begin{bmatrix} y_i \\ u_i \end{bmatrix} - (1 - \omega_i(\tau_i))\bar{\gamma}_i W_i^2 \tag{2.71}
$$

with $\omega_i(\tau_i)$ as in (2.46) and $\bar{\gamma}_i$ as in (2.45).

2.6 Numerical example

In this section we illustrate the use of the above analysis in synthesizing the ETMs in (2.6)-(2.7) for decentralized and output-based NCSs. First, a linear example is presented, which reveals trade-offs between robustness (in terms of MADs), performance (in terms of the $\mathcal{L}_2$-gain of the overall system) and network utilization (in terms of MIETs and average inter-event times). Secondly, we consider a nonlinear example. For both examples, we compare the dynamic event-triggering condition (2.6) with the more commonly used static event-triggering condition (2.47). Let us remark that for both the linear as the nonlinear example, we consider decentralized output-based feedback subject to (variable) transmission delays and disturbances. To the best of our knowledge, only the ETC method proposed in this chapter is applicable to this situation. For this reason, we do not compare the numerical result with other ETC methods reported in literature. Moreover, both examples employ the sampled-data protocol for the local networks. For a numerical example considering the RR and TOD protocol, see [71]. The simulation results are obtained using the Hybrid Systems Simulation Toolbox [200] in Matlab/Simulink.

2.6.1 Linear example

We study in the first example the problem of stabilizing two coupled cart-pendulum systems $\mathcal{P}_i, i \in \{1,2\}$, with the pendula in their (unstable) upright equilibria. Each subsystem consists of a moving support (cart) with mass M_i, a rigid massless beam of length l_i, and a point mass m_i attached to the end of the beam, $i \in \{1,2\}$. The end points of the pendula are coupled via a linear spring of stiffness k. The system is actuated via input forces u_i, $i \in \{1,2\}$. Linearizing the pendula around their unstable upright equilibria, we find, with parameter values $M_1 = M_2 = 25$, $m_1 = m_2 = 5$, $l_1 = l_2 = 2$, $k = 0.1$ and gravitational acceleration $g = 10$,

$$\mathcal{P}_i : \begin{cases} \dot{x}_{p,i} &= A_{p,i,i}x_{p,i} + A_{p,i,j(i)}x_{p,j(i)} + B_{p,i}u_i + E_{p,i}w \\ y_i &= C_{p,i}x_{p,i}, \end{cases}$$

for $i \in \{1,2\}$, where $j(1) = 2$ and $j(2) = 1$ and where $x_{p,i}$ is the state of subsystem $\mathcal{P}_i$, $i \in \{1,2\}$. The matrices $A_{p,i,j}$, $B_{p,i}$, $E_{p,i}$ and $C_{p,i}$, for $i, j \in \{1,2\}$, are then given by

$$\begin{aligned} A_{p,1,1} = A_{p,2,2} &= \begin{bmatrix} 0 & 1 & 0 & 0 \\ 2.9058 & 0 & -0.0054 & 0 \\ 0 & 0 & 0 & 1 \\ -1.6633 & 0 & 0.0017 & 0 \end{bmatrix} \\ A_{p,1,2} = A_{p,2,1} &= \begin{bmatrix} 0 & 0 & 0 & 0 \\ 0.0108 & 0 & 0.0054 & 0 \\ 0 & 0 & 0 & 0 \\ -0.0033 & 0 & -0.0017 & 0 \end{bmatrix} \\ B_{p,1} = B_{p,2} &= \begin{bmatrix} 0 & -0.0042 & 0 & 0.0167 \end{bmatrix}^\top \\ E_{p,1} = B_{p,1}, \qquad & E_{p,2} = \begin{bmatrix} 0 & 0 & 0 & 0 \end{bmatrix}^\top \\ C_{p,1} = C_{p,2} &= \begin{bmatrix} 1 & 0 & 0 & 0 \\ 0 & 0 & 1 & 0 \end{bmatrix}. \end{aligned}$$

Each subsystem has its own, observer-based controller $\mathcal{C}_i$ collocated with the actuator (and thus $\hat{u}_i = u_i$, $i \in \{1,2\}$), given by

$$\mathcal{C}_i : \begin{cases} \dot{x}_{c,i} &= (A_{p,i,i} + B_{p,i}K_i)x_{c,i} + L_i(C_{p,i}x_{c,i} - \hat{y}_i) \\ u_i &= K_i x_{c,i}, \end{cases}$$

where $x_{c,i}$ is the state of controller $\mathcal{C}_i$ (and an estimate of $x_{p,i}$), and where K_i and L_i are such that the eigenvalues of $A_{K,1} := A_{p,1,1} + B_{p,1}K_1$ and $A_{L,1} := A_{p,1,1} + L_1C_{p,1}$ are $-1, -2, -3, -4$, and the eigenvalues of $A_{K,2} := A_{p,2,2} + B_{p,2}K_2$

and $A_{L,2} := A_{p,2,2} + L_2 C_{p,2}$ are $-2, -3, -4, -5$. Particularly,

$$K_1 = \begin{bmatrix} 11321 & 7161.8 & 556.68 & 1190.4 \end{bmatrix}$$
$$L_1 = \begin{bmatrix} -5.998 & -10.902 & 0.052 & 1.785 \\ 0.063 & 0.164 & -4.002 & -3.006 \end{bmatrix}^\top$$
$$K_2 = \begin{bmatrix} 29071 & 18058 & 2833.3 & 3674.6 \end{bmatrix}$$
$$L_2 = \begin{bmatrix} -7.702 & -16.687 & 0.703 & 4.112 \\ 0.721 & 2.529 & -6.298 & -9.038 \end{bmatrix}^\top.$$

For each $i \in \{1, 2\}$, the output y_i is transmitted over network $\mathcal{N}_i$ using the sampled-data protocol (so $h_i = 0$ for $i = 1, 2$), leading to the control setup as shown in Figure 2.2. By defining $x_i := (x_{p,i}, x_{c,i} - x_{p,i})$, the closed loops

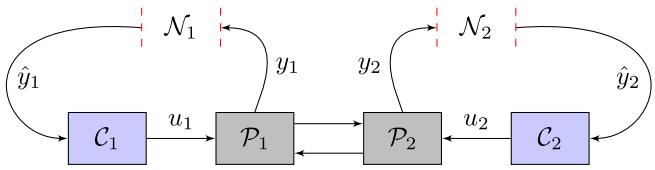

Fig. 2.2. Networked control setup of the two coupled cart-pendulum systems.

dynamics of (x_1, x_2) can be described by (2.59), where

$$A_{11} = \begin{bmatrix} A_{K,1} & B_{p,1}K_1 & A_{p,1,2} & 0 \\ 0 & A_{L,1} & -A_{p,1,2} & 0 \\ A_{p,2,1} & 0 & A_{K,2} & B_{p,2}K_2 \\ -A_{p,2,1} & 0 & 0 & A_{L,2} \end{bmatrix}$$

and where

$$A_{12} = \operatorname{diag}\left(\begin{bmatrix} 0 \\ -L_1 \end{bmatrix}, \begin{bmatrix} 0 \\ -L_2 \end{bmatrix} \right),$$
$$A_{13} = \begin{bmatrix} E_{p,1}^\top & -E_{p,1}^\top & E_{p,2}^\top & -E_{p,2}^\top, \end{bmatrix}^\top,$$

and by defining $e_i := \hat{y}_i - y_i$, the closed loop dynamics of e_i is given by (2.61) with

$$C_1 = -\begin{bmatrix} C_{p,1} & 0 & 0 & 0 \end{bmatrix}$$
$$C_2 = -\begin{bmatrix} 0 & 0 & C_{p,2} & 0 \end{bmatrix}.$$

The performance output is chosen as $z = C_z x$, where $x = (x_1, x_2)$ and $C_z = (\mathbf{0}_{10}^\top, 1, \mathbf{0}_5^\top)$. By using the results in Section 2.5.3, we have that $W_i = |e_i|$,

$c_i = 1$, $0 < \lambda_i < 1$, $\lambda_{W,i} = 1$, $\underline{\alpha}_{W,i} = \bar{\alpha}_{W,i} = 1$, $H_i = |A_{21,i}x + A_{23,i}w|$ and $M_{e,i} = \sqrt{\lambda_{max}(A_{22,i}^\top A_{22,i})}$, $i \in 1, 2$. Furthermore, we choose ϱ_i according to (2.68) with

$$Q_1 = 0.5 \begin{bmatrix} 100 & 0 \\ 0 & 1 \end{bmatrix}, \; Q_2 = 0.3 \begin{bmatrix} 100 & 0 \\ 0 & 1 \end{bmatrix}. \tag{2.72}$$

Now, we can minimize γ_i, $i = 1, 2$, subject to (2.70) for various values of θ and find τ^i_{miet} and τ^i_{mad} trade-off curves by solving (2.29) and (2.30), respectively, for various λ_i, $\phi_{0,i}(0)$ and $\phi_{1,i}(0)$ that satisfy $\gamma_{1,i}\phi_{1,i}(0) \geqslant \gamma_{0,i}\phi_{0,i}(0) > \lambda_i^2\gamma_{1,i}\phi_{1,i}(0) > 0$ where $\gamma_{l_i,i}$, $l_i \in \{0, 1\}$, $i \in \{1, 2\}$ follow from (2.57). The corresponding dynamic event-triggering condition (2.6), (2.7) and the corresponding static event-triggering condition (2.47) are constructed by taking Ψ_i as in (2.71).

In Figure 2.3, τ^i_{miet} versus τ^i_{mad} trade-off curves for both networks, corresponding to the case where an $\mathcal{L}_2$-gain of $\theta = 0.01$ is guaranteed, are shown. In this figure, also the τ^i_{mati} versus τ^i_{mad} trade-off curves are shown that can be obtained in a similar matter, as explained in Remark 2.3. Observe that the MATI of the time-triggered case is slightly larger than the MIET of the event-triggered setup. The average inter-event times τ^i_{avg}, for $i \in \{1, 2\}$, are obtained by simulating the system on the time interval $[0, 40]$ for both the static and dynamic triggering conditions with $w(t)$ zero-mean Gaussian noise with variance 10 for the time-intervals $[0, 20) \cup [30, 40)$, and $w(t) = 0$ for the time interval $[20, 30)$ and initial conditions $x_1(0) = x_2(0) = (10^{-2}, 0, 0, 0, 0, 0, 0, 0)$. The corresponding τ^i_{mad}, $i \in \{1, 2\}$, are chosen such that $\tau^1_{mad} = \tau^2_{mad}$. However, observe that in principle τ^i_{mad} can be chosen independently for each network $\mathcal{N}_i$, for $i \in \{1, 2\}$. Based on Figure 2.3, we can conclude that robust performance in terms of MADs comes at the cost of more network utilization in terms of both minimum inter-event times and average inter-event times being smaller. Furthermore, observe that the dynamic triggering condition indeed yields larger inter-event times than the static triggering condition as mentioned in Remark 2.5.

Figure 2.4 illustrates the trade-off between performance and network utilization in terms of an $\mathcal{L}_2$-gain and MIETs, MATIs and average inter-event times, respectively, for the case that $\tau^1_{mad} = \tau^2_{mad} = 10^{-3}$. The average inter-event times displayed in Figure 2.4 show that for this system, better performance (in terms of a smaller $\mathcal{L}_2$-gain) comes at the cost of more network utilization. Figure 2.5 shows the inter-event times of the coupled cart-pendulum systems for the case that $\tau^1_{mad} = \tau^2_{mad} = 10^{-3}$ and a guaranteed $\mathcal{L}_2$-gain of $\theta = 0.01$ with corresponding τ^1_{miet} and τ^2_{miet} as indicated by the asterisk $(*)$ in Figure 2.3 for both the static and the dynamic event generators. As can be seen in this figure, the static event-triggering mechanism generates smaller inter-event times than the dynamic event-triggering mechanism, even when no disturbances are present (in this case on the time interval $[20, 30)$). Note that the static triggering reduces (when the system is close to the origin, *e.g.*, in the time interval $[20, 30)$) to periodic triggering with the "sampling period" equal to the enforced lower

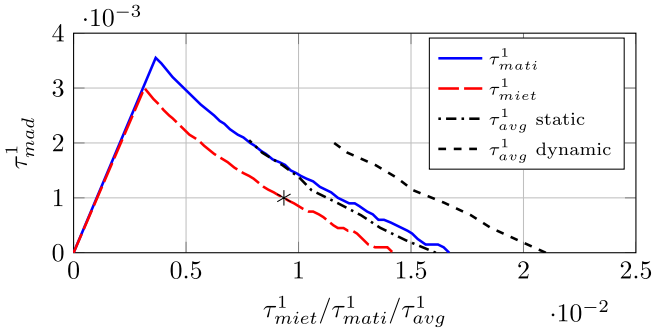

(a) Network $\mathcal{N}_1$

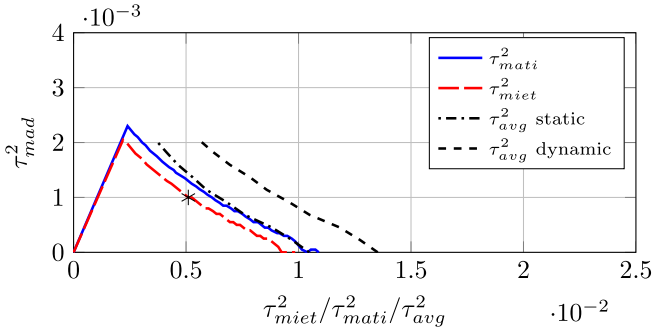

(b) Network $\mathcal{N}_2$

Fig. 2.3. Tradeoff curves of τ_{miet} versus τ_{mad} for the event-triggered setup and τ_{mati} versus τ_{mad} for the time-based specifications as discussed in 2.3. The black curves represent the average inter-event times τ^i_{avg} obtained by means of simulations of the ETC system for various MADs, where τ^i_{mad}, $i = 1, 2$, are chosen such that $\tau^1_{mad} = \tau^2_{mad}$. The asterisk $(*)$ in each plot corresponds to the τ_{miet} / τ_{mad} combination that was used to produce Figure 2.5.

bound τ_{miet} on the MIET, while the dynamic ETC does not have this property (see also Example 3 in [71]) as indicated by property (iii) mentioned in the introduction. Even though for both networks the MIET is (slightly) smaller than the MATI, the *average* inter-event times generated by the dynamic ETM is significantly larger than the MATIs in contrast to the inter-event times generated by the static ETM.

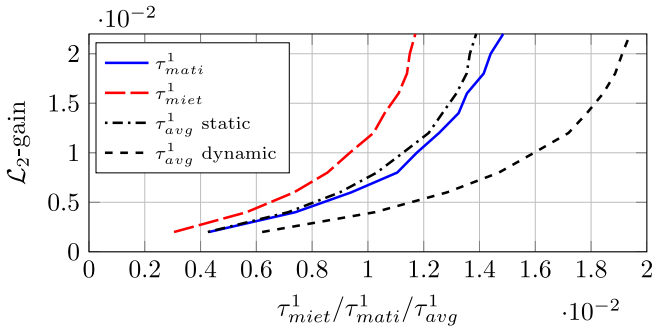

(a) Network $\mathcal{N}_1$

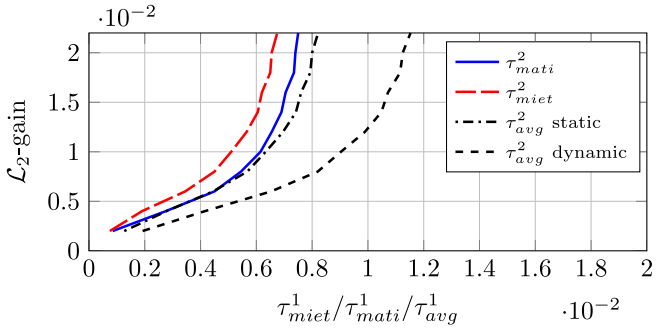

(b) Network $\mathcal{N}_2$

Fig. 2.4. Tradeoff curves of MIET, MATI and average inter-event times versus $\mathcal{L}_2$-gain for the case that $\tau^1_{mad} = \tau^2_{mad} = 10^{-3}$.

2.6.2 Non-linear example

Consider again the control setup as shown in Figure 2.2, now with the plants $\mathcal{P}_i$, $i\{\in 1, 2\}$ given by

$$\mathcal{P}_1 : \dot{x}_1 = x_1^2 - x_1^3 + x_2 + u_1 \tag{2.73a}$$
$$\mathcal{P}_2 : \dot{x}_2 = x_2^2 - x_2^3 + x_1 + u_2, \tag{2.73b}$$

and with the controllers $\mathcal{C}_i : u_i = -2\hat{y}_i$ for $i \in \{1, 2\}$, and where $\hat{y}_i$ denotes the most recently received measurement of the output $y_i = x_i$. The example is inspired by [128], but differs in the way the subsystems are interconnected. Observe that in open loop, *i.e.*, $u_i = 0$, the system has multiple equilibria and that the origin is an unstable equilibrium point. The objective of the controller is to stabilize the origin. By defining $e_i = \hat{x}_i - x_i$ for $i = 1, 2$, we have that

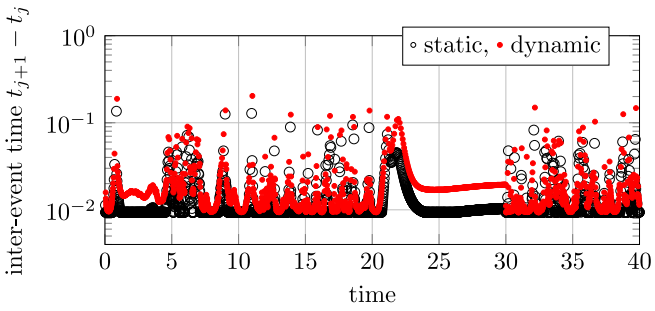

(a) Network $\mathcal{N}_1$

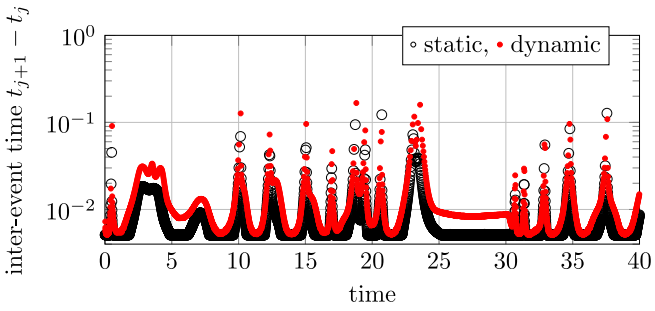

(b) Network $\mathcal{N}_2$

Fig. 2.5. Inter-event times for the static and dynamic event triggering mechanisms.

$u_i = -2(x_i + e_i)$ and the closed-loop system can be described by

$$\dot{x}_i = x_i^2 - x_i^3 + x_{j(i)} - 2(x_i + e_i) \tag{2.74a}$$

$$\dot{e}_i = -x_i^2 + x_i^3 - x_{j(i)} + 2(x_i + e_i), \tag{2.74b}$$

where $i \in \{1, 2\}$ with $j(1) = 2$ and $j(2) = 1$, as before. By taking $W_i(\kappa_i, e_i) = |e_i|$, and thus $c_i = 1$, we find by means of (2.74b) that

$$|\dot{e}_i| \leqslant |2x_i - x_i^2 + x_i^3 - x_{j(i)}| + 2W_i(e_i), \tag{2.75}$$

and thereby (2.51) is satisfied with $M_{e,i} = 2$ and $H_{x,i}(x) = |2x_i - x_i^2 + x_i^3 - x_{j(i)}|$ for $i \in \{1, 2\}$. Consider the candidate Lyapunov function

$$V(x) = \sigma^2 \sum_{i=1}^{2} \left[\left(\alpha \frac{x_i^2}{2} + \beta \frac{x_i^4}{4} \right) \right], \tag{2.76}$$

where $\alpha, \beta, \sigma \in \mathbb{R}_{>0}$. By means of (2.74a) we find that

$$\langle \nabla V(x), f(x,e) \rangle = \sigma^2 \Bigg(\sum_{i=1}^{2} \Big[\alpha x_i^3 - \alpha x_i^4 - 2\alpha x_i^2 - 2\alpha x_i e_i + \beta x_i^5 - \beta x_i^6 - 2\beta x_i^4 - 2\beta x_i^3 e_i \Big] + 2\alpha x_1 x_2 + \beta x_1^3 x_2 + \beta x_1 x_2^3 \Bigg). \quad (2.77)$$

Using Lemma 1 (with $\varepsilon = 1$) for the terms $2\alpha x_i e_i$, $2\beta x_i^3 e_i$ and $2\alpha x_1 x_2$ yields

$$\langle \nabla V(x), f(x,e) \rangle \leqslant \sigma^2 \Bigg(\sum_{i=1}^{2} \Big[(\alpha^2 + \beta^2) e_i^2 + (-\beta + 1) x_i^6 + \beta x_i^5 + (-\alpha - 2\beta) x_i^4 + \alpha x_i^3 + (-\alpha + 1) x_i^2 \Big] + \beta x_1^3 x_2 + \beta x_1 x_2^3 \Bigg) \quad (2.78)$$

To find α, β and σ such that (2.54) holds, we add and subtract $\varepsilon W_i^2(\kappa_i, e_i)$, $H_{x,i}^2(x)$, $\varrho(x_i)_i$, $i \in \{1,2\}$ and $\rho(|x|)$ with $\varrho(r) = qr^2$ for some constant $q \in \mathbb{R}_{\geqslant} 0$ and with $\rho(r) = \varepsilon r^2$ for some constant $\varepsilon \in \mathbb{R}_{>0}$

$$\langle \nabla V(x), f(x,e) \rangle \leqslant \Bigg(\sum_{i=1}^{2} \Big[-(\varepsilon + q) x_i^2 - \varepsilon e_i^2 - H_{x,i}^2(x) + \sigma^2 (\alpha^2 + \beta^2 + \sigma^{-2}\varepsilon) e_i^2 \Big] + \sigma^2 p(x) \Bigg) \quad (2.79)$$

with

$$p(x) := \sum_{i=1}^{2} \Big[x_i^2 \Big(-\alpha + 1 + \sigma^{-2}(10 + \varepsilon + q) + (\alpha - 8\sigma^{-2}) x_i + (-\alpha - 2\beta + 10\sigma^{-2}) x_i^2 + (\beta - 4\sigma^{-2}) x_i^3 + (-\beta + 1 + 2\sigma^{-2}) x_i^4 \Big) \Big] + \beta x_1^3 x_2 + \beta x_1 x_2^3, \quad (2.80)$$

where we used that $H_{x,i}^2(x) \leqslant 2\left(2x_i - x_i^2 + x_i^3\right)^2 + 2x_{j(i)}^2$. Note that if α, β, ε, σ and q are chosen such that $p(x) \leqslant 0$ for all $x \in \mathbb{R}^2$, V satisfies (2.54) with $\gamma = \sigma\sqrt{\alpha^2 + \beta^2 + \sigma^{-2}\varepsilon}$. We determined numerically $[\alpha, \beta, \varepsilon, \sigma, q]$ as $[3.01, 1.47, 0.01, 2.48, 0.5]$ to ensure that $p(x) \leqslant 0$ for all $x \in \mathbb{R}^2$ which yields $\gamma = 8.305$. By solving (2.29) and (2.30) with $\lambda_i = 0.18$, $\phi_{0,i}(0) = \lambda^{-1}$ and $\phi_{1,i}(0) = 12.9$, for $i \in \{1,2\}$, and with $L_{0,i}$, $L_{1,i}$, $\gamma_{0,i}$ and $\gamma_{1,i}$, $i \in 1,2$ according to Proposition 2.4, we obtain that $\tau_{miet}^i = 0.0995$ and $\tau_{mad}^i = 0.01$, $i = 1,2$. Now if we choose Ψ_i, $i \in 1,2$ according to (2.45), it follows from Theorem 2.2

that the system is UGAS under both the static and the dynamic ETM described by (2.6) and (2.47), respectively. By simulating the system 250 times on a time interval $[0, 5]$ with the initial conditions $x_1(0)$ and $x_2(0)$ chosen randomly from the interval $[-5, 5]$, we obtained that $\tau^1_{avg,static} = \tau^2_{avg,static} = 0.101$ and $\tau^1_{avg,dynamic} = \tau^2_{avg,dynamic} = 0.137$. The minimum and average inter-event times are the same for both networks as both systems are identical. Observe that although no disturbances are present, the average inter-event time generated by the static ETM is relatively close to the MIET in contrast to average inter-event time generated by the dynamic ETM.

2.7 Conclusions

In this work, a novel *dynamic* ETC strategy for a class of nonlinear feedback systems was proposed that can simultaneously guarantee a finite $\mathcal{L}_p$-gain and a strictly positive lower bound on the inter-event times (which guarantees Zeno-freeness). In addition to these two important properties, the new ETC approach has other favorable properties: The controllers and event generators can be synthesized in an output-based and/or decentralized form with multiple asynchronously operating networks, the design takes the specific medium access protocol into account, and robustness to (variable) transmission delays is guaranteed by design. When the states of the system are close to the origin, the triggering does not reduce to periodic time-triggered control (with inter-event times equal to the enforced lower bound of the MIET). Key to obtaining all these beneficial properties is the unique combination of *dynamic* event-triggering conditions and time regularization. The design of this class of dynamic event-triggered controllers is systematic. Interestingly, the MIET and the MAD bounds of the presented ETC strategy are close to or equal to the MATI and MAD bounds derived for time-based specifications for stability and guaranteed $\mathcal{L}_p$-gains of NCSs, but the inter-event times significantly larger. Indeed, we presented two numerical examples in which we showed that dynamic ETMs yield significantly larger average inter-event times than time-based communication and ETC strategies with static event generators, even for the case when no disturbances are present. Furthermore, we showed that the developed theory leads to trade-offs curves between robustness (in terms of MADs), performance (in terms of an $\mathcal{L}_p$-gain of the overall system) and network utilization (in terms of MIETs and average inter-event times).

Chapter 3

Riccati-Based Design of Event-Triggered Controllers for Linear Systems with Delays

Abstract – In event-triggered control (ETC) systems, the measured state or output of the plant is sent to the controller at so-called *event times*. In many ETC systems these event times are generated based on a static function of the current state or output measurement of the system and its sampled-and-held version that is available to the controller. Hence, the event-generator does not include any dynamics of its own. In contrast, *dynamic* event-generators trigger events based on additional dynamic variables, whose dynamics depend on the state or output of the system.

In this chapter we propose new static and dynamic continuous event-generators (which require continuous measuring of the plant output) and periodic event-generators (which only require periodic sampling of the plant output) for linear control systems with communication delays. All event-generators we propose lead to closed-loop systems which are globally exponentially stable with a guaranteed decay rate, $\mathcal{L}_2$-stable with a guaranteed $\mathcal{L}_2$-gain, and have a guaranteed positive minimum inter-event time. By using new Riccati-based analysis tools tailored to linear systems, the conservatism in our decay rate and $\mathcal{L}_2$-gain estimates is small. The dynamic event-generators even further reduce this conservatism, and as a result typically generate significantly fewer events than their static counterparts, while guaranteeing the same control performance. The benefits of these new event-generators are demonstrated via two numerical examples.

This chapter is based on [40] and has been published as a preliminary version in [39].

3.1 Introduction

In most digital control systems, the measured output of the plant is periodically transmitted to the controller, regardless of the state the system is in. This possibly leads to a waste of (e.g., computation, communication, and energy) resources, as many of the transmissions are actually not necessary to achieve the desired performance guarantees. To mitigate this potential waste of valuable resources, many *event-triggered control* (ETC) strategies have been proposed, which generate the transmission times based on a triggering condition involving the current state or output measurement of the plant and the most recently transmitted measurement data, see, e.g., [52,54,117,163,224] and the references therein. This brings a *feedback* mechanism into the sampling and communication process, such that measurement data is only transmitted to the controller when needed in order to guarantee the required stability and performance properties of the system.

ETC strategies can be divided into *static* and *dynamic* strategies, or into *continuous* and *periodic* strategies. In static ETC strategies, events are based on a static function of the current state or output measurement and its sampled-and-held version that is available to the controller (using, e.g., a zero-order-hold, a first-order-hold, or even a model-based-hold function). In contrast, in dynamic ETC strategies, events are based on an additional dynamic variable with dynamics that depend on the state or output of the system. Continuous event-triggered control (CETC) strategies require continuous measuring of the plant output (which is sometimes difficult to implement on digital platforms), while periodic event-triggered control (PETC) strategies only require periodic sampling of the plant output.

Static CETC strategies have been proposed in [52,92,114,155,163,224,251]. However, the event-generators in these works that lead to asymptotic stability of the CETC system can typically also lead to Zeno behavior (an infinite number of events in finite time) in the presence (and sometimes even in the absence) of disturbances [41,78], and those that do not exhibit Zeno behavior only lead to practical stability and not to asymptotic stability [41]. To prevent Zeno behavior, static CETC strategies with waiting times (also called 'time regularization') have been proposed in, e.g., [7,44,87,117,205,225,228].

Dynamic CETC strategies for nonlinear systems have been proposed in [72, 96,168,191]. In [191], a dynamic strategy is used to extend the inter-event times compared to a time-triggered system, and in [72,96,168], dynamic strategies are used to extend the inter-event times compared to static CETC systems. In these works the guaranteed control performance and minimum inter-event time of the proposed dynamic CETC system are identical to its static (or time-triggered) counterpart, while it is demonstrated that the average number of events in the dynamic CETC system is typically much smaller.

While the results above show that for CETC systems the inclusion of a

dynamic variable in the event-generator can clearly lead to a significant further reduction of the consumption of communication and energy resources, there are currently no *dynamic* PETC strategies available in literature. Indeed, only static PETC strategies have been proposed, see, e.g., [54,55,112,113,117,184,243,260] for linear systems and [43,188,247] for nonlinear systems.

In this chapter, we provide new (static and dynamic) CETC and PETC strategies tailored to linear systems with (varying) communication delays. We are able to guarantee a positive minimum inter-event time by design, and we provide tight estimates of the $\mathcal{L}_2$-gains and exponential decay rates of the resulting closed-loop systems, by making use of analysis tools specific to the domain of linear systems. These analysis tools are based on Lyapunov/storage functions exploiting matrix Riccati differential equations and computationally friendly semi-definite programming, using ideas from [112]. In addition, we also provide even less conservative conditions for global exponential stability and $\mathcal{L}_2$-stability based on piecewise quadratic Lyapunov functionals. Based on these conditions, we are able to provide trade-offs of guaranteed control performance versus minimum and average inter-event times. Interestingly, for identical control performance guarantees, the dynamic ETC strategies produce significantly larger average inter-event times than their static counterparts, and hence require much less communication. These results, based on exploiting the linearity of the underlying plants and controllers, provide significantly better results than the application of the results obtained for nonlinear systems [72]. In fact, to the best of our knowledge, the proposed continuous event-generators are the least conservative in literature, and we are the first to propose dynamic periodic event-generators. Preliminary results have appeared in [44, 45], in which we did not consider communication delays. Moreover, the conditions provided in [44, 45], are significantly more conservative in guaranteeing global exponential stability and $\mathcal{L}_2$-stability than the novel conditions provided here.

The chapter is organized as follows. In Section 3.2 we present the control setup that we consider in this chapter, for which we present our new static and dynamic CETC strategies in Section 3.3, and our new static and dynamic PETC strategies in Section 3.4. In both sections we provide tight bounds on the $\mathcal{L}_2$-gains and decay rates of the resulting closed-loop systems. In Section 3.5 we provide even tighter bounds based on less conservative conditions using state-space partitioning and piecewise quadratic Lyapunov/storage functionals. Finally, we demonstrate our results in Section 3.6 and provide concluding remarks in Section 3.7. All proofs are given in Appendix B.

3.1.1 Notation

For a vector $x \in \mathbb{R}^{n_x}$, we denote by $|x| := \sqrt{x^\top x}$ its Euclidean norm. For a symmetric matrix $A \in \mathbb{R}^{n\times n}$, we denote by $\lambda_{max}(A)$ and $\lambda_{min}(A)$ its maximum and minimum eigenvalue, respectively. For a matrix $P \in \mathbb{R}^{n\times n}$, we write $P \succ 0$

($P \succeq 0$) if P is symmetric and positive (semi-)definite, and $P \prec 0$ ($P \preceq 0$) if P is symmetric and negative (semi-)definite. By I and O we denote the identity and zero matrix of appropriate dimensions, respectively. For a measurable signal $w : \mathbb{R}_{\geqslant 0} \to \mathbb{R}^{n_w}$, we write $w \in \mathcal{L}_2$ if $\|w\|_{\mathcal{L}_2} < \infty$, where $\|w\|_{\mathcal{L}_2} := \left(\int_0^\infty |w(t)|^2 \mathrm{d}t\right)^{1/2}$ denotes its $\mathcal{L}_2$-norm, and we write $w \in \mathcal{L}_\infty$ if $\|w\|_{\mathcal{L}_\infty} < \infty$, where $\|w\|_{\mathcal{L}_\infty} := \operatorname{ess\,sup}_t |w(t)|$ denotes its $\mathcal{L}_\infty$-norm. By $\mathbb{N}$ we denote the set of natural numbers including zero, i.e., $\mathbb{N} := \{0, 1, 2, \dots\}$. A function $\gamma : \mathbb{R}_{\geqslant 0} \to \mathbb{R}_{\geqslant 0}$ is a $\mathcal{K}$-function if it is continuous, strictly increasing and $\gamma(0) = 0$, and a $\mathcal{K}_\infty$-function if it is a $\mathcal{K}$-function and, in addition, $\gamma(s) \to \infty$ as $s \to \infty$. A function $\beta : \mathbb{R}_{\geqslant 0} \times \mathbb{R}_{\geqslant 0} \to \mathbb{R}_{\geqslant 0}$ is a $\mathcal{KL}$-function if for each fixed $t \in \mathbb{R}_{\geqslant 0}$ the function $\beta(\cdot, t)$ is a $\mathcal{K}$-function and for each fixed $s \in \mathbb{R}_{\geqslant 0}$, $\beta(s, t)$ is decreasing in t and $\beta(s, t) \to 0$ as $t \to \infty$. For vectors $x_i \in \mathbb{R}^{n_i}$, $i \in \{1, 2, \dots, N\}$, we denote by $(x_1, x_2, \cdots, x_N)$ the vector $[x_1^\top x_2^\top \cdots x_N^\top]^\top \in \mathbb{R}^n$ with $n = \sum_{i=1}^N n_i$. For a vector $y \in \mathbb{R}^n$ we write $y \geqslant 0$ if $y_i \geqslant 0$ for all $i \in \{1, 2, \dots, n\}$. For brevity, we sometimes write symmetric matrices of the form $\left[\begin{smallmatrix} A & B \\ B^\top & C \end{smallmatrix}\right]$ as $\left[\begin{smallmatrix} A & B \\ \star & C \end{smallmatrix}\right]$ or $\left[\begin{smallmatrix} A & \star \\ B^\top & C \end{smallmatrix}\right]$. For a left-continuous signal $f : \mathbb{R}_{\geqslant 0} \to \mathbb{R}^n$ and $t \in \mathbb{R}_{\geqslant 0}$, we use $f(t^+)$ to denote the limit $f(t^+) = \lim_{s \to t, s > t} f(s)$.

3.2 Control setup

In this chapter, we consider the event-triggered control setup of Fig. 3.1, in which the plant $\mathcal{P}$ is given by

$$\mathcal{P} : \begin{cases} \frac{\mathrm{d}}{\mathrm{d}t} x_p(t) = A_p x_p(t) + B_p u(t) + B_{pw} w(t) \\ \qquad y(t) = C_y x_p(t) + D_y u(t) \\ \qquad z(t) = C_z x_p(t) + D_z u(t) + D_{zw} w(t) \end{cases} \tag{3.1}$$

and the controller $\mathcal{C}$ is given by

$$\mathcal{C} : \begin{cases} \frac{\mathrm{d}}{\mathrm{d}t} x_c(t) = A_c x_c(t) + B_c \hat{y}(t) \\ \qquad u(t) = C_u x_c(t) + D_u \hat{y}(t). \end{cases} \tag{3.2}$$

Here, $x_p(t) \in \mathbb{R}^{n_{x_p}}$ denotes the state of the plant $\mathcal{P}$, $y(t) \in \mathbb{R}^{n_y}$ its measured

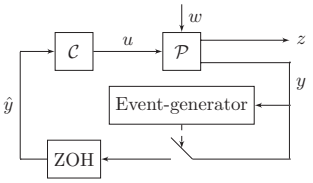

Fig. 3.1. Event-triggered control setup considered in this chapter.

output, $z(t) \in \mathbb{R}^{n_z}$ the performance output, and $w(t) \in \mathbb{R}^{n_w}$ the disturbance at

time $t \in \mathbb{R}_{\geqslant 0}$. Furthermore, $x_c(t) \in \mathbb{R}^{n_{x_c}}$ denotes the state of the controller $\mathcal{C}$, $u(t) \in \mathbb{R}^{n_u}$ is the control input, $\hat{y}(t) \in \mathbb{R}^{n_y}$ denotes the output that is available at the controller, given by

$$\hat{y}(t) = y(t_k),\ t \in (t_k + \tau_k, t_{k+1} + \tau_{k+1}], \tag{3.3}$$

where the sequence $\{t_k\}_{k\in\mathbb{N}}$ satisfying

$$t_0 = 0,\ t_{k+1} - t_k \geqslant h, \tag{3.4}$$

denotes the event (or transmission) times with $h \in \mathbb{R}_{>0}$ the minimum inter-event time, and where the sequence $\{\tau_k\}_{k\in\mathbb{N}}$ with $\tau_k \in \mathcal{D} := \{d_1, d_2, \ldots, d_{n_d}\}$ for all $k \in \mathbb{N}$ denotes the communication delays. The set $\mathcal{D}$ contains the $n_d \in \mathbb{N}$ possible delays, $d_i \in \mathbb{R}_{\geqslant 0}$, and satisfies the following small-delay assumption.

Assumption 3.1. $\mathcal{D} := \{d_1, d_2, \ldots, d_{n_d}\} \subset [0, h]$.

By making use of Assumption 3.1, we ensure that each data packet has arrived at its destination before a new transmission is triggered.

In Sections 3.3, 3.4, and 3.5 we will propose a number of methods to generate the transmission times (3.4), such that the closed-loop system is globally exponentially stable with decay rate ρ and $\mathcal{L}_2$-stable with $\mathcal{L}_2$-gain θ.

3.3 Main results for the CETC case

In this section we will propose *continuous* event-generators, which require continuous measuring of the plant output y. First, in Section 3.3.1, we will propose a *static* continuous event-generator, and in 3.3.2 we will propose a *dynamic* continuous event-generator, which generates the transmission times based on an additional dynamic variable $\eta \in \mathbb{R}$ that is included in the event-generator.

To describe the closed-loop system, we first have to introduce a number of variables, inspired by, e.g., the works [72,120]. We introduce the memory variable $s \in \mathbb{R}^{n_y}$, the timer $\tau \in \mathbb{R}_{\geqslant 0}$, the integer $\kappa \in \mathbb{N}$, and the boolean $l \in \{0, 1\}$. The role of these variables will be explained below. Finally, we define $\zeta := (y, s) \in \mathbb{R}^{2n_y}$ and the state $\xi := (x_p, x_c, \hat{y}, s) \in \mathbb{R}^{n_\xi}$ with $n_\xi = n_{x_p} + n_{x_c} + n_y + n_y$.

The dynamic variable $\eta \in \mathbb{R}$ that will be included in the event-generator will evolve according to

$$\tfrac{\mathrm{d}}{\mathrm{d}t}\eta(t) = \Psi(o(t)), \qquad t \in \mathbb{R}_{\geqslant 0} \setminus \{t_k\}_{k\in\mathbb{N}}, \tag{3.5a}$$

$$\eta(t^+) = \eta_T(o(t)), \qquad t \in \{t_k\}_{k\in\mathbb{N}}, \tag{3.5b}$$

where the signal $o : \mathbb{R}_{\geqslant 0} \to \mathbb{R}^{2n_y} \times \mathbb{R}_{\geqslant 0} \times \mathbb{N} \times \{0, 1\} \times \mathbb{R}$ given by

$$o(t) := (\zeta(t), \tau(t), \kappa(t), l(t), \eta(t)). \tag{3.6}$$

is the information that is available to the continuous event-generator, and where the functions $\Psi : \mathbb{R}^{2n_y} \times \mathbb{R}_{\geqslant 0} \times \mathbb{N} \times \{0,1\} \times \mathbb{R} \to \mathbb{R}$ and $\eta_T : \mathbb{R}^{2n_y} \times \mathbb{R}_{\geqslant 0} \times \mathbb{N} \times \{0,1\} \times \mathbb{R} \to \mathbb{R}$ are to be designed.

Now, we can write the closed-loop system as the impulsive system [106]

$$\frac{\mathrm{d}}{\mathrm{d}t}\begin{bmatrix}\xi(t)\\ \tau(t)\\ \kappa(t)\\ l(t)\\ \eta(t)\end{bmatrix} = \begin{bmatrix}A\xi(t)+Bw(t)\\ 1\\ 0\\ 0\\ \Psi(o(t))\end{bmatrix}, \quad \begin{array}{l} t \in \mathbb{R}_{\geqslant 0} \\ t \notin \{t_k\}_{k\in\mathbb{N}} \\ t \notin \{t_k+\tau_k\}_{k\in\mathbb{N}}\end{array} \tag{3.7a}$$

$$\begin{bmatrix}\xi(t^+)\\ \tau(t^+)\\ \kappa(t^+)\\ l(t^+)\\ \eta(t^+)\end{bmatrix} = \begin{bmatrix}J_0\xi(t)\\ 0\\ \kappa(t)\\ 1\\ \eta_T(o(t))\end{bmatrix}, \quad \begin{array}{l} l = 0 \\ t \in \{t_k\}_{k\in\mathbb{N}}\end{array} \tag{3.7b}$$

$$\begin{bmatrix}\xi(t^+)\\ \tau(t^+)\\ \kappa(t^+)\\ l(t^+)\\ \eta(t^+)\end{bmatrix} = \begin{bmatrix}J_1\xi(t)\\ \tau(t)\\ \kappa(t)+1\\ 0\\ \eta(t)\end{bmatrix}, \quad \begin{array}{l} l = 1 \\ t \in \{t_k+\tau_k\}_{k\in\mathbb{N}}\end{array} \tag{3.7c}$$

$$z(t) = C\xi(t) + Dw(t), \tag{3.7d}$$

where

$$A = \begin{bmatrix}A_p & B_pC_u & B_pD_u & O\\ O & A_c & B_c & O\\ O & O & O & O\\ O & O & O & O\end{bmatrix}, \; B = \begin{bmatrix}B_{pw}\\ O\\ O\\ O\end{bmatrix},$$

$$C = \begin{bmatrix}C_z & D_zC_u & D_zD_u & O\end{bmatrix}, \; D = D_{zw},$$

$$J_0 = \begin{bmatrix}I & O & O & O\\ O & I & O & O\\ O & O & I & O\\ C_y & D_yC_u & D_yD_u & O\end{bmatrix}, \text{ and}$$

$$J_1 = \begin{bmatrix}I & O & O & O\\ O & I & O & O\\ O & O & O & I\\ O & O & O & I\end{bmatrix}.$$

In this model, the memory variable $s \in \mathbb{R}^{n_y}$ stores the value of $y(t_k)$ that has been transmitted to the controller (and which will arrive at the update time $t_k + \tau_k$), the timer $\tau \in \mathbb{R}_{\geqslant 0}$ keeps track of the time that has elapsed since the latest transmission, the integer $\kappa \in \mathbb{N}$ is used to count the number of (received) transmissions, and the boolean $l \in \{0,1\}$ indicates whether the next jump is

a transmission (when $l = 0$) or an update (when $l = 1$). Furthermore, (3.7b) models the jumps at transmission times t_k, $k \in \mathbb{N}$, (3.7c) models the jumps at update times $t_k + \tau_k$, $k \in \mathbb{N}$ (when the transmitted data arrives at the controller), and (3.7a) models the flow in between transmissions and updates.

The sequence of transmission times $\{t_k\}_{k\in\mathbb{N}}$ will be generated by the dynamic continuous event-generator

$$t_0 = 0,\ t_{k+1} = \inf\{t \geqslant t_k + h \mid \eta(t) \leqslant 0 \wedge \zeta^\top(t) Q \zeta(t) \geqslant 0\}, \tag{3.8}$$

where the timer threshold $h \in \mathbb{R}_{\geqslant 0}$ and the matrix $Q \in \mathbb{R}^{2n_y \times 2n_y}$ are design variables, in addition to the functions Ψ and η_T in (3.5). The time threshold h acts as a *waiting time* or *time regularization*, and ensures that (3.4) holds.

With the model (3.5), (3.8) we can also capture *static* event-generators by choosing $\eta(0) = 0$ and

$$\Psi(o) = 0 \tag{3.9a}$$

$$\eta_T(o) = 0 \tag{3.9b}$$

for all $o \in \mathbb{R}^{2n_y} \times \mathbb{R}_{\geqslant 0} \times \mathbb{N} \times \{0, 1\} \times \mathbb{R}$, as then we have that $\eta(t) = 0$ for all $t \in \mathbb{R}_{\geqslant 0}$, and the dynamic event-generator (3.8) reduces to the static event-generator

$$t_0 = 0,\ t_{k+1} = \inf\{t \geqslant t_k + h \mid \zeta^\top(t) Q \zeta(t) \geqslant 0\}, \tag{3.10}$$

which only has h and Q as design parameters.

While tuning h is straightforward as it is a scalar, choosing a suitable Q is more difficult. However, a possible design for Q can be derived from [224] and is given by

$$Q = \begin{bmatrix} (1 - \sigma^2) I & -I \\ -I & I \end{bmatrix} \tag{3.11}$$

with $\sigma \in (0, 1)$. With this choice of Q, (3.10) reduces to

$$t_0 = 0,\ t_{k+1} = \inf\{t \geqslant t_k + h \mid |s(t) - y(t)|^2 \geqslant \sigma^2 |y(t)|^2\},$$

which can be seen as the event-generator proposed in [224] with waiting time h.

In case $h = 0$, the setup (3.7), (3.10) can exhibit Zeno behavior in the presence of disturbances, as shown in [41]. Therefore, we often take $h > 0$, which leads to static event-triggered controllers with time regularization, see, e.g., [117,228]. Other control setups and other choices of Q are also possible, see e.g., [112].

We will consider the following two notions of stability.

Definition 3.1. *The CETC system* (3.7)-(3.8) *is said to be input-to-state exponentially stable (ISES), if there exist functions $\alpha \in \mathcal{K}_\infty$, $\beta \in \mathcal{KL}$, and scalars $c > 0$, $\gamma > 0$, and $\rho > 0$ such that for any initial condition $\xi(0) = \xi_0 \in \mathbb{R}^{n_\xi}$, $\tau(0) = 0$, $\kappa(0) = 0$, $l(0) = 0$, $\eta(0) = 0$, and any sequence of delays $\{\tau_k\}_{k\in\mathbb{N}}$ with*

$\tau_k \in \mathcal{D}$ for all $k \in \mathbb{N}$, all corresponding solutions to (3.7)-(3.8) *with $w \in \mathcal{L}_\infty$ satisfy $|\xi(t)| \leqslant ce^{-\rho t}|\xi_0| + \gamma\|w\|_{\mathcal{L}_\infty}$ and $|\eta(t)| \leqslant \beta(|\xi_0|, t) + \alpha(\|w\|_{\mathcal{L}_\infty})$ for all $t \in \mathbb{R}_{\geqslant 0}$. In this case, we call ρ a (lower bound on the) decay rate.*

Note that our definition of ISES is a variation of the one in [102], which uses the 'max' formulation. Moreover, we only require exponential decay of the state variable ξ, as we are mainly interested in the control performance regarding the plant and controller states, which are captured in ξ. In addition, we require that η stays bounded by a $\mathcal{KL}$-function for practical implementability. We do not put any constraint on the variables τ, κ, and l, as these are only used for modelling purposes. In case $\|w\|_{\mathcal{L}_\infty} = 0$ we have $|\xi(t)| \leqslant ce^{-\rho t}|\xi_0|$ and $|\eta(t)| \leqslant \beta(|\xi_0|, t)$, and thus ISES implies global exponential stability (GES) in the absence of disturbances.

Definition 3.2. *The CETC system* (3.7)-(3.8) *is said to have an $\mathcal{L}_2$-gain from w to z smaller than or equal to θ, if there exists a function $\delta \in \mathcal{K}_\infty$ such that for any initial condition $\xi(0) = \xi_0 \in \mathbb{R}^{n_\xi}$, $\tau(0) = 0$, $\kappa(0) = 0$, $l(0) = 0$, $\eta(0) = 0$, and any sequence of delays $\{\tau_k\}_{k\in\mathbb{N}}$ with $\tau_k \in \mathcal{D}$ for all $k \in \mathbb{N}$, all corresponding solutions to* (3.7)-(3.8) *with $w \in \mathcal{L}_2$ satisfy $\|z\|_{\mathcal{L}_2} \leqslant \delta(|\xi_0|) + \theta\|w\|_{\mathcal{L}_2}$.*

Before proceeding, we introduce the matrix $Y \in \mathbb{R}^{2n_y \times n_\xi}$

$$Y := \begin{bmatrix} C_y & D_yC_u & D_yD_u & O \\ O & O & O & I \end{bmatrix} \tag{3.12}$$

such that $\zeta = (y, s) = Y\xi$, and the transformation matrix $T \in \mathbb{R}^{n_\xi \times (n_{x_p}+n_{x_c}+n_y)}$

$$T := \begin{bmatrix} I & O & O \\ O & I & O \\ O & O & I \\ O & O & I \end{bmatrix}, \tag{3.13}$$

such that

$$T \begin{bmatrix} x_p \\ x_c \\ s \end{bmatrix} = \begin{bmatrix} x_p \\ x_c \\ s \\ s \end{bmatrix}. \tag{3.14}$$

3.3.1 Static CETC

Before designing the dynamics of (3.5) and analyzing ISES and $\mathcal{L}_2$-stability of the system (3.7) with the dynamic event-generator (3.8), we will first consider *static* continuous event-generators with time regularization of the form (3.10).

To analyze ISES and $\mathcal{L}_2$-stability of the static CETC system (3.7) with (3.9) and (3.10), we will use the Lyapunov/storage function U given by

$$U(\xi, \tau, \kappa, l, \eta) = V(\xi, \tau, \kappa, l) + \eta \tag{3.15}$$

with V given by

$$V(\xi,\tau,\kappa,l)=\begin{cases}\xi^\top P_1^{\tau_\kappa}(\tau)\xi, & \tau\in[0,\tau_\kappa] \text{ and } l=1,\\ \xi^\top P_0(\tau)\xi, & \tau\in[\tau_\kappa,h] \text{ and } l=0,\\ \xi^\top P_0(h)\xi, & \tau\in[h,\infty) \text{ and } l=0.\end{cases} \tag{3.16}$$

Here, $P_0:[0,h]\to\mathbb{R}^{n_\xi\times n_\xi}$ is a continuously differentiable function with $P_0(\tau)\succ 0$ for $\tau\in[0,h]$, and for all $d\in\mathcal{D}$, $P_1^d:[0,d]\to\mathbb{R}^{n_\xi\times n_\xi}$ is a continuously differentiable function with $P_1^d(\tau)\succ 0$ for $\tau\in[0,d]$. The functions P_0, P_1^d, $d\in\mathcal{D}$, will be chosen such that (3.15) becomes a storage function [241, 254] for the CETC system (3.7) with (3.9) and (3.10), with the supply rate $\theta^{-2}z^\top z-w^\top w$ and decay rate 2ρ. In particular, we will select the functions P_0, P_1^d, $d\in\mathcal{D}$, to satisfy the Riccati differential equation

$$\tfrac{\mathrm{d}}{\mathrm{d}\tau}P_0(\tau)=R(P_0(\tau)) \tag{3.17}$$

$$\tfrac{\mathrm{d}}{\mathrm{d}\tau}P_1^d(\tau)=R(P_1^d(\tau)),\ d\in\mathcal{D}, \tag{3.18}$$

where R denotes the Riccati operator

$$\begin{aligned}R(P)=&-A^\top P-PA-Y^\top N_F Y-2\rho P-\theta^{-2}C^\top C\\&-(PB+\theta^{-2}C^\top D)M(B^\top P+\theta^{-2}D^\top C).\end{aligned} \tag{3.19}$$

Here, $M:=(I-\theta^{-2}D^\top D)^{-1}$ is assumed to exist and to be positive definite, which corresponds to $\theta^2>\lambda_{max}(D^\top D)$, and $N_F\in\mathbb{R}^{2n_y\times 2n_y}$, $N_F\succeq 0$, is an arbitrary matrix, which we will use as a design parameter in Section 3.3.2.

Note that V given by (3.16) depends on the delay τ_κ of the current transmission, and thus the Lyapunov/storage function U is parametrized by the delay sequence $\{\tau_k\}_{k\in\mathbb{N}}$. However, as we will see below, based on this parametrized function U we are able to guarantee ISES and $\mathcal{L}_2$-stability for *any* sequence of delays $\{\tau_k\}_{k\in\mathbb{N}}$ with $\tau_k\in\mathcal{D}$ and $\mathcal{D}$ satisfying Assumption 3.1. For ease of notation, we will not make this dependence on $\{\tau_k\}_{k\in\mathbb{N}}$ explicit in (3.15) and (3.16).

In order to find the explicit expressions for the functions P_0, P_1^d, $d\in\mathcal{D}$, we introduce the Hamiltonian matrix

$$H:=\begin{bmatrix}A+\rho I+\theta^{-2}BMD^\top C & BMB^\top\\ -C^\top LC-Y^\top N_F Y & -\big(A+\rho I+\theta^{-2}BMD^\top C\big)^\top\end{bmatrix}$$

in which $L:=(\theta^2 I-DD^\top)^{-1}$, and we define the matrix exponential

$$F(\tau):=e^{-H\tau}=\begin{bmatrix}F_{11}(\tau) & F_{12}(\tau)\\ F_{21}(\tau) & F_{22}(\tau)\end{bmatrix}. \tag{3.20}$$

To guarantee that solutions to $\frac{\mathrm{d}}{\mathrm{d}\tau}P_0(\tau)=R(P_0(\tau))$ are well defined on $[0,h]$ and that solutions to $\frac{\mathrm{d}}{\mathrm{d}\tau}P_1^d(\tau)=R(P_1^d(\tau))$ are well defined on $[0,d]$, $d\in\mathcal{D}$, we will make use of the following assumption, see also [112].

Assumption 3.2. *$F_{11}(\tau)$ is invertible for all $\tau \in [0, h]$.*

Assumption 3.2 can always be satisfied by choosing h sufficiently small, as $F_{11}(0) = I$ and F_{11} is a continuous function. Note that larger h can be allowed by reducing ρ or increasing θ.

In the delay-free case with periodic sampling and $\rho = 0$, the $\mathcal{L}_2$-gain θ of the system (3.7) can be determined *exactly* (so without conservatism) by using a lifting-based approach as in, e.g., [24, 113]. These works also require that Assumption 3.2 (or an equivalent thereof) holds. Moreover, if an $\mathcal{L}_2$-gain θ cannot be achieved with periodic sampling with sampling period h and without communication delays, this will also not be possible with event-triggered sampling with minimum inter-event time h. Hence, Assumption 3.2 is not restrictive in that sense.

The function $P_0 : [0, h] \to \mathbb{R}^{n_\xi \times n_\xi}$ is now explicitly defined for $\tau \in [0, h]$ by

$$P_0(\tau) = (F_{21}(h-\tau) + F_{22}(h-\tau)P_0(h)) \\ (F_{11}(h-\tau) + F_{12}(h-\tau)P_0(h))^{-1}, \quad (3.21)$$

and the functions $P_1^d : [0, d] \to \mathbb{R}^{n_\xi \times n_\xi}$, $d \in \mathcal{D}$, are now explicitly defined for $\tau \in [0, d]$ by

$$P_1^d(\tau) = \big(F_{21}(d-\tau) + F_{22}(d-\tau)P_1^d(d)\big) \\ \big(F_{11}(d-\tau) + F_{12}(d-\tau)P_1^d(d)\big)^{-1}, \quad (3.22)$$

where $P_0(h), P_1^d(d) \succ 0$, $d \in \mathcal{D}$, are to be selected. See [22, 112] for further details.

Before stating the next theorem, let us introduce the notation $P_{00} = P_0(0)$, $P_{0d} = P_0(d)$, $P_{0h} = P_0(h)$, $P_{10}^d = P_1^d(0)$, $P_{1d}^d = P_1^d(d)$, the functions

$$G_0(\tau) := F_{11}(\tau)^{-\top} P_{0h} F_{11}(\tau)^{-1} + F_{21}(\tau) F_{11}(\tau)^{-1} \quad (3.23)$$

for $\tau \in [0, h]$,

$$G_1^d(\tau) := F_{11}(\tau)^{-\top} P_{1d}^d F_{11}(\tau)^{-1} + F_{21}(\tau) F_{11}(\tau)^{-1} \quad (3.24)$$

for $\tau \in [0, d]$, $d \in \mathcal{D}$, and finally a matrix function $S : [0, h] \to \mathbb{R}^{n_\xi \times n_\xi}$ that satisfies $S(\tau)S(\tau)^\top := -F_{11}(\tau)^{-1}F_{12}(\tau)$ for $\tau \in [0, h]$. A matrix $S(\tau)$ exists under Assumption 3.2, because this assumption will guarantee that the matrix $-F_{11}(\tau)^{-1}F_{12}(\tau)$ is positive semi-definite [112].

Theorem 3.1. *If Assumption 3.1 holds, and there exist matrices $N_F, N_T, N_N \in \mathbb{R}^{2n_y \times 2n_y}$ with $N_F, N_T, N_N \succeq 0$, $P_{0h}, P_{1d}^d \in \mathbb{R}^{n_\xi \times n_\xi}$ with $P_{0h}, P_{1d}^d \succ 0$, and scalars $\theta, \rho, \beta, \mu^d \in \mathbb{R}_{\geqslant 0}$, $d \in \mathcal{D}$, such that Assumption 3.2 holds and the matrix*

inequalities

$$\begin{bmatrix} T^\top(A^\top P_{0h} + P_{0h}A + Y^\top(N_N - \beta Q)Y)T & \star \\ B^\top P_{0h} T & O \end{bmatrix} \preceq \begin{bmatrix} T^\top(-2\rho P_{0h} - \theta^{-2}C^\top C)T & -\theta^{-2}T^\top C^\top D \\ \star & I - \theta^{-2}D^\top D \end{bmatrix}, \quad (3.25)$$

$$\begin{bmatrix} J_0^\top G_1^d(d) J_0 & J_0^\top F_{11}(d)^{-\top} P_{1d}^d S(d) \\ \star & S(d)^\top P_{1d}^d S(d) \end{bmatrix} \prec \begin{bmatrix} P_{0h} - Y^\top(N_T + \mu^d Q)Y & O \\ O & I \end{bmatrix}, \quad (3.26)$$

and

$$\begin{bmatrix} J_1^\top G_0(h-d) J_1 & J_1^\top F_{11}(h-d)^{-\top} P_{0h} S(h-d) \\ \star & S(h-d)^\top P_{0h} S(h-d) \end{bmatrix} \prec \begin{bmatrix} P_{1d}^d & O \\ O & I \end{bmatrix}, \quad (3.27)$$

hold for all $d \in \mathcal{D}$, then the static CETC system (3.7) *with* (3.9) *and* (3.10) *is ISES with decay rate ρ, and has an $\mathcal{L}_2$-gain from w to z smaller than or equal to θ.*

Inequalities (3.25), (3.26), and (3.27) depend nonlinearly on the parameters N_F, ρ, and θ. However, once these parameters are *fixed*, also the matrices M, L, $F_{ij}(\tau)$, and $S(\tau)$ become fixed matrices. The matrices $G_0(\tau)$ and $G_1^d(\tau)$, $d \in \mathcal{D}$, then only depend *linearly* on the matrices P_{0h} and P_{10}^d, $d \in \mathcal{D}$. Hence, inequalities (3.25), (3.26), and (3.27) then become linear matrix inequalities (LMIs), and the parameters P_{0h}, P_{10}^d, N_N, N_T, β, and μ^d, $d \in \mathcal{D}$, can be synthesized numerically via semi-definite programming (e.g., using Yalmip/SeDuMi [153] in MATLAB).

The $\mathcal{L}_2$-gain estimate θ can be optimized via bisection when N_F and ρ are fixed. Although the optimization is non-convex and we should expect to find local optima, good results can be found with proper initial estimates. The same holds for the decay rate ρ when N_F and θ are fixed.

As the term $-Y^\top N_F Y$ in (3.19) leads to an extra decrease $-\zeta^\top N_F \zeta$ in V during flow (3.7a) with $\tau \in [0, h]$, an increase in N_F will typically lead to an increase in θ or a decrease in ρ. Hence, to analyse ISES and $\mathcal{L}_2$-stability of the static CETC system (3.7) with (3.9) and (3.10), it is often best to choose $N_F = O$. However, for dynamic CETC it can sometimes be useful to choose $N_F \neq O$, as we will see in the next section.

3.3.2 Dynamic CETC

In this section we present our design for a *dynamic* continuous event-generator, which follows from the analysis in Section 3.3.1. The idea is as follows. In Section 3.3.1, the function V (and, hence, also the Lyapunov/storage function U) has an 'extra' decrease $-\zeta^\top N_F \zeta$ during flow (3.7a) with $\tau \in [0, h]$, and

an 'extra' decrease $-\zeta^\top(N_N - \beta Q)\zeta$ during flow (3.7a) with $\tau \in [h, \infty)$ and $\zeta^\top Q \zeta \leqslant 0$. Additionally, V is often strictly decreasing along jumps (3.7b), while we only require that U is nonincreasing along jumps [98]. To get even less conservative results, we can store this 'unnecessary' decrease of V in the dynamic variable η (as much as possible), which acts as a buffer. When a transmission is necessary according to the static event-generator (i.e., when $\tau \in [h, \infty)$ and $\zeta^\top Q \zeta \geqslant 0$) the term $-\zeta^\top(N_N - \beta Q)\zeta$ can become positive, in which case the function V will start to increase with the excess amount $-\zeta^\top(N_N - \beta Q)\zeta$ if we do not transmit. However, as long as $\eta > 0$, we can compensate for this excess increase in V by reducing η, and thus we can postpone the transmission until the buffer η becomes empty ($\eta = 0$). As a result, the conservatism in the stability analysis is reduced, and the same $\mathcal{L}_2$-gain and decay rate can be guaranteed with typically less transmissions, as will also be demonstrated by a numerical example in Section 3.6.1. In this way, our design will lead to a dynamic CETC system with *the same* $\mathcal{L}_2$-gain θ and decay rate ρ as the static CETC system (3.7) with (3.9) and (3.10), but with a significant reduction in the number of transmissions.

We select the flow dynamics (3.5a) of η as

$$\Psi(o) = \begin{cases} -2\rho\eta + \zeta^\top N_F \zeta, & \tau \in [0, h) \quad (3.28a) \\ -2\rho\eta + \zeta^\top (N_N - \beta Q)\zeta, & \tau \in [h, \infty). \quad (3.28b) \end{cases}$$

For the function η_T we provide the following two different designs.

1) State-based dynamic CETC:

$$\eta_T(o) = \eta + \min_{d \in \mathcal{D}} \xi^\top \left(P_{0h} - J_0^\top P_{10}^d J_0 \right) \xi. \quad (3.29)$$

2) Output-based dynamic CETC:

$$\eta_T(o) = \eta + \zeta^\top N_T \zeta. \quad (3.30)$$

Here, the scalars ρ and β, and the matrices N_F, N_T, N_N, P_{0h}, $P_{10}^d \in \mathbb{R}^{n_\xi \times n_\xi}$, $d \in \mathcal{D}$, follow from the stability analysis of the static CETC system in Theorem 3.1.

The first design requires that the full state $\xi(t_k)$ is known to the event-generator at transmission time t_k. This is the case when Assumption 3.1 holds and $y = (x_p, x_c)$ (e.g., when $\mathcal{C}$ is a static state-feedback controller in which case $y = x_p$ and $n_{x_c} = 0$), as then $\hat{y}(t_k) = s(t_k)$, $k \in \mathbb{N}$, and $\xi(t_k) = T\zeta(t_k)$. Note that when the set of possible delays $\mathcal{D}$ contains only a single element, a copy of the controller could be included in the event-generator in order to track the controller state x_c. In case $\mathcal{D}$ contains multiple elements, this is not possible, as the exact input $\hat{y}$ to the controller is then unknown.

The second design is more conservative, but can also be used in case the event-generator does not have access to the full state ξ. Hence, this choice can be used for output-based dynamic CETC.

Theorem 3.2. *If the conditions of Theorem 3.1 hold, then the dynamic CETC system* (3.7) *with* (3.8), (3.28), *and* η_T *given by* (3.29) *or* (3.30) *is ISES with decay rate* ρ*, and has an* $\mathcal{L}_2$*-gain from* w *to* z *smaller than or equal to* θ*.*

While the static continuous event-generator only has design parameters h and Q, the state-based dynamic event-generator has design parameters h, Q, ρ, N_F, N_N, β, P_{0h}, and P_{10}^d, $d \in \mathcal{D}$, and the output-based dynamic event-generator has design parameters h, Q, ρ, N_F, N_N, β, and N_T.

However, these extra design parameters directly follow from the ISES and $\mathcal{L}_2$-gain analysis of the static CETC system in Theorem 3.1. Hence, the design of these extra parameters follows directly and naturally from the design and stability analysis of the static event-generator. Of course, manual tuning of one or more of these parameters is also possible, but can be difficult given the large design space.

In contrast to the static CETC case, in the dynamic CETC case it can make sense to choose $N_F \neq O$, as η grows with (3.28a) during flow with $\tau \in [0, h]$, and thus the average inter-event times might become larger when N_F is increased. This indicates the presence of a trade-off between control performance and resource utilization, as an increase in N_F typically also leads to an increase in θ or a decrease in ρ. On the other hand, as we can give hard guarantees on the minimum inter-event time (given by h), but not on the average inter-event time, it often makes more sense to choose $N_F = O$ and to make the trade-off between control performance and resource utilization via the parameter h.

Remark 3.1. Even though we will often choose $N_F = O$, the parameter N_F can be useful in some cases. For example, in our work [44], we chose $N_F \neq O$ in order to model the dynamic continuous event-generator of [72] in our proposed new framework.

Remark 3.2. In [72] we were able to guarantee GAS and $\mathcal{L}_p$-stability for all possible delays $\tau_k \in [0, \tau_{mad}]$, where $\tau_{mad} \in \mathbb{R}_{\geqslant 0}$ is the maximum allowable delay. In contrast, here we guarantee ISES and $\mathcal{L}_2$-stability for a finite set $\mathcal{D}$ of possible delays. As an engineering solution, we can approach the situation of [72] by including sufficiently many delays out of the set $[0, \tau_{mad}]$ in the set $\mathcal{D}$ (gridding). Assuming that the ETC system has a small amount of robustness against deviations of the delays from the set $\mathcal{D}$, this could also lead to a stability guarantee for all possible delays $\tau_k \in [0, \tau_{mad}]$, $k \in \mathbb{N}$, cf. [89], which uses a similar approach for the stability analysis of networked control system with varying transmission intervals.

3.4 Main results for the PETC case

Consider again the control setup of Fig. 3.1 with plant $\mathcal{P}$ given by (3.1) and controller $\mathcal{C}$ given by (3.2). Instead of continuously monitoring the output y (which is sometimes difficult to realize in digital implementations), we now *periodically*

sample the output y at sample times $\{s_n\}_{n\in\mathbb{N}}$ given by $s_n = nh$, where $h \in \mathbb{R}_{>0}$ is the sample period. At each sample time s_n, $n \in \mathbb{N}$, the event-generator decides whether the sampled output should be transmitted to the controller or not.

In the PETC case, the dynamic variable η will evolve according to

$$\frac{\mathrm{d}}{\mathrm{d}t}\eta(t) = \Psi(\hat{o}(t)), \qquad t \in \mathbb{R}_{\geqslant 0} \setminus \{s_n\}_{n\in\mathbb{N}}, \tag{3.31a}$$

$$\eta(t^+) = \eta_T(\hat{o}(t)), \qquad t \in \{t_k\}_{k\in\mathbb{N}}, \tag{3.31b}$$

$$\eta(t^+) = \eta_N(\hat{o}(t)), \qquad t \in \{s_n\}_{n\in\mathbb{N}} \setminus \{t_k\}_{k\in\mathbb{N}}, \tag{3.31c}$$

where the functions Ψ, η_T, and η_N are to be designed and where the signal $\hat{o} : \mathbb{R}_{\geqslant 0} \to \mathbb{R}^{2n_y} \times [0, h] \times \mathbb{N} \times \{0, 1\} \times \mathbb{R}$ given by

$$\hat{o}(t) := (\zeta(s_n), \tau(t), \kappa(t), l(t), \eta(t)), \quad t \in (s_n, s_{n+1}] \tag{3.32}$$

is the information that is available to the periodic event-generator.

We can now describe the closed-loop system as

$$\frac{\mathrm{d}}{\mathrm{d}t}\begin{bmatrix}\xi(t)\\ \tau(t)\\ \kappa(t)\\ l(t)\\ \eta(t)\end{bmatrix} = \begin{bmatrix}A\xi(t) + Bw(t)\\ 1\\ 0\\ 0\\ \Psi(\hat{o}(t))\end{bmatrix}, \quad \begin{array}{l} t \in \mathbb{R}_{\geqslant 0} \\ t \notin \{s_n\}_{n\in\mathbb{N}} \\ t \notin \{t_k + \tau_k\}_{k\in\mathbb{N}}\end{array} \tag{3.33a}$$

$$\begin{bmatrix}\xi(t^+)\\ \tau(t^+)\\ \kappa(t^+)\\ l(t^+)\\ \eta(t^+)\end{bmatrix} = \begin{bmatrix}J_0\xi(t)\\ 0\\ \kappa(t)\\ 1\\ \eta_T(\hat{o}(t))\end{bmatrix}, \quad \begin{array}{l} l = 0 \\ t \in \{t_k\}_{k\in\mathbb{N}}\end{array} \tag{3.33b}$$

$$\begin{bmatrix}\xi(t^+)\\ \tau(t^+)\\ \kappa(t^+)\\ l(t^+)\\ \eta(t^+)\end{bmatrix} = \begin{bmatrix}J_1\xi(t)\\ \tau(t)\\ \kappa(t)+1\\ 0\\ \eta(t)\end{bmatrix}, \quad \begin{array}{l} l = 1 \\ t \in \{t_k + \tau_k\}_{k\in\mathbb{N}}\end{array} \tag{3.33c}$$

$$\begin{bmatrix}\xi(t^+)\\ \tau(t^+)\\ \kappa(t^+)\\ l(t^+)\\ \eta(t^+)\end{bmatrix} = \begin{bmatrix}\xi(t)\\ 0\\ \kappa(t)\\ l(t)\\ \eta_N(\hat{o}(t))\end{bmatrix}, \quad \begin{array}{l} l = 0 \\ t \in \{s_n\}_{n\in\mathbb{N}} \\ t \notin \{t_k\}_{k\in\mathbb{N}}\end{array} \tag{3.33d}$$

$$z(t) = C\xi(t) + Dw(t). \tag{3.33e}$$

In this model, $\tau \in [0, h]$ tracks the time that has elapsed since the last *sample time*, in contrast with the CETC case, in which τ tracked the time since the last *transmission*. All other variables have the same interpretation as in the CETC case. Furthermore, (3.33b) models the jumps at transmission times t_k,

$k \in \mathbb{N}$, (3.33c) models the jumps at update times $t_k + \tau_k$, $k \in \mathbb{N}$ (when the transmitted data arrives at the controller), (3.33d) models the jumps at sample times $s_n \neq t_k$, $n, k \in \mathbb{N}$, at which no transmission occurs, and (3.7a) models the flow in between jumps.

In the PETC case, the sequence of transmission times $\{t_k\}_{k\in\mathbb{N}}$ will be generated by the dynamic periodic event-generator

$$t_0 = 0,\ t_{k+1} = \min\{t > t_k \mid \eta_N(\hat{o}(t)) \leqslant 0 \wedge \zeta^\top(t) Q \zeta(t) \geqslant 0, t \in \{s_n\}_{n\in\mathbb{N}}\}. \tag{3.34}$$

As in the CETC case, the model (3.31), (3.34) can also capture *static* periodic event-generators by choosing $\eta(0) = 0$ and

$$\Psi(\hat{o}) = \eta_T(\hat{o}) = \eta_N(\hat{o}) = 0 \tag{3.35}$$

for all $\hat{o} \in \mathbb{R}^{2n_y} \times [0, h] \times \mathbb{N} \times \{0, 1\} \times \mathbb{R}$, as then we have that $\eta(t) = 0$ for all $t \in \mathbb{R}_{\geqslant 0}$, and the dynamic periodic event-generator (3.34) reduces to the static periodic event-generator

$$t_0 = 0,\ t_{k+1} = \min\{t > t_k \mid \zeta(t)^\top Q \zeta(t) \geqslant 0, t \in \{s_n\}_{n\in\mathbb{N}}\}. \tag{3.36}$$

Definitions for ISES and $\mathcal{L}_2$-stability of the PETC system (3.33)-(3.34) can be given mutatis mutandis, but are omitted for space reasons.

3.4.1 Static PETC

As in the CETC case, we will first consider *static* periodic event-generators of the form (3.36).

To analyze ISES and $\mathcal{L}_2$-stability of the static PETC system (3.33) with (3.35) and (3.36), we will again use the Lyapunov/storage function U given by (3.15), but now with V given by

$$V(\xi, \tau, \kappa, l) = \begin{cases} \xi^\top P_1^{\tau_\kappa}(\tau)\xi, & \tau \in [0, \tau_\kappa] \text{ and } l = 1, \\ \xi^\top P_0(\tau)\xi, & \tau \in [0, h] \text{ and } l = 0, \end{cases} \tag{3.37}$$

where again $P_0 : [0, h] \to \mathbb{R}^{n_\xi \times n_\xi}$ is a continuously differentiable function satisfying (3.17) and for all $d \in \mathcal{D}$, $P_1^d : [0, d] \to \mathbb{R}^{n_\xi \times n_\xi}$ is a continuously differentiable function satisfying (3.18).

Theorem 3.3. *If Assumption 3.1 holds, and there exist matrices $N_F, N_T, N_N \in \mathbb{R}^{2n_y \times 2n_y}$ with $N_F, N_T, N_N \succeq 0$, $P_{0h}, P_{1d}^d \in \mathbb{R}^{n_\xi \times n_\xi}$ with $P_{0h}, P_{1d}^d \succ 0$, and scalars $\theta, \rho, \beta, \mu^d \in \mathbb{R}_{\geqslant 0}$, $d \in \mathcal{D}$, such that Assumption 3.2 holds and inequalities* (3.26), (3.27), *and*

$$\begin{bmatrix} T^\top G_0(h) T & T^\top F_{11}(h)^{-\top} P_{0h} S(h) \\ \star & S(h)^\top P_{0h} S(h) \end{bmatrix} \prec \begin{bmatrix} T^\top \left(P_{0h} - Y^\top (N_N - \beta Q) Y\right) T & O \\ \star & I \end{bmatrix}, \tag{3.38}$$

hold for all $d \in \mathcal{D}$, then the static PETC system (3.33) *with* (3.35) *and* (3.36) *is ISES with decay rate ρ, and has an $\mathcal{L}_2$-gain from w to z smaller than or equal to θ.*

Note that Theorem 3.3 extends [112, Theorem III.2] to the case with delays. When particularized to the delay-free case, Theorem 3.3 becomes equivalent to [112, Theorem III.2], see also [45].

3.4.2 Dynamic PETC

In this section we present our design for a *dynamic* periodic event-generator, which follows from the analysis in Section 3.4.1. As in Section 3.3.2, the idea is to store the 'extra' decrease of V in the dynamic variable η, which is then used to reduce the number of transmissions while maintaining the same $\mathcal{L}_2$-gain θ and decay rate ρ as the static PETC system.

We select the flow dynamics (3.31a) of η as

$$\Psi(\hat{o}) = -2\rho\eta, \text{ for } \tau \in [0, h]. \tag{3.39}$$

Remark 3.3. As $\eta^+ = \eta$ at update times $t_k + \tau_k$, $k \in \mathbb{N}$, and Ψ is given by (3.39), it follows that $\eta(s_{n+1}) = e^{-2\rho h}\eta(s_n^+)$. Thus, since the event-generator only needs to know the value of η at sample times s_n, $n \in \mathbb{N}$, the variable η does not need to continuously evolve according to (3.31a) in the event-generator. Instead we can use the discrete-time dynamics just described.

For the functions η_T and η_N we will provide the following two different designs.

1) State-based dynamic PETC:

$$\eta_T(\hat{o}) = \eta + \min_{d\in\mathcal{D}} \xi^\top \left(P_{0h} - J_0^\top P_{10}^d J_0\right) \xi, \tag{3.40a}$$

$$\eta_N(\hat{o}) = \eta + \xi^\top (P_{0h} - P_{00})\xi. \tag{3.40b}$$

2) Output-based dynamic PETC:

$$\eta_T(\hat{o}) = \eta + \zeta^\top N_T \zeta, \tag{3.41a}$$

$$\eta_N(\hat{o}) = \eta + \zeta^\top \left(N_N - \beta Q\right) \zeta. \tag{3.41b}$$

Here, the scalars ρ and β, and the matrices N_T, N_N, $P_{00}, P_{0h}, P_{10}^d \in \mathbb{R}^{n_\xi \times n_\xi}$, $d \in \mathcal{D}$, follow from the stability analysis of the static PETC system in Theorem 3.3.

The first design requires that the full state $\xi(s_n)$ is known to the event-generator at sample times s_n, $n \in \mathbb{N}$. The second design is more conservative, but can also be used in case the event-generator does not have access to the full state ξ. Hence, this choice can be used for output-based dynamic PETC.

Theorem 3.4. *If the conditions of Theorem 3.3 hold, then the dynamic PETC system* (3.33) *with* (3.34), (3.39), *and* η_T *and* η_N *given by* (3.40) *or* (3.41) *is ISES with decay rate* ρ*, and has an* $\mathcal{L}_2$*-gain from* w *to* z *smaller than or equal to* θ*.*

Remark 3.4. Note that in contrast to the CETC case, (3.39) does not include the term $\zeta^\top N_F \zeta$, as in the PETC case we do not continuously measure the output y. Hence, our dynamic PETC designs do not involve the matrix N_F, and we can simply let $N_F = O$ in Theorems 3.3 and 3.4. The matrix N_N appears linearly in the LMI (3.38), and thus can be easily synthesized numerically via semi-definite programming.

3.5 Reduced conservatism using state-space partitioning

The ISES and $\mathcal{L}_2$-gain analysis in Sections 3.3 and 3.4 are based on the 'common' (timer-dependent) quadratic Lyapunov function V, in the sense that the same matrix functions P_0 and $P_1^{\tau_\kappa}$ are used for all $\xi \in \mathbb{R}^{n_\xi}$. In this section, we present even less conservative conditions to analyze ISES and $\mathcal{L}_2$-stability of the proposed CETC and PETC systems, using a *piecewise quadratic* Lyapunov/storage functional technique as proposed in [243] for static PETC systems without delays.

Define the regions

$$\mathcal{X}_i := \{\xi \in \mathbb{R}^{n_\xi} \mid X_i \xi \geqslant 0\}, i \in \{1, 2, \ldots, N\}, N \in \mathbb{N}, \tag{3.42}$$

where the matrices $X_i \in \mathbb{R}^{n_\xi \times n_\xi}$, $i \in \{1, 2, \ldots, N\}$, are such that $\{\mathcal{X}_1, \mathcal{X}_2, \ldots, \mathcal{X}_N\}$ forms a partition of $\mathbb{R}^{n_\xi}$, i.e., the sets $\mathcal{X}_i$, $i \in \{1, 2, \ldots, N\}$, have nonempty interior, $\bigcup_{i=1}^N \mathcal{X}_i = \mathbb{R}^{n_\xi}$, and $\mathcal{X}_i \cap \mathcal{X}_j$ is of zero measure for all $i \neq j$, $i, j \in \{1, 2, \ldots, N\}$.

3.5.1 CETC

Consider the CETC system (3.7), (3.8), and define the functional

$$V(\xi, \tau, \kappa, l, w, t) = \begin{cases} \max\limits_{\substack{i \in \{1,2,\ldots,N\} \\ s.t.\ \bar{\xi}(t_\kappa + \tau_\kappa - t, \xi, w_t) \in \mathcal{X}_i}} \xi^\top P_{i,1}^{\tau_\kappa}(\tau)\xi, & \tau \in [0, \tau_\kappa],\ l = 1 \\ \max\limits_{\substack{i \in \{1,2,\ldots,N\} \\ s.t.\ \bar{\xi}(t_{\kappa+1} - t, \xi, w_t) \in \mathcal{X}_i}} \xi^\top P_{i,0}(\tau)\xi, & \tau \in [\tau_\kappa, h],\ l = 0 \\ \max\limits_{\substack{i \in \{1,2,\ldots,N\} \\ s.t.\ \bar{\xi}(t_{\kappa+1} - t, \xi, w_t) \in \mathcal{X}_i}} \xi^\top P_{i,0}(h)\xi, & \tau \in [h, \infty),\ l = 0, \end{cases} \tag{3.43}$$

where $w_t : \mathbb{R}_{\geqslant 0} \to \mathbb{R}^{n_w}$ denotes the time-shifted signal given by $w_t(s) = w(s+t)$ for $s \geqslant 0$, and $\bar{\xi}(t, \xi, w)$ denotes the solution to $\frac{\mathrm{d}}{\mathrm{d}t}\bar{\xi} = A\bar{\xi} + Bw$ at time t with initial condition $\bar{\xi}(0) = \xi$ and disturbance signal $w : \mathbb{R}_{\geqslant 0} \to \mathbb{R}^{n_w}$. Furthermore, $P_{i,0} : [0, h] \to \mathbb{R}^{n_\xi \times n_\xi}$, $i \in \{1, 2, \ldots, N\}$, are continuously differentiable functions satisfying (3.17) and $P^d_{i,1} : [0, d] \to \mathbb{R}^{n_\xi \times n_\xi}$, $d \in \mathcal{D}$, $i \in \{1, 2, \ldots, N\}$, are continuously differentiable functions satisfying (3.18)

Note that V given by (3.43) depends on the value of $\xi(t_k + \tau_k)$ for $t \in [t_k, t_k + \tau_k]$ when $l = 1$ (as in this interval the index i depends on the value $\xi(t_k + \tau_k)$), and depends on the value of $\xi(t_{k+1})$ for $t \in [t_k, t_{k+1}]$ when $l = 0$, (as in this interval the index i depends on the value $\xi(t_{k+1})$. Hence, V depends not only on the delay sequence $\{\tau_k\}_{k\in\mathbb{N}}$, but also on *future* values of the disturbance w. As such, we have a trajectory/disturbance-dependent Lyapunov/storage functional, which deviates from the common literature on GES and $\mathcal{L}_2$-gain analysis, as usually the Lyapunov/storage function only depends on the current (and sometimes past) values of the state, but typically not on future values. Even though the interpretation of $U = V + \eta$ as a genuine storage function is now less natural, we will see below that we are still able to prove ISES and $\mathcal{L}_2$-stability for *any* sequence of delays $\{\tau_k\}_{k\in\mathbb{N}}$ with $\tau_k \in \mathcal{D}$ and $\mathcal{D}$ satisfying Assumption 3.1 and *any* disturbance $w : \mathbb{R}_{\geqslant 0} \to \mathbb{R}^{n_w}$ with $w \in \mathcal{L}_2$.

Before defining the dynamics of η and stating our next theorem, let us introduce the notation $P_{i,00} = P_{i,0}(0)$, $P_{i,0d} = P_{i,0}(d)$, $P_{i,0h} = P_{i,0}(h)$, $P^d_{i,10} = P^d_{i,1}(0)$, $P^d_{i,1d} = P^d_{i,1}(d)$, and the functions

$$G_{i,0}(\tau) := F_{11}(\tau)^{-\top} P_{i,0h} F_{11}(\tau)^{-1} + F_{21}(\tau) F_{11}(\tau)^{-1} \tag{3.44}$$

for $\tau \in [0, h]$, $i \in \{1, 2, \ldots, N\}$, and

$$G^d_{i,1}(\tau) := F_{11}(\tau)^{-\top} P^d_{i,1d} F_{11}(\tau)^{-1} + F_{21}(\tau) F_{11}(\tau)^{-1} \tag{3.45}$$

for $\tau \in [0, d]$, $i \in \{1, 2, \ldots, N\}$, $d \in \mathcal{D}$.

For the dynamics of η, we again select Ψ as in (3.28). For the state-based dynamic continuous event-generator, we now select η_T as

$$\eta_T(o) = \eta + \max_{\substack{i\in\{1,2,\ldots,N\} \\ s.t.\ \xi\in\mathcal{X}_i}} \min_{\substack{d\in\mathcal{D} \\ j\in\{1,2,\ldots,N\}}} \xi^\top \left(P_{i,0h} - J_0^\top P^d_{j,10} J_0\right) \xi, \tag{3.46}$$

and for the output-based dynamic continuous event-generator, we again select η_T as in (3.30).

To understand (3.46), some comments are in order. At the transmission time t_k, we know which matrix function $P_{i,0}$, $i \in \{1, 2, \ldots, N\}$ we should have used in the interval $t \in [t_{k-1} + \tau_{k-1}, t_k]$. However, we do not know yet which matrix function $P^d_{j,1}$, $j \in \{1, 2, \ldots, N\}$, $d \in \mathcal{D}$, we should use in the interval $t \in [t_k, t_k + \tau_k]$. Hence, to make sure that the Lyapunov/storage function $U = V + \eta$ does not increase along transmissions (3.7b), we therefore take the minimum over all $j \in \{1, 2, \ldots, N\}$ and all $d \in \mathcal{D}$ in (3.46).

Theorem 3.5. *If Assumption 3.1 holds, and there exist matrices* $N_F, N_T, N_N \in \mathbb{R}^{2n_y \times 2n_y}$ *with* $N_F, N_T, N_N \succeq 0$, $P_{i,0h}, P_{i,1d}^d \in \mathbb{R}^{n_\xi \times n_\xi}$ *with* $P_{i,0h}, P_{i,1d}^d \succ 0$, $U_{ij}^d, W_{ij}^d \in \mathbb{R}_{\geqslant 0}^{n_\xi \times n_\xi}$ *with* $U_{ij}^d = {U_{ij}^d}^\top$ *and* $W_{ij}^d = {W_{ij}^d}^\top$, *and scalars* $\beta \geqslant 0$ *and* $\mu_{ij}^d \geqslant 0$, $d \in \mathcal{D}$, $i, j \in \{1, 2, \ldots, N\}$, *such that Assumption 3.2 holds and the matrix inequalities*

$$\begin{bmatrix} T^\top (A^\top P_{i,0h} + P_{i,0h} A + Y^\top (N_N - \beta Q) Y) T & \star \\ B^\top P_{i,0h} T & O \end{bmatrix} \preceq \begin{bmatrix} T^\top (-2\rho P_{i,0h} - \theta^{-2} C^\top C) T & -\theta^{-2} T^\top C^\top D \\ \star & I - \theta^{-2} D^\top D \end{bmatrix}, \quad (3.47)$$

$$\begin{bmatrix} J_0^\top G_{i,1}^d(d) J_0 & J_0^\top F_{11}(d)^{-\top} P_{i,1d}^d S(d) \\ \star & S(d)^\top P_{i,1d}^d S(d) \end{bmatrix} \prec \begin{bmatrix} P_{j,0h} - Y^\top (N_T + \mu_{ij}^d Q) Y - X_j^\top U_{ij}^d X_j & O \\ O & I \end{bmatrix}, \quad (3.48)$$

and

$$\begin{bmatrix} J_1^\top G_{i,0}(h-d) J_1 & J_1^\top F_{11}(h-d)^{-\top} P_{i,0h} S(h-d) \\ \star & S(h-d)^\top P_{i,0h} S(h-d) \end{bmatrix} \prec \begin{bmatrix} P_{j,1d}^d - X_j^\top W_{ij}^d X_j & O \\ O & I \end{bmatrix}, \quad (3.49)$$

hold for all $d \in \mathcal{D}$ *and all* $i, j \in \{1, 2, \ldots, N\}$, *then the dynamic CETC system* (3.7) *with* (3.8), (3.28), *and* (3.46) *or* (3.30) *is ISES with decay rate* ρ, *and has an* $\mathcal{L}_2$*-gain from* w *to* z *smaller than or equal to* θ.

Corollary 3.6. *If the conditions of Theorem 3.5 hold, then the static CETC system* (3.7) *with* (3.9) *and* (3.10) *is ISES with decay rate* ρ, *and has an* $\mathcal{L}_2$*-gain from* w *to* z *smaller than or equal to* θ.

Remark 3.5. When increasing the number of regions N, the ISES and $\mathcal{L}_2$-gain analysis becomes less conservative at the cost of higher computational complexity. Moreover, the update (3.46) becomes more computationally intensive, leading to more complex event-generators. On the other hand, (3.30) is independent of N and thus do not lead to more complex event-generators when increasing N.

3.5.2 PETC

Consider the PETC system (3.33), (3.34), and define the functional

$$V(\xi,\tau,\kappa,l,w,t)=\begin{cases}\max\limits_{\substack{i\in\{1,2,\dots,N\}\\ s.t.\ \bar{\xi}(\tau_\kappa-\tau,\xi,w_t)\in\mathcal{X}_i}} \xi^\top P_{i,1}^{\tau_\kappa}(\tau)\xi, & \tau\in[0,\tau_\kappa],\ l=1\\ \max\limits_{\substack{i\in\{1,2,\dots,N\}\\ s.t.\ \bar{\xi}(h-\tau,\xi,w_t)\in\mathcal{X}_i}} \xi^\top P_{i,0}(\tau)\xi, & \tau\in[0,h],\ l=0,\end{cases} \tag{3.50}$$

where again $P_{i,0}:[0,h]\to\mathbb{R}^{n_\xi\times n_\xi}$, $i\in\{1,2,\dots,N\}$, are continuously differentiable functions satisfying (3.17), and $P_{i,1}^d:[0,d]\to\mathbb{R}^{n_\xi\times n_\xi}$, $d\in\mathcal{D}$, $i\in\{1,2,\dots,N\}$, are continuously differentiable functions satisfying (3.18).

For the dynamics of η, we again choose Ψ as in (3.39). For the state-based dynamic periodic event-generator, we now select η_T and η_N as

$$\eta_T(\hat{o})=\eta+\max_{\substack{i\in\{1,2,\dots,N\}\\ s.t.\ \xi\in\mathcal{X}_i}}\ \min_{\substack{d\in\mathcal{D}\\ j\in\{1,2,\dots,N\}}} \xi^\top\left(P_{i,0h}-J_0^\top P_{j,10}^d J_0\right)\xi, \tag{3.51a}$$

$$\eta_N(\hat{o})=\eta+\max_{\substack{i\in\{1,2,\dots,N\}\\ s.t.\ \xi\in\mathcal{X}_i}}\ \min_{j\in\{1,2,\dots,N\}} \xi^\top\left(P_{i,0h}-P_{j,00}\right)\xi, \tag{3.51b}$$

and for the output-based dynamic periodic event-generator, we again select η_T and η_N as in (3.41).

Theorem 3.7. *If Assumption 3.1 holds, and there exist matrices $N_F,N_T,N_N\in\mathbb{R}^{2n_y\times 2n_y}$ with $N_F,N_T,N_N\succeq 0$, $P_{i,0h},P_{i,1d}^d\in\mathbb{R}^{n_\xi\times n_\xi}$ with $P_{i,0h},P_{i,1d}^d\succ 0$, $U_{ij}^d,W_{ij}^d,V_{ij}\in\mathbb{R}^{n_\xi\times n_\xi}_{\geqslant 0}$ with $U_{ij}^d={U_{ij}^d}^\top$, $W_{ij}^d={W_{ij}^d}^\top$, and $V_{ij}={V_{ij}}^\top$, and scalars $\beta\geqslant 0$ and $\mu_{ij}^d\geqslant 0$, $d\in\mathcal{D}$, $i,j\in\{1,2,\dots,N\}$, such that Assumption 3.2 holds and the matrix inequalities* (3.48), (3.49), *and*

$$\begin{bmatrix} T^\top\left(P_{j,0h}-Y^\top(N_N-\beta Q)Y-X_j^\top V_{ij}X_j\right)T & O\\ \star & I\end{bmatrix} \succ \begin{bmatrix} T^\top G_{i,0}(h)T & T^\top F_{11}(h)^{-\top}P_{i,0h}S(h)\\ \star & S(h)^\top P_{i,0h}S(h)\end{bmatrix} \tag{3.52}$$

hold for all $d\in\mathcal{D}$ and all $i,j\in\{1,2,\dots,N\}$, then the dynamic PETC system (3.33) *with* (3.34), (3.39), *and* (3.51) *or* (3.41) *is ISES with decay rate ρ, and has an $\mathcal{L}_2$-gain from w to z smaller than or equal to θ.*

Corollary 3.8. *If the conditions of Theorem 3.7 hold, then the static PETC system* (3.33) *with* (3.35) *and* (3.36) *is ISES with decay rate ρ, and has an $\mathcal{L}_2$-gain from w to z smaller than or equal to θ.*

3.6 Numerical examples

In [45], we have already shown that in the delay-free case our new dynamic PETC designs provide the same control performance guarantees with less communication than the static PETC designs of [112, 113].

Here, we will demonstrate our static and dynamic CETC and PETC designs for the case with delays via two numerical examples.

3.6.1 Unstable batch reactor

Consider the unstable batch reactor of [120, 173, 245], with $n_{x_p} = 4$, $n_{x_c} = 2$, $n_y = n_w = n_u = n_z = 2$, and plant and controller dynamics given by (3.1) and (3.2) with

$$A_p = \begin{bmatrix} 1.3800 & -0.2077 & 6.7150 & -5.6760 \\ -0.5814 & -4.2900 & 0.0000 & 0.6750 \\ 1.0670 & 4.2730 & -6.6540 & 5.8930 \\ 0.0480 & 4.2730 & 1.3430 & -2.1040 \end{bmatrix},$$

$$B_p = \begin{bmatrix} 0.0000 & 0.0000 \\ 5.6790 & 0.0000 \\ 1.1360 & -3.1460 \\ 1.1360 & 0.0000 \end{bmatrix}, \; B_{pw} = \begin{bmatrix} 10 & 0 \\ 0 & 5 \\ 10 & 0 \\ 0 & 5 \end{bmatrix},$$

$$C_y = C_z = \begin{bmatrix} 1 & 0 & 1 & -1 \\ 0 & 1 & 0 & 0 \end{bmatrix}, \; C_u = \begin{bmatrix} -2 & 0 \\ 0 & 8 \end{bmatrix},$$

$$D_y = D_z = D_{zw} = A_c = \begin{bmatrix} 0 & 0 \\ 0 & 0 \end{bmatrix},$$

$$B_c = \begin{bmatrix} 0 & 1 \\ 1 & 0 \end{bmatrix}, \text{ and } \; D_u = \begin{bmatrix} 0 & -2 \\ 5 & 0 \end{bmatrix},$$

and $\mathcal{D} = \{0.01,\ 0.0125,\ 0.0150,\ 0.0175,\ 0.02\}$. Note that for this system $y \neq (x_p, x_c)$, and thus we cannot use (3.29), (3.40), (3.46), or (3.51), but we have to resort to (3.30) for the dynamic CETC case and to (3.41) for the dynamic PETC case.

We choose $h = 0.1$, Q given by (3.11), $N_F = O$, and $\rho = 0.05$. For each choice of σ we minimize the $\mathcal{L}_2$-gain θ, using Theorem 3.1 for the CETC case and Theorem 3.3 for the PETC case, from which also the matrices N_T and N_N follow.

Fig. 3.2a shows the guaranteed $\mathcal{L}_2$-gain θ as a function of σ for both the CETC and PETC approaches. Fig. 3.2b shows the average inter-event times τ_{avg} = (total number of events)/(simulation time) for the static and (output-based) dynamic event-generators, which have been obtained by simulating the

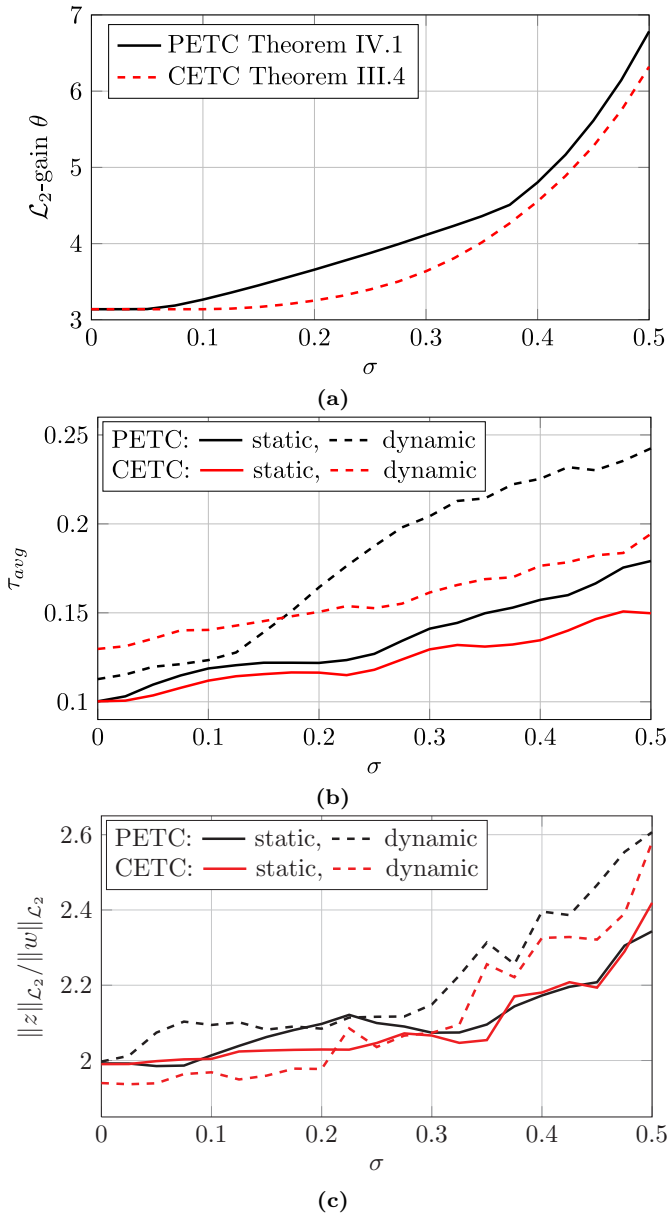

Fig. 3.2. Guaranteed $\mathcal{L}_2$-gain θ for varying σ (a), average inter-event times τ_{avg} for disturbance w given by (3.53) and different event-generators (b), and actual ratio $\|z\|_{\mathcal{L}_2}/\|w\|_{\mathcal{L}_2}$ for disturbance w given by (3.53) (c).

system 10 times for 40 time units with $\xi(0) = 0$ and disturbance w given by

$$w(t) = e^{-0.2t} \begin{bmatrix} 5\sin(3.5t) \\ -\cos(3t) \end{bmatrix}. \tag{3.53}$$

Finally, Fig. 3.2c shows the actual ratio $\|z\|_{\mathcal{L}_2}/\|w\|_{\mathcal{L}_2}$ for disturbance w given by (3.53), which has been obtained from the same simulations.

In Fig. 3.2c we see that, while the control performance guarantees for the dynamic CETC and PETC systems are identical to the performance guarantees for their static counterparts, the dynamic event-generators exploit (part of) the conservatism in the $\mathcal{L}_2$-gain analysis of Theorems 3.1 and 3.3 to postpone the transmissions. This leads to higher ratios $\|z\|_{\mathcal{L}_2}/\|w\|_{\mathcal{L}_2}$ (but still below the guaranteed bounds in Fig. 3.2b), but also to consistently larger τ_{avg}, as can be seen in Fig. 3.2b.

To compare these results with [72], note that for given ρ and θ the waiting time h (or τ_{MIET} in the terminology of [72]) of the continuous event-generator proposed in [72] cannot exceed the maximally allowable transmission interval (MATI) of [120]. Moreover, for the same example in [120, Section IV] we can calculate that when using the sampled-data protocol, no notion of stability can be guaranteed for MATI larger than 0.063, even without delays. In contrast, here we guarantee ISES and $\mathcal{L}_2$-stability for $h = 0.1$, in the presence of delays. Hence, our new framework tailored to linear systems is clearly much less conservative than our previous results for nonlinear systems in [72]. See also [44] for a direct comparison between the static and dynamic continuous event-generators in Section 3.3 and the event-generators proposed in [72], for the case without delays.

3.6.2 Reduced conservatism using Section 3.5

In this example, we show how the conservatism of the ISES and $\mathcal{L}_2$-stability analysis can be further reduced by partitioning the state-space as in Section 3.5.

Consider the example from [41, Section VI.B], with $n_{x_p} = 2$, $n_{x_c} = 0$, $n_y = n_w = n_u = n_z = 1$, and matrices

$$A_p = \begin{bmatrix} 0 & 1 \\ 0 & -3 \end{bmatrix},\ B_p = B_{pw} = \begin{bmatrix} 0 \\ 1 \end{bmatrix},\ D_u = \begin{bmatrix} -3 \end{bmatrix},$$
$$C_y = C_z = \begin{bmatrix} 1 & 0 \end{bmatrix},\ \text{ and }\ D_y = D_z = D_{zw} = \begin{bmatrix} 0 \end{bmatrix}.$$

We will control the system using a periodic event-generator, and choose $h = 1$, $\mathcal{D} = \{0,\ 0.1,\ 0.2\}$, Q as in (3.11), $N_F = O$, and $\rho = 0.05$.

We partition the state-space as in (3.42), with $N = 10$ and matrices

$$X_i = \begin{bmatrix} -\sin(\phi_i) & \cos(\phi_i) & 0 & 0 \\ \sin(\phi_{i+1}) & -\cos(\phi_{i+1}) & 0 & 0 \\ 0 & 0 & 0 & 0 \\ 0 & 0 & 0 & 0 \end{bmatrix}, \tag{3.54}$$

with

$$\phi_i = (i-1)\frac{2\pi}{N}, \text{ for } i \in \{1, 2, \ldots, N+1\}. \tag{3.55}$$

Fig. 3.3 shows the guaranteed $\mathcal{L}_2$-gain θ as a function of σ for the PETC approach using Theorem 3.3, and using the less conservative conditions of Theorem 3.7 with the state-space partition as defined above. The matrices N_T

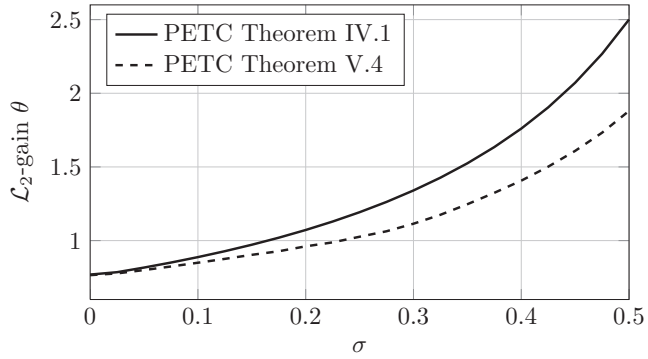

Fig. 3.3. Guaranteed $\mathcal{L}_2$-gain θ for varying σ.

and N_N and the scalar β were found numerically based on Theorem 3.3. In Theorem 3.7 we then used the same values for N_N, N_T, and β, such that the resulting design for the output-based dynamic periodic event-generator is identical for both theorems, and any difference in θ can be solely attributed to the partitioning of the state-space and the use of piecewise quadratic Lyapunov functions.

Clearly, by using piecewise quadratic Lyapunov/storage functionals even tighter guarantees on the $\mathcal{L}_2$-gain can be achieved. However, while the performance guarantees become tighter when the number of regions N in the partition is increased, also the computational complexity of the required calculations becomes larger.

3.7 Conclusions

In this chapter, we proposed a new method for the design of static and dynamic *continuous* event-generators (which require continuous measuring of the plant output) and static and dynamic *periodic* event-generators (which only require periodic sampling of the plant output) for linear control systems with communication delays. All proposed event-generators lead to global exponential stability and $\mathcal{L}_2$-stability with guaranteed decay rates and $\mathcal{L}_2$-gains, and have a guaranteed positive minimum inter-event time.

Our designs exploit Riccati-based tools tailored to linear systems, leading to a significant reduction in conservatism compared to existing results in the

literature (which focus on more general nonlinear systems). In fact, we showed via a numerical example that the conservatism in the guaranteed $\mathcal{L}_2$-gain (for any of the proposed event-generators) is small.

Moreover, to the best of the authors' knowledge, the proposed dynamic periodic event-generators are the first in literature that can deal with communication delays.

Chapter 4

Input-to-state Stabilizing Event-triggered Control for Linear Systems with Distributed and Quantized Output Measurements

Abstract – In this chapter, we study output-based stabilization of linear time-invariant (LTI) systems affected by unknown external disturbances. The plant outputs are measured by a collection of distributed sensors, which transmit their feedback information to the controller in an asynchronous fashion over different communication channels. To save communication resources, the transmission instants of each sensor are determined by event-triggering mechanisms that only depend on locally available information. Before being sent over the network, each sensor measurement is subject to quantization, which is carried out by means of dynamic quantizers. The proposed event-triggering and dynamic quantization mechanisms ensure an input-to-state stability (ISS) property of a set around the origin with respect to the external disturbances. Moreover, the proposed approach prevents the occurrence of Zeno behaviour on the transmission instants and the quantization updates. An additional feature of the proposed scheme is that transmission instants can only be generated when the sampling error becomes larger than the quantizer error bound, which helps in avoiding redundant usage of the network. The trade-off between transmissions and quantization is characterized in terms of design parameters. The effectiveness of the approach is illustrated on a numerical example.

4.1 Introduction

The increasing popularity of networked control systems (NCS) has motivated an extensive research effort on this subject during the last few decades. In NCS, the sensors, the controller, and the actuators communicate with each other over a shared channel. This configuration offers several advantages compared to dedicated point-to-point connections in terms of increased flexibility, lower cost, and ease of maintenance. However, the communication resources of the network are often limited, which induces new challenges on the analysis and the design of control systems [23,120]. In this context, event-triggered control (ETC) schemes have been proposed in the literature as an alternative to traditional time-triggered platforms. The idea of ETC is to generate transmission events based on locally available output measurements of the system instead of purely on time as in most traditional digital control setups. In this way, unnecessary access to the network can be prevented, leading to more efficient usage of the communication resources, see, e.g., [115,191] and the references therein. One of the main difficulties in the synthesis of event-triggering conditions is to guarantee appropriate stability/performance properties while preventing the occurrence of Zeno (an infinite number of transmissions in finite time); certainly when only the plant output is available for feedback instead of the full state [78] and/or when the control system is subject to exogenous inputs [41].

Besides reducing the amount of transmissions over the network, quantization is another important and challenging aspect in NCS [116, 167, 175]. The use of quantization is unavoidable due to the digital nature of the communication channel and the fact that only a finite amount of data can be transmitted over the network. Quantization requires a careful handling as well since the closed-loop stability may no longer be guaranteed when state or output measurements are quantized with insufficient number of quantization regions, see, e.g., [144] and the references therein. Most existing techniques reported in the literature are developed for static quantizers in which the quantizer range and the quantizer error bound are fixed. Therefore, to guarantee that the feedback information remains within range of the static quantizer, i.e., to make sure that the quantizer does not saturate, it is often assumed in the analysis of static quantizers that the quantizer range is infinite [242]. This requirement is impractical due to the finite size of the transmitted data packages. To overcome this requirement, the authors of [48] have proposed to dynamically adjust the quantizer range and the quantizer error bound according to the available feedback information, which leads to so-called dynamic quantizers. To that end, a zoom variable is used to either increase the quantizer range to avoid saturation (referred to as the zoom-out stage) or decrease the quantizer range to extract more precise information (referred to as the zoom-in stage). As such, with dynamic quantizers, saturation can be avoided while using only a small number of quantization regions (and thus less number of bits need to be communicated). Hence, in the context of NCS,

dynamic quantizers create a balance between the desired control performance and utilization of the communication resources, which show their advantages over static quantizers. However, the use of dynamic quantizers also introduces new challenges in the stability analysis and practical implementation, which need to be carefully handled. For instance, since the zoom actions are state-dependent, the accumulation of zoom instants need to be avoided. Moreover, chattering between the zoom-in and the zoom-out stages should be prevented, and the zoom variable should remain bounded, see also, e.g., [145].

In this chapter, we consider the event-triggered stabilization of linear time-invariant (LTI) systems. The plant may be affected by external disturbances and, as in many applications, only the output of the plant can be measured and not the full the state. These output measurements are assumed to be distributed, i.e., they are collected by multiple network nodes and asynchronously transmitted over different channels. Each of these network nodes employs an event-triggering condition, which only depends on locally available information, to decide when to transmit measurement data. It is important to emphasize that when both event-triggering and quantization are considered in NCS, the combined analysis becomes more complicated since the design of the event-triggering mechanism and the quantizer are directly coupled. For instance, the sampling-induced error of the feedback information is in general not reset to zero at each transmission instant due to the effect of quantization [116, 167, 175]. This issue may have negative impact on the closed-loop stability and the handling of this behaviour is far from trivial. Moreover, the combined event-triggering mechanism and the dynamic quantizer for each node should be designed such that, at each transmission instant, the transmitted information is more accurate with respect to the current output measurement than the information already available at the receiving node. Obviously, the latter is important to avoid redundant usage of the network. In addition, since we consider the case of distributed output measurements with asynchronous transmissions, more attention has to be paid in the modeling and the analysis of the closed-loop system.

The event-triggering mechanism that we construct is inspired by [72, 96, 191] and ensures the existence of a strictly positive lower bound on the inter-transmission times of each node. Before being sent to the controller, the sensor measurement is quantized by means of a dynamic quantizer associated to its node. To prevent the accumulation of zoom actions, the quantizer is only allowed to update its range (and consequently its error bound) at the transmission instants of the respective node. To be more specific, the required zoom variable updates by the quantizer need to be performed before the data is being sent over the network. The overall event-triggering and dynamic quantization strategy achieves the following properties:

(i) an input-to-state stability property is guaranteed for a set around the origin with respect to the external disturbances and Zeno behaviour is excluded;

(ii) at each transmission event, the output measurement is within the quantizer range;

(iii) the transmitted information is more accurate with respect to the current output measurement than the information already available at the receiving node;

(iv) the size of the data packages that are transmitted is bounded for each distributed quantizer.

Sufficient design conditions of the event-triggering mechanism and the quantizer are provided, under which the above properties are guaranteed. The required conditions are formulated in terms of the feasibility of a linear matrix inequality (LMI). Interestingly, the proposed design strategy reveals the intuitive trade-off between the amount of transmissions and the number of quantization levels (and thereby the size of each transmitted data package). The effectiveness of the approach is illustrated on a numerical example.

Despite the practical importance of synthesizing both event-triggered controllers and dynamic quantizers for NCS, only few results in the literature have addressed this problem [141,150,221,229,231]. The techniques of [141,150,221,229] are dedicated to the case of *state feedback* control and only the result of [231] is developed for the case of *output feedback* control, to the best of our knowledge. Moreover, the authors of [229] only focus on the zoom-in stage while the authors of [150, 231] assume that the plant dynamics is not affected by external disturbances. Furthermore, the practical aspects that we consider in (i)-(iv) have not been studied in the previously mentioned works. To the best of our knowledge, this is the first work on the design of input-to-state stabilizing event-triggered controllers with dynamic quantization of the *output feedback* information that deals with all the previously mentioned issues in (i)-(iv). In addition, we handle the implementation scenario where the plant outputs are distributed and transmitted in an asynchronous fashion. A preliminary version of this work has been reported in [3]. Compared to [3], the approach is adapted to a more general scenario than the setup in [21], where the latter result is dedicated to the case where the plant outputs are sent over a single node in a centralized fashion. Moreover, in this chapter, we provide more insights on the problem and all proofs are included.

The remainder of the chapter is organised as follows. Preliminaries are given in Section 4.2. The problem is formulated in Section 4.3. The hybrid model is given in Section 4.4. We present the main results in Section 4.5. Numerical simulations are given in Section 4.6. Conclusions are provided in Section 4.7. The proofs are given in the Appendix.

4.2 Preliminaries

Let $\mathbb{R} := (-\infty, \infty)$, $\mathbb{R}_{\geqslant 0} := [0, \infty)$, $\mathbb{N} := \{0, 1, 2, \ldots\}$, $\mathbb{N}_{>0} := \{1, 2, \ldots\}$ and $\mathbb{Z}$ the set of integers. For a countable set S, $\mathrm{card}(S)$ denotes its cardinality. A continuous function $\gamma : \mathbb{R}_{\geqslant 0} \to \mathbb{R}_{\geqslant 0}$ is of class $\mathcal{K}$ if it is zero at zero and strictly increasing. It is of class $\mathcal{K}_\infty$ if, in addition, $\gamma(s) \to \infty$ as $s \to \infty$. A continuous function $\gamma : \mathbb{R}^2_{\geqslant 0} \to \mathbb{R}_{\geqslant 0}$ is of class $\mathcal{KL}$ if for each fixed $t \in \mathbb{R}_{\geqslant 0}$, $\gamma(\cdot, t)$ is of class $\mathcal{K}$, and for each fixed $s \in \mathbb{R}_{\geqslant 0}$, $\gamma(s, .)$ is nonincreasing and satisfies $\lim_{t\to\infty} \gamma(s, t) = 0$. A function $V : \mathcal{X} \subset \mathbb{R}^n \to \mathbb{R}_{\geqslant 0}$ is locally Lipschitz continuous if for each $x \in \mathcal{X}$, there exists a neighborhood $\mathcal{U}_x$ and a constant $M > 0$ such that $|V(y) - V(z)| \leqslant M|y - z|$ for all $y, z \in \mathcal{U}_x$. A set-valued mapping from a set X to a set Y, associates, with every point $x \in X$, a subset of Y. The notation $F : X \rightrightarrows Y$, indicates that F is a set-valued mapping from X to Y with $F(x) \subset Y$ for all $x \in X$. A set-valued mapping $F : X \rightrightarrows Y$ is said to be outer semicontinuous at a point $x \in X$ if for every sequence of points x_i convergent to x and any convergent sequence of points $y_i \in F(x_i)$, one has $y \in F(x)$, where $\lim_{i\to\infty} y_i = y$. The mapping F is outer semicontinuous if it is outer semicontinuous at each point $x \in X$.

We denote the minimum and maximum eigenvalues of the real symmetric matrix A as $\lambda_{\min}(A)$ and $\lambda_{\max}(A)$, respectively. We write A^T to denote the transpose of A, and $\mathbb{I}_n$ stands for the identity matrix of dimension n. The symbol $\star$ stands for symmetric blocks. We denote by $\mathbf{0}_n$ and $\mathbf{1}_n$ the vectors in $\mathbb{R}^n$ whose all elements are 0 or 1, respectively. We write $(x, y) \in \mathbb{R}^{n_x+n_y}$ to represent the vector $[x^T, y^T]^T$ for $x \in \mathbb{R}^{n_x}$ and $y \in \mathbb{R}^{n_y}$. For a vector $x \in \mathbb{R}^{n_x}$, we denote by $|x| := \sqrt{x^T x}$ its Euclidean norm and, for a matrix $A \in \mathbb{R}^{n\times m}$, $|A| := \sqrt{\lambda_{\max}(A^T A)}$. Given a set $\mathcal{A} \subset \mathbb{R}^n$ and a vector $x \in \mathbb{R}^n$, the distance of x to $\mathcal{A}$ is defined as $|x|_{\mathcal{A}} := \inf_{y\in\mathcal{A}} |x - y|$. We use the following regularized *ceiling* function, for $x \in \mathbb{R}$

$$\lceil x \rceil := \begin{cases} \{\min\{k \in \mathbb{Z} : k > x\}\}, & x \notin \mathbb{Z} \\ \{x, x + 1\}, & x \in \mathbb{Z}. \end{cases} \tag{4.1}$$

Note that this (set-valued) regularized ceiling function is outer semicontinuous in the sense that for each $x \in \mathbb{R}$, each sequence of points $x_i \in \mathbb{R}$ that converge to x, and each sequence of points $y_i \in \mathbb{R}$ that converge to y, $y \in \lceil x \rceil$.

We consider hybrid systems of the following form [49, 99]

$$\dot{x} \in F(x, w) \quad x \in \mathcal{C}, \quad x^+ \in G(x) \quad x \in \mathcal{D}, \tag{4.2}$$

where $x \in \mathbb{R}^{n_x}$ is the state, $w \in \mathbb{R}^{n_w}$ is an exogenous input, $\mathcal{C}$ is the flow set, F is the flow map, $\mathcal{D}$ is the jump set and G is the jump map. Solutions to system (4.2) are defined on *hybrid time domains*. We call a subset $E \subset \mathbb{R}_{\geqslant 0} \times \mathbb{N}$ a *compact hybrid time domain* if $E = \bigcup_{j=0}^{J-1} ([t_j, t_{j+1}], j)$ for some finite sequence

of times $0 = t_0 \leqslant t_1 \leqslant ... \leqslant t_J$ and it is a *hybrid time domain* if for all $(T, J) \in E, E \cap ([0, T] \times \{0, 1, ..., J\})$ is a compact hybrid time domain. A *hybrid signal* is a function defined on a hybrid time domain. A hybrid signal $w : \operatorname{dom} w \to \mathbb{R}^{n_w}$ is called a *hybrid input* if $w(\cdot, j)$ is measurable and locally essentially bounded for each j. A hybrid signal $x : \operatorname{dom} x \to \mathbb{R}^{n_x}$ is called a hybrid arc if $x(\cdot, j)$ is locally absolutely continuous for each j. A hybrid arc $x : \operatorname{dom} x \to \mathbb{R}^{n_x}$ and a hybrid input $w : \operatorname{dom} w \to \mathbb{R}^{n_w}$ form a *solution pair* (x, w) to system (4.2) if $\operatorname{dom} w = \operatorname{dom} x$, $x(0, 0) \in \mathcal{C} \cup \mathcal{D}$, and:

(i) for all $j \in \mathbb{N}$, and almost all t such that $(t, j) \in \operatorname{dom} x$, $x(t, j) \in \mathcal{C}$ and $\dot{x}(t, j) \in F(x(t, j), w(t, j))$;

(ii) for all $(t, j) \in \operatorname{dom} x$ such that $(t, j + 1) \in \operatorname{dom} x$, $x(t, j) \in \mathcal{D}$ and $x(t, j + 1) \in G(x(t, j))$.

A solution pair (x, w) to system (4.2) is *nontrivial* if $\operatorname{dom} x$ contains at least two points, *maximal* if it cannot be extended, it is *complete* if its domain, $\operatorname{dom} x$, is unbounded, it is *Zeno* if it is complete and $\sup_t \operatorname{dom} x < \infty$, where $\sup_t \operatorname{dom} x := \sup\{t \in \mathbb{R}_{\geqslant 0} : \exists j \in \mathbb{N}_{>0} \text{ such that } (t, j) \in \operatorname{dom} x\}$, and it is t-complete if $\operatorname{dom} x$ is unbounded in the t-direction, i.e., $\sup_t \operatorname{dom} x = \infty$.

We use the following definition of $\mathcal{L}_\infty$-norm for hybrid signals [49, 176].

Definition 4.1. *For a hybrid signal w, with domain $\operatorname{dom} w \subset \mathbb{R}_{\geqslant 0} \times \mathbb{N}$, and a scalar $T \in \mathbb{R}_{\geqslant 0}$, the T-truncated $\mathcal{L}_\infty$-norm is given by*

$$\|w_{[T]}\|_\infty := \sup_{j \in \mathbb{N}} \left\{ \operatorname*{ess\,sup}_{t \in \mathbb{R}_{\geqslant 0} | (t,j) \in \operatorname{dom} w,\, t+j \leqslant T} |w(t, j)| \right\}. \tag{4.3}$$

The $\mathcal{L}_\infty$-norm of w is given by

$$\|w\|_\infty := \lim_{T \to T^*} \|w_{[T]}\|_\infty, \tag{4.4}$$

where $T^* := \sup\{t + j : (t, j) \in \operatorname{dom} w\}$. Moreover, we say that $w \in \mathcal{L}_\infty$ whenever the above limit exists and is finite. □

We adopt the following ISS notion for hybrid systems [49].

Definition 4.2. *Consider the hybrid system (4.2), a set $\mathcal{A} \subset \mathbb{R}^{n_x}$ and a set $\mathbb{X}_0 \subseteq \mathbb{R}^{n_x}$. The set $\mathcal{A}$ is input-to-state stable (ISS) w.r.t. w and initial state set $\mathbb{X}_0$ if there exist $\beta \in \mathcal{KL}$ and $\psi \in \mathcal{K}$ such that, for each $x(0, 0) \in \mathbb{X}_0$ and $w \in \mathcal{L}_\infty$, each maximal solution pair (x, w) is t-complete[1] and satisfies for all $(t, j) \in \operatorname{dom} x$.*

$$|x(t, j)|_{\mathcal{A}} \leqslant \max\{\beta(|x(0, 0)|_{\mathcal{A}}, t + j), \psi(||w||_\infty)\}. \tag{4.5}$$

□

[1] In general, t-completeness is not required in the ISS property for hybrid systems as mentioned in [49, Remark 2.2]. However, in the context of NCSs, it is desired that all solutions are t-complete and is therefore explicitly required in this definition.

4.3 Problem formulation

Consider the continuous-time plant model

$$\begin{aligned} \dot{x}_p &= A_p x_p + B_p u + E_p w \\ y &= C_p x_p, \end{aligned} \tag{4.6}$$

where $x_p \in \mathbb{R}^{n_p}$ is the plant state, $u \in \mathbb{R}^{n_u}$ is the control input, $w \in \mathbb{R}^{n_w}$ is unknown plant disturbance, and $y \in \mathbb{R}^{n_y}$ is the measured output. The disturbance w is assumed to be Lebesgue measurable and locally bounded. The plant is stabilized by a dynamic controller of the form

$$\begin{aligned} \dot{x}_c &= A_c x_c + B_c \hat{y}_q \\ u &= C_c x_c + D_c \hat{y}_q, \end{aligned} \tag{4.7}$$

where $x_c \in \mathbb{R}^{n_c}$ is the controller state and $\hat{y}_q \in \mathbb{R}^{n_y}$ denotes the most recent quantized output measurement available at the controller, see Figure 4.1. The controller (4.7) is designed by an emulation approach in the sense that we assume that the closed-loop system given by (4.6) and (4.7) is stable when the effects of both the quantization and the network are absent, i.e., when $\hat{y}_q = y$.

4.3.1 Setup description

We consider the scenario where the controller is directly connected to the plant while the output measurement y is transmitted to the controller over a digital channel. In particular, we assume that the plant output y is partitioned into l components, i.e., $y = (y_1, y_2, \ldots, y_l)$, which are measured by l distributed sensors. The sensors communicate with the controller over l different communication channels at discrete time instants t_k^i, $k \in \mathbb{N}, i \in \{1, 2, \ldots, l\}$. At any node $i \in \{1, 2, \ldots, l\}$, the measured output $y_i \in \mathbb{R}^{n_{y_i}}$ is collected, quantized, encoded and the resulting encrypted data is sent over the communication channel, see Figure 4.1. This encryption is required to make sure that at each transmission, only a limited number of bits is sent. Let $\hat{y}_q = (\hat{y}_{q,1}, \hat{y}_{q,2}, \ldots, \hat{y}_{q,l})$, where $\hat{y}_{q,i}$, $i \in \{1, 2, \ldots, l\}$, denotes the most recent quantized value of y_i available at the controller. The value of $\hat{y}_{q,i}$ is kept constant between two consecutive transmission instants of node i in a zero-order-hold (ZOH) fashion, i.e., $\dot{\hat{y}}_{q,i} = 0$. We ignore communication and computation delays in this study, although it would be possible to include them by using the techniques in, e.g., [72, 120].

4.3.2 Event-triggering mechanism

The sequence of transmission instants of each node i is generated by an independent event-triggering condition in the sense that the event-triggering condition

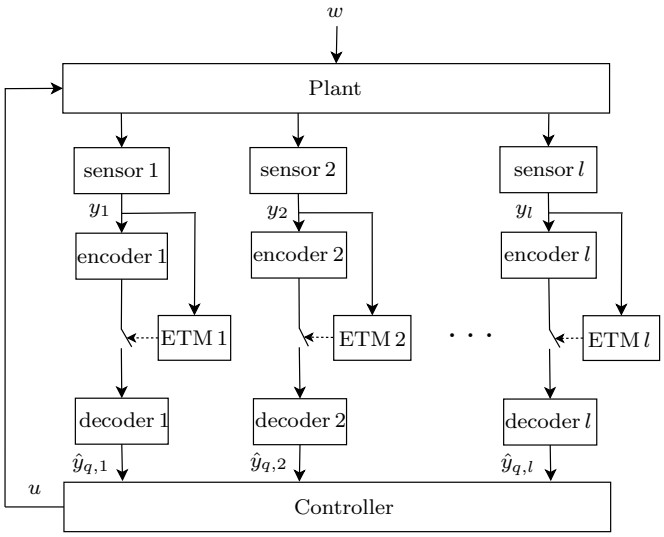

Fig. 4.1. NCS with distributed and quantized output measurements.

only depends on locally available information at node i. Each triggering mechanism determines the next transmission instant t_k^i, $k \in \mathbb{N}, i \in \{1, 2, \ldots, l\}$ based on the actual values of the output measurement y_i of node i and the most recent transmitted (quantized) value $\hat{y}_{q,i}$. The triggering mechanism at each node $i \in \{1, 2, \ldots, l\}$, is dynamic, in the sense of [72, 96, 191], and takes the following form

$$t_{k+1}^i = \inf\{t > t_k^i + T_i \mid \eta_i(t) = 0\}, \tag{4.8}$$

where $t_0^i = 0$, $T_i > 0$, $\eta_i \in \mathbb{R}_{\geqslant 0}$. The time constant $T_i > 0, i \in \{1, 2, \ldots, l\}$ is a strictly positive lower bound on the inter-transmission times of the output y_i that we enforce to prevent the occurrence of Zeno with respect to transmission events at node i. The variable $\eta_i, i \in \{1, 2, \ldots, l\}$, is the solution to the dynamical system

$$\dot{\eta}_i \in \Psi_i(o_i) \quad t \in (t_k^i, t_{k+1}^i), \qquad \eta_i((t_k^i)^+) = \eta_{0,i}(o_i), \tag{4.9}$$

where $o_i \in \mathbb{R}^{n_{o_i}}$ represents locally available information at the event-triggering mechanism. The time constant T_i and the functions Ψ_i and $\eta_{0,i}$ are to be designed and will be specified in Section 4.5.

4.3.3 Dynamic quantization

As mentioned before, at each transmission instant t_k^i, $k \in \mathbb{N}, i \in \{1, 2, \ldots, l\}$, the value of y_i is quantized before being sent over the network. A quantizer is essentially a piecewise constant function $q_i : \mathbb{R}^{n_{y_i}} \to Q_i \subseteq \mathbb{R}^{n_{y_i}}$ with Q_i a

finite countable subset of $\mathbb{R}^{n_{y_i}}$. As such, a quantizer induces a partition in $\mathbb{R}^{n_{y_i}}$ consisting of $\text{card}(Q_i)$ *quantization regions* described by $\{z \in \mathbb{R}^{n_{y_i}} : q_i(z) = x\}$, $x \in Q_i$. We assume that the function q_i satisfies the following assumption as proposed in [143], see also [116, 145, 175].

Assumption 4.1. *[143] There exist constants M_i, Δ_i, $i \in \{1, 2, \ldots, l\}$, such that for all $y_i \in \mathbb{R}^{n_{y_i}}$, it holds that*

$$|y_i| \leqslant M_i \quad \Rightarrow \quad |q_i(y_i) - y_i| \leqslant \Delta_i. \tag{4.10}$$

Moreover, there exists a constant $\delta > 0$ such that for all $z \in \mathbb{R}^{n_{y_i}}$ with $|z| \leqslant \delta$, it holds that $q(z) = 0$. □

This assumption in essence states that the magnitude of the quantization error $|q_i(y_i) - y_i|$ is upper bounded by Δ_i, as long as the quantizer is not saturated, i.e., the output measurement y_i is within the range of its respective quantizer. Moreover, it states that $q_i(z) = 0$ for z in some neighborhood around the origin (and implies $0 \in Q_i$). Let us remark that Assumption 4.1 allows the quantizer regions to have arbitrary shapes. In the remainder of the chapter, we will refer to M_i and Δ_i as the initial quantizer range and initial error bound of node $i \in \{1, 2, \ldots, l\}$, respectively.

In this chapter, we consider dynamic quantizer functions $q_i^{\mu_i}$, $i \in \{1, 2, \ldots, l\}$, which, as in [48, 143, 145], are defined as

$$q_i^{\mu_i}(y_i) := \mu_i q_i \left(\frac{y_i}{\mu_i} \right), \tag{4.11}$$

where $\mu_i \in \mathbb{R}_{\geqslant \underline{\mu}_i}$, $i \in \{1, 2, \ldots, l\}$, are dynamic variables referred to as the zoom variables and where q_i satisfies Assumption 4.1 for some $M_i, \Delta_i > 0$ and where $\underline{\mu}_i > 0$ is a lower-bound on μ_i to be specified.. The zoom variables μ_i, $i \in \{1, 2, \ldots, l\}$, are used to adjust the quantizer range initially equal to $M_i > 0$ and the quantizer error bound initially equal to $\Delta_i > 0$ of node i based on the magnitude of the output measurement y_i. To be more specific, the range and the error bound of the dynamic quantizer as in (4.10) are given by $M_i\mu_i$ and $\Delta_i\mu_i$, respectively. As such, property (4.10) becomes $|y_i| \leqslant \mu_i M_i \quad \Rightarrow$ $|q_i^{\mu_i}(y_i) - y_i| \leqslant \mu_i \Delta_i$. Note that the number of quantization regions of dynamic quantizers remains constant all the time.

In the context of NCSs, it is of importance that at each transmission instant, before data is actually transmitted, the dynamic quantizer is set such that property (ii) and (iii) mentioned in Section 4.1 are satisfied. To achieve these two properties, the zoom variable μ_i is adapted at transmission instants $t_k^i, k \in \mathbb{N}$, $i \in \{1, 2, \ldots, l\}$, according to

$$\mu_i^+ \in \Theta_i(y_i, \mu_i) := \Omega_{\text{in},i}^{\kappa_{\text{in},i}(y_i,\mu_i)} \Omega_{\text{out},i}^{\kappa_{\text{out},i}(y_i,\mu_i)} \mu_i \tag{4.12}$$

where $\Omega_{\text{in},i} \in (0,1), \Omega_{\text{out},i} > 1$, are the zoom-in and zoom-out factors, respectively, and where we omitted the time arguments for sake of compactness. The functions $\kappa_{\text{in},i}, \kappa_{\text{out},i} : \mathbb{R}^{n_{y_i}} \times \mathbb{R}_{>0} \rightrightarrows \mathbb{N}$ determine the number of zoom-in or zoom-out actions that need to be performed at each transmission[2].

Let us elaborate on the dynamic adjustment strategy of μ_i, $i \in \{1,2,\ldots,l\}$. At any transmission instant t_k^i, $k \in \mathbb{N}, i \in \{1,2,\ldots,l\}$, if the magnitude of $|y_i|$ is close to the range of the quantizer, we increase the value of μ_i with the factor $\sigma_{\text{out},i} \in \Omega_{\text{out},i}^{\kappa_{\text{out},i}(y_i,\mu_i)}$ with $\sigma_{\text{out},i} > 1$ in order to make sure that the transmitted information is within range of the quantizer (which corresponds to property (ii) stated in Section 4.1). We refer to this action as the zoom-out event. On the other hand, if $|y_i|$ is small with respect to the current quantizer error bound, we decrease μ_i by means of the zoom-in factor $\sigma_{\text{in},i} \in \Omega_{\text{in},i}^{\kappa_{\text{in},i}(y_i,\mu_i)}$ with $\sigma_{\text{in},i} \in (0,1)$ such that more precise information is transmitted (which corresponds to property (iii) stated in Section 4.1). We refer to this action as the zoom-in event. See, e.g., [145] for more details on dynamic quantizers.

Let us emphasize that the zoom variable μ_i in (4.12) is only updated at transmission instants t_k^i, $k \in \mathbb{N}, i \in \{1,2,\ldots,l\}$ and held constant in between transmissions, i.e., $\dot{\mu}_i = 0$ for $t \in (t_k^i, t_{k+1}^i)$. Consequently, in each node $i \in \{1,2,\ldots,l\}$, the time in between the zoom events is lower bounded by the minimum inter-transmission time T_i ensured by the local triggering condition (4.8).

To be able to successfully reconstruct the broadcast encoded information, the zoom variable μ_i of both the encoder and the decoder at any channel should be initialized at the same value, see Remark 1 in [116] for an in-depth discussion on this point. Then, at each update instant t_k^i, we only transmit the index of the quantization region, the number of required zoom actions corresponding to the transmission and a boolean (one bit) that indicates whether these zoom actions are zoom-in or zoom-out events. By means of these three (two integers and one boolean) quantities, the decoder on the other side of the network can reconstruct μ_i and thereby the quantized output $\hat{y}_{q,i}$ using (4.11), which then can be used by the controller according to (4.7).

4.3.4 Problem statement

Our objective is to design both the event-triggering mechanism (4.8), (4.9) (i.e., to design the time-constant T_i and the functions Ψ_i and $\eta_{0,i}$ for $i \in \{1,2,\ldots,l\}$) and the dynamic quantization strategy (4.12) (i.e., to design the parameters $\Delta_i, M_i, \Omega_{\text{in},i}, \Omega_{\text{out},i}$ and the functions $\kappa_{\text{in},i}, \kappa_{\text{out},i}$ for $i \in \{1,2,\ldots,l\}$) such that properties (i)-(iv) mentioned in Section 4.1 are achieved for the closed-loop system.

[2] In (4.12), we use $\Omega_{\text{in},i}^{\kappa_{\text{in},i}(y_i,\mu_i)}$ to denote the set $\{\Omega_{\text{in},i}^{\kappa} \mid \kappa \in \kappa_{\text{in},i}(y_i,\mu_i)\}$ and $\Omega_{\text{out},i}^{\kappa_{\text{out},i}(y_i,\mu_i)}$ to denote the set $\{\Omega_{\text{out},i}^{\kappa} \mid \kappa \in \kappa_{\text{out},i}(y_i,\mu_i)\}$.

4.4 Hybrid model

In this section, we present a formal description of the closed-loop system using the modelling framework for hybrid dynamical systems as advocated in [99]. We define the network-induced error as $e_{s,i} := \hat{y}_{q,i} - q_i^{\mu_i}(y_i)$, which is reset to zero at each transmission instant $t_k^i, k \in \mathbb{N}$. We also define the quantization error as $e_{q,i} := q_i^{\mu_i}(y_i) - y_i$. The total network-induced error at each node $i \in \{1, 2, \ldots, l\}$, is given by

$$e_i := e_{s,i} + e_{q,i} = \hat{y}_{q,i} - y_i. \tag{4.13}$$

Since at each transmission instant t_k^i, $k \in \mathbb{N}, i \in \{1, 2, \ldots, l\}$, the sampling error of node i is set to zero, we have that $e_i(t_k^{i\,+}) = e_{q,i}(t_k^{i\,+})$. Observe that in general e_i is not reset to zero at each transmission instant due to the effect of quantization. This issue induces nontrivial challenges to the design of event-triggered control mechanisms, compared to the case where quantization is not considered, and requires careful handling. In fact, this phenomenon may have a negative impact on the closed-loop stability, as we will explain later. Let $x := (x_p, x_c) \in \mathbb{R}^{n_x}$ and $e := (e_1, e_2, \ldots, e_l) \in \mathbb{R}^{n_y}$. Then, in view of (4.6), (4.7), (4.13), the flow dynamics of x is given by

$$\begin{aligned} \dot{x} = & \begin{bmatrix} A_p + B_p D_c C_p & B_p C_c \\ B_c C_p & A_c \end{bmatrix} x + \begin{bmatrix} B_p D_c \\ B_c \end{bmatrix} e + \begin{bmatrix} E_p \\ 0 \end{bmatrix} w \\ =: & \mathcal{A}_1 x + \mathcal{B}_1 e + \mathcal{E}_1 w. \end{aligned} \tag{4.14}$$

Let the matrix C_p in (4.6) be partitioned as $C_p = \begin{bmatrix} C_{p,1}^T & \ldots & C_{p,l}^T \end{bmatrix}^T$ with $C_{p,i} \in \mathbb{R}^{n_{y_i}} \times \mathbb{R}^{n_p}$ such that $y_i = C_{p,i} x_p \in \mathbb{R}^{n_{y_i}}$ for $i \in \{1, 2, \ldots, l\}$. Then, because of the ZOH implementation, the flow dynamics of e_i is

$$\begin{aligned} \dot{e}_i = & -\dot{y}_i = -C_{p,i} \dot{x}_p \\ = & \begin{bmatrix} -C_{p,i}(A_p + B_p D_c C_p) & -C_{p,i} B_p C_c \end{bmatrix} x - C_{p,i} B_p D_c e \\ & - C_{p,i} E_p w \\ =: & \mathcal{A}_{2i} x + \mathcal{B}_{2i} e + \mathcal{E}_{2i} w. \end{aligned} \tag{4.15}$$

In view of (4.15), the flow dynamics of the overall e is

$$\begin{aligned} \dot{e} = & \begin{bmatrix} \mathcal{A}_{21} \\ \vdots \\ \mathcal{A}_{2l} \end{bmatrix} x + \begin{bmatrix} \mathcal{B}_{21} \\ \vdots \\ \mathcal{B}_{2l} \end{bmatrix} e + \begin{bmatrix} \mathcal{E}_{21} \\ \vdots \\ \mathcal{E}_{2l} \end{bmatrix} w \\ =: & \mathcal{A}_2 x + \mathcal{B}_2 e + \mathcal{E}_2 w. \end{aligned} \tag{4.16}$$

We introduce auxiliary variables $\tau_i \in \mathbb{R}_{\geqslant 0}$ and $p_i \in \{0,1\}$ for $i \in \{1,2,\ldots,l\}$. The variable τ_i represents the time elapsed since the last transmission instant of node i. It has the dynamics

$$\dot{\tau}_i = 1 \quad t \in (t_k^i, t_{k+1}^i), \qquad \tau_i((t_k^i)^+) = 0 \quad \text{for } k \in \mathbb{N}. \tag{4.17}$$

The variable p_i is a boolean that keeps track of whether at the next event, the zoom-variable is updated ($p_i = 0$) or a transmission occurs ($p_i = 1$) (recall that at each transmission instant t_k^i, the zoom variable μ_i is updated before y_i is transmitted). Let $\xi := (x, e, \mu, \tau, \eta, p) \in \mathbb{X}$ with $\mathbb{X} = \mathbb{R}^{n_x} \times \mathbb{R}^{n_y} \times (\mathbb{R}_{\geqslant \underline{\mu}_1} \times \ldots \times \mathbb{R}_{\geqslant \underline{\mu}_l}) \times \mathbb{R}_{\geqslant 0}^l \times \mathbb{R}_{\geqslant 0}^l \times \{0,1\}^l$ be the concatenation of the state variables, where $\mu := (\mu_1, \ldots, \mu_l) \in \mathbb{R}_{\geqslant 0} \times \ldots \times \mathbb{R}_{\geqslant 0}$, $\tau := (\tau_1, \ldots, \tau_l) \in \mathbb{R}_{\geqslant 0}^l$, $\eta := (\eta_1, \ldots, \eta_l) \in \mathbb{R}_{\geqslant 0}^l$, and $p := (p_1, \ldots, p_l) \in \{0,1\}^l$. Then, in view of (4.8) and (4.9), the flow set $\mathcal{C}$ and the jump set $\mathcal{D}$ are given by

$$\begin{aligned} \mathcal{C} &:= \Big\{ \xi \in \mathbb{X} : p = 0 \Big\} \\ \mathcal{D} &:= \textstyle\bigcup_{i=1}^l \mathcal{D}_i \end{aligned} \tag{4.18}$$

with

$$\mathcal{D}_i := \Big\{ \xi \in \mathbb{X} : (\eta_i = 0 \text{ and } \tau_i \geqslant T_i) \text{ or } p_i = 1 \Big\}. \tag{4.19}$$

Note that the triggering condition related to $\eta_i(t) = 0$, $i \in \{1,2,\ldots,l\}$, in (4.8) is embedded in the flow set $\mathcal{C}$ via the definition of $\mathbb{X}$ ($\xi \in \mathbb{X}$ implies $\eta_i \geqslant 0$ for each $i \in \{1,2,\ldots,l\}$). Given (4.18), we obtain the hybrid system[3]

$$\begin{aligned} \dot{\xi} \in F(\xi, w) := \begin{pmatrix} \mathcal{A}_1 x + \mathcal{B}_1 e + \mathcal{E}_1 w \\ \mathcal{A}_2 x + \mathcal{B}_2 e + \mathcal{E}_2 w \\ \mathbf{0}_l \\ \mathbf{1}_l \\ \Psi(o) \\ \mathbf{0}_l \end{pmatrix} \qquad & \xi \in \mathcal{C} \\ \xi^+ \in G(\xi) \qquad & \xi \in \mathcal{D}, \end{aligned} \tag{4.20}$$

[3]With no loss of generality, we assume that before the first hybrid time instant, i.e., $(t,j) = (0,0)$, the system is properly initialized in the sense that at least one successful transmission per node has occurred. The latter is important to make sure that both the sensors and the controller have the same knowledge on $\hat{y}_q$ at the initial time. This prevents the system to start in and undesired equilibrium due to the mismatch between the controller and the sensor on the last transmitted value $\hat{y}_q$, see also, e.g., [4, 74, 78].

where $\Psi(o) := (\Psi_1(o_1), \ldots, \Psi_l(o_l))$ with $o_i := (y_i, e_i, \tau_i, \eta_i) \in \mathbb{R}^{n_{o_i}}$. The jump map is given by $G(\xi) := \bigcup_{i=1}^{l} G_i(\xi)$, where

$$G_i(\xi) := \begin{cases} \left\{G_i^{\mu}(\xi)\right\} & \text{for } \xi \in \mathcal{D}_i \wedge p_i = 0 \\ \left\{G_i^{y}(\xi)\right\} & \text{for } \xi \in \mathcal{D}_i \wedge p_i = 1 \\ \emptyset & \text{for } \xi \notin \mathcal{D}_i \end{cases} \tag{4.21}$$

with

$$\begin{aligned} G_i^{\mu}(\xi) &:= \begin{pmatrix} x \\ e \\ \bar{\Lambda}_i \Theta_i(y_i, \mu_i) + (\mathbb{I}_l - \bar{\Lambda}_i)\mu \\ \tau \\ \eta \\ \bar{\Lambda}_i \mathbf{1}_l + (\mathbb{I}_l - \bar{\Lambda}_i)p \end{pmatrix} \\ G_i^{y}(\xi) &:= \begin{pmatrix} x \\ \Lambda_i e_q + (\mathbb{I}_{n_y} - \Lambda_i)e \\ \mu \\ (\mathbb{I}_l - \bar{\Lambda}_i)\tau \\ \bar{\Lambda}_i \eta_0(e) + (\mathbb{I}_l - \bar{\Lambda}_i)\eta \\ (\mathbb{I}_l - \bar{\Lambda}_i)p \end{pmatrix}, \end{aligned} \tag{4.22}$$

where $\Lambda_i := \operatorname{diag}\{\delta_{1i}\mathbb{I}_{n_{y1}}, \ldots, \delta_{li}\mathbb{I}_{n_{yl}}\}, i \in \{1, 2, \ldots, l\}$, $\bar{\Lambda}_i := \operatorname{diag}\{\delta_{1i}, \ldots, \delta_{li}\}$ with δ_{ji} the Kronecker delta, which takes the value $\delta_{ji} = 1$ when $i = j$ and $\delta_{ji} = 0$ when $i \neq j$, $\eta_0(e) := (\eta_{0,1}(e_1), \ldots, \eta_{0,l}(e_l))$, $e_q := (e_{q,1}, \ldots, e_{q,l})$, the function $\Theta_i : \mathbb{R}^{n_{y_i}} \times \mathbb{R}_{\geqslant 0} \rightrightarrows \mathbb{R}_{\geqslant 0}$ as in (4.12) with the functions $\kappa_{\text{in},i}, \kappa_{\text{out},i} : \mathbb{R}^{n_{y_i}} \times \mathbb{R}_{\geqslant 0} \rightrightarrows \mathbb{N}$ to be specified.

System (4.20) flows on $\mathcal{C}$ as long as the triggering conditions are not satisfied and $p = 0$. When $\xi \in \mathcal{D}_i$ and $p_i = 0$, ξ can jump according to $\xi^+ \in G_i^{\mu}(\xi)$ corresponding to an update of the quantizer settings. To be more specific, when the state jumps according to $\xi^+ \in G_i^{\mu}(\xi)$, the quantizer variable μ_i, $i \in \{1, 2, \ldots, l\}$, is updated and p_i is changed to 1. Consequently, ξ^+ lies into the jump set $\mathcal{D}_i$ with $p_i = 1$. Since the system is not allowed to flow when $p_i = 1$ for some $i \in \{1, 2, \ldots, l\}$, since, in view of (4.18), $\xi \notin \mathcal{C}$ when $p_i = 1$ for some $i \in \{1, 2, \ldots, l\}$, a transmission is generated and p_i is reset to 0, in view of the jump map $G_i^{y}(\xi)$. As such, the boolean variable p_i ensures that at any transmission instant t_k^i, the quantizer variable μ_i is updated before transmitting $q_i^{\mu_i}(y_i)$, which is fundamental for realizing properties (ii) and (iii) as mentioned in the introduction.

Let us remark that the hybrid system in (4.20) satisfies the following conditions

- $\mathcal{C}$ and $\mathcal{D}$ are closed sets
- $F : \mathbb{X} \times \mathbb{R}^{n_w} \rightrightarrows \mathbb{Y}$ is outer semicontinuous and locally bounded, and $F(\xi, w)$ is non-empty and convex for all $(\xi, w) \in \mathcal{C} \times \mathbb{R}^{n_w}$.
- $G : \mathbb{X} \rightrightarrows \mathbb{Y}$ is outer semicontinuous and locally bounded, and $G(\xi, w)$ is non-empty for all $(\xi, w) \in \mathcal{D}$,

where $\mathbb{Y} = \mathbb{R}^{n_x} \times \mathbb{R}^{n_y} \times \mathbb{R}^l \times \mathbb{R}^l_{\geqslant 0} \times \mathbb{R}^l \times \{0,1\}^l$. These conditions assure that the hybrid system $\mathcal{H}$ described by (4.18) and (4.20), is well-posed, see also, [99, Chapter 6].

Remark 4.1. We note that the update strategy of the zoom variable μ_i, $i \in \{1, 2, \ldots, l\}$, in (4.12), (4.20) and (4.22) is essentially different from related techniques in the context of quantized control systems (QCS) [145,207,232] from two points of view. First, in the proposed scheme, the zoom actions are carried out based on the past (true) values of y_i and not based on the quantized feedback information $q_i^{\mu_i}(y_i)$ as in [145,207,232] for instance. To that end, we rely on the assumption that the true values of y_i can be accessed by the corresponding encoder at node i. Indeed, this requirement is relevant if the communication network is the reason of quantization, such as in e.g., [56,194,209,231] and as we consider in this study, but not the sensor, see [207] for further discussion on this point. Second, unlike [145,207], we do not reset the control input to zero during a zoom-out event, which allows to avoid large overshoot during the zoom-out event. □

4.5 Main result

4.5.1 Assumptions

We make the following assumption on system (4.20).

Assumption 4.2. *Consider system (4.20). There exist a positive definite symmetric real matrix P, real numbers $\varepsilon_x, \varepsilon_w > 0$ and $\varepsilon_{y_i}, \gamma_i > 0$ for $i \in \{1, 2, \ldots, l\}$, such that*

$$\begin{pmatrix} \Sigma & \star & \star \\ \mathcal{B}_1^T P + \overline{\mathcal{B}}_2^T \mathcal{A}_2 & -\Gamma^2 + \overline{\mathcal{B}}_2^T \overline{\mathcal{B}}_2 & \star \\ \mathcal{E}_1^T P + \mathcal{E}_2^T \mathcal{A}_2 & \mathcal{E}_2^T \overline{\mathcal{B}}_2 & \mathcal{E}_2^T \mathcal{E}_2 - \varepsilon_w \mathbb{I}_{n_w} \end{pmatrix} \leqslant 0, \tag{4.23}$$

where $\Sigma := \mathcal{A}_1^T P + P\mathcal{A}_1 + \varepsilon_x \mathbb{I}_{n_x} + \mathcal{A}_2^T \mathcal{A}_2 + \overline{C}_p^T \Upsilon \overline{C}_p$ *with* $\overline{C}_p := [C_p \quad 0]$ *and* $\Upsilon := \mathrm{diag}\{\varepsilon_{y_1}\mathbb{I}_{n_{y_1}}, \ldots, \varepsilon_{y_l}\mathbb{I}_{n_{y_l}}\}$, $\Gamma := \mathrm{diag}\{\gamma_1 \mathbb{I}_{n_{y_1}}, \ldots, \gamma_l \mathbb{I}_{n_{y_l}}\}$, *and where* $\overline{\mathcal{B}}_2 = \begin{bmatrix} \overline{\mathcal{B}}_{21}^T & \ldots & \overline{\mathcal{B}}_{2l}^T \end{bmatrix}^T$ *with* $\overline{\mathcal{B}}_{2i} := \mathcal{B}_{2i}(\mathbb{I}_{n_y} - \Lambda_i)$. □

The LMI condition (4.23) in essence establishes an $\mathcal{L}_2$-gain stability property for the system $\dot{x} = \mathcal{A}_1 x + \mathcal{B}_1 e + \mathcal{E}_1 w$ from (e, w) to $(\mathcal{A}_2 x + \overline{\mathcal{B}}_2 e + \mathcal{E}_2 w, y)$. Indeed, if we define $V(x) := x^T P x$ for all $x \in \mathbb{R}^{n_x}$, then in view of (4.20) and the definitions of $\Upsilon, \Gamma, \Lambda$, the feasibility of (4.23) implies for all $(x, e, w) \in \mathbb{R}^{n_x + n_e + n_w}$ that

$$\begin{aligned} \langle \nabla V(x), \mathcal{A}_1 x + \mathcal{B}_1 e + \mathcal{E}_1 w \rangle &\leqslant -\varepsilon_x |x|^2 - \sum_{i=1}^{l} \varepsilon_{y_i} |y_i|^2 \\ &- \sum_{i=1}^{l} \left| \mathcal{A}_{2i} x + \overline{\mathcal{B}}_{2i} e + \mathcal{E}_{2i} w \right|^2 + \sum_{i=1}^{l} \gamma_i^2 |e_i|^2 + \varepsilon_w |w|^2. \end{aligned} \tag{4.24}$$

This property is needed to design the enforced minimum time $T_i, i \in \{1, 2, \ldots, l\}$ on the inter-transmission times of each node and to design the dynamics of $\eta_i, i \in \{1, 2, \ldots, l\}$ in (4.18) such that closed-loop stability (in an appropriate sense) is guaranteed.

4.5.2 Design conditions for the event-triggering mechanism

The dynamics of the functions $\eta_i, i \in \{1, 2, \ldots, l\}$, in (4.9) are defined by the functions Ψ_i and $\eta_{0,i}$, inspired by [72], where quantization was not considered, and are given by[4]

$$\begin{aligned} \Psi_i(o_i) &:= \varepsilon_{y_i} \max\left\{|y_i|^2, \Delta_{0,i}^2\right\} - (1 - \omega_i(\tau_i))\tilde{\gamma}_i |e_i|^2 - \vartheta_i \eta_i, \\ \eta_{0,i}(e_i) &:= \gamma_i(\tilde{\lambda}_i - \lambda_i)|e_i|^2, \end{aligned} \tag{4.25}$$

where

$$\omega_i(\tau_i) := \begin{cases} \{1\}, & \text{for } \tau_i \in [0, T_i) \\ [0, 1], & \text{for } \tau_i = T_i \\ \{0\}, & \text{for } \tau_i > T_i, \end{cases} \tag{4.26}$$

and where $o_i = (y_i, e_i, \tau_i, \eta_i)$, as before, $\vartheta_i > 0$, $\Delta_{0,i} > 0$, $\lambda_i \in (0, 1)$, $\tilde{\lambda}_i \in [\lambda_i, \lambda_i^{-1})$, $\tilde{\gamma}_i := \gamma_i^2 + \gamma_i^2 \tilde{\lambda}_i^2 + 2\gamma_i \tilde{\lambda}_i \tilde{L}_i$ with $\tilde{L}_i := L_i + \nu_i$ for any $\nu_i > 0$ and $L_i := |\mathcal{B}_{2i}\Lambda_i| = |b_{2i,i}|$, with $b_{2i,i}$ such that $\mathcal{B}_{2i} = \begin{bmatrix} b_{2i,1} & \ldots & b_{2i,l} \end{bmatrix}$, and the constants ε_{y_i},

[4] In (4.25), we use $\varepsilon_{y_i} \max\left\{|y_i|^2, \Delta_{0,i}^2\right\} - (1 - \omega_i(\tau_i))\tilde{\gamma}_i |e_i|^2 - \vartheta_i \eta_i$ to denote the set $\{\varepsilon_{y_i} \max\left\{|y_i|^2, \Delta_{0,i}^2\right\} - (1 - \omega)\tilde{\gamma}_i |e_i|^2 - \vartheta_i \eta_i \mid \omega \in \omega_i(\tau_i)\}$.

γ_i as in Assumption 4.2. The time constant T_i of any node $i \in \{1, 2, \ldots, l\}$, is taken such that $T_i = \mathcal{T}_i(\lambda_i, \tilde{\lambda}_i, \gamma_i, \tilde{L}_i)$, where

$$\mathcal{T}_i(\lambda_i, \tilde{\lambda}_i, \gamma_i, \tilde{L}_i) := \begin{cases} \frac{1}{\tilde{L}_i r_i} \arctan\left(\frac{r_i(1-\lambda_i\tilde{\lambda}_i)}{\frac{\gamma_i}{\tilde{L}_i}(\lambda_i+\tilde{\lambda}_i)+1+\lambda_i\tilde{\lambda}_i}\right), & \gamma_i > \tilde{L}_i \\ \frac{1}{\tilde{L}_i} \frac{1-\lambda_i\tilde{\lambda}_i}{\lambda_i\tilde{\lambda}_i+\lambda_i+\tilde{\lambda}_i+1}, & \gamma_i = \tilde{L}_i \\ \frac{1}{\tilde{L}_i r_i} \operatorname{arctanh}\left(\frac{r_i(1-\lambda_i\tilde{\lambda}_i)}{\frac{\gamma_i}{\tilde{L}_i}(\lambda_i+\tilde{\lambda}_i)+1+\lambda_i\tilde{\lambda}_i}\right), & \gamma_i < \tilde{L}_i \end{cases} \tag{4.27}$$

with $r_i := \sqrt{\left|(\frac{\gamma_i}{\tilde{L}_i})^2 - 1\right|}$. When $\tilde{\lambda}_i = \lambda_i$, the time $\mathcal{T}_i(\lambda_i, \tilde{\lambda}_i, \gamma_i, \tilde{L}_i)$ corresponds to the *maximally allowable transmission interval* (MATI) of time-triggered controllers [51] for NCSs without quantization. Let us remark that λ_i also has an important role in the design of the quantizer as we will discuss in later in Section 4.5.5. The time-constant T_i as given in (4.27) is derived as the time it takes for the function $\phi_i : \mathbb{R}_{\geqslant 0} \to \mathbb{R}_{\geqslant 0}$ to decrease from $\phi_i(0) = \lambda_i^{-1}$ to $\phi_i(T_i) = \tilde{\lambda}_i$, where ϕ_i satisfies, see also [51, 72],

$$\frac{d\phi_i}{d\tau_i} = -2\tilde{L}_i\phi_i(\tau_i) - \gamma_i(\phi_i^2(\tau_i) + 1). \tag{4.28}$$

Remark 4.2. We observe that, in view of (4.27) and its interpretation in terms of (4.28), when $\tilde{\lambda}_i \in [\lambda_i, \lambda_i^{-1})$ is increased, the guaranteed minimum time T_i between two transmission instants of node i will be reduced. However, by increasing $\tilde{\lambda}_i$, the value of $\eta_{0,i}$ in (4.25) will increase. Consequently, this may lead to increase the time it takes for η_i to decrease to 0, i.e., it may enlarge the inter-transmission times. Hence, the tuning of $\tilde{\lambda}_i$ may generate a trade-off between the guaranteed minimum inter-transmission time T_i and the average inter-transmission times. □

4.5.3 Design conditions for the dynamic quantizer

In this subsection, we specify how to design the parameters $\Delta_i, M_i, \Omega_{\text{in},i}, \Omega_{\text{out},i}$ and the functions $\kappa_{\text{in},i}, \kappa_{\text{out},i}$ for $i \in \{1, 2, \ldots, l\}$, see (4.12). For each node $i \in \{1, 2, \ldots, l\}$, we design the initial quantizer range M_i, the initial error bound Δ_i, the zoom-in parameters $\Omega_{\text{in},i} \in (0, 1)$, and the zoom-out parameters $\Omega_{\text{out},i} > 1$ such that

$$\frac{M_i}{\Delta_i} \geqslant \left(\kappa_i + \frac{2\sqrt{\tilde{\gamma}_i}}{\sqrt{\varepsilon_{y_i}}\Omega_{\text{in},i}\lambda_i}\right) \tag{4.29}$$

$$\kappa_i > \max\left\{1, \frac{(\Omega_{\text{in},i}\Omega_{\text{out},i} - 1)M_i + \Delta_i}{\Omega_{\text{in},i}\Omega_{\text{out},i}\Delta_i}\right\}. \tag{4.30}$$

Moreover, the functions $\kappa_{\text{in},i}$ and $\kappa_{\text{out},i}$ for $i \in \{1, 2, \ldots, l\}$, are, for $y_i \in \mathbb{R}^{n_{y_i}}$ and $\mu_i \in \mathbb{R}_{\geqslant 0}$, given by

$$\begin{aligned} \kappa_{\text{in},i}(y_i, \mu_i) &:= \left\lceil \max\left\{ -\varsigma, \frac{\log\left(\max\{|y_i|, \Delta_{0,i}\}/(\ell_{\text{in},i}\mu_i) \right)}{\log \Omega_{\text{in},i}} \right\} \right\rceil \\ \kappa_{\text{out},i}(y_i, \mu_i) &:= \left\lceil \max\left\{ -\varsigma, \frac{\log\left(|y_i|/(\ell_{\text{out},i}\mu_i) \right)}{\log \Omega_{\text{out},i}} \right\} \right\rceil, \end{aligned} \tag{4.31}$$

where

$$\ell_{\text{in},i} := \Omega_{\text{in},i}(M_i - \kappa_i \Delta_i), \qquad \ell_{\text{out},i} := M_i - \Delta_i \tag{4.32}$$

with κ_i as in (4.30), $\Delta_{0,i}$ as in (4.25) and where the constant $\varsigma \in (0, 1)$ can be chosen arbitrarily.

The functions $\kappa_{\text{in},i}$ and $\kappa_{\text{out},i}$ and the constants $\ell_{\text{in},i}$ and $\ell_{out,i}$ are specified such that the following properties are satisfied. For all $y_i \in \mathbb{R}^{n_{y_i}}$ and $\mu_i \in \mathbb{R}_{\geqslant 0}$, $i \in \{1, 2, \ldots, l\}$, we have that

(a) $\kappa_{\text{in},i}(y_i, \mu_i), \kappa_{\text{out},i}(y_i, \mu_i) \subset \mathbb{N}$

(b) $\kappa_{\text{in},i}(y_i, \mu_i) \neq \{0\} \Rightarrow |y_i| < \ell_{\text{out},i}\mu_i$. Moreover, $\kappa_{\text{out},i}(y_i, \mu_i) = \{0\}$

(c) $\kappa_{\text{out},i}(y_i, \mu_i) \neq \{0\} \Rightarrow \ell_{\text{in},i}\mu_i < \max\{|y_i|, \Delta_{0,i}\}$. Moreover, $\kappa_{\text{in},i}(y_i, \mu_i) = \{0\}$.

Moreover, for each $\mu_i^+ \in \Omega_{\text{in},i}^{\kappa_{\text{in},i}(y_i,\mu_i)}\mu_i$ with $y_i \in \mathbb{R}^{n_{y_i}}$ and $\mu_i \in \mathbb{R}_{\geqslant 0}$, it holds that

(d) $\frac{\Omega_{\text{in},i}}{\ell_{\text{in},i}} \max\{|y_i|, \Delta_{0,i}\} \leqslant \mu_i^+ \leqslant \frac{\max\{|y_i|, \Delta_{0,i}\}}{\ell_{\text{in},i}}$,

and, for each $\mu_i^+ \in \Omega_{\text{out},i}^{\kappa_{\text{out},i}(y_i,\mu_i)}\mu_i$ with $y_i \in \mathbb{R}^{n_{y_i}}$ and $\mu_i \in \mathbb{R}_{\geqslant 0}$, it holds that

(e) $\frac{|y_i|}{\ell_{\text{out},i}} \leqslant \mu_i^+ \leqslant \frac{\Omega_{\text{out},i}}{\ell_{\text{out},i}}|y_i|$.

Property (a) follows from the fact that $\lceil -\varsigma \rceil = \{0\}$ for any $\varsigma \in (0, 1)$. Properties (b) and (c) are due to the fact that according to (4.32) and (4.30), $0 < \ell_{\text{in},i} < \ell_{\text{out},i} < M_i$. At last, properties (d) and (e) follow directly from the definitions of $\kappa_{\text{in},i}(y_i, \mu_i)$ and $\kappa_{\text{out},i}(y_i, \mu_i)$, respectively. Let us remark that property (c) implies that $\kappa_{\text{in},i}(y_i, \mu_i) = 0$ when $\ell_{\text{in},i}\mu_i < \Delta_{0,i}$. As we will show, this property is important to ensure that the values of $\kappa_{\text{in},i}(y_i, \mu_i)$ and $\kappa_{\text{out},i}(y_i, \mu_i)$ remain finite at all time, especially when y_i crosses zero at any transmission instant t_k^i. Similar conditions have been used in [143, 145, 232]. Moreover, observe that properties (b) and (c) imply that when the quantizer is updated, either a zoom-in or zoom-out event occurs or neither of them.

4.5.4 Stability result

We obtain the following result.

Theorem 4.1. *Consider system (4.20) with the flow and the jump sets as in (4.18) with $\Psi_i, \eta_{0,i}$ specified in (4.25) and T_i defined in (4.27). Suppose that Assumptions 4.1, 4.2 are satisfied and that the dynamic quantizer is designed as in (4.29)-(4.30). Let $\mathbb{X}_0 := \{\xi \in \mathbb{X} : \eta_i > 0, p_i = 0\}$. Then*

(i) the set $\mathcal{A} := \{\xi \in \mathbb{X} : R(\xi) \leqslant c\}$ is input-to-state stable w.r.t. w, where where

$$R(\xi) := x^T P x + \sum_{i=1}^{l} \left(\gamma_i \tilde{\phi}_i(\tau_i) |e_i|^2 + \eta_i \right), \tag{4.33}$$

$$\tilde{\phi}_i(\tau_i) := \begin{cases} \phi_i(\tau) & \text{when } \tau \leqslant T_i \\ \phi_i(T_i) & \text{when } \tau > T_i, \end{cases} \tag{4.34}$$

and $c := \frac{\sum_{i=1}^{l} \varepsilon_{y_i} \Delta_{0,i}^2}{\epsilon \min\{\varepsilon_x / \lambda_{\max}(P), 2 \min_i \nu_i, \min_i \vartheta_i\}}$ with $P, \gamma_i, \varepsilon_x, \varepsilon_{y_i}$ as in Assumption 4.2, $\Delta_{0,i}$ as in (4.12) and where $\epsilon \in (0,1)$ can be chosen arbitrarily.

Moreover, for each maximal solution pair (ξ, w) with $\xi(0,0) \in \mathbb{X}_0$ and $w \in \mathcal{L}_\infty$, it holds that, when $p_i(t,j) = 1$,

(ii) $|y_i(t,j)| \leqslant M_i \mu_i(t,j)$;

(iii) $|e_{s,i}(t,j)| > |e_{q,i}(t,j)|$;

(iv) $\kappa_{\text{in},i}(y_i(t,j), \mu_i(t,j)) \subseteq \{0, 1, \ldots, \kappa^*_{\text{in},i}\}$ and $\kappa_{\text{out},i}(y_i(t,j), \mu_i(t,j)) \subseteq \{0, 1, \ldots, \kappa^*_{\text{out},i}\}$, where

$$\kappa^*_{\text{in},i} := \max\left(\left\lceil \frac{\log\left(\Delta_{0,i} / (\ell_{\text{in},i} \bar{\mu}_i)\right)}{\log \Omega_{\text{in},i}} \right\rceil \right), \tag{4.35}$$

$$\kappa^*_{\text{out},i} := \max\left(\left\lceil \frac{\log\left(\bar{y}_i / (\ell_{\text{out},i} \underline{\mu}_i)\right)}{\log \Omega_{\text{out},i}} \right\rceil \right) \tag{4.36}$$

with

$$\bar{\mu}_i := \max\{\Omega_{\text{out},i}^{\kappa^*_{\text{out},i}} \frac{\bar{y}_i}{\ell_{\text{out},i}}, \mu_i(0,0)\}, \tag{4.37}$$

$$\underline{\mu}_i := \frac{\Omega_{\text{in},i} \Delta_{0,i}}{\ell_{\text{in},i}}, \tag{4.38}$$

and

$$\bar{y}_i := \sqrt{\frac{\lambda_{\max}(C_{p,i}^\top C_{p,i})}{\lambda_{\min}(P)}} \left(\sqrt{R(\xi(0,0))} + \sqrt{\frac{\varepsilon_w}{\rho}} \|w\|_\infty \right). \tag{4.39}$$

□

Observe that properties (i)-(iv) above correspond to properties (i)-(iv) introduced in Section 4.1, respectively. Let us first remark that the guaranteed ISS property implies that, in the absence of disturbances, the state trajectory converges to a neighbourhood of the origin whose size depends on $\sum_{i=1}^{l} \Delta_{0,i}$. This is due to the fact that μ_i does not eventually go to zero since no zooming-in occurs when $\mu_i < \frac{\Delta_{0,i}}{\ell_{\text{in},i}}$ according to (4.12) in combination with (4.31), which is also the case in, e.g., [143, 145]. Property (ii) implies that at each transmission event, the output measurement y_i is within the range of the associated quantizer. As a consequence, the quantization error is always smaller than or equal to the quantization error bound at each transmission event. Property (iii) implies that at each transmission event, *i.e.*, when $\xi \in \mathcal{D}_i$ and $p_i = 1$, $i \in \{1, 2, \ldots, l\}$, the magnitude of sampling-induced error is larger than the error due to quantization which implies that the transmitted information is more accurate than the information already available at the corresponding receiving node. As such, property (iii) helps in avoiding redundant usage of the network. Finally, property (iv) shows that at transmissions, the elements of the sets $\kappa_{\text{in},i}(y_i, \mu_i)$ and $\kappa_{\text{out},i}(y_i, \mu_i)$, $i \in \{1, 2, \ldots, l\}$, are bounded by $\kappa^*_{\text{in},i}$ and $\kappa^*_{\text{out},i}$, respectively. The latter property is important to make sure that the amount of data sent over the network per transmission is bounded. Let us remark that the quantities $\bar{\mu}_i$ and $\bar{y}_i$, $i \in \{1, 2, \ldots, l\}$, represent upper-bounds on $\|\mu_i\|_\infty$ and $\|y_i\|_\infty$, respectively.

Let us highlight that the maximum number of bits that is required to capture the encoded quantized output measurement of the i-th node in a single data package is given by

$$N_{bits,i} = \min \left(\left\lceil \frac{\log(\text{card}(Q_i) + \max\{\kappa^*_{\text{in},i}, \kappa^*_{\text{out},i}\} + 1)}{\log 2} \right\rceil \right), \tag{4.40}$$

for $i \in \{1, 2, \ldots, l\}$, where $\text{card}(Q_i)$ is equal to the number of quantization regions as before. As such, the requirements for the communication channel in terms of bits per data package, can be determined a priori.

4.5.5 Design procedure of the ETM and quantizer

In this subsection, we discuss the design of the ETM and the quantizer. Note that, in view of (4.27), (4.29), that the design parameters $\tilde{\gamma}_i, \varepsilon_{y_i}, \lambda_i, \tilde{\lambda}_i$ $i \in \{1, 2, \ldots, l\}$, create a strong coupling between the design of the event-triggering mechanism and the design of the dynamic quantizer.

The first step of the design procedure is to find suitable γ_i, $i \in \{1, 2, \ldots, l\}$, by minimizing the weighted sum $\sum_{i=1}^{l} \pi_i \gamma_i$ subject to (4.23) with $\pi_i \in (0, 1)$, $i \in \{1, 2, \ldots, l\}$, such that $\sum_{i=1}^{l} \pi_i = 1$. The selection of π_i allows to balance the communication resource utilization among the different nodes. The parameters $\Omega_{\text{in},i}$ and $\Omega_{\text{out},i}$, $i \in \{1, 2, \ldots, l\}$, allow to balance the required number of quantization regions that is needed to satisfy (4.30) and the maximum number of zoom-in and zoom-out events per transmission as given in (4.35) and (4.36), respectively. The next step is to select κ_i as small as possible to minimize the lower-bound on M_i/Δ_i as given in (4.30). The latter is desired as M_i/Δ_i typically reflects the number of quantization regions. After $\Omega_{\text{in},i}$, $\Omega_{\text{out},i}$ and κ_i, $i \in \{1, 2, \ldots, l\}$, are obtained, we take M_i, Δ_i such that (4.30) holds. Finally, the tuning of λ_i can be used to obtain an intuitive trade-off between the number of transmissions and the amount of data that needs to be transmitted per transmission. When λ_i is reduced, the value of T_i in (4.27) will increase and, depending on the choice of $\tilde{\lambda}_i$, the value of $\tilde{\gamma}$ will decrease, which may result in a reduction in the amount of transmissions. However, by reducing λ_i, the right-hand side of (4.29) will also increase. Hence, the value of $\frac{M_i}{\Delta_i}$ needs to be increased which typically implies that more quantization regions are required, in order to ensure that (4.29) holds. We will illustrate this also with an example in the next section.

4.6 Illustrative example

We consider the following LTI plant model

$$\begin{aligned} \dot{x}_p &= \begin{bmatrix} 0 & 1 \\ -2 & -1 \end{bmatrix} x_p + \begin{bmatrix} 0 \\ -1 \end{bmatrix} u + \begin{bmatrix} 0 \\ 1 \end{bmatrix} w \\ y &= \begin{bmatrix} 1 & 0 \\ 1 & 1 \end{bmatrix} x_p. \end{aligned} \tag{4.41}$$

The plant is controlled by the dynamic controller

$$\begin{aligned} \dot{x}_c &= \begin{bmatrix} 0 & -2 \\ 0 & -3 \end{bmatrix} x_c + \begin{bmatrix} 0 & 0 \\ 1 & 0 \end{bmatrix} \hat{y}_q \\ u &= \begin{bmatrix} -1 & -2 \end{bmatrix} x_c. \end{aligned} \tag{4.42}$$

We assume that the two outputs of the plant are transmitted asynchronously and independently over two different networks. By solving the LMI (4.23), we obtain $\varepsilon_{y_1} = 2.1780$, $\varepsilon_{y_2} = 1.0049$, $L_1 = L_2 = 0$, $\gamma_1 = 9.4274$, $\gamma_2 = 6.1258$. We take $\lambda_1 = \lambda_2 = 0.5$, $\tilde{\lambda}_1 = 0.6, \tilde{\lambda}_2 = 0.5$, $\nu_1 = \nu_2 = 0.01$ and we compute the values of T_1, T_2 by using (4.27), which yields $T_1 = 0.0601$ and $T_2 = 0.1049$. Furthermore,

we obtain $\tilde{\gamma}_1 = 120.9841$ and $\tilde{\gamma}_2 = 51.1083$. Finally, we set $\vartheta_1 = \vartheta_2 = 0.01$ and, hence, all the required parameters for the event-triggering functions in (4.25) are defined. Next, we set the range of the quantizers to be $M_1 = 150, M_2 = 100$ and we take $\Delta_1 = \Delta_2 = 1.5$, $\Delta_{01} = \Delta_{02} = 1 \times 10^{-6}$, $\Omega_{\text{in},1} = \Omega_{\text{in},2} = 0.5, \Omega_{\text{out},1} = \Omega_{\text{out},2} = 2$ and $\kappa_1 = \kappa_2 = 10$, which verify conditions (4.29), (4.30) and lead to $\ell_{\text{in},1} = 67.5$, $\ell_{\text{in},2} = 42.5$, $\ell_{\text{out},1} = 148.5$ and $\ell_{\text{out},2} = 98.5$. We run simulations for 50 seconds with the initial conditions $x(0,0) = (40, -50, 30, -20)$, $e(0,0) = (0,0)$, $\eta(0,0) = (0,0)$, $\phi(0,0) = (\lambda_1^{-1}, \lambda_2^{-1})$, $\mu(0,0) = (1,1)$ and with the external disturbance w satisfying $w(t,j) = 2\sin(2\pi t)$ for all $(t,j) \in \operatorname{dom} w$ with $t \in [0,10]$, $w(t,j) = 0$ for all $(t,j) \in \operatorname{dom} w$ with $t \in (10,30]$ and $w(t,j) = 0.2$ for all $(t,j) \in \operatorname{dom} w$ with $t \in (30,50]$. The observed minimum and average inter-transmission times, respectively denoted by $\tau_{\min}$ and τ_{avg}, are summarized in Table 4.1. We note that $\tau_{\min,1} > T_1$ while $\tau_{\min,2} \approx T_2$, which supports the

	T_i	$\tau_{\min,i}$	$\tau_{\text{avg},i}$
y_1	0.0601	0.0644	0.2173
y_2	0.1049	0.1051	0.2563

Table 4.1. Minimum and average inter-transmission times.

observation of Remark 4.2 on the choice of $\tilde{\lambda}_i$ since $\tilde{\lambda}_1 > \lambda_1$ and $\tilde{\lambda}_2 = \lambda_2$. The state trajectories of the plant and the dynamic controller are shown in Figure 4.2, where we note that the state converges to a small neighborhood of the origin as expected. The output trajectories y_1, y_2 are shown in Figure 4.3 and Figure

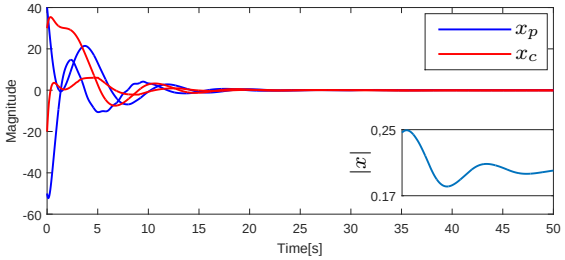

Fig. 4.2. State trajectory for the plant and the controller.

4.4, where we note that the trajectories y_1, y_2 exhibit oscillations, which makes it necessary to incorporate the zoom-out event to avoid the quantizers saturation.

The zoom-in/zoom-out events by the respective dynamic quantizers are shown in Figure 4.5 and Figure 4.6 during the first 3 seconds. We note that at any transmission instant $t_k^i, k \in \mathbb{N}$, only a zoom-in event or a zoom-out event occurs but not both of them due to the design conditions in Section 4.5.3 that imply properties (b) and (c) below (4.38).

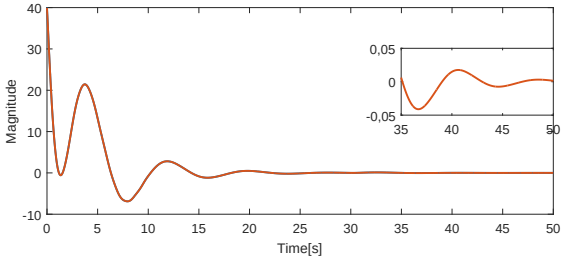

Fig. 4.3. Plant output y_1.

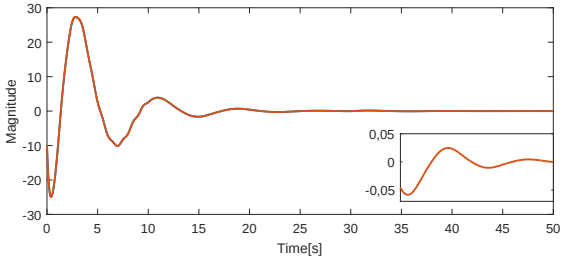

Fig. 4.4. Plant output y_2.

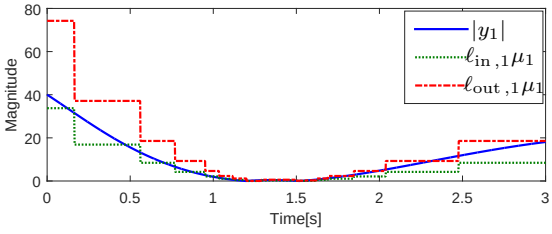

Fig. 4.5. Zoom actions for y_1 for the first 3 seconds.

Figure 4.7 and Figure 4.8 present the generated transmission instants and the zoom instants during the first 3 seconds for nodes 1 and 2, respectively. We observe that the zoom actions are only executed at transmission instants as described in Section 4.3.3 and that at some transmission instants, no zoom action occurs. The latter is the case when none of the zoom conditions is met at those instants. The trade-off between transmissions and number of quantization regions is illustrated in Figure 4.9 and 4.10 for node 1 and 2, respectively. These figures are generated by varying λ_i in (4.27), (4.29) from 0.01 to 0.99 and by taking $\tilde{\lambda}_i = \lambda_i$. Observe that larger values of $\frac{M_i}{\Delta_i}, i \in \{1, 2\}$ which for this case implies more quantization regions, lead to larger values of the guaranteed mini-

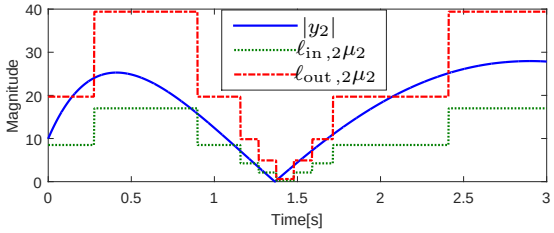

Fig. 4.6. Zoom actions for y_2 for the first 3 seconds.

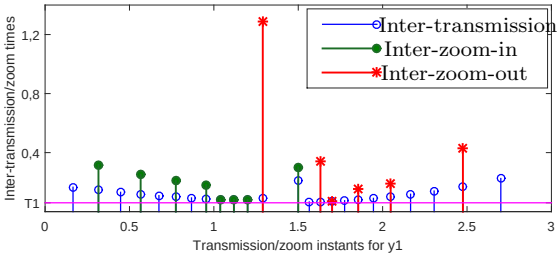

Fig. 4.7. Transmission/zoom instants for y_1 for the first 3 seconds.

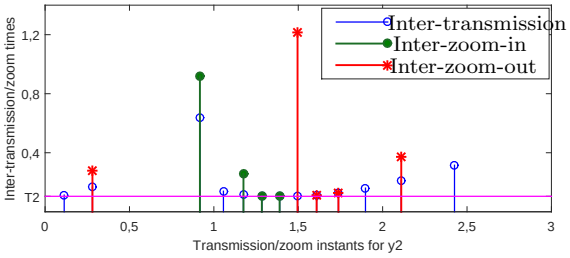

Fig. 4.8. Transmission/zoom instants for y_2 for the first 3 seconds.

mum time T_i between two consecutive transmissions/zooms at the corresponding node and vice versa, as discussed in Section 4.5.5.

4.7 Conclusions

In this chapter, we addressed the problem of input-to-state stabilization of linear systems over digital communication networks. We considered three important features of the communication network. First of all, our problem involved quantization of the measured variables. In networked control systems, quantization

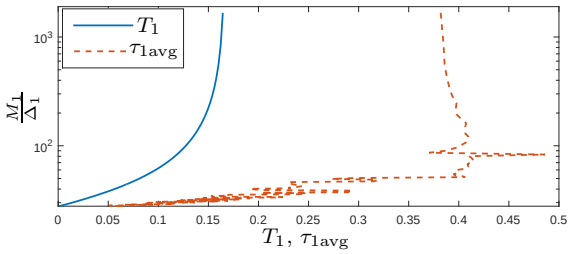

Fig. 4.9. Tradeoff curves between number of quantization regions and transmissions for y_1.

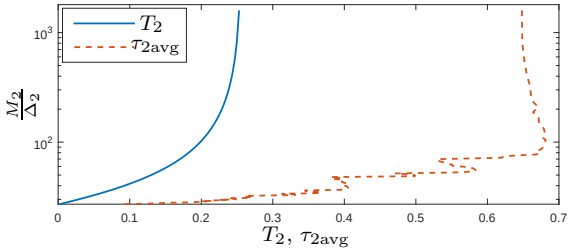

Fig. 4.10. Tradeoff curves between number of quantization regions and transmissions for y_2.

mechanisms are inevitable as the packets to be transmitted have a finite size in terms of bits. Secondly, we employed a resource-aware control paradigm (in particular, event-triggered control) to utilize the bandwidth-limited communication channels only when needed. Thirdly, we studied the scenario where multiple sensor nodes transmit their information asynchronously. We provided a complete design solution for this setup for a linear plant in the presence of disturbances and only based on output measurements, which is known to be a difficult problem. Our main design framework solves the co-design problem of synthesizing both the dynamic quantizers and the event-triggering mechanisms that are provided for each individual sensor node. Interestingly, the intuitive trade-off between the number of quantization levels (and thus the size of the information/data packet that has to be transmitted) and the number of transmissions naturally appears in our main theoretical results and the design methods. In fact, the design of quantizers and event generators is directly coupled and reflecting this essential trade-off. The proposed event-triggering mechanism enforces the existence of a strictly positive lower bound on the inter-transmission times of each channel, which prevents the occurrence of Zeno behavior. Moreover, the dynamic quantization strategy prevents the accumulation of zoom actions since the zoom actions only take place at transmission instants. The zoom parameter of

the dynamic quantizer is shown to be always bounded. The chattering between the zoom-in stage and the zoom-out stage is avoided and the redundant access of the network is prevented.

The framework laid down in this chapter can be extended in different directions, such as the inclusion of delays based on the work in [120], combined with co-design of the controllers [8]. Also, it might be the case in some practical scenarios that the event-triggering mechanism only has access to the quantized output measurement but not the current (true) value of the plant output as we have considered in this study. This would call for a new analysis corresponding to the case where in Figure 4.1 the sensor and the encoder are reversed in the control loop. Also the extension of the approach to nonlinear systems is a challenging and a relevant problem for the future.

Chapter 5

Event-triggered Control Systems under Packet Losses

Abstract – Networked control systems (NCSs) offer many benefits in terms of increased flexibility and maintainability but might also suffer from inevitable imperfections such as packet dropouts and limited communications resources. In this chapter, (static and dynamic) event-triggered control (ETC) strategies are proposed that aim at reducing the utilization of communication resources while guaranteeing desired stability and performance criteria and a strictly positive lower bound on the inter-event times despite the presence of packet losses. For the packet losses, we consider both configurations with an acknowledgment scheme (as, *e.g.*, in the transmission control protocol (TCP)) and without an acknowledgment scheme (as, *e.g.*, in the user datagram protocol (UDP)). The proposed design methodology will be illustrated by means of a numerical example which reveals trade-offs between the maximum allowable number of successive packet dropouts, (minimum and average) inter-event times and $\mathcal{L}_p$-gains of the closed-loop NCS.

5.1 Introduction

Networked control systems (NCSs) differ from traditional control setups as they rely on shared communication media instead of dedicated point-to-point connections to transmit the sensor and actuation data. This offers many benefits as NCSs are typically easier to install and maintain. Moreover, in case the communication is wireless, the physical limitations of wired links are not present. Nonetheless, before all the benefits of NCSs can be fully exploited, many issues regarding the inherent imperfections of (packet-based) networked communica-

This chapter is based on [73, 74].

tion, such as, limited communication resources and packet dropouts, need to be resolved.

To deal with the fact that, in the context of NCSs, communication resources are often limited and possibly shared with other users, new control strategies need to be developed that do not only guarantee desired stability and closed-loop performance properties but also aim to reduce the utilization of the communication channel. In addition, these control strategies should also guarantee the desired closed-loop behavior in case packet dropouts are present. Traditional (digital) control setups, in which data packages are typically sent in a *time-triggered* fashion according to a fixed sampling rate often lead to inefficient use of communication resources as the scheduling of transmission instants is purely based on time and not on the actual status of the plant. Hence, it seems more natural to use resource-aware control methodologies that determine the transmission instants on the basis of state or output information to allow a better balance between communication efficiency and control performance. Examples of resource-aware control methods include *event-triggered* control and *self-triggered* control, see [114] for a recent overview.

In event-triggered control (ETC) strategies, transmission times are determined by means of a triggering rule that depends on, *e.g.*, state or output measurements of the system. This enables ETC strategies to reduce the number of transmissions while maintaining desired stability and performance criteria. Although many ETC strategies were proposed before, the majority of them do not consider the occurrence of packet losses despite the facts that these packet losses are often present in practical NCSs and that they deteriorate the performance and might even lead to instability of the closed-loop system. Obviously, due to the latter, the performance and stability results of existing ETC strategies in which the occurrence of packet losses are not taken into account are not valid in the presence of packet losses. In addition, in the context of ETC systems, the presence of packet losses might annul the existence of a *positive minimum inter-event time* (MIET). The latter property is essential for enabling practical implementation of the ETC strategy. Because of the above mentioned reasons, it is of interest to study ETC strategies that do take into account the presence of packet losses. Examples of such ETC strategies include [37, 156, 164, 165] in which stochastic optimal control approaches are used to minimize a cost function consisting of a quadratic control cost and a communication cost. A key assumption there is that acknowledgment signals are available, *e.g.* as in transmission control protocols (TCP), such that it is known whether a transmitted package has been received or not. In [103, 104, 138, 259], a different approach is presented which combines time-triggered and event-triggered solutions in the sense that in case a packet loss is detected, the ETC scheme is interrupted and transmissions are scheduled according to time-based specifications until the controller successfully receives the plant measurements. Clearly, this approach requires an acknowledgment scheme as well. In [251] it was shown that the design of

a triggering rule of the form as in [224] can be adapted such that a maximum allowable number of successive packet drops (MANSD) can be tolerated. This setup does not require any acknowledgment scheme and is thereby compatible with, *e.g.*, the user datagram protocol (UDP). However, as shown in [41], this approach does not guarantee a strictly positive lower bound on the inter-event times in case disturbances are present. In [184] a periodic event-triggered control (PETC) scheme is considered in the sense that the triggering condition is only evaluated at equidistant instances in time. As such, a lower-bound on the inter-event times is enforced despite the presence of disturbances. In a similar spirit as in [251], it was shown that the design of such a PETC rule can be adapted to tolerate a MANSD without the need for an acknowledgment scheme.

A significant drawback of the aforementioned approaches is that they rely on the availability of full state information which may not be the case in practice. Since, especially in the presence of disturbances, it is far from trivial to modify existing *state-based* ETC schemes to *output-based* ETC schemes as shown in [7, 41, 78], it is of interest to study *output-based* ETC schemes subject to packet losses. To the best of our knowledge, the output-based case in the context of packet dropouts has not been addressed in literature so far. Therefore, we propose a new design framework for *output-based* event-triggering strategies for NCSs that are subject to packet losses and disturbances. Motivated by UDP and TCP protocols, we consider both the case with acknowledgments and the case without acknowledgments. Interestingly, the design framework proposed in this chapter can lead to both *dynamic* event-triggering mechanisms (ETMs), see also [71, 72, 96, 191], and the more commonly studied *static* ETMs.

The remainder of this chapter is organized as follows. First, we present the necessary preliminaries and notational conventions in Section 5.2, followed by the introduction of the event-triggered NCS setup considered in this chapter and the problem statement in Section 5.3. In Section 5.4, we describe the event-triggered NCS by means of the hybrid modeling framework as presented in [98] leading to a more mathematically rigorous problem formulation. In Section 5.5 and Section 5.6 we present design conditions for the proposed *static* and *dynamic* event-triggering strategies for the case with and without acknowledgments, respectively. Finally, we demonstrate how the presented theory leads to trade-offs between the maximum allowable number of successive packet dropouts (MANSD), (minimum and average) inter-event times and $\mathcal{L}_p$-gains by means of a numerical example in Section 5.7. We provide concluding remarks in Section 5.8.

5.2 Definitions and preliminaries

$\mathbb{N}$ denotes the set of all non-negative integers, $\mathbb{N}_{>0}$ the set of positive integers, $\mathbb{R}$ the field of real numbers and $\mathbb{R}_{\geqslant 0}$ the set of all non-negative reals. For N vectors $x_i \in \mathbb{R}^{n_i}$, $i \in \bar{N}$, we denote the vector obtained by stacking all vectors

in one (column) vector $\bar{x} \in \mathbb{R}^n$ with $n = \sum_{i=1}^{N} n_i$ by $(x_1, x_2, \ldots, x_N)$, *i.e.*, $(x_1, x_2, \ldots, x_N) = \begin{bmatrix} x_1^\top & x_2^\top & \cdots & x_N^\top \end{bmatrix}^\top$. By $|\cdot|$ and $\langle \cdot, \cdot \rangle$ we denote the Euclidean norm and the usual inner product of real vectors, respectively. I denotes the identity matrix of appropriate dimensions. A function $\alpha : \mathbb{R}_{\geqslant 0} \to \mathbb{R}_{\geqslant 0}$ is said to be of class $\mathcal{K}$ if it is continuous, strictly increasing and $\alpha(0) = 0$. It is said to be of class $\mathcal{K}_\infty$ if it is of class $\mathcal{K}$, and in addition, it is unbounded. A function $\beta : \mathbb{R}_{\geqslant 0} \times \mathbb{R}_{\geqslant 0} \to \mathbb{R}_{\geqslant 0}$ is said to be a $\mathcal{KL}$ function if it is continuous, $\beta(\cdot, t)$ is of class $\mathcal{K}$ for each $t \geqslant 0$ and $\beta(s, \cdot)$ is nonincreasing and satisfies $\lim_{t \to \infty} \beta(s, t) = 0$. A function $f : \mathbb{R}^n \to \mathbb{R}^n$ is said to be locally Lipschitz continuous if for each $x_0 \in \mathbb{R}^n$ there exist constants $\delta > 0$ and $L > 0$ such that $|x - x_0| \leqslant \delta \Rightarrow |f(x) - f(x_0)| \leqslant L|x - x_0|$. A set-valued mapping from a set X to a set Y, associates, with every point $x \in X$, a subset of Y. The notation $F : X \rightrightarrows Y$, indicates that F is a set-valued mapping from X to Y with $F(x) \subset Y$ for all $x \in X$.

In this chapter, we model NCSs as hybrid systems $\mathcal{H}$ of the form

$$\dot{\xi} = F(\xi, w), \text{ when } \xi \in C, \tag{5.1a}$$

$$\xi^+ \in G(\xi), \quad \text{when } \xi \in D. \tag{5.1b}$$

where F describes the flow dynamics, G the jump dynamics, C the flow set and D the jump set. We denote the hybrid system as in (5.1) with $\mathcal{H} = (C, D, F, G)$ or by $\mathcal{H}$ in short. We now recall some definitions given in [98] on the solutions of such hybrid system.

A *compact hybrid time domain* is a set $\mathcal{D} = \bigcup_{j=0}^{J-1} [t_j, t_{j+1}] \times \{j\} \subset \mathbb{R}_{\geqslant 0} \times \mathbb{N}$ with $J \in \mathbb{N}_{>0}$ and $0 = t_0 \leq t_1 \ldots \leq t_J$. A *hybrid time domain* is a set $\mathcal{D} \subset \mathbb{R}_{\geqslant 0} \times \mathbb{N}$ such that $\mathcal{D} \cap ([0, T] \times \{0, \ldots, J\})$ is a compact hybrid time domain for each $(T, J) \in \mathcal{D}$. A *hybrid signal* is a function defined on a hybrid time domain. In this chapter, the hybrid signal $w : \operatorname{dom} w \to \mathbb{R}_w^n$ is referred to as a *hybrid input*. A hybrid signal $\xi : \operatorname{dom} \xi \to \mathbb{R}^n$ is called a *hybrid arc* if $\xi(\cdot, j)$ is locally absolutely continuous for each j.

For the hybrid system $\mathcal{H}$ given by the state space $\mathbb{R}^n$, the input space $\mathbb{R}^{n_w}$ and the data (F, G, C, D), where flow map $F : \mathbb{R}^n \times \mathbb{R}^{n_w} \to \mathbb{R}^n$ is continuous, the jump map $G : \mathbb{R}^n \rightrightarrows \mathbb{R}^n$ is a set-valued map, and the flow set C and jump set D are subsets of $\mathbb{R}^n$, a hybric arc $\xi : \operatorname{dom} \xi \to \mathbb{R}^n$ and a hybrid input $w : \operatorname{dom} w \to \mathbb{R}^{n_w}$ is a *solution pair* (ξ, w) to $\mathcal{H}$ if

1) $\operatorname{dom} \xi = \operatorname{dom} w$,

2) For all $j \in \mathbb{N}$ and for almost all t such that $(t, j) \in \operatorname{dom} \xi$, we have $\xi(t, j) \in C$ and $\dot{\xi}(t, j) = F(\xi(t, j), w(t, j))$.

3) For all $(t, j) \in \operatorname{dom} \xi$ such that $(t, j + 1) \in \operatorname{dom} \xi$, we have $\xi(t, j) \in D$ and $\xi(t, j + 1) \in G(\xi(t, j))$.

Let us remark that the hybrid systems considered in this chapter have time regularization (or dwell time) and external inputs only appearing in the flow map. The latter allow us to employ the following signal norm definitions inspired

by [21]. For $p \in [1, \infty)$, we introduce the $\mathcal{L}_p$-norm of a function ξ defined on a hybrid time domain $\operatorname{dom} \xi = \bigcup_{j=0}^{J-1} [t_j, t_{j+1}] \times \{j\}$ with J possibly ∞ and/or $t_J = \infty$ by

$$\|\xi\|_p = \Big(\sum_{j=0}^{J-1} \int_{t_j}^{t_{j+1}} |\xi(t,j)|^p dt \Big)^{1/p} \tag{5.2}$$

provided the right-hand side is well-defined and finite. In case $\|\xi\|_p$ is finite, we say that $\xi \in \mathcal{L}_p$.

5.3 NCS model and problem statement

In this section, we present the event-triggered NCS setup considered in this chapter and discuss how this NCS is affected by packet losses. Based on these descriptions, we provide an initial problem formulation, which will be formalized later in Section 5.4.

5.3.1 Networked control configuration

In this chapter, we consider the output-based feedback control configuration as illustrated in Fig. 5.1. The dynamics of plant $\mathcal{P}$ is given by

$$\mathcal{P} : \begin{cases} \dot{x}_p = f_p(x_p, u, w) \\ y = g_p(x_p), \end{cases} \tag{5.3}$$

where $x_p \in \mathbb{R}^{n_{x_p}}$ represents the state vector of the plant, $w \in \mathbb{R}^{n_w}$ is a disturbance input, $u \in \mathbb{R}^{n_u}$ is the control input, and $y \in \mathbb{R}^{n_y}$ the measurable output. The function $f_p : \mathbb{R}^{n_{x_p}} \times \mathbb{R}^{n_u} \times \mathbb{R}^{n_w} \to \mathbb{R}^{n_{x_p}}$ is assumed to be locally Lipschitz continuous and the function $g_p : \mathbb{R}^{n_{x_p}} \to \mathbb{R}^{n_y}$ is assumed to be continuously differentiable. The controller $\mathcal{C}$ is given by

$$\mathcal{C} : \begin{cases} \dot{x}_c = f_c(x_c, \hat{y}) \\ u = g_c(x_c, \hat{y}), \end{cases} \tag{5.4}$$

where $x_c \in \mathbb{R}^{n_{x_c}}$ denotes the state of the controller and where $\hat{y} \in \mathbb{R}^{n_y}$ represents the most recently received output measurement by the controller $\mathcal{C}$. The function $f_c : \mathbb{R}^{n_{x_c}} \times \mathbb{R}^{n_y} \to \mathbb{R}^{n_{x_c}}$ is assumed to be locally Lipschitz continuous and the function $g_c : \mathbb{R}^{n_{x_c}} \times \mathbb{R}^{n_y} \to \mathbb{R}^{n_u}$ is assumed to be continuously differentiable. Notice that we ignore the effect of discretization and quantization due to the implementation on a digital platform. The performance output is given by

$$z = q(x), \tag{5.5}$$

where $z \in \mathbb{R}^{n_z}$, $x = (x_p, x_c) \in \mathbb{R}^{n_x}$ with $n_x := n_{x_p} + n_{x_c}$ and where $q : \mathbb{R}^{n_x} \to \mathbb{R}^{n_z}$ a continuous function.

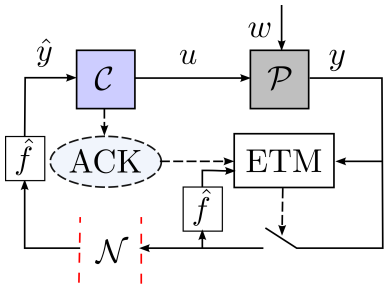

Fig. 5.1. Schematic representation of the event-triggered control configuration of an NCS discussed in this chapter.

In general, the communication in NCSs is packet-based in the sense that only discrete packages containing finite amounts of data can be sent across the network at countable instants in time. In particular, transmissions are attempted at times t_l, $l \in \mathbb{N}$, that satisfy $0 \leqslant t_0 < t_1 < t_2 < \ldots$. Since packet losses might occur, the most recent sensor measurement information $\hat{y}$ available at the controller is only updated according to $\hat{y}^+ = y$, in terms of the framework of [98], if the transmission has been received successfully at time t_l. Otherwise, the packet is considered to be lost with the consequence that the sensor information available at the controller cannot be updated, and we will have $\hat{y}^+ = \hat{y}$.

To be able to guarantee the desired behaviour of the closed-loop system in presence of these packet losses, we adopt the following assumption, which has been used in several works before, see, *e.g.*, [103, 104, 120, 138, 184, 251].

Assumption 5.1. *The number of successive packet dropouts $\delta \in \mathbb{N}$ that might occur since the last successful transmission is upper bounded by δ_{max}, where $\delta_{max} \in \mathbb{N}$ represents the* maximum allowable number of successive dropouts *(MANSD).*

In between updates, $\hat{y}$ evolves according to

$$\dot{\hat{y}} = \hat{f}(\hat{y}), \tag{5.6}$$

where $\hat{f}$ is a locally Lipschitz function. Notice that a zero-order hold device (ZOH), in which $\hat{y}$ is kept constant between transmissions, can simply be modeled by taking $\hat{f} = 0$ in (5.6). Furthermore, the framework presented in this chapter also allows extensions in the direction of, *e.g.*, model-based holding devices that, for the output-based case, require additional dynamics, see [93, 259] for more details. For ease of exposition, we do not consider these type of holding devices in the remainder of this chapter.

Remark 5.1. For the sake of simplicity, we assume that the controller is connected to actuators of the plant via a dedicated point-to-point link, *i.e.*, the

control signal u is continuously available at plant $\mathcal{P}$ and only the output y is transmitted over a network in a packet-base manner. However, in a similar fashion as in [6, 72], the framework presented in this chapter allows for extensions towards other control configurations as well such as configurations in which (parts of) the output y and/or the control input u are asynchronously transmitted over a network. Moreover, for brevity of exposition, we do not consider the presence of transmission delays. Although, in case a ZOH device is employed, we foresee that, by building upon the work in [72, 110, 120], the current work can *mutatis mutandis* be extended to ETM design for NCSs in which variable communication delays are present.

5.3.2 Event-based communication

As mentioned in the introduction, in *time-triggered* NCSs, the scheduling of transmission instants is purely based on time. As a consequence, desired stability and performance criteria of these *time-triggered* schemes can only be guaranteed if all transmission intervals satisfy $\epsilon \leqslant t_{l+1} - t_l \leqslant \tau_{mati}$, $l \in \mathbb{N}$, independent of the status of the system. Here $\epsilon \in (0, \tau_{mati}]$ is an arbitrarily small positive constant to guarantee Zeno-freeness and where τ_{mati} represents the so-called *maximum allowable transmission interval* (MATI) as used in [51, 120, 173, 245]. Hence, this time-based specification is typically chosen on the basis of the worst-case situation of the system. Since in the context of NCSs, the communication resources are often scarce, we consider *event-triggered* control (ETC) schemes in this chapter in which transmission instants are determined on the basis of state or output measurements. In this way, the transmission intervals are no longer restricted to the worst-case value, which may result in significantly larger average inter-event times while (the same) stability and performance properties can be guaranteed.

The fact that in ETC schemes, transmission instant are determined on the basis of output measurements instead of time as in time-triggered control schemes also lead to new challenges. To be more specific, one of the main difficulties for constructing an event-triggering mechanism (ETM), for the output-case and in presence of disturbances in particular, is to exclude Zeno-behavior, *i.e.*, to avoid an infinite number of transmissions in finite time and still provide stability and performance guarantees. As such, it is important to guarantee the existence of a strictly positive lower bound on the inter-event times, often referred to as the *minimal inter-event time* (MIET), despite the presence of disturbances. This MIET is crucial in order to implement the ETC scheme in practice. The event-triggering conditions determining the transmission attempts as considered in this chapter (for the case with acknowledgments) have the form

$$t_{l+1} := \inf \{ t > t_l + \tau_{miet} \mid \Psi(o(t), 0) < 0 \}, \tag{5.7}$$

and

$$t_{l+1} := \inf \{t > t_l + \tau_{miet} \mid \eta(t) < 0\}, \tag{5.8}$$

for $l \in \mathbb{N}_{>\delta_{max}+1}$ where $\eta \in \mathbb{R}_{\geqslant 0}$ is the triggering variable which evolves according to

$$\begin{cases} \dot{\eta}(t) & = \Psi(o(t), \eta(t)), \text{ when } \eta(t) \geqslant 0, \\ \eta(t^+) & = \eta_0(o(t)), \text{ when } \eta(t) = 0 \text{ and transmission successful,} \\ \eta(t^+) & = \eta(t), \text{ when } \eta(t) = 0 \text{ and transmission failed,} \end{cases} \tag{5.9}$$

where $o \in \mathbb{O}$ denotes all the information which is locally available at the ETM such as the sensor measurements $y \in \mathbb{R}^{n_y}$. The first $\delta_{max} + 1$ transmission instants are given by

$$t_{l+1} := t_l + \tau_{miet}, \tag{5.10}$$

for $l \in 1, 2, \ldots, \delta_{max}$, where $t_0 = 0$. These (time-triggered) transmission instants are used to make sure that at least one sensor measurement has successfully been received at the controller side before the ETMs are active (independent whether an acknowledgments scheme is present or not). Observe that when employing ETC, also for the case in which there are no packet losses, *i.e.*, when $\delta_{max} = 0$, it is in general required to have at least one transmission instant before the ETM is active to make sure that the transmission error $e := y - \hat{y}$, which is often used by the ETM, is available at the sensor side. See also [4, 78] in which this issue is also discussed for ETC systems without packet losses. Let us remark that also for the case without acknowledgments, in which the transmission error e is not known at the sensor side, it is also required that the first δ_{max} transmission are scheduled in a time-triggered fashion as we will discuss later in more detail.

In (5.7) and (5.9), the functions $\Psi : \mathbb{O} \times \mathbb{R}_{\geqslant 0} \to \mathbb{R}$ and $\eta_0 : \mathbb{O} \to \mathbb{R}$ are to be designed to guarantee proper behavior of the closed-loop system. Observe that the ETMs given in (5.7) and (5.8) use time-regularization in the sense that the next transmission instant always occurs after at least τ_{miet} time units, despite the presence of disturbances. Hence, a robust positive MIET exists by design in case $\tau_{miet} > 0$. To the best our knowledge, only periodic event-triggered control schemes,*e.g.*, see [112], or event-triggered control schemes equipped with this time-regularization are able to both guarantee Zeno-freeness and finite $\mathcal{L}_p$-gains for output-based systems subject to disturbances. See also [41, 71, 72] for a more detailed discussion on adopting time-regularization. Be aware that the variable τ_{miet} in the ETMs described by (5.7) and (5.8) can not be chosen arbitrarily but must be designed such that the closed-loop system yields the desired stability and performance properties.

Observe that in contrast to the ETM in (5.7), the triggering mechanism presented in (5.8) employs the triggering variable η, which is a dynamic variable evolving according to the dynamical system given in (5.9). For this reason, the ETM in (5.7) is referred to as a *static* ETM and the in ETM in (5.8) as a *dynamic* ETM. The main motivation for using *dynamic* ETMs is that, in contrast to the

commonly studied *static* ETMs, the generated inter-event times do not converge to the enforced lower bound in presence of disturbances when the output is close to zero, as observed in [41, 71], and typically lead to larger inter-event times. See also [71, 72, 96, 191] for more details on *dynamic* ETMs. On the other hand, from a practical point of view, *static* ETMs might be easier to implement.

5.3.3 Problem formulation

Time-triggered control schemes can relatively easy deal with packet losses in the sense that packet losses can simply be regarded as prolongation of the transmission interval. To be more concrete, the desired stability and performance guarantees can be guaranteed by taking the MATI as

$$\tau'_{mati} := \frac{\tau_{mati}}{\delta_{max} + 1}, \tag{5.11}$$

where τ_{mati} corresponds to the MATI bound derived for the case in which packet losses do not occur. This bound can be computed using tools as in, *e.g.*, [51].

For ETC schemes, it is not possible to subdivide the transmission intervals in case of packet losses (as in (5.11) for time-triggered control) since the next transmission instant depends on the (future) evolution of the system, which is in general not exactly known. Given this technical difficulty and the fact that packet losses do typically occur, considering ETC schemes that are robust with respect to packet losses is an important problem to be tackled. For this reason, the problem consider in this chapter is formulated as follows.

Problem 5.1. *Propose design conditions for τ_{miet}, Ψ and η_0 such that the ETMs given by (5.7), (5.8) and (5.9) result in closed-loop stability and finite $\mathcal{L}_p$-gain ($p \in [1, \infty)$) guarantees for the plant/controller combination given by (5.3) and (5.4) despite the occurrence of packet losses.*

The problem is formulated more formally in the next section. In the remainder of the chapter, we discuss two scenarios. First, we discuss the situation in which the communication protocol employs an acknowledgment scheme as in the transmission control protocol (TCP), in the sense that the transmitting device "knows" whether a transmission instant was successful or not. After that, we consider the case in which the communication protocol does not employ an acknowledgment scheme as in the user datagram protocol (UDP) which forms an additional challange. In this case, the transmitting device can not distinguish between a successful and a failed transmission. In the remainder of this chapter, we refer to these two scenarios in short as the *case with acknowledgments* and the *case without acknowledgments*, respectively.

5.4 Hybrid model of the ETC scheme with acknowledgements

To facilitate the ($\mathcal{L}_p-$)stability analysis, we cast the event-triggered NCS setup subject to packet losses discussed in the previous section in the hybrid system framework as developed in [98] inspired by [51,71,120,173,191]. For the moment, we only consider the case with acknowledgments.

To capture packet dropouts, we introduce the auxiliary variables $\delta \in \Delta$, where $\Delta := \{0, 1, \ldots, \delta_{max}\}$. The integer variable $\delta \in \mathbb{N}$ is used to keep track of the number of successive packet losses since the most recent successful transmission attempt. Moreover, we introduce an internal clock variable $\tau \in \mathbb{R}$, which captures the time elapsed since the most recent transmission attempt and the integer variable $\kappa \in \mathbb{N}$, which represents the total number of transmission attempts. Let $e \in \mathbb{R}^{n_y}$ denote the network-induced error $e := \hat{y} - y$. By using this variable and the auxiliary variables τ, κ and δ, we can now write the closed-loop system described by (5.3)-(5.9) in terms of flow and jump equations as in (5.1) resulting in the hybrid system $\mathcal{H}$ in which the flow map is given by

$$F(\xi, w) = \big(f(x, e, w), g(x, e, w), 0, 1, 0, \Psi(o, \eta)\big), \tag{5.12}$$

where $\xi := (x, e, \delta, \tau, \kappa, \eta) \in \mathbb{X} := \mathbb{R}^{n_x} \times \mathbb{R}^{n_y} \times \Delta \times \mathbb{R}_{\geqslant 0} \times \mathbb{N} \times \mathbb{R}_{\geqslant 0}$ and where $o = (y, e, \tau, \delta) \in \mathbb{O} := \mathbb{R}^{n_y} \times \mathbb{R}^{n_y} \times \mathbb{R}_{\geqslant 0} \times \Delta$. By combining $e = \hat{y} - y$ with (5.3), (5.4) and (5.6), we find that for $x \in \mathbb{R}^{n_x}$, $e \in \mathbb{R}^{n_y}$ and $w \in \mathbb{R}^{n_w}$

$$f(x, e, w) = \begin{bmatrix} f_p(x_p, g_c(x_c, g_p(x_p) + e), w) \\ f_c(x_c, g_p(x_p) + e) \end{bmatrix}, \tag{5.13}$$

$$g(x, e, w) = \hat{f}(g_p(x_p) + e) - \frac{\partial g_p}{\partial x_p}(x_p) f_p(x_p, g_c(x_c, g_p(x_p) + e), w). \tag{5.14}$$

The functions Ψ and η_0 are part of the ETM design and will be specified in Section 5.5.

The jump map G is given by

$$G(\xi, w) := \begin{cases} \{G_0(\xi, w), G_1(\xi, w)\} & \text{when } \delta < \delta_{max} \\ \{G_0(\xi, w)\} & \text{when } \delta \geqslant \delta_{max} \end{cases} \tag{5.15}$$

for $\xi \in \mathbb{X}$ and $w \in \mathbb{R}^{n_w}$ with

$$G_0(\xi, w) := \big(x, 0, 0, 0, \kappa + 1, \eta_0(o)\big), \tag{5.16a}$$

$$G_1(\xi, w) := \big(x, e, \delta + 1, 0, \kappa + 1, \eta\big). \tag{5.16b}$$

Note that the function G_0 describes the jump of ξ when a successful transmission attempt occurs and that G_1 describes the jump of ξ when a transmission attempt fails due to a packet loss. Furthermore, observe that the definition of jump map

G is in correspondence with Standing Assumption 5.1 in the sense that after δ_{max} successive packet-losses have occurred (when $\delta = \delta_{max}$), it is enforced that a successful transmission occurs, *i.e.*, that the system jumps according to G_0.

On the basis of (5.7) and (5.10), we find that the flow set C_s and the jump set D_s corresponding to the *static* event-triggering condition are given by

$$C_s := \Big\{ \xi \in \mathbb{X} \mid \tau \leqslant \tau_{miet} \text{ or } (\Psi(o,0) \geqslant 0 \text{ and } \kappa > \delta_{max}) \Big\} \tag{5.17a}$$

$$D_s := \Big\{ \xi \in \mathbb{X} \mid \tau \geqslant \tau_{miet} \text{ and } (\Psi(o,0) \leqslant 0 \text{ or } \kappa \leqslant \delta_{max}) \Big\}. \tag{5.17b}$$

Observe that for the case of a static triggering condition, the variable η is redundant. The flow set C_d and jump set D_d corresponding to the *dynamic* triggering condition as given in (5.8) and (5.10), are given by

$$C_d := \Big\{ \xi \in \mathbb{X} \mid \tau \leqslant \tau_{miet} \text{ or } \kappa > \delta_{max} \Big\} \tag{5.18a}$$

$$D_d := \Big\{ \xi \in \mathbb{X} \mid \tau \geqslant \tau_{miet} \text{ and } (\eta = 0 \text{ or } \kappa \leqslant \delta_{max}) \Big\}. \tag{5.18b}$$

Note that the triggering condition related to $\eta < 0$ in (5.8) is embedded via the definition of $\mathbb{X}$ ($\xi \in \mathbb{X}$ implies $\eta \geqslant 0$). The resulting hybrid systems corresponding to the *static* triggering condition and the *dynamic* triggering condition can now be defined as

$$\mathcal{H}_s := (C_s, D_s, F, G) \tag{5.19}$$

$$\mathcal{H}_d := (C_d, D_d, F, G), \tag{5.20}$$

respectively, with F, G, C_s, D_s, C_d and D_d as in (5.12)-(5.18). Observe that the choices for C_s, D_s, C_d and D_d lead to more solutions than induced by the triggering conditions given by (5.7), (5.8) and (5.9), respectively, due to the non-strictness of the inequalities in (5.17) and (5.18). Moreover, it is important to note that for the hybrid models described above, o in (5.7) and (5.9) is given by $o = (y, e, \tau, \delta)$ and that indeed this information is available at the ETM in case an acknowledgment scheme is employed. However, for the case without acknowledgments e and δ are *not* known, providing even more challenging design issues.

To establish definitions for stability and performance properties, we first introduce the following definition [98].

Definition 5.1. *A hybrid system $\mathcal{H}$ is said to be* persistently flowing *with respect to initial state set $\mathbb{X}_0$ if all maximal solution pairs*[1] *(ξ, w) with $\xi(0,0) \in \mathbb{X}_0$ and $w \in \mathcal{L}_p$ have unbounded domains in the t-direction, i.e.,* $\sup\{t \in \mathbb{R}_{\geqslant 0} : \exists j \in \mathbb{N} \text{ such that } (t,j) \in \text{dom } \xi\} = \infty$.

[1] A solution pair (ξ, w) is said to be maximal if there does not exist another solution pair (ξ', w') such that (ξ, w) is a truncation of (ξ', w') to some proper subset of dom ξ'. See, *e.g.*, [199] for more details.

To formalize the problem informally stated in the previous section (Problem 1), consider the following definitions.

Definition 5.2. *A hybrid system $\mathcal{H}$ with initial state set $\mathbb{X}_0$ is said to be* uniformly globally asymptotically stable *(UGAS) if the system is persistently flowing for $w = 0$ with respect to initial state set $\mathbb{X}_0$ and if there exists a function $\beta \in \mathcal{KL}$ such that for any initial condition $\xi(0,0) \in \mathbb{X}_0$ all corresponding solutions ξ of $\mathcal{H}$ with $w = 0$ satisfy*

$$|\,(x(t,j), e(t,j), \eta(t,j))\,| \leqslant \beta\,(|\,(x(0,0), e(0,0), \eta(0,0))\,|, t)\,, \tag{5.21}$$

for all $(t,j) \in dom\,\xi$.

In case disturbances are present, *i.e.*, $w \neq 0$, we consider the performance output $z = q(x)$ as in (5.5).

Definition 5.3. *A hybrid system $\mathcal{H}$ with initial state set $\mathbb{X}_0$ is said to be $\mathcal{L}_p$-stable with an $\mathcal{L}_p$-gain less than or equal to θ from input w to output z, if the system is persistently flowing for $w \neq 0$ and there exists a $\mathcal{K}_\infty$-function β such that for any exogenous input $w \in \mathcal{L}_p$, and any initial condition $\xi(0,0) \in \mathbb{X}_0$, each corresponding solution to $\mathcal{H}$ satisfies*

$$\|z\|_p \leq \beta(|(x(0,0), e(0,0)|) + \theta\|w\|_p. \tag{5.22}$$

The problem statement corresponding to the TCP case can now be formulated as follows.

Problem 5.2. *Given the event-triggered NCSs described by hybrid systems $\mathcal{H}_s$ and $\mathcal{H}_d$, a desired $\mathcal{L}_p$-gain $\theta \in \mathbb{R}_{\geqslant 0}$ and a maximum number of successive packet dropouts δ_{max}, determine conditions for the positive scalar τ_{miet} and for the functions Ψ and η_0 as in (5.9), such that the systems $\mathcal{H}_s$ and $\mathcal{H}_d$ are UGAS in case $w = 0$ and, in the presence of disturbances, $\mathcal{L}_p$-stable with an $\mathcal{L}_p$-gain less than or equal to θ.*

5.5 ETM design with acknowledgments of packet losses

In the first part of this section, we present well-known conditions as used in [51, 120, 173] for the $\mathcal{L}_p$-stability analysis of NCSs. To be more concrete, these conditions are used to construct a positive semi-definite *storage function* S, for a hybrid system $\mathcal{H}$ that satisfies, loosely speaking, $\dot{S} \leq \theta^p|w|^p - |z|^p$ during flow and $S^+ \leqslant S$ during jumps, where $p \in [1, \infty)$ and where w and z represent the external disturbance and performance output, respectively. The existence of such a storage function is a sufficient condition for system $\mathcal{H}$ to be $\mathcal{L}_p$-stable with $\mathcal{L}_p$-gain less than or equal to θ (provided that the solutions are well-defined).

In the second part of this section, we exploit these conditions to construct ETMs as given in (5.8) and (5.9) that lead to $\mathcal{L}_p$-stability of system $\mathcal{H}_s$ and $\mathcal{H}_d$ (and thus including packet drops).

5.5.1 Preliminaries

Consider the following condition inspired by the work in [51, 120, 173, 174].

Condition 5.1. *There exist a locally Lipschitz function $W : \mathbb{R}^{n_y} \to \mathbb{R}_{\geqslant 0}$, a continuous function $H : \mathbb{R}^{n_x} \times \mathbb{R}^{n_w} \to \mathbb{R}_{\geqslant 0}$ and constants $\underline{\alpha}_W$, $\bar{\alpha}_W \in \mathbb{R}_{>0}$ and $L \in \mathbb{R}_{\geqslant 0}$, such that*

- *for all $e \in \mathbb{R}^{n_y}$, $W(e)$ satisfies*

$$\underline{\alpha}_W |e| \leqslant W(e) \leqslant \bar{\alpha}_W |e|, \tag{5.23}$$

- *for all $x \in \mathbb{R}^{n_x}$, $w \in \mathbb{R}^{n_w}$ and almost all $e \in \mathbb{R}^{n_y}$ it holds that*

$$\left\langle \frac{\partial W(e)}{\partial e}, g(x, e, w) \right\rangle \leqslant LW(e) + H(x, w). \tag{5.24}$$

In addition, there exist a locally Lipschitz function $V : \mathbb{R}^{n_x} \to \mathbb{R}_{\geqslant 0}$, $\mathcal{K}_\infty$-functions $\underline{\alpha}_V$ and $\bar{\alpha}_V$, positive definite continuous functions $\rho, \sigma : \mathbb{R} \to \mathbb{R}_{\geqslant 0}$ and $\varrho : \mathbb{R}^{n_x} \to \mathbb{R}_{\geqslant 0}$, and a constant $\gamma > 0$, such that

- *for all $x \in \mathbb{R}^{n_x}$*

$$\underline{\alpha}_V(|x|) \leqslant V(x) \leqslant \bar{\alpha}_V(|x|). \tag{5.25}$$

- *for almost all $x \in \mathbb{R}^{n_x}$, $w \in \mathbb{R}^{n_w}$ and all $e \in \mathbb{R}^{n_y}$*

$$\begin{aligned} \langle \nabla V(x), f(x, e, w) \rangle \leqslant & -\rho(|x|) - \varrho(y) - H^2(x, w) \\ & - \sigma(W(e)) + \gamma^2 W^2(e) + \mu(\theta^p |w|^p - |q(x, w)|^p) \end{aligned} \tag{5.26}$$

  for some $\mu > 0$ and $\theta \geqslant 0$.

For linear systems, it is possible to construct functions V and W that satisfy Condition 5.1 via a linear matrix inequality (LMI) optimization problem, see [71, 120] for more details. The conditions presented above also apply to several classes of nonlinear systems as also illustrated by a nonlinear example in Section 5.7.

Besides the conditions above, we adopt the following condition for τ_{miet}.

Condition 5.2. *The time-constant $\tau_{miet} \in \mathbb{R}_{>0}$ satisfies*

$$(\delta_{max} + 1)\tau_{miet} < \mathcal{T}(\gamma, L) \tag{5.27}$$

where $\mathcal{T} : \mathbb{R}_{\geqslant 0} \times \mathbb{R}_{\geqslant 0} \to \mathbb{R}_{\geqslant 0}$ *is given by*

$$\mathcal{T}(\gamma, L) := \begin{cases} \frac{1}{Lr} arctan\,(r)\,, & \gamma > L \\ \frac{1}{L}, & \gamma = L \\ \frac{1}{Lr} arctanh\,(r)\,, & \gamma < L \end{cases} \tag{5.28}$$

with $r = \sqrt{|(\gamma/L)^2 - 1|}$.

Let us remark that $\mathcal{T}(\gamma, L)$ is related to the *maximum allowable transmission interval* (MATI) for time-based control schemes as presented in [51, 174]. Moreover, consider the function $\phi : \mathbb{R}_{\geqslant 0} \to \mathbb{R}$ that satisfies

$$\dot{\phi} = -2L\phi - \gamma(\phi^2 + 1), \tag{5.29}$$

where $\phi(0) = \lambda^{-1}$ with $\lambda \in (0, 1)$ such that $\phi(s) \in [\lambda^{-1}, \lambda]$ and $\dot{\phi}(s) < 0$ for all $s \in [0, \tau_{miet}(\delta_{max} + 1)]$. As can be shown based on [51, 174], under Condition 5.2, the latter properties always hold if $\lambda \in (0, 1)$ is taken sufficiently small.

5.5.2 Main result

In this section, we present the definitions of the functions Ψ and η_0 such that the ETM as given in (5.8) leads to the desired stability and performance criteria for the case with acknowledgments.

Theorem 5.1. *Consider the systems* $\mathcal{H}_s$ *and* $\mathcal{H}_d$*, as in (5.19) and (5.20), respectively, with initial state set* $\mathbb{X}_0 := \{\xi \in \mathbb{X} \mid \kappa = 0\}$ *that satisfy Condition 5.1, a desired* $\mathcal{L}_p$*-gain* $\theta \in \mathbb{R}_{\geqslant 0}$ *and a MANSD* $\delta_{max} \in \mathbb{N}$*. Suppose that the function* $\Psi : \mathbb{O} \times \mathbb{R}_{\geqslant 0} \to \mathbb{R}$ *is given by*

$$\Psi(o, \eta) := \begin{cases} \varrho(y) - \chi(\eta), & \text{for } \tau \leqslant \tau_{miet}, \\ \varrho(y) - \bar{\gamma}(\delta) W^2(e) - \chi(\eta), & \text{for } \tau > \tau_{miet}, \end{cases} \tag{5.30}$$

where $\bar{\gamma}(\delta) := \gamma(2\phi((\delta+1)\tau_{miet})L + \gamma(1 + \phi^2((\delta+1)\tau_{miet}))$ *with* τ_{miet} *satisfying Condition 5.2 and the function* ϕ *as in (5.29) and where* χ *is a locally Lipschitz* $\mathcal{K}_\infty$*-function. Moreover, suppose that the function* $\eta_0 : \mathbb{O} \to \mathbb{R}_{\geqslant 0}$ *is given by*

$$\eta_0(o) := \gamma\phi((\delta + 1)\tau_{miet}) W^2(e). \tag{5.31}$$

Then, $\mathcal{H}_s$ *and* $\mathcal{H}_d$ *with initial state set* $\mathbb{X}_0$ *are UGAS and, in presence of disturbances,* $\mathcal{L}_p$*-stable with an* $\mathcal{L}_p$*-gain less than or equal to* θ *and with a lower-bound on the MIET equal to* τ_{miet}*.*

Let us remark that the dynamics of the variable η given by (5.8), (5.9), (5.30) and (5.31) is chosen such that if Condition 5.1 holds, $U(\xi) = V(x) + \gamma\tilde{\phi}(\delta, \tau) W^2(e) + \eta$ with $\tilde{\phi}(\delta, \tau) := \phi(\delta\tau_{miet} + \min(\tau, \tau_{miet}))$, constitutes a valid Lyapunov/storage function establishing the desired stability and performance properties. The complete proof is provided in the appendix.

Remark 5.2. The *static* and *dynamic* ETMs given by (5.7), (5.8) and (5.9) are related to the *static* and *dynamic* ETMs presented in [72], in which the presence of packet dropouts is not considered. However, observe that due to this presence of packet losses, besides having a different τ_{miet}, it is required that the ETMs given by (5.7), (5.8) and (5.9) explicitly depend on the number of successive packet dropouts, which was not the case in [72] and require new technical derivations as shown in the proof of Theorem 1.

Remark 5.3. Observe that the ETMs as given by (5.7), (5.8), (5.9), (5.30) and (5.31) require that transmitted acknowledgments are being received instantaneously. However, let us remark that these ETMs can easily be adjusted such that this requirement can be relaxed. For example, by letting the ETMs keep track of the evolution of η for both the case that the most recent transmission has been successful or denied. In this case, the acknowledgment is allowed to be delayed with at most τ_{miet} time units since it is known that within this time frame, no other transmission is scheduled. For brevity of exposition, this feature has, however, not been included formally.

Remark 5.4. The choice of the positive semi-definite continuous function $\varrho : \mathbb{R}^{n_y} \to \mathbb{R}_{\geqslant 0}$ in (5.26) and the time-constant $\tau_{miet} \in (0, \mathcal{T}(\gamma, L))$ with $\mathcal{T}$ in (5.28) is part of the ETM design. This choice typically relies on a trade-off between the minimum inter-event time τ_{miet} and the expected average inter-event time due to the following facts. Observe from (5.30) that ϱ affects the size of Ψ and thus the inter-event times. In addition, we can see from (5.26) that ϱ also affects γ and thus $\mathcal{T}(\gamma, L)$ which restricts the choice for τ_{miet}. Furthermore, for the *dynamic* ETM, we can see from (5.31) that τ_{miet} determines the size of η_0 (and thus of η) at jump times.

5.6 ETM design conditions without acknowledgments of packet losses

If the communication protocol does not employ an acknowledgment scheme, the ETM has no knowledge about whether a transmission attempt was successful or not. As a consequence, the number of successive packet losses δ and therefore also the transmission error e, which depends on the most recent sensor measurement information $\hat{y}$ available at the controller, are not available at the ETM in case acknowledgments are absent. It is obvious that the ETMs presented in the previous section are not suitable for the case without acknowledgments since these ETM, among others, rely on the availability of the transmission error e. However, given that the number of successive packet losses is upper-bounded by δ_{max}, it is known that the most recent successful transmission instant has occurred at most δ_{max} transmission attempts ago. To be more concrete, for all $t \in (t_l, t_{l+1})$, $l \in \mathbb{N}$, the time instant at which the most recent *successful* transmission occurred is

contained in the set $\{t_{\max\{0,l-\delta_{max}\}}, t_{\max\{0,l-\delta_{max}+1\}} \ldots, t_l\} \subset \mathbb{R}_{\geqslant 0}$. In the remainder of this section, we exploit this fact to modify the ETM design for the case with acknowledgments presented above, to obtain an ETM suitable for the case without acknowledgments.

5.6.1 A modified ETM setup

To construct an ETM suitable for the case without acknowledgments, *i.e*, an ETM that does not rely on availability of the number of successive packet losses δ or the transmission error e, we proposed to track of all possible values that the variable $\hat{y}$ can possibly attain. For this reason, we augment the state $\xi \in \mathbb{X}$ with the variables

$$\bar{\hat{y}} = (\hat{y}_1, \hat{y}_2, \ldots, \hat{y}_{\delta_{max}+1}) \in \mathbb{R}^{(\delta_{max}+1)n_y}, \tag{5.32}$$

where the i-th element of this sequence corresponds to the hypothesis that $i-1$ successive dropouts have occurred since the most recent successful transmission attempt. To comply with the latter, the dynamics of the variables $\hat{y}_i$, $i \in \tilde{\Delta} := \{1, 2, \ldots, \delta_{max}+1\}$ need to be defined and initialized such that when $\delta \in \Delta$ successive packet losses have occurred since the most recent successful transmission attempt, it holds that $\hat{y}_\delta = \hat{y}$. Observe from (5.6) and (5.12) that the flow dynamics of $\hat{y}$ does not explicitly depend on δ. As such, the flow dynamics of $\hat{y}_i$ for all $i \in \tilde{\Delta}$ is similar to the flow dynamics of $\hat{y}$ and given by

$$\dot{\hat{y}}_i = \hat{f}(\hat{y}_i). \tag{5.33}$$

As mentioned before, when a transmission instant is successful, $\hat{y}$ is updated according to $\hat{y}^+ = y$. Hence, the jump equation of the variable $\hat{y}_1$, that corresponds to the hypothesis that the most recent transmission attempt has been successful, is given by

$$\hat{y}_1^+ = y \tag{5.34}$$

Moreover, the jump map in (5.15) shows that when a transmission instant is unsuccessful, the state variables e and y (and thus $\hat{y}$) do not jump. From this fact, we can deduce that the jump equations for the variables $\hat{y}_i$, $i \in \{2, 3, \ldots, \delta_{max}+1\}$ are given by

$$\hat{y}_i^+ = \hat{y}_{i-1}, \tag{5.35}$$

for all $i \in \{2, 3, \ldots, \delta_{max}+1\}$.

As already mentioned, the state variables δ and e are unknown as no acknowledgment scheme is employed. For this reason, we propose to use a more robust triggering condition than the ETM given in (5.7) and (5.8) in the sense that it triggers on the basis of the worst-case situation. As such, we propose to use the definitions (where in line with (5.7) and (5.8), we use t instead of the hybrid time (t, j))

$$t_{l+1} := \inf \Big\{ t > t_l + \tau_{miet} \mid \min_{k \in \tilde{\Delta}} \Psi(o_k(t), 0) < 0 \Big\}, \tag{5.36}$$

and

$$t_{l+1} := \inf\{t > t_l + \tau_{miet} \mid \Phi_\eta(\bar{\eta}(t)) < 0\}, \tag{5.37}$$

for $l \in \mathbb{N}_{>\delta_{max}+1}$, where $o_k := (y, \hat{y}_k - y, \tau, k-1)$, $k \in \tilde{\Delta}$, $\bar{\eta} = (\eta_1, \eta_2, \ldots, \eta_{\delta_{max}+1}) \in \mathbb{R}_{\geqslant 0}^{\delta_{max}+1}$ and where the function $\Phi_\eta : \mathbb{R}_{\geqslant 0}^{\delta_{max}+1} \to \mathbb{R}_{\geqslant 0}$ is given by

$$\Phi_\eta(\bar{\eta}) := \min_{k \in \tilde{\Delta}} \eta_k. \tag{5.38}$$

As before in the case with acknowledgments, the first $\delta_{max} + 1$ transmission instants are generated in a time-based fashion according to (5.10). The triggering variables $(\eta_1, \eta_2, \ldots, \eta_{\delta_{max}+1})$ behave as follows. During flows, the variable η_i evolves according to

$$\dot{\eta}_i = \Psi(o_i, \eta_i), \tag{5.39}$$

for all $i \in \tilde{\Delta}$, and, at jumps, according to

$$\eta_i^+ = \eta_{i-1} \tag{5.40a}$$

$$\eta_1^+ = \min_{k \in \tilde{\Delta}} \gamma\phi(k\tau_{miet})W^2(\hat{y}_k - y). \tag{5.40b}$$

for all $i \in \{2, 3, \ldots, \delta_{max} + 1\}$. The resulting augmented state is now given by $\tilde{\xi} := (x, e, \delta, \tau, \kappa, \eta, \tilde{\hat{y}}, \bar{\eta}) \in \tilde{\mathbb{X}} := \mathbb{X} \times \mathbb{R}^{(\delta_{max}+1)n_y} \times \mathbb{R}_{\geqslant 0}^{\delta_{max}+1}$.

It is important to note that the ETMs given by (5.36) and (5.37) do not require the availability of η, δ or e at the sensor side. Instead, they need to keep track of $2\delta_{max} + 2$ auxiliary variables whose updates only depend on the locally available output measurement y and the most recently transmitted value of y, regardlessly whether the corresponding transmission attempt was successful or not. Hence, the ETMs given in (5.36) and (5.37) are indeed suitable for the case without acknowledgments.

By means of (5.32)-(5.40), we can now specify the augmented systems $\tilde{\mathcal{H}}_s$ and $\tilde{\mathcal{H}}_d$ corresponding to NCSs with a *static* and *dynamic* ETM, respectively, as

$$\tilde{\mathcal{H}}_s := (\tilde{C}_s, \tilde{D}_s, \tilde{F}, \tilde{G}) \tag{5.41}$$

$$\tilde{\mathcal{H}}_d := (\tilde{C}_d, \tilde{D}_d, \tilde{F}, \tilde{G}) \tag{5.42}$$

where

$$\tilde{C}_s := \left\{ \tilde{\xi} \in \tilde{\mathbb{X}} \mid \tau \leqslant \tau_{miet} \text{ or } \left(\min_{k \in \tilde{\Delta}} \Psi(o_k, 0) \geqslant 0 \text{ and } \kappa > \delta_{max} \right) \right\} \tag{5.43a}$$

$$\tilde{D}_s := \left\{ \tilde{\xi} \in \tilde{\mathbb{X}} \mid \tau \geqslant \tau_{miet} \text{ and } \left(\min_{k \in \tilde{\Delta}} \Psi(o_k, 0) \leqslant 0 \text{ or } \kappa \leqslant \delta_{max} \right) \right\}, \tag{5.43b}$$

and where

$$\tilde{C}_d := \left\{ \tilde{\xi} \in \tilde{\mathbb{X}} \mid \tau \leqslant \tau_{miet} \text{ or } \kappa > \delta_{max} \right\} \tag{5.44a}$$

$$\tilde{D}_d := \left\{ \tilde{\xi} \in \tilde{\mathbb{X}} \mid \tau \geqslant \tau_{miet} \text{ and } (\Phi_\eta(\bar{\eta}) = 0 \text{ or } \kappa \leqslant \delta_{max}) \right\}. \tag{5.44b}$$

Note that the triggering condition related to $\Phi_\eta(\bar{\eta}) < 0$ in (5.37) is embedded via the definition of $\tilde{\mathbb{X}}$ ($\tilde{\xi} \in \tilde{\mathbb{X}}$ implies $\eta_i \geqslant 0$ for all $i \in \tilde{\Delta}$). The flow map $\tilde{F}$ and the jump map $\tilde{G}$ can be obtained straightforwardly from (5.12), (5.15), (5.33)-(5.34) and (5.39)-(5.40). Observe from (5.43) and (5.44) that, similar as for the ETMs presented in (5.7) and (5.8), we consider that the first $\delta_{max} + 1$ transmission instants are generated in a time-triggered fashion according to (5.10) which makes sure that at least one transmission has been successful before the ETM is active. This is needed for establishing the aforementioned desired relationships between $\bar{\hat{y}}$ (which is only available at the sensor side) and the actual values of $\hat{y}$ ($g_p(x_p) + e$) (which is only available at the controller side), namely,

$$\hat{y}(t, j) = \hat{y}_{\delta(t,j)+1}(t, j), \tag{5.45}$$

for all $(t, j) \in \operatorname{dom} \tilde{\xi}$ for which $j \geqslant \delta_{max} + 1$.

5.6.2 Main result

Theorem 5.2. *Consider the systems $\tilde{\mathcal{H}}_s$ and $\tilde{\mathcal{H}}_d$ with initial state set $\tilde{\mathbb{X}}_0 := \{\xi \in \tilde{\mathbb{X}} \mid \kappa = 0\}$ as given in (5.41) and (5.41), respectively, that satisfy Condition 5.1, a desired $\mathcal{L}_p$-gain $\theta \in \mathbb{R}_{\geqslant 0}$ and a MANSD $\delta_{max} \in \mathbb{N}$. Suppose that the function $\Psi : \mathbb{O} \times \mathbb{R}_{\geqslant 0} \to \mathbb{R}$ is given by (5.30) with τ_{miet} satisfying Condition 5.2, then the ETM given by (5.37) guarantees that the systems $\tilde{\mathcal{H}}_s$ and $\tilde{\mathcal{H}}_d$ with initial state set $\tilde{\mathbb{X}}_0$ are UGAS and, in presence of disturbances, $\mathcal{L}_p$-stable with an $\mathcal{L}_p$-gain less than or equal to θ and with a lower-bound on the MIET equal to τ_{miet}.*

The proof is provided in the appendix.

Remark 5.5. Observe that, under the same circumstances, the inter-event times generated by the ETM given in (5.8) (corresponding to the case with acknowledgments) are larger than or equal to the inter-event times generated by the ETM given in (5.37) (corresponding to the case without acknowledgments) due to the fact that $\Phi_\eta(\bar{\eta}(t, j)) \leqslant \eta(t, j)$ for all $(t, j) \in \operatorname{dom} \tilde{\xi}$ (see the proof of Theorem 2 in the Appendix). This is natural given that much more information is available in the case with acknowledgments when compared to the case without acknowledgments.

5.7 Numerical example

In this section, we present a numerical example that illustrates how to apply the developed framework to systematically design an ETM for a nonlinear system

both for the case with and without acknowledgments. Furthermore, we show that this procedure leads to trade-offs between performance (in terms of an induced $\mathcal{L}_2$-gain), robustness (in terms of MANSD) and the utilization of communication resources (in terms of the MIET and average inter-event times).

5.7.1 Model description

Consider the nonlinear system

$$\mathcal{P}: \begin{cases} \dot{x}_1 = -2x_1 + x_2 + x_1^2 - x_1^3 \\ \dot{x}_2 = x_1 + x_2^2 - x_2^3 + u + w \\ y = z = x_2, \end{cases} \tag{5.46}$$

where $x_1, x_2 \in \mathbb{R}$, $u \in \mathbb{R}$. The example is inspired by the numerical example considered in [72]. We consider the control law $u = -2\hat{y}$ and suppose it is implemented in a ZOH fashion, *i.e.*, $\dot{\hat{y}} = 0$. Recalling that $\hat{y} = e + x_2$, we obtain that f and g as in (5.12) are given by

$$f(x, e, w) = \begin{bmatrix} -2x_1 + x_2 + x_1^2 - x_1^3 \\ x_1 - 2x_2 + x_2^2 - x_2^3 - 2e + w \end{bmatrix}, \tag{5.47a}$$

$$g(x, e, w) = -x_1 + 2x_2 - x_2^2 + x_2^3 + 2e - w. \tag{5.47b}$$

5.7.2 Storage function analysis and ETM design

To construct the ETMs given by (5.8) and (5.37) for the case with and without acknowledgments, respectively, we first need to find functions H and W and constants L, γ, k, and θ that satisfy Condition 5.1 for the system described in (5.47). Consider the function $W(e) = |e|$. Then the inequality given by (5.24) is satisfied with $L = 2$ and $H(x_1, x_2, w) = |-x_1 + 2x_2 - x_2^2 + x_2^3 - w|$.

To find γ and θ, consider the candidate storage function

$$V(x) = \varsigma^2 \sum_{i=1}^{2} \left[\left(\alpha \frac{x_i^2}{2} + \beta \frac{x_i^4}{4} \right) \right], \tag{5.48}$$

where $\alpha, \beta, \varsigma \in \mathbb{R}_{>0}$. Recalling (5.47a), we have that

$$\begin{aligned} \langle \nabla V(x), f(x, e, w) \rangle \leqslant \varsigma^2 \Big(& 2\alpha x_1 x_2 + \beta x_1^3 x_2 + \beta x_2^3 x_1 \\ & + \sum_{i=1}^{2} \left[-2\alpha x_i^2 + \alpha x_i^3 - (\alpha + 2\beta) x_i^4 + \beta x_i^5 - \beta x_i^6 \right] \\ & - 2\alpha x_2 e - 2\beta x_2^3 e + \alpha x_2 w + \beta x_2^3 w \Big). \end{aligned} \tag{5.49}$$

By using the facts that for all $x_2, e, w \in \mathbb{R}$, $-2\alpha x_2 e \leqslant x_2^2 + \alpha^2 e^2$, $\alpha x_2 w \leqslant \frac{1}{2}x_2^2 + \frac{1}{2}\alpha^2 w^2$ and $-2\beta x_2^3 e \leqslant x_2^6 + \beta^2 e^2$, we obtain

$$\begin{aligned}\langle \nabla V(x), f(x,e,w)\rangle \leqslant \varsigma^2\Big(&2\alpha x_1 x_2 + \beta x_1^3 x_2 + \beta x_2^3 x_1 \\ &+ \sum_{i=1}^{2}\left[-2\alpha x_i^2 + \alpha x_i^3 - (\alpha+2\beta)x_i^4 + \beta x_i^5 - \beta x_i^6\right] \\ &+ \frac{3}{2}x_2^2 + \frac{3}{2}x_2^6 + (\alpha^2+\beta^2)e^2 + \frac{1}{2}(\alpha^2+\beta^2)w^2\Big). \quad (5.50)\end{aligned}$$

To find the values of γ and θ for which the dissipation inequality given in (5.26) holds, we take the functions ϱ, σ and ρ as given in Condition 5.1 as $\varrho(y) := q_1 y^2 + q_2 y^4 + q_3 y^6$, $\sigma(W(e)) := \varsigma^2 \varepsilon W(e)$ and $\rho(|x|) := \varsigma^2 \varepsilon |x|$ with $\varepsilon \in \mathbb{R}_{>0}$, and we add $H^2(x,w)$, $\varrho(y)$, $-\gamma^2 W^2(e)$, $\sigma(W(e))$ and $\rho(|x|)$ to both sides of (5.50). This leads to

$$\begin{aligned}\langle \nabla V(x), f(x,e,w)\rangle + H^2(x,w) + \varrho(y) - \gamma^2 W^2(e) &\\ + \sigma(W(e)) + \rho(x) \leqslant (\alpha^2+\beta^2+\varepsilon-\varsigma^{-2}\gamma^2)e^2 &\\ + \varsigma^2\Big(p(x) - \nu\left(2\alpha - \varepsilon - \frac{3}{2} - (8+q_1)\varsigma^{-2}\right)x_2^2 &\\ + \frac{1}{2}(\alpha^2+\beta^2+5\varsigma^{-2})w^2\Big), \quad (5.51)\end{aligned}$$

where

$$\begin{aligned}p(x) = (2\alpha - 4\varsigma^{-2})x_1 x_2 + (\varepsilon - 2\alpha + \varsigma^{-2})x_1^2 + \beta x_1^3 x_2 &\\ + \beta x_2^3 x_1 + (1-\nu)(\varepsilon + \frac{3}{2} - 2\alpha + (8+q_1)\varsigma^{-2})x_2^2 &\\ + \sum_{i=1}^{2}\left[\alpha x_i^3 - (\alpha+2\beta)x_i^4 + \beta x_i^5 - \beta x_i^6\right] - 4\varsigma^{-2}x_2^3 &\\ + (4+q_2)\varsigma^{-2}x_2^4 - 2\varsigma^{-2}x_2^5 + \left(\frac{3}{2} + (2+q_3)\varsigma^{-2}\right)x_2^6\Big). \quad (5.52)\end{aligned}$$

Let us remark that we used the fact that $H^2(x,w) \leqslant -4x_1x_2 + x_1^2 + 8x_2^2 - 4x_2^3 + 4x_2^4 - 2x_2^5 + 2x_2^6 + 5w^2$ to obtain the inequalities above.

Observe from (5.51) that if $p(x) \leqslant 0$, (5.26) holds for $\gamma = \varsigma\sqrt{\alpha^2+\beta^2+\epsilon}$, $\mu = \varsigma^2\nu(2\alpha - \varepsilon - 3/2 - (8+q1)\varsigma^{-2})$ and $\theta = \sqrt{\frac{\alpha^2+\beta^2+10\varsigma^{-2}}{2\nu(2\alpha-\varepsilon-3/2-(8+q1)\varsigma^{-2})}}$. As such, the parameters α, β, ς, q_1, q_2, q_3 and ε need to be chosen such that $p(x) \leqslant 0$. We numerically determined that $[\alpha, \beta, \varsigma, q_1, q_2, q_3, \varepsilon] = [10.20, 3.29, 1.69, 2, 2, 2, 10^{-4}]$ constitutes a valid choice, which results in $\theta = 3.58$, $\mu = 13.20$ and $\gamma = 18.12$. Moreover, by means of (5.2) we obtain that τ_{miet} should satisfy $(\delta_{max}+1)\tau_{miet} <$

0.0811. In this example, we take $\tau_{miet} = 0.0691$ such that the conditions under (5.29) are satisfied with $\lambda = 0.1$.

Based on the analysis above, we can now construct the ETMs according to (5.7), (5.8), (5.36) and (5.37), with the function Ψ as in (5.30), where we choose $\chi(\eta) = \varepsilon|\eta|$ for all $\eta \in \mathbb{R}_{\geqslant 0}$.

5.7.3 Simulation results

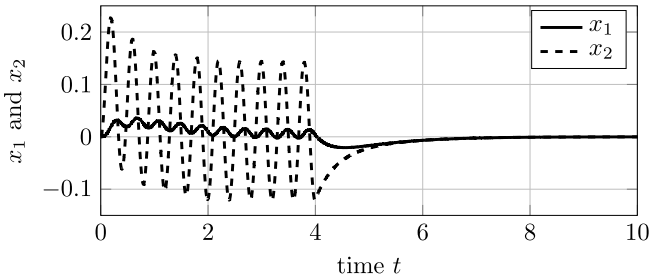

Fig. 5.2. Evolution of $x(t, j)$ (corresponding to the case with acknowledgments with a dynamic ETM) with $\delta_{max} = 2$.

Given the system and ETMs as described above, we present next the simulation results for both the case with and without acknowledgments. To evaluate the system in terms of utilization of communication resources, we consider average inter-event times τ_{avg} based on the average over 100 simulations of the system on the time interval $[0, 10]$, with the external disturbance w being $w(t, j) = 2\sin(5\pi t)$ for all $(t, j) \in \operatorname{dom} w$ for which $t \in [0, 4]$, and $w(t, j) = 0$ for all $(t, j) \in \operatorname{dom} w$ for which $t \in (4, 10]$ and with initial condition $x_1(0, 0) = x_2(0, 0) = 0$. Furthermore, in case the MANSD has not been exceeded, *i.e.*, in case $\delta < \delta_{max}$, the probability that the next transmission attempt results in a packet dropout set for simulation purposes to $p = 0.5$.

In Figure 5.2, the evolution of x is shown for the case with acknowledgments and with the dynamic ETM as given in (5.8) for the case that $\delta_{max} = 2$. Observe that the oscillations in the first four seconds is due to the disturbances acting on the system. The evolution of x for the case without acknowledgments and/or with a static ETM looks similar and is therefore omitted. The inter-event times $t_{j+1} - t_j$ resulting from the static ETM given in (5.7) and the dynamic ETM given in (5.8) corresponding to the case with acknowledgments and from the static ETM given in (5.36) and the dynamic ETM given in (5.37) corresponding to the case without acknowledgments, are shown in Figure 5.3. Observe that for this example, both dynamic ETMs as given in (5.8) and (5.37) corresponding to the case with and without acknowledgments, respectively, lead to a significant reduction of communication in comparison with time-triggered control schemes

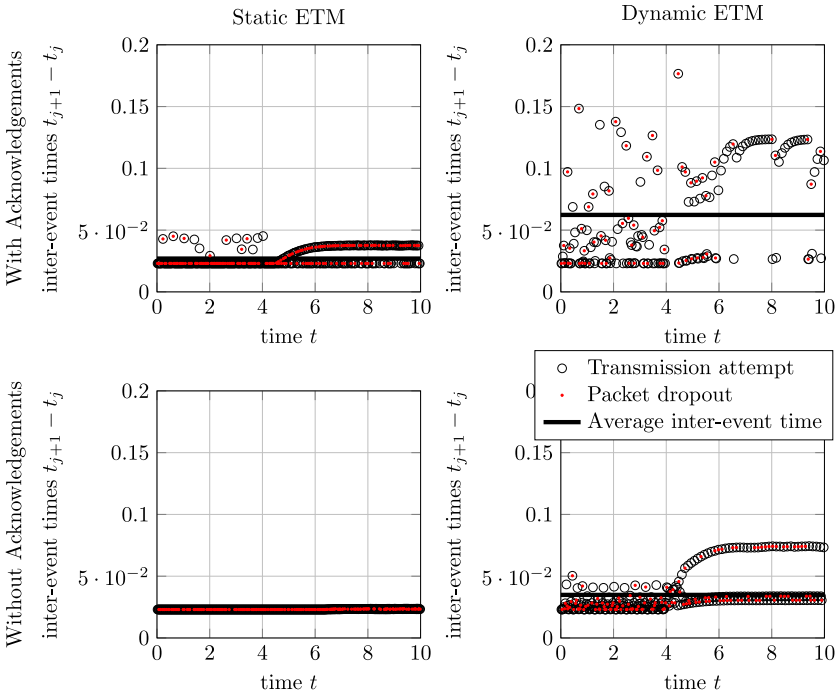

Fig. 5.3. The top plots show the inter-event times $t_{j+1} - t_j$ that result from the static ETM (left) given in (5.7) and the dynamic ETM (right) given in (5.8) for the case with acknowledgments. The bottom plots show the inter-event times $t_{j+1} - t_j$ that result from the static ETM (left) given in (5.36) and the dynamic ETM (right) given in (5.37) for the case without acknowledgments. In all four plots, the MANSD is equal to $\delta_{max} = 2$

in which the inter-event times would be upper bounded by $\mathcal{T}(\gamma, L)/(\delta_{max}+1) = 0.027$. Furthermore, as discussed in Remark 5.5, it clearly shows that the ETC scheme corresponding to the case with acknowledgments yields average larger inter-event times (indicated with a solid line) than the ETC schemes in which acknowledgments are absent.

Figure 5.4 illustrates the influence of the MANSD δ_{max} on the average inter-event times τ_{avg} relative to the minimal inter-event time τ_{miet} for all four ETMs given in (5.7), (5.8), (5.36) and (5.37).

5.8 Conclusions

In this chapter, we proposed a systematic design procedure for *static* and *dynamic* event-triggered control (ETC) schemes such that in absence of disturbances,

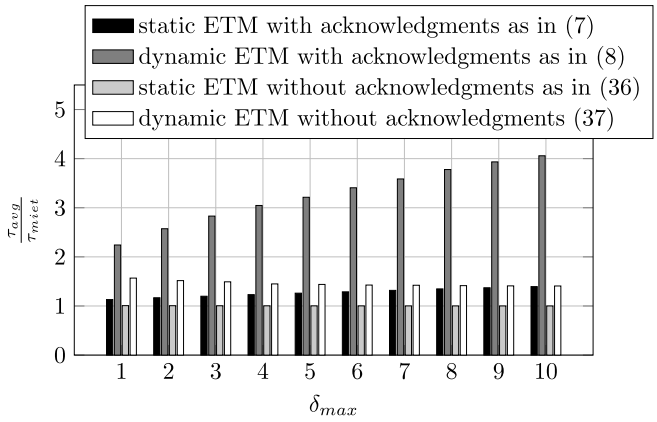

Fig. 5.4. Tradeoff between the maximum allowable number of successive packet losses and the relative average inter-event time τ_{avg}/τ_{miet} for the static ETM given in (5.7) and the dynamic ETM given in (5.8) corresponding to the case with acknowledgments and for the static ETM given in (5.36) and the dynamic ETM given in (5.37) corresponding to the case without acknowledgments.

the resulting closed-system is UGAS, and in the presence of disturbances, the resulting closed-loop system has a guaranteed $\mathcal{L}_p$-gain with respect to its performance output and external disturbances. Moreover, by design, a robust positive MIET can be guaranteed, even for the case where disturbances and packet dropouts are present. In fact, the ETMs proposed in this chapter can admit a maximum allowable number of successive packet dropouts (MANSD) while still maintaining the desired stability and performance properties. Two different ETC schemes were proposed depending on the situation if an acknowledgment scheme is employed (as, *e.g.*, in TCP) or not (as, *e.g.*, in UDP).

The presented theory was illustrated by means of a nonlinear numerical example, which showed that the dynamic ETC schemes can be systematically designed and yield significantly larger inter-event times than time-triggered or static ETC strategies. Moreover, the numerical example validated that ETC schemes relying on acknowledgments yield larger inter-event times than the ETC schemes for the case without acknowledgments for the same performance guarantees.

Chapter 6

Event-triggered Control Systems under Denial-of-Service Attacks

Abstract – In this chapter, we propose a systematic design framework for output-based dynamic event-triggered control (ETC) systems under Denial-of-Service (DoS) attacks. These malicious DoS attacks are intended to interfere with the communication channel causing periods in time at which transmission of measurement data is impossible. We show that the proposed ETC scheme, if well designed, can tolerate a class of DoS signals characterized by frequency and duration properties without jeopardizing the stability, performance and Zeno-freeness of the ETC system. In fact, the design procedure of the ETC condition allows trade-offs between performance, robustness to DoS attacks and utilization of communication resources. The main results will be illustrated by means of a numerical example.

6.1 Introduction

The field of *cyber-physical systems* (CPS) and, in particular, networked control systems (NCSs) is rapidly emerging due to a wide range of potential applications. However, there is a strong need for novel analysis and synthesis tools in control theory to guarantee safe and secure operation despite the presence of possible malicious attacks [198]. Especially for safety-critical applications such as intelligent transport systems and power grids, this is of high importance and requires the integration of cyber-security and control strategies.

One of the main concerns in NCSs with respect to security are *deception* attacks and *denial-of-service* (DoS) attacks. Deception attacks are intended to tamper transmitted data packages causing false feedback information, see for more details, *e.g.*, [183] and the reference therein, whereas DoS attacks, induced

This chapter is based on [76, 77].

by radio interference signals (also referred to as *jamming* signals), typically cause periods in time at which communication is not possible, see, for instance, [253]. In the present chapter, we focus on the latter type of attack. To be more concrete, we are interested in creating control strategies that render the overall closed-loop system resilient to DoS attacks which occur according to some *unknown* strategy with the aim to impede the communication of sensor measurements.

In addition to this resilience requirement described above, the control strategy needs to deal with the inherent imperfections of networked communication. Communication in NCSs is in general packet-based and thus measurement data can only be transmitted at discrete time instants. Moreover, especially since a communication network is often shared with multiple devices, the communication resources are restricted. Hence, a *resource-aware* and *resilient* control approach, which aims to only schedule the transmission of data when needed to maintain the desired stability and performance criteria, is a requisite. In a nutshell, the control problem addressed in this chapter is to design a control law that limits the transmission of sensor data while realizing desired closed-loop stability and performance criteria despite the presence of DoS attacks.

The proposed solution to this challenging design problem is to adopt an event-triggered control (ETC) strategy, in which transmission times are determined online by means of well-design triggering rules which rely on, *e.g.*, sensor measurements of the system. The introduction of this feedback in the sampling process enables ETC schemes to reduce the utilization of communication resources without jeopardizing control performance. In contrast to periodic time-triggered control schemes, ETC schemes aim to only transmit data when needed to maintain desired closed-loop properties. However, the majority of the literature on ETC strategies do not consider cyber-security issues like DoS attacks. Notable exceptions are [63, 64, 88]. In [88], a method was proposed to identify features of DoS attacks in order to improve the scheduling of transmissions in the sense that the DoS periods are being avoided. However, this approach turns out to be effective only when the DoS attacks are "well-structured" over time, e.g., in case of a periodic jamming signal. In [63, 64], a more general and more realistic DoS attack model is used based on the frequency and duration of the attacker's actions. These constraints are quite natural, as in reality, also the jammers resources are not infinite and several provisions can be taken to mitigate these DoS attacks. Additionally, no assumptions regarding the underlying jamming strategy of the attacker are made. Moreover, in contrast to stochastic packet dropout models, this characterization allows to capture a wide class of DoS attacks including *trivial*, *periodic*, *random* and *protocol-aware* jamming attacks [65, 253].

A drawback of the approaches in [63, 64, 88] is that these approaches are restricted to the case of static state feedback which requires the availability of full state information. Clearly, in practice, this is a strong assumption as only in very rare cases the full state variable is available for feedback. For this rea-

son, it is of interest to study event-triggered NCSs subject to DoS attacks that rely on output measurements only. To the best of our knowledge, the output feedback case in the context of DoS attacks has never been addressed in literature. This is not surprising as, especially in the presence of disturbances, extending existing ETC schemes that rely on state-feedback to the *output-based* ETC schemes (even without DoS attacks) is far from trivial as shown in [41,78]. Therefore, we propose in this chapter a novel systematic design methodology for *output-based resilient* and *resource-aware* dynamic ETC strategies for a class of nonlinear systems subject to disturbances. We prove that under the proposed design conditions, the resulting closed-loop system is input-to-output stable with finite induced $\mathcal{L}_\infty$-gains (*peak-to-peak gains*). Interestingly, this result is of independent interest in the context of switched systems under average-dwell time conditions, see also [124].

To enable practical implementation of the ETC scheme, it is important to guarantee that the time between consecutive transmission attempts is strictly positive and preferably lower bounded by a positive constant. By exploiting the Zeno-freeness property of the ETC scheme presented in [71, 72], we show that for the proposed ETC scheme, such a positive minimal-inter event time (MIET) exists by design despite the presence of disturbances and/or DoS attacks. By employing the DoS characterization as presented in [63,64], the obtained results hold for wide classes of relevant DoS attacks. As a matter of fact, as already mentioned, no assumptions regarding the underlying strategy of the attacker are needed, which makes the proposed scheme applicable in many contexts. The design procedure is demonstrated on a case study of cooperative adaptive cruise control. The numerical example reveals that illustrates a trade-off between robustness with respect to DoS attacks, network utilization and performance guarantees.

The remainder of this chapter is organized as follows. After presenting the necessary preliminaries and notational conventions in Section 6.2, we introduce the event-triggered networked control setup subject to DoS attacks in Section 6.3 leading to the problem statement. This event-triggered NCS setup is formalized in Section 6.4 by means of hybrid models resulting in a mathematically rigorous problem formulation. In Section 6.5, we characterize DoS attacks in terms of frequency and duration and, based on this characterization, we provide design conditions for the proposed dynamic event-triggered strategy such that stability and performance properties are satisfied. The obtained design framework is illustrated by means of a numerical example in Section 6.6. Finally, we provide the concluding remarks in Section 6.7.

6.2 Definitions and preliminaries

The following notational conventions will be used in this chapter. $\mathbb{N}$ denotes the set of all non-negative integers, $\mathbb{N}_{>0}$ the set of all positive integers, $\mathbb{R}$ the

field of all real numbers and $\mathbb{R}_{\geqslant 0}$ the set of all non-negative reals. For $N \in \mathbb{N}$, we write the set $\{1, 2, \ldots, N\}$ as $\bar{N}$. For N vectors $x_i \in \mathbb{R}^{n_i}, i \in \bar{N}$, we denote the vector obtained by stacking all vectors in one (column) vector $x \in \mathbb{R}^n$ with $n = \sum_{i=1}^{N} n_i$ by $(x_1, x_2, \ldots, x_N)$, *i.e.*, $(x_1, x_2, \ldots, x_N) = \begin{bmatrix} x_1^\top & x_2^\top & \cdots & x_N^\top \end{bmatrix}^\top$. The vectors in $\mathbb{R}^N$ consisting of all ones and zeros are denoted by $\mathbf{1}_N$ and $\mathbf{0}_N$, respectively. By $|\cdot|$ and $\langle \cdot, \cdot \rangle$ we denote the Euclidean norm and the usual inner product of real vectors, respectively. For a real symmetric matrix A, $\lambda_{\max}(A)$ denotes the largest eigenvalue of A. I_N denotes the identity matrix of dimension $N \times N$ and if N is clear for the context, we write I. A function $\alpha : \mathbb{R}_{\geqslant 0} \to \mathbb{R}_{\geqslant 0}$ is said to be of class $\mathcal{K}$ if it is continuous, strictly increasing and $\alpha(0) = 0$. It is said to be of class $\mathcal{K}_\infty$ if it is of class $\mathcal{K}$ and it is unbounded. A continuous function $\beta : \mathbb{R}_{\geqslant 0} \times \mathbb{R}_{\geqslant 0} \to \mathbb{R}_{\geqslant 0}$ is said to be of class $\mathcal{KL}$ if, for each fixed s, the mapping $r \mapsto \beta(r, s)$ belongs to class $\mathcal{K}$, and for each fixed r, the mapping $\beta(r, s)$ is decreasing with respect to s and $\beta(r, s) \to 0$ as $s \to \infty$. A continuous function $\gamma : \mathbb{R}_{\geqslant 0} \times \mathbb{R}_{\geqslant 0} \times \mathbb{R}_{\geqslant 0} \to \mathbb{R}_{\geqslant 0}$ is said to be of class $\mathcal{KLL}$ if, for each $r \geqslant 0$, both $\gamma(\cdot, \cdot, r)$ and $\gamma(\cdot, r, \cdot)$ belong to class $\mathcal{KL}$. A function $f : \mathbb{R}^n \to \mathbb{R}^n$ is said to be locally Lipschitz continuous if for each $x_0 \in \mathbb{R}^n$ there exist constants $\delta > 0$ and $L > 0$ such that for all $x \in \mathbb{R}^n$ we have that $|x - x_0| \leqslant \delta \Rightarrow |f(x) - f(x_0)| \leqslant L|x - x_0|$.

6.3 NCS model and problem statement

In this section, we present the networked control setup and the dynamic event-triggering mechanism employed by this NCS. Moreover, we describe how this NCS is affected by *denial-of-service* (DoS) attacks. Based on these descriptions, we formulate the problem statement.

6.3.1 Networked control configuration

Consider the feedback control configuration depicted in Figure 6.1. In this configuration, the sensor measurements of a plant $\mathcal{P}$ are being transmitted to a (dynamic) *output-based* controller $\mathcal{C}$ over a network $\mathcal{N}$. The continuous-time plant $\mathcal{P}$ is given by

$$\mathcal{P} : \begin{cases} \dot{x}_p = f_p(x_p, u, w) \\ y = g_p(x_p), \end{cases} \tag{6.1}$$

where $w \in \mathbb{R}^{n_w}$ is a disturbance input, $x_p \in \mathbb{R}^{n_p}$ the state vector, $u \in \mathbb{R}^{n_u}$ is the control input, $y \in \mathbb{R}^{n_y}$ is the measured output of plant $\mathcal{P}$. The (dynamic) output-based controller $\mathcal{C}$ is given by

$$\mathcal{C} : \begin{cases} \dot{x}_c = f_c(x_c, \hat{y}) \\ u = g_c(x_c, \hat{y}), \end{cases} \tag{6.2}$$

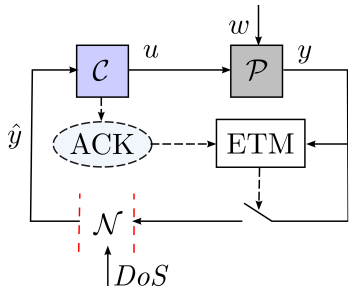

Fig. 6.1. Schematic representation of the event-triggered NCS considered in this chapter which consists of the interconnection of $\mathcal{P}$, $\mathcal{C}$ and $\mathcal{N}$ and where the transmission instants are determined by an event-triggering mechanism (ETM). Moreover, we assume an acknowledgement scheme is available meaning that the ETM has knowledge about reception of packages at the controller side.

where $x_c \in \mathbb{R}^{n_c}$ denotes the controller state, $\hat{y} \in \mathbb{R}^{n_y}$ represents the most recently received output measurement of the plant at the controller $\mathcal{C}$ and $u \in \mathbb{R}^{n_u}$ is the controller output. The performance output is given by $z = q(x)$, where $z \in \mathbb{R}^{n_z}$ and $x = (x_p, x_c)$.

Typically, the communication over the network $\mathcal{N}$ is packet-based, which implies that the output measurements y can only be transmitted at discrete instants in time, *i.e.*, at times t_j, $j \in \mathbb{N}$, satisfying $0 \leqslant t_0 < t_1 < t_2 < \ldots$. Hence, at each transmission instant t_j, $j \in \mathbb{N}$, the value of $\hat{y}$ is updated/jumps according to $\hat{y}(t_j^+) = y(t_j)$, for all $j \in \mathbb{N}$ (assuming for the moment that no DoS attacks are present). Here we consider $\hat{y}$ as a left-continuous signal in the sense that $\hat{y}(t) = \lim_{s \to t} \hat{y}(s)$. Furthermore, we assume that the value of $\hat{y}$ evolves in a zero-order-hold (ZOH) fashion in the sense that in between updates, the variable $\hat{y}$ is held constant, *i.e.*, $\dot{\hat{y}}(t) = 0$ for all $t \in (t_j, t_{j+1})$ with $j \in \mathbb{N}$. The functions f_p and f_c are assumed to be continuous and the functions g_p and g_c are assumed to be continuously differentiable.

Remark 6.1. For the sake of brevity, we consider the control configuration presented in Figure 6.1 in which we consider dynamic controllers as in (6.2) and only sensor measurements are transmitted over the network. However, the framework presented in this chapter also applies to other configurations such as decentralized control setups as described in [42, 72].

6.3.2 DoS attacks

A *denial-of-service* (DoS) attack is defined as a period in time at which the communication is blocked by a malicious attacker. Hence, when a transmission of $y(t_j)$ is attempted at transmission time t_j and a DoS attack is active, the

attempt will fail and thus the value of $\hat{y}$ can not be updated to $y(t_j)$. Obviously, this can have detrimental effects on the stability and performance of the closed-loop system.

In general, DoS attacks lead to a sequence of time intervals $\{H_n\}_{n\in\mathbb{N}}$, where the n-th time interval H_n, given by $H_n := \{h_n\} \cup [h_n, h_n + \tau_n)$, represents the n-th DoS attack (period). Hence, $h_n \in \mathbb{R}_{\geqslant 0}$ denotes the time instant at which the n-th DoS interval commences and $\tau_n \in \mathbb{R}_{\geqslant 0}$ denotes the length of the n-th DoS interval. The collection of all sequences $\{H_n\}_{n\in\mathbb{N}}$ of DoS attacks without overlap, *i.e.*, satisfy $0 \leqslant h_0 \leqslant h_0 + \tau_0 < h_1 \leqslant h_1 + \tau_1 < h_2 < \ldots$, is denoted by $\mathcal{I}_{DoS}$.

Moreover, for a given $\{H_n\}_{n\in\mathbb{N}} \in \mathcal{I}_{DoS}$, we define the collection of times at which a DoS attack is active by

$$\mathcal{T} := \bigcup_{n\in\mathbb{N}} H_n, \tag{6.3}$$

where we do not explicitly write the dependency of $\mathcal{T}$ on $\{H_n\}_{n\in\mathbb{N}} \in \mathcal{I}_{DoS}$ assuming it is clear from the context. By means of this definition, we can now describe the jump/update of $\hat{y}$ as in (6.2) for each transmission attempt at time $t_j \in \mathbb{R}_{\geqslant 0}$, $j \in \mathbb{N}$ as

$$\hat{y}(t_j^+) = \begin{cases} y(t_j), & \text{when } t_j \notin \mathcal{T} \\ \hat{y}(t_j), & \text{when } t_j \in \mathcal{T}, \end{cases}$$

and, accordingly, the update of the transmission error $e := \hat{y} - y$ as

$$e(t_j^+) = \begin{cases} 0, & \text{when } t_j \notin \mathcal{T} \\ e(t_j), & \text{when } t_j \in \mathcal{T}, \end{cases} \tag{6.4}$$

for each $j \in \mathbb{N}$.

6.3.3 Event-based communication

As already mentioned in the introduction, in comparison with time-triggered control, event-triggered control (ETC) is much more suitable for balancing network utilization and control performance. See also [18,20,54,224] for some early approaches of ETC and see [114] for a recent overview.

In this chapter, we we follow a design philosophy based on a *dynamic* event-triggered control scheme [71,72,96,189,190,248], which has several advantages over their *static* counterparts, see [71,73,96,189,248] for more details on these advantages. A dynamic triggering condition in the context of this chapter will take the form

$$t_0 = 0,\ t_{j+1} := \inf\left\{ t > t_j + \tau_{miet}^{m(t)} \mid \eta(t) < 0 \right\}, \tag{6.5}$$

for all $j \in \mathbb{N}$, $\eta(0) = 0$, where $m(t) \in \{0, 1\}$ is an auxiliary variable used to keep track of whether the most recent transmission attempt at time $t \in \mathbb{R}_{\geqslant 0}$ was successful ($m(t) = 0$) or not ($m(t) = 1$) (due to DoS attacks), $\tau^0_{miet}, \tau^1_{miet} \in \mathbb{R}_{>0}$ are (enforced) lower bounds on the *minimum inter-event times* (MIETs) for the cases that $m(t) = 0$ and $m(t) = 1$, respectively, and $\eta \in \mathbb{R}$ is an auxiliary variable. Let us remark that in general, if possible, it is helpful to schedule transmission attempts more often when a DoS attack is active in order to determine earlier when the DoS attack is over. For this reason, we consider two different waiting times τ^0_{miet}, τ^1_{miet} and we choose $\tau^1_{miet} \leqslant \tau^0_{miet}$. The variable η evolves according to

$$\dot{\eta}(t) = \tilde{\Psi}(m(t), o(t), \eta(t)), \text{ when } t \in (t_j, t_{j+1}] \tag{6.6}$$

$$\eta(t_j^+) = \begin{cases} \eta_0(e(t_j)), & \text{when } t_j \notin \mathcal{T} \\ \eta(t_j), & \text{when } t_j \in \mathcal{T}, \end{cases} \tag{6.7}$$

where $o = (y, e, \tau, \phi) \in \mathbb{O} := \mathbb{R}^{n_y} \times \mathbb{R}^{n_y} \times \mathbb{R}_{\geqslant 0} \times \left[\lambda, \lambda^{-1}\right]$ with $\lambda \in (0, 1)$ representing the information *locally* available at the event-triggering mechanism (ETM) (see Figure 6.1) including the output measurements $y \in \mathbb{R}^{n_y}$, the transmission error $e := \hat{y} - y$ and the auxiliary variables $\tau \in \mathbb{R}_{\geqslant 0}$ and $\phi \in \left[\lambda, \lambda^{-1}\right]$. The variables τ and ϕ are discussed in more detail in Section 6.4. Observe that by taking $\tau^0_{miet}, \tau^1_{miet} \in \mathbb{R}_{>0}$ Zeno-behavior is excluded from the ETC system since the next event can only occur after at least τ^1_{miet} time units have elapsed, *i.e.*, $t_{j+1} - t_j \geqslant \tau^1_{miet}$, for each $j \in \mathbb{N}$. In Section 6.5.2 and Section 6.5.3, we specify how to select τ^0_{miet}, τ^1_{miet}, $\tilde{\Psi}$ and η_0 such that desirable closed-loop stability and performance requirements are met.

6.3.4 Problem formulation

Given the descriptions above, the problem considered in this work can now roughly be stated as follows: *Propose a systematic design procedure for $\tilde{\Psi}$, η_0, τ^0_{miet} and τ^1_{miet} such that the interconnection $(\mathcal{P}, \mathcal{C}, \mathcal{N})$ with $\mathcal{P}$ and $\mathcal{C}$ as in (6.1) and (6.2), respectively, and the transmission attempts being generated by (6.5)-(6.7), satisfies desired asymptotic stability criteria and performance criteria, in terms of the so-called* peak-to-peak *gain despite the presence of the DoS attacks $\{H_n\}_{n\in\mathbb{N}} \in \mathcal{I}_{DoS}$ that satisfy constraints in terms of frequency and duration.*

In the next section, we introduce a complete mathematical (hybrid) model for the event-triggered closed-loop NCS setup, definitions of DoS frequency and duration, and relevant stability and performance notions, leading to a more formal problem formulation.

6.4 Mathematical formulation of the ETC setup

In this section, we reformulate the dynamics of the event-triggered NCS subject to DoS attacks in the form of the hybrid model $\mathcal{H}_\mathcal{T}$ given by,

$$\dot{\xi} = F(\xi, w), \quad \text{when } \xi \in C, \tag{6.8a}$$

$$\xi^+ = G_\mathcal{T}(\xi), \quad \text{when } \xi \in D, \tag{6.8b}$$

see [98] for details on this hybrid modelling framework.

Let us remark that the hybrid systems considered in this chapter have time regularization (or dwell time) and external inputs only appearing in the flow map. The latter allow us to employ the following signal norm definitions inspired by [21]. For any hybrid signal $\zeta(\cdot,\cdot)$ defined on $\operatorname{dom}\zeta \subset \mathbb{R}_{\geqslant 0} \times \mathbb{N}$ we define the $\mathcal{L}_\infty$-norm of ζ as $\|\zeta\|_\infty := \sup_{j\in\mathbb{N}} \left(\operatorname{ess\,sup}_{\{t\in\mathbb{R}|(t,j)\in\operatorname{dom}\,\zeta\}} |\zeta(t,j)|\right)$. Observe that this signal norm definition is similar to the corresponding classical continuous-time norm. In this chapter, we employ the same notation for the $\mathcal{L}_\infty$-norm of hybrid time signals and conventional continuous-time signals. Moreover, due to the aforementioned properties and notational convenience, we consider the disturbance input $w : \mathbb{R}_{\geqslant 0} \to \mathbb{R}^{n_w}$ to be a time signal instead of a hybrid signal and use the usual definition for $\mathcal{L}_\infty$-norm.

6.4.1 Hybrid model

To describe the NCS setup as discussed before in terms of flow equations (6.8a) and jump equations (6.8b), we first need to introduce a few auxiliary variables, namely, the timer variables s, $\tau \in \mathbb{R}_{\geqslant 0}$ representing the overall time and the time elapsed since the most recent transmission attempt, respectively. Moreover, we we also introduce an additional auxiliary variable $\phi \in \left[\lambda, \lambda^{-1}\right]$, where $\lambda \in (0,1)$ is a tuning parameter to be specified, used in the triggering condition and part of o as already mentioned in Section 6.3.3. By combining these auxiliary variables with (6.1), (6.2) and (6.7), the flow map of the interconnection $(\mathcal{P}, \mathcal{C}, \mathcal{N})$ can be defined as

$$F(\xi, w) := \Big(f(x,e,w), g(x,e,w), 1, 1, 0, \tilde{\Psi}(m,o,\eta), f_\phi(\tau,m,\phi)\Big), \tag{6.9}$$

where $\xi = (x, e, \tau, s, m, \eta, \phi) \in \mathbb{X} := \mathbb{R}^{n_x} \times \mathbb{R}^{n_y} \times \mathbb{R}_{\geqslant 0} \times \mathbb{R}_{\geqslant 0} \times \{0,1\} \times \mathbb{R}_{\geqslant 0} \times \left[\lambda, \lambda^{-1}\right]$ with $n_x = n_p + n_c$ and $\lambda \in (0,1)$. Moreover, the functions f and g follow from (6.1) and (6.2) and are given by

$$f(x,e,w) = \begin{bmatrix} f_p(x_p, g_c(x_c, g_p(x_p)+e), w) \\ f_c(x_c, g_p(x_p)+e) \end{bmatrix}, \tag{6.10}$$

$$g(x,e,w) = -\frac{\partial g_p}{\partial x_p}(x_p) f_p(x_p, g_c(x_c, g_p(x_p)+e), w), \tag{6.11}$$

and f_ϕ will be specified later. In accordance with (6.5), we define the flow set as

$$C := \{\xi \in \mathbb{X} \mid \tau \leqslant \tau^m_{miet} \vee \eta \geqslant 0\}. \tag{6.12}$$

Based on (6.7) and (6.4), we specify the jump map as

$$G_{\mathcal{T}}(\xi) := \begin{cases} G_0(\xi), & \text{when } \xi \in D \wedge s \notin \mathcal{T} \\ G_1(\xi), & \text{when } \xi \in D \wedge s \in \mathcal{T}, \end{cases} \tag{6.13}$$

where

$$G_0(\xi) = (x, 0, 0, s, 0, \eta_0(e), \lambda) \tag{6.14}$$
$$G_1(\xi) = (x, e, 0, s, 1, \eta, \phi), \tag{6.15}$$

such that $\xi^+ = G_0(\xi)$ corresponds to a successful transmission attempt and $\xi^+ = G_1(\xi)$ to a failed transmission attempt.

Finally, the jump set is given by

$$D := \{\xi \in \mathbb{X} \mid \tau \geqslant \tau^m_{miet} \wedge \eta \leqslant 0\}. \tag{6.16}$$

The time-constants τ^0_{miet} and τ^1_{miet} and the functions $\tilde{\Psi}$, η_0 and f_ϕ are specified in Section 6.5. Observe that the hybrid system description presented above leads to more solutions than induced by the triggering condition given by (6.5) and (6.7).[1]

Moreover, observe that the hybrid system $\mathcal{H}_{\mathcal{T}}$ as described by (6.8)-(6.16) is parameterized by the collection of time-intervals at which DoS attacks are active as defined in (6.3). Therefore, we write explicitly the dependence of $\mathcal{H}_{\mathcal{T}}$ on $\mathcal{T}$.

6.4.2 Constraints on DoS sequence

Since it is reasonable to assume that the attacker's resources are not infinite and measures can be taken to mitigate malicious DoS attacks, a natural characterization of DoS attacks can be given in terms of both the DoS *frequency* and the DoS *duration* as in [63], see also Remark 6.2 below. Therefore, we define the collection of times within the interval $[T_1, T_2]$, with $T_2 \geqslant T_1 \geqslant 0$, at which DoS attacks are active as

$$\Xi(T_1, T_2) := [T_1, T_2] \cap \mathcal{T} \tag{6.17}$$

[1] We foresee that the results in [98, Chapter 6, Chapter 7] on well-posed hybrid systems can relatively easily be used to obtain robustness properties with respect to arbitrarily small vanishing perturbations on the flow map jump map and all states. Note, however, that the focus of this chapter is to obtain robustness result with respect to DoS attacks, which require different and new techniques. To not complicate the exposition of the novel techniques by introducing more technicalities needed to address also the robustness properties studied in [98], we describe only the new results, although they can be combined with the existing robustness results of [98].

with $\mathcal{T}$ as in (6.3) and the collection of time instants within the interval $[T_1, T_2]$ at which communication is possible as

$$\Theta(T_1, T_2) := [T_1, T_2] \backslash \Xi(T_1, T_2).$$

Consider a collection $\{I_i\}$, $i \in \bar{N}$ of N intervals that do not overlap, *i.e.*, $I_i \cap I_j = \emptyset$ for all $i, j \in \bar{N}$, $i \neq j$, and let $I = \bigcup_{i \in \bar{N}} I_i$. We denote with $|I|$ the sum of the lengths of all intervals I_i, $i \in \bar{N}$. Consequently, $|\Xi(T_1, T_2)|$ denotes the total length of the DoS attacks within the interval $[T_1, T_2]$. Consider the following definitions.

Definition 6.1. [64] (DoS frequency*). Let* $\{H_n\}_{n \in \mathbb{N}} \in \mathcal{I}_{DoS}$ *and let* $n(T_1, T_2)$ *denote the number of DoS* off/on *transitions occurring in the interval* $[T_1, T_2)$, i.e., $n(T_1, T_2) = card\{n \in \mathbb{N} \mid h_n \in [T_1, T_2)\}$, *where card denotes the number of elements in the set. We say that a given sequence of DoS attacks* $\{H_n\}_{n \in \mathbb{N}}$ *satisfies the* DoS frequency *constraint for a given* $\tau_D \in \mathbb{R}_{>0}$, *and a given* $\nu \in \mathbb{R}_{\geqslant 0}$, *if for all* $T_1, T_2 \in \mathbb{R}_{\geqslant 0}$ *with* $T_2 \geqslant T_1$

$$n(T_1, T_2) \leqslant \nu + \frac{T_2 - T_1}{\tau_D}. \tag{6.18}$$

We denote the class of sequences of DoS intervals that satisfy this DoS frequency *constraint by* $\mathcal{I}_{DoS,freq}(\nu, \tau_D)$.

Definition 6.2. [64] (DoS duration*). We say that a sequence of DoS attacks specified by* $\{H_n\}_{n \in \mathbb{N}} \in \mathcal{I}_{DoS}$ *satisfies the* DoS duration *constraint for a given* $T \in \mathbb{R}_{>1}$ *and a given* $\varsigma \in \mathbb{R}_{\geqslant 0}$, *if for all* $T_1, T_2 \in \mathbb{R}_{\geqslant 0}$ *with* $T_2 \geqslant T_1$

$$|\Xi(T_1, T_2)| < \varsigma + \frac{T_2 - T_1}{T}. \tag{6.19}$$

We denote the class of all sequences of DoS intervals that satisfy this DoS duration *constraint by* $\mathcal{I}_{DoS,dur}(\varsigma, T)$.

We will also use the notation $\mathcal{I}_{DoS}(\nu, \tau_D, \varsigma, T)$ for $\nu, \varsigma \in \mathbb{R}_{\geqslant 0}$, $\tau_D \in \mathbb{R}_{>0}$ and $T \in \mathbb{R}_{>1}$ to denote the intersection $\mathcal{I}_{DoS,freq}(\nu, \tau_D) \cap \mathcal{I}_{DoS,dur}(\varsigma, T)$. We call a sequence of DoS attacks that satisfies $\{H_n\}_{n \in \mathbb{N}} \in \mathcal{I}_{DoS}(\nu, \tau_D, \varsigma, T)$, a $(\nu, \tau_D, \varsigma, T)$-DoS sequence for short. Moreover, we also define the class of hybrid systems, which are generated by $(\nu, \tau_D, \varsigma, T)$-DoS sequences as $\mathcal{H}(\nu, \tau_D, \varsigma, T) := \{\mathcal{H}_\mathcal{T} \mid \mathcal{T}$ as in (6.3) with $\{H_n\}_{n \in \mathbb{N}} \in \mathcal{I}_{DoS}(\nu, \tau_D, \varsigma, T)\}$.

Remark 6.2. Observe that Definition 6.1 and Definition 6.2 make no assumptions regarding the attacker's underlying strategy as they only indicate limitations in terms of the frequency and duration of DoS attacks. From a practical point of view, Definition 6.1 and Definition 6.2 are natural as well since there exist several techniques to *mitigate* jamming attacks, for example, spreading techniques and high-pass filtering. As a consequence, the frequency and duration of DoS attacks can indeed be restrained by exploiting such techniques, see, *e.g.*, [65, 253].

Of course, desired control objectives can in general not be achieved in case the DoS frequency and/or DoS duration can be arbitrarily large, *i.e.*, in case $\tau_D \to 0$ or $T = 1$, respectively, as in that case every communication attempt can be blocked by the attacker with the consequence that the system is in open loop all the time. Fortunately, as already mentioned in Remark 6.2, several provisions can be taken in order to mitigate DoS attacks with the aim to limit the frequency and duration of the time intervals over which communication is effectively denied.

6.4.3 Mathematical problem formulation

To specify desirable stability and performance properties, we introduce the following definitions that use the concepts of hybrid time domains and corresponding solutions [98]. In this chapter, we assume that all hybrid trajectories start in the set

$$\mathbb{X}_0 := \{\xi \in \mathbb{X} \mid \tau \geqslant \tau^0_{miet}, s = 0, \eta = 0, \phi = \phi_{miet}\}, \tag{6.20}$$

where ϕ_{miet} will be specified in Section 6.5.2. Observe that this assumption only reflects the initialization of the ETM variables, which can be freely chosen, while we do not put any (initial) constraints on the plant and the controller states $x = (x_p, x_c)$ and the initial knowledge of $\hat{y}$ at the controller side.

Definition 6.3. *A hybrid system $\mathcal{H}_\mathcal{T}$ is said to be* persistently flowing *with respect to initial state set $\mathbb{X}_0$ if all maximal solutions*[2] *ξ with $\xi(0,0) \in \mathbb{X}_0$ have unbounded domains in the t-direction, i.e.,* $\sup_t \operatorname{dom} \xi = \infty$.

Definition 6.4. *Let $\nu, \varsigma \in \mathbb{R}_{\geqslant 0}$, $\tau_D \in \mathbb{R}_{>0}$ and $T \in \mathbb{R}_{>1}$ be given. A closed set $\mathcal{A} \subset \mathbb{X}$ is said to be* uniformly globally asymptotically stable *(UGAS) for the class of hybrid systems $\mathcal{H}(\nu, \tau_D, \varsigma, T)$ with respect to initial state set $\mathbb{X}_0$ if all systems $\mathcal{H}_\mathcal{T} \in \mathcal{H}(\nu, \tau_D, \varsigma, T)$ are persistently flowing with respect to initial state set $\mathbb{X}_0$ and there exists a function $\beta \in \mathcal{KLL}$ such that for any $\mathcal{H}_\mathcal{T} \in \mathcal{H}(\nu, \tau_D, \varsigma, T)$ and for any initial condition $\xi(0,0) \in \mathbb{X}_0$, all corresponding solutions ξ of $\mathcal{H}_\mathcal{T}$ with $w = 0$ satisfy*

$$|\xi(t,j)|_\mathcal{A} \leqslant \beta\left(|\xi(0,0)|_\mathcal{A}, t, j\right) \tag{6.21}$$

for all $(t,j) \in \operatorname{dom}\xi$. The closed set $\mathcal{A}$ is said to be uniformly globally exponentially stable *(UGES) for the class of hybrid systems $\mathcal{H}(\nu, \tau_D, \varsigma, T)$, if the above holds with $\beta(r,t,j) = Mr\exp(-\varrho(t+j))$ for some $M \geqslant 0$ and $\varrho > 0$.*

Definition 6.5. *Let $\vartheta, \nu, \varsigma \in \mathbb{R}_{\geqslant 0}$, $\tau_D \in \mathbb{R}_{>0}$ and $T \in \mathbb{R}_{>1}$ be given. A closed set $\mathcal{A} \subset \mathbb{X}$ is said to be $\mathcal{L}_\infty$-stable with an induced $\mathcal{L}_\infty$-gain less than or equal to ϑ for the class of hybrid systems $\mathcal{H}(\nu, \tau_D, \varsigma, T)$, if all systems $\mathcal{H}_\mathcal{T} \in \mathcal{H}(\nu, \tau_D, \varsigma, T)$*

[2] [98, Chapter 2] A solution ξ to $\mathcal{H}_\mathcal{T}$ is maximal if there does not exist another solution $\bar{\xi}$ to $\mathcal{H}_\mathcal{T}$ such that dom ξ is a proper subset of dom $\bar{\xi}$ and $\xi(t,j) = \bar{\xi}(t,j)$ for all $(t,j) \in$ dom ξ.

are persistently flowing with respect to initial state set $\mathbb{X}_0$ *and there exists a* $\mathcal{K}_\infty$*-function* β *such that for any* $\mathcal{H}_\mathcal{T} \in \mathcal{H}(\nu, \tau_D, \varsigma, T)$*, exogenous input* $w \in \mathcal{L}_\infty$*, and any initial condition* $\xi(0,0) \in \mathbb{X}_0$*, each corresponding solution to* $\mathcal{H}_\mathcal{T}$ *satisfies*

$$\|z\|_{\mathcal{L}_\infty} \leqslant \beta(|\xi(0,0)|_\mathcal{A}) + \vartheta\|w\|_{\mathcal{L}_\infty}. \tag{6.22}$$

We can now formalize the problem, which was loosely stated at the end of Section 6.3.

Problem 6.1. *Given* $\nu \in \mathbb{R}_{\geqslant 0}$*,* $\tau_D \in \mathbb{R}_{>0}, \varsigma \in \mathbb{R}_{\geqslant 0}$ *and* $T \in \mathbb{R}_{>1}$*, provide design conditions for the values of* $\tau^0_{miet}, \tau^1_{miet} \in \mathbb{R}_{>0}$ *and the functions* $\tilde{\Psi}$*,* η_0 *as in the event generator given by (6.5) and (6.7) and* f_ϕ *as in (6.9), such that the closed set* $\mathcal{A} := \{\xi \in \mathbb{X} \mid x = 0,\, e = 0\}$ *is UGES and/or, in the presence of disturbances, has a finite induced* $\mathcal{L}_\infty$*-gain for the class of hybrid systems* $\mathcal{H}(\nu, \tau_D, \varsigma, T)$ *.*

6.5 Design conditions and stability guarantees

In Section 6.5.2 and Section 6.5.3, the time-constants τ^0_{miet} and τ^1_{miet}, and the function f_ϕ are specified and design conditions for the functions $\tilde{\Psi}$ and η_0 are presented leading to a solution for Problem 6.1. In order to specify the design conditions, we first start with the required preliminaries consisting of stability and performance conditions for *time-triggered* NCSs taken from [51, 120] in Section 6.5.1.

6.5.1 Preliminaries

Consider the following condition.

Condition 6.1. *([51, 120]) There exist a locally Lipschitz function* $W : \mathbb{R}^{n_y} \to \mathbb{R}_{\geqslant 0}$*, a continuous function* $H : \mathbb{R}^{n_x} \times \mathbb{R}^{n_w} \to \mathbb{R}$*, and constants* $L \geqslant 0$*,* $\underline{c}_W$*, and* $\bar{c}_W$*, such that*

- *for all* $e \in \mathbb{R}^{n_e}$ *it holds that*

$$\underline{c}_W|e| \leqslant W(e) \leqslant \bar{c}_W|e|, \tag{6.23}$$

- *for all* $x \in \mathbb{R}^{n_x}$*, and almost all* $e \in \mathbb{R}^{n_y}$ *it holds that*

$$\left\langle \frac{\partial W(e)}{\partial e}, g(x,e,w) \right\rangle \leqslant LW(e) + H(x,w). \tag{6.24}$$

In addition, there exist a locally Lipschitz function $V : \mathbb{R}^{n_x} \to \mathbb{R}_{\geqslant 0}$*, and a positive semi-definite function* $\varrho : \mathbb{R}^{n_y} \to \mathbb{R}_{\geqslant 0}$ *and constants* $\rho_V, \rho_W, \gamma, \underline{c}_V, \bar{c}_V, c_z > 0$*, such that*

- *for all* $x \in \mathbb{R}^{n_x}$

$$\underline{c}_V |x|^2 \leqslant V(x) \leqslant \bar{c}_V |x|^2,\ c_z |q(x)|^2 \leqslant V(x), \tag{6.25}$$

- *for all* $e \in \mathbb{R}^{n_y}$, $w \in \mathbb{R}^{n_w}$ *and almost all* $x \in \mathbb{R}^{n_x}$

$$\begin{aligned}\langle \nabla V(x), f(x,e,w) \rangle \leqslant -\rho_V V(x) - \varrho(|y|) - H^2(x,w) \\ + (\gamma^2 - \rho_W) W^2(e) + \theta^2 |w|^2,\end{aligned} \tag{6.26}$$

- *the constants* ρ_W *and* γ *satisfy* $\rho_W \leqslant \gamma^2$.

Let us remark that for linear systems the conditions above can be obtained systematically by solving a multi-objective linear matrix inequality (LMI) problem, see [71, 72, 120] for more details. Also several classes of nonlinear systems satisfy these conditions, see [72].

6.5.2 Minimal inter-event time

As already mentioned, τ^0_{miet} and τ^1_{miet} (and ϕ_{miet}, $\tilde{\Psi}$, f_ϕ and η_0) should be chosen appropriately in the sense that desirable closed-loop stability and performance requirements can be achieved. To do so, we specify the function[3] $f_\phi : \mathbb{R}_{\geqslant 0} \times \mathbb{N} \times \mathbb{R}_{\geqslant 0} \to \mathbb{R}$, as

$$f_\phi(\tau, m, \phi) := \begin{cases} (m-1)\left(2L\phi + \gamma(\phi^2+1)\right), & \text{for } \tau \leqslant \tau^0_{miet}, \\ 0, & \text{for } \tau > \tau^0_{miet}, \end{cases} \tag{6.27}$$

with L and γ as given in Condition 6.1. The time-constants τ^0_{miet} and τ^1_{miet} can be chosen less than or equal to the *maximally allowable transmission interval* bound (in this work referred to as $\bar{\tau}_{miet}$) given in [51] as

$$\bar{\tau}_{miet} := \begin{cases} \frac{1}{Lr} \arctan\left(\frac{r(1-\lambda)}{2\frac{\lambda}{1+\lambda}\left(\frac{\gamma}{L}-1\right)+1+\lambda} \right), & \gamma > L \\ \frac{1}{L}\frac{1-\lambda}{1+\lambda}, & \gamma = L \\ \frac{1}{Lr} \operatorname{arctanh}\left(\frac{r(1-\lambda)}{2\frac{\lambda}{\lambda+1}\left(\frac{\gamma}{L}-1\right)+1+\lambda} \right), & \gamma < L, \end{cases} \tag{6.28}$$

where $r = \sqrt{|(\gamma/L)^2 - 1|}$. Note that by selecting τ^0_{miet} and τ^1_{miet} equal to the right-hand side of (6.28) indeed longer (average) transmission intervals are realized compared to time-based (worst-case) specifications as discussed in Section 6.3.3.

[3] Observe that the flow map F as given in (6.9) is discontinuous in τ due to (6.27). However, due to the facts that $\dot{\tau} = 1$ and the right hand-side of (6.27) is Lipschitz continuous, we find by means of the Carathéodory's existence theorem that this does not cause any problems in the uniqueness and existence of solutions.

Lemma 6.1. *[51] Let $\bar{\tau}_{miet}$ be given by (6.28), then the solution to*

$$\dot{\tilde{\phi}} = -2L\tilde{\phi} - \gamma\left(\tilde{\phi}^2 + 1\right) \tag{6.29}$$

with $\tilde{\phi}(0) = \lambda^{-1}$ satisfies $\tilde{\phi}(t) \in [\lambda, \lambda^{-1}]$ for all $t \in [0, \bar{\tau}_{miet}]$, and $\tilde{\phi}(\bar{\tau}_{miet}) = \lambda$.

Finally, we define

$$\phi_{miet} := \tilde{\phi}(\tau^0_{miet}), \tag{6.30}$$

where $\tilde{\phi}$ is the solution to (6.29) with $\tilde{\phi}(0) = \lambda^{-1}$ and note again that $\tau^1_{miet} \leqslant \tau^0_{miet} \leqslant \bar{\tau}_{miet}$.

6.5.3 Stability and performance guarantees

Theorem 6.2. *Consider the class of hybrid systems $\mathcal{H}(\nu, \tau_D, \varsigma, T)$ with $\nu, \varsigma \in \mathbb{R}_{\geqslant 0}$, $\tau_D \in \mathbb{R}_{>0}$, $T \in \mathbb{R}_{>1}$ and let Condition 6.1 be satisfied with $\tau^1_{miet} \leqslant \tau^0_{miet} \leqslant \bar{\tau}_{miet}$ with $\bar{\tau}_{miet}$ as in (6.28) and with f_ϕ and ϕ_{miet} as in (6.27) and (6.30), respectively. Moreover, suppose that the following three conditions hold:*

i) The DoS frequency parameter τ_D and the DoS duration parameter T satisfy

$$\frac{\tau^1_{miet}}{\tau_D} + \frac{1}{T} < \frac{\omega_1}{\omega_1 + \omega_2}, \tag{6.31}$$

where

$$\omega_1 = \min\left(\rho_V, \frac{\lambda\rho_W}{\gamma}\right), \omega_2 = \frac{(\bar{\gamma} - \rho_W)}{\gamma\phi_{miet}} \tag{6.32}$$

and

$$\bar{\gamma} := \gamma\left(2\phi_{miet}L + \gamma(1 + \phi^2_{miet})\right). \tag{6.33}$$

ii) The function $\tilde{\Psi}$ is given by

$$\tilde{\Psi}(m, o, \eta) = \begin{cases} \Psi(o) - \sigma(\eta), & \text{when } m = 0, \\ -(1 - \omega(\tau, m)), & \text{when } m = 1, \end{cases} \tag{6.34}$$

where σ is a $\mathcal{K}_\infty$-function that satisfies $\sigma(s) \geqslant \omega_1 s$ for all $s \in \mathbb{R}_{\geqslant 0}$, the function $\Psi : \mathbb{O} \to \mathbb{R}$ is given by

$$\Psi(o) = \varrho(|y|) + \bar{\gamma}\omega(\tau, m)W^2(e) \tag{6.35}$$

with

$$\omega(\tau, m) := \begin{cases} 1, & \text{for } 0 \leqslant \tau \leqslant \tau^m_{miet} \\ 0, & \text{for } \tau > \tau^m_{miet}, \end{cases} \tag{6.36}$$

for $\tau \in \mathbb{R}_{\geqslant 0}$ and with $\bar{\gamma}$ as given in (6.33).

iii) The function η_0 is given by $\eta_0(e) = \gamma\phi_{miet}W^2(e)$.

Then the closed set $\mathcal{A} = \{\xi \in \mathbb{X} \mid x = 0, e = 0\}$ is UGES and is $\mathcal{L}_\infty$-stable with a finite induced $\mathcal{L}_\infty$-gain less than or equal to $\theta\sqrt{\frac{\kappa}{c_z\beta^*}}$ with c_z as in (6.25) and where $\kappa := e^{\varsigma_*(\omega_1+\omega_2)}$, $\varsigma_* := \varsigma + \nu\tau^1_{miet}$, $\beta_* = \omega_1 - (\omega_1+\omega_2)/T_*$ and $T_* := \tau_D T/(\tau_D + \tau^1_{miet}T)$, for the class of hybrid systems $\mathcal{H}(\nu, \tau_D, \varsigma, T)$.

The proof is provided in the Appendix. Observe that the condition given in item i) imposes restrictions on the DoS parameters τ_D and T in terms of other system parameters. As such, the frequency and duration of the allowable DoS attacks are limited. Moreover, observe that the DoS parameters ν, τ_D, ς and T affect the guaranteed $\mathcal{L}_\infty$-gain of the system which illustrates the trade-off between robustness with respect to DoS attacks and performance in the sense that in general, robustness comes at cost of performance.

Observe that in case communication is allowed, the transmissions are scheduled in an event-based fashion (to save valuable communication resources) whereas in case the communication is denied, the next transmission is scheduled again after τ^1_{miet} time units (to determine when the DoS attack is over) since when $m = 1$, which implies that $\eta = 0$ at the previous transmission attempt, $\tilde{\Psi}(m, o, \eta) = 0$ for $0 \leqslant \tau \leqslant \tau^1_{miet}$ and $\tilde{\Psi}(m, o, \eta) = -1$ for $\tau > \tau^1_{miet}$. Hence, when $m = 1$ and $\tau > \tau^1_{miet}$ a next jump occurs as flow condition $\eta \geqslant 0$ will be violated.

Remark 6.3. Note that this implementation requires the knowledge about when DoS attacks are blocking transmissions, which could be realized by means of acknowledgements as illustrated in Figure 6.1. Let us remark that the ETM can easily be adjusted such that it is not required that acknowledgements are being received instantaneously. For example, the acknowledgement is allowed to be delayed with at most τ^1_{miet} time units if after each transmission instant, the ETM keeps track of the evolution of η for both the cases that the transmission has been successful or denied. For the brevity of exposition, this feature has, however, been omitted.

The presented framework does not require an acknowledgement scheme when purely periodic sampling with inter-sampling time τ^1_{miet} is employed. The same design conditions lead to the same guarantees in this case.

Remark 6.4. The proposed framework can also be used for the design of a *static* triggering mechanism, namely

$$t_{j+1} := \inf\left\{t > t_j + \tau^{m(t)}_{miet} \mid \Psi(o) \leqslant 0\right\}, \tag{6.37}$$

with $t_0 = 0$ and with Ψ as in (6.35).

6.6 Case study on cooperative adaptive cruise control

In this section, we illustrate the main result by means of a case study on cooperative adaptive cruise control (CACC). As shown in [187], in the context of vehicle platooning, wireless communication between vehicles can have a significant contribution to improving traffic throughput and safety. For a platoon of two identical vehicles equipped with CACC, the functions f and g as in (6.9) are given by $f(x,e,w) = A_{11}x + A_{12}e + A_{13}w$ and $g(x,e,w) = A_{21}x + A_{22}e + A_{23}w$, where

$$A_{11} = \begin{bmatrix} -\frac{1}{\tau_c} & \frac{1}{\tau_c} & 0 & 0 & 0 & 0 \\ 0 & -\frac{1}{h} & 0 & 0 & 0 & 0 \\ 0 & 0 & 0 & 1 & -h & 0 \\ 1 & 0 & 0 & 0 & -1 & 0 \\ 0 & 0 & 0 & 0 & -\frac{1}{\tau_c} & \frac{1}{\tau_c} \\ 0 & \frac{1}{h} & \frac{k_p}{h} & \frac{k_d}{h} & -k_d & -\frac{1}{h} \end{bmatrix}$$

$$A_{12} = \begin{bmatrix} 0 & 0 & 0 & 0 & 0 & \frac{1}{h} \end{bmatrix}^\top,$$

$$A_{13} = \begin{bmatrix} 0 & \frac{1}{h} & 0 & 0 & 0 & 0 \end{bmatrix}^\top,$$

$$A_{21} = \begin{bmatrix} 0 & \frac{1}{h} & 0 & 0 & 0 & 0 \end{bmatrix},\ A_{22} = 0,\ A_{23} = -\frac{1}{h}$$

with $\tau_c \in \mathbb{R}_{>0}$ a time-constant corresponding to the driveline dynamics, $h \in \mathbb{R}_{>0}$ the time headway (desired time between the two vehicles) and k_p, $k_d \in \mathbb{R}_{>0}$ the controller gains. Moreover, the input w represents the control input of the leading vehicle. See, *e.g.*, [187] for more details. For this example, we use the following parameter values $\tau_c = 0.15$, $h = 0.6$, $k_p = 0.2$, $k_d = 0.7$. To comply with safety, one of the control objectives is to keep the error with respect to the vehicle desired distance small and therefore we define the performance output as $z = C_z x$, where

$$C_z = \begin{bmatrix} 0 & 0 & 1 & 0 & 0 & 0 \end{bmatrix},$$

which corresponds to the spacing error between the two vehicles. The measured output y as in (6.1) is the desired acceleration of the leading vehicle and is given by $y = C_y x$, where

$$C_y = \begin{bmatrix} 0 & 1 & 0 & 0 & 0 & 0 \end{bmatrix},$$

and is available at the ETM to determine the transmission instants.

Before the ETM design and the stability and performance analysis, we first have to guarantee that Condition 6.1 is met. For the vehicle platoon system described above, we can take $W(e) = |e|$. Observe that with this choice, (6.23) and (6.24) are met with $\underline{c}_W = \bar{c}_W = 1$, $L = 0$ and $H(x,w) = |A_{21}x + A_{21}w|$. To comply with (6.25) and (6.26), we take $\varrho(r) = qr^2$ and $V(x) = x^\top P x$,

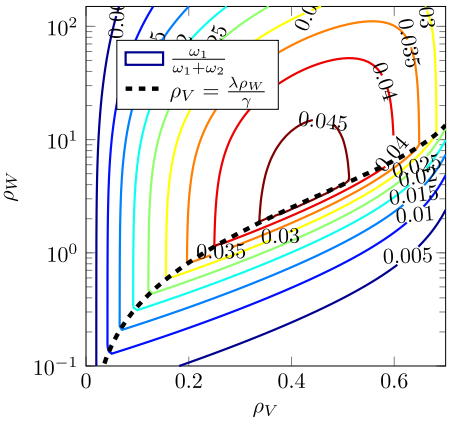

(a) The achievable robustness in terms of $\frac{\omega_1}{\omega_1+\omega_2}$ for various values of ρ_V and ρ_W. The dashed line represents the points for which $\omega_1 = \rho_V = \frac{\lambda\rho_W}{\gamma}$.

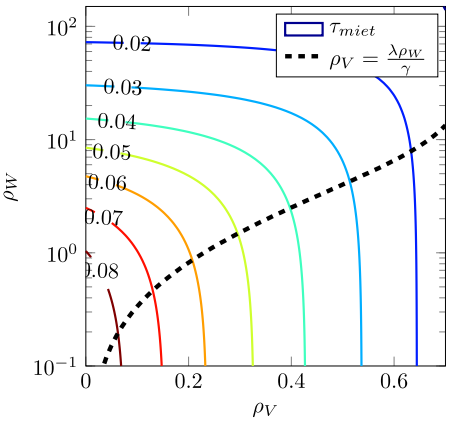

(b) The minimal inter-event time for various values of ρ_V and ρ_W. The dashed line represents the points for which $\omega_1 = \rho_V = \frac{\lambda\rho_W}{\gamma}$.

Fig. 6.2. Achievable robustness and minimal inter-event times for various values of ρ_V and ρ_W.

$\underline{c}_V = \lambda_{\min}(P)$ and $\bar{c}_V = \lambda_{\max}(P)$ where P can be obtained by minimizing $\gamma + \theta$ subject to the LMI given by

$$\begin{pmatrix} R_{11} & R_{12} & R_{13} \\ \star & R_{22} & R_{23} \\ \star & \star & R_{33} \end{pmatrix} \preceq 0,\ P \succeq 0, C_y^\top C_y \preceq P, \tag{6.38}$$

where

$$\begin{aligned} R_{11} &:= A_{11}^\top P + P A_{11} + \rho_V P + A_{21}^\top A_{21} + C^\top Q C, & R_{12} &:= P A_{12}, \\ R_{13} &:= P A_{13} + A_{21}^\top A_{23}, & R_{22} &:= (\rho_W - \gamma^2) I, & R_{23} &:= 0, \\ R_{33} &:= A_{23}^\top A_{23} - \theta^2 I. \end{aligned}$$

To illustrate the design procedure, we take $\lambda = 0.7$ and compute $\bar{\tau}_{miet}$ (as in (6.28)) for various ρ_V and ρ_W. By taking $\lambda = 0.7$, $c_z = 1$ and $\tau_{miet}^0 = \tau_{miet}^1 = \frac{1}{2}\bar{\tau}_{miet}$, we obtain Figure 6.2a and Figure 6.2b, which illustrate robustness in terms of $\frac{\omega_1}{\omega_1+\omega_2}$ which corresponds to the right-hand side of (6.31) and network utilization in terms of τ_{miet}^1, respectively.

Let us now study the influence of four DoS attacks of length zero on the performance of the system described above. For this reason, we take $\nu = 4$, $\varsigma = 0$ and we take $\beta^* = \frac{3}{4}\omega_1$ which implies that τ_D and T should satisfy $\frac{\tau_{miet}}{\tau_D} + \frac{1}{T} \leqslant \frac{1}{4}\frac{\omega_1}{\omega_1+\omega_2}$. The $\mathcal{L}_\infty$-gains for this case for various ρ_V and ρ_W are shown in Figure

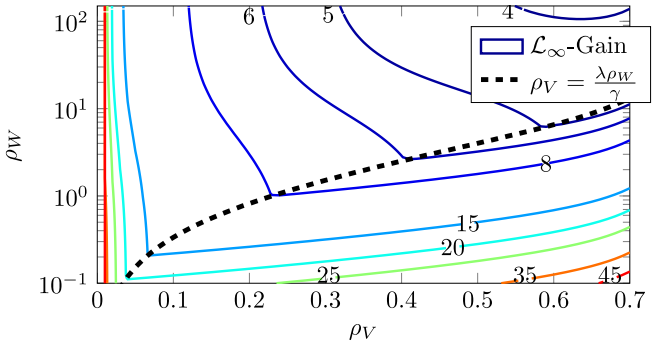

Fig. 6.3. The $\mathcal{L}_\infty$-gain for various values of ρ_V and ρ_W. The dashed line represents the points for which $\omega_1 = \rho_V = \frac{\lambda \rho_W}{\gamma}$.

6.3. Let us remark that other choices for ς and ν such as, *e.g.*, $\varsigma = \tau_{miet}$ and $\nu = 2\tau_{miet}$ lead to identical results in terms of the $\mathcal{L}_\infty$-gain but allow for different classes of DoS Attacks. The dashed-line In Figure 6.2a, Figure 6.3 and Figure 6.2b represents the points at which $\omega_1 = \rho_V = \frac{\lambda \rho_W}{\gamma}$. Observe that below this line, the trade-off between robustness, network utilization and performance is unfavorable for $\rho_V \geqslant \frac{\lambda \rho_W}{\gamma}$, since for this case, a smaller ρ_W leads to a relatively steep decline in both robustness and performance in contrast to the minimal inter-event time τ^1_{miet} that barely changes.

In Figure 6.4, the distance error/performance output z and the inter-event times $t_{j+1} - t_j$ are displayed for the case that $\rho_V = 0.5$, $\rho_W = 5$ and w as illustrated the figure resulting in an $\mathcal{L}_\infty$-gain less than or equal to 5.35, $\frac{\omega_1}{\omega_1+\omega_2} = 0.0454$ and $\tau^0_{miet} = \tau^1_{miet} = 0.0307$. Although in general, it is difficult to obtain the worst-case DoS attack and disturbance, the simulation results show that for this particular system, the derived $\mathcal{L}_\infty$-bound is a somewhat conservative. In fact, more consecutive transmission failures can be tolerated as shown in Figure 6.4. To obtain better performance in terms of lower $\mathcal{L}_\infty$-bounds, λ and/or c_z could be chosen larger and τ^0_{miet} and τ^1_{miet} could be chosen smaller. However, this comes at cost of increased network utilization and/or reduced robustness with respect to DoS attacks.

6.7 Conclusions

In this work, we addressed the design of *resource-aware* and *resilient* control strategies for networked control systems (NCS) subject to malicious *Denial-of-service* (DoS) attacks. In particular, the control and communication strategy was based on an *output-based* event-triggered control scheme applicable to a class of nonlinear feedback systems that are subject to exogenous disturbances.

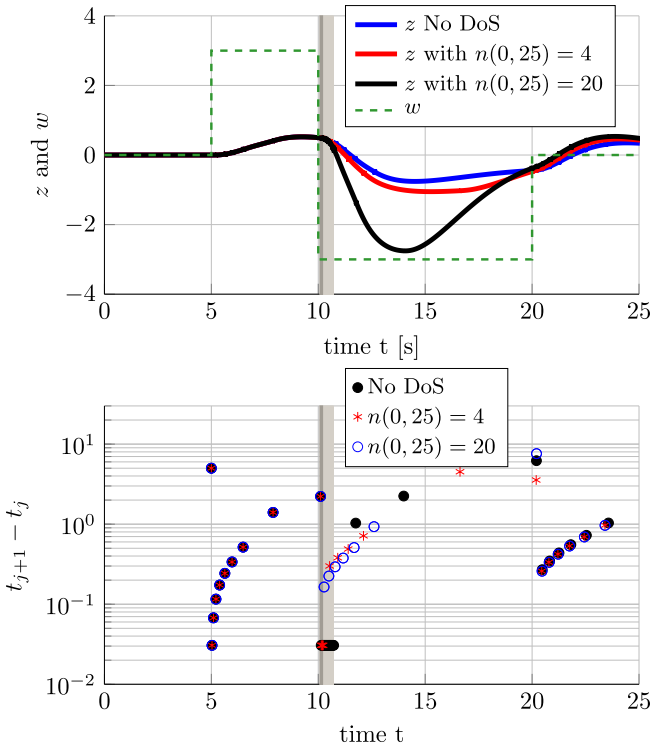

Fig. 6.4. In the top plot, the trajectory of the distance error z of the vehicle platoon for DoS-attacks of various sizes and the input w are given. In the bottom plot, the inter-event times of the dynamic event triggering mechanism described by (6.5) and (6.7) are given. Both plots were generated by taking $\rho_V = 0.5$ and $\rho_W = 5$ resulting in $\mathcal{L}_\infty$-gain less than or equal to 5.35, $\frac{\omega_1}{\omega_1+\omega_2} = 0.0454$ and $\tau_{miet} = 0.0307$. The dark and light gray boxes show where the DoS attacks take place that block 4 and 20 consecutive transmissions, respectively.

The proposed framework led to guarantees regarding the existence of a robust strictly positive lower bound on the inter-event times despite the presence of disturbances and DoS attacks. Additionally, based on the natural assumption that DoS attacks are restricted in terms of frequency and duration, we showed that desired stability and performance criteria in terms of induced $\mathcal{L}_\infty$-gains can be guaranteed.

Chapter 7

Event-triggered Control of Nonlinear Multi-agent systems subject to Non-uniform Time-Varying Delays

Abstract – In this chapter, we consider a class of nonlinear multi-agent systems (MAS) subject to disturbances and the inevitable imperfections induced by packet-based networked communication. These imperfections include non-uniform time-varying transmission delays and intervals, limited communication resources and communication constraints. To reduce the utilization of the (scarce) communication resources, we propose a design procedure for distributed event-triggered control schemes that result in aperiodic transmission of information. Under suitable conditions, the designed event-triggered controllers lead to a MAS that is dissipative with respect to a desired supply rate (and thus can be used to study, *e.g.*, $\mathcal{L}_p$-gains, input-to-state stability (ISS) and passivity properties), strictly positive lower bounds on the inter-event times and robustness to non-uniform time-varying delays in terms of maximum allowable delays. Moreover, the framework allows for the consideration of destination protocols which determine, at each transmission instant, to which (groups of) agent(s) a local output measurement is being transmitted. In addition, the proposed event-triggered control schemes also apply in the context of packet losses and denial-of-service attacks thereby showing the generality of the new design framework.

7.1 Introduction

Recently, the interest in multi-agent systems (MAS) has grown significantly due to the wide-range of applications. Examples include the distributed con-

trol of a platoon or a formation of vehicles [67, 83] and distributed state estimation in large-scale processes such as power grids and building automation [66, 161, 162, 235, 236], see also [179, 196] and the reference therein for overviews of some early approaches in consensus seeking MAS. In many of these applications, the sensor and the actuator data are sent over shared (packet-based) communication networks which, in contrast to dedicated point-to-point links, offer many benefits in terms of flexibility, maintenance and ease of installation. In fact, in some applications, such as in vehicle platooning, the use of (wireless) communication networks is unavoidable. However, these shared communication networks also come with inevitable imperfections including time-varying transmission delays, asynchronous transmission instants, limited communication resources and communication constraints requiring scheduling protocols. Moreover, in the context of MAS, broadcast data is typically not received and processed simultaneously by each connected agent. Due to the latter fact, the transmission delays in MAS are time-varying and often non-uniform in the sense that the time between the transmission and receipt of a data package might vary per connected agent. As a consequence, the information available at each agent is not consistent. Given the above mentioned network-induced artifacts inherent to networked control systems (NCSs) (and MAS in particular), there is a need for novel analysis tools and control algorithms for MAS that take these imperfections into account.

Despite this need, the majority of the available literature on MAS only consider a subset of the aforementioned network-induced imperfections. For instance, the approaches presented in [67, 146, 222, 230], which consider non-uniform time-varying delays, hold under the assumption that communication is continuous instead of packet-based and thereby they do not take into account the sampled-data and digital nature of the communication links. At the opposite side, [69, 93, 94, 104, 105, 133, 140, 148, 160, 185, 206, 251, 262] proposed to use event-triggered control (ETC) strategies for MAS to cope with these limited communication resources. These ETC strategies aim to reduce the utilization of communication resources by letting the transmission instants depend on state measurements of the system. If well-designed, these schemes can still guarantee desired closed-loop behavior in terms of stability and performance, see, *e.g.*, [15, 41, 72, 78, 165, 191, 224, 236] for more details on ETC. However, the ETC approaches presented in [69, 93, 105, 133, 140, 148, 160, 185] do not consider delays and the approaches in [206, 262] assume that the delays are uniform and constant. Notable exceptions that study event-triggered MAS under non-uniform time-varying delays include [94, 104, 251]. In [94], a periodic ETC approach is presented that can deal with non-uniform delays. However, it is assumed that the sizes of the delays are known. Hence, this approach requires that the internal clocks of all agents are perfectly synchronized. In [104, 251], it was proposed to use transmission protocols that rely on acknowledgment and permission signals in order to make sure that the information available at each individual agent

is updated simultaneously. However, the latter approach might put a burden on the communication channel due to the presence of additional acknowledgment and permission signals. In addition, it might not be practically feasible to realize acknowledgment and permission signals that can be sent and received instantaneously. For this reason, [104] also proposed an ETC scheme that does not require permission signals. However, this approach does not consider the presence of disturbances.

In the current work, we present a systematic and general design framework for families of event-triggered controllers for classes of nonlinear MAS subject to disturbances, network-induced imperfections such as *unknown* non-uniform time-varying transmission delays, asynchronous transmission instants, limited communication resources and communication constraints. The proposed framework leads to MASs that are dissipative with respect to a desired supply rate (and thus can be used to guarantee, *e.g.*, $\mathcal{L}_p$-gains, input-to-state stability (ISS) and passivity properties) and strictly positive lower bounds on the inter-event times. Let us emphasize that the proposed scheme does *not* require clock synchronization, acknowledgment signals that need to be transmitted and received instantaneously, or any knowledge about the sizes of the transmission delays. In addition, we show that the concept of network scheduling protocols, which are typically used in the context of NCSs (see, *e.g.*, [173, 245]), can be used for the design of so-called *destination protocols*. These destination protocols determine, at each transmission instant, to which (groups of) agent(s) a local output measurement is being transmitted. The latter feature is useful, for example, in the context of intelligent transportation systems that rely on the GeoNetworking protocol [81]. This protocol uses geographical addressing to establish *ad hoc* communication networks and allows for both unicast (transmission of data directed to a single agent) and broadcast (transmission of data directed to multiple agents) as communication types, see [81] for more details. As shown in [134], the performance of the communication network is significantly better under unicast communication types compared to broadcast communication types. Hence, the use of destination protocols can be beneficial for relevant applications thereby making the possibility of analysis, as done in this paper, important. Interestingly, the proposed concept of destination protocols also allows to capture packet-losses, see, *e.g.*, [74, 103, 104, 138], and even (malicious) denial-of-service attacks, which are intended to interfere with the communication channel, see, *e.g.*, [64, 77]. The latter result is of independent interest.

The proposed ETC design framework is general in the sense that it can not only deal with malicious attacks, packet losses, (destination) protocols, time-varying non-uniform delays, varying transmission intervals but also supports the use of model-based holding devices. As shown in, *e.g.*, [92, 93, 111, 138, 258], the use of model-based holding devices generally allow the system to be in open-loop for a longer period in time thereby saving valuable communication resources. As such, model-based ETC schemes typically outperform conventional ETC

schemes equipped with zero-order hold devices in terms of (average) inter-event times. One of the main challenges in the design of a model-based ETC scheme, however, is to incorporate the presence of communication delays. In [92], solutions to this challenge are proposed for two particular cases. In the first case, the delays are assumed to be constant and known. In the second case, it is assumed that the clock of the sending and receiving node are synchronized and time-stamping is used to compensate for the effect of the delays. In the current chapter, as mentioned before, we consider unknown delays and the proposed ETC scheme does not required clock synchronization. To the best of our knowledge, the latter situation has not been studied in literature before, not even for centralized control schemes.

The remainder of this chapter is organized as follows. After presenting the necessary preliminaries and notational conventions in Section 7.2, we introduce the multi-agent control setup and the problem statement in Section 7.3, which are formalized in Section 7.4 by a hybrid model representing the entire closed-loop system. The design conditions of the proposed event-triggered mechanism and the main result is presented in Section 7.5. In Section 7.6, we discuss the applicability of the proposed framework in the presence of packet losses and denial-of-service attacks. The proofs of all technical results can be found in the appendix.

7.2 Definitions and preliminaries

7.2.1 Definitions

The following notational conventions will be used in this chapter. The set $\mathbb{N}$ denotes the set of non-negative integers, $\mathbb{N}_{>0}$ the set of all positive integers, $\mathbb{R}$ the field of all real numbers and $\mathbb{R}_{\geqslant 0}$ the set of all non-negative reals. For N vectors $x_i \in \mathbb{R}^{n_i}, i \in \{1, 2, \ldots, N\}$, we denote the vector obtained by stacking all vectors in one (column) vector $x \in \mathbb{R}^n$ with $n = \sum_{i=1}^{N} n_i$ by $(x_1, x_2, \ldots, x_N)$, *i.e.*, $(x_1, x_2, \ldots, x_N) = \begin{bmatrix} x_1^\top & x_2^\top & \cdots & x_N^\top \end{bmatrix}^\top$. The vectors in $\mathbb{R}^N$ whose elements are all ones or all zeros are denoted by $\mathbf{1}_N$ and $\mathbf{0}_N$, respectively. By $|\cdot|$ and $\langle \cdot, \cdot \rangle$ we denote the Euclidean norm and the usual inner product of real vectors, respectively. Moreover, for $x \in \mathbb{R}^n$ and a given closed non-empty set $\mathcal{A} \subset \mathbb{R}^n$, $|x|_{\mathcal{A}} = \inf_{y \in \mathcal{A}} |x - y|$. For a real symmetric matrix A, $\lambda_{\max}(A)$ denotes the largest eigenvalue of A. For a matrix M of dimensions $N \times N$, $M_{i,\cdot}$ denotes the i-th row of matrix M. I_N denotes the identity matrix of dimension $N \times N$ and if N is clear for the context, we write I. For two matrices $A \in \mathbb{R}^{m \times n}$ and $B \in \mathbb{R}^{p \times q}$, the Kronecker product $A \otimes B \in \mathbb{R}^{mp \times nq}$ is given by

$$A \otimes B = \begin{bmatrix} a_{1,1}B & \cdots & a_{1,n}B \\ \vdots & \ddots & \vdots \\ a_{n,1}B & \cdots & a_{n,n} \end{bmatrix}, \tag{7.1}$$

where $a_{i,j}$ denotes the element in row i and column j of matrix A. A function $\alpha : \mathbb{R}_{\geqslant 0} \to \mathbb{R}_{\geqslant 0}$ is said to be of class $\mathcal{K}$ if it is continuous, strictly increasing and $\alpha(0) = 0$. It is said to be of class $\mathcal{K}_\infty$ if it is of class $\mathcal{K}$ and it is unbounded. A continuous function $\beta : \mathbb{R}_{\geqslant 0} \times \mathbb{R}_{\geqslant 0} \to \mathbb{R}_{\geqslant 0}$ is said to be of class $\mathcal{KL}$ if, for each fixed s, the mapping $r \mapsto \beta(r, s)$ belongs to class $\mathcal{K}$, and for each fixed $r > 0$, the mapping $\beta(r, s)$ is decreasing with respect to s and $s \mapsto \beta(r, s) \to 0$ as $s \to \infty$. A function $f : \mathbb{R}^n \to \mathbb{R}^n$ is said to be locally Lipschitz continuous if for each $x_0 \in \mathbb{R}^n$ there exist constants $\delta > 0$ and $L > 0$ such that for all $x \in \mathbb{R}^n$ we have that $|x - x_0| \leqslant \delta \Rightarrow |f(x) - f(x_0)| \leqslant L|x - x_0|$. A function $V : \mathbb{R}^n \to \mathbb{R}_{\geqslant 0}$ is called proper with respect to a set $\mathcal{A}$ if $V(x) \to \infty$ whenever $|x|_{\mathcal{A}} \to \infty$. A set-valued mapping from a set X to a set Y, associates, with every point $x \in X$, a subset of Y. The notation $F : X \rightrightarrows Y$, indicates that F is a set-valued mapping from X to Y with $F(x) \subset Y$ for all $x \in X$.

7.2.2 Graph theory notions

Here we recall some basic definitions and properties from graph theory as adopted in [36,68]. A *graph* is a pair $\mathcal{G} = (\mathcal{V}, \mathcal{E})$ composed of a vertex set $\mathcal{V}$ and a set of edges $\mathcal{E} \subset \mathcal{V} \times \mathcal{V}$. The cardinality of $\mathcal{V}$, denoted by $N \in \mathbb{N}_{>0}$, is the number of vertices in $\mathcal{V}$. An ordered pair $(i, j) \in \mathcal{E}$ with $i, j \in \mathcal{V}$ is said to be an edge *directed* from i to j. A graph is called *undirected* if it holds that $(i, j) \in \mathcal{E}$ if and only if $(j, i) \in \mathcal{E}$. Otherwise, the graph is a *directed* graph, also referred to as a digraph. A vertex j is said to be a neighbor of i if $(j, i) \in \mathcal{E}$. The set of neighbors of a vertex i is denoted by $\mathcal{V}_i^{\text{in}}$ and defined as $\mathcal{V}_i^{\text{in}} := \{j \in \mathcal{V} \mid (j, i) \in \mathcal{E}\}$ and the set of vertices for which vertex i is a neighbor is denoted by $\mathcal{V}_i^{\text{out}}$ and defined as $\mathcal{V}_i^{\text{out}} := \{j \in \mathcal{V} \mid (i, j) \in \mathcal{E}\}$. Clearly, for *undirected* graphs, it holds that $\mathcal{V}_i^{\text{in}} = \mathcal{V}_i^{\text{out}}$ for all $i \in \mathcal{V}$. The cardinality of $\mathcal{V}_i^{\text{in}}$ is denoted by N_i. An edge $(i, i) \in \mathcal{E}$ is called a *self-loop*. A *directed path* from i to j is a (finite) sequence of edges starting in i and ending at j. A digraph $\mathcal{G}$ is connected if there exists a path, regardless of its direction, between all vertices $i, j \in \mathcal{V}$.

7.3 Multi-agent control setup and problem statement

7.3.1 Distributed control configuration

In this chapter, we consider a collection of agents $\mathcal{A}_1, \mathcal{A}_2, \ldots, \mathcal{A}_N$ that are interconnected according to a connected and time-invariant directed graph $\mathcal{G}(\mathcal{V}, \mathcal{E})$. The dynamics of the i-th agent $\mathcal{A}_i$ for $i \in \mathcal{V}$ are given by

$$\mathcal{A}_i : \begin{cases} \dot{x}_{p,i} & = f_{p,i}(x_p, u_i, w) \\ y_i & = g_{p,i}(x_{p,i}), \end{cases} \tag{7.2}$$

where $x_{p,i} \in \mathbb{R}^{n_{x_{p,i}}}$ represents the local state vector, $u_i \in \mathbb{R}^{n_{u_i}}$ the local control input, $w \in \mathbb{R}^{n_w}$ the disturbance or external input, $y_i \in \mathbb{R}^{n_y}$ the local (measurable) output and $x_p = (x_{p,1}, x_{p,2}, \ldots, x_{p,N}) \in \mathbb{R}^{n_{x_p}}$ with $n_{x_p} = \sum_{i\in\mathcal{V}} n_{x_{p,i}}$. Observe that dimensions of the local state state vectors of the agents are not necessarily equal. The dimensions of the local outputs, however, are the same for each agent. Moreover, we consider control laws of the form

$$\begin{cases} \dot{x}_{c,i} &= f_{c,i}(x_{c,i}, y_i, \hat{y}^i) \\ u_i &= g_{c,i}(x_{c,i}, y_i, \hat{y}^i), \end{cases} \tag{7.3}$$

where $\hat{y}^i = \left(\hat{y}^i_1, \hat{y}^i_2, \ldots, \hat{y}^i_N\right) \in \mathbb{R}^{Nn_y}$. We use $\hat{y}^i_j$ with $i \in \mathcal{V}^{\text{out}}_j$ and $j \in \mathcal{V}$, to denote the local estimate of the output y_j of agent $\mathcal{A}_j$, y_j, available at agent $\mathcal{A}_i$. Let us remark that the variable $\hat{y}^i_j$, $i \in \mathcal{V}^{\text{out}}_j$ and $j \in \mathcal{V}$, corresponds to the edge $(j,i) \in \mathcal{E}$ of graph $\mathcal{G}$. Observe that the variables $\hat{y}^i_j$ for which $i \notin \mathcal{V}^{\text{out}}_j$ with $j \in \mathcal{V}$, i.e., $(j,i) \notin \mathcal{E}$, are non existent in practice and thus in principle redundant due to the communication topology. However, for ease of notation, we still use these variables and assume that $\hat{y}^i_j(t) = 0$ for all $i \notin \mathcal{V}^{\text{out}}_j$ with $j \in \mathcal{V}$ and all $t \in \mathbb{R}_{\geqslant 0}$.

Due to the presence of network-induced imperfections such as time-varying transmission delays, packet-based communication, time-varying transmission intervals and scheduling protocols, we typically have that $\hat{y}^i_j \neq y_j$, for all $i \in \mathcal{V}^{\text{out}}_j$ and $j \in \mathcal{V}$. In this chapter, we consider the case that each agent $\mathcal{A}_i$, $i \in \mathcal{V}^{\text{out}}_j$ and $j \in \mathcal{V}$, employs the same holding device to obtain the estimate $\hat{y}^i_j$. Nonetheless, we employ the notation $\hat{y}^i_j$ since, in general, estimates of y_i differ per agent, i.e., $\hat{y}^i_j \neq \hat{y}^l_j$, for $j \in \mathcal{V}$ and $i,l \in \mathcal{V}^{\text{out}}_j$ with $i \neq l$. This inconsistency is, for example, caused by the fact that a broadcast output measurement is not necessarily received at the same time by each connected agent due to the presence of *non-uniform delays*, which we will discuss in more detail in Section 7.3.2.

7.3.2 Networked communication

As already mentioned, (packet-based) networked communication induces inherent imperfections such as the fact that data can only be transmitted at discrete instants in time (sampled-data communication) and the presence of unknown non-uniform time-varying delays. To be more concrete, the output y_i, $i \in \mathcal{V}$, is only sampled and transmitted over the network at discrete time instants t^i_k, $k \in \mathbb{N}$, that satisfy $0 = t^i_0 < t^i_1 < \ldots$, for all $i \in \mathcal{V}$. After the k-th transmission is sent by agent $\mathcal{A}_i$, $i \in \mathcal{V}$, the data is received by the agent(s) $\mathcal{A}_j$, $j \in \mathcal{V}^{\text{out}}_i$, after a communication delay of $\Delta^{ij}_k \geqslant 0$ time units, $k \in \mathbb{N}$. In other words, at time $t^i_k + \Delta^{ij}_k$, $i,j \in \mathcal{V}, k \in \mathbb{N}$, the estimate $\hat{y}^j_i$ is updated according to

$$\hat{y}^j_i((t^i_k + \Delta^{ij}_k)^+) \;=\; z_i(k, \bar{e}_i(t^i_k), j) y_i(t^i_k) + (1 - z_i(k, \bar{e}_i(t^i_k), j))\hat{y}^j_i(t^i_k + \Delta^{ij}_k), \tag{7.4}$$

for all $i \in \mathcal{V}$ and $j \in \mathcal{V}_i^{\text{out}}$, where $\bar{e}_i := (\delta_i(1)e_i^1, \delta_i(2)e_i^2, \ldots, \delta_i(N)e_i^N) \in \bar{\mathbb{E}}_i \subseteq \mathbb{R}^{Nn_y}$, where $\bar{\mathbb{E}}_i := \mathbb{E}_i(1) \times \mathbb{E}_i(2) \times \ldots \times \mathbb{E}_i(N)$ with

$$\mathbb{E}_i(j) := \begin{cases} \{0\}, \text{ when } j \notin \mathcal{V}_i^{\text{out}} \\ \mathbb{R}^{n_y}, \text{ otherwise,} \end{cases}$$

$$\delta_i(j) := \begin{cases} 0, \text{ when } j \notin \mathcal{V}_i^{\text{out}} \\ 1, \text{ otherwise,} \end{cases} \tag{7.5}$$

and where $e_i^j \in \mathbb{R}^{n_y}$, $i, j \in \mathcal{V}$ represents the estimation error given by

$$e_i^j := \hat{y}_i^j - y_i, \tag{7.6}$$

for $i \in \mathcal{V}$ and $j \in \mathcal{V}_i^{\text{out}}$. Hence, e_i^j denotes the error present in the information $\hat{y}_i^j$ available at agent $\mathcal{A}_j$ regarding the output y_i of agent $\mathcal{A}_i$, also referred to as the transmission error. Note that $\bar{e}_i$ does not depend on the redundant variables $e_i^j \in \mathbb{R}^{n_y}$ for which $i \in \mathcal{V}$ and $j \notin \mathcal{V}_i^{\text{out}}$ due to the presence of $\delta(i)_j$.

The function $z_i : \mathbb{N} \times \bar{\mathbb{E}}_i \times \mathcal{V} \to \{0, 1\}$, $i \in \mathcal{V}$, which we will refer to as the *destination protocol*, is related to the transmission decision of agent $\mathcal{A}_i$. To be more specific, at each transmission time t_k^i, $i \in \mathcal{V}$, $k \in \mathbb{N}$, the function z_i specifies on the basis of k and $\bar{e}_i(t_k^i)$, to which of the connected agents $\mathcal{A}_j$, $j \in \mathcal{V}_i^{\text{out}}$, the most recent local output measurement of agent $\mathcal{A}_i$, *i.e.*, $y_i(t_k^i)$, is transmitted. In case the output measurement y_i should be transmitted to agent $\mathcal{A}_j$, $j \in \mathcal{V}_i^{\text{out}}$, at transmission time t_k^i, $i \in \mathcal{V}$, $k \in \mathbb{N}$, then $z_i(k, \bar{e}_i(t_k^i), j) = 1$. If it should not be transmitted to agent $\mathcal{A}_j$, $j \in \mathcal{V}_i^{\text{out}}$, then $z_i(k, \bar{e}_i(t_k^i), j) = 0$.

Interestingly, as we will show in Section 7.6, the function z_i also allows to capture packet losses and denial-of-service attacks, which are results of independent interest.

In this chapter, we focus on small-delay scenarios meaning that an agent is only allowed to transmit after the previous broadcast information of that agent has been received by all targeted agents. In addition, we assume that the delays are bounded from above by a time-constant called the *maximum allowable delay* (MAD). To be more precise, we adopt the following assumption.

Assumption 7.1. *For each $i \in \mathcal{V}$, there is a time-constant τ_{mad}^i such that the transmission delays are bounded according to $0 \leqslant \Delta_k^{ij} \leqslant \tau_{mad}^i \leqslant t_{k+1}^i - t_k^i$, $j \in \mathcal{V}_i^{out}$ for all $k \in \mathbb{N}$, where τ_{mad}^i denotes the* maximum allowable delay.

The values of the delay Δ_k^{ij}, $i, j \in \mathcal{V}$, $k \in \mathbb{N}$, for which $j \notin \{p \in \mathcal{V}_i^{\text{out}} \mid z_i(k, \bar{e}_i(t_k^i), p) = 1\}$ have no physical meaning since for these cases, agent $\mathcal{A}_i$ does not transmit any information to agent $\mathcal{A}_j$ at transmission time t_k^i due to the communication topology specified by the communication graph $\mathcal{G}$ and/or the destination protocol given by z_i. Therefore, we simply take $\Delta_k^{ij} = 0$ for $i, j \in \mathcal{V}$ for which $j \notin \{p \in \mathcal{V}_i^{\text{out}} \mid z_i(k, \bar{e}_i(t_k^i), p) = 1\}$.

Remark 7.1. Destination protocols are modeled in a similar fashion as network scheduling protocols as described in [173, 245]. As such, we can be inspired by the framework presented in [173,245] for the design of destination protocols. For example, the destination protocols could be based on well-known network scheduling protocols such as the Sample-Data (SD), the Round-Robin (RR) and the Try-Once-Discard (TOD) protocol. The framework presented also allows to generate new classes of protocols that are meaningful in the context of multi-agent systems such as destination protocols that capture switching communication topologies.

In time periods in which agent $\mathcal{A}_j$ does not receive new information of agent $\mathcal{A}_i$, the estimate $\hat{y}_i^j$ evolves according to

$$\dot{\hat{y}}_i^j(t) = \hat{f}_i(\hat{y}_i^j(t)), \tag{7.7}$$

for all $t \in (t_k^i + \Delta_k^{ij}, t_{k+1}^i + \Delta_{k+1}^{ij})$, with $i \in \mathcal{V}$, $j \in \mathcal{V}_i^{\text{out}}$, $k \in \mathbb{N}$, where $\hat{f}_i : \mathbb{R}^{n_y} \to \mathbb{R}^{n_y}$ describes the holding device. Let us highlight that the setup described above allows for model-based networked control schemes in which, in between update events, the control input is computed by means of a model of the system, see, *e.g*, also [111,166,259]. As shown in [148,149], model-based control schemes also facilitate in consensus/synchronization problems.

Remark 7.2. Observe from (7.4) that since the sizes of the transmission delays are in general unknown, the estimate $\hat{y}_i^j$, $i \in \mathcal{V}$, $j \in \mathcal{V}_i^{\text{out}}$, is typically not available at agent $\mathcal{A}_i$. As such, in practice, it is in general not possible to implement a destination protocol that depends on $\bar{e}_i$ such as the TOD protocol. Let us remark, however, that in case zero-order hold (ZOH) devices are employed, *i.e.*, when $\hat{f}_i(\hat{y}_i^j) = 0$ for all $\hat{y}_i^j \in \mathbb{R}^{n_y}$, it is possible to practically implement protocols that depend on $\bar{e}_i$ as we will discuss later on.

7.3.3 Dynamic event-triggered communication

Conventional (digital) control schemes often employ a time-triggered execution of control tasks meaning that sampling instants of measurements are purely based on time, often according to a fixed sampling rate. Typically, this fixed sampling rate is determined *a priori* and therefore needs to be selected such that even for the worst-case situation, the system satisfies the desired closed-loop stability and performance criteria, see, *e.g.*, [51, 120, 173]. Hence, in these time-triggered control schemes transmission are generated irregardless the state system and therefore often lead to redundant utilization of communication resources. The latter is not desirable, in particular, when the communication resources are scarce such as, for instance, in networked control systems (NCSs).

In this work, we consider event-triggered control (ETC) schemes in which the transmission instants are determined based on state- or output measurements, see, *e.g.*, [15, 18, 20, 41, 72, 78, 165, 191, 224, 236] and the references therein. By

introducing this mechanism, the communication resources are only used when necessary to maintain desired closed-loop behaviour, which reduces the utilization of communication resources (and corresponding energy resources). In this chapter, we consider *dynamic* event-generators of the form as proposed in [72] that schedule transmission instants according to

$$t_0^i = 0,\, t_{k+1}^i := \inf\left\{t > t_k^i + \tau_{miet}^i \mid \eta_i(t) \leqslant 0\right\}, \tag{7.8}$$

for $i \in \mathcal{V}$ and $k \in \mathbb{N}$ and where $\eta_i \in \mathbb{R}$ is the triggering variable of agent $\mathcal{A}_i$ that evolves according to

$$\dot{\eta}_i(t) = \Psi_i(o_i(t)) - \sigma_i(\eta_i), \text{ when } \eta_i(t) \geqslant 0 \tag{7.9a}$$

$$\eta_i(t^+) = \eta_i^0(o_i(t)), \text{ when } \eta_i(t) = 0, \tag{7.9b}$$

where the functions $\Psi_i : \mathbb{O}_i \to \mathbb{R}$, $\sigma_i : \mathbb{R}_{\geqslant 0} \to \mathbb{R}_{\geqslant 0}$ and $\eta_i^0 : \mathbb{O}_i \to \mathbb{R}_{\geqslant 0}$ and the time constant τ_{miet}^i are to be properly designed as we discuss in Section 7.5. The variable o_i represents information locally available at agent $\mathcal{A}_i$, such as the output y_i, the local estimates $\hat{y}_j^i$, $j \in \mathcal{V}_i^{\text{in}}$, and the most recently transmitted output measurement. Note that the time constant τ_{miet}^i is an enforced lower bound on the inter-transmission times for agent $\mathcal{A}_i$ referred to as the *minimum inter-event time* (MIET). Clearly, we have that $t_{k+1}^i - t_j^i \geqslant \tau_{miet}^i$ and thus that Zeno-behaviour is excluded from the event-triggering mechanism (ETM). The latter property is obviously important to enable implementation of the ETC scheme in practice. In accordance with Assumption 7.1, we select $\tau_{miet}^i \geqslant \tau_{mad}^i$.

The ETM described by (7.8) and (7.9) is referred to as a *dynamic* ETM because the transmission instants are determined based on dynamic variables such as η_i in contrast to the commonly adopted *static* ETMs which rely on a static expression dependent on the locally available information o_i, see also [72, 96, 191]. Employing dynamic ETMs instead of static versions has several advantages including significant larger average inter-event times in many cases, see [72, 96] for more details.

As mentioned before, typically, the sizes of the transmission delays are time-varying and unknown. As a consequence, the estimate $\hat{y}_i^m$, $i \in \mathcal{V}$, $m \in \mathcal{V}_i^{\text{out}}$, as in (7.4) and (7.7), is not available at agent $\mathcal{A}_i$. To deal with the latter fact, each agent $\mathcal{A}_i$, $i \in \mathcal{V}$, keeps track of a local estimate of the information available at agent $\mathcal{A}_m$, $m \in \mathcal{V}_i^{\text{out}}$, regarding the local output y_i. We denote this local estimate with $\tilde{y}_i^m$. To be more specific, for all t_k^i, $k \in \mathbb{N}$, $i \in \mathcal{V}$, $\tilde{y}_i^m$, $m \in \mathcal{V}_i^{\text{out}}$, is updated according to

$$\tilde{y}_i^m({t_k^i}^+) = z_i(k, \bar{e}_i(t_k^i), j) y_i(t_k^i) + (1 - z_i(k, \bar{e}_i(t_k^i), j)) \tilde{y}_i^m(t_k^i), \tag{7.10}$$

and in between transmission instants, $\tilde{y}_i^m$ evolves according to

$$\dot{\tilde{y}}_i^m(t) = \hat{f}_i(\tilde{y}_i^m(t)), \tag{7.11}$$

for $t \in (t_k^i, t_{k+1}^i)$. It is important to note that the dynamics of $\tilde{y}_i^m$, $i \in \mathcal{V}$, $m \in \mathcal{V}_i^{\text{out}}$, are identical to the dynamics of $\hat{y}_i^m$ as described in (7.4) except from the fact that $\tilde{y}_i^m$ is immediately updated at a transmission instant. For this reason, we typically have that $\tilde{y}_i^m \neq \hat{y}_i^m$. Observe that in case communication delays are absent, *i.e.*, $\Delta_k^{ij} = 0$ for all $i \in \mathcal{V}$, $j \in \mathcal{V}_i^{\text{out}}$ and $k \in \mathbb{N}$, we have that $\tilde{y}_i^m = \hat{y}_i^m$.

Let us emphasize that the ETM of agent $\mathcal{A}_i$ described by (7.8) and (7.9) will *not* rely on the continuous availability of output measurements of other agents, *i.e.*, y_j, $j \in \mathcal{V}_i^{\text{in}}$, and will *not* require clock synchronization, acknowledgment signals that need to be transmitted and received instantaneously or knowledge about the sizes of the transmission delays.

7.3.4 Problem formulation

Given the descriptions above, the problem considered in this chapter can now be stated informally as follows.

Problem 7.1. *Consider a collection of agents $\mathcal{A}_1, \mathcal{A}_2, \ldots, \mathcal{A}_N$ described by (7.2) and a collection of maximum allowable delays τ_{mad}^i, $i \in \mathcal{V}$. Propose design conditions for the time constants $\tau_{miet}^i (\geqslant \tau_{mad}^i)$ and the functions z_i, Ψ_i and η_i^0, $i \in \mathcal{V}$, such that the control laws given by (7.3) and the ETM given by (7.8) and (7.9) result in a multi-agent system with the desired (and to be specified) closed-loop stability and robustness properties.*

As we will discuss in the next section, we will consider general dissipativity properties that can reflect a broad range of control objectives.

7.4 Mathematical formulation of the event-triggered multi-agent system

In this section, we formulate the event-triggered multi-agent system in terms of a hybrid model to facilitate the stability analysis in Section 7.5 and we formalize the problem stated at the end of Section 7.3.

7.4.1 Hybrid model

A hybrid model $\mathcal{H}(\mathcal{C}, F, \mathcal{D}, G)$ with state $\xi \in \mathbb{X}$ and disturbance $w \in \mathbb{R}^{n_w}$ describes the system in terms of flow and jump equations and takes the form

$$\dot{\xi} = F(\xi, w), \qquad \text{when } \xi \in \mathcal{C}, \tag{7.12a}$$

$$\xi^+ \in G(\xi), \qquad \text{when } \xi \in \mathcal{D}, \tag{7.12b}$$

where F and G denote the flow and the jump map, respectively, $\mathcal{C}$ and $\mathcal{D}$ the flow and the jump set, respectively, and where ξ^+ denotes the updated value of

ξ right after a jump, see [50, 98] for profound definitions regarding this hybrid modeling framework.

To model the updates (in terms of (7.12b)) of e_i^j at update times $t_k^i + \Delta_k^{ij}$, we first obtain from (7.4) and (7.6), that for all $i, j \in \mathcal{V}$ and $k \in \mathbb{N}$ for which $z_i(k, \bar{e}_i(t_k^i)), j) = 1$,

$$\begin{aligned} e_i^j((t_k^i + \Delta_k^{ij})^+) &= \hat{y}_i^j((t_k^i + \Delta_k^{ij})^+) - y_i((t_k^i + \Delta_k^{ij})^+) \\ &= y_i(t_k^i) - y_i(t_k^i + \Delta_k^{ij}). \end{aligned} \tag{7.13}$$

As in [72, 120], to capture the updates of e_i^j in terms of jump equations, we need to distinguish two types of jumps, namely, jumps corresponding to time instants at which an agent $\mathcal{A}_i$, $i \in \mathcal{V}$, transmits a new measurement to the agent(s) $\mathcal{A}_j$, $j \in \mathcal{V}_i^{\text{out}}$ (referred to as transmission events/jumps), and jumps corresponding to time instants at which an agent $\mathcal{A}_j$, $j \in \mathcal{V}_i^{\text{out}}$, receives a new measurement from agent $\mathcal{A}_i$, $i \in \mathcal{V}_j^{\text{in}}$ (referred to as update events/jumps). To keep track of these two jump types, we introduce auxiliary variables $l_i^j \in \{0, 1\}$, that indicate whether the *next* jump corresponds to the transmission of an output measurement by agent $\mathcal{A}_i$, $i \in \mathcal{V}$ ($l_i^j = 0$ for all $j \in \mathcal{V}$), or to the reception of an output measurement by agent $\mathcal{A}_j$ from agent $\mathcal{A}_i$ ($l_i^j = 1$). Moreover, we introduce memory variable $r_i \in \mathbb{R}^{n_y}$, $i \in \mathcal{V}$, to store the value of y_i at times t_k^i, $k \in \mathbb{N}$, *i.e.*, at each transmission instant t_k^i, we have that

$$r_i({t_k^i}^+) = y_i(t_k^i). \tag{7.14}$$

In between transmissions, the variable r_i is held constant, *i.e.*,

$$\dot{r}_i = 0 \tag{7.15}$$

for all $t \in (t_k^i, t_{k+1}^i)$, $i \in \mathcal{V}$ and $k \in \mathbb{N}$. Given the description above, the update of e_i^j, $i \in \mathcal{V}$, $j \in \mathcal{V}_i^{\text{out}}$, as described in (7.13) can be rewritten as

$$e_i^j((t_k^i + \Delta_k^{ij})^+) = r_i(t_k + \Delta_k^{ij}) - y_i(t_k + \Delta_k^{ij}). \tag{7.16}$$

To secure that Assumption 7.1 holds and to keep track of the time elapsed since the most recent transmission, we adopt the timer variable $\tau_i \in \mathbb{R}_{\geqslant 0}$, $i \in \mathcal{V}$. To be more concrete, τ_i, $i \in \mathcal{V}$, represents the time elapsed since the most recent transmission instant of agent $\mathcal{A}_i$, *i.e.*, $\tau_i = \inf_{\{k \in \mathbb{N} | t_k^i < t\}}(t - t_k^i)$. Moreover, we let $\kappa_i \in \mathbb{N}$ denote the transmission counter of agent $\mathcal{A}_i$. Observe that the state variables e_i^j and l_i^j, $i \in \mathcal{V}$, $j \notin \mathcal{V}_i^{\text{out}}$, are in principle redundant due to the communication topology. However, for notational consistency and simplicity, we keep these variables in the hybrid model presented next.

To write the entire multi-agent system in the form as given in (7.12), consider the state vector $\xi := (x, e, \tau, \kappa, r, \tilde{y}, l, \eta) \in \mathbb{X}$ with $\mathbb{X} := \Big\{(x, e, \tau, \kappa, r, \tilde{y}, l, \eta) \in$

$\mathbb{R}^{n_x} \times \mathbb{R}^{N^2 n_y} \times \mathbb{R}^N_{\geqslant 0} \times \mathbb{N}^N \times \mathbb{R}^{N n_y} \times \mathbb{R}^{N^2 n_y} \times \{0,1\}^{N^2} \times \mathbb{R}^N_{\geqslant 0} \mid \forall i,j \in \mathcal{V}, ((l_i^j = 0) \vee (l_i^j = 1 \wedge \tau_i \in [0, \tau_{mad}^i]))\Big\}$, where $\tau = (\tau_1, \tau_2, \ldots, \tau_N) \in \mathbb{R}^N_{\geqslant 0}$, $\kappa = (\kappa_1, \kappa_2, \ldots, \kappa_N) \in \mathbb{N}^N$, $r = (r_1, r_2, \ldots, r_N) \in \mathbb{R}^{N n_y}$, $\tilde{y} = (\tilde{y}_1^1, \tilde{y}_2^1, \ldots, \tilde{y}_N^1, \tilde{y}_1^2, \tilde{y}_2^2, \ldots, \tilde{y}_N^N) \in \mathbb{R}^{N^2 n_y}$, $l = (l_1^1, l_2^1, \ldots, l_N^1, l_1^2, l_2^2, \ldots, l_N^N) \in \{0,1\}^{N^2}$ and $\eta = (\eta_1, \eta_2, \ldots, \eta_N) \in \mathbb{R}^N_{\geqslant 0}$. The flow map $F : \mathbb{X} \times \mathbb{R}^{n_w} \to \mathbb{Y}$ with $\mathbb{Y} := \mathbb{R}^{n_x} \times \mathbb{R}^{N^2 n_y} \times \mathbb{R}^N_{\geqslant 0} \times \mathbb{N}^N \times \mathbb{R}^{N n_y} \times \mathbb{R}^{N^2 n_y} \times \{0,1\}^{N^2} \times \mathbb{R}^N_{\geqslant 0}$, is given by

$$F(\xi, w) := \big(f(x,e,w), g(x,e,w), \mathbf{1}_N, \mathbf{0}_N, \mathbf{0}_{N^2 n_y}, \hat{f}(\tilde{y}), \mathbf{0}_{N^2}, \Psi(y, \hat{y}, \tilde{y}, e, \tau) - \sigma(\eta)\big), \quad (7.17)$$

where $\hat{f}(\tilde{y}) = (\hat{f}_1(\tilde{y}_1^1), \hat{f}_2(\tilde{y}_2^1), \ldots, \hat{f}_N(\tilde{y}_N^1), \hat{f}_1(\tilde{y}_1^2), \hat{f}_2(\tilde{y}_2^2), \ldots, \hat{f}_N(\tilde{y}_N^N))$. Based on (7.2) and (7.3), we define $f(x,e,w) := (f_1(x, e^1, w), f_2(x, e^2, w), \ldots, f_N(x, e^N, w))$ with $x = (x_{p,1}, x_{c,1}, x_{p,2}, x_{c,2}, \ldots, x_{p,N}, x_{c,N})$ and

$$f_i(x, e^i, w) := \begin{bmatrix} f_{p,i}(x_p, g_{c,i}(x_{c,i}, g_{p,i}(x_{p,i}), g_p(x_p) + e^i), w) \\ f_{c,i}(x_{c,i}, g_{p,i}(x_{p,i}), g_p(x_p) + e^i) + e^i) \end{bmatrix}. \quad (7.18)$$

According to (7.6), we have that $\dot{e}_i^j = \dot{\hat{y}}_i^j - \dot{y}_i$. By combining the latter with (7.2), (7.3) and (7.7), we obtain that $g(x,e,w) := (g_1^1(x,e,w)), g_2^1(x,e,w)), \ldots, g_N^1(x,e,w), g_1^2(x,e,w), g_2^2(x,e,w), \ldots, , g_N^N(x,e,w))$ where

$$g_i^j(x,e,w) := \hat{f}_i(g_{p,i}(x_{p,i}) + e_i^j) + f_{y,i}^j(x, e^i, w) \quad (7.19)$$

with

$$f_{y,i}^j(x, e^i, w) := -\frac{\partial g_{p,i}}{\partial x_{p,i}} f_{p,i}(x_p, g_{c,i}(x_{c,i}, g_{p,i}(x_{p,i}), g_p(x_p) + e^i), w). \quad (7.20)$$

Observe that $f_{y,i}^j$ is such that $f_{y,i}^j(x, e^i, w) = -\dot{y}_i$. The functions $\Psi(y, \hat{y}, \tilde{y}, e, \tau) = (\Psi_1(o_1), \Psi_2(o_2), \ldots, \Psi_N(o_N))$ with Ψ_i, $i \in \mathcal{V}$, as in (7.9) and $o_i = (y_i, \hat{y}^i, \bar{\tilde{y}}_i, \bar{e}_i, \tau_i)$, where $\bar{\tilde{y}}_i := (\delta_i(1)\tilde{y}_i^1, \delta_i(2)\tilde{y}_i^2, \ldots, \delta_i(N)\tilde{y}_i^N) \in \bar{\mathbb{E}}_i \subseteq \mathbb{R}^{N n_y}$ with $\delta_i(j)$, $j \in \mathcal{V}$ as in 7.5, and $\sigma(\eta) = (\sigma_1(\eta_1), \sigma_2(\eta_2), \ldots, \sigma_N(\eta_N))$ with $\sigma_i \in \mathcal{K}_\infty$, are to be designed.

The flow set $\mathcal{C} \subseteq \mathbb{X}$ can be derived from (7.9) and Assumption 7.1, and is given by $\mathcal{C} := \bigcap_{i,j \in \mathcal{V}} \mathcal{C}_{i,j}$ with

$$\mathcal{C}_{i,j} := \Big\{\xi \in \mathbb{X} \mid \Big(l_i^j = 0\Big) \vee \Big(0 \leqslant \tau_i \leqslant \tau_{mad}^i \wedge l_i^j = 1\Big)\Big\}. \quad (7.21)$$

Let us emphasize that the triggering condition in (7.8) is embedded via the definition of $\mathbb{X}$ (note that $\xi \in \mathbb{X}$ implies $\eta_i \geqslant 0$ for all $i \in \mathcal{V}$).

To describe the jump map $G : \mathbb{X} \rightrightarrows \mathbb{Y}$, we define Γ_i as a $N \times N$ matrix of which the ii-th (diagonal) entry is equal to one and all other entries are zero, $\tilde{\Gamma}_i(\kappa_i, \bar{e}_i) := (Z_i(\kappa_i, \bar{e}_i) \otimes \Gamma_i)$ with $Z_i(\kappa_i, \bar{e}_i) := \mathrm{diag}(z_i(\kappa_i, \bar{e}_i, 1), z_i(\kappa_i, \bar{e}_i, 2), \ldots,$

$z_i(\kappa_i, \bar{e}_i, N))$ and $\Gamma_{i,j} := \Gamma_j \otimes \Gamma_i$. Given these definitions, we obtain the jump map $G(\xi) = \bigcup_{i\in\mathcal{V}} \bigcup_{j\in\mathcal{V}} G_{i,j}(\xi)$, where

$$G_{i,j}(\xi) := \begin{cases} \{G_i^0(\xi)\}, & \text{when } \xi \in D_{i,j} \wedge l_i^j = 0 \\ \{G_{i,j}^1(\xi)\}, & \text{when } \xi \in D_{i,j} \wedge l_i^j = 1 \\ \emptyset, & \text{when } \xi \notin D_{i,j} \end{cases} \tag{7.22}$$

with

$$\begin{aligned} G_i^0(\xi) := \big(x, e, (I_N - \Gamma_i)\tau, \kappa + \Gamma_i \mathbf{1}_N, (\Gamma_i \otimes I_{n_y})y + (I_{Nn_y} - \Gamma_i \otimes I_{n_y})r, \\ (\tilde{\Gamma}_i(\kappa_i, \bar{e}_i) \otimes I_{n_y})(\mathbf{1}_N \otimes y) + (I_{N^2 n_y} - \tilde{\Gamma}_i(\kappa_i, \bar{e}_i)) \otimes I_{n_y})\tilde{y}, \\ l + \tilde{\Gamma}_i(\kappa_i, \bar{e}_i)\mathbf{1}_{N^2}, \Gamma_i \eta_i^0(o_i) + (I - \Gamma_i)\eta\big) \end{aligned} \tag{7.23}$$

and

$$\begin{aligned} G_{i,j}^1(\xi) := \big(x, (\Gamma_{i,j} \otimes I_{n_y})(\mathbf{1}_N \otimes r - e - \mathbf{1}_N \otimes y) + e, \\ \tau, \kappa, r, \tilde{y}, l - \Gamma_{i,j}\mathbf{1}_{N^2}, \eta\big). \end{aligned} \tag{7.24}$$

The function G_i^0, $i \in \mathcal{V}$ describes the jump of the state ξ at transmission events of agent $\mathcal{A}_i$. Observe that for this case, $\tilde{y}_i^j$ and r_i are set to y_i for all $i \in \mathcal{V}$ and all $j \in \mathcal{V}$ for which $z_i(\kappa_i, \bar{e}_i, j) = 1$, as described in (7.10) and (7.14), respectively. Moreover, observe that $l_i^{j^+} = 1$, for all $i \in \mathcal{V}$, and $j \in \mathcal{V}_i^{\text{out}}$ for which $z_i(\kappa_i, \bar{e}_i, j) = 1$. The latter ensures that first update events occur, *i.e.* that the broadcast information of agent $\mathcal{A}_i$, $i \in \mathcal{V}$, is received by all targeted agents, before the next transmission is scheduled.

The function $G_{i,j}^1$, $i \in \mathcal{V}$, $j \in \mathcal{V}_i^{\text{out}}$, describes the jump of the state ξ at update events at agent $\mathcal{A}_j$ due to a transmission/broadcast of agent $\mathcal{A}_i$. Observe that indeed, e_i^j is set to $r_i - y_i$ as described in (7.16). Moreover, observe that l_i^j is set back to 0.

The jump set $\mathcal{D} \subseteq \mathbb{X}$ is given by $\mathcal{D} := \bigcup_{i\in\mathcal{V}} \bigcup_{j\in\mathcal{V}_i^{\text{out}}} \mathcal{D}_{i,j}$, where

$$\mathcal{D}_{i,j} := \Big\{\xi \in \mathbb{X} \mid \Big(\tau_i \geqslant \tau_{miet}^i \wedge \eta_i = 0 \wedge l_i^j = 0\Big) \vee \Big(l_i^j = 1\Big)\Big\}. \tag{7.25}$$

By means of (7.17)-(7.25), we define the hybrid model $\mathcal{H}(\mathcal{C}, F, \mathcal{D}, G)$ of the form (7.12).

7.4.2 Mathematical problem formulation

To specify the various desired stability and performance properties in a general sense, we introduce the following definitions that use the concepts of *hybrid time domains*, *hybrid inputs*, corresponding *solution pairs* and *maximal solutions*, see [50, 98] for more details.

Definition 7.1. *Given any hybrid input $w : dom\ w \to \mathbb{R}^{n_w}$. Define $\|w\|_\infty := \sup_{j\in\mathbb{N}} \left(\operatorname{ess\,sup}_{\{t\in\mathbb{R}|(t,j)\in dom\ w\}} |w(t,j)|\right)$. A hybrid input is said to be of class $\mathcal{L}_\infty^{n_w}$ if $w(t,j) \in \mathbb{R}^{n_w}$ for all $(t,j) \in dom\ w$ and $\|w\|_\infty < \infty$.*

Definition 7.2. *The hybrid system $\mathcal{H}$ is said to be* persistently flowing *if all maximal solution pairs (ξ, w) with $\xi(0,0) \in \mathcal{C} \cup \mathcal{D}$ and $w \in \mathcal{L}_\infty^{n_w}$ have unbounded domains in the t-direction, i.e.,* $\sup_t dom\ \xi = \infty$.

Definition 7.3. *The system $\mathcal{H}$ is said to be* flow-dissipative *with respect to the supply rate $\tilde{s}\mathbb{X} \times \mathbb{R}^{n_w} \to \mathbb{R}$ if there exists a locally Lipschitz function $U : \mathbb{X} \to \mathbb{R}_{\geqslant 0}$, referred to as the storage function, such that*

1. *for almost all $\xi \in \mathcal{C}$*
$$\langle \nabla U, F(\xi, w)\rangle \leqslant \tilde{s}(\xi, w) \tag{7.26a}$$
2. *for all $\xi \in \mathcal{D}$*
$$U(G(\xi)) - U(\xi) \leqslant 0. \tag{7.26b}$$

Problem 1 can now be formalized as follows.

Problem 7.2. *Given the event-triggered MAS represented by $\mathcal{H}(\mathcal{C}, F, \mathcal{D}, G)$ with data F, G, $\mathcal{C}$ and $\mathcal{D}$ as described in (7.17)-(7.25), the functions z_i, $i \in \mathcal{V}$, as in (7.4) and maximum allowable delays τ_{mad}^i, $i \in \mathcal{V}$. Provide design conditions for the time-constants $\tau_{miet}^i \in \mathbb{R}_{>0}$ with $\tau_{miet}^i \geqslant \tau_{mad}^i$ and the functions Ψ_i and η_i^0 as in (7.8) and (7.9), for $i \in \mathcal{V}$, such that, under Assumption 1, the system $\mathcal{H}$ is persistently flowing and flow-dissipative with respect to the supply rate $\tilde{s} : \mathbb{X} \times \mathbb{R}^{n_w} \to \mathbb{R}$ given for $\xi \in \mathbb{X}$ and $w \in \mathbb{R}^{n_w}$ by*

$$\tilde{s}(x, e, w, \eta) := s(x, e, w) - \sigma\eta. \tag{7.27}$$

As shown in, for example, [80, 170, 241, 254], the dissipation inequalities in (7.26) allow to consider various system properties such as asymptotic stability, input-to-state stability, $\mathcal{L}_p$-stability with $p \in [1, \infty)$ and passivity, from a common point of view. Hence, Problem 7.2 captures a wide range of relevant multi-agent/distributed control problems addressed in the literature including output-regulation problems (of which the consensus-seeking problem is a particular case) and vehicle-platooning problems (in which $\mathcal{L}_p$-contractivity, $p \in [1, \infty)$, is of interest).

To illustrate the latter, we discuss the case of input-to-state stability. Consider the following definitions.

Definition 7.4. *A nonempty closed set $\mathcal{A} \subset \mathbb{X}$ is* input-to-state stable *(ISS) for the hybrid system $\mathcal{H}$ from input w to state ξ, if it is persistently flowing and there exist functions $\beta \in \mathcal{KL}$ and $\gamma \in \mathcal{K}$ such that for any initial condition $\xi(0,0) \in \mathcal{C} \cup \mathcal{D}$, every solution pair (ξ, w) to $\mathcal{H}$ with $w \in \mathcal{L}_\infty^{n_w}$ satisfies*

$$|\xi(t,j)|_{\mathcal{A}} \leqslant \max\{\beta(|\xi(0,0)|_{\mathcal{A}}, t), \gamma(\|w\|_\infty)\} \tag{7.28}$$

for all $(t,j) \in dom\ \xi$.

As shown in [50], the existence of an ISS Lyapunov function, as defined below, implies ISS of system. Inspired by [50], we consider the following definition.

Definition 7.5. *Let $U^* : \mathbb{X} \to \mathbb{R}_{\geqslant 0}$ be a locally Lipschitz function. Consider system (7.12). Under the assumption that* (7.12) *is persistently flowing, we call a function U^* an ISS Lyapunov function for the system* (7.12) *with respect to the nonempty closed set $\mathcal{A} \subset \mathbb{X}$ and input w if the function is proper with respect to $\mathcal{A}$ and if there exist $\alpha, \underline{\alpha}, \bar{\alpha} \in \mathcal{K}_\infty$ and $\gamma \in \mathcal{K}$ such that*

1. *for almost all $\xi \in \mathcal{C}$,*

$$\langle \nabla U^*, F(\xi, w) \rangle \leqslant -\alpha(|\xi|_{\mathcal{A}}) + \gamma(|w|) \tag{7.29a}$$

2. *for all $\xi \in \mathcal{D}$,*

$$U^*(G(\xi)) - U^*(\xi) \leqslant 0. \tag{7.29b}$$

Observe that the condition in (7.29) is equivalent to (7.26) for U proper and $\tilde{s}(\xi, w) = -\alpha(|\xi|_{\mathcal{A}}) + \gamma(|w|)$. Let us remark that in case no disturbances are present, *i.e.*, when $w(t, j) = 0$ for all $(t, j) \in \operatorname{dom} \xi$ and that $\mathcal{A} = \{\xi \in \mathbb{X} \mid e = 0, \eta = 0, x_i = x_j \text{ for all } i, j \in \mathcal{V}\}$, we obtain conditions for asymptotic consensus, see also [179, 196].

Remark 7.3. Since we are interested in persistently flowing systems as these are often relevant from a physical point of view, we weakened the ISS conditions provided in [50], see also [192] and [98, Proposition 3.27].

7.5 Design conditions and main result

In this section, we present design conditions for the destination protocol z_i, the time constants τ^i_{miet}, τ^i_{mad} and the functions Ψ_i and η^0_i, $i \in \mathcal{V}$. At the end of the section, we present the main result of the chapter.

7.5.1 Design of the destination protocols

As already mentioned in Remark 7.1, the destination protocols considered in this chapter can be modeled in a similar fashion as the network scheduling protocols as described in [51, 173]. As such, we can exploit the conditions on network protocols as introduced in [51, 173] for the design of suitable destination protocols. Thereto, let $h_i(k, \bar{e}_i) := \Big((1 - z_i(k, \bar{e}_i, 1))e^1_i, (1 - z_i(k, \bar{e}_i, 2))e^2_i, \ldots, (1 - z_i(k, \bar{e}_i, N))e^N_i\Big)$ for all $a \in \mathbb{R}^{n_y}$ and $k \in \mathbb{N}$. Consider the following condition.

Condition 7.1. *[51, 173] A destination protocol $z_i : \mathbb{N} \times \mathbb{R}^{Nn_y} \times \mathcal{V} \to \{0, 1\}$, $i \in \mathcal{V}$, is said to be* uniformly globally exponentially *stable (UGES) if there*

exists a Lyapunov function $W_i : \mathbb{N} \times \mathbb{R}^{Nn_y} \to \mathbb{R}_{\geqslant 0}$ *that is locally Lipschitz in its second argument such that for all* $k \in \mathbb{N}$ *and all* $\bar{e}_i \in \mathcal{E}_i$ *it holds that*

$$\underline{\alpha}_{W,i}|\bar{e}_i| \leqslant W_i(k, \bar{e}_i) \leqslant \bar{\alpha}_{W,i}|\bar{e}_i| \tag{7.30a}$$

$$W_i(k+1, h_i(k, \bar{e}_i)) \leqslant \lambda_i W_i(k, \bar{e}_i) \tag{7.30b}$$

for constants $0 < \underline{\alpha}_{W,i} \leqslant \bar{\alpha}_{W,i}$ *and any* $0 < \lambda_i < 1$.

As shown in [173], the condition above is equivalent to the UGES property of the following discrete-time system

$$q(k+1) = h_i(k, q),\ k \in \mathbb{N}, \tag{7.31}$$

where $q \in \mathbb{R}^{Nn_y}$. Hence, Condition 7.1 is only related to the destination protocol and not to the other dynamics of the system. In fact, in case the system described by (7.31) is UGES for a given protocol z_i, the corresponding Lyapunov function W_i satisfying (7.30a) and (7.30b) can be specified as

$$W_i(k, \bar{e}_i) = \sqrt{\sum_{m=k}^{\infty} |\psi(m, k, \bar{e}_i)|^2}, \tag{7.32}$$

where $\psi(m, k, \bar{e}_i)$ denotes the solution of (7.31) at discrete time instant m with initial condition $\bar{e}_i$ and initial time k, see also [173, Proposition 3].

The well-known Round-Robin (RR) protocol and Try-Once-Discard (TOD) protocol but also many other protocols are known to be UGES protocols as well, see also [120,173]. For a TOD protocol, we can take the function $W_{i,TOD}(\kappa_i, e_i) = |e_i|$, for which (7.30a) holds with $\underline{\alpha}_{W,i,TOD} = \bar{\alpha}_{W,i,TOD} = 1$ and (7.30b) with $\lambda_{i,TOD} = \sqrt{(N_i - 1)/N_i}$. For the RR protocol, there exists a function $W_{i,RR}$ that satisfies (7.30a) with $\underline{\alpha}_{W,i,RR} = 1$ and $\bar{\alpha}_{W,i,RR} = \sqrt{N_i}$, and (7.30b) with $\lambda_{i,RR} = \sqrt{(N_i - 1)/N_i}$, see [173] for more details. For the sampled-data (SD) protocol, corresponding to the case that at each transmission instant an agent $\mathcal{A}_i$, $i \in \mathcal{V}$ broadcasts its output measurement to all connected agents $\mathcal{A}_j$, $j \in \mathcal{V}_i^{\text{out}}$, we can take $W_i(k, \bar{e}_i) = |\bar{e}_i|$, $\underline{\alpha}_{W,i} = \bar{\alpha}_{W,i} = 1$ and $\lambda_i > 0$.

Next to Condition 7.1, we also consider the following condition.

Condition 7.2. *([72, 120]) For each* $i \in \mathcal{V}$ *and for all* $k \in \mathbb{N}$, $\bar{e}_i \in \mathcal{E}_i$

$$W_i(k+1, \bar{e}_i) \leqslant \lambda_{W,i} W_i(k, \bar{e}_i) \tag{7.33}$$

for some constant $\lambda_{W,i} \geqslant 1$, *and that for almost all* $e_i^j \in \mathbb{R}^{n_y}$ *and all* $i \in \mathcal{V}$, $j \in \mathcal{V}_i^{out}$ *and* $k \in \mathbb{N}$

$$\left| \frac{\partial W_i(k, \bar{e}_i)}{\partial \bar{e}_i} \right| \leqslant c_i \tag{7.34}$$

for some constant $c_i \in \mathbb{R}_{>0}$. *Moreover, for each* $i \in \mathcal{V}$, *there exist functions* $H_{e,i} : \mathbb{R}^{n_x} \times \mathbb{R}^{Nn_y} \times \mathbb{R}^{n_w} \to \mathbb{R}_{\geqslant 0}$ *and* $H_{y,i} : \mathbb{R}^{n_x} \times \mathbb{R}^{Nn_y} \times \mathbb{R}^{n_w} \to \mathbb{R}_{\geqslant 0}$ *and constants* $L_{1,i}, L_{2,i} > 0$ *such that for all* $j \in \mathcal{V}_i^{out}$, $x \in \mathbb{R}^{n_x}$, $e \in \mathbb{R}^{N^2 n_y}$ *and* $w \in \mathbb{R}^{n_w}$, *it holds that*

$$c_i |g_i^j(x, e, w)| \leqslant H_{e,i}(x, e^i, w) + L_{1,i}|e_i^j| + L_{2,i}|e_i^i|, \tag{7.35}$$

and

$$c_i |f_{y,i}^j(x, e^i, w)| \leqslant H_{y,i}(x, e^i, w) + L_{2,i}|e_i^i| \tag{7.36}$$

with the functions g_i^j *and* $f_{y,i}^j$ *as in (7.19) and (7.20), respectively.*

Observe that (7.33) and (7.34) are only related to the destination protocol z_i. For the TOD, RR and SD protocol, we can take $\lambda_{W,i,TOD} = 1$, $c_{i,TOD} = 1$, $c_{i,RR} = \sqrt{N_i}$, $\lambda_{W,i,RR} = \sqrt{N_i}$ and $c_{i,SD} = 1$, $\lambda_{W,i,SD} = 1$, respectively.

7.5.2 Lower-bounds on the minimum inter-event times and maximum allowable delays

To obtain the lower-bounds on the minimum inter-event time and the maximum allowable delay for each agent $\mathcal{A}_i$, $i \in \mathcal{V}$, we first characterize the influence of the transmission errors e_i^j, $j \in \mathcal{V}_i^{\text{out}}$, on the state x and the desired stability/performance property by means of the following condition.

Condition 7.3. *There exist a proper locally Lipschitz function* $V : \mathbb{R}^{n_x} \to \mathbb{R}_{\geqslant 0}$, *functions* $\varrho_i : \mathbb{R}^{n_y} \times \mathbb{R}^{Nn_y} \to \mathbb{R}_{\geqslant 0}$, *constants* $\gamma_{\ell,i} > 0$, $\ell \in \{0, 1\}$, *such that for all* $e \in \mathbb{R}^{N^2 n_y}$, $w \in \mathbb{R}^{n_w}$, $\kappa \in \mathbb{N}^N$, $l \in \{0, 1\}^{N^2}$, *and almost all* $x \in \mathbb{R}^{n_x}$

$$\langle \nabla V(x), f(x, e, w) \rangle \leqslant s(x, e, w) + \sum_{i \in \mathcal{V}} \Big(- \varrho_i(g_{y,i}(x), g_y(x) + e^i) - N_i H_i^2(x, e^i, w, l_i) + \gamma^2_{\bar{l}_i(l_i),i} W_i^2(\kappa_i, \bar{e}_i) \Big) \tag{7.37}$$

with $l_i := (l_i^1, l_i^2, \ldots l_i^N)$ *and* $s(x, e, w)$ *as in (7.27), where the function* $H_i : \mathbb{R}^{n_x} \times \mathbb{R}^{Nn_y} \times \mathbb{R}^{n_w} \times \{0, 1\}^N \to \mathbb{R}_{\geqslant 0}$ *is given by*

$$H_i(x, e^i, w, l_i) := \max\{H_{e,i}(x, e^i, w), \tilde{l}_i(l_i) H_{y,i}(x, e^i, w)\}, \tag{7.38}$$

with the functions $H_{e,i}$ *and* $H_{y,i}$ *as in (7.35) and (7.36), respectively, and where the function* $\tilde{l}_i : \{0, 1\}^N \to \{0, 1\}$ *is given by*

$$\tilde{l}_i(l_i) := \begin{cases} 0, & \text{when } \sum_{j \in \mathcal{V}_i^{out}} l_i^j = 0 \\ 1, & \text{when } \sum_{j \in \mathcal{V}_i^{out}} l_i^j > 0. \end{cases} \tag{7.39}$$

In essence, (7.37) constitutes a dissipation inequality for the system $\dot{x} = f(x, e, w)$ and, in particular, an $\mathcal{L}_2$-gain condition from $(W_1, W_2, \ldots, W_N)$ to $(H_1, H_2, \ldots, H_N)$. The constants $\gamma_{\ell,i}$, $\ell \in \{0, 1\}$, resulting from this inequality indicate the influence of the transmission errors e_i^j, $j \in \mathcal{V}_i^{\text{out}}$, on the state x and the desired stability/performance property. The constants $\gamma_{\ell,i}$, $\ell \in \{0, 1\}$ are used to determine τ_{miet}^i and τ_{mad}^i, $i \in \mathcal{V}$, via the following condition.

Condition 7.4. *There exist positive real constants τ_{miet}^i and τ_{mad}^i, $i \in \mathcal{V}$, with $\tau_{miet}^i \geqslant \tau_{mad}^i$ satisfying*

$$\tilde{\gamma}_i(0)\phi_{0,i}(\tau_{miet}^i) \geqslant \lambda_i^2 \tilde{\gamma}_i(1)\phi_{1,i}(0), \tag{7.40}$$

$$\tilde{\gamma}_i(1)\phi_{1,i}(\tau_i) \geqslant \tilde{\gamma}_i(0)\phi_{0,i}(\tau_i), \text{ for all } \tau_i \in [0, \tau_{mad}^i], \tag{7.41}$$

where $\phi_{\ell,i}$, $\ell \in \{0, 1\}$, evolve according to

$$\frac{d}{d\tau_i}\phi_{\ell,i} = -\left(2\tilde{L}_i(\ell)\phi_{\ell,i} + \tilde{\gamma}_i(\ell)(\phi_{\ell,i}^2 + 1)\right), \tag{7.42}$$

for some fixed initial conditions $\phi_{\ell,i}(0)$, $\ell \in \{0, 1\}$, that satisfy $\gamma_i(1)\phi_{1,i}(0) \geqslant \gamma_i(0)\phi_{0,i}(0) > \lambda_i^2\gamma_i(1)\phi_{1,i}(0) > 0$, where the function $\tilde{L}$ and the constants $\gamma_{0,i}$ and $\gamma_{1,i}$ are given by

$$\tilde{L}_i(\ell) := \underline{\alpha}_{W,i}^{-1}\zeta_i^{-\ell} \max\left\{L_{1,i}, \sqrt{N_i}L_{2,i}\right\}, \tag{7.43}$$

$$\tilde{\gamma}_i(\ell) := \zeta_i^{-\ell}\gamma_{\ell,i} \tag{7.44}$$

with $\zeta_i := \frac{\lambda_i}{\lambda_{W,i}} \frac{\underline{\alpha}_{W,i}}{\overline{\alpha}_{W,i}}$ and where $\gamma_{\ell,i}$ satisfies Condition 3 and with λ_i as in (7.30b).

Condition 7.3 and Condition 7.4 might seem difficult to satisfy at first sight. However, the conditions above can be obtained systematically for, *e.g.*, systems with linear plant and controller dynamics. In fact, we will show that, in a similar fashion as in [120], the result above leads to intuitive trade-off curves between τ_{mad}^i and τ_{miet}^i, which can be used to find appropriate values for λ_i, $\phi_{0,i}(0)$ and $\phi_{1,i}(0)$, $i \in \mathcal{V}$.

Remark 7.4. Observe from (7.42) that $\frac{d}{d\tau_i}\phi_{\ell,i}(\tau_i) < 0$, $\ell \in \{0, 1\}$ for $\tau_i \in [0, \tau_{miet}^i]$, (since $\phi_{\ell,i}(\tau_i) > 0$ for $\tau_i \in [0, \tau_{miet}^i]$), and that a larger γ_i leads to faster decay of $\phi_{\ell,i}$. By combining (7.40) and (7.41) with the latter fact, we can see that larger γ_i leads to less favorable $(\tau_{mad}^i, \tau_{miet}^i)$-combinations.

7.5.3 Event-triggering mechanism design

The dynamics of the triggering variables η_i, $i \in \mathcal{V}$, which, according to (7.8), are used to determine the transmission instants, are defined by the functions Ψ_i

and η_i^0. For all $(t,j) \in \operatorname{dom} \xi$, the functions $\Psi_i : \mathbb{O} \to \mathbb{R}$ and $\eta_i^0 : \mathbb{O} \to \mathbb{R}_{\geqslant 0}$, $i \in \mathcal{V}$, as in (7.9), are given by

$$\begin{aligned}\Psi_i(o_i(t,j)) &:= \varrho_i(y_i(t,j), \hat{y}^i(t,j)) \\ &\quad - (1-\omega_i(\tau_i(t,j)))\bar{\gamma}_i \sum_{j \in \mathcal{V}_i^{\text{out}}} \max_{\tau \in [0,\tau_{mad}^i]} |\tilde{y}_i^j(t-\tau,j) - y_i(t,j)|^2 \end{aligned} \tag{7.45}$$

and

$$\eta_i^0(o_i(t,j)) := \varepsilon_\eta \sum_{j \in \mathcal{V}_i^{\text{out}}} \min_{\tau \in [0,\tau_{mad}^i]} |\tilde{y}_i^j(t-\tau,j) - y_i(t,j)|^2 \tag{7.46}$$

with $\varepsilon_\eta := \underline{\alpha}_{W,i}\left(\tilde{\gamma}_i(0)\phi_{0,i}(\tau_{miet}^i) - \tilde{\gamma}_i(1)\phi_{1,i}(0)\lambda_i^2\right)$, respectively, where

$$\omega_i(\tau_i) := \begin{cases} 1, & \text{for } \tau_i \in [0, \tau_{miet}^i] \\ 0, & \text{for } \tau_i > \tau_{miet}^i, \end{cases} \tag{7.47}$$

and where

$$\bar{\gamma}_i := \overline{\alpha}_{W,i}\tilde{\gamma}_i(0)\Big(2\tilde{L}_i(0)\phi_{0,i}(\tau_{miet}) + \tilde{\gamma}_i(0)(1+\phi_{0,i}^2(\tau_{miet}))\Big). \tag{7.48}$$

Observe that the constant λ_i and the function ϱ_i, $i \in \mathcal{V}$, are part of the ETM described by (7.8), (7.9), (7.45) and (7.46). Hence, the design of λ_i and ϱ_i have a significant influence on the average inter-event times generated by this ETM.

Remark 7.5. In case ZOH devices are employed, *i.e.*, in case $\dot{\hat{y}}_i^j(t,j) = 0$, when $\xi \in \mathcal{C}$ for all $i \in \mathcal{V}$, $j \in \mathcal{V}_i^{\text{out}}$, it holds that $\hat{y}_i^j(t,j) = \tilde{y}_i^j(t,j)$ for all $(t,j) \in \operatorname{dom} \xi$ for which $\tau_i(t,j) \geqslant \tau_{miet}^i$ due to Assumption 7.1. As such, for this case, we can choose the functions Ψ_i and η_i^0 as

$$\begin{aligned}\Psi_i(o_i(t,j)) &:= \varrho_i(y_i(t,j), \hat{y}_i(t,j)) \\ &\quad - (1-\omega_i(\tau_i(t,j)))\bar{\gamma}_i \sum_{j \in \mathcal{V}_i^{\text{out}}} |\tilde{y}_i^j(t,j) - y_i(t,j)|^2, \end{aligned} \tag{7.49}$$

and

$$\eta_i^0(o_i(t,j)) := \varepsilon_\eta \sum_{j \in \mathcal{V}_i^{\text{out}}} |\tilde{y}_i^j(t,j) - y_i(t,j)|^2. \tag{7.50}$$

In addition, as already mentioned in Remark 7.2, note that for the ZOH case, it is indeed possible to practically implement destination protocols that explicitly depend on $\bar{e}_i$ since $\hat{y}_i^j(t,j)$ is known for all $(t,j) \in \operatorname{dom} \xi$ for which $\tau_i(t,j) \geqslant \tau_{miet}^i$.

Remark 7.6. The event-triggering condition presented in (7.8) can be modified to a *static* event-triggered condition by taking

$$t_0^i = 0,\ t_{k+1}^i := \inf\left\{t > t_k^i + \tau_{miet}^i \mid \Psi_i(o_i) \leqslant 0\right\}. \tag{7.51}$$

This modification does not affect the stability and/or performance guarantees.

7.5.4 Main result

Given the conditions and the ETM design presented above, we can now state the following result.

Theorem 7.1. *Consider the system $\mathcal{H}(\mathcal{C}, F, \mathcal{D}, G)$ with data $\mathcal{C}$, F, $\mathcal{D}$ and G as described in (7.17)-(7.25) that satisfies Condition 7.1-7.4. Moreover, suppose that Ψ_i and η_i^0 are given by (7.45) and (7.46), respectively. Then the MAS described by $\mathcal{H}$ is flow-dissipative with respect to the supply rate $\tilde{s} : \mathbb{X} \times \mathbb{R}^{n_w} \to \mathbb{R}$ as given in (7.27). In addition, if there exist constants $c_V, c_W \in \mathbb{R}_{\geqslant 0}$ and a function $\sigma_w \in \mathcal{K}_\infty$ such that $\tilde{s}(\xi, w) \leqslant c_V V(x) + c_W \sum_{i\in\mathcal{V}} |\bar{e}_i|^2 + \sigma_w(|w|)$, then the system $\mathcal{H}$ is persistently flowing.*

The proof is provided in the appendix.

7.6 Packet losses and Denial-of-Service attacks

As mentioned before, the function z_i can also capture packet losses and denial-of-service attacks. In this section, we show that under reasonable assumptions, the resulting protocols are still UGES in the sense of Condition 7.1 and consequently the claims of Theorem 7.1 still hold.

7.6.1 Packet losses

To model the presence of packet losses, we take the function z_i as follows, for all $i \in \mathcal{V}$, $j \in \mathcal{V}_i^{\text{out}}$, $k \in \mathbb{N}$,

$$z_i(k, \bar{e}_i(t_k^i), j) = \begin{cases} 0, & \text{when packet loss at time } t_k^i, \\ 1, & \text{when no packet loss at time } t_k^i. \end{cases} \tag{7.52}$$

Observe from (7.4) that with this protocol function, the estimate $\hat{y}_i^j$, $i \in \mathcal{V}$, $j \in \mathcal{V}_i^{\text{out}}$, is only updated if the transmission attempt of agent $\mathcal{A}_i$ at time t_k^i, $k \in \mathbb{N}$, has been successful. In this chapter, we adopt the following assumption regarding the presence of packet losses.

Assumption 7.2. *The number of successive packet dropouts of transmissions from agent $\mathcal{A}_i$, $i \in \mathcal{V}$, to agent $\mathcal{A}_j$, $j \in \mathcal{V}_i^{out}$, that might occur since the last successful transmission is upper bounded by δ_{max}^i, where $\delta_{max}^i \in \mathbb{N}$ represents the maximum allowable number of successive dropouts (MANSD).*

Let us remark that the assumption above has been used in several works before, see, *e.g.*, [74, 103, 104, 120, 138, 184, 251].

Remark 7.7. Observe from (7.52) that we do not consider the combination of destination protocols and the presence packet losses although we envision this

is possible. However, in this case, the destination protocol design should take the dropout model into account such that resulting protocol function z_i is still UGES.

Given (7.52) and Assumption 7.2, consider the following proposition

Proposition 7.2. *Suppose Assumption 7.2 holds, then the protocol function z_i given by (7.52) is UGES with the Lyapunov function W_i as in (7.32). Moreover, we can take $\underline{\alpha}_{W,i} = 1$, $\bar{\alpha}_{W,i} = \sqrt{\delta^i_{max} + 1}$ and $\lambda_i = \sqrt{\frac{\delta^i_{max}}{\delta^i_{max}+1}}$*

Proof of Proposition 7.2: Consider the discrete-time system as given in (7.31) with function z_i as (7.52). The solution ψ satisfies $\psi(k, k, \bar{e}_i) = |\bar{e}_i| \leqslant W_i(k, \bar{e}_i)$ with W_i as in (7.32), and thus that $\underline{\alpha}_{W,i} = 1$. Moreover, observe that for all $k \in \mathbb{N}$ and all $m \geqslant \delta^i_{max} + 1$, we have that $\psi(m + k, k, \bar{e}_i) = 0$. By combining the latter fact with (7.32), we obtain that $W(k, \bar{e}_i) \leqslant \sqrt{\delta^i_{max} + 1}|\bar{e}_i|$, and thus that $\bar{\alpha}_{W,i} = \sqrt{\delta^i_{max} + 1}$. From (7.31), (7.32) and by recalling the facts that $\psi(k, k, \bar{e}_i) = |\bar{e}_i|$, we obtain that

$$W_i(k+1, h_i(\bar{e}_i)) = \sqrt{\sum_{m=k}^{\infty} |\psi(m, k, \bar{e}_i)|^2 - |\bar{e}_i|^2} \leqslant \sqrt{\frac{\delta^i_{max}}{\delta^i_{max}+1}} W_i(k, \bar{e}_i),$$

for all $\bar{e}_i \in \mathbb{R}^{Nn_y}$, $i \in \mathcal{V}$, $j \in \mathcal{V}_i^{\text{out}}$ and all $k \in \mathbb{N}$. Hence, (7.30b) holds for $\lambda_i = \sqrt{\frac{\delta^i_{max}}{\delta^i_{max}+1}}$, which completes the proof. □

It is important to note that under packet losses, the ETM described by (7.8), (7.9), (7.45) and (7.46), requires an acknowledgments in order to obtain $\tilde{y}_i^j$, $i \in \mathcal{V}$, $j \in \mathcal{V}_i^{\text{out}}$. Observe, however, that this acknowledgment is allowed to be delayed with τ^i_{miet} time units. See [74] for ETC approaches with packet losses without acknowledgments schemes.

7.6.2 Denial-of-Service attacks

A *denial-of-service* (DoS) attack is defined as a period in time at which the communication is blocked by a malicious attacker. Hence, in case an agent $\mathcal{A}_i$, $i \in \mathcal{V}$, attempts to transmit a new measurement to agent $\mathcal{A}_j$, $j \in \mathcal{V}_i^{\text{out}}$, at transmission time t_j and a DoS attack is active, the attempt will fail and agent i can not update $\hat{y}_i^j$. Obviously, the latter might endanger the stability and performance of the closed-loop system.

In general, DoS attacks can be described by a sequence of time intervals $\{H_n\}_{n\in\mathbb{N}}$, where the n-th time interval H_n, given by $H_n := \{h_n\} \cup [h_n, h_n + d_n)$, represents the n-th DoS attack (period). Hence, $h_n \in \mathbb{R}_{\geqslant 0}$ denotes the time instant at which the n-th DoS interval commences and $d_n \in \mathbb{R}_{\geqslant 0}$ denotes the length of the n-th DoS interval. The intervals in $\{H_n\}_{n\in\mathbb{N}}$ do not overlap, *i.e.*,

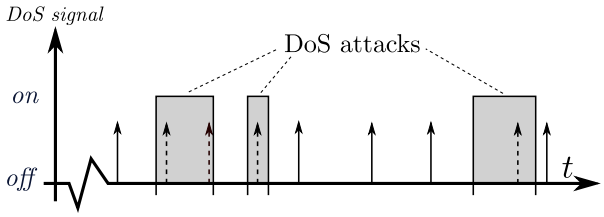

Fig. 7.1. Schematic representation of a sequence of DoS attacks. The solid arrows indicate successful transmissions and the dashed arrows transmissions that are blocked by the attacker. The gray areas indicate the presence of a DoS attack.

$0 \leqslant h_0 \leqslant h_0 + d_0 < h_1 \leqslant h_1 + d_1 < h_2 < \ldots$. For a given sequence $\{H_n\}_{n\in\mathbb{N}}$, the set of time instants at which a DoS attack is active is defined as

$$\mathcal{T} := \bigcup_{n\in\mathbb{N}} H_n. \tag{7.53}$$

To capture the presence of these DoS attacks, we consider the following protocol function, for all $i \in \mathcal{V}$, $j \in \mathcal{V}_i^{\text{out}}$, $k \in \mathbb{N}$, $\mathcal{T} \subseteq \mathbb{R}_{\geqslant 0}$ and all $t_k^i \in \mathbb{R}_{\geqslant 0}$

$$\tilde{z}_i(k, \bar{e}_i(t_k^i), j, \mathcal{T}, t_k^i) = \begin{cases} 1, & \text{when } t_k^i \notin \mathcal{T} \\ 0, & \text{when } t_k^i \in \mathcal{T}. \end{cases} \tag{7.54}$$

Observe from (7.4) that indeed, $\hat{y}_i^j$, $i \in \mathcal{V}$, $j \in \mathcal{V}_i^{\text{out}}$, is not updated in case a DoS attack is active at time instant t_k^i, $k \in \mathbb{N}$. The latter is also illustrated in Figure 7.1.

Moreover, observe that in contrast to the destination protocols as discussed in Section 7.5.1, the protocol presented in (7.54) explicitly depends on $\mathcal{T}$ and the sequence of transmission instants $\{t_k^i\}_{k\in\mathbb{N}}$, $i \in \mathcal{V}$. Hence, to analyze the UGES property for the protocol in (7.54), we need to study the UGES property of the following discrete-time system

$$q(k+1) = \tilde{h}_i(k, q, \mathcal{T}, t_k^i),\ k \in \mathbb{N}, \tag{7.55}$$

where $\tilde{h}_i(k, q, \mathcal{T}, t_k^i) := \Big((1 - \tilde{z}_i(k, q, 1, \mathcal{T}, t_k^i))q_1, (1 - z_i(k, q, 2, \mathcal{T}, t_k^i))q_2, \ldots, (1 - z_i(k, q, N, \mathcal{T}, t_k^i))q_N\Big)$ for all $q \in \mathbb{R}^{Nn_y}$, $i \in \mathcal{V}$, $j \in \mathcal{V}_i^{\text{out}}$, $k \in \mathbb{N}$, $\mathcal{T} \subseteq \mathbb{R}_{\geqslant 0}$ and all $t_k^i \in \mathbb{R}_{\geqslant 0}$.

In the context of DoS attacks, it is reasonable to assume that the attacker's resources are not infinite, see also [63,64,77]. Therefore, we characterize the DoS attacks in terms of the DoS *frequency* and the DoS *duration*. To do so, let us

define the collection of times within the interval $[T_1, T_2]$, with $T_2 \geqslant T_1 \geqslant 0$, at which DoS attacks are active as

$$\Xi(T_1, T_2) := [T_1, T_2] \cap \mathcal{T} \tag{7.56}$$

with $\mathcal{T}$ as in (7.53) and the number of DoS *off/on* transitions occurring in the interval $[T_1, T_2]$ as

$$n(T_1, T_2) := |\{n \in \mathbb{N} \mid h_n \in [T_1, T_2]\}|. \tag{7.57}$$

Moreover, we use $|\Xi(T_1, T_2)|$ to denote the total length of the DoS attacks within the interval $[T_1, T_2]$. Now, consider the following definitions.

Definition 7.6. [64, 124] (DoS frequency*). A given sequence of DoS attacks* $\{H_n\}_{n\in\mathbb{N}}$ *is said to satisfy the* DoS frequency *constraint for a given* $\tau_D \in \mathbb{R}_{>0}$*, and a given* $\nu \in \mathbb{R}_{\geqslant 0}$*, if for all* $T_1, T_2 \in \mathbb{R}_{\geqslant 0}$ *with* $T_2 \geqslant T_1$

$$n(T_1, T_2) \leqslant \nu + \frac{T_2 - T_1}{\tau_D}. \tag{7.58}$$

Definition 7.7. [64] (DoS duration*). A given sequence of DoS attacks* $\{H_n\}_{n\in\mathbb{N}}$ *is said to satisfy the* DoS duration *constraint for a given* $T \in \mathbb{R}_{>1}$ *and a given* $\varsigma \in \mathbb{R}_{\geqslant 0}$*, if for all* $T_1, T_2 \in \mathbb{R}_{\geqslant 0}$ *with* $T_2 \geqslant T_1$

$$|\Xi(T_1, T_2)| \leqslant \varsigma + \frac{T_2 - T_1}{T}. \tag{7.59}$$

Let us highlight that no assumptions regarding the underlying strategy of the attacker are made in Definition 7.6 and Definition 7.7.

To deal with the presence of denial-of-service attacks, we modify the ETM described by (7.8) to the following

$$t_{k+1}^i := \begin{cases} \inf\left\{t > t_k^i + \tau_{miet}^i \mid \eta_i(t) \leqslant 0\right\}, & \text{when } t_k^i \notin \mathcal{T} \\ t_k^i + \tau_{miet}^i, & \text{when } t_k^i \in \mathcal{T} \end{cases} \tag{7.60}$$

with $t_0^i = 0$. Observe that in case no DoS attack is present at a transmission instant, *i.e.*, when $t_k^i \notin \mathcal{T}$, the next transmission instant is determined in an event-based fashion, similar as in (7.8). However, in case a DoS attack is present, *i.e.*, when $t_k^i \in \mathcal{T}$, which, for example, can be detected by using communication with acknowledgments, the next-time instant is scheduled after τ_{miet}^i, $i \in \mathcal{V}$, time units. The latter is necessary to probe when the network is available again. In that sense, dealing with packet losses as described in Section 7.6 is different from dealing with DoS attacks.

Proposition 7.3. *The protocol $\tilde{z}_i$ given by (7.54) is UGES under the DoS frequency and duration constraints with the Lyapunov function W_i as in (7.32). Moreover, we can take $\underline{\alpha}_{W,i} = 1$, $\bar{\alpha}_{W,i} = \sqrt{\chi^i + 1}$ and $\lambda_i = \sqrt{\frac{\chi^i}{\chi^i+1}}$, where*

$$\chi^i := \left\lceil \left(\frac{\varsigma + \nu\tau^i_{miet}}{\tau^i_{miet}} \right) \left(1 - \frac{1}{T} - \frac{\tau^i_{miet}}{\tau_d} \right)^{-1} + 1 \right\rceil . \tag{7.61}$$

Proof of Proposition 7.3: To prove Proposition 7.3, we show that χ^i is equal to the maximum amount of consecutive transmission attempts that are blocked by the DoS attack. As shown in [84], the maximum time in between two successful transmissions is given by

$$d_{\max} := \left(\varsigma + \nu\tau^i_{miet}\right) \left(1 - \frac{1}{T} - \frac{\tau^i_{miet}}{\tau_d} \right)^{-1} + \tau^i_{miet} \tag{7.62}$$

Given that the minimum time between two consecutive transmission is equal to τ^i_{miet}, we indeed obtain that χ^i is equal to the maximum amount of consecutive transmission attempts that are blocked by the DoS attack. The proof can now be completed by using the same arguments as in the proof of Proposition 7.2. □

7.7 Conclusions

In this work, we presented a systematic design methodology for *event-triggered* control strategies for a class of nonlinear multi-agent systems (MAS) subject to disturbances resulting in strictly positive lower bounds on the inter-event times. The proposed framework leads to MASs that are dissipative with respect to a desired supply rate which can capture many relevant control problems. Furthermore, robustness to *non-uniform* and *time-varying* delays is guaranteed by design. In addition to event-triggering mechanisms, we introduced so-called destination protocols that at each transmission instant, locally determine to which agents local output measurements are transmitted. Moreover, we showed that this concept can also be exploited in the context of packet losses and denial-of-service attacks, thereby laying down a general framework for ETC design for MASs with many different features.

Chapter 8

Event-triggered Control for String-Stable Vehicle Platooning

Abstract – Cooperative Adaptive Cruise Control (CACC) is a promising technology that is proven to enable the formation of vehicle platoons with small inter-vehicle distances while avoiding amplifications of disturbances along the vehicle string. As such, CACC systems can potentially improve road safety, traffic throughput and fuel consumption due to the reduction in aerodynamic drag. Dedicated Short Range Communication (DSRC) is a key ingredient in CACC systems to overcome the limitations of onboard sensors. However, wireless communication also involves inevitable network-induced imperfections, such as a limited communication bandwidth and time-varying transmission delays. Moreover, excessive utilization of communication resources jeopardizes the reliability of the DSRC channel. The latter might restrict the minimum time gap that can be realized safely. As a consequence, to harvest all the benefits of CACC, it is important to limit the communication to only the information that is actually required to establish a (string-)stable platoon over the wireless network and to avoid unnecessary transmissions. For this reason, an event-triggered control scheme and communication strategy is developed that takes into account the aforementioned network-induced imperfections and that aims to reduce the utilization of communication resources while maintaining the desired closed-loop performance properties. The resulting $\mathcal{L}_2$ string-stable control strategy is experimentally validated by means of a platoon of three passenger vehicles.

This chapter is based on [75].

8.1 Introduction

8.1.1 Cooperative adaptive cruise control

The main objective of Cooperative Adaptive Cruise Control (CACC) systems is to maintain a desired, not necessarily constant, (small) distance between vehicles, while ensuring that disturbances are attenuated throughout the string of vehicles. The latter property is also referred to as *string stability*, see, *e.g.*, [31,187,223], and in essence constitutes an $\mathcal{L}_p$-stability property (for $p \in [1, \infty)$) [241]. Vehicle platoons that are string unstable lead to so-called phantom traffic jams due to excessive braking. Hence, string stability forms an important property in enhancing traffic flow. Besides this string stability property, it is desired to realize a small inter-vehicle distance as it increases the road capacity and reduces fuel consumption. Well-known Adaptive Cruise Control (ACC) systems allow vehicles to maintain a desired distance or time gap, based on measurements of the distance and distance rate that are obtained via onboard sensors such as a radar and/or camera. Cooperative Adaptive Cruise Control systems (CACC) offer to enhance the behavior of traffic flow in terms of string stability while realizing small inter-vehicle distances commonly expressed in terms of the *time gap*, being the distance between a leader and a follower vehicle, divided by the follower vehicle speed (typically less than 1 second). A key ingredient to achieve these two (somehow conflicting) goals simultaneously, is the wireless vehicle-to-vehicle (V2V) communication via Dedicated Short Range Communication (DSRC) channel. It is shown in, *e.g.*, [171,187], that CACC significantly improves the attenuation of disturbances along the vehicle string with small time gaps compared to conventional ACC systems.

8.1.2 Wireless communication

The use of wireless communication also has drawbacks as it comes with inevitable network-induced imperfections caused by the digital nature of the communication network. To be more concrete, the communication is packet-based, where the rate at which these data-packages can be transmitted is limited and the communication channel is subject to communication delays. As shown in [67,85,90,130,151,180,181,187,203], these communication imperfections can have a significant influence on the performance of CACC systems in the sense that if the communication delays are too large and/or the rate at which transmissions occur is too small, string stability and other performance properties for a given time gap might no longer be guaranteed. Hence, the number of transmissions in time should be sufficiently large and communication delays sufficiently small in order to obtain the desired platooning behavior. The latter is not trivial to realize as high communication rates degrade the reliability of the DSRC channel and increase the transmission delays as reported in [28,134,152]. This, in turn, might put restrictions on the minimum time gap that can be achieved safely

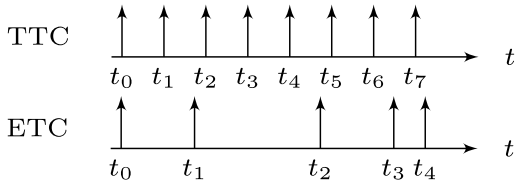

Fig. 8.1. Paradigm shift in digital control from time-triggered control (TTC) systems to event-triggered control (ETC) systems.

in dense traffic and might as a consequence impede the benefits of CACC with respect to traffic throughput and fuel consumption, see also [187]. Hence, in order to secure the reliability and the quality of the network (in terms of communication delays), it is of importance that only the information that is actually required to establish a string-stable platoon is being transmitted and that the transmission of unnecessary information is avoided. Despite the growing interest in vehicle platooning, only a few works available in the literature address this important topic, including [130, 147, 180, 181, 203].

8.1.3 Time-triggered versus event-triggered communication

In CACC systems, the desired acceleration is transmitted over the DSRC channel. Due to the packet-based nature of DSRC, these transmissions only occur at discrete instants in time, which we denote by t_k, $k \in \mathbb{N}$, satisfying $0 = t_0 < t_1 < t_2 < \ldots$. In traditional (digital) control setups, these transmission instants are scheduled in a time-triggered fashion, typically according to a fixed sampling rate as illustrated in Figure 8.1. Since the scheduling of transmission instants is purely based on time and not on the actual status of the plant, time-triggered communication often leads to inefficient use of communication resources which, in the context of CACC, is not desirable as discussed before. Hence, it seems more natural to use resource-aware control methods that determine the transmission instants on the basis of output measurements to allow a better balance between communication efficiency and control performance. Such a resource-aware control method is offered by *event-triggered control* (ETC).

In ETC schemes, the transmission instants are determined on-line by means of a "smart" triggering condition that depends on, *e.g.*, output measurements of the system such that, as illustrated in Figure 8.1, transmission are only scheduled when needed in order to guarantee stability, safety and performance properties. As a consequence, event-triggered control has the potential to offer a better balance between the utilization of communication resources and the control performance than time-triggered control. An event-triggering mechanism (ETM) takes, for instance, the form

$$t_0 = 0,\ t_{k+1} := \inf\left\{t \geqslant t_k \mid |\hat{y}(t) - y(t)| \geqslant \sigma|y(t)|\right\}, \tag{8.1}$$

where y denotes the output measurement (*e.g.*, the desired acceleration of the vehicle equipped with this ETM) and $\hat{y}$ the most recently transmitted value of y, and where $\sigma \in (0, 1)$. Observe that if the most recent transmitted value of y, $\hat{y}$, is relatively close to the actual value of y, no transmission takes place. On the other hand, if the difference between $\hat{y}$ and y, also referred to as the *network-induced error*, is relatively large, a new transmission instant is generated. As such, transmissions only take place when there is a significant change in the value of y with respect to the most recently transmitted value. See also [18, 20, 54, 117, 224] for some early approaches and [115] for a recent overview on event-triggered control systems.

One of the main challenges in the design of such an *event-triggering mechanism* (ETM) is to guarantee the desired control performance, *e.g.*, in terms of $\mathcal{L}_2$-stability, together with a *positive minimum inter-event time* (MIET) despite the presence of disturbances [41, 72]. Obviously, the latter two properties are essential in the context of event-triggered vehicle platooning. The control performance guarantee is needed to establish a string-stable platoon and a positive MIET is required to avoid Zeno-behavior (an infinite number of events in finite time) and to enable practical implementation of the ETC system. In addition, the resulting ETC systems should be robust to time-varying communication delays induced by the DSRC channel. Although many ETC methods are available in the literature, in [41] it is shown that many of the proposed ETMs, including the ETM described by (8.1), do not have a positive MIET that is robust with respect to the presence of external disturbances. To deal with the aforementioned issue, recent works on ETC either use *time regularization* [7, 87, 112, 117, 225, 227, 228], in the sense that the next event transmission can only occur after a specific "waiting time" δ since the last transmission has elapsed, or *periodic event-triggered control* (PETC) [54, 112, 117, 126, 164, 184], in the sense that the triggering condition is checked at fixed periodic sampling time instants with sampling period h, such that the MIET is larger than or equal to δ or h, respectively. However, none of these works provides an output-based event-triggered control method that leads to the combination of $\mathcal{L}_2$-stability and robustness guarantees with respect to time-varying delays, which is required in the context of CACC.

8.1.4 Event-triggered cooperative adaptive cruise control

In this chapter, the recently developed framework presented in [72] is used to construct an event-triggered control strategy that does comply with the aforementioned criteria. To be more specific, the proposed ETC framework offers an ETC strategy for a class of nonlinear feedback systems and results in

- a finite $\mathcal{L}_2$-gain,
- a strictly positive lower bound on the inter-event times (which guarantees

Zeno-freeness),

- robustness guarantees with respect to (time-varying) transmission delays.

Key to obtaining all these beneficial properties is the unique combination of *dynamic* event-triggering conditions and time regularization. As shown in the present chapter, the design of this class of dynamic event-triggered controllers is systematic. The proposed control methodology is experimentally validated by means of a platoon of three passenger vehicles.

8.1.5 Organization of the chapter

The remainder of this chapter is organized as follows. After presenting some preliminaries and notational conventions in Section 8.2, we introduce the platoon model and the control objectives in Section 8.3 leading to the problem statement. In Section 8.4, we shortly discuss the tuning of a CACC system for the network-free situation. In Section 8.5, we discuss the imperfections induced by the wireless communication network and we provide a brief introduction on (*dynamic*) event-triggered control. Moreover, we adapt aforementioned the platoon model to include these network-induced errors. In Section 8.6 this model is used to obtain design conditions for the proposed *dynamic* event-triggered strategy such that string stability is guaranteed under event-triggered communication.

Finally, we provide the concluding remarks in Section 8.8.

8.2 Definitions and preliminaries

The following notational conventions will be used in this chapter. $\mathbb{N}$ denotes the set of all non-negative integers, $\mathbb{N}_{>0}$ the set of all positive integers, $\mathbb{R}$ the field of all real numbers and $\mathbb{R}_{\geqslant 0}$ the set of all non-negative reals. For $N \in \mathbb{N}$, we write the set $\{1, 2, \ldots, N\}$ as $\bar{N}$. By $|\cdot|$ and $\langle \cdot, \cdot \rangle$ we denote the Euclidean norm and the usual inner product of real vectors, respectively. For a matrix $P \in \mathbb{R}^{n \times n}$, we write $P \succ 0$ ($P \succeq 0$) if P is symmetric and positive (semi-)definite, *i.e.*, $x^\top P x > 0$ ($x^\top P x \geq 0$) for all $x \neq 0$. Likewise, we write $P \prec 0$ ($P \preceq 0$) if P is symmetric and negative (semi-)definite, *i.e.* $x^\top P x < 0$ ($x^\top P x \leq 0$) for all $x \neq 0$. A function $\alpha : \mathbb{R}_{\geqslant 0} \to \mathbb{R}_{\geqslant 0}$ is said to be of class $\mathcal{K}$ if it is continuous, strictly increasing and $\alpha(0) = 0$. It is said to be of class $\mathcal{K}_\infty$ if it is of class $\mathcal{K}$ and it is unbounded. For a signal $f : \mathbb{R}_{\geqslant 0} \to \mathbb{R}^n$, $n \in \mathbb{N}_{>0}$ and $t \in \mathbb{R}_{\geqslant 0}$, $f(t^+)$ denotes the limit $f(t^+) = \lim_{s \to t, s > t} f(s)$, provided it exists.

In this chapter, we will use hybrid systems $\mathcal{H}$ of the form

$$\dot{\xi} = F(\xi, w), \text{ when } \xi \in \mathcal{C}, \tag{8.2a}$$

$$\xi^+ = G(\xi), \quad \text{when } \xi \in \mathcal{D}, \tag{8.2b}$$

where $F : \mathbb{R}^n \times \mathbb{R}^{n_w} \to \mathbb{R}^n$ describes the flow dynamics, $G : \mathbb{R}^n \to \mathbb{R}^n$ the jump dynamics, $\mathcal{C} \subset \mathbb{R}^n$ the flow set and $\mathcal{D} \subset \mathbb{R}^n$ the jump set. A hybrid system with the data $\mathcal{C}$, F, $\mathcal{D}$ and G as above is denoted by $\mathcal{H} = (\mathcal{C}, F, \mathcal{D}, G)$ or, in short, $\mathcal{H}$. We now recall some definitions given in [98] regarding the solutions of such hybrid systems.

A *compact hybrid time domain* is a set $\mathcal{E} = \bigcup_{j=0}^{J-1} [t_j, t_{j+1}] \times \{j\} \subset \mathbb{R}_{\geqslant 0} \times \mathbb{N}$ with $J \in \mathbb{N}_{>0}$ and $0 = t_0 \leq t_1 \ldots \leq t_J$. A *hybrid time domain* is a set $\mathcal{D} \subset \mathbb{R}_{\geqslant 0} \times \mathbb{N}$ such that $\mathcal{E} \cap ([0, T] \times \{0, \ldots, J\})$ is a compact hybrid time domain for each $(T, J) \in \mathcal{D}$. A *hybrid signal* is a function defined on a hybrid time domain. A hybrid signal $\xi : \operatorname{dom} \xi \to \mathbb{R}^n$ is called a *hybrid arc* if $\xi(\cdot, j)$ is locally absolutely continuous for each j.

For the hybrid system $\mathcal{H}$ given by the state space $\mathbb{R}^n$, the input space $\mathbb{R}^{n_w}$ and the data $(\mathcal{C}, F, \mathcal{D}, G)$, a hybric arc $\xi : \operatorname{dom} \xi \to \mathbb{R}^n$ and a hybrid input signal $w : \operatorname{dom} w \to \mathbb{R}^{n_w}$ is called a *solution pair* (ξ, w) to $\mathcal{H}$ if

1) $\operatorname{dom} \xi = \operatorname{dom} w$,

2) For all $j \in \mathbb{N}$ and for almost all t such that $(t, j) \in \operatorname{dom} \xi$, we have $\xi(t, j) \in \mathcal{C}$ and $\dot{\xi}(t, j) = F(\xi(t, j), w(t, j))$.

3) For all $(t, j) \in \operatorname{dom} \xi$ such that $(t, j + 1) \in \operatorname{dom} \xi$, we have $\xi(t, j) \in \mathcal{D}$ and $\xi(t, j + 1) = G(\xi(t, j))$.

For the motivation and more details on these definitions, the interested reader is referred to [98]. We will often not mention $\operatorname{dom} \xi$ explicitly, and understand that with each hybrid solution pair (ξ, w) comes a hybrid time domain $\operatorname{dom} \xi = \operatorname{dom} w$. A solution pair (ξ, w) to system (8.2) is *nontrivial* if $\operatorname{dom} \xi$ contains at least two points, *maximal* if there does not exist another solution ξ' to $\mathcal{H}$ such that $\operatorname{dom} \xi$ is a proper subset of $\operatorname{dom} \xi'$ and $\xi(t, j) = \xi'(t, j)$ for all $(t, j) \in \operatorname{dom} \xi$, it is *complete* if its domain, $\operatorname{dom} \xi$, is unbounded, it is *Zeno* if it is complete and $\sup_t \operatorname{dom} \xi < \infty$, where $\sup_t \operatorname{dom} \xi := \sup\{t \in \mathbb{R}_{\geq 0} : \exists j \in \mathbb{N} \text{ such that } (t, j) \in \operatorname{dom} \xi\}$, and it is t-complete if $\operatorname{dom} \xi$ is unbounded in the t-direction, i.e., $\sup_t \operatorname{dom} \xi = \infty$.

In addition, we introduce the $\mathcal{L}_2$-norm of a function ξ defined on a hybrid time domain $\operatorname{dom} \xi = \bigcup_{j=0}^{J-1} [t_j, t_{j+1}] \times \{j\}$ with J possibly ∞ and/or $t_J = \infty$ by

$$\|\xi\|_{\mathcal{L}_2} = \sqrt{\sum_{j=0}^{J-1} \int_{t_j}^{t_{j+1}} |\xi(t, j)|^2 dt} \tag{8.3}$$

provided the right-hand side is well-defined and finite. In case $\|\xi\|_{\mathcal{L}_2}$ is finite, we say that $\xi \in \mathcal{L}_2$. Note that this definition is essentially identical to the usual $\mathcal{L}_2$-norm in case a function is defined on a subset of $\mathbb{R}_{\geqslant 0}$.

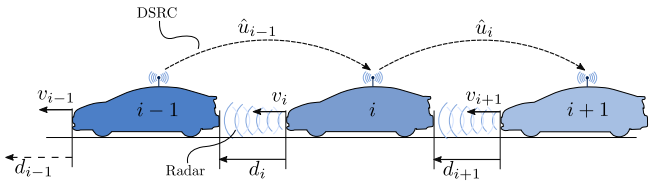

Fig. 8.2. Homogeneous vehicle platoon consisting of N vehicles equipped with radar and DSRC communication. The variable d_i, $i \in \bar{N}$ represents the distance between vehicle i and its predecessor (vehicle $i-1$), v_i the velocity of vehicle i and $\hat{u}_i$ denotes the most recently transmitted measurement of the desired acceleration of vehicle i.

8.3 Model description, control objectives and problem formulation

In this section, we introduce a generic model of a homogeneous platoon consisting of N vehicles. Moreover, we provide formal definitions of *individual vehicle stability* and *string stability*, which are used to formalize the problem statement considered in this chapter.

8.3.1 Platooning dynamics

In this chapter, we consider a vehicle platoon consisting of N identical vehicles as illustrated in Figure 8.2. The main objective of each vehicle i, $i \in \bar{N}$, in the platoon is to maintain a desired distance $d_{r,i}$ with respect to its predecessor (defined as vehicle $i-1$). In this chapter, we consider a constant time gap policy in which the desired distance at time $t \in \mathbb{R}_{\geqslant 0}$ is given by

$$d_{r,i}(t) = r_i + hv_i(t), \tag{8.4}$$

where $v_i(t)$ denotes the velocity of vehicle i at time t, r_i the standstill distance and where $h \in \mathbb{R}_{>0}$ represents the desired constant *time gap*.

Let $d_i(t)$ represent the actual distance between vehicle i and its preceding vehicle at time $t \in \mathbb{R}_{\geqslant 0}$, then we define the spacing error $e_i(t)$, $i \in \bar{N} \backslash \{1\}$, at time $t \in \mathbb{R}_{\geqslant 0}$ as

$$\begin{aligned} e_i(t) &:= d_i(t) - d_{r,i}(t) \\ &= (q_{i-1}(t) - q_i(t) - L_i) - (r_i + hv_i(t)), \end{aligned} \tag{8.5}$$

where $q_i(t)$ denotes the (curvilinear) position of vehicle i at time t, L the length of the vehicle i, r the standstill distance and h the time gap as before. Since we consider a homogeneous vehicle platoon, h does not depend on the index i. The first vehicle in the platoon (corresponding to $i = 1$) follows a *virtual reference vehicle* (corresponding to index $i = 0$). As such, we defined e_1 as the spacing error between the first vehicle and its virtual predecessor.

The dynamics of the virtual reference vehicle are given by

$$\mathcal{V}_0 : \begin{cases} \dot{v}_0(t) = a_0(t) \\ \dot{a}_0(t) = -\frac{1}{\tau_d} a_0(t) + \frac{1}{\tau_d} u_0(t), \end{cases} \tag{8.6}$$

where $u_0(t)$ is the exogenous input of the vehicle platoon at time t. The plant dynamics of the i-th vehicle $\mathcal{V}_i$, $i \in \bar{N}$, are given by

$$\dot{e}_i(t) = v_{i-1}(t) - v_i(t) - h a_i(t) \tag{8.7a}$$

$$\mathcal{V}_i : \begin{cases} \dot{v}_i(t) &= a_i(t) \\ \dot{a}_i(t) &= -\frac{1}{\tau_d} a_i(t) + \frac{1}{\tau_d} u_i(t) \end{cases} \tag{8.7b}$$

$$\dot{u}_i(t) = -\frac{1}{h} u_i(t) + \frac{1}{h} \chi_i(t) \tag{8.7c}$$

where $v_i(t)$ denotes the velocity at time t, $a_i(t)$ the acceleration at time t, $u_i(t)$ the desired acceleration at time t, $\chi_i(t)$ the control input at time t and $\tau_d \in \mathbb{R}_{>0}$ the characteristic time constant of the vehicle drive-line of vehicle i. Note that (8.7a) is in correspondence with (8.5). Moreover, observe from (8.7b) that the vehicles are assumed to be acceleration-controlled since the dynamic behavior of the acceleration $a_i(t)$, $i \in \bar{N}$, is described by a first-order model. The latter can be realized by means of feedback linearization as described in [97, 208]. At last, observe from (8.7c) that the signal $\chi_i(t)$ is filtered by a first order low-pass filter before it is fed into the vehicle drive line. This low-pass filter is used as a pre-compensator for the time-gap policy as in [187]. The latter is illustrated in Figure 8.3, where H represents the spacing policy filter which is given by $H(s) = hs + 1$. Let us remark that this filter is such that the variable $e_i(t)$ in Figure 8.3 corresponds to the spacing error $e_i(t)$, $i \in \bar{N}$, as defined in (8.5). The transfer function H^{-1} represents the inverse of the spacing policy filter which corresponds to (8.7c). Observe that the control configuration is such that the asymptotic stability properties of the control-loop of vehicle i do not depend on h due to the cancellation of the poles and zeros of H^{-1} and H in the dynamics of the closed-loop system. This is desirable as it enables the driver to set different time-gaps h without jeopardizing the individual vehicle stability which we formally define below in Section 8.3.2.

Typically, a CACC scheme consists of a feedback controller $\mathcal{C}_i$, $i \in \bar{N}$, that depends on the spacing error and a feedforward component being the direct feedthrough of the predecessor's desired acceleration $u_{i-1}(t)$ as illustrated in Figure 8.2. The feedback controller often relies on measurements of a forward-looking radar whereas the feedforward component is obtained via dedicated short range communication (DSRC). In this chapter, we consider a control law of the form

$$\chi_i(t) = \underbrace{k_p e_i(t) + k_d \dot{e}_i(t)}_{\mathcal{C}_i} + \underbrace{\hat{u}_{i-1}(t)}_{\text{feedforward}}, \; i \in \bar{N}, \tag{8.8}$$

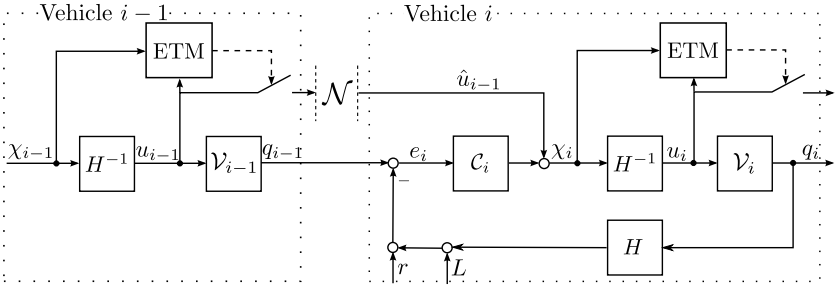

Fig. 8.3. Schematic representation of the proposed event-triggered CACC setup.

where k_p and k_d are controller gains to be specified. Observe from (8.5) and (8.8) that a *one-vehicle look-ahead control strategy* is considered in the sense that the control law of vehicle i only depends on local information and information of its predecessor, vehicle $i-1$. The first two terms of (8.8) form the feedback controller $\mathcal{C}_i$ and $\hat{u}_{i-1}(t)$ the feedforward of the predecessors desired acceleration $u_{i-1}(t)$ that is sent over the DSRC channel as illustrated in Figure 8.3. We employ the notation $\hat{u}_{i-1}(t)$ to denote the most recently received information regarding $u_{i-1}(t)$ by vehicle i at time t. Due to the packet based-nature of the communication channel and the presence of communication delays, we typically have that $\hat{u}_{i-1}(t) \neq u_{i-1}(t)$ for $t \in \mathbb{R}_{\geqslant 0}$. Note that in case these communication delays are absent and the communication network is infinitely fast, it would hold that $\hat{u}_{i-1}(t) = u_{i-1}(t)$ for all $t \in \mathbb{R}_{\geqslant 0}$. Observe from Figure 8.3 that, as discussed in the introduction, the time instants at which u_i will be transmitted over the network are determined by means of an event-triggering mechanism (ETM).

Remark 8.1. Besides the aforementioned time gap policy, also other spacing policies are reported in the literature such as a *constant (velocity independent) spacing policy* ($h = 0$). However, as shown in [171], in one vehicle look-ahead platoons, *i.e.*, platoons in which the vehicles can only obtain information of their predecessors, string stability properties can only be achieved when the spacing policy is velocity dependent. For this reason, we only focus on the constant time gap policy in this chapter.

Remark 8.2. To streamline the exposition of the chapter, we only consider a platoon of N vehicles whose dynamics are given by (8.6), (8.7), $i \in \bar{N}$, and (8.8). However, as shown in [72], the event-triggered control framework and design methodology used in this chapter can be used for a broad class of systems and thus can be applied to a much larger class of vehicle platoons that employ a one-vehicle look-ahead control strategy with possibly other vehicle, spacing policy and controller dynamics.

8.3.2 Problem formulation

A well-designed CACC has to comply with two objectives: The first objective is vehicle following, *i.e.*, regulating the spacing errors as given in (8.5) towards zero while realizing a small time-gap h (typically less than 1 second). This property is also referred to as *individual vehicle stability*. The second objective is to attenuate disturbances/shock waves along the vehicle platoons. The latter property is also referred to as *string stability* which, as mentioned in the introduction, forms an important property to enhance traffic flows and avoid so-called phantom traffic jams. To be more concrete, the platoon system consisting of N vehicles whose dynamics are given by (8.7), $i \in \bar{N}$, (8.6) and (8.8), should satisfy the following two control objectives.

(i) *Individually vehicle stability:* For each vehicle i, it should hold that if $v_{i-1}(t) = c$ with c some constant velocity, and $\hat{u}_{i-1}(t) = 0$ for all $t \in \mathbb{R}_{\geqslant 0}$, then all corresponding solutions to (8.7), $i \in \bar{N}$, and (8.6) with the corresponding controller as in (8.8), satisfy

$$\lim_{t\to\infty} e_i(t) = 0. \tag{8.9}$$

(ii) *String stability:* For any exogenous input $u_0 \in \mathcal{L}_2$ and any $x(0) \in \mathbb{R}^{(4N+3)}$ with $x^\top = \begin{bmatrix} x_0^\top & x_1^\top & \dots & x_N^\top \end{bmatrix}^\top$ the lumped state vector, it should hold that for all $i \in \bar{N}$, there exists a $\mathcal{K}_\infty$-function $\beta_i : \mathbb{R}_{\geqslant 0} \to \mathbb{R}_{\geqslant 0}$ such that the corresponding solution to (8.7), $i \in \bar{N}$, and (8.6) with the corresponding controller as in (8.8), satisfies

$$\|\chi_i\|_{\mathcal{L}_2} \leqslant \|u_0\|_{\mathcal{L}_2} + \beta_i(\|x(0)\|). \tag{8.10}$$

Let us remark that the string stability objective is closely related to the notion of $\mathcal{L}_2$-stability, see, *e.g.*, [131]. In particular, if the system given by (8.7), $i \in \bar{N}$, (8.6) and (8.8) is string-stable, then the system is $\mathcal{L}_2$-stable with respect to exogenous input $u_0 \in \mathcal{L}_2$ and every output $\chi_i \in \mathcal{L}_2$, $i \in \bar{N}$, with an $\mathcal{L}_2$-gain less than or equal to one. Moreover, let us remark that the notion of string stability as presented above is similar to the weak string stability as presented in [181].

As already mentioned, Cooperative Adaptive Cruise Control (CACC) is a promising technology that is proven to be an effective method to achieve both individual vehicle stability and string stability while realizing small time-gaps. The wireless communication via DSRC forms an important ingredient to these conflicting goals. The use of wireless communication, however, also has drawbacks due to inevitable network-induced imperfections that result from the digital (packet-based) nature of the communication network. These imperfections include the presence of (time-varying) delays and a limited communication

bandwidth. As already mentioned in the introduction, the aforementioned artifacts potentially degrade the performance of CACC systems in the sense that if the communication delays are too large and/or the time in between two consecutive transmission is too large, string stability for a given time-gap might no longer be guaranteed, see also [90, 130, 151, 180, 181, 203]. A second issue that arises when using wireless communication is that excessive use of the communication resources might lead to degradation of the reliability of the DSRC channel in terms of packet losses and transmission delays as reported in [28]. As such, it is important that unnecessary communication is avoided. Only relevant information should be transmitted over the DSRC channels. Given these facts and the objectives above, we can formulate the problem considered in this chapter as follows.

Problem 8.1. *Consider a homogeneous platoon consisting of N vehicles and whose dynamics are given by (8.6), (8.7), $i \in \bar{N}$, and (8.8). Propose a resource-aware (event-triggered) CACC system with guaranteed individual vehicle stability and string stability in the presence of time-varying communication delays (given upper bounds on the maximal delay values) and that significantly reduces the number of unnecessary transmissions compared to control methods that employ fixed transmission rates.*

To address the problem stated above, we will adopt an emulation approach meaning that we first design the CACC system as in (8.8) such that the desired stability criteria are satisfied when the network-induced imperfections are ignored, *i.e.*, when $\hat{u}_{i-1}(t) = u_{i-1}(t)$, $i \in \bar{N}$, for all $t \in \mathbb{R}_{\geqslant 0}$. Secondly, we provide the design of the ETM. This triggering mechanism determines at which time instants a vehicle transmits a data package, containing its desired acceleration, to its successor. If the ETM is well-designed, the desired properties of the network-free system can still be preserved despite the presence of (event-based) packet-based communication and time-varying communication delays as we will show. In short, the proposed design procedure of a resource-aware controller consists of two steps: (i) the design of the CACC system for the network-free situation and (ii) the design of the ETM. One of the main advantages of this approach is that any control design method for continuous linear time-invariant systems can be used for the design of the CACC system in step (i), although here we focus on the setup as in (8.8). We will discuss the tuning of this control law in the next section.

8.4 Tuning of the network-free CACC system

The controller gains k_p and k_d as in (8.8) need to be tuned such that in absence of network-induced imperfections, *i.e.*, when $\hat{u}_{i-1}(t) = u_{i-1}(t)$ for all $t \geqslant 0$, each vehicle in the platoon is individually stable and that the platoon system itself is string-stable. As shown in [187], individual vehicle stability and string stability

for the system given by (8.6), (8.7), $i \in \bar{N}$, and (8.8) are obtained for any h, k_d, $k_p > 0$ for which $k_d - k_p\tau_d > 0$ with τ_d as in (8.7), $i \in \bar{N}$. It is important to notice that, in contrast to the string stability property, the individual vehicle stability is not affected by the network-induced imperfections and thus also not by the design of the ETMs.

In the remainder of the chapter, we describe the effect of network-induced imperfections on the platoon dynamics given by (8.6), (8.7), $i \in \bar{N}$, and (8.8). Moreover, we will propose a triggering rule that aims to only communicate when necessary to achieve string stability.

8.5 Wireless and event-triggered communication

As mentioned before, typically we have that $\hat{u}_{i-1}(t) \neq u_{i-1}(t)$, $t \in \mathbb{R}_{\geqslant 0}$, due to the presence of network-induced imperfections. In this section, we describe the effect of the network-induced imperfections more thoroughly by reformulating the platoon model given by (8.6), (8.7), $i \in \bar{N}$, and (8.8) in terms of network-induced errors defined by

$$e_{u_{i-1}}(t) := \hat{u}_{i-1}(t) - u_{i-1}(t),\ i \in \bar{N}. \tag{8.11}$$

To do so, we first discuss the evolution of $\hat{u}_i$ over time.

8.5.1 Wireless communication

To model the packet-based communication and the presence of delays, note that at each transmission instant t_k^{i-1}, $k \in \mathbb{N}$, a new measurement of u_{i-1} is collected and transmitted to vehicle i. After a communication delay of Δ_k^{i-1}, $i \in \bar{N}_{>0}$, $k \in \mathbb{N}$, time units, the value of $\hat{u}_{i-1}$ is updated according to

$$\hat{u}_{i-1}((t_k^{i-1} + \Delta_k^{i-1})^+) = u_{i-1}(t_k^{i-1}). \tag{8.12}$$

In between two update events, the value of $\hat{u}_i$, $i \in \bar{N}$, is kept constant in a zero-order hold fashion (ZOH). As such, we adopt the following assumption.

Assumption 8.1. *For all $t \in (t_k^{i-1} + \Delta_k^{i-1}, t_{k+1}^{i-1} + \Delta_{k+1}^{i-1})$, with $i \in \bar{N} \setminus \{1\}$ and $k \in \mathbb{N}$, it holds that*

$$\dot{\hat{u}}_{i-1}(t) = 0. \tag{8.13}$$

As in [72, 120], we can distinguish two types of events, namely, events that correspond to time instants at which a vehicle $i-1$, transmits a new measurement to its successor (referred to as *transmission events*), and events corresponding to time instants at which vehicle i receives a new measurement from its predecessor (referred to as *update events*).

In this chapter, it is assumed that the communication delays Δ_k^{i-1}, $i \in \bar{N} \setminus \{1\}$, $k \in \mathbb{N}$, are bounded from above by a (known) time-constant called the

maximum allowable delay (MAD). In addition, we assume that before a vehicle transmits new information, the most recently transmitted information of that vehicle has been received by its succeeding vehicle. To be more specific, we adopt the following assumption.

Assumption 8.2. *The transmission delays are bounded according to* $0 \leqslant \Delta_k^{i-1} \leqslant \tau_{mad} \leqslant t_{k+1}^{i-1} - t_k^{i-1}$ *for all* $i \in \bar{N} \setminus \{1\}$ *and* $k \in \mathbb{N}$*, where* τ_{mad} *denotes the* maximum allowable delay *of transmissions sent by a vehicle in the platoon.*

Observe that τ_{mad} does not depend on index i as we consider a homogeneous vehicle string. Let us remark that Assumption 8.2 is indeed reasonable to make as in case of DSRC communication, the inter-transmission times are typically larger than the delays as shown in [152].

8.5.2 Event-based communication

In this chapter, we consider event-triggered control (ETC) schemes that determine the transmission instants by means of a triggering condition that depends on locally available output measurements, see, *e.g.*, [15,41,71,72,78,165,191,224,236] and the references therein for more details on ETC. In this way, the communication resources are only used when necessary to maintain desired closed-loop behavior and the utilization of communication resources is reduced.

In particular, we consider *dynamic* event-generators for vehicle $i \in \bar{N}$ of the form as proposed in [72] that schedule transmission instants according to

$$t_0^i = 0,\ t_{k+1}^i := \inf\left\{t \geqslant t_k^i + \tau_{miet} \mid \eta_i(t) < 0\right\}, \tag{8.14}$$

for $k \in \mathbb{N}$ and where $\eta_i(t)$ is the triggering variable at time t that evolves according to

$$\dot{\eta}_i(t) = \Psi_i(\chi_i(t), u_i(t), e_{u_i}(t), \tau_i(t)), \tag{8.15}$$

for all $t \in \mathbb{R}_{\geqslant 0}$, and where the function $\Psi_i : \mathbb{R} \times \mathbb{R} \times \mathbb{R} \times \mathbb{R}_{\geqslant 0} \to \mathbb{R}$ and the time-constant $\tau_{miet} \in \mathbb{R}_{>0}$, are to be properly designed as we will discuss in the next section. Observe that the time-constant $\tau_{miet} \in \mathbb{R}_{>0}$ enforces a strictly positive lower-bound on the *minimum inter-event time* (MIET), *i.e.*, the minimum time in between two consecutive transmissions. This strictly positive lower-bound is important to enable implementation of the ETC scheme in practice. Moreover, observe that Assumption 8.2 is satisfied when $\tau_{miet} > \tau_{mad}$, where τ_{mad} typically follows from the timing specifications of the DSRC channel.

Given the control law in (8.8) with k_d, $k_p > 0$ and $k_d - k_p\tau_d > 0$ (which leads to individual vehicle stability as discussed before) and the ETM described by (8.14) and (8.15), the remaining part of Problem 8.1 can be reformulated as follows: provide design conditions for the time-constant $\tau_{miet} \in \mathbb{R}_{>\tau_{mad}}$ and the function Ψ_i such that the system described by (8.6)-(8.8), and (8.11)-(8.15),

$i \in \bar{N}$, is string-stable despite the presence of time-varying delays (that are upper bounded by a given τ_{mad}) and such that the (average) time in between two consecutive transmission instants, also referred to as the inter-event times, is significantly larger than for time-triggered control schemes with a fixed transmission rate.

8.5.3 State space formulation of platoon model

Since we are interested in string stability, it is of interest to evaluate the input-output behavior in terms of $\mathcal{L}_2$-gains with respect to χ_{i-1} (as input) and χ_i (as output). As already illustrated in Figure 8.3 and as we will show later, this input-output behavior is not affected by other vehicles in the platoon. To describe this input-output behavior, let us define

$$\tilde{x}_i := \begin{bmatrix} v_{i-1} & a_{i-1} & u_{i-1} & e_i & v_i & a_i & u_i \end{bmatrix}^\top, \tag{8.16}$$

for $i \in \bar{N}\backslash\{1\}$. Then the platoon dynamics in between the update events, as given in (8.6)-(8.8), can be formulated in terms of the following state-space model

$$\dot{\tilde{x}}_i(t) = A\tilde{x}_i(t) + B\chi_{i-1}(t) + E\hat{u}_{i-1}(t), \tag{8.17}$$

for $t \in \mathbb{R}_{\geqslant 0} \setminus \{t_k^{i-1} + \Delta_{k+1}^{i-1}\}_{k\in\mathbb{N}}$, $i \in \bar{N}\backslash\{1\}$, and $k \in \mathbb{N}$, where

$$A = \begin{bmatrix} 0 & 1 & 0 & 0 & 0 & 0 & 0 \\ 0 & -\frac{1}{\tau_d} & \frac{1}{\tau_d} & 0 & 0 & 0 & 0 \\ 0 & 0 & -\frac{1}{h} & 0 & 0 & 0 & 0 \\ 1 & 0 & 0 & 0 & -1 & -h & 0 \\ 0 & 0 & 0 & 0 & 1 & 0 & 0 \\ 0 & 0 & 0 & 0 & 0 & -\frac{1}{\tau_d} & \frac{1}{\tau_d} \\ \frac{k_d}{h} & 0 & 0 & \frac{k_p}{h} & -\frac{k_d}{h} & -k_d & -\frac{1}{h} \end{bmatrix} \tag{8.18}$$

$$B = \begin{bmatrix} 0 & 0 & \frac{1}{h} & 0 & 0 & 0 & 0 \end{bmatrix}^\top \tag{8.19}$$

$$E = \begin{bmatrix} 0 & 0 & 0 & 0 & 0 & 0 & \frac{1}{h} \end{bmatrix}^\top, \tag{8.20}$$

and where $\hat{u}_{i-1}$ evolves according to (8.12) and (8.13).

The input-output relation of u_0 and χ_1 does not involve network-induced imperfections since the first vehicle follows a virtual reference vehicle, *i.e.*, $\hat{u}_0(t) = u_0(t)$ for all $t \in \mathbb{R}_{\geqslant 0}$. Let us define $\tilde{x}_1 := \begin{bmatrix} v_0 & a_0 & e_1 & v_1 & a_1 & u_1 \end{bmatrix}^\top$, then the input-output relation of u_0 and χ_1 can be described by the following state space model

$$\dot{\tilde{x}}_1(t) = A_0\tilde{x}_1(t) + B_0u_0(t), \tag{8.21a}$$

$$\chi_1(t) = C_0\tilde{x}_1(t) + D_0u_0(t), \tag{8.21b}$$

for all $t \in \mathbb{R}_{\geqslant 0}$, where

$$A_0 = \begin{bmatrix} 0 & 1 & 0 & 0 & 0 & 0 \\ 0 & -\frac{1}{\tau_d} & 0 & 0 & 0 & 0 \\ 1 & 0 & 0 & -1 & -h & 0 \\ 0 & 0 & 0 & 0 & 1 & 0 \\ 0 & 0 & 0 & 0 & -\frac{1}{\tau_d} & \frac{1}{\tau_d} \\ \frac{k_d}{h} & 0 & \frac{k_p}{h} & -\frac{k_d}{h} & -k_d & -\frac{1}{h} \end{bmatrix}, B_0 = \begin{bmatrix} 0 \\ \frac{1}{\tau_d} \\ 0 \\ 0 \\ 0 \\ \frac{1}{h} \end{bmatrix}$$
$$C_0 = \begin{bmatrix} k_d & 0 & k_p & -k_d & -k_d h & 0 \end{bmatrix}, D_0 = 1. \tag{8.22}$$

Let us remark that for all $h, \tau_d, k_p, k_d \in \mathbb{R}_{>0}$, a minimal realization of (A_0, B_0, C_0, D_0) is given by $\chi_1(t) = u_0(t)$, $t \in \mathbb{R}_{\geqslant 0}$. In other words, for the zero initial condition, *i.e.*, when $\tilde{x}_1(0) = \begin{bmatrix} 0 & 0 & 0 & 0 & 0 & 0 \end{bmatrix}^\top$, the solution to (8.21) satisfies $\chi_1(t) = u_0(t)$, $t \in \mathbb{R}_{\geqslant 0}$. Given the latter, we find that (8.10) holds for $i = 1$ and $k_d, k_p > 0$ with $k_d - k_p \tau_d > 0$ (which leads to individual vehicle stability as discussed in Section 8.4).

In essence, the dynamical system corresponding to the lumped state vector $\tilde{x} = \begin{bmatrix} \tilde{x}_1^\top & \tilde{x}_2^\top & \dots & \tilde{x}_N^\top \end{bmatrix}^\top$ that can be obtained by means of (8.17)-(8.22), $i \in \bar{N}$, constitutes an overlapping decomposition of the entire platoon model given by (8.6), (8.7), $i \in \bar{N}$, and (8.8), see also [214]. The main advantages of having this decomposition is that we now only have to evaluate the input-output properties of these (overlapping) subsystems. In fact, by recalling that (8.10) holds for $i = 1$, we only need to evaluate the $\mathcal{L}_2$-gains of (8.17) with respect to χ_{i-1} (as input) and χ_i (as output) for $i \in \bar{N} \setminus \{1\}$. Since we consider a homogeneous platoon, we only have to examine the $\mathcal{L}_2$-gain of a single subsystem. This leads to conditions that are computationally more tractable since the state-dimension of $\tilde{x}_i$, $i \in \bar{N}$, is in general much smaller than the state-dimension of x. More importantly, if these conditions are satisfied, the string stability property as given in (8.10) holds for any arbitrary platoon length N. Let us remark, however, that it is not trivial to extend this result to platoons with other communication topologies such as a two-vehicle look-ahead communication topology as described in, *e.g.*, [186].

8.5.4 Hybrid system formulation of platoon model

To facilitate the $\mathcal{L}_2$-gains with respect to χ_{i-1} (as input) and χ_i (as output), we reformulate the model given in (8.17) using the hybrid system formulation as presented in (8.2), see also [98]. Moreover, we express the model in terms of the network-induced errors $e_{u_{i-1}}$, $i \in \bar{N} \setminus \{1\}$, as given in (8.11), which was also employed in [51, 72, 73, 120, 173, 191].

Before we reformulated the platoon model in terms of a hybrid system, we first discuss the dynamics of $e_{u_{i-1}}$, $i \in \bar{N} \setminus \{1\}$, as in (8.11) at update events. By recalling that at update events, $\hat{u}_{i-1}$ is updated according to (8.12), we find

that the dynamics of $e_{u_{i-1}}$, $i \in \bar{N} \setminus \{1\}$, at update events are given by

$$\begin{aligned} e_{u_{i-1}}((t_k^{i-1}+\Delta_k^{i-1})^+) &= \hat{u}_{i-1}((t_k^{i-1}+\Delta_k^{i-1})^+) - u_{i-1}(t_k^{i-1}+\Delta_k^{i-1}) \\ &= u_{i-1}(t_k^{i-1}) - \hat{u}_{i-1}(t_k^{i-1}+\Delta_k^{i-1}) + \hat{u}_{i-1}(t_k^{i-1}+\Delta_k^{i-1}) - u_{i-1}(t_k^{i-1}+\Delta_k^{i-1}) \\ &\overset{(8.13)}{=} \underbrace{u_{i-1}(t_k^{i-1}) - \hat{u}_{i-1}(t_k^{i-1})}_{-e_{u_{i-1}}(t_k^{i-1})} + \underbrace{\hat{u}_{i-1}(t_k^{i-1}+\Delta_k^{i-1}) - u_{i-1}(t_k^{i-1}+\Delta_k^{i-1})}_{e_{u_{i-1}}(t_k^{i-1}+\Delta_k^{i-1})} \\ &= -e_{u_{i-1}}(t_k^{i-1}) + e_{u_{i-1}}(t_k^{i-1}+\Delta_k^{i-1}). \end{aligned} \tag{8.23}$$

Let us highlight that for the third equality, we used Assumption 8.1.

To formulate the platoon dynamics in terms of jump and flow equations as in (8.2), we introduce the auxiliary variables $\tau_i \in \mathbb{R}_{\geqslant 0}$, $l_i \in \{0,1\}$, $s_i \in \mathbb{R}$, $i \in \bar{N}$. The variable τ_i constitutes a local timer that keeps track on the time elapsed since the most recent transmission of vehicle i. The variable l_i indicates whether the next event at vehicle i is a transmission ($l_i = 0$) or an update event ($l_i = 1$). The variable s_i is used as a memory variable to store the value of $-e_{u_i}$ at transmission instants t_k^i, $i \in \bar{N}$, $k \in \mathbb{N}$. Consider the state vector

$$\xi_i = (\tilde{x}_i, e_{u_{i-1}}, \tau_{i-1}, l_{i-1}, s_{i-1}, \eta_{i-1}) \in \mathbb{X}_i, i \in \bar{N} \setminus \{1\} \tag{8.24}$$

with $\mathbb{X}_i := \mathbb{R}^7 \times \mathbb{R} \times \mathbb{R}_{\geqslant 0} \times \{0,1\} \times \mathbb{R} \times \mathbb{R}_{\geqslant 0}$. Based on (8.14) and Assumption 8.2, we find that the flow and jump sets are given by

$$\mathcal{C}_i := \{\xi_i \in \mathbb{X}_i \mid l_{i-1} = 0 \vee (0 \leqslant \tau_{i-1} \leqslant \tau_{mad} \wedge l_{i-1} = 1)\}, \tag{8.25}$$

and

$$\mathcal{D}_i := \{\xi_i \in \mathbb{X}_i \mid (\eta_{i-1} = 0 \wedge \tau_{i-1} \geqslant \tau_{miet}) \vee l_{i-1} = 1\}, \tag{8.26}$$

respectively. Observe that indeed, the system jumps in case the triggering condition given in (8.14) is violated. The flow dynamics are given by $\dot{\xi}_i = F_i(\xi_i, \chi_{i-1})$ with the flow map $F_i : \mathbb{X} \times \mathbb{R} \to \mathbb{X}$ defined as

$$\begin{aligned} F_i(\xi_i, \chi_{i-1}) := \Big(& f(\tilde{x}_i, e_{u_{i-1}}, \chi_{i-1}), g(\tilde{x}_i, \chi_{i-1}), 1, 0, 0, \\ & \Psi_{i-1}(\chi_{i-1}, u_{i-1}, e_{u_{i-1}}, \tau_{i-1})). \end{aligned} \tag{8.27}$$

By substituting (8.11) in (8.17), we obtain that $f(\tilde{x}_i, e_{u_{i-1}}, \chi_{i-1})$ is given by

$$f(\tilde{x}_i, e_{u_{i-1}}, \chi_{i-1}) := A_{11}\tilde{x}_i + A_{12}e_{u_{i-1}} + A_{13}\chi_{i-1}, \tag{8.28}$$

where

$$A_{11} = A + EC, \qquad A_{12} = E, \qquad A_{13} = B, \tag{8.29}$$

and where $C := \begin{bmatrix} 0 & 0 & 1 & 0 & 0 & 0 & 0 \end{bmatrix}$, such that $u_{i-1} = C\tilde{x}_i$. The expression for $g(\tilde{x}_i, \chi_{i-1})$ can be obtained from the fact that $\dot{e}_{u_{i-1}} = -\dot{u}_{i-1}$ when $\xi_i \in \mathcal{C}_i$, $i \in \bar{N} \setminus \{1\}$, due to Assumption 8.1. As such, $g(\tilde{x}_i, \chi_{i-1})$ is given by

$$g(\tilde{x}_i, \chi_{i-1}) := \frac{1}{h} C\tilde{x}_i - \frac{1}{h}\chi_{i-1}. \tag{8.30}$$

The jump dynamics are given by $\xi_i^+ = G_i(\xi_i)$ with the jump map $G_i : \mathbb{X} \to \mathbb{X}$ defined as

$$G_i(\xi_i) := (\tilde{x}_i, e_{u_{i-1}} + l_{i-1}s_{i-1}, l_{i-1}\tau_{i-1}, -(1-l_{i-1})e_{u_{i-1}}, 1-l_{i-1}, \eta_{i-1}). \tag{8.31}$$

Observe that, when $l_i = 0$, the variable l_i jumps to the value 1, and, when $l_i = 1$, l_i jumps to the value 0. The latter ensures that the a transmission event can only be followed by an update event and vice versa. Hence, the flow and jump sets and maps comply with Assumption 8.2. Moreover, observe that the timer τ_i is set to zero at transmission event (when $l_i = 0$).

Observe that the jump map in (8.31) is defined such that s_{i-1}, $i \in \bar{N} \setminus \{1\}$, is assigned the value of $-e_{u_{i-1}}$ at a transmission event (when $l_i = 0$). Given the latter and the fact that $\dot{s}_{i-1} = 0$ for $\xi_i \in \mathcal{C}_i$, we can see that the jump dynamics of $e_{u_{i-1}}$ defined by (8.31) are in correspondence with (8.23). Note that the variable s_{i-1} is set to zero at update events (when $l_i = 1$).

The input-output relation of χ_{i-1} and χ_i subject to network-induced errors is now described by the hybrid system $\mathcal{H}_i = (\mathcal{C}_i, F_i, \mathcal{D}_i, G_i)$, $i \in \bar{N} \setminus \{1\}$ with $\mathcal{C}_i$, F_i, $\mathcal{D}_i$ and G_i as in (8.25), (8.27), (8.26) and (8.31), respectively, and where the output χ_i, $i \in \bar{N}\setminus\{1\}$, as in (8.8) is given by

$$\chi_i = C_z\tilde{x}_i + D_z e_{u_{i-1}}, \tag{8.32}$$

where

$$C_z = \begin{bmatrix} k_d & 0 & 1 & k_p & -k_d & -k_d h & 0 \end{bmatrix}, \; D_z = 1. \tag{8.33}$$

It is important to notice that this relation indeed only depends on (part of) the states of vehicle $i-1$ and the states of vehicle i and that it does not depend on states of other vehicles in the platoon.

Consider the following definition.

Definition 8.1. *The hybrid system $\mathcal{H}_i$, $i \in \bar{N} \setminus \{1\}$, is said to be $\mathcal{L}_2$-stable from input χ_{i-1} to output χ_i with an $\mathcal{L}_2$-gain less than or equal to θ, if there exists a $\mathcal{K}_\infty$-function β such that for any exogenous input $\chi_{i-1} \in \mathcal{L}_2$, and any initial condition $\xi_i(0,0) \in \mathbb{X}_{0,i}$ with $\mathbb{X}_{0,i} = \{\xi_i \in \mathbb{X} \mid l_{i-1} = 0\}$, each corresponding maximal solution to $\mathcal{H}_i$ is t-complete and satisfies*

$$\|\chi_i\|_{\mathcal{L}_2} \leqslant \beta(|\left(\tilde{x}_i(0,0), e_{u_{i-1}}(0,0), s_{i-1}(0,0), \eta_{i-1}(0,0)\right)|) + \theta\|\chi_{i-1}\|_{\mathcal{L}_2}. \tag{8.34}$$

Consider the following problem.

$$\begin{pmatrix} A_{11}^\top P + PA_{11} + \mu C_z^\top C_z + (\varrho + \frac{1}{h^2})C^\top C & PA_{12} + \mu C_z^\top D_z & PA_{13} + \frac{1}{h^2}C^\top \\ A_{12}^\top P + \mu D_z^\top C_z & \mu D_z^T D_z - \gamma^2 & 0 \\ A_{13}^\top P + \frac{1}{h^2}C & 0 & \frac{1}{h^2} - (1+\epsilon)\mu \end{pmatrix} \preceq 0,\ P \succeq 0. \tag{8.35}$$

Problem 8.2. *Determine the time constants $\tau_{miet}, \tau_{mad} \in \mathbb{R}_{>0}$ with $\tau_{mad} \leqslant \tau_{miet}$, the function Ψ_{i-1}, $i \in \bar{N} \setminus \{1\}$ (as in the event generator given by (8.14) and (8.15)), such that each system $\mathcal{H}_i = (\mathcal{C}_i, F_i, \mathcal{D}_i, G_i)$, $i \in \bar{N} \setminus \{1\}$ with $\mathcal{C}_i$, F_i, $\mathcal{D}_i$ and G_i as in (8.25), (8.27), (8.26) and (8.31), respectively, is $\mathcal{L}_2$-stable from input χ_{i-1} to output χ_i with an $\mathcal{L}_2$-gain less than or equal to one, with a strictly positive τ_{miet} to assure Zeno-freeness and with large (average) inter-event times $t_{j+1}^{i-1} - t_j^{i-1}$, $j \in \mathbb{N}$.*

By recalling that the individual vehicle stability is not affected by the ETM design and the fact that (8.10) holds for $i = 1$, we can conclude that solving Problem 8.2 is sufficient for solving the problem loosely stated at the end of Section 8.3.2. In the next subsection, we present the design procedure for the time constants τ_{mad} and τ_{miet} and the function Ψ_{i-1}, $i \in \bar{N} \setminus \{1\}$, such that the criteria mentioned in Problem 8.2 are satisfied.

8.6 ETM Design with string stability guarantees

In the first part of this section, we specify the conditions for the design of τ_{mad}, τ_{miet} and Ψ_i as in (8.15) based on the result in [71, 72] and for obtaining string stability guarantees. Based on these conditions, we provide a systematic design procedure in the second part of this section, resulting in intuitive trade-off curves between robustness in terms of τ_{mad} and utilization of communication resources in terms of τ_{miet}.

8.6.1 Stability analysis

Consider the following condition regarding the flow-dynamics of $\tilde{x}_i$, $i \in \bar{N} \setminus \{1\}$, as given in (8.27).

Condition 8.1. *There exist constants γ, ϵ, $\varrho \in \mathbb{R}_{\geqslant 0}$ and $\mu \in \mathbb{R}_{>0}$ such that (8.35) holds with A_{11}, A_{12} and A_{13} as in (8.29)*

Let us remark that Condition 1 in essence constitutes an $\mathcal{L}_2$-gain condition on the linear system given in (8.17), where $\sqrt{1+\epsilon}$ is an $\mathcal{L}_2$-gain upper bound with respect to χ_{i-1} and χ_i and γ an $\mathcal{L}_2$-gain upper bound related to the influence of the transmission error $e_{u_{i-1}}$ on the state $\tilde{x}_i$.

In addition, we consider the following condition regarding the time-constants τ_{mad} and τ_{miet}.

Condition 8.2. *There exists a pair of time-constants* $(\tau_{mad}, \tau_{miet})$ *such that*

$$\gamma_1\phi_1(\tau) \geqslant \gamma_0\phi_0(\tau), \text{ for all } \tau \in [0, \tau_{mad}], \tag{8.36a}$$

$$\gamma_0\phi_0(\tau_{miet}) \geqslant \lambda^2\gamma_1\phi_1(0) \tag{8.36b}$$

with $\tau_{miet} \geqslant \tau_{mad}$, $\lambda \in (0,1)$ *and the constants* γ_0 *and* γ_1 *given by*

$$\gamma_0 := \gamma, \qquad \gamma_1 := \frac{\gamma}{\lambda}, \tag{8.37}$$

and where $\phi_l : \mathbb{R}_{\geqslant 0} \to \mathbb{R}$, $l \in \{0,1\}$, *satisfies*

$$\frac{d}{d\tau}\phi_l = -\gamma_l(\phi_l^2 + 1) \tag{8.38}$$

with $\phi_l(0) > 0$.

At last, we consider that the function $\Psi_{i-1} : \mathbb{R} \times \mathbb{R} \times \mathbb{R} \to \mathbb{R}$, $i \in \bar{N} \setminus \{1\}$, is of the form

$$\begin{aligned}\Psi_{i-1}(\chi_{i-1}, u_{i-1}, e_{u_{i-1}}, \tau_{i-1}) = \varrho u_{i-1}^2 \\ + \omega(\tau_{i-1})\left(\frac{1-\varepsilon}{h^2}(\chi_{i-1} - u_{i-1})^2 - \bar{\gamma}e_{u_i-1}^2\right),\end{aligned} \tag{8.39}$$

where

$$\omega(\tau_{i-1}) := \begin{cases} 0, & \text{for } \tau_{i-1} \leqslant \tau_{miet} \\ 1, & \text{for } \tau_{i-1} > \tau_{miet} \end{cases} \tag{8.40}$$

with

$$\bar{\gamma} = \gamma^2\left(1 + \frac{1}{\varepsilon}\phi_0^2(\tau_{miet})\right), \tag{8.41}$$

and where $\varepsilon \in (0,1)$ and $\varrho \in \mathbb{R}_{\geqslant 0}$ are tuning parameters.

Observe from (8.39) that $\Psi_{i-1}(\chi_{i-1}, u_{i-1}, e_{u_{i-1}}, \tau_{i-1}) \geqslant 0$, $i \in \bar{N} \setminus \{1\}$, for $\tau_{i-1} \leqslant \tau_{miet}$. As such, the triggering variable η_i as in (8.15) does not decrease when $\tau_{i-1} \leqslant \tau_{miet}$. Moreover, observe from (8.39) that $\Psi_{i-1}(\chi_{i-1}, u_{i-1}, e_{u_{i-1}}, \tau_{i-1}) \leqslant 0$, $i \in \bar{N} \setminus \{1\}$ (and thus that the triggering variable η_{i-1} is decreasing) when the transmission error $e_{u_{i-1}}$ is relatively large with respect to $u_{i-1}^2 + \frac{1-\varepsilon}{h^2}(\chi_{i-1} - u_{i-1})^2$. Given the latter, we can conclude from (8.14) that a new transmission is scheduled if the transmission error $e_{u_{i-1}}$ is relatively large over time. Hence, in essence, this mechanism is similar to the ETM presented in the introduction, given by (8.1). The difference, however, is that for the ETM given by (8.14), (8.15) and (8.39), a robust positive MIET exists by design. Moreover, the ETM given by (8.14), (8.15) and (8.39) is a *dynamic* ETM as it employs the dynamic variable η_i to determine the transmission instants. The main motivation for using *dynamic* ETMs is that, in contrast to the commonly

studied *static* ETMs (such as the ETM in (8.1)), the generated inter-event times do not converge to the enforced lower bound in presence of disturbances when the output is close to zero, as observed in [41, 71], and typically lead to larger inter-event times.

By means of the Condition 1, Condition 2 and the definition of Ψ_{i-1}, $i \in \bar{N} \setminus \{1\}$, we can now establish the following result.

Theorem 8.1. *Consider the system $\mathcal{H}_i = (\mathcal{C}_i, F_i, \mathcal{D}_i, G_i)$, $i \in \bar{N} \setminus \{1\}$, with $\mathcal{C}_i$, F_i, $\mathcal{D}_i$ and G_i as in (8.25), (8.27), (8.26) and (8.31), respectively, and with Ψ_{i-1} given by (8.39) and suppose that Condition 1 with $\epsilon = 0$ and Condition 2 hold. Then the system $\mathcal{H}_i$ is $\mathcal{L}_2$-stable from input χ_{i-1} to output χ_i with an $\mathcal{L}_2$-gain less than or equal to one and thus the platoon system given by (8.7), $i \in \bar{N}$, (8.6) and (8.8) is string stable.*

The proof is provided in Appendix G.

It is important to notice that Condition 1 and Condition 2 do not depend on index i due to the homogeneous nature of the vehicle string.

8.6.2 ETM design

The first step of the design procedure is to compute the constants γ, μ and the matrix P. The constants γ, μ and the matrix P can be obtained via a Linear Matrix Inequality (LMI) optimization problem in which γ is minimized subject to the LMI given in (8.35) where the constant ϱ is a tuning parameter and ϵ is typically selected small. This LMI optimization problem can, for example, be solved using MATLAB with the YALMIP interface [153] and the SeDuMi solver [220]. Let us remark that if the system described by (8.6)-(8.8) is string-stable in the absence of network-induced imperfections, i.e., when $\hat{u}_{i-1}(t) = u_i(t)$ for all $t \in \mathbb{R}_{\geqslant 0}$, the LMI in (8.35) is always feasible for sufficiently large γ and sufficiently small ϱ.

As mentioned before, the constant γ is related the influence of the transmission error $e_{u_{i-1}}$ on the state $\tilde{x}_i$. To be more specific, when γ is large, then the influence of transmission error $e_{u_{i-1}}$ on the state $\tilde{x}_i$ is also large and more transmissions might be needed in order to realize desirable closed-loop results.

The second step in the design procedure is to determine the $(\tau_{mad}, \tau_{miet})$-trade-off curves. To do so, we solve (8.38) for $\phi_0(0) = \frac{1}{\lambda}$ and $\phi_1(0) \in \left(\frac{\phi_0\gamma_0}{\gamma_1}, \frac{\phi_0\gamma_0}{\gamma_1\lambda^2}\right]$ with $\lambda \in (0, 1)$. The corresponding $(\tau_{mad}, \tau_{miet})$-combinations can be obtained by computing intersection of the functions $\gamma_0\phi_0$ and $\gamma_1\phi_1$ (which corresponds to τ_{mad}) and the intersection of $\gamma_0\phi_0$ and $\lambda^2\gamma_1\phi_1(0)$ (which correspond to τ_{miet}), see also [120].

The latter procedure is also illustrated in Figure 8.4 in which (8.38) was solved for $\gamma = 8.442$, $\lambda = 0.305$, $\phi_0(0) = 3.279$ and $\phi_1(0) = 8.557$. As shown in Figure 8.4, this results in $(\tau_{mad}, \tau_{miet}) = (0.026, 0.072)$.

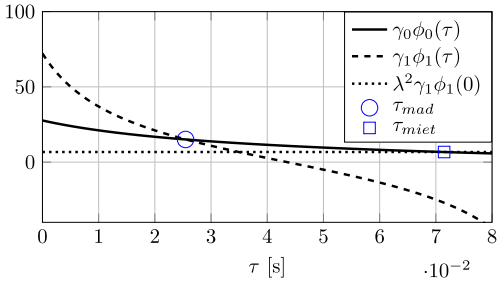

Fig. 8.4. Evolution of $\gamma_l\phi_l(\tau)$, $l \in \{0, 1\}$, with ϕ_l the solutions of (8.38) for $\gamma = 8.442$, $\lambda = 0.305$, $\phi_0(0) = 3.279$ and $\phi_1(0) = 8.557$. The circle represents the point at which $\gamma_0\phi_0(\tau) = \gamma_1\phi_1(\tau)$, which corresponds to $\tau_{mad} = 0.026$ and the rectangle represents the point at which $\gamma_0\phi_0(\tau) = \lambda^2\gamma_1\phi_1(0)$, which corresponds to $\tau_{miet} = 0.072$.

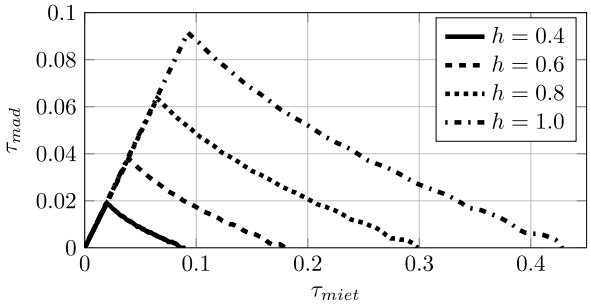

Fig. 8.5. $(\tau_{mad}, \tau_{miet})$-trade-off curves corresponding to the platoon system described by (8.7), $i \in \bar{N}$, (8.6) and (8.8) with $\tau_d = 0.1$, $k_p = 0.2$, $k_d = 0.7$, $h \in \{0.4, 0.6, 0.8, 1.0\}$, $\varrho = 0.04$ and $\epsilon = 0.01$.

By repeating the procedure described above for various values of λ, and $\phi_1(0)$, other $(\tau_{mad}, \tau_{miet})$-combinations can be obtained which are then used to establish the $(\tau_{mad}, \tau_{miet})$-trade-off curve. This trade-off curve provides an intuitive way to find appropriate values λ, $\phi_0(0)$ and thus $\phi_0(\tau_{miet})$ which are part of the ETM given by (8.14), (8.15) and (8.39). As such, although the design procedure might seem difficult to carry out at first sight, the required conditions can be verified in a systematic manner and the procedure results in intuitive trade-off curves. In Figure 8.5, the $(\tau_{mad}, \tau_{miet})$-trade-off curves are shown for the platoon system described by (8.7), $i \in \bar{N}$, (8.6) and (8.8) with $\tau_d = 0.1$, $k_p = 0.2$, $k_d = 0.7$, $h \in \{0.4, 0.6, 0.8, 1.0\}$, $\varrho = 0.04$ and $\epsilon = 0.01$. The $(\tau_{mad}, \tau_{miet})$-combinations that are confined by the trade-off curves and the horizontal axis lead to a string-stable platoon.

As mentioned before, if the system is string-stable when network-induced errors are absent, *i.e.*, when $\hat{u}_{i-1}(t) = u_{i-1}(t)$ for all $t \in \mathbb{R}_{\geqslant 0}$, one can always find a matrix P and constants γ, ϵ and ϱ that satisfy (8.35). Consequently,

after the constants γ, ϵ and ϱ are obtained, one can always find (possibly small) time-constants τ_{miet} and τ_{mad} such that string stability is preserved.

Remark 8.3. The LMI condition as given in (8.35) yields an $\mathcal{L}_2$-gain upper bound with respect to χ_{i-1} and χ_i of $\sqrt{1+\epsilon}$. Hence, strictly speaking (and as indicated in Theorem 1), the vehicle platoon described by (8.6) and (8.7) is only guaranteed to be string-stable if $\epsilon = 0$. Let us remark, however, that the $\mathcal{L}_2$-gain is also lower-bounded by 1 due to the individual vehicle stability objective. As such, the LMI optimization problem stated in (8.35) is hard to solve from a numerical point of view. For this reason, we typically take ϵ small ($\epsilon \sim 10^{-2}$) but strictly positive to make the LMI computationally tractable. Let us remark that ϵ is typically chosen such that its size is small with respect to the uncertainties introduced by the inevitable noise on radar and accelerometer measurements.

Remark 8.4. The variable ϱ constitutes a tuning parameter of the ETC system. To be more specific, from (8.39) we can see that the variable ϱ is part of the ETM given in (8.14) and (8.15), and therefore can have a significant influence on the average inter-event times generated by this ETM. Let us remark, however, that a bit of performance is sacrifice by choosing ϱ positive in the sense that it affects ϵ.

Remark 8.5. Important to notice is that the triggering condition given by (8.14), (8.15) and (8.39) indeed only depends on locally available information since the variables χ_{i-1}, u_{i-1}, $\hat{u}_{i-1}$ and τ_{i-1}, are available at vehicle $i-1$.

8.7 Experimental validation

To validate the proposed resource-aware control design and to demonstrate its technical feasibility, the event-triggered CACC strategy has been implemented on a platoon of three (almost) identical passenger vehicles. The Toyota Prius III Executive is selected as benchmark vehicle and is equipped with long-range radar, GPS and a communication module that uses the IEEE 802.11p-based ETSI ITS G5 standard for DSRC, see also Figure 8.6. Let us remark that the same test-bed was used in [187]. A schematic overview of the vehicle architecture is provided in Figure 8.7. Observe that the vehicle gateway provides access to the CAN-bus of the vehicle that is connected to the vehicle's actuators and sensors, which among others consists of the hybrid drive line, the accelerometer, the long-range radar measurements and the wheel speed encoders. Besides CAN-bus access, the vehicle gateway includes the low-level acceleration controller as discussed below (8.7) and safety-functionalities including a mechanism that allows the driver to overrule the system at any time.

The control design strategy is implemented on a real-time target, which provides reference commands to the vehicle gateway. Moreover, the real-time target, which runs MATLAB Simulink Real-Time applications at 100 Hz, is connected

Fig. 8.6. Benchmark platoon consisting of three passenger cars equipped with long-range radar and DSRC.

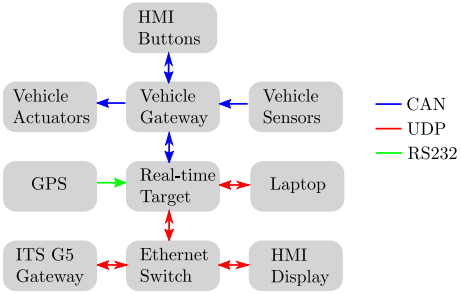

Fig. 8.7. Schematic overview of the vehicle architecture.

to the ITS G5 communication module and an HMI display that informs the driver about the target tracking functionalities, for example, it shows whether or not a wireless connection with the preceding vehicle is established.

The characteristic time constant of the drive line is $\tau_d = 0.1$. As experimentally verified in [187], the first-order model used to described the drive line which, neglecting the actuation delay, adequately described the longitudinal dynamics. To include the actuation delay of 0.2 seconds in the model, we use a 12^{th}-order Padé approximation to obtain a model including actuation delays that is used for the ETM design. For the experiments, we choose the controller gains as in (8.8) as $k_p = 0.2$ and $k_d = 0.7$, the desired following distance as in (8.4) with $r = 2.5$ meters and $h = 0.6$ seconds and the ETM parameters as in (8.39) and (35) as $\varrho = 0.04$, $\varepsilon = 0.5$ and $\epsilon = 0.01$, which yield $(\tau_{mad}, \tau_{miet})$-trade-off curves as depicted in Figure 8.5. Based on these trade-off curves, we choose $(\tau_{mad}, \tau_{miet}) = (0.026, 0.072)$, which corresponds to $\gamma = 8.442$, $\lambda = 0.305$, $\phi_0(0) = 3.279$ and $\phi_1(0) = 8.557$ and coincides with the situation illustrated in Figure 8.4.

To enable the implementation of the ETM as described by (8.14), (8.15) and (8.39) on a digital real-time platform, we use exact discretization in order to obtain a triggering condition that is only verified as discrete-time instants. Let us remark that in this discrete implementation a triggering event is scheduled before it actually violates (8.14) in order to compensate for the sampling effect of the real-time target. Moreover, as the signal-to-noise ratio is large when u_i is close to zero, it is desirable to avoid transmissions due to this measurement

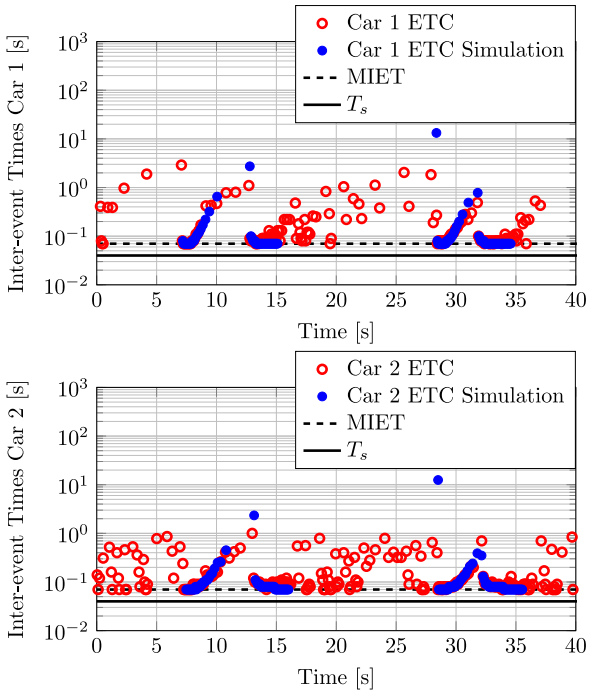

Fig. 8.8. Inter-event times generated by the ETM as given in (8.14), (8.15) and (8.39) resulting from the experiments (indicated in red) and from simulation (indicated in blue). The horizontal lines represent the minimum inter-event times τ_{miet} and the fixed transmission period $T_s = 0.04$ seconds as used in the benchmark TTC scheme.

noise when u_i is close to zero. As such, we employ, next to the ETM as given in (8.14) and (8.15), a constant threshold in the sense that no transmissions are being issued when $|u_i| \leqslant 0.05$.

To evaluate the proposed ETC method in terms of performance (in this case the spacing error) and utilization of communication resources (in this case the inter-event times), the experimental results are compared with the results obtained using a time-triggered control (TTC) scheme, in which the transmission instants are determined according to fixed transmission rate of $1/T_s = 25$ Hz, as benchmark. The experimental results are shown in Figure 8.8 and Figure 8.9. To be more specific, in Figure 8.8, the inter-event times generated by the first and second car of the platoon are shown. Moreover, to indicate the predictability of the proposed ETC scheme, also the simulation results are included. Observe from Figure 8.8 and Figure 8.9 that the inter-event times generated by the ETM are only small in case there is a significant change in the desired acceleration and otherwise, significantly larger than the enforced lower-bound τ_{miet} or the

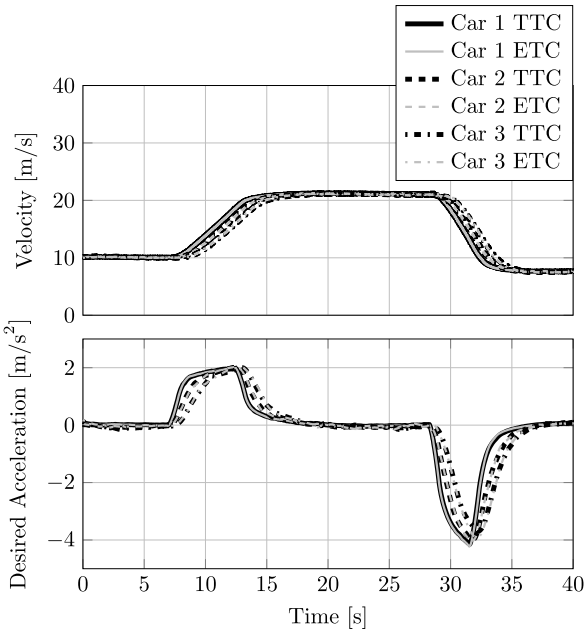

Fig. 8.9. Time response of the platoon of 3 passenger vehicles. In the top plot, the velocity $v_i(t)$, $i \in \{1, 2, 3\}$, at time t, of each vehicle is displayed. The bottom plot shows the desired acceleration $\chi_i(t)$, $i \in \{1, 2, 3\}$ at time t, for all three vehicles.

communication period T_s of the TTC scheme (showing that "communication is only used when really needed"). In fact, the average inter-event times generated by the ETM in vehicle 1 and in vehicle 2, are $\tau^1_{avg} = 0.24$ and $\tau^2_{avg} = 0.16$, respectively, which is clearly larger than τ_{miet} and T_s.

In Figure 8.9 the time-response of the velocity and desired acceleration for both the proposed ETC and the benchmark TTC strategy and all three vehicles are plotted. Observe that the responses corresponding to the ETC scheme look similar to the responses corresponding to the TTC scheme despite the significant reduction in communication achieved by the ETC scheme. The maximum absolute value of the spacing error (as defined in (8.5)) is approximately 0.8 m for both the TTC and the ETC implementation showing that the performance of the ETC implementation is similar to the performance of the TTC scheme. Summarizing, the experimental results illustrate the potential benefits of event-triggered communication for CACC systems, namely, having significantly larger inter-event times while realizing similar control performance in comparison with conventional time-triggered control methods.

8.8 Conclusions

Dedicated Short Range Communication (DSRC) is a key ingredient in Cooperative Adaptive Cruise Control (CACC) systems to overcome the physical limitations of onboard sensors and enables to form string-stable platoons with small inter-vehicle distances. However, excessive utilization of communication resources can have a negative impact on the reliability of the DSRC channel and the size of the transmission delays. For this reason, a resource-aware CACC control strategy was proposed in this chapter, which aims to reduce the utilization of communication resources in comparison with conventional time-triggered control method while preserving the individual vehicle stability and string-stability guarantees. In addition, robustness with respect to time-varying delays and the presence of a strictly positive lower-bound on the minimum inter-event times (to avoid Zeno-behavior) is guaranteed by design. The proposed resource-aware control method relies on a recently developed ETC strategy that exploits the unique combination of *dynamic* event-triggered control and time-regularization ("waiting times"). Moreover, a systematic design procedure for this ETC strategy was provided that results in intuitive trade-off curves between robustness in terms of the maximum allowable delay (MAD) and utilization of communication resources in terms of the minimum inter-event time (MIET). The proposed resource-aware CACC strategy was experimentally validated by means of a platoon of three passenger vehicles employing a time-gap of only $h = 0.6$ seconds. The experimental results clearly demonstrated the potential benefits of event-triggered control, namely, having significantly larger inter-event times while realizing string stability and similar control performance in comparison with conventional time-triggered control methods. This result might be one of the important steps in order to realise the implementation of CACC on a large scale without introducing congestion of V2V communication network and/or the need to increase the time-gaps in the platoon.

Chapter 9

Conclusions, Recommendations and Final Thoughts

9.1 Concluding remarks

The field of networked control systems (NCSs) offers many novel promising applications with enormous societal impacts. However, control systems operating over possibly shared and wireless communication channels also introduce many new challenges due to the inherent network-induced imperfections of NCSs and their vulnerabilities with respect to malicious attacks. In general, these artifacts degrade the performance of the closed-loop system and might even lead to instability. As such, it is, on the one hand, important to take them into account in the control design. On the other hand, the control architecture itself might also affect the quality of the communication channel. For example, excessive use of communication resources typically leads to larger transmission delays and/or more packet losses. Hence, in NCSs, there is a strong interaction between the design of the control architecture and the design of the ICT infrastructure, and as a result, it is not optimal to consider them separately. For this reason, there is a strong need for integrated design approaches.

In this thesis, we addressed the design of resource-aware and resilient control schemes for safety-critical NCSs and thereby provided an important step towards a more integrated systems design. In fact, we considered event-triggered control (ETC) systems that aim to minimize the utilization of communication resources while guaranteeing desired stability and/or performance properties by introducing feedback in the sampling and communication processes. The feedback in sampling and communication is introduced by an event-generator, also referred to as the *event-triggering mechanism* (ETM), which determines the sampling

instants on the basis of current (and possibly previous) output measurements and other available information.

The contributions of this thesis can be summarized as follows:

(i) The development of novel design frameworks for ETC algorithms for output-based feedback systems that aim to reduce the utilization of communication resources and take into account the inevitable network-induced imperfections (Chapter 2-5).

(ii) The development of resilient ETC algorithms for output-based feedback systems that, in addition to the resource-aware requirement, realize desired closed-loop behavior despite the presence of malicious denial-of-service attacks (Chapter 6).

(iii) The development of ETC algorithms for multi-agent systems (Chapter 7).

(iv) Experimental validation of the proposed resource-aware control strategy on a relevant safety-critical system (Chapter 8).

Each of these contribution are discussed in more detail below.

9.1.1 Design frameworks for ETC algorithms

One of the main difficulties in the design of ETC schemes is to design the ETM such that a strictly positive *minimum-inter event time* (MIET) is obtained, while guaranteeing important stability and performance properties despite the presence of network-induced imperfections and disturbances. The latter property is particularly difficult to realize for systems that rely on output-based feedback. In Chapter 2, a novel ETC strategy for a class of nonlinear output-based feedback systems was presented. The proposed framework results in closed-loop systems with guaranteed finite $\mathcal{L}_p$-gains and strictly positive lower bounds on the inter-event times. Moreover, the controllers and event generators can be synthesized in an output-based and/or decentralized form with multiple asynchronously operating networks, the design takes the specific medium access protocol into account, and robustness to (variable) transmission delays (in terms of the maximum allowable delays (MADs)) is guaranteed by design. In addition, it was shown that for linear systems, the provided design conditions can be verified systematically based on Linear Matrix Inequalities (LMIs). Key to obtaining all these beneficial properties is the unique combination of *dynamic* event-triggering conditions and time regularization. Interestingly, the MIET and the MAD bounds of the presented ETC strategy are close to or equal to the maximal allowable transmission interval (MATI) and MAD bounds derived for time-based specifications for stability and guaranteed $\mathcal{L}_p$-gains of NCSs, but the (average) inter-event times significantly larger.

One of the strengths of the dynamic ETC approach presented in Chapter 2 is that it is a general framework encompassing many nonlinear systems while still guaranteeing the important properties mentioned above. However, it is of interest to examine if less conservative design techniques can be obtained when a particular class of systems is considered, for example, linear systems. In Chapter 3, we presented novel ETC schemes that exploit Riccati-based tools tailored to linear systems. This Riccati-based approach leads to a further improvement of ETC schemes compared to the results presented in Chapter 2 in the sense that a larger MIET can be obtained under the same $\mathcal{L}_2$-gain guarantees. In addition, Chapter 3 also considered (dynamic) *periodic* ETC schemes, which only require access to output measurements at discrete instants in time. The benefit of periodic ETC strategies is that they are more easy to implement in practice as it is not needed to continuously measure and monitor the outputs of the plant, but only at specific sampling times. Many of the ETC schemes of Chapter 2 will eventually be implemented on digital platforms and thereby take the form of PETC systems. Therefore, it is important to have analysis and design tools for these controllers. All the event-generators that have been proposed in Chapter 3, have a strictly positive MIET, can be synthesized in an output-based form and are robust to (variable) transmission delays by design.

In Chapter 4, we built upon the resource-aware control paradigm introduced in Chapter 2 and considered the quantization of the output measurements. In NCSs, quantization mechanisms are inevitable due to the fact that the bandwidth of the communication channel is limited, which imposes restrictions on the size of the transmitted packets (in terms of bits). For this reason, a design framework was presented in Chapter 4 for synthesizing the dynamic quantizers and the event-triggering mechanisms for each individual sensor node, simultaneously. Interestingly, the intuitive trade-off between the size of the data packet that has to be transmitted and the number of transmissions naturally appears in the main theoretical results and the design methods. In fact, the design of quantizers and event generators is directly coupled and reflects this essential trade-off. Similar as in Chapter 2, (dynamic) ETMs with time regularization were used in order to enforce the existence of a strictly positive MIET. Moreover, the proposed dynamic quantization strategy prevents the accumulation of zoom actions since the zoom actions only take place at transmission instants. The number of bits that need to be sent over the network per transmission instant is finite and can be determined a priori.

In NCSs, the presence of packet losses is often unavoidable. In Chapter 5, a systematic design procedure was proposed for static and dynamic ETC schemes under packet losses. The resulting closed-loop system was shown to be UGAS in absence of disturbances, and $\mathcal{L}_p$-stable with respect to its performance output and external disturbances in the presence of disturbances. Moreover, it was shown that a robust positive MIET is guaranteed by design, even for the case where disturbances and packet dropouts are present. In fact, the ETMs

proposed in this chapter can admit a maximum allowable number of successive packet dropouts (MANSD) while still maintaining the desired stability and performance properties. Two different ETC configurations were proposed, namely, a configuration that is equipped with an acknowledgment scheme (as, *e.g.*, in TCP) and a configuration which is not (as, *e.g.*, in UDP). By means of a numerical example, it was shown that, under the same performance guarantees, ETC schemes relying on acknowledgments yield larger inter-event times than the ETC schemes without acknowledgments schemes.

9.1.2 Resilient ETC algorithms

Cyber-security forms a crucial aspect in the design of NCSs. Chapter 6 addressed the design of ETC algorithms for NCSs that, next to the resource-aware requirement, are resilient to malicious *Denial-of-service* (DoS) attacks. In particular, the control and communication strategy was inspired by the ETC scheme proposed in Chapter 2 and thereby applicable to a class of nonlinear output-based feedback systems which have not been covered by existing results in the literature. The proposed framework led to guarantees regarding stability and performance in terms of $\mathcal{L}_\infty$ gains and guarantees regarding the existence of a robust strictly positive lower bound on the inter-event times despite the presence of disturbances and DoS attacks. These guarantees could be given under the assumption that the DoS attacks are restricted in terms of frequency and duration. The latter assumption is reasonable in many practical scenarios due to several provisions that can be taken to mitigate DoS attacks.

9.1.3 ETC algorithms for multi-agent systems

Chapter 7 discussed a systematic design methodology for ETC strategies for a class of nonlinear multi-agents systems (MAS) subject to disturbances resulting in strictly positive MIETs. The proposed framework can capture many relevant control problems as it leads to MASs that are dissipative with respect to a desired supply rate and supports the use of model-based holding devices. As particular cases, it captures consensus seeking, output-regulation and leader following problems. Furthermore, robustness to *non-uniform* and *time-varying* delays is guaranteed by design. In addition to ETMs, so-called destination protocols were introduced. These protocols locally determine to which of the connected agents, local output measurements are transmitted at each transmission instant. Interestingly, this concept can also be exploited in the context of packet losses and denial-of-service attacks. In short, Chapter 7 provided a general framework that covers many relevant control problems for event-triggered MASs subject to network-induced imperfections and malicious DoS attacks.

9.1.4 Experimental validation

As mentioned before, ETC systems offer significant reductions in the utilization of communication resources while guaranteeing desired control performance, which are crucial in many practical applications. A particular application for which this concept is useful, is Cooperative Adaptive Cruise Control (CACC). CACC systems exploit Dedicated Short Range Communication (DSRC) to enable the formation of string-stable platoons with small inter-vehicle distances. However, it is shown that excessive utilization of communication resources can have a negative impact on the reliability and the quality of the DSRC channel and thereby the functionality of CACC systems. For this reason, ETC is an important enabling technology for harvesting all the potential benefits of CACC systems and realizing the introduction of CACC systems on a large scale without introducing congestion of V2V communication network. In Chapter 8, the proposed ETC method in Chapter 2 was experimentally validated by means of a platoon of three passenger vehicles equipped with CACC employing a time-gap of only 0.6 seconds. The experimental results showed that in comparison with conventional time-triggered solutions, the proposed resource-aware CACC strategy indeed leads to significant reductions in the utilization of communication resources while preserving the individual vehicle stability and string-stability guarantees. This provides a proof-of-concept of the main results in this thesis.

9.2 Recommendations

As mentioned in the introduction, the field of cyber-physical systems (CPSs) and NCSs in particular, is relatively young and there are still many interesting challenges to be solved. On the basis of the results presented in this dissertation, several directions were identified.

Improved design procedures for ETC systems: The ETC designs methods presented in this dissertation rely on an emulation-based approach in which the controller and the ETM are designed separately. To be more specific, in this approach, first the feedback law is designed such that the closed-loop system attains the desired stability and/or performance properties in absence of network-induced imperfections. Subsequently, the ETM is designed such that these desired properties are preserved. Although this separation in the design procedure allows to exploit well-known methods for the design of feedback laws, it might lead to a tedious iteration process before the satisfactory results are obtained. This problem can be tackled by considering two research directions. The first direction is to study and characterize the influences of the ETM on the system before the loop is closed which facilitates in developing more intuitive and effective design procedures. For example, the lifting-based techniques presented in [113] allow to characterize linear plants with a class of ETMs in terms of a piecewise linear discrete-time system. Using this perspective, discrete-time

control design can be exploited to design a feedback law that takes into account the presence of an ETM. The second direction is the development of synthesis methods in which the feedback law and the ETM are synthesized simultaneously. In [8,233], based on the scheme presented in Chapter 2, such a co-design method is proposed by using congruence transformation techniques for the linear matrix inequalities (LMIs). However, this approach requires additional LMI constraints which, in particular for controllers with feed-through term, might lead to conservative and even infeasible synthesis formulations. As a consequence, how to effectively design an ETC system can still be considered as an important open problem.

Riccati-based ETC design for decentralized control configurations: The numerical examples in Chapter 3 demonstrated that by exploiting Riccati-based tools for linear systems, significantly better performance bounds can be obtained for ETC systems in comparison with the more general approach presented in Chapter 2. However, the approach presented in Chapter 2 on the other hand, captures a larger class of control setups such as decentralized control configurations. As shown in [112], the Riccatti-based approach could be extended to decentralized control configurations. However, the approach presented in [112] requires the internal clocks of all sensor and actuator nodes to be synchronized. The latter requirement might be impractical. For this reason, it is of interest to develop novel decentralized ETC methods that do not require clock-synchronization but are still able to exploit the benefits of the Riccati-based approach.

Analyzing flexible large-scale systems: One of the main motivations for using (wireless) NCSs is that NCSs offer flexibility in the sense that it relatively easy to expand and reconfigure a networked systems. However, the majority of the literature of NCSs including the approaches presented in the current dissertation consider fixed network configurations and systems with fixed state dimensions. As a consequence, the control design procedure has to be repeated for every configuration that the system can attain. For this reason, it is of interest to study NCSs in which components can be added, removed or reconfigured without the need to reconsider the (local) control architectures. These systems are also referred to as open systems. In Chapter 8, it is shown that unidirectional vehicle strings are flexible in the sense that vehicles can join or leave the platoon without consequences for the overall string stability property of the platoon. However, it is still an open question if it is possible to have this property for other communication topologies such as a bidirectional topology or a two-vehicle lookahead topology. In the context of cyber-security, it might also be useful to examine the flexibility of the NCS. Indeed, by being able to break links and establish new links during operation, the resilience of an NCS can be improved as it allows the system to actively respond to malicious attacks by disconnecting certain compromised parts of the NCS and thereby to reduce the vulnerability of the system. In [46], it is shown that by using small-gain arguments, it is

possible to assess the input-to-state stability of the overall NCS based on local conditions that only involve local dynamics. However, the resulting time-based specifications are in general conservative. A step in reducing this conservatism could be to examine the techniques used for spatially (invariant) systems, see, *e.g.*, [59, 122, 123], and overlapping-decompositions, see, *e.g.*, [214].

Resource-aware distributed model-predictive control: Model predictive control (MPC) is a control strategy, which can effectively deal with constraints and which has widely been applied in process industry over the last few decades, see, *e.g.*, [33, 91]. The current trend in process industry is to move from centralized control systems that rely on dedicated wired connections to distributed control systems that rely on wireless networked communication and battery-powered sensors, see, *e.g.*, [255]. As such, there is a strong need for distributed resource-aware MPC methods. Despite this need, works in the literature that address this topic are rare. For these reasons, the topic of resource-aware distributed MPC design methods forms an interesting and important direction for future research. A first step could be to build upon [217] in which sequential MPC configurations are considered. Similar as in distributed MPC schemes, the approach in [217] relies on local prediction models that do no capture the dynamics of the entire system. It is shown that if the MPC laws are well-designed, it is possible to bound the uncertainty induced by the local prediction models. Consequently, by means of robust MPC methods, desired closed-loop behavior could still be guaranteed. The same principle might be applicable to distributed configurations with additional uncertainties induced by the networked communication.

Resource-aware multi-agent systems with cloud-based communication: In the multi-agent setting considered in Chapter 7, it is assumed that agents can directly exchange information via a possibly shared communication channel. In some applications, for example in swarms of autonomous underwater vehicles, communication is only possible via a common cloud repository that stores the output information of all agents. An agent can only access this information and update its own output information that is available in the cloud after a connection with the cloud has been established. Typically, agents can only connect to the cloud at discrete instants in time, often in an asynchronous fashion, and they are unable to detect when other agents are connected to the cloud. As such, there is no direct information exchange among agents. The latter has a significant impact on the time between the moment at which an output measurement is being collected and updated in the cloud and the moment at which it is received and processed by other agents. As such, cloud-based communication for MASs requires different resource-aware communication strategies than MASs that rely on a shared communication channels that enable direct exchange of information. Early approaches that tackle this problem include [10, 11, 47, 178]. However, these approaches do not consider the presence of disturbances, which, as advocated in this dissertation, is not trivial to account for. Hence, it would

be interesting to examine whether the ETC framework presented in Chapter 7 can be generalized to resource-aware MASs with cloud-based communication.

9.3 Final thoughts

The developments in information and communication technology (ICT) over the last few decades have enabled many novel interesting control applications that will have a major impact on our future. For this reason, the field of cyber-physical systems, and, in particular, NCSs have become prominent within the control community. Although many significant advances are made in fundamental system theory related NCSs as well as in experimental exploration and validation, there are still many interesting open challenges of which a selection has been discussed above. Given the potential benefits and impacts of NCSs, it is of importance to encourage the industry to shift from separate design approaches for the control architecture and the ICT infrastructure to integrated design approaches, from centralized control solutions to distributed control solutions and from conventional time-triggered digital control paradigms to resource-aware and resilient control paradigms. These shifts can be accelerated by focusing on the development of accessible and intuitive tools for the analysis and design of reliable NCSs and providing proof-of-concepts. The present thesis contributed to these important research areas. Moreover, it was shown that relevant results on safety-critical cyber-physical systems that rely on resource-aware and resilient control strategies do not only exist in theory but actually work in practice as well.

Appendix A

Proofs of Chapter 2

Proof of Lemma 2.5: According to (2.46) we have that $1-\omega_i(\tau_i)=0$ for $0 \leqslant \tau_i \leqslant \tau^i_{miet}$. Hence, $(1-\omega_i(\tau_i))\bar{\gamma}\tilde{W}_i^2 = (1-\omega_i(\tau_i))\bar{\gamma}W_i^2 = 0$ when $0 \leqslant \tau_i \leqslant \tau^i_{miet}$. Furthermore, given the fact that $\tau^i_{mad} \leqslant \tau^i_{miet}$ due to Standing Assumption 2.1, then for $\tau_i > \tau_{miet}$, the next event in network $\mathcal{N}_i$ is a transmission event, *i.e.*, $l_i = 0$. Since, $s_i = 0$ for $l_i = 0$ when $\tau_i > \tau^i_{miet}$ according to (2.10) and (2.15), we can see that $\tilde{W}_i = \max\big\{W_i(\kappa_i, e_i), W_i(\kappa_i, e_i + s_i)\big\} = W_i$ for $\tau_i > \tau^i_{miet}$, which completes the proof. □

Proof of Theorem 2.2: Consider the candidate Lyapunov function

$$U(\xi) = \tilde{V}(x) + \sum_{i=1}^{N} \Big(\gamma_{l_i,i}\phi_{l_i,i}(\tau_i)\tilde{W}_i^2(\kappa_i, l_i, e_i, s_i) + \eta_i\Big). \tag{A.1}$$

By means of the Comparison Lemma (see, *e.g.*, [131, p. 102-103]), we can conclude from (2.7) and (2.32) that $\eta_i(t,j) \geqslant 0$ when $0 \leqslant \tau_i \leqslant \tau^i_{miet}$. Given this fact, observe that the triggering mechanism given by (2.6) and (2.7) ensures that $\eta_i(t,j) \geqslant 0$ for all $t \in \mathbb{R}_{\geqslant 0}$[1]. Combining this with the fact that $\phi_{l_i,i}(\tau_i) > 0$ for all $\tau_i \in \mathbb{R}_{\geqslant 0}$ and for all $i \in \bar{N}$, and the radial unboundedness of functions $\tilde{V}$ and $\tilde{W}_i$, for all $i \in \bar{N}$, due to Condition 2.2 and Condition 2.1, respectively, we can conclude that U is radially unbounded in the sense that there exist $\mathcal{K}_\infty$-functions $\underline{\beta}_U$ and $\bar{\beta}_U$ such that

$$\underline{\beta}_U(|\hat{\xi}|) \leqslant U(\xi) \leqslant \bar{\beta}_U(|\hat{\xi}|),$$

for all $\xi \in \mathbb{X}$ where $\hat{\xi} = \big(x, e, s, \eta\big) \in \mathbb{R}^{n_x} \times \mathbb{R}^{n_v} \times \mathbb{R}^{n_v} \times \mathbb{R}_{\geqslant 0}$. Hence, U constitutes a suitable candidate Lyapunov function.

[1] Note that this also implies that when $\xi \in D_i \wedge l_i = 0$, the jump $\eta_i^+ = \eta_i$ is equivalent to $\eta_i^+ = 0$.

Let ξ be a solution to $\mathcal{H}$ defined on the hybrid time domain $\operatorname{dom}\xi = \bigcup_{j=0}^{J-1}[t_j, t_{j+1}] \times \{j\}$ with J possibly ∞ and $t_J = \infty$ for initial condition $\xi(0,0)$ and input $w \in \mathcal{L}_p$. The function U given by (A.1) constitutes a valid Lyapunov function for hybrid system $\mathcal{H}$ if we can show that

$$\begin{aligned} &\langle \nabla U(\xi), F(\xi)\rangle \leqslant -\tilde{\rho}(|x|) - \delta_\eta(\eta) - \sigma_l(\tilde{W}), && \text{when } \xi \in C,\\ &U(\xi^+) - U(\xi) \leqslant 0, && \text{when } \xi \in D, \end{aligned}$$

for some positive definite functions $\tilde{\rho}$, δ_η and σ_l [98]. Note that non-strictness in the second (jump) condition is sufficient since all solutions are defined for all $t \in \mathbb{R}_{\geqslant 0}$. We can see from (2.15) and (2.28) that at transmission events, *i.e.*, if $\xi \in D_i \wedge l_i = 0$, for some $i \in \bar{N}$ (and thus $\tau_i \geqslant \tau^i_{miet}$), we have that for all (κ_i, e_i)

$$\begin{aligned} U(\xi^+) - U(\xi) = &-\gamma_{0,i}\phi_{0,i}(\tau^i_{miet})\tilde{W}_i^2(\kappa_i, 0, e_i, s_i)\\ &+ \gamma_{1,i}\phi_{1,i}(0)\tilde{W}_i^2(\kappa_i + 1, 1, e_i, h_i(\kappa_i, e_i) - e_i). \end{aligned}$$

The conditions given in (2.22) and (2.29) ensure that

$$\begin{aligned} U(\xi^+) - U(\xi) &\leqslant -\gamma_{0,i}\phi_{0,i}(\tau^i_{miet})\tilde{W}_i^2(\kappa_i, 0, e_i, s_i)\\ &\quad + \gamma_{1,i}\phi_{1,i}(0)\lambda_i^2\tilde{W}_i^2(\kappa_i, 0, e_i, s_i),\\ &\leqslant 0, \end{aligned} \tag{A.2}$$

when $\xi \in D_i \wedge l_i = 0$ for some $i \in \bar{N}$. At update events, *i.e.*, if $\xi \in D_i \wedge l_i = 1$ for some $i \in \bar{N}$, we have that due to (2.15)

$$\begin{aligned} U(\xi^+) - U(\xi) = &-\gamma_{1,i}\phi_{1,i}(\tau_i)\tilde{W}_i^2(\kappa_i, 1, e_i, s_i)\\ &+ \gamma_{0,i}\phi_{0,i}(\tau_i)\tilde{W}_i^2(\kappa_i, 0, s_i + e_i, 0). \end{aligned} \tag{A.3}$$

By using the condition given by (2.23), we obtain that

$$\begin{aligned} U(\xi^+) - U(\xi) \leqslant &-\gamma_{1,i}\phi_{1,i}(\tau_i)\tilde{W}^2(\kappa_i, 1, e_i, s_i)\\ &+ \gamma_{0,i}\phi_{0,i}(\tau_i)\tilde{W}_i^2(\kappa_i, 1, e_i, s_i). \end{aligned} \tag{A.4}$$

Now given the fact that, according to (2.19), $\xi \in D_i \wedge l_i = 1$ implies $\tau_i \leqslant \tau^i_{mad}$, the condition given in (2.30) ensures that when $\xi \in D_i \wedge l_i = 1$ for some $i \in \bar{N}$,

$$U(\xi^+) - U(\xi) \leqslant 0.$$

With some abuse of notation, we consider the quantity $\langle \nabla U(\xi), F(\xi)\rangle$ with $F(\xi)$ given by (2.10), even though $\tilde{W}$ is not differentiable with respect to κ and l. Since $\dot{\kappa} = 0$ and $\dot{l} = 0$ in between jumps, this does not cause any problems. We also omit the argument of $H_{l_i,i}$. From (2.25), (2.26) and (2.28), we can derive

that for all $\tau \in \mathbb{R}^N_{\geqslant 0}$, all $\kappa \in \mathbb{N}^N$, all $l \in \{0,1\}^N$ and almost all $(x,e) \in \mathbb{R}^{n_x} \times \mathbb{R}^{n_v}$

$$\begin{aligned}\langle \nabla U(\xi), F(\xi) \rangle &\leqslant \sum_{i=1}^{N} \Big[-\tilde{\varrho}_i(v_i) - H_{l_i,i}^2 + \gamma_{l_i,i}^2 \tilde{W}_i^2 \\ &+ 2\gamma_{l_i,i}\phi_{l_i,i}\tilde{W}_i \left(L_{l_i,i}\tilde{W}_i + H_{l_i,i} \right) - \sigma_{l_i,i}(\tilde{W}_i) + \Psi_i \\ &- \omega_i(\tau_i)\gamma_{l_i,i}\tilde{W}_i^2 \left(2L_{l_i,i}\phi_{l_i,i} + \gamma_{l_i,i} \left(\phi_{l_i,i}^2 + 1 \right) \right) \Big] - \tilde{\rho}(|x|) \\ &= \sum_{i=1}^{N} \Big[-M_i(\xi) - \sigma_{l_i,i}(\tilde{W}_i) + \Psi_i \Big] - \tilde{\rho}(|x|), \end{aligned} \tag{A.5}$$

with $\omega_i(\tau_i)$ as in (2.46), and where $M_i, i \in \bar{N}$, is given by (2.33). Since Ψ_i is upper bounded by $M_i(\xi) - \delta_{\eta_i}(\eta_i)$ according to (2.31), we obtain from (A.5) that

$$\langle \nabla U(\xi), F(\xi) \rangle \leqslant -\tilde{\rho}(|x|) - \sum_{i=1}^{N} \left(\delta_{\eta_i}(\eta_i) + \sigma_{l_i,i}(\tilde{W}_i) \right), \tag{A.6}$$

which completes the proof using standard Lyapunov arguments, see, *e.g.*, [98, 131]. □

Proof of Theorem 2.3: Following the same steps as in the proof of Theorem 2.2, we can conclude that $U(\xi)$ is positive definite. Furthermore, we obtain that at jumps

$$U(\xi(t_{j+1}, j+1)) \leqslant U(\xi(t_{j+1}, j)) \tag{A.7}$$

and during flows

$$\langle \nabla U(\xi), F(\xi, w) \rangle \leqslant \mu(\theta^p |w|^p - |q(x,w)|^p). \tag{A.8}$$

As shown in [120], (A.7) and (A.8) imply that system $\mathcal{H}$ is $\mathcal{L}_p$-stable with an $\mathcal{L}_p$-gain less than or equal to θ which completes the proof. □

Appendix B

Proofs of Chapter 3

Proof of Theorem 3.1: The proof is based on the storage function U given by (3.15) with V as defined in (3.16), P_0 satisfying (3.17), and P_1^d, $d \in \mathcal{D}$, satisfying (3.18). However, we only need to consider the function V, as it holds that $\eta(t) = 0$ for all $t \in \mathbb{R}_{\geqslant 0}$ (cf. (3.9)) and thus in this case $U = V$.

The proof consists of showing that V is a proper storage function and satisfies for all $\xi \in \mathbb{R}^{n_\xi}$, $\tau \in \mathbb{R}_{\geqslant 0}$, $\kappa \in \mathbb{N}$, and all $l \in \{0, 1\}$,

$$c_1|\xi|^2 \leqslant V(\xi, \tau, \kappa, l) \leqslant c_2|\xi|^2 \tag{B.1}$$

with $c_2 \geqslant c_1 > 0$, has a supply rate $\theta^{-2} z^\top z - w^\top w$ [241, 254] and decay rate 2ρ during flow (3.7a), and is nonincreasing along jumps (3.7b) and (3.7c).

The first property follows from Assumption 3.2, as this assumption guarantees that $P_0(\tau) \succ 0$ for all $\tau \in [0, h]$ and $P_1^d(\tau) \succ 0$ for all $\tau \in [0, d]$, $d \in \mathcal{D}$, see [22, 112]. Hence, (B.1) holds with

$$c_1 = \min \left\{ \min_{\tau \in [0,h]} \lambda_{min}(P_0(\tau)), \min_{\substack{d \in \mathcal{D} \\ \tau \in [0,d]}} \lambda_{min}\left(P_1^d(\tau)\right) \right\} \tag{B.2a}$$

$$c_2 = \max \left\{ \max_{\tau \in [0,h]} \lambda_{max}(P_0(\tau)), \max_{\substack{d \in \mathcal{D} \\ \tau \in [0,d]}} \lambda_{max}\left(P_1^d(\tau)\right) \right\}, \tag{B.2b}$$

where $c_2 \geqslant c_1 > 0$.

For brevity, we will use the notation $V(t) = V(\xi(t), \tau(t), \kappa(t), l(t))$ in the remainder of the proof.

Following the derivations in the proof of [112, Theorem III.2] it can be shown

that (3.17), (3.18), and (3.19) imply that

$$\tfrac{\mathrm{d}}{\mathrm{d}t}V(t) \leqslant -2\rho V(t) - \theta^{-2} z(t)^\top z(t) + w(t)^\top w(t) - \zeta(t)^\top N_F \zeta(t) \quad \text{(B.3)}$$

during flow (3.7a) with ($\tau \in [0, \tau_\kappa]$ and $l = 1$) or ($\tau \in [0, h]$ and $l = 0$). Additionally, during flow (3.7a) with $\tau \in [h, \infty)$, $l = 0$, and $\zeta^\top Q \zeta \leqslant 0$, it holds that $\hat{y} = s$, which implies that

$$\begin{bmatrix} x_p(t) \\ x_c(t) \\ \hat{y}(t) \\ s(t) \end{bmatrix} = T \begin{bmatrix} x_p(t) \\ x_c(t) \\ s(t) \end{bmatrix} \text{ when } t \in (t_k + h, t_{k+1}],$$

and thus it follows from (3.25) that

$$\tfrac{\mathrm{d}}{\mathrm{d}t}V(t) \leqslant -2\rho V(t) - \theta^{-2} z(t)^\top z(t) + w(t)^\top w(t) - \zeta(t)^\top (N_N - \beta Q)\zeta(t). \quad \text{(B.4)}$$

Equations (B.3) and (B.4) together with $N_F, N_N \succeq 0$, $\beta \geqslant 0$, and $\zeta(t)^\top Q \zeta(t) \leqslant 0$ for $t \in [t_k + h, t_{k+1}]$ show that

$$\tfrac{\mathrm{d}}{\mathrm{d}t}V(t) \leqslant -2\rho V(t) - \theta^{-2} z(t)^\top z(t) + w(t)^\top w(t) \quad \text{(B.5)}$$

holds during flow (3.7a), proving the second property.

Finally, we show that V does not increase along jumps. In [112], it is shown that (3.21) evaluated at $\tau = d$, $d \in \mathcal{D}$, leads to

$$P_{0d} = G_0(h-d) + F_{11}(h-d)^{-\top}\big(P_{0h} S(h-d)\big(I - S(h-d)^\top P_{0h} S(h-d)\big)^{-1} S(h-d)^\top P_{0h}\big) F_{11}(h-d)^{-1}, \quad \text{(B.6)}$$

and for $d \in \mathcal{D}$, (3.22) evaluated at $\tau = 0$, leads to

$$P_{10}^d = G_1^d(d) + F_{11}(d)^{-\top}\big(P_{1d}^d S(d)\big(I - S(d)^\top P_{1d}^d S(d)\big)^{-1} S(d)^\top P_{1d}^d\big) F_{11}(d)^{-1}. \quad \text{(B.7)}$$

Here, the existence of $\big(I - S(h-d)^\top P_{0h} S(h-d)\big)^{-1}$ and $\big(I - S(d)^\top P_{1d}^d S(d)\big)^{-1}$ is guaranteed by Assumption 3.2 and $P_{0h}, P_{1d}^d \succ 0$, $d \in \mathcal{D}$, cf. [112]. By applying a Schur complement it follows from (3.26), $N_T \succeq 0$, and $\mu^d \geqslant 0$ for all $d \in \mathcal{D}$ that along transmissions (3.7b) (when $\tau \in [h, \infty)$, $l = 0$, and $\zeta^\top Q \zeta \geqslant 0$) we have

$$V(t^+) = \xi(t)^\top J_0^\top P_{10}^{\tau_\kappa(t)} J_0 \xi(t)$$

$$\leqslant \xi(t)^\top P_{0h}\xi(t) - \zeta(t)^\top (N_T + \mu^{\tau_\kappa(t)} Q)\zeta(t) \tag{B.8a}$$
$$\leqslant \xi(t)^\top P_{0h}\xi(t) = V(t), \tag{B.8b}$$

and it follows from (3.27) that along updates (3.7c) (when $\tau = \tau_\kappa$ and $l = 1$) we have

$$V(t^+) = \xi(t)^\top J_1^\top P_{0\tau_\kappa(t)} J_1 \xi(t) \leqslant \xi(t)^\top P_{1\tau_\kappa(t)}^{\tau_\kappa(t)} \xi(t) = V(t). \tag{B.9}$$

Combining (B.1), (B.5), (B.8b), and (B.9) establishes the upper bound θ on the $\mathcal{L}_2$-gain of the ETC system (3.7), (3.10) [112].

Furthermore, it follows that

$$\begin{aligned} V(t) &\leqslant e^{-2\rho t} V(0) + \int_0^t e^{-2\rho(t-s)} \|w\|_{\mathcal{L}_\infty}^2 \mathrm{d}s \\ &\leqslant e^{-2\rho t} V(0) + \frac{1}{2\rho}(1 - e^{-2\rho t})\|w\|_{\mathcal{L}_\infty}^2 \\ &\leqslant e^{-2\rho t} V(0) + \frac{1}{2\rho}\|w\|_{\mathcal{L}_\infty}^2 \end{aligned}$$

and thus

$$|\xi(t)| \leqslant ce^{-\rho t}|\xi(0)| + (2\rho c_1)^{-1/2}\|w\|_{\mathcal{L}_\infty} \tag{B.10}$$

with $c = \sqrt{c_1/c_2}$, which proves that the system is ISES with decay rate ρ. □

Proof of Theorem 3.2: Consider again the Lyapunov/storage function U given by (3.15) with V as defined in (3.16).

First, we show that U is a proper storage function, by showing that $\eta(t) \geqslant 0$ for all $t \in \mathbb{R}_{\geqslant 0}$, and that U satisfies for all $\xi \in \mathbb{R}^{n_\xi}$, $\tau \in \mathbb{R}_{\geqslant 0}$, $\kappa \in \mathbb{N}$, $l \in \{0, 1\}$, and all $\eta \geqslant 0$,

$$c_1|\xi|^2 + |\eta| \leqslant U(\xi, \tau, \kappa, l, \eta) \leqslant c_2|\xi|^2 + |\eta|, \tag{B.11}$$

where c_1 and c_2 are given by (B.2). As $\eta(0) = 0$, it follows from (3.28a), $N_F \succeq 0$, and the comparison lemma [131, Lemma 3.4] that $\eta(t) \geqslant 0$ for all $t \in [0, h)$. Next, η flows according to (3.28b) on $[h, t_1)$, i.e., as long as $\eta \geqslant 0$ or $\zeta^\top Q\zeta \leqslant 0$ (see (3.8)). However, note that η can only become negative when $\eta = 0$ and $\zeta^\top Q\zeta > 0$ (see (3.28b) as $N_N \succeq 0$), in which case a transmission (3.7b) would be triggered. Hence, $\eta(t_1) = 0$. The relation $\eta_T(o(t_1)) \geqslant 0$ then follows from (B.8b) when η_T is given by (3.29), or from $N_T \succeq 0$ when η_T is given by (3.30). Hence, in both cases it holds that $\eta(t_1^+) \geqslant 0$. It now follows by induction that $\eta(t) \geqslant 0$ for all $t \in \mathbb{R}_{\geqslant 0}$. Property (B.11) then follows by combining (B.1) and (3.15).

It remains to show that U has a supply rate $\theta^{-2} z^\top z - w^\top w$ and decay rate 2ρ during flow (3.7a), and is nonincreasing along jumps (3.7b) and (3.7c). For brevity, we will use the notation $U(t) = U(\xi(t), \tau(t), \kappa(t), l(t), \eta(t))$ and $V(t) = V(\xi(t), \tau(t), \kappa(t), l(t))$ in the remainder of the proof.

From (3.19) and (3.28a) it follows (using (B.3)) that

$$\tfrac{\mathrm{d}}{\mathrm{d}t} U(t) \leqslant -2\rho V(t) - 2\rho\eta(t) - \theta^{-2} z(t)^\top z(t) + w(t)^\top w(t)$$

$$= -2\rho U(t) - \theta^{-2} z(t)^\top z(t) + w(t)^\top w(t) \tag{B.12}$$

holds during flow (3.7a) with $\tau \in [0, h]$, and from (3.19) and (3.28b) it follows (using (B.4)) that (B.12) holds during flow (3.7a) with $\tau \in [h, \infty)$.

Finally, we show that

$$U(t^+) \leqslant U(t), \tag{B.13}$$

holds along jumps. When using (3.29), we find along transmissions (3.7b) that (cf. (B.8))

$$\begin{aligned} U(t^+) &= \xi(t)^\top J_0^\top P_{10}^{\tau_\kappa(t)} J_0 \xi(t) \\ &\quad + \eta(t) + \min_{d \in \mathcal{D}} \xi(t)^\top \left(P_{0h} - J_0^\top P_{10}^d J_0 \right) \xi(t) \\ &\leqslant \xi(t)^\top P_{0h} \xi(t) + \eta(t) = U(t). \end{aligned}$$

Alternatively, when using (3.30), we find (using (B.8a) and $\mu^{\tau_\kappa(t)} \zeta(t)^\top Q \zeta(t) \geqslant 0$) along transmissions (3.7b) that

$$\begin{aligned} U(t^+) &= \xi(t)^\top J_0^\top P_{10}^{\tau_\kappa(t)} J_0 \xi(t) + \eta(t) + \zeta(t)^\top N_T \zeta(t) \\ &\leqslant \xi(t)^\top P_{0h} \xi(t) + \eta(t) = U(t). \end{aligned}$$

Along updates (3.7c), (B.13) follows from (B.9) (which follows from (3.27)) and $\eta(t^+) = \eta(t)$.

Equations (B.11), (B.12), and (B.13) together prove that the system has an $\mathcal{L}_2$-gain from w to z smaller than or equal to θ [241,254]. Furthermore, it follows that

$$\begin{aligned} U(t) &= V(t) + |\eta(t)| \\ &\leqslant e^{-2\rho t} V(0) + e^{-2\rho t} |\eta(0)| + \int_0^t e^{-2\rho(t-s)} \|w\|_{\mathcal{L}_\infty}^2 \mathrm{d}s \\ &\leqslant e^{-2\rho t} V(0) + e^{-2\rho t} |\eta(0)| + \frac{1}{2\rho} \|w\|_{\mathcal{L}_\infty}^2 \end{aligned}$$

and, since $\eta(0) = 0$, it follows that

$$|\xi(t)| \leqslant c e^{-\rho t} |\xi(0)| + (2\rho c_1)^{-1/2} \|w\|_{\mathcal{L}_\infty}, \text{ and} \tag{B.14}$$

$$|\eta(t)| \leqslant c_2 e^{-2\rho t} |\xi(0)|^2 + (2\rho)^{-1} \|w\|_{\mathcal{L}_\infty}^2 \tag{B.15}$$

with $c = \sqrt{c_1/c_2}$, which proves that the system is ISES with decay rate ρ. □

Proof of Theorem 3.3: Consider the Lyapunov function U given by (3.15), with V given by (3.37). As in the proof of Theorem 3.1, we only need to consider the function V, as it holds that $\eta(t) = 0$ for all $t \in \mathbb{R}_{\geqslant 0}$ and thus in this case $U = V$.

In the proof of Theorem 3.1 it is shown that (B.1) holds with c_1 and c_2 given by (B.2), that (B.5) holds during flow (3.33a), that (B.8b) holds along transmissions (3.33b), and that (B.9) holds along updates (3.33c),

It remains to show that V is decreasing along non-transmission jumps (3.33d). From (B.6) it follows that (3.21) evaluated at $\tau = 0$, leads to

$$P_{00} = G_0(h) + F_{11}(h)^{-\top}\big(P_{0h}S(h) \big(I - S(h)^\top P_{0h}S(h)\big)^{-1} S(h)^\top P_{0h}\big)F_{11}(h)^{-1}. \quad \text{(B.16)}$$

By applying a Schur complement it follows from (3.38) and $\hat{y}(t^+) = \hat{y}(t) = s(t) = s(t^+)$ that along jumps (3.33d) (when $\tau = h$ and $\zeta^\top Q\zeta \leqslant 0$) we have

$$\begin{aligned} V(t^+) &= \xi(t)^\top P_{00}\xi(t) \\ &\leqslant \xi(t)^\top P_{0h}\xi(t) - \zeta(t)^\top (N_N - \beta Q)\zeta(t) && \text{(B.17a)} \\ &\leqslant \xi(t)^\top P_{0h}\xi(t) = V(t), && \text{(B.17b)} \end{aligned}$$

as $N_N \succeq 0$.

Similar arguments as in the proof of Theorem 3.1 lead to ISES with decay rate ρ and $\mathcal{L}_2$-stability with $\mathcal{L}_2$-gain θ. □

Proof of Theorem 3.4: Consider again the Lyapunov function U given by (3.15), with V given by (3.37).

First, we show that U is a proper storage function, by showing that $\eta(t) \geqslant 0$ for all $t \in \mathbb{R}_{\geqslant 0}$, and that U satisfies (B.11) for all $\xi \in \mathbb{R}^{n_\xi}$, $\tau \in [0, h]$, $\kappa \in \mathbb{N}$, $l \in \{0, 1\}$, and all $\eta \geqslant 0$. As $\eta(0) = 0$, it follows from (3.39) that $\eta(t) \geqslant 0$ for all $t \in [0, h]$, and hence, that $\eta(s_1) \geqslant 0$. Next, given event-generator (3.34), a transmission (3.33b) occurs in case $\zeta(s_1)^\top Q\zeta(s_1) \geqslant 0$ and $\eta_N(\hat{o}(s_1)) \leqslant 0$. In this case, $\eta_T(\hat{o}(s_1)) \geqslant 0$ follows from (B.8b) when η_T is given by (3.40a), or from $N_T \succeq 0$ when η_T is given by (3.41a). Otherwise, if $\zeta(s_1)^\top Q\zeta(s_1) < 0$ or $\eta_N(\hat{o}(s_1)) > 0$, no transmission occurs, and the state jumps according to (3.33d). Observe however that when $\zeta(s_1)^\top Q\zeta(s_1) < 0$ it holds that $\eta_N(\hat{o}(s_1)) \geqslant 0$, which follows from (B.17b) when η_N is given by (3.40b), or from $N_N \succeq 0$ and $\beta \geqslant 0$ when η_N is given by (3.41b). Hence, in all cases it holds that $\eta(s_1^+) \geqslant 0$. It now follows by induction that $\eta(t) \geqslant 0$ for all $t \in \mathbb{R}_{\geqslant 0}$. Property (B.11) then follows by combining (B.1) and (3.15), where c_1 and c_2 are given by (B.2).

From (3.19) and (3.39), it follows that (B.12) holds during flow (3.33a), and thus that U has a supply rate $\theta^{-2}z^\top z - w^\top w$ and decay rate 2ρ during flow.

It remains to show that (B.13) holds along jumps. For transmissions (3.33b) and updates (3.33c), this has already been shown in the proof of Theorem 3.2, as the functions (3.40a) and (3.29), and (3.41a) and (3.30) are identical. Along jumps (3.33d), we find when using (3.40b) that

$$\begin{aligned} U(t^+) &= \xi(t)^\top P_{00}\xi(t) + \eta(t) + \xi(t)^\top \left(P_{0h} - P_{00}\right)\xi(t) \\ &= \xi(t)^\top P_{0h}\xi(t) + \eta(t) = U(t). \end{aligned}$$

Alternatively, when using (3.41b), we find using (B.17a) (which also holds along jumps (3.33d) when $\tau = h$ and $\zeta^\top Q\zeta > 0$) that

$$\begin{aligned} U(t^+) &= \xi(t)^\top P_{00}\xi(t) + \eta(t) + \zeta(t)^\top (N_N - \beta Q)\zeta(t) \\ &\leqslant \xi(t)^\top P_{0h}\xi(t) + \eta(t) = U(t). \end{aligned}$$

This completes the proof. □

Proof of Theorem 3.5: The proof directly follows from the proof of Theorem 3.2 by using V as defined in (3.43) and noting that for all $d \in \mathcal{D}$ and all $i \in \{1, 2, \ldots, N\}$ it holds that $X_j^\top U_{ij}^d X_j \geqslant 0$ and $X_j^\top W_{ij}^d X_j \geqslant 0$ when $\xi \in \mathcal{X}_j$, $j \in \{1, 2, \ldots, N\}$. □

Proof of Theorem 3.7: The proof directly follows from the proof of Theorem 3.4 by using V as defined in (3.50) and noting that for all $d \in \mathcal{D}$ and all $i \in \{1, 2, \ldots, N\}$ it holds that $X_j^\top U_{ij}^d X_j \geqslant 0$, $X_j^\top W_{ij}^d X_j \geqslant 0$, and $X_j^\top V_{ij} X_j \geqslant 0$ when $\xi \in \mathcal{X}_j$, $j \in \{1, 2, \ldots, N\}$. □

Appendix C

Proofs of Chapter 4

Proof of Theorem 4.1.

Before we provide the proof for ISS for the set $\mathcal{A}$, we first consider statement (ii) and (iii), which form important ingredients for the stability analysis of system $\mathcal{H}$ described by (4.18) and (4.20). In the proof, we often omit the time arguments of the solution ξ of hybrid system $\mathcal{H}$ and we do not mention $\operatorname{dom}\xi$ explicitly.

Proof of statement (ii)

By recalling that $\mathbb{X}_0 := \{\xi \in \mathbb{X} : \eta_i > 0, p_i = 0\}$, we can see from (4.21) that $p_i(t,j) = 1$ is only possible if the system has jumped according to the jump map $G_i^\mu(\xi)$. To be more concrete, we can conclude from (4.21) that for all $(t,j) \in \operatorname{dom}\xi$ for which $p_i(t,j) = 1$, there exists an $n \in \mathbb{N}$ such that $\xi(t, j-n) \in G_i^\mu(\mathcal{D}_i)$ and that $\xi(t,\bar{j}) \in \bigcup_{k\in\{1,2,\dots,l\}\setminus\{i\}} (\{G_k^\mu(\mathcal{D}_i)\} \cup \{G_k^y(\mathcal{D}_i)\})$ for all $\bar{j} \in \{j-n+1,\dots,j\}$. Since μ_i is only affected by the jump map $G_i^\mu(\mathcal{D}_i)$ (corresponding to a zoom-update event at node i), we only need to show that $|y_i(t,j)| \leqslant M_i\mu_i(t,j)$ for all $\xi(t,j) \in G_i^\mu(\mathcal{D}_i)$ with $(t,j) \in \operatorname{dom}\xi$. To do so, we consider the cases that a zoom-in event occurs, a zoom-out event occurs and that none of the zoom conditions are violated.

In case of a zoom-in event, i.e., when $\xi \in \mathcal{D}_i$, and the system jumps according to $\xi \in G_i^\mu(\xi)$ with $\mu_i^+ \in \Omega_{\text{in},i}^{\kappa_{\text{in},i}(y_i,\mu_i)}\mu_i$ and $y_i^+ = y_i$, we have that

$$\ell_{\text{out},i}\mu_i^+ \overset{(4.31)}{\geqslant} \Omega_{\text{in},i}\frac{\ell_{\text{out},i}}{\ell_{\text{in},i}}\max\{|y_i|,\Delta_{0,i}\} \overset{(4.32)}{\geqslant} \frac{M_i-\Delta_i}{M_i-\kappa_i\Delta_i}|y_i|. \tag{C.1}$$

Since according to (4.30), $\kappa_i > 1$, we obtain that $\ell_{\text{out},i}\mu_i^+ \overset{(C.1)}{\geqslant} |y_i|$ and thus $M_i\mu_i^+ \geqslant |y_i^+|$.

In case of a zoom-out event, i.e., when $\xi(t,j) \in \mathcal{D}_i$ and the system jumps according to $\xi^+ \in G_i^\mu(\xi)$ with $\mu_i^+ \in \Omega_{\text{out},i}^{\kappa_{\text{out},i}(y_i,\mu_i)}\mu_i$ and $y_i^+ = y_i$, it immediately follows from (4.31) that $\ell_{\text{out},i}\mu_i^+ \geqslant |y_i^+|$ and thus $M_i\mu_i^+ \geqslant |y_i^+|$ as $\ell_{\text{out},i} = M_i - \Delta_i \leqslant M_i$.

In case none of the zoom-conditions are violated, i.e., when $\xi \in \mathcal{D}_i$ and the system jumps according to $\xi^+ \in G_i^\mu(\xi)$ with $\mu_i^+ = \mu_i$ and $y_i^+ = y_i$ we have that $\kappa_{\text{out},i}(y_i,\mu_i) = 0$ which, per definition of $\kappa_{\text{out},i}$, implies that $|y_i| \leqslant \ell_{\text{out},i}\mu_i$ and thus $M_i\mu_i^+ \geqslant |y_i^+|$. Hence, statement (ii) in Theorem 4.1 holds.

Proof of statement (iii)

Consider the following claim.

Claim C.1. *Let the hypotheses of Theorem 1 hold. Consider a solution pair (ξ, w) to (4.20) with $\xi(0,0) \in \mathbb{X}_0$ with $\mathbb{X}_0$ as defined in Theorem 4.1. Then, it holds for all $(t,j) \in \operatorname{dom}\xi$ with $\xi(t,j) \in \mathcal{D}_i$ that*

$$\tilde{\gamma}_i |e_i(t,j)|^2 \geqslant \varepsilon_{y_i} \max\{|y_i^2(t,j)|, \Delta_{0,i}^2\}, \quad i \in \{1,2,\ldots,l\}$$

. □

Proof of Claim C.1.

To prove this claim, we use the following lemma.

Lemma C.1. *Consider $f : \mathbb{R}_{\geq 0} \to \mathbb{R}$ that is continuously differentiable at an open interval containing $(T_1, T_2]$ with $f(t) \geqslant 0$ $t \in (T_1, T_2]$ for $T_2 > T_1 > 0$ and $f(T_2) = 0$, then $\dot{f}(T_2) \leqslant 0$.* □

Moreover, let us define $\bar{E}_i := \{(t,j) \in \operatorname{dom}\xi : \xi(t,j) \in \mathcal{C} \cap \mathcal{D}_i\}$ for all $i \in \{1,2,\ldots,l\}$. Observe from (4.25) that $\Psi_i(o_i(t,j)) > 0$ for all $(t,j) \in \operatorname{dom}\xi$ for which $\eta_i(t,j) = 0$ and $0 \leqslant \tau_i(t,j) < T_i$. By means of the latter, and by recalling (4.9) and the fact that, per definition of $\mathbb{X}_0$, $\eta_i(0,0) > 0$ for all $i \in \{1,2,\ldots,l\}$, we obtain that $\eta_i(t,j) > 0$ for all $(t,j) \in \operatorname{dom}\xi$ for which $\tau_i(t,j) = T_i$. Since $\eta_i(t,j) = 0$ and $\tau_i(t,j) \geqslant T_i$ when $\xi(t,j) \in \mathcal{D}_i$, we can consequently conclude that for each $(t,j) \in \bar{E}_i$, there exists a $t' < t$ such that $(t',j) \in \mathcal{C}$ with $\tau_i(t',j) > T_i$. By using the latter, the fact that, for all $(t,j) \in \operatorname{dom}\xi$, $\eta_i(t,j) \geqslant 0$, per definition of $\mathbb{X}$ and Lemma C.1, we obtain that for all $(t,j) \in \bar{E}_i$, $\dot{\eta}(t,j) \leqslant 0$. Observe from (4.25) that $\dot{\eta}_i(t,j) \geqslant \varepsilon_{y_i} \max\left\{|y_i(t,j)|^2, \Delta_{0,i}^2\right\} - \tilde{\gamma}_i|e_i(t,j)|^2 - \vartheta_i\eta_i(t,j)$ for all $(t,j) \in \operatorname{dom}\xi$. Hence, we have that for all $i \in \{1,2,\ldots,l\}$, and all $(t,j) \in \bar{E}_i$, $\tilde{\gamma}_i|e_i(t,j)|^2 \geqslant \varepsilon_{y_i} \max\{|y_i^2(t,j)|, \Delta_{0,i}^2\}$.

To complete the proof, we need to show that the property $\tilde{\gamma}_i|e_i(t,j)|^2 \geqslant \varepsilon_{y_i} \max\{|y_i^2(t,j)|, \Delta_{0,i}^2\}$ also holds for all $(t,j) \in \operatorname{dom}\xi$ for which $\xi(t,j) \in \mathcal{D}_i \setminus \mathcal{C}$. Observe that $\xi(t,j) \in \mathcal{D}_i \setminus \mathcal{C}$ implies that $p_i(t,j) = 1$ for all $(t,j) \in \operatorname{dom}\xi$. As mentioned before, $p_i(t,j) = 1$ implies that there exists an $n \in \mathbb{N}$ such that $\xi(t, j-n) = G_i^\mu(\mathcal{D}_i)$ and that $\xi(t,\bar{j}) \in \bigcup_{k\in\{1,2,\ldots,l\}\setminus\{i\}} (\{G_k^\mu(\mathcal{D}_i)\} \cup \{G_k^y(\mathcal{D}_i)\})$

for all $\bar{j} \in \{j-n+1, \dots, j\}$. Since y_i and e_i are not affected after the jumps maps $G_i^{\mu}(\xi)$ or $G_k^{y}(\xi)$, $i \in \{1,2,\dots,l\}$, $k \in \{1,2,\dots,l\} \setminus \{i\}$ are applied, Claim C.1 follows. □

Claim C.2. *Let the hypotheses of Theorem 1 hold. Consider a solution pair (ξ, w) to (4.20) with $\xi(0,0) \in \mathbb{X}_0$ with $\mathbb{X}_0$ as defined in Theorem 4.1. Then, it holds for all $(t,j) \in \operatorname{dom}\xi$ with $p_i(t,j) = 1$ that*

$$\ell_{\text{in},i}\mu_i(t,j) \leqslant \max\{|y_i(t,j)|, \Delta_{0,i}\}$$

. □

Proof of Claim C.2 following similar arguments as in the proof of statement (ii), we only need to show that $\ell_{\text{in},i}\mu_i \leqslant \max\{|y_i|, \Delta_{0,i}\}$ for all $\xi \in G_i^{\mu}(\mathcal{D}_i)$. To do so, we consider three cases, namely, the cases that a zoom-in event occurs, that a zoom-out occurs and that none of the zoom conditions are violated.

In case of a zoom-in event, i.e., when $\xi \in \mathcal{D}_i$ and the system jumps according to $\xi^+ \in G_i^{\mu}(\xi)$ with $\mu_i^+ \in \Omega_{\text{in},i}^{\kappa_{\text{in},i}(y_i,\mu_i)}\mu_i$ and $y_i^+ = y_i$, we can immediately conclude from (4.31) that $\ell_{\text{in},i}\mu_i^+ \leqslant \max\{|y_i^+|, \Delta_{0,i}\}$

In case of a zoom-out event, i.e., when $\xi \in \mathcal{D}_i$ and the system jumps according to $\xi^+ \in G_i^{\mu}(\xi)$ with $\mu_i^+ \in \Omega_{\text{out},i}^{\kappa_{\text{out},i}(y_i,\mu_i)}\mu_i$ and $y_i^+ = y_i$, we obtain that

$$\begin{aligned}\ell_{\text{in},i}\mu_i^+ &\overset{(4.31)}{\leqslant} \Omega_{\text{out},i}\frac{\ell_{\text{in},i}}{\ell_{\text{out},i}}|y_i| \overset{(4.32)}{=} \Omega_{\text{out},i}\Omega_{\text{in},i}\frac{M_i-\kappa_i\Delta_i}{M_i-\Delta_i}|y_i| \\ &\overset{(4.30)}{\leqslant} \max\{|y_i^+|, \Delta_{0,i}\}. \end{aligned} \tag{C.2}$$

Let us remark that for the last inequality, we used the fact that the bound on κ_i given in (4.30) is such that $\Omega_{\text{out},i}\Omega_{\text{in},i}\frac{M_i-\kappa_i\Delta_i}{M_i-\Delta_i} < 1$.

Finally, we consider the case that no zoom condition is violated, i.e., when $\xi \in \mathcal{D}_i$ and the system jumps according to $\xi^+ \in G_i^{\mu}(\xi)$ with $\mu_i^+ = \mu_i$ and $y_i^+ = y_i$. In this case $\kappa_{\text{in},i}(y_i,\mu_i) = \kappa_{\text{out},i}(y_i,\mu_i) = \{0\}$, and thus it holds trivially that $\ell_{\text{in},i}\mu_i^+ \leqslant \max\{|y_i^+|, \Delta_{0,i}\}$, which completes the proof of Claim C.2. □

To complete the proof of statement (iii), we proceed with observing that in view of (4.29), $M_i - \kappa_i\Delta_i \geqslant \frac{2\sqrt{\tilde{\gamma}_i}}{\sqrt{\varepsilon_{y_i}}\Omega_{\text{in},i}\lambda_i}\Delta_i$. Hence, in view of the definition of $\ell_{\text{in},i}$ in (4.32), we have

$$2\Delta_i\frac{\sqrt{\tilde{\gamma}_i}}{\lambda_i\sqrt{\varepsilon_{y_i}}} \leqslant \Omega_{\text{in},i}(M_i - \kappa_i\Delta_i) = \ell_{\text{in},i}. \tag{C.3}$$

Hence, $\frac{2\Delta_i}{\lambda_i} \leqslant \frac{\sqrt{\varepsilon_{y_i}}\ell_{\text{in},i}}{\sqrt{\tilde{\gamma}_i}}$. By multiplying both sides by $\mu_i(t,j)$ we have that, for all $\xi(t,j) \in \mathcal{D}$ for which $p_i(t,j) = 1$ with $(t,j) \in \operatorname{dom}\xi$, $\frac{2\Delta_i\mu_i(t,j)}{\lambda_i} \leqslant \frac{\sqrt{\varepsilon_{y_i}}\ell_{\text{in},i}\mu_i(t,j)}{\sqrt{\tilde{\gamma}_i}}$, which leads to

$$\frac{2\Delta_i\mu_i(t,j)}{\lambda_i} \overset{\text{Claim C.2}}{\leqslant} \frac{\sqrt{\varepsilon_{y_i}}\max\{|y_i(t,j)|, \Delta_{0,i}}}{\sqrt{\tilde{\gamma}_i}},$$

$$\overset{\text{Claim C.1}}{\leqslant} |e_i(t,j)| \overset{(4.13)}{\leqslant} |e_{s,i}(t,j)| + |e_{q,i}(t,j)| \tag{C.4}$$

By means of statement (ii) of Theorem 4.1 and (4.10), we obtain that $|e_{q,i}(t,j)| \leqslant \Delta_i \mu_i(t,j)$ for all $\xi(t,j) \in \mathcal{D}$ for which $p_i(t,j) = 1$ with $(t,j) \in \operatorname{dom} \xi$. Combining the latter fact with (C.4) yields

$$|e_{s,i}(t,j)| \geqslant \frac{2-\lambda_i}{\lambda_i} \Delta_i \mu_i(t,j), \tag{C.5}$$

for all $\xi(t,j) \in \mathcal{D}$ for which $p_i(t,j) = 1$ with $(t,j) \in \operatorname{dom} \xi$. Since $\lambda_i \in (0,1)$, it holds that, for all $\xi(t,j) \in \mathcal{D}_i \wedge p_i(t,j) = 1$, $|e_{s,i}(t,j)| > \Delta_i \mu_i(t,j) \geqslant |e_{q,i}(t,j)|$. Thus, statement (iii) of Theorem 4.1 is proven. □

Proof of ISS property of the set $\mathcal{A}$

To prove the ISS property of the set $\mathcal{A}$, we show that there exists an ISS Lyapunov function U for the hybrid system $\mathcal{H}$ described by (4.18) and (4.20). To be more specific, we aim to find a locally Lipschitz non-negative function U that satisfies the following properties. For some functions $\alpha_1, \alpha_2 \in \mathcal{K}_\infty$ such that for all $\chi \in \mathcal{C} \cup \mathcal{D} \cup G(\mathcal{D})$, it holds that

$$\alpha_1(|\chi|_{\mathcal{A}}) \leqslant U(\chi) \leqslant \alpha_2(|\chi|_{\mathcal{A}}) \tag{C.6}$$

Moreover, for each solution pair (ξ, w) with $\xi(0,0) \in \mathbb{X}_0$ and $w \in \mathcal{L}_\infty$, there exist some functions $\tilde{\rho} \in \mathcal{K}_\infty$ and $\sigma \in \mathcal{K}$, such that for all $(t,j) \in \operatorname{dom} \xi$, it holds that when $\xi(t,j) \in \mathcal{D}$,

$$U(G(\xi(t,j))) - U(\xi(t,j)) \leqslant 0, \tag{C.7}$$

and for almost all $(t,j) \in \operatorname{dom} \xi$, when $\xi(t,j) \in \mathcal{C}$, it holds that

$$\langle \nabla U \xi(t,j), F(\xi(t,j), w(t,j)) \rangle \leqslant -\tilde{\rho}(U(\xi(t,j))) + \sigma(|w(t,j)|). \tag{C.8}$$

Observe that the ISS conditions above are closely related to the ISS conditions presented in [121, Definition 3.2]. Note that the ISS condition in (C.6)-(C.8) are relaxed compared to [121]. This is possible as we will have that the all maximal solutions of $\mathcal{H}$ described by (4.18) and (4.20) are t-complete, see also Proposition 3.27 in [99], Lemma III.3 in [78], [193].

Consider the function

$$U(\xi) := \max\{0, R(\xi) - c\} \tag{C.9}$$

with the function R as in Theorem 4.1. Observe that $U(\xi) = 0$ for $\xi \in \mathcal{A}$. Moreover, note that, in view of (4.28) and (4.34), $\tilde{\phi}_i(\tau_i(t,j)) > 0$ for all $(t,j) \in \operatorname{dom} \xi$ and $i \in \{1, 2, \ldots, l\}$. Hence, since $\eta_i(t,j) \geqslant 0$ for all $(t,j) \in \operatorname{dom} \xi$ in view of the definition of $\mathbb{X}$, we deduce that the function U satisfies the inequality in (C.6) and thereby constitutes an appropriate candidate ISS Lyapunov function.

Lemma C.2. *For all $\xi \in \mathcal{C} \setminus \mathcal{A}$, it holds that*

$$\epsilon\Big(\varepsilon_x|x|^2 + \sum_{i=1}^{l} 2\nu_i\gamma_i\tilde{\phi}_i(\tau_i)|e_i|^2 + \sum_{i=1}^{l}\vartheta_i\eta_i\Big) \geqslant \sum_{i=1}^{l}\varepsilon_{y_i}\Delta_{0,i}^2. \tag{C.10}$$

Proof of Lemma C.2. In view of the definition of $\mathcal{A}$, it holds for all $\xi \in \mathcal{C} \setminus \mathcal{A}$ that $R(\xi) \geqslant c$ with c as defined in Theorem 4.1, i.e.,

$$x^\top P x + \sum_{i=1}^{l}\Big(\gamma_i\tilde{\phi}_i(\tau_i)|e_i|^2 + \eta_i\Big) \geqslant \frac{\sum_{i=1}^{l}\varepsilon_{y_i}\Delta_{0,i}^2}{\epsilon\min\{\varepsilon_x/\lambda_{\max}(P),\, 2\min_i \nu_i,\, \min_i \vartheta_i\}}. \tag{C.11}$$

Hence, we deduce from (C.11) for all $\xi \in \mathcal{C} \setminus \mathcal{A}$ that

$$\begin{aligned}&\epsilon\min\{\varepsilon_x/\lambda_{\max}(P),\, 2\min_i \nu_i,\, \min_i \vartheta_i\}\times\\ &\Big(\lambda_{\max}(P)|x|^2 + \sum_{i=1}^{l}\Big(\gamma_i\tilde{\phi}_i(\tau_i)|e_i|^2 + \eta_i\Big)\Big) \geqslant \sum_{i=1}^{l}\varepsilon_{y_i}\Delta_{0,i}^2.\end{aligned} \tag{C.12}$$

Consequently, by using the fact that for $r \in \mathbb{N}$, $\min_{i\in\{1,2,\ldots,r\}}\alpha_i\left(\sum_{j=1}^{r}\beta_j\right) \leqslant \sum_{j=1}^{r}\alpha_j\beta_j$ for all $\alpha_j,\, \beta_j \in \mathbb{R}_{\geqslant 0}$, we can conclude that (C.10) indeed it holds for all $\xi \in \mathcal{C} \setminus \mathcal{A}$. □

Dynamics of U at jumps

In view of the jump map in (4.21), we distinguish two type of jumps.

- When $\xi \in \mathcal{D}_i$ with $p_i = 0$, $i \in \{1, 2, \ldots, l\}$, and the system jumps according to $\xi^+ = G_i^\mu(\xi)$. This case corresponds to an update of the quantizer at node i. Since τ_i, e_i and η_i are not affected by the jump map G_i^μ, we obtain

$$\begin{aligned}R(G(\xi)) - R(\xi) &= \gamma_i\tilde{\phi}_i(\tau_i^+)|e_i^+|^2 + \eta_i^+ - \gamma_i\tilde{\phi}_i(\tau_i)|e_i|^2 - \eta_i\\ &\overset{(4.21)}{=} 0.\end{aligned} \tag{C.13}$$

- When $\xi \in \mathcal{D}_i$ with $p_i = 1$, $i \in \{1, 2, \ldots, l\}$, and the system jumps according to $\xi^+ = G_i^y(\xi)$. This case corresponds to a new transmission generated at some node i. In view of (4.20), (4.21) and by using the fact that $\tilde{\phi}(\tau_i^+) = \phi(\tau_i^+) = \lambda_i^{-1}$, we have that

$$\begin{aligned}R(G(\xi)) - R(\xi) &= \gamma_i\tilde{\phi}_i(\tau_i^+)|e_i^+|^2 + \eta_i^+ - \gamma_i\tilde{\phi}_i(\tau_i)|e_i|^2 - \eta_i\\ &\overset{(4.21)}{=} \gamma_i\lambda_i^{-1}|e_{q,i}|^2 + \eta_{0,i}(e_i) - \gamma_i\tilde{\phi}_i(\tau_i)|e_i|^2\\ &\overset{(4.10)}{\leqslant} \gamma_i\lambda_i^{-1}\Delta_i^2\mu_i^2 + \eta_{0,i}(e_i) - \gamma_i\tilde{\phi}_i(\tau_i)|e_i|^2\\ &\overset{(C.4)}{\leqslant} \gamma_i\lambda_i^{-1}\lambda_i^2|e_i|^2 + \eta_{0,i}(e_i) - \gamma_i\tilde{\phi}_i(\tau_i)|e_i|^2\\ &\overset{(4.25)}{=} \gamma_i\lambda_i|e_i|^2 + \gamma_i(\tilde{\lambda}_i - \lambda_i)|e_i|^2 - \gamma_i\tilde{\phi}_i(\tau_i)|e_i|^2\\ &\overset{(4.28)}{\leqslant} \gamma_i\lambda_i|e_i|^2 + \gamma_i(\tilde{\lambda}_i - \lambda_i)|e_i|^2 - \gamma_i\tilde{\lambda}_i|e_i|^2 \leqslant 0.\end{aligned} \tag{C.14}$$

As a result, in view of (C.13) and (C.14), we have that when $\xi \in \mathcal{D}$, $R(G(\xi)) \leqslant R(\xi)$. In the view of the definition of $\mathcal{A}$, we also have that $G(\xi) \in \mathcal{A}$ when $\xi \in \mathcal{A}$. Given the latter facts, we can conclude that (C.7) holds for all $(t, j) \in \operatorname{dom} \xi$.

Dynamics of U during flows

Recall that $F(\xi, w) = (\mathcal{A}_1 x + \mathcal{B}_1 e + \mathcal{E}_1 w, \mathcal{A}_2 x + \mathcal{B}_2 e + \mathcal{E}_2 w, \mathbf{0}_l, \mathbf{1}_l, \Psi(o), \mathbf{0}_l)$. Consequently, in view of (4.20), (4.24), (4.28), we obtain for $\xi \in \mathcal{C}$ (recall that $\tilde{L}_i = L_i + \nu_i$, $i \in \{1, 2, \ldots, l\}$)

$$
\begin{aligned}
&\langle \nabla R, F(\xi, w) \rangle = \langle \nabla V(x), \mathcal{A}_1 x + \mathcal{B}_1 e + \mathcal{E}_1 w \rangle \\
&+ \sum_{i=1}^{l} 2\gamma_i \tilde{\phi}_i(\tau_i)|e_i| \left\langle \tfrac{\partial}{\partial e_i}|e_i|, \mathcal{A}_{2i} x + \mathcal{B}_{2i} e + \mathcal{E}_{2i} w \right\rangle + \sum_{i=1}^{l} \gamma_i \dot{\tilde{\phi}}_i(\tau_i)|e_i|^2 + \sum_{i=1}^{l} \dot{\eta}_i \\
&\leqslant -\varepsilon_x |x|^2 - \sum_{i=1}^{l} |\mathcal{A}_{2i} x + \mathcal{B}_{2i} e + \mathcal{E}_{2i} w|^2 - \sum_{i=1}^{l} \varepsilon_{y_i} |y_i|^2 + \sum_{i=1}^{l} \gamma_i^2 |e_i|^2 + \varepsilon_w |w|^2 \\
&+ \sum_{i=1}^{l} 2L_i \gamma_i \tilde{\phi}_i(\tau_i)|e_i|^2 + \sum_{i=1}^{l} 2\gamma_i \tilde{\phi}_i(\tau_i)|e_i||\mathcal{A}_{2i} x + \overline{\mathcal{B}}_{2i} e + \mathcal{E}_{2i} w| \\
&- \sum_{i=1}^{l} \tilde{\omega}_i(\tau_i) \left(2\tilde{L}_i \gamma_i \tilde{\phi}_i(\tau_i) + \gamma_i^2 (\tilde{\phi}_i^2(\tau_i) + 1) \right) |e_i|^2 + \sum_{i=1}^{l} \tilde{\Psi}_i(y_i, e_i, \tau_i, \eta_i)
\end{aligned}
$$

for some $\tilde{\omega}_i(\tau_i) \in \omega_i(\tau_i)$ and $\tilde{\Psi}_i(y_i, e_i, \tau_i, \eta_i) \in \Psi_i(y_i, e_i, \tau_i, \eta_i)$.

By using the fact that $2\gamma_i \tilde{\phi}_i(\tau_i)|e_i||\mathcal{A}_{2i} x + \overline{\mathcal{B}}_{2i} e + \mathcal{E}_{2i} w| \leqslant \gamma_i^2 \tilde{\phi}_i^2(\tau_i)|e_i|^2 + |\mathcal{A}_{2i} x + \overline{\mathcal{B}}_{2i} e + \mathcal{E}_{2i} w|^2$ and since, in view of (4.25), $\Psi_i(y_i, e_i, \tau_i, \eta_i) \in \varepsilon_{y_i} \max\left\{|y_i|^2, \Delta_{0,i}^2\right\} - (1 - \omega_i(\tau_i))\tilde{\gamma}_i |e_i|^2 - \vartheta_i \eta_i$, we have that for all $\xi \in \mathcal{C}$

$$
\begin{aligned}
&\langle \nabla R, F(\xi, w) \rangle \leqslant -\varepsilon_x |x|^2 - \sum_{i=1}^{l} \varepsilon_{y_i} |y_i|^2 + \varepsilon_w |w|^2 \\
&+ \sum_{i=1}^{l} \left(2L_i \gamma_i \tilde{\phi}_i(\tau_i) + \gamma_i^2 (\tilde{\phi}_i^2(\tau_i) + 1) \right) |e_i|^2 \\
&- \sum_{i=1}^{l} \tilde{\omega}_i(\tau_i) \left(2\tilde{L}_i \gamma_i \tilde{\phi}_i(\tau_i) + \gamma_i^2 (\tilde{\phi}_i^2(\tau_i) + 1) \right) |e_i|^2 \\
&+ \sum_{i=1}^{l} \varepsilon_{y_i} \max\left\{|y_i|^2, \Delta_{0,i}^2\right\} - (1 - \tilde{\omega}_i(\tau_i))\tilde{\gamma}_i |e_i|^2 - \vartheta_i \eta_i
\end{aligned}
$$

for some $\tilde{\omega}_i(\tau_i) \in \omega_i(\tau_i)$.

By recalling that $\tilde{\gamma}_i = \gamma_i^2 + \gamma_i^2 \tilde{\lambda_i}^2 + 2\gamma_i \tilde{\lambda_i}^2 \tilde{L}_i$, $\tilde{L}_i = L_i + \nu_i$ and $\tilde{\phi}_i(\tau_i) = \phi_i(T_i) = \tilde{\lambda}_i$ for $\tau_i \geqslant T_i$ according to (4.28) and using the fact that $\max\left\{|y_i|^2, \Delta_{0,i}^2\right\} - |y_i|^2 \leqslant \Delta_{0,i}^2$, we obtain that

$$
\langle \nabla R, F(\xi, w) \rangle \leqslant -\varepsilon_x |x|^2 + \sum_{i=1}^{l} \varepsilon_{y_i} \Delta_{0,i}^2 + \varepsilon_w |w|^2 - \sum_{i=1}^{l} 2\nu_i \gamma_i \tilde{\phi}_i(\tau_i)|e_i|^2 - \sum_{i=1}^{l} \vartheta_i \eta_i. \tag{C.15}
$$

Now by means of Lemma C.2, we obtain that for $\epsilon \in (0,1)$ and for all $(t,j) \in \operatorname{dom}\xi$ for which $\xi(t,j) \in \mathcal{C} \setminus \mathcal{A}$, it holds that

$$\begin{aligned}\langle \nabla R, F(\xi,w)\rangle \leqslant & -(1-\epsilon)\varepsilon_x|x|^2 + \varepsilon_w|w|^2 - (1-\epsilon)\sum_{i=1}^{l} 2\nu_i\gamma_i\tilde{\phi}_i(\tau_i)|e_i|^2 \\ & -(1-\epsilon)\sum_{i=1}^{l}\vartheta_i\eta_i.\end{aligned} \tag{C.16}$$

By recalling the fact that $U(\xi) = 0$ when $\xi \in \mathcal{A}$, we can conclude that for all $(t,j) \in \operatorname{dom}\xi$ for which $\xi(t,j) \in \mathcal{C}$

$$\langle \nabla U(\xi, F(\xi,w))\rangle \leqslant -\rho U(\xi) + \varepsilon_w|w|^2, \tag{C.17}$$

where $\rho := (1-\epsilon)\min\{\frac{\varepsilon_x}{\lambda_{\max}(P)}, 2\min_i \nu_i, \min_i \vartheta_i\}$ and thus that (C.8) holds.

t-completeness of maximal solutions

We investigate t-completeness of maximal solutions. To do so, we verify the conditions provided in [99, Proposition 6.10]. First of all, observe that $G(\mathcal{D}) \subset \mathcal{C} \cup \mathcal{D}$ since for all $\xi \in G(\mathcal{D})$, it holds that $\tau_i^+ \geqslant 0$, $\eta_i^+ \geqslant 0$, $\mu_i^+ \geqslant \frac{\Omega_{\text{in},i}}{\ell_{\text{in},i}}\Delta_{0,i}$ and $p_i^+ \in \{0,1\}$ due to (4.20), (4.25) and property (d) below (4.38). Next, we show that for any $\varphi \in \mathcal{C}\setminus\mathcal{D}$ there exists a neighborhood S of ξ such that, it holds for every $\varphi \in S \cap \mathcal{C}$ that $F(\varphi,w) \cap T_{\mathcal{C}}(\varphi) \neq \emptyset$, where $T_{\mathcal{C}}(\varphi)$ is the tangent cone[1] to $\mathcal{C}$ at φ. Observe that for each $\xi \in \mathcal{C}$ (recall that $\xi = (x,e,\mu,\tau,\eta,p)$), $T_{\mathcal{C}}(\xi) = \mathbb{R}^{n_x}\times\mathbb{R}^{n_y}\times(T_{\mathbb{R}_{\geqslant \underline{\mu}_1}}(\mu_1)\times\ldots\times T_{\mathbb{R}_{\geqslant \underline{\mu}_l}}(\mu_l))\times(T_{\mathbb{R}_{\geqslant 0}}(\tau_1)\times\ldots\times T_{\mathbb{R}_{\geqslant 0}}(\tau_l))\times(T_{\mathbb{R}_{\geqslant 0}}(\eta_1)\times\ldots\times T_{\mathbb{R}_{\geqslant 0}}(\eta_l))\times\{0\}^l$. Observe also from (4.18) that $\mathcal{C}/\mathcal{D} = \bigcap_{i=1}^{l}\{\xi \in \mathbb{X} : p_i = 0 \text{ and } (\tau_i < T_i \text{ or } \eta_i > 0)\}$. Given the facts that, for all $i \in \{1,2,\ldots,l\}$, $\dot{\tau}_i = 1$ and $\dot{\mu}_i = 0$ due to (4.21) and that $\dot{\eta}_i > 0$ when $\tau_i < T_i$ and $\eta_i = 0$ due to (4.9) and (4.25), it indeed follows that for any $\xi \in \mathcal{C}\setminus\mathcal{D}$ there exists a neighborhood S of ξ such that, it holds for every $\varphi \in S \cap \mathcal{C}$ that $F(\varphi,w) \cap T_{\mathcal{C}}(\varphi) \neq \emptyset$. To conclude the proof for t-completeness, finite escape times should be excluded which is the case due to (C.8). Hence, indeed all maximal solutions (4.20), (4.21) with $\xi(0,0) \in \mathbb{X}_0$ and $w \in \mathcal{L}_\infty$ are t-complete.

Proof of statement (iv)

To obtain the upper-bound for $\kappa_{\text{out},i}(y_i,\mu_i)$, we first derive an upper-bound for y_i. From (C.17), we obtain that

$$U(\xi(t,j)) \leqslant e^{-\rho t}U(\xi(0,0)) + \varepsilon_w\int_0^t e^{-\rho(t-s)}|w(s)|^2\mathrm{d}s. \tag{C.18}$$

By combining the latter with the fact that $U(\xi(t,j)) \geqslant x^\top(t,j)Px(t,j) - c \geqslant \frac{\lambda_{\min}(P)}{\lambda_{\max}(C_{p,i}^\top C_{p,i})y(t,j)} - c$, we can conclude that $\|y_i\|_\infty \leqslant \bar{y}_i$ with $\bar{y}_i$ as in (4.39).

[1] The tangent cone to a set $S \subset \mathbb{R}^n$ at a point $x \in \mathbb{R}^n$, denoted $T_S(x)$, is the set of all vectors $\omega \in \mathbb{R}^n$ for which there exist $x_i \in S, \tau_i > 0$ with $x_i \to x, \tau \to 0$ as $i \to \infty$ such that $\omega = \lim_{i\to\infty}(x_i - x)/\tau_i$ (see Definition 5.12 in [99]).

Consequently, in view of (4.31) and the fact $\mu_i(t,j) \geqslant \underline{\mu}_i$ for all $(t,j) \in \operatorname{dom}\xi$, we can conclude that the elements of $\kappa_{\text{out},i}(y_i,\mu_i)$ are upper bounded by $\kappa^*_{\text{out},i}$ as in (4.36).

To obtain the upper-bound for $\kappa_{\text{in},i}(y_i,\mu_i)$, we first derive an upper-bound for μ_i. By recalling the fact that μ_i, $i \in \{1,2,\ldots,l\}$, is only increased when $|y_i| \geqslant \ell_{\text{out},i}\mu_i$ (see also property (b) below (4.38), we obtain that $\|\mu_i\|_\infty \leqslant \bar{\mu}_i$ with $\bar{\mu}_i$ as in (4.37). Given the latter, we can obtain from (4.31) that the elements of $\kappa_{\text{in},i}(y_i,\mu_i)$ are upper bounded by $\kappa^*_{\text{in},i}$ as in (4.35).

All the statements of Theorem 4.1 are now proved. □

Appendix D

Proofs of Chapter 5

Proof of Theorem 5.1 To streamline the proof of Theorem 5.1, we first consider only the closed-loop system $\mathcal{H}_d$. After that, we show that also the closed-loop system $\mathcal{H}_s$ has the same stability and performance guarantees as $\mathcal{H}_d$. Let us define $\mathcal{R}_d(\mathbb{X}_0)$ as the set of all reachable states for hybrid system $\mathcal{H}_d$ with initial condition $\xi(0,0) \in \mathbb{X}_0$ and any input $w \in \mathcal{L}_p$, *i.e.*, $\mathcal{R}_d(\mathbb{X}_0) = \{\bar{\xi} \in \mathbb{X} \mid$ there exists a solution pair (ξ, w) of $\mathcal{H}_d$ with $\xi(0,0) \in \mathbb{X}_0$, $w \in \mathcal{L}_p$ such that for some $(t,j) \in \operatorname{dom} \xi$, $\bar{\xi} = \xi(t,j)\}$.

Lemma D.1. *For all $\chi \in \mathcal{R}_d(\mathbb{X}_0)$, there exists a positive constant c such that $\phi(\delta\tau_{miet} + \min(\tau, \tau_{miet})) \leqslant \lambda$, where $\lambda > 0$.*

Before we discuss the proof of Lemma D.1, let us first remark that in the remainder of the proof, we often omit the time arguments of the solution pair (ξ, w) of a hybrid system $\mathcal{H}_d$ and we do not mention $\operatorname{dom} \xi = \operatorname{dom} w$ explicitly for shortness.

Proof of Lemma D.1: Observe that since $\delta \in \Delta$ and $\dot{\tau} = 1$ for all $(t,j) \in \operatorname{dom} \xi$, we have that $0 \leqslant \delta\tau_{miet} + \min(\tau, \tau_{miet}) \leqslant \tau_{miet}(\delta_{max} + 1)$. By recalling the facts that when $(\delta_{max}+1)\tau_{miet} < \mathcal{T}(\gamma, L)$ and the constant λ is chosen sufficiently small (as indicated after Condition 5.2), $\phi(s) \in [\lambda, \lambda^{-1}]$ and $\dot{\phi}(s) < 0$ for all $s \in [0, \tau_{miet}(\delta_{max}+1)]$, the statement follows immediately, which completes the proof. □

Consider the function

$$U(\xi) = V(x) + \gamma\tilde{\phi}(\delta, \tau)W^2(e) + \eta, \tag{D.1}$$

where $\tilde{\phi}(\delta, \tau) := \phi(\delta\tau_{miet} + \min(\tau, \tau_{miet}))$. Using Lemma D.1 with the facts that the functions V and W are positive definite and radially unbounded due to Condition 5.1 and that $\eta \geqslant 0$ per definition of $\mathbb{X}$, we can conclude that U is

a positive definite and radially unbounded function with respect to (x, e, η) in the sense that there exist $\mathcal{K}_\infty$-functions $\underline{\beta}_U$ and $\bar{\beta}_U$ such that $\underline{\beta}_U(|\hat{\xi}|) \leqslant U(\xi) \leqslant \bar{\beta}_U(|\hat{\xi}|)$, for all $\xi \in \mathbb{X}$ where $\hat{\xi} = \big(x, e, \eta\big) \in \mathbb{R}^{n_x} \times \mathbb{R}^{n_y} \times \mathbb{R}_{\geqslant 0}$. Hence, U constitutes a suitable candidate storage/Lyapunov function for our purpose.

Consider the storage function U given by (D.1). We can see from (5.1) that at a packet loss (*i.e.*, if $\xi \in D_d$ and jumps according to (5.16b)), $U(\xi^+) - U(\xi) = 0$, since $x^+ = x$, $e^+ = e$, $\eta^+ = \eta$ and $\tilde{\phi}(\delta^+, \tau^+) = \tilde{\phi}(\delta, \tau)$. The latter follows the fact that $\delta^+ \tau_{miet} + \min(\tau^+, \tau_{miet}) = (\delta + 1)\tau_{miet} = \delta\tau_{miet} + \min(\tau, \tau_{miet})$, where in the last equality we used that $\tau \geqslant \tau_{miet}$ when $\xi \in D_d$ (and thus $\tau_{miet} = \min(\tau, \tau_{miet})$). When a transmission is successful (*i.e.*, if $\xi \in D_d$ and jumps according to (5.16a)), we have, due to (5.31) and the fact that $\eta = 0$ when $\xi \in D_d$, that

$$U(\xi^+) - U(\xi) = \eta_0(o) - \gamma\tilde{\phi}(\delta, \tau)W^2(e). \tag{D.2}$$

By recalling that $\tau_{miet} = \min(\tau, \tau_{miet})$ when $\xi \in D_d$, we obtain that $\phi((\delta + 1)\tau_{miet}) = \tilde{\phi}(\delta, \tau)$ and thus $U(\xi^+) - U(\xi) = 0$ for all $\xi \in D_d$. With some abuse of notation, we consider the quantity $\langle \nabla U(\xi), F(\xi, w)\rangle$ with $F(\xi, w)$ as in (5.12) even though U is not differentiable with respect to δ and κ. Instead, the elements of $\nabla U(\xi)$ corresponding to partial derivative with respect to δ and κ can be considered as zero. This is justified since the components in $F(\xi, w)$ corresponding to δ and κ are zero. From the imposed conditions (5.24) and (5.26), we can derive that when $\tau \in [0, \tau_{miet}]$ and almost all (x, e)

$$\begin{aligned}
\langle \nabla U(\xi), F(\xi, w)\rangle &\leqslant -\rho(|x|) - \varrho(y) - H^2(x, w) \\
&\quad - \sigma(W(e)) + \gamma^2 W^2(e) + \mu(\theta^p|w|^p - |q(x, w)|^p) \\
&\quad + 2\gamma\tilde{\phi}(\delta, \tau)W(e)\left(LW(e) + H(x, w)\right) \\
&\quad - \gamma W^2(e)\left(2L\tilde{\phi}(\delta, \tau) + \gamma\left(\tilde{\phi}^2(\delta, \tau) + 1\right)\right) + \Psi(o, \eta) \\
&= -M_1(o, w) - \rho(|x|) - \sigma(W(e)) + \Psi(o, \eta) + \mu(\theta^p|w|^p - |q(x, w)|^p),
\end{aligned} \tag{D.3}$$

where $M_1(o, w) := \varrho(y) + \big(H(x, w) - \gamma\tilde{\phi}(\delta, \tau)W(e)\big)^2$. Observe that $\Psi(o, \eta) \leqslant M_1(o, w) - \chi(\eta)$. Hence, we obtain from (D.3) that in case $w = 0$,

$$\langle \nabla U(\xi), F(\xi, 0)\rangle \leqslant -\rho(|x|) - \sigma(W(e)) - \chi(\eta), \tag{D.4}$$

and, in case disturbances are present, that

$$\langle \nabla U(\xi), F(\xi, w)\rangle \leqslant \mu(\theta^p|w|^p - |q(x, w)|^p). \tag{D.5}$$

When $\tau > \tau_{miet}$, $\dot{\tilde{\phi}} = 0$ since $\tilde{\phi}(\delta, \tau) = \phi((\delta + 1)\tau_{miet})$ for $\tau > \tau_{miet}$ and $\dot{\delta} = 0$. Hence, for almost all $\xi \in C_d$ for which $\tau > \tau_{miet}$, we obtain

$$\begin{aligned}\langle \nabla U(\xi), F(\xi,w)\rangle &\leqslant -\rho(|x|) - \varrho(y) - H^2(x,w)\\ &\quad - \sigma(W(e)) + \gamma^2 W^2(e) + \mu(\theta^p|w|^p - |q(x,w)|^p)\\ &\quad + 2\gamma\tilde{\phi}(\delta,\tau)W(e)\left[LW(e) + H(x,w)\right] + \Psi(o)\\ &= -M_2(o,w) - \rho(|x|) - \sigma(W(e)) + \Psi(o) + \mu(\theta^p|w|^p - |z(x,w)|^p), \quad \text{(D.6)}\end{aligned}$$

where

$$M_2(o,w) := \varrho(y) + H^2(x,w) - 2\gamma\tilde{\phi}(\delta,\tau)W(e)H(x,w) - \left(\gamma^2 + 2\gamma\tilde{\phi}(\delta,\tau)L\right)W^2(e).$$

By using the fact that $2\gamma\tilde{\phi}(\delta,\tau)W(e)H(x,w) \leqslant H^2(x,w) + \tilde{\phi}^2(\delta,\tau)\gamma^2 W^2(e)$, we obtain that $\Psi(o,\eta) \leqslant M_2(o,w) - \chi(\eta)$ when $\tau > \tau_{miet}$. Given the latter, we can see from (D.6) that the inequalities (D.4) and (D.5) are also satisfied when $\tau > \tau_{miet}$. Hence, for each maximal solution pair (ξ, w) of the system $\mathcal{H}_d$ with $\xi(0,0) \in \mathbb{X}_0$, it holds that during flows, *i.e.*, when $\xi(t,j) \in C_d$, $(t,j) \in \operatorname{dom}\xi$ the storage function U satisfies (D.4) and (D.5) for the cases that $w = 0$ and $w \neq 0$, respectively. Furthermore, at jumps, *i.e.*, when $\xi(t,j) \in D_d$, $(t,j) \in \operatorname{dom}\xi$, U satisfies (D.2). As shown in [60, 120], this implies that system $\mathcal{H}_d$ is UGAS for the case $w = 0$ (see also [98, Proposition 3.27]) and, in presence of disturbances, $\mathcal{L}_p$-stable with an $\mathcal{L}_p$-gain less than or equal to θ provided we can show that $\mathcal{H}_d$ is persistently flowing.

To show that the system $\mathcal{H}_d$ is indeed persistently flowing, we verify the conditions provided in [98, Proposition 6.10]. First, observe that $G(D_d) \subset C_d$ since according to (5.15) and (5.31), at each jump we have that $\tau^+ = 0$ and $\xi^+ \in \mathbb{X}$. The latter follows from the facts that δ is being reset to zero after at most δ_{max} jumps, *i.e.*, $\delta^+ \in \Delta$, and that $\eta_0(o) \geqslant 0$ for all $o \in \mathbb{O}$ due to Lemma D.1 since $\gamma > 0$ and $W^2(e) \geqslant 0$ for all $e \in \mathbb{R}^{n_y}$, which implies $\eta^+ \geqslant 0$ (for both the cases that the system jumps according to G_0 and G_1 as in (5.16a) and (5.16b), respectively). Secondly, we need to show that for each point $p \in C_d \backslash D_d$ there exists a neighborhood U of p such that for all $q \in U \cap C_d$, $F(q,w) \in T_{C_d}(q)$ where $T_{C_d}(q)$ denotes the tangent cone to the set C_d at point p.[1] Based on (5.18), we obtain that for the system $\mathcal{H}_d$, $C_d \backslash D_d = \{\xi \in \mathbb{X} \mid \tau < \tau_{miet} \text{ or } (\eta > 0 \text{ and } \kappa > \delta_{max})\}$. The tangent cone $T_{C_d}(q)$ for each $q \in C_d$, is given for the relevant cases below:

(i) For $q \in \{\xi \in \mathbb{X} \mid \big((0 < \tau < \tau_{miet}) \text{ or } (\tau \geqslant \tau_{miet} \text{ and } \kappa > \delta_{max})\big) \text{ and } \eta > 0\}$, $T_{C_d}(q) = \mathbb{R}^{n_x} \times \mathbb{R}^{n_y} \times \{0\} \times \mathbb{R} \times \{0\} \times \mathbb{R}$.

(ii) For $q \in \{\xi \in \mathbb{X} \mid \tau = 0 \text{ and } \eta > 0\}$, $T_{C_d}(q) = \mathbb{R}^{n_x} \times \mathbb{R}^{n_y} \times \{0\} \times \mathbb{R}_{\geqslant 0} \times \{0\} \times \mathbb{R}$.

[1] [98, Definition 5.12] The tangent cone to a set $S \subset \mathbb{R}^n$ at a point $x \in \mathbb{R}^n$, denoted by $T_S(x)$, is the set of all vectors $q \in \mathbb{R}^n$ for which there exist sequences $\{x_i\}_{i\in\mathbb{N}}$ and $\{\tau_i\}_{i\in\mathbb{N}}$ with $x_i \in S$, $\tau_i > 0$ and with $x_i \to x$, $\tau_i \downarrow 0$ $(i \to \infty)$, and $q = \lim_{i\to\infty} \frac{x_i - x}{\tau_i}$.

(iii) For $q \in \{\xi \in \mathbb{X} \mid \big((0 < \tau < \tau_{miet}) \text{ or } (\tau \geqslant \tau_{miet} \text{ and } \kappa > \delta_{max})\big) \text{ and } \eta = 0\}$, $T_{C_d}(q) = \mathbb{R}^{n_x} \times \mathbb{R}^{n_y} \times \{0\} \times \mathbb{R} \times \{0\} \times \mathbb{R}_{\geqslant 0}$.

(iv) For $q \in \{\xi \in \mathbb{X} \mid \tau = 0 \text{ and } \eta = 0\}$, $T_{C_d}(q) = \mathbb{R}^{n_x} \times \mathbb{R}^{n_y} \times \{0\} \times \mathbb{R}_{\geqslant 0} \times \{0\} \times \mathbb{R}_{\geqslant 0}$.

Observe from (5.12) that $\dot{\tau} = 1$, $\dot{\delta} = 0$ and $\dot{\kappa} = 0$ for all $q \in C_d$. Based on the latter facts it follows trivially that $F(q, w) \in T_{C_d}(q)$ for $q \in C_d \backslash D_d$ with $\eta > 0$ (corresponding to item (i) and (ii) above). Moreover, for each $q \in C_d \backslash D_d$ with $\eta = 0$ (corresponding to item (iii) and (iv)), it holds that $0 \leqslant \tau < \tau_{miet}$. Observe from (5.9) and (5.30) that for the latter situation it holds that $\dot{\eta} \geqslant 0$ since $\Psi(o, 0) \geqslant 0$ when $0 \leqslant \tau < \tau_{miet}$ due to the fact that ϱ is a positive definite continuous function (as indicated in Condition 5.1). As such, $F(q, w) \in T_{C_d}(q)$ also holds for $q \in C_d \backslash D_d$ with $\eta = 0$, which leads to the conclusion that for each point $p \in C_d \backslash D_d$, there exists a neighborhood U of p such that for all $q \in U \cap C_d$, $F(q, w) \in T_{C_d}(q)$. The latter implies that there exists a non-trivial solution pair (ξ, w) to $\mathcal{H}_d$ with $\xi(0, 0) \in \mathbb{X}_0$ meaning that dom ξ consists of at least two points, see also [98, Proposition 6.10]. In addition, due the time regularization employed in the jump set (5.18b) and the absence of finite-escape times due to the bounds generated by the Lyapunov/storage function, we can conclude that the system $\mathcal{H}_d$ is indeed persistently flowing, which completes the proof.

To prove the stability and performance results for system $\mathcal{H}_s$ (which employs the *static* triggering condition given by (5.7)), let us first recall that $\mathcal{H}_s$ and $\mathcal{H}_d$ have the same flow and jump dynamics. As a consequence, we can use the same candidate storage/Lyapunov function and follow the same arguments as used in the proof of the stability and performance results for system $\mathcal{H}_d$. To be more specific, for each maximal solution pair (ξ, w) of the system $\mathcal{H}_s$ with $\xi(0, 0) \in \mathbb{X}_0$, the storage/Lyapunov function as given in (D.1) satisfies (D.4) and (D.5) for the cases that $w = 0$ and $w \neq 0$, respectively, during flows, *i.e.*, when $\xi(t, j) \in C_s$, $(t, j) \in \text{dom } \xi$ and satisfies $U(\xi^+) - U(\xi) = 0$ at jumps, *i.e.*, when $\xi(t, j) \in D_s$, $(t, j) \in \text{dom } \xi$. Observe, however, to obtain the desired UGAS and $\mathcal{L}_p$-stability properties, we still need to show that $\mathcal{H}_s$ is persistently flowing as $C_s \neq C_d$ and $D_s \neq D_d$.

Based on (5.17), we obtain that for the system $\mathcal{H}_s$, $C_s \backslash D_s = \{\xi \in \mathbb{X} \mid \tau < \tau_{miet} \text{ or } (\Psi(o, 0) > 0 \text{ and } \kappa > \delta_{max})\}$. By recalling $C_d \backslash D_d$ and the description of $T_{C_d}(q)$ as in items (i)-(iv) above, we can obtain that the tangent cone $T_{C_s}(q) = T_{C_d}(q)$ for each $q \in C_s \backslash D_s$. Let us recall that due to (5.12), $\dot{\tau} = 1$, $\dot{\delta} = 0$ and $\dot{\kappa} = 0$ for all $q \in C_s$. Moreover, we have that for all $q \in C_s \backslash D_s$ for which $0 \leqslant \tau < \tau_{miet}$, $\dot{\eta} \geqslant 0$ since $\Psi(o, 0) \geqslant 0$ when $0 \leqslant \tau < \tau_{miet}$. Observe from (5.17b) that for each $q \in C_s \backslash D_s$ for which $\tau \geqslant \tau_{miet}$, $\kappa > \delta_{max}$ and $\eta = 0$, $\dot{\eta} > 0$ since then $\Psi(o, 0) > 0$. Hence, we can conclude that for each point $p \in C_s \backslash D_s$, there exists a neighborhood U of p such that for all $q \in U \cap C_s$, $F(q, w) \in T_{C_s}(q)$. As mentioned before, this implies that there exists a non-trivial solution pair (ξ, w) to $\mathcal{H}_s$ with $\xi(0, 0) \in \mathbb{X}_0$ meaning that dom ξ consists of

at least two points. Moreover, due the time regularization employed in the jump set (5.17b) and the absence of finite-escape times due to the bounds generated by the Lyapunov/storage function, we can conclude the system $\mathcal{H}_s$ is indeed persistently flowing, which completes the proof. Hence, indeed the closed-loop system $\mathcal{H}_s$ has the same UGAS and $\mathcal{L}_p$-gain properties as the closed-loop system $\mathcal{H}_d$, which completes the proof. □

Proof of Theorem 5.2: Similar as in Theorem 5.1, we first only consider the closed-loop system $\tilde{\mathcal{H}}_d$. After that, we show that also the closed-loop system $\tilde{\mathcal{H}}_s$ has the same stability and performance guarantees as $\tilde{\mathcal{H}}_d$. By following the same arguments as in the proof of Theorem 5.1, we can conclude that $\tilde{U}(\tilde{\xi}) = V(x) + \gamma\tilde{\phi}(\delta,\tau)W^2(e) + \eta$ constitutes a suitable candidate storage function for the system $\tilde{\mathcal{H}}_d$ given by (5.44) in the sense that the function $\tilde{U}$ is positive definite and radially unbounded with respect to (x,e,η) in the sense that there exist $\mathcal{K}_\infty$-functions $\underline{\beta}_{\tilde{U}}$ and $\bar{\beta}_{\tilde{U}}$ such that $\underline{\beta}_{\tilde{U}}(|\hat{\xi}|) \leqslant \tilde{U}(\tilde{\xi}) \leqslant \bar{\beta}_{\tilde{U}}(|\hat{\xi}|)$, for all $\tilde{\xi} \in \tilde{\mathbb{X}}$ where $\hat{\xi} = \big(x,e,\eta\big) \in \mathbb{R}^{n_x} \times \mathbb{R}^{n_y} \times \mathbb{R}_{\geqslant 0}$. Moreover, we can obtain that for each maximal solution pair $(\tilde{\xi},w)$ of the system $\tilde{\mathcal{H}}_d$ with $\tilde{\xi}(0,0) \in \tilde{\mathbb{X}}_0$, $\tilde{U}(\tilde{\xi}^+) - \tilde{U}(\tilde{\xi}) = 0$ at jumps and that in case $w = 0$, $\Big\langle \nabla\tilde{U}(\tilde{\xi}), F(\tilde{\xi},w) \Big\rangle \leqslant -\rho(|x|) - \sigma(W(e)) - \chi(\eta)$ and, in case disturbances are present, that $\Big\langle \nabla\tilde{U}(\tilde{\xi}), F(\tilde{\xi},w) \Big\rangle \leqslant \mu(\theta^p|w|^p - |q(x,w)|^p)$ at flows since the dynamics of x, e and η has not been changed with respect to system $\mathcal{H}_d$. However, as the triggering condition has been changed to (5.37), we again have to show that $\tilde{\mathcal{H}}_d$ is persistently flowing with respect to initial state set $\tilde{X}_0$.

First of all, observe that $\tilde{G}(\tilde{D}_d) \subset \tilde{C}_d$ since $\tilde{\xi}^+ \in \tilde{\mathbb{X}}$ (as shown in the proof of Theorem 5.1), $\eta_i^+ \in \mathbb{R}_{\geqslant 0}$, $i \in \tilde{\Delta}$ due to (5.40) and the fact that $\gamma\phi(k\tau_{miet})W^2(\hat{y}_k - y) \geqslant 0$ for all $k \in \tilde{\Delta}$.

Now, let $\tilde{\mathcal{R}}_d(\tilde{\mathbb{X}}_0)$ denote the set of all the reachable states of hybrid system $\tilde{\mathcal{H}}_d$ with initial condition $\tilde{\xi}(0,0) \in \tilde{\mathbb{X}}_0$ and some input $w \in \mathcal{L}_p$ and consider the following lemma.

Lemma D.2. *For all $\tilde{\chi} \in \tilde{\mathcal{R}}_d\left(\tilde{\mathbb{X}}_0\right)$ for which $\tau \geqslant \tau_{miet}$ and $\eta = 0$ and $\kappa > \delta_{max}$, it holds that $\Phi_\eta(\bar{\eta}) = 0$.*

Proof of Lemma D.2: Consider the following hypothesis. Suppose $(\tilde{\xi},w)$ is a maximal solution pair of the system $\tilde{\mathcal{H}}_d$ with $\xi(\tilde{0},0) \in \tilde{\mathbb{X}}_0$, then for each $j \in \{\bar{\kappa},\dots,J\}$ with $J = \sup_j \operatorname{dom}\tilde{\xi}$, it holds that $\eta(t,j) \geqslant \eta_{\delta(t,j)+1}(t,j)$ for all $t \in [t_j,t_{j+1}]$, where $\bar{\kappa} := \inf\{j \mid \delta(t,j) = 0, (t,j) \in \operatorname{dom}\tilde{\xi}\}$ such that $\bar{\kappa} \leqslant \delta_{max}$ due to Assumption 5.1.To prove the aforementioned hypothesis, we use an induction argument. First, we show that the hypothesis holds for $j = \bar{\kappa}$. We have that $\eta(t_{\bar{\kappa}},\bar{\kappa}) \geqslant \eta_{\delta(t_{\bar{\kappa}},\bar{\kappa})+1}(t_{\bar{\kappa}},\bar{\kappa})$ since $\delta(t_{\bar{\kappa}},\bar{\kappa}) = 0$ and $\eta_1(t_{\bar{\kappa}},\bar{\kappa}) \overset{(5.40b)}{=} \min_{k\in\tilde{\Delta}} \gamma\phi(k\tau_{miet})W^2(\hat{y}_k(t_{\bar{\kappa}},\bar{\kappa}) - y(t_{\bar{\kappa}},\bar{\kappa})) \overset{(5.45)}{\leqslant} \gamma\phi(\delta(t_{\bar{\kappa}},\bar{\kappa}) + 1)\tau_{miet}W^2(e) \overset{(5.15),(5.31)}{\leqslant} \eta(t_{\bar{\kappa}},\bar{\kappa})$. Observe that $\dot{\eta}_{\delta(t,j)+1} = \Psi(y,\hat{y}_{\delta(t,j)+1} - y,\tau,$

$\eta_{\delta(t,j)+1}, \delta(t,j)+1) = \Psi(y, e, \tau, \eta_{\delta(t,j)+1}, \delta(t,j)+1)$ for all $(t,j) \in [t_{\bar{\kappa}}, t_{\bar{\kappa}+1}] \times \{\bar{\kappa}\}$ since $e(t,j) = \hat{y}_{\delta(t,j)+1}(t,j) - y(t,j)$ for all $(t,j) \in \operatorname{dom} \xi$ due to (5.45). Recalling the facts that $\dot{\eta} = \Psi(y, e, \tau, \eta, \delta)$ and that the function $\Psi(\cdot,\cdot,\cdot,\eta,\cdot)$ is locally Lipschitz in $\eta \in \mathbb{R}_{\geqslant 0}$, we can now obtain by means of the Comparison Lemma (see, *e.g.*, [131, p. 102-103]) that $\eta(t,j) \geqslant \eta_{\delta(t,j)+1}(t,j)$ for all $(t,j) \in [t_{\bar{\kappa}}, t_{\bar{\kappa}+1}] \times \{\bar{\kappa}\}$. Hence, the hypothesis holds for $j = \bar{\kappa}$. Now suppose that the hypothesis is true for some $j > \bar{\kappa}$, then we know that $\eta(t_{j+1}, j) \geqslant \eta_{\delta(t_{j+1},j)+1}(t_{j+1}, j)$. In case the transmission at time t_{j+1} is successful (if (5.16a) holds), we have that $\eta(t_{j+1}, j+1) = \gamma\phi W^2(e(t_{j+1}, j+1))$ and $\eta_{\delta(t_{j+1},j+1)+1}(t_{j+1}, j+1) = \eta_1(t_{j+1}, j+1) \overset{(5.40b)}{=} \min_i \gamma\phi_i W^2(\hat{y}_i(t_{j+1}, j+1) - y(t_{j+1}, j+1))$. Since $\gamma\phi W^2(e(t_{j+1}, j+1)) \overset{(5.45)}{\geqslant} \min_i \gamma\phi_i W^2(\hat{y}_i(t_{j+1}, j+1) - y(t_{j+1}, j+1))$, we obtain that if the transmission attempt is successful, $\eta(t_{j+1}, j+1) \geqslant \eta_{\delta(t_{j+1},j+1)+1}(t_{j+1}, j+1)$ holds. In case of a packet loss (if (5.16b) holds), we have that $\eta(t_{j+1}, j+1) = \eta(t_{j+1}, j)$ and $\eta_{\delta(t_{j+1},j+1)+1}(t_{j+1}, j+1) = \eta_{\delta(t_{j+1},j)+2}(t_{j+1}, j+1) \overset{(5.40a)}{=} \eta_{\delta(t_{j+1},j)+1}(t_{j+1}, j)$. Hence, at a transmission attempt at time t_{j+1}, we have that $\eta(t_{j+1}, j+1) \geqslant \eta_{\delta(t_{j+1},j+1)+1}(t_{j+1}, j+1)$ holds. By using the same arguments based on the Comparison Lemma used for the case $j = 0$, we find that $\eta(t,j) \geqslant \eta_{\delta(t,j)+1}(t,j)$ for $(t,j) \in [t_{j+1}, t_{j+2}] \times \{j+1\}$ and thus the hypothesis holds for $j+1$. Observe however that induction argument is not complete yet as the total number of jumps in $\operatorname{dom} \tilde{\xi}$ might be finite, *i.e.*, $J < \infty$. As such, to complete the proof by induction, we need to show that $\eta(t,j) \geqslant \eta_{\delta(t,j)+1}(t,j)$ for all $(t,j) \in [t_J, T] \times \{J\}$ with $T \geqslant t_j$ finite or $T = \infty$. Note however, that we can use the same arguments as before to verify the previous statement, namely, by using the fact that $\gamma\phi W^2(e(t_J, J)) \overset{(5.45)}{\geqslant} \min_{i \in \tilde{\Delta}} \gamma\phi_i W^2(\hat{y}_i(t_J, J) - y(t_J, J))$ to show that $\eta(t_J, J) \geqslant \eta_{\delta(t_J,J)+1}(t_J, J)$, and by using the Comparison Lemma to show that $\eta(t,j) \geqslant \eta_{\delta(t,j)+1}(t,j)$ for all $(t,j) \in [t_J, T] \times \{J\}$. Hence, for each $j \in \{\bar{\kappa}, \ldots, J\}$ with $J = \sup_j \operatorname{dom} \tilde{\xi}$, it indeed holds that $\eta(t,j) \geqslant \eta_{\delta(t,j)+1}(t,j)$ for all $t \in [t_j, t_{j+1}]$. Using the fact that $\Phi_\eta(\bar{\eta}(t,j)) \leqslant \eta_{\delta(t,j)+1}(t,j)$ due to (5.38), we can now conclude that $\Phi_\eta(\bar{\eta}(t,j)) \leqslant \eta(t,j)$ for all $(t,j) \in \operatorname{dom} \tilde{\xi}$. The previous inequality implies that for all $\tilde{\chi} \in \tilde{\mathcal{R}}_d(\tilde{\mathbb{X}}_0)$ for which $\tau \geqslant \tau_{miet}$ and $\eta = 0$, it holds that $\Phi_\eta(\bar{\eta}(t,j)) = 0$, which completes the proof. □

Let us define $\tilde{D}_d^* := \left\{\tilde{\xi} \in \tilde{\mathbb{X}} \mid \tau \geqslant \tau_{miet} \text{ and } \left(\Phi_\eta(\bar{\eta}) = 0 \text{ or } \eta = 0 \text{ or } \kappa \leqslant \delta_{max}\right)\right\}$. Observe that $\tilde{D}_d^* \backslash \tilde{D}_d = \left\{\tilde{\xi} \in \tilde{\mathbb{X}} \mid \tau \geqslant \tau_{miet} \text{ and } \Phi_\eta(\bar{\eta}) > 0 \text{ and } \eta = 0 \text{ and } \kappa > \delta_{max}\right\}$. From Lemma D.2, it follows that $(\tilde{D}_d^* \backslash \tilde{D}_d) \cap \tilde{\mathcal{R}}_d(\tilde{\mathbb{X}}_0) = \emptyset$. As such, the hybrid system $\tilde{\mathcal{H}}_d^* := (\tilde{C}_d, \tilde{D}_d^*, \tilde{F}, \tilde{G})$ is equivalent to the system $\tilde{\mathcal{H}}_d$ for initial state set $\tilde{\mathbb{X}}_0$ in the sense that each solution pair $(\tilde{\xi}^*, w^*)$ of $\tilde{\mathcal{H}}_d^*$ with $\tilde{\xi}^*(0,0) \in \tilde{\mathbb{X}}_0$ and $w^* \in \mathcal{L}_p$, is equal to the solution pair $(\tilde{\xi}, w)$ of $\tilde{\mathcal{H}}_d$ with $\tilde{\xi}(0,0) = \tilde{\xi}^*(0,0)$ and $w(t,j) = w^*(t,j)$ for all $(t,j) \in \operatorname{dom} w$ and vice versa. The latter fact implies that $\tilde{\mathcal{H}}_d$ is persistently flowing with respect to initial state set

$\tilde{\mathbb{X}}_0$ if and only if $\tilde{\mathcal{H}}_d^*$ is persistently flowing with respect to initial state set $\tilde{\mathbb{X}}_0$. Let us recall that $\tilde{G}(\tilde{D}_d) \subset \tilde{C}_d$ and observe that, due to the bounds generated by the Lyapunov/storage function as mentioned before, finite-escape times are absent for all solution pairs $(\tilde{\xi}, w)$ of $\tilde{\mathcal{H}}_d$ with $\tilde{\xi}(0,0) = \tilde{\xi}^*(0,0)$ and $w \in \mathcal{L}_p$. By combining the previous facts, we obtain (in the spirit of [98, Proposition 6.10]) that $\tilde{\mathcal{H}}_d$ is persistently flowing with respect to initial state set $\tilde{\mathbb{X}}_0$, if and only if for each point $\tilde{p} \in \tilde{C}_d \backslash \tilde{D}_d^*$, there exists a neighborhood U of $\tilde{p}$ such that for all $\tilde{q} \in U \cap \tilde{C}_d$, $\tilde{F}(\tilde{q}, w) \in T_{\tilde{C}_d}(\tilde{q})$

By recalling the descriptions of $\tilde{D}_d^*$ and $C_d \backslash D_d$, and by means of (5.44a), we obtain that $\tilde{C}_d \backslash \tilde{D}_d^* = (C_d \backslash D_d) \times \mathbb{R}^{(\delta_{max}+1)n_y} \times \mathbb{R}_{>0}^{\delta_{max}+1}$. Moreover, observe from (5.18a) and (5.44a) that $\tilde{C}_d = C_d \times \mathbb{R}^{(\delta_{max}+1)n_y} \times \mathbb{R}_{\geqslant 0}^{\delta_{max}+1}$. By means of the latter, we find that $T_{\tilde{C}_d}(\tilde{q}) = T_{C_d}(q) \times \mathbb{R}^{(\delta_{max}+1)n_y} \times T_{\mathbb{R}_{\geqslant 0}}(\eta_1) \times T_{\mathbb{R}_{\geqslant 0}}(\eta_2) \times \ldots \times T_{\mathbb{R}_{\geqslant 0}}(\eta_{\delta_{max}+1})$ for all $\tilde{q} \in \tilde{C}_d$, where

$$T_{\mathbb{R}_{\geqslant 0}}(r) = \begin{cases} \mathbb{R}_{\geqslant 0}, & \text{when } r = 0 \\ \mathbb{R}, & \text{when } r > 0, \end{cases} \tag{D.7}$$

for all $r \in \mathbb{R}_{\geqslant 0}$. In the proof of Theorem 5.1, we already showed that for each point $p \in C_d \backslash D_d$ there exists a neighborhood U of p such that for all $q \in U \cap C_d$, $F(q, w) \in T_{C_d}(q)$. As such, we only need to show that for each $\tilde{p} \in \tilde{C}_d \backslash \tilde{D}_d$, $\dot{\eta}_i \in T_{\mathbb{R}_{\geqslant 0}}(\eta_i)$, $i \in \tilde{\Delta}$. Observe from (D.7) that the latter holds trivially for $\eta_i > 0$. For $\tilde{p} \in \tilde{C}_d \backslash \tilde{D}_d$ with $\eta_i = 0$, we have that $\tau \leqslant \tau_{miet}$ and, according to (5.30), that $\Psi(o_i, 0) \geqslant 0$ and thus $\dot{\eta}_i \geqslant 0$. Hence, it indeed holds that $\dot{\eta}_i \in T_{\mathbb{R}_{\geqslant 0}}(\eta_i)$, $i \in \tilde{\Delta}$ for all $\tilde{p} \in \tilde{C}_d \backslash \tilde{D}_d$. As such, we can conclude that $\tilde{\mathcal{H}}_d$ is indeed UGAS for the case $w = 0$ and, in presence of disturbances, $\mathcal{L}_p$-stable with an $\mathcal{L}_p$-gain less than or equal to θ.

The fact that $\tilde{\mathcal{H}}_s$ (which employs the *static* triggering condition given by (5.36)) is UGAS for the case $w = 0$ and, in presence of disturbances, is $\mathcal{L}_p$-stable follows from similar arguments as used at the end of the proof of Theorem 5.1. This completes the proof. □

Appendix E

Proofs of Chapter 6

Proof of Theorem 6.2: The main idea behind the proof is to regard the closed-loop system $\mathcal{H}_{\mathcal{T}}$ as a system switching between a stable hybrid model (when effectively no DoS attack is active) and an unstable mode (when effectively a DoS attack is active). Inspired by the concept of *average dwell-time* [124], we can then exploit the duration and frequency constraints of the DoS attacks to conclude UGES (or $\mathcal{L}_\infty$-stability a finite induced $\mathcal{L}_\infty$-gain) of the set $\mathcal{A}$ for the class of hybrid systems $\mathcal{H}(\nu, \tau_D, \varsigma, T)$. For clarity of exposition, the proof consists of four steps. In the proof, we often omit the time arguments of the solution ξ of a hybrid system $\mathcal{H}_{\mathcal{T}}$ and we do not mention dom ξ explicitly.

Step I. *Lyapunov/storage function analysis.* Let $\mathcal{R}(\mathbb{X}_0)$ denote all the reachable states of a hybrid system $\mathcal{H}_{\mathcal{T}} \in \mathcal{H}(\nu, \tau_D, \varsigma, T)$ for $\xi(0,0) \in \mathbb{X}_0$, see also [98, Chapter 6].

Lemma E.1. *For any $\chi \in \mathcal{R}(\mathbb{X}_0)$ it holds that*

- $\{m = 1 \vee \tau \geqslant \tau^0_{miet}\} \Leftrightarrow \phi = \phi_{miet}$
- $\lambda^{-1} \geqslant \phi \geqslant \phi_{miet}$
- $\eta \geqslant 0$

Moreover, for all $\chi \in \mathcal{R}(\mathbb{X}_0) \backslash D$ there exists an $\varepsilon > 0$ and an absolutely continuous function $z : [0, \varepsilon] \to \mathbb{R}^n$ such that $z(0) = \chi$, $\dot{z}(t) = F(z(t))$ for almost all $t \in [0, \varepsilon]$ and $z(t) \in C$ for all $t \in (0, \varepsilon]$.

The proof is omitted for the sake of brevity. Consider the candidate Lyapunov/storage function,

$$U(\xi) = V(x) + \gamma \phi W^2(e) + \eta. \tag{E.1}$$

Given the second and third item of Lemma E.1 and the fact that according to Condition 6.1, V and W satisfy (6.25) and (6.23), respectively, and $\gamma > 0$, we find that there exists a positive constant $\underline{c}_U \in \mathbb{R}_{\geqslant 0}$ such that

$$\underline{c}_U |\xi|_{\mathcal{A}}^2 \leqslant U(\xi), \tag{E.2}$$

for all $\xi \in \mathcal{R}(\mathbb{X}_0)$ where $\mathcal{A} = \{\xi \in \mathbb{X} \mid x = 0,\, e = 0\}$. Hence, U constitutes a suitable candidate Lyapunov/storage function for the cases $w = 0$ and $w \neq 0$, respectively.

To study the stability and the performance, we will discuss how the function U evolves over time by considering both jumps (when $\xi \in D$), and flows (when $\xi \in C$).

Jumps: We can see from (6.14) and (6.27) that at transmission events when communication is possible, *i.e.,* if $\xi \in \mathcal{R}(\mathbb{X}_0)$ and $\xi \in D$ and $s \notin \mathcal{T}$ (and thus $\eta = 0$), we have that $U(\xi^+) - U(\xi) = -\gamma\phi W^2(e) + \eta_0(e)$. By recalling that $\eta_0 = \gamma\phi_{miet} W^2(e)$, the first item of Lemma E.1 and by using the fact that $\tau \geqslant \tau^0_{miet}$ when $\xi \in D$, we have that

$$U(\xi^+) - U(\xi) = 0, \tag{E.3}$$

when $\xi \in \mathcal{R}(\mathbb{X}_0) \cap D$ and $s \notin \mathcal{T}$ (and thus $\tau \geqslant \tau^0_{miet}$). At transmission times during a DoS attack, *i.e.,* when $\xi \in D$, and $s \in \mathcal{T}$, (E.3) holds as well since $e^+ = e$, $\phi^+ = \phi$, $\eta^+ = \eta = 0$ and $x^+ = x$.

Flows: For the bounds on U during flow we consider two cases depending on whether the most recent transmission attempt was successful ($m = 0$) or not ($m = 1$).

Case I ($m = 0$): From (6.24), (6.26) and (6.27), we can derive that for almost all $\xi \in \mathcal{R}(\mathbb{X}_0)$ with $m = 0$ and for $w \in \mathbb{R}^{n_w}$,

$$\begin{aligned}
\langle \nabla U(\xi), F(\xi, w) \rangle &\leqslant -\varrho(|y|) - H^2(x,w) + \gamma^2 W^2(e) \\
&+2\gamma\phi W(e)\left(LW(e) + H(x,w)\right) - \omega(\tau,0)\gamma W^2(e)\left(2L\phi + \gamma\left(\phi^2+1\right)\right) \\
&-\rho_W W^2(e) - \rho_V V(x) + \tilde{\Psi}(m,o,\eta) + \theta^2|w|^2 \\
&\leqslant -\rho_V V(x) - \rho_W W^2(e) - M(\xi,w) + \tilde{\Psi}(m,o,\eta) + \theta^2|w|^2,
\end{aligned} \tag{E.4}$$

with $\omega(\tau, m)$ as in (6.36) and where M given by

$$M(\xi,w) = \begin{cases} M_1(\xi,w), & \text{for } 0 \leqslant \tau \leqslant \tau^0_{miet}, \\ M_2(\xi,w), & \text{for } \tau > \tau^0_{miet}, \end{cases} \tag{E.5}$$

where for all $\xi \in \mathbb{X}$ and $w \in \mathbb{R}^{n_w}$

$$M_1(\xi,w) := \varrho(|y|) + \left(H(x,w) - \gamma\phi W(e)\right)^2, \tag{E.6}$$

$$M_2(\xi,w) := \varrho(|y|) + H^2(x,w) - 2\gamma\phi W(e) H(x,w) - \left(\gamma^2 + 2\gamma\phi L\right) W^2(e). \tag{E.7}$$

By using the fact that $2\gamma\phi W(e)H(x,w) \leqslant \gamma^2\phi^2 W^2(e) + H^2(x,w)$, we can conclude from (6.35) and (E.5) that $\Psi(o) \leqslant M(\xi,w)$ for all $o \in \mathbb{O}$. Using the latter fact, we obtain from (6.34) and (E.4) that for $m=0$, $\langle \nabla U(\xi), F(\xi,w)\rangle \leqslant -\rho_V V(x) - \rho_W W^2(e) - \omega_1\eta + \theta^2|w|^2$. By using Lemma E.1 and the fact that $V(x) \leqslant c_{\bar{V}}|x|^2$ due to (6.25), we can conclude that for almost all $\xi \in \mathcal{R}(\mathbb{X}_0)$ with $m=0$ and for $w \in \mathbb{R}^{n_w}$, we have that

$$\langle \nabla U(\xi), F(\xi,w)\rangle \leqslant -\omega_1 U(\xi) + \theta^2|w|^2, \tag{E.8}$$

with ω_1 as in (6.32).

Case II ($m=1$): Observe that for $m=1$, we have that $\dot{\phi}=0$ and $\dot{\eta}=0$ due to (6.7), (6.27) and (6.34), respectively. Hence, it holds that for almost all $\xi \in \mathcal{R}(\mathbb{X}_0)$ with $m=1$ and for all $w \in \mathbb{R}^{n_w}$

$$\begin{aligned}\langle \nabla U(\xi), F(\xi,w)\rangle &\leqslant -\varrho(|y|) - H^2(x,w) + \gamma^2 W^2(e)\\ &+2\gamma\phi W(e)\left(LW(e) + H(x,w)\right) - \rho_W W(e) - \rho_V V(x) + \theta^2|w|^2.\end{aligned}$$

Using the fact that $2\gamma\phi W(e)H(x,w) \leqslant \gamma^2\phi^2 W^2(e) + H^2(x,w)$, and Lemma E.1 we obtain that $\langle \nabla U(\xi), F(\xi,w)\rangle \leqslant (\bar{\gamma} - \rho_W)W^2(e) + \theta^2|w|^2$ with $\bar{\gamma}$ as in (6.33). Hence, it holds that for almost all $\xi \in \mathcal{R}(\mathbb{X}_0)$ with $m=1$ and all $w \in \mathbb{R}^{n_w}$

$$\langle \nabla U(\xi), F(\xi,w)\rangle \leqslant \omega_2 U(\xi) + \theta^2|w|^2 \tag{E.9}$$

with ω_2 as in (6.32). In fact, observe that since $\omega_2 >$ due to Condition 6.1, (E.9) also holds when $m=0$.

Observe that a system $\mathcal{H}_{\mathcal{T}} \in \mathcal{H}(\nu, \tau_D, \varsigma, T)$ does not exhibit Zeno-behaviour due to a strictly positive MIET. Moreover, observe that finite escape-times are excluded from the system due to the bounds on the states x and e as in (E.2), (E.3), (E.8), (E.9) and the fact that the trajectories of the state variables τ, s, m, η, and ϕ do not exhibit finite escape-times. Given the aforementioned facts and the last property mentioned in Lemma E.1, we can conclude that a system $\mathcal{H}_{\mathcal{T}} \in \mathcal{H}(\nu, \tau_D, \varsigma, T)$ with $\xi(0,0) \in \mathbb{X}_0$ is indeed persistently flowing with respect to initial state set $\mathbb{X}_0$.

Step II. *Characterization of stable and unstable modes.* In the previous step, we have shown how the Lyapunov/storage function behaves for both the cases where $m=0$ and $m=1$, see (E.8) ($m=0$) and (E.9) ($m=1$). To use average dwell-time arguments, it is needed to determine the collection of time instants at which either $m=0$ or $m=1$. Unfortunately, this can not directly be related to $\mathcal{T}$, since the value of $\hat{y}$ is typically not updated immediately after a DoS interval has ended due to τ^1_{miet} being a lower bound on the inter-event times $t_{j+1} - t_j$, $j \in \mathbb{N}$, for which transmission time t_j corresponds to an unsuccessful transmission attempt. For this reason, we will consider the "effective" DoS attacks, decompose the time axis accordingly and relate these "effective" DoS attacks to $\mathcal{T}$ via the collection of DoS intervals as given in (6.17). To do so, we

first define for a given maximal solution ξ, the collection of time instants in the interval $[T_1, T_2]$, with $T_2 \geqslant T_1$, at which the most recent transmission attempt was successful and at which no DoS attack is active as

$$\bar{\Theta}_\xi(T_1, T_2) := \big\{\bar{t} \in (T_1, T_2) \mid \bar{t} \notin \mathcal{T} \text{ and } \forall j \in \mathbb{N}, (\bar{t}, j) \in \operatorname{dom} \xi \Rightarrow m(\bar{t}, j) = 0\big\}. \quad \text{(E.10)}$$

The system $\mathcal{H}_\mathcal{T}$ is said to be in the *stable mode* (satisfying (E.8)) at a time instant t if $t \in \bar{\Theta}_\xi(0, \infty)$. In addition, we define the collection of "effective" DoS attacks in the interval $[T_1, T_2]$, with $T_2 \geqslant T_1$ as

$$\overline{\Xi}_\xi(T_1, T_2) := [T_1, T_2]/\bar{\Theta}_\xi(T_1, T_2). \quad \text{(E.11)}$$

Likewise, the system is said to be in the *unstable mode* (satisfying (E.9)) at a time instant t if $t \in \overline{\Xi}_\xi(0, \infty)$. Since for $T_1, T_2 \in \mathbb{R}_{\geqslant 0}$ with $T_2 \geqslant T_1$, $\bar{\Theta}_\xi(T_1, T_2) \cup \overline{\Xi}_\xi(T_1, T_2) = [T_1, T_2]$, we can write $\bar{\Theta}_\xi(T_1, T_2)$ and $\overline{\Xi}_\xi(T_1, T_2)$ as follows

$$\overline{\Xi}_\xi(T_1, T_2) := \bigcup_{k \in \mathbb{N}} Z_k \cap [T_1, T_2], \quad \text{(E.12)}$$

and

$$\bar{\Theta}_\xi(T_1, T_2) := \bigcup_{k \in \mathbb{N}} W_{k-1} \cap [T_1, T_2], \quad \text{(E.13)}$$

where for $k \in \mathbb{N}$

$$Z_k := \begin{cases} [\zeta_k, \zeta_k + v_k) & \text{when } v_k > 0, \\ \{\zeta_k\} & \text{when } v_k = 0, \end{cases}$$

$$W_k := \begin{cases} [\zeta_k + v_k, \zeta_{k+1}) & \text{when } v_k > 0, \\ (\zeta_k, \zeta_{k+1}) & \text{when } v_k = 0, \end{cases}$$

where v_k denotes the time elapsed between ζ_k and the next successful transmission attempt, and where $\zeta_0 := h_0$ where $W_{-1} = [0, \zeta_0)$ when $h_0 > 0$ and $W_{-1} = \emptyset$ when $h_0 = 0$. The collection of *effective* DoS attacks can be related to the *original* collection of DoS intervals as given in (6.17) as

$$|\overline{\Xi}_\xi(T_1, T_2)| \leqslant |\Xi(T_1, T_2)| + (1 + n(T_1, T_2))\tau^1_{miet}, \quad \text{(E.14)}$$

for all $T_1, T_2 \in \mathbb{R}_{\geqslant 0}$ with $T_2 \geqslant T_1$, where $n(T_1, T_2)$ denotes the number of DoS attacks in the interval $[T_1, T_2)$. Indeed, due to the finite sampling rate, the effective DoS interval $\bar{H}_n$ is extended with maximally τ^1_{miet} time units compared to H_n, $n \in \mathbb{N}$. Since this extension might also occur at the beginning of an interval $[T_1, T_2)$, the collection of effective DoS attacks over the interval $[T_1, T_2)$ is at most prolonged with $(1+n(T_1, T_2))\tau^1_{miet}$ time units. Observe that the latter is not the case if $T_1 \in \big[\big(\bigcup_{k \in \mathbb{N}} W_{k-1}\big) \cup \{0\}\big] \cap [0, t]$, *i.e.*,

$$|\overline{\Xi}_\xi(T_1, T_2)| \leqslant |\Xi(T_1, T_2)| + n(T_1, T_2)\tau^1_{miet}, \quad \text{(E.15)}$$

for all $T_1 \in \left[\left(\bigcup_{k\in\mathbb{N}} W_{k-1}\right) \cup \{0\}\right] \cap [0,t]$ and all $T_2 \in \mathbb{R}_{\geqslant T_1}$. By means of Definition 6.1 and Definition 6.2 for the specific values of τ_D and T, we find that according to (E.15)

$$|\overline{\Xi}_\xi(T_1,T_2)| \leqslant \varsigma_* + \frac{T_2-T_1}{T_*}, \tag{E.16}$$

where $\varsigma_* := \varsigma + \nu\tau^1_{miet}$ and $T_* := \tau_D T/(\tau_D + \tau^1_{miet} T)$ for all $T_1 \in \Big[\left(\bigcup_{k\in\mathbb{N}} W_{k-1}\right) \cup \{0\}\Big] \cap [0,t]$ and all $T_2 \in \mathbb{R}_{\geqslant T_1}$.

In summary, in this second step of the proof, we defined effective DoS sequences, which led to the intervals Z_k and W_k, $k \in \mathbb{N}$, representing the *stable* and (possibly) *unstable* mode of the system, respectively. Furthermore, we showed how this effective DoS is related to the original DoS sequence. This relation will be important in the stability and performance analysis.

Step III. *Time-trajectory bounds on Lyapunov/storage function.* As already mentioned, the collection of time instants at which either $m = 0$ or $m = 1$ can not directly be related to $\mathcal{T}$. However, we can deduce the following implications regarding a trajectory ξ with $\xi(0,0) \in \mathbb{X}_0$ and the *stable* and *unstable* mode descriptions

$$\begin{aligned}(t,j) \in &(W_k \times \mathbb{N}) \cap \operatorname{dom}\xi \Rightarrow m(t,j) = 0,\\ (t,j) \in &(Z_k \times \mathbb{N}) \cap \operatorname{dom}\xi \Rightarrow (m(t,j) = 0 \text{ or } m(t,j) = 1).\end{aligned}$$

Based on these implications, (E.3), (E.8) and (E.9), we have that for all $(t,j) \in (W_k \times \mathbb{N}) \cap \operatorname{dom}\xi$, $k \in \mathbb{N} \cup \{-1\}$

$$U(\xi(t,j)) \leqslant e^{-\omega_1(t-\zeta_k-v_k)} U(\xi(\zeta_k+v_k,j)) + \theta^2 \int\limits_{(\zeta_k+v_k)}^{t} e^{-\omega_1(t-s)}|w(s)|^2 \mathrm{d}s \tag{E.17}$$

and for all $(t,j) \in (Z_k \times \mathbb{N}) \cap \operatorname{dom}\xi$, $k \in \mathbb{N}$

$$U(\xi(t,j)) \leqslant e^{\omega_2(t-\zeta_m)} U(\xi(\zeta_k,j)) + \theta^2 \int\limits_{\zeta_k}^{t} e^{\omega_2(t-s)}|w(s)|^2 \mathrm{d}s. \tag{E.18}$$

In essence, the right-hand sides of (E.17) and (E.18) reflect bounds on the Lyapunov/storage function U over (hybrid) time for the stable and unstable modes, respectively. In order to asses the performance of a system $\mathcal{H}_\mathcal{T} \in \mathcal{H}(\nu,\tau_D,\varsigma,T)$, we require an upper-bound that holds for all $(t,j) \in \operatorname{dom}\xi$. For this reason, consider the following statement.

Lemma E.2. *For all $(t,j) \in$ dom ξ, it holds that*

$$U(\xi(t,j)) \leqslant \Upsilon(0,t) U(\xi(0,0)) + \theta^2 \int_0^t \Upsilon(s,t)|w(s)|^2 ds \tag{E.19}$$

with $\Upsilon(s,t) := e^{-\omega_1|\bar{\Theta}_\xi(s,t)|}e^{\omega_2|\overline{\Xi}_\xi(s,t)|}$.

Proof of Lemma E.2: We will prove Lemma E.2 by induction. First, we need to prove that (E.19) holds for all $(t,j) \in [0,\zeta_0) \times \mathbb{N} \cap \operatorname{dom} \xi$. To do so, observe that for all $(t,j) \in W_{-1} \times \mathbb{N} \cap \operatorname{dom} \xi$ it holds that $|\bar{\Theta}_\xi(0,t)| = t$ and $|\overline{\Xi}_\xi(0,t)| = 0$. By substituting the latter in (E.19), we can conclude that for all $(t,j) \in W_{-1} \times \mathbb{N} \cap \operatorname{dom} \xi$, the inequality given in (E.19) coincides with (E.17). As such, (E.19) holds for all $(t,j) \in W_{-1} \times \mathbb{N} \cap \operatorname{dom} \xi$ and thus for all $(t,j) \in [0,\zeta_0) \times \mathbb{N} \cap \operatorname{dom} \xi$. Now assume (E.19) holds for all $(t,j) \in [0,\zeta_p) \times \mathbb{N} \cap \operatorname{dom} \xi$, where $p \in \mathbb{N}$. By means of this hypothesis and the inequality in (E.18), we find that for all $(t,j) \in (Z_p \times \mathbb{N}) \cap \operatorname{dom} \xi$,

$$U(\xi(t,j)) \leqslant e^{\omega_2(t-\zeta_p)}\Upsilon(0,\zeta_p)U(\xi(0,0)) + \theta^2 e^{\omega_2(t-\zeta_p)} \int_0^{\zeta_p} \Upsilon(s,\zeta_p)|w(s)|^2 \mathrm{d}s + \theta^2 \int_{\zeta_p}^{t} e^{\omega_2(t-s)}|w(s)|^2 \mathrm{d}s. \quad \text{(E.20)}$$

Since for all $t \in Z_p$ and all $s \in [0,t]$, $|\bar{\Theta}_\xi(s,\zeta_p)| = |\bar{\Theta}_\xi(s,t)|$ and $t - \zeta_p + |\overline{\Xi}_\xi(s,\zeta_p)| = |\overline{\Xi}_\xi(s,t)|$, we have that $e^{\omega_2(t-\zeta_p)}\Upsilon(s,\zeta_p) = \Upsilon(s,t)$ for all $t \in Z_p$ and all $s \in [0,t]$. Substitution of the latter in (E.20) yields that for all $(t,j) \in (Z_p \times \mathbb{N}) \cap \operatorname{dom} \xi$,

$$U(\xi(t,j)) \leqslant \Upsilon(0,t)U(\xi(0,0)) + \theta^2 \int_0^{\zeta_p} \Upsilon(s,t)|w(s)|^2 \mathrm{d}s + \theta^2 \int_{\zeta_p}^{t} e^{\omega_2(t-s)}|w(s)|^2 \mathrm{d}s. \quad \text{(E.21)}$$

Note that for all $t \in Z_p$ and $s \in [\zeta_p, t]$, $t - s = |\overline{\Xi}_\xi(s,t)|$ and in accordance with (E.13), $|\bar{\Theta}_\xi(s,t)| = 0$ and thus $e^{\omega_2(t-s)} = \Upsilon(s,t)$ for all $t \in Z_p$ and $s \in [\zeta_p, t]$. By combining the latter with (E.21), we can see that (E.19) holds for all $(t,j) \in ([0,\zeta_p + v_p) \times \mathbb{N}) \cap \operatorname{dom} \xi$, $p \in \mathbb{N}$.

Now we consider the interval W_p. Using (E.17), we have that for all $(t,j) \in (W_p \times \mathbb{N}) \cap \operatorname{dom} \xi$,

$$U(\xi(t,j)) \leqslant e^{-\omega_1(t-\zeta_p-v_p)}\Upsilon(0,\zeta_p+v_p)U(\xi(0,0)) + \theta^2 e^{-\omega_1(t-\zeta_p-v_p)} \int_0^{\zeta_p+v_p} \Upsilon(s,\zeta_p+v_p)|w(s)|^2 \mathrm{d}s + \theta^2 \int_{\zeta_p+v_p}^{t} e^{-\omega_1(t-s)}|w(s)|^2 \mathrm{d}s. \quad \text{(E.22)}$$

Since $t-\zeta_p-v_p+|\bar{\Theta}_\xi(s,\zeta_p+v_p)|=|\bar{\Theta}_\xi(s,t)|$ and $|\overline{\Xi}_\xi(s,\zeta_p+v_p)|=|\overline{\Xi}_\xi(s,t)|$ for all $t\in W_p$ and all $s\in[0,t]$, we obtain

$$e^{-\omega_1(t-\zeta_p)}\Upsilon(s,\zeta_p)=\Upsilon(s,t) \tag{E.23}$$

for all $t\in W_p$ and all $s\in[0,t]$. Substitution of (E.23) in (E.22) yields that for all $(t,j)\in(W_p\times\mathbb{N})\cap\operatorname{dom}\xi$,

$$U(\xi(t,j))\leqslant\Upsilon(0,t)U(\xi(0,0))+\theta^p\int_0^{\zeta_p}\Upsilon(s,t)|w(s)|^2\mathrm{d}s + \theta^p\int_{\zeta_p}^{t}e^{-\omega_1(t-s)}|w(s)|^2\mathrm{d}s. \tag{E.24}$$

Combining (E.23) with the fact that for all $t\in W_p$ and $s\in[\zeta_p+v_p,t]$, $t-s=|\bar{\Theta}_\xi(s,t)|$ and in accordance with (E.12), $|\overline{\Xi}_\xi(s,t)|=0$, we can see that $e^{-\omega_1(t-s)}=\Upsilon(s,t)$ for all $t\in W_p$ and $s\in[\zeta_p+v_p,t]$. By means of the latter, we can conclude that (E.19) coincides with (E.24) and thus (E.19) holds for all $(t,j)\in([0,\zeta_{p+1})\times\mathbb{N})\cap\operatorname{dom}\xi$, which concludes the proof of Lemma E.2. □

Step IV. *Stability and performance analysis.* In the last step of the proof, we show that under (ν,τ_D,ς,T)-DoS sequences with τ_D and T satisfying (6.31), the system $\mathcal{H}_\mathcal{T}$ is UGES, and has a finite *induced* $\mathcal{L}_\infty$*-gain*. By means of (E.16) and the fact that $|\bar{\Theta}_\xi(T_1,T_2)|=T_2-T_1-|\overline{\Xi}_\xi(T_1,T_2)|$, we obtain that

$$\Upsilon(T_1,T_2)\leqslant\kappa e^{-\beta_*(T_2-T_1)}, \tag{E.25}$$

for all $T_2\in\mathbb{R}_{\geqslant0}$ and all $T_1\in\big[\big(\bigcup_{k\in\mathbb{N}}W_{k-1}\big)\cup\{0\}\big]\cap[0,T_2]$, where $\kappa:=e^{\varsigma_*(\omega_1+\omega_2)}$ and where $\beta_*:=\omega_1-(\omega_1+\omega_2)/T_*$. Important to note is that condition (6.31) assures that $\beta_*>0$.

The inequality given in (E.25) does not only hold for $T_1\in\big[\big(\bigcup_{k\in\mathbb{N}}W_{k-1}\big)\cup\{0\}\big]\cap[0,T_2]$. In fact, the inequality holds for all $T_1,T_2\in\mathbb{R}_{\geqslant0}$ with $T_1\leqslant T_2$ due to the following. Let $0\leqslant T_1\leqslant T_2$ be arbitrary and consider

$$T_1^*=\sup\left\{\tilde{T}\leqslant T_1\mid\tilde{T}\in\left(\bigcup_{k\in\mathbb{N}}W_k\right)\cup\{0\}\right\}.$$

Since $|\Theta(T_1^*,T_1)|=0$, we can write $\Upsilon(T_1^*,T_2)=\Upsilon(T_1,T_2)e^{\omega_2(T_1-T_1^*)}$ for all $T_1,T_2\in\mathbb{R}_{\geqslant0}$ with $T_1\leqslant T_2$. Hence, we have that $\Upsilon(T_1,T_2)\leqslant\Upsilon(T_1^*,T_2)$. Due to (E.25) and the facts that $\beta^*>0$ and $T_1^*\in\overline{\big[\big(\bigcup_{k\in\mathbb{N}}W_k\big)\cup\{0\}\big]\cap[0,T_2]}$, we have that $\Upsilon(T_1^*,T_2)\leqslant\kappa e^{-\beta_*(T_2-T_1^*)}\leqslant\kappa e^{-\beta_*(T_2-T_1)}$. for all $T_1,T_2\in\mathbb{R}_{\geqslant0}$ with $T_1\leqslant T_2$. Hence, (E.25) holds for all $T_1,T_2\in\mathbb{R}_{\geqslant0}$ with $T_1\leqslant T_2$.

1) Stability analysis for the case $w=0$. By combining (E.25) and (E.19) for the case $w=0$, we find that for all $(t,j)\in\operatorname{dom}\xi$

$$U(\xi(t,j))\leqslant\kappa e^{-\beta_*t}U(\xi(0,0)).$$

Using (6.23), (6.25), (E.2) and the fact that $\eta(0,0)=0$, we obtain

$$|\xi(t,j)|_{\mathcal{A}} \leqslant \sqrt{\frac{\kappa \max\left(\bar{c}_V, \tilde{c}_W\right)}{\underline{c}_U}} e^{-(\beta_*/2)t} |\xi(0,0)|_{\mathcal{A}},$$

where $\tilde{c}_W := \gamma \phi_{miet} \bar{c}_W^2$. Given the fact that due to (6.31) $\beta_* > 0$, we can conclude that $\mathcal{H}_{\mathcal{T}}$ is UGES under $(\nu, \tau_D, \varsigma, T)$-DoS sequences.

2) Performance analysis for the case $w \neq 0$ in terms of induced $\mathcal{L}_\infty$-gain. Substitution of (E.25) in (E.19) yields

$$U(\xi(t,j)) \leqslant \kappa U(\xi(0,0)) + \kappa\theta^2 \int_0^t e^{-\beta_*(t-s)} \mathrm{d}s \|w\|_{\mathcal{L}_\infty}^2.$$

The facts that $U(\xi(t,j)) \geqslant V(x(t,j)) \geqslant c_z |z(t,j)|^2$ and $U(\xi(0,0)) \leqslant \max\left(\bar{c}_V, \tilde{c}_W\right) |\xi(0,0)|_{\mathcal{A}}^2$, we now obtain that for all $(t,j) \in \operatorname{dom} \xi$

$$\|z\|_{\mathcal{L}_\infty} \leqslant \sqrt{\frac{\kappa}{c_z} \max\left(\bar{c}_V, \tilde{c}_W\right)} |\xi(0,0)|_{\mathcal{A}} + \theta \sqrt{\frac{\kappa}{c_z \beta^*}} \|w\|_{\mathcal{L}_\infty}.$$

Hence, (6.22) is satisfied with $\beta(r) = \sqrt{\frac{\kappa}{c_z} \max\left(\bar{c}_V, \tilde{c}_W\right)} r$ and $\vartheta = \theta \sqrt{\frac{\kappa}{c_z \beta^*}}$ for $p = \infty$ which completes the proof. □

Appendix F

Proofs of Chapter 7

Proof of Theorem 1 To verify the passivity properties of the MAS with respect to the supply rate $\tilde{s}(\xi, w)$, we aim to construct a storage function that satisfies (7.26).

For clarity of exposition, the construction of the storage function is composed of five steps. At first, we present a candidate storage function. In the second, third and fourth step, we study the individual terms of this candidate storage function. At last, we show that the overall candidate storage function indeed satisfies (7.26).

Step I. *Candidate storage function.* Consider the candidate storage function

$$U(\xi) \;=\; V(x) \;+\; \sum_{i\in\mathcal{V}} \eta_i \;+\; \sum_{i\in\mathcal{V}} \tilde{\gamma}_i(\tilde{l}_i(l_i))\tilde{\phi}_{\tilde{l}_i(l_i),i}(\tau_i)\tilde{W}_i^2(\kappa_i, l_i, y_i, \bar{e}_i, r_i) \quad \text{(F.1)}$$

with $l_i := (l_i^1, l_i^2, \dots l_i^N)$ and the function $\tilde{l}_i : \{0,1\}^N \to \{0,1\}$ as in (7.39), and where the function $V : \mathbb{R}^{n_x} \to \mathbb{R}_{\geqslant 0}$ satisfies (7.37), the function $\tilde{\phi}_{\ell,i} : \mathbb{R}_{\geqslant 0} \to \mathbb{R}_{\geqslant 0}$, $\ell \in \{0,1\}$, is given by

$$\tilde{\phi}_{\ell,i}(\tau_i) := \begin{cases} \phi_{\ell,i}(\tau) & \text{when } \tau_i \leqslant \tau_{miet}^i \\ \phi_{\ell,i}(\tau_{miet}^i) & \text{when } \tau_i > \tau_{miet}^i \end{cases} \quad \text{(F.2)}$$

with the function $\phi_{\ell,i}$ as in (7.42), and the function $\tilde{W}_i : \mathbb{N} \times \{0,1\}^N \times \mathbb{R}^{Nn_y} \times \mathbb{R}^{Nn_y} \times \mathbb{R}^{n_y} \to \mathbb{R}_{\geqslant 0}$ is given by

$$\tilde{W}_i(\kappa_i, l_i, y_i, \bar{e}_i, r_i) := \max\Big\{ W_i(\kappa_i, \bar{e}_i + \bar{s}_i(l_i, y_i, \bar{e}_i, r_i)),$$

$$\zeta_i \max_{\mathcal{S}\subset\mathcal{S}_i(l_i)} \left\{ W_i \left(\kappa_i, \bar{e}_i + \sum_{l\in\mathcal{S}} Y_l \bar{s}_i(l_i, y_i, \bar{e}_i, r_i) \right) \right\} \Big\}, \quad \text{(F.3)}$$

where $Y_l := (\Gamma_l \otimes I_{n_y})$, $\mathcal{S}_i(l_i) := \{j \in \mathcal{V}_i^{\text{out}} \mid l_i^j = 1\}$, which is the set of agents that are about to receive a transmitted measurement by agent $\mathcal{A}_i$, ζ_i is as below (7.44), and where

$$\bar{s}_i(l_i, y_i, \bar{e}_i, r_i) = \sum_{l\in\mathcal{S}_i(l_i)} Y_l(-\mathbf{1}_N \otimes y_i - \bar{e}_i + \mathbf{1}_N \otimes r_i) \quad \text{(F.4)}$$

with the variables $\tilde{\gamma}_{\ell,i} \in \mathbb{R}_{\geqslant 0}$, $\ell \in \{0, 1\}$, as in (7.44).

Before analyzing the jump and the flow behavior of U, we first present several properties of $\tilde{W}_i$.

Step II. *Properties of* $\tilde{W}_i$. Consider the following lemma.

Lemma F.1. *Consider the function* $\tilde{W}_i$ *as in (F.3) with* W_i *satisfying Condition 7.1 and 7.2. For each* $i \in \mathcal{V}$, $j \in \mathcal{V}_i^{out}$ *and for all* $\kappa_i \in \mathbb{N}$, $\bar{e}_i \in \mathbb{R}^{Nn_y}$, $r_i \in \mathbb{R}^{n_y}$ *and* $0 < \lambda_i < 1$, *the function* $\tilde{W}_i$ *satisfies*

$$\tilde{W}_i(\kappa_i, l_i - \Gamma_j \mathbf{1}_N, y_i, \bar{e}_i + Y_j \bar{s}_i(l_i, y_i, \bar{e}_i, r_i), r_i) \leqslant \tilde{W}_i(\kappa_i, l_i, y_i, \bar{e}_i, r_i), \quad \text{(F.5)}$$

$$\tilde{W}_i(\kappa_i + 1, Z_i(\kappa_i, \bar{e}_i)\mathbf{1}_N, y_i, \bar{e}_i, \kappa_i, \bar{e}_i, y_i) \leqslant \lambda_i \tilde{W}_i(\kappa_i, \mathbf{0}_N, y_i, \bar{e}_i, r_i), \quad \text{(F.6)}$$

$$\tilde{W}_i(\kappa_i, \mathbf{0}_N, y_i, \bar{e}_i + Y_j \bar{s}_i(\Gamma_j \mathbf{1}_N, y_i, \bar{e}_i, r_i), r_i) \leqslant \tilde{W}_i(\kappa_i, \Gamma_j \mathbf{1}_N, y_i, \bar{e}_i, r_i), \quad \text{(F.7)}$$

where $Y_j := (\Gamma_j \otimes I_{n_y})$ *and* $\bar{Y}_j := (I_{Nn_y} - \Gamma_j \otimes I_{n_y})$.

Proof of Lemma F.1: Observe that (F.5) with $\tilde{W}$ as in (F.3), is equivalent to

$$\begin{aligned}
\max \Bigg\{ & W_i(\kappa_i, \bar{e}_i + Y_j \bar{s}_i(l_i, y_i, \bar{e}_i, r_i) + \bar{s}_i(l_i - \Gamma_j \mathbf{1}_N, y_i, \bar{e}_i, r_i)), \\
& \zeta_i \Big[\max_{\mathcal{S}\subset\mathcal{S}_i(l_i - \Gamma_j \mathbf{1}_N)} \Big\{ W_i \Big(\kappa_i, \bar{e}_i + Y_j \bar{s}_i(l_i, y_i, \bar{e}_i, r_i) \\
& + \sum_{l\in\mathcal{S}} Y_l \bar{s}_i(l_i - \Gamma_j \mathbf{1}_N, y_i, \bar{e}_i + Y_j(\bar{s}_i(l_i, y_i, \bar{e}_i, r_i)), r_i) \Big) \Big\} \Big] \Bigg\} \\
& \leqslant \max \big\{ W_i(\kappa_i, \bar{e}_i + \bar{s}_i(l_i, y_i, \bar{e}_i, r_i)), \\
& \quad \zeta_i \max_{\mathcal{S}\subset\mathcal{S}_i(l_i)} \{ W_i(\kappa_i, \bar{e}_i + \sum_{l\in\mathcal{S}} Y_l \bar{s}_i(l_i, y_i, \bar{e}_i, r_i)) \} \big\} \quad \text{(F.8)}
\end{aligned}$$

for each $i \in \mathcal{V}$, $j \in \mathcal{V}_i^{\text{out}}$. By means of (F.4), we find that

$$W_i(\kappa_i, \bar{e}_i + Y_j \bar{s}_i(l_i, y_i, \bar{e}_i, r_i) + \bar{s}_i(l_i - \Gamma_j \mathbf{1}_N, y_i, \bar{e}_i, r_i))$$

$$= W_i(\kappa_i, \bar{e}_i + \bar{s}_i(l_i, y_i, \bar{e}_i, r_i)) \quad \text{(F.9)}$$

Moreover, given the fact that $Y_l Y_j = 0$ for $l \neq j$, we have that

$$\begin{aligned}
&\max_{\mathcal{S}\subset\mathcal{S}_i(l_i-\Gamma_j\mathbf{1}_N)} \Big\{ W_i\Big(\kappa_i, \bar{e}_i + Y_j\bar{s}_i(l_i, y_i, \bar{e}_i, r_i) \\
&\qquad + \sum_{l\in\mathcal{S}} Y_l\bar{s}_i(l_i - \Gamma_j\mathbf{1}_N, y_i, \bar{e}_i + Y_j\bar{s}_i(l_i, y_i, \bar{e}_i, r_i), r_i)\Big)\Big\} \\
&\quad = \max_{\mathcal{S}\subset\mathcal{S}_i(l_i-\Gamma_j\mathbf{1}_N)} \Big\{ W_i\Big(\kappa_i, \bar{e}_i + \sum_{l\in\mathcal{S}\cup\{j\}} Y_l\bar{s}_i(l_i, y_i, \bar{e}_i, r_i)\Big)\Big\} \\
&\qquad \leqslant \max_{\mathcal{S}\subset\mathcal{S}_i(l_i)} \Big\{ W_i\Big(\kappa_i, \bar{e}_i + \sum_{l\in\mathcal{S}} Y_l\bar{s}_i(l_i, y_i, \bar{e}_i, r_i)\Big)\Big\} \quad \text{(F.10)}
\end{aligned}$$

By combining (F.8) with (F.9) and (F.10), we can conclude that (F.5) indeed holds.

The condition given in (F.6) is equivalent to

$$\begin{aligned}
&\max\Bigg\{ W_i\Big(\kappa_i + 1, \bar{e}_i + \bar{s}_i(Z_i(\kappa_i, \bar{e}_i)\mathbf{1}_N, y_i, \bar{e}_i, y_i)\Big), \\
&\quad \zeta_i \max_{\mathcal{S}\subset\mathcal{S}_i(Z_i(\kappa_i,\bar{e}_i)\mathbf{1}_N)} \Big\{ W_i(\kappa_i + 1, \bar{e}_i + \sum_{l\in\mathcal{S}} Y_l\bar{s}_i(Z_i(\kappa_i, \bar{e}_i)\mathbf{1}_N, y_i, \bar{e}_i, y_i)\Big)\Big\}\Bigg\} \\
&\qquad \leqslant \lambda_i \max\{W_i(\kappa_i, \bar{e}_i)\} \quad \text{(F.11)}
\end{aligned}$$

for each $i \in \mathcal{V}$. By using the fact that, according to (F.4),

$$\bar{s}_i(Z_i(\kappa_i, \bar{e}_i)\mathbf{1}_N, y_i, \bar{e}_i, y_i) = -Z_i(\kappa_i, \bar{e}_i)\bar{e}_i,$$

we find that (F.11) is equivalent to

$$\begin{aligned}
&\max\Bigg\{ W_i\Big(\kappa_i + 1, h_i(\kappa_i, \bar{e}_i)\Big), \zeta_i \max_{\mathcal{S}\subset\mathcal{S}_i(Z_i(\kappa_i,\bar{e}_i)\mathbf{1}_N)} \Big\{ W_i(\kappa_i + 1, \bar{e}_i - \sum_{l\in\mathcal{S}} Y_l\bar{e}_i\Big\}\Bigg\} \\
&\qquad \leqslant \lambda_i W_i(\kappa_i, \bar{e}_i). \quad \text{(F.12)}
\end{aligned}$$

By combining the fact that

$$\begin{aligned}
&\zeta_i \max_{\mathcal{S}\subset\mathcal{S}_i(Z_i(\kappa_i,\bar{e}_i)\mathbf{1}_N)} \Big\{ W_i(\kappa_i + 1, \bar{e}_i - \sum_{l\in\mathcal{S}} Y_l\bar{e}_i\Big)\Big\} \\
&\qquad \overset{(7.30a),(7.33)}{\leqslant} \frac{\lambda_i}{\overline{\alpha}_{W,i}} \max_{\mathcal{S}\subset\mathcal{S}_i(Z_i(\kappa_i,\bar{e}_i)\mathbf{1}_N)} |\bar{e}_i - \sum_{l\in\mathcal{S}} Y_l\bar{e}_i| \leqslant \lambda_i W_i(\kappa_i, \bar{e}_i) \quad \text{(F.13)}
\end{aligned}$$

with (7.30b), we can conclude that (F.12) holds and therefore also (F.6).

The inequality given in (F.7) is equivalent to

$$W_i(\kappa_i, \bar{e}_i + Y_j \bar{s}_i(\Gamma_j \mathbf{1}_N, y_i, \bar{e}_i, r_i)) \leqslant \max \Bigg\{ W_i\left(\kappa_i, y_i, \bar{e}_i + \bar{s}_i(\Gamma_j \mathbf{1}_N, y_i, \bar{e}_i, r_i)\right), \\ \zeta_i \max_{\mathcal{S} \subset \mathcal{S}_i(\Gamma_j \mathbf{1}_N)} \left\{ W_i\left(\kappa_i, \bar{e}_i + \sum_{l \in \mathcal{S}} Y_l \bar{s}_i(l_i, y_i, \bar{e}_i, r_i)\right) \right\} \Bigg\} \quad \text{(F.14)}$$

for each $j \in \mathcal{V}_i^{\text{out}}$ and each $i \in \mathcal{V}$. Observe from (F.4) that $Y_j \bar{s}_i(\Gamma_j \mathbf{1}_N, y_i, \bar{e}_i, r_i) = \bar{s}_i(\Gamma_j \mathbf{1}_N, y_i, \bar{e}_i, r_i)$. Hence, we can see from (F.14) that (F.7) indeed holds, which completes the proof of Lemma F.1. □

Consider the following lemma.

Lemma F.2. *Consider the function $\tilde{W}_i$ as in (F.3) with W_i satisfying Condition 7.1 and 7.2 and the function H_i as in (7.38). Then for all $\kappa_i \in \mathbb{N}$, $l_i \in \{0,1\}^N$, $r_i \in \mathbb{R}^{n_y}$, $x \in \mathbb{R}^{n_x}$, $e^i \in \mathbb{R}^{N n_y}$, $w \in \mathbb{R}^{n_w}$ and almost all $\bar{e}_i \in \mathbb{R}^{N n_y}$, it holds that*

$$\left\langle \frac{\partial \tilde{W}_i\left(\kappa_i, l_i, y_i, \bar{e}_i, r_i\right)}{\partial(\bar{e}_i, y_i)}, \left(\bar{g}_i(x,e,w), \bar{f}_{y,i}(x, e^i, w)\right) \right\rangle \\ \leqslant \sqrt{N_i} H_i(x, e^i, w, l_i) + \tilde{L}_i(\tilde{l}_i(l_i)) \tilde{W}_i\left(\kappa_i, l_i, y_i, \bar{e}_i, r_i\right), \quad \text{(F.15)}$$

where $\bar{g}_i(x,e,w) := (\delta_i(1) g_i^1(x,e,w), \delta_i(2) g_i^2(x,e,w), \ldots, \delta_i(N) g_i^N(x,e,w))$ and where $\bar{f}_{y,i}(x,e,w) := (\delta_i(1) f_{y,i}^1(x,e^i,w), \delta_i(2) f_{y,i}^2(x,e^i,w), \ldots, \delta_i(N) f_{y,i}^N(x,e^i,w))$ with $\delta_i(j)$, $g_i^j(x,e,w)$ and $f_i^j(x,e^i,w)$, $i \in \mathcal{V}$, $j \in \mathcal{V}_i^{out}$ as in (7.5), (7.19) and (7.20), respectively.

Proof of Lemma F.2: To prove Lemma F.2, we need to consider two cases that are based on (F.15).

Case 1: $\tilde{W}_i\left(\kappa_i, l_i, y_i, \bar{e}_i, r_i\right) = W_i\left(\kappa_i, \bar{e}_i + \bar{s}_i(l_i, y_i, \bar{e}_i, r_i)\right)$. For this case, we have that

$$\left\langle \frac{\partial \tilde{W}_i\left(\kappa_i, l_i, y_i, \bar{e}_i, r_i\right)}{\partial(\bar{e}_i, y_i)}, \left(\bar{g}_i, \bar{f}_{y,i}\right) \right\rangle \\ = \left\langle \frac{\partial W_i\left(\kappa_i, \bar{e}_i + \bar{s}_i(l_i, y_i, \bar{e}_i, r_i)\right)}{\partial(\bar{e}_i, y_i)}, \left(\bar{g}_i, \bar{f}_{y,i}\right) \right\rangle \\ \overset{(7.34)-(7.36)}{\leqslant} \sqrt{(N_i - |\mathcal{S}_i(l_i)|) c_i^2 \bar{g}_i^2(x,e,w) + |\mathcal{S}_i(l_i)| c_i^2 \bar{f}_{y,i}^2(x,e^i,w)} \\ \overset{(7.35),(7.36)}{\leqslant} \sqrt{N_i} \max\{H_{e,i}(x,e^i,w), \tilde{l}_i(l_i) H_{y,i}(x,e^i,w)\} + \max\{L_{1,i}, \sqrt{N_i} L_{2,i}\} |\bar{e}_i| \\ \overset{(7.38),(7.44)}{\leqslant} \sqrt{N_i} H_i(x,e^i,w,l_i) + \tilde{L}_i(\tilde{l}_i(l_i)) W_i(\kappa_i, \bar{e}_i)$$

$$\overset{(F.3)}{\leqslant} \sqrt{N_i} H_i(x, e^i, w, l_i) + \tilde{L}_i(\tilde{l}_i(l_i)) \tilde{W}_i\left(\kappa_i, l_i, y_i, \bar{e}_i, r_i\right). \quad \text{(F.16)}$$

Case 2: $\tilde{W}_i\left(\kappa_i, l_i, y_i, \bar{e}_i, r_i\right) = \zeta_i \max_{\mathcal{S} \subset \mathcal{S}_i(l_i)} \left\{ W_i\left(\kappa_i, \bar{e}_i + \sum_{l \in \mathcal{S}} Y_l \bar{s}_i(l_i, y_i, \bar{e}_i, r_i)\right)\right\}$ (and thus $\tilde{l}_i(l_i) = 1$). For this case, we have that

$$\begin{aligned}
&\left\langle \frac{\partial \tilde{W}_i\left(\kappa_i, l_i, y_i, \bar{e}_i, r_i\right)}{\partial(\bar{e}_i, y_i)}, \left(\bar{g}_i, \bar{f}_{y,i}\right)\right\rangle \\
&\qquad = \zeta_i \left\langle \frac{\partial W_i\left(\kappa_i, \bar{e}_i + \sum_{l \in \mathcal{S}^*} Y_l \bar{s}_i(l_i, y_i, \bar{e}_i, r_i)\right)}{\partial(\bar{e}_i, y_i)}, \left(\bar{g}_i, \bar{f}_{y,i}\right)\right\rangle \\
&\qquad \overset{(7.34)}{\leqslant} \zeta_i \sqrt{(N_i - |\mathcal{S}^*|) c_i^2 \bar{g}_i^2(x, e, w) + |\mathcal{S}^*| c_i^2 \bar{f}_{y,i}^2(x, e^i, w)} \\
&\overset{(7.35),(7.36)}{\leqslant} \zeta_i \sqrt{N_i} \max\{H_{e,i}(x, e^i, w), H_{y,i}(x, e^i, w)\} + \zeta_i \max\{L_{1,i}, \sqrt{N_i} L_{2,i}\} |\bar{e}_i| \\
&\qquad \overset{(7.38),(7.44)}{\leqslant} \sqrt{N_i} H_i(x, e^i, w, l_i) + \tilde{L}_i(1) W_i(\kappa_i, \bar{e}_i) \\
&\qquad \overset{(F.3)}{\leqslant} \sqrt{N_i} H_i(x, e^i, w, l_i) + \tilde{L}_i(1) \tilde{W}_i\left(\kappa_i, l_i, y_i, \bar{e}_i, r_i\right), \quad \text{(F.17)}
\end{aligned}$$

where

$$\mathcal{S}^* := \arg \max_{\mathcal{S} \subset \mathcal{S}_i(l_i)} \left\{ W_i\left(\kappa_i, \bar{e}_i + \sum_{l \in \mathcal{S}} Y_l \bar{s}_i(l_i, y_i, \bar{e}_i, r_i)\right)\right\}. \quad \text{(F.18)}$$

Based on (F.16) and (F.17), we can conclude that (F.15) is true, which completes the proof of Lemma F.2. □

Step III. *Properties of V.* Consider the following lemma.

Lemma F.3. *Consider the system $\mathcal{H}(\mathcal{C}, F, \mathcal{D}, G)$ with data $\mathcal{C}$, F, $\mathcal{D}$ and G as described in (7.17)-(7.25), the function V satisfying (7.37) and the function H_i as in (7.38). Then for all $e \in \mathbb{R}^{N^2 n_y}$, $r \in \mathbb{R}^{N n_y}$, $w \in \mathbb{R}^{n_w}$, $\kappa \in \mathbb{N}^N$, $l \in \{0,1\}^{N^2}$ and all $x \in \mathbb{R}^{n_x}$, it holds that*

$$\begin{aligned}
\langle \nabla V(x), f(x, e, w) \rangle \leqslant -s(x, e, w) + \sum_{i=1}^{N} \Big(&- \varrho_i(y_i, \hat{y}^i) \\
&- N_i H_i^2(x, e^i, w, l_i) + \tilde{\gamma}_i^2(\tilde{l}_i(l_i) \tilde{W}_i\left(\kappa_i, l_i, y_i, \bar{e}_i, r_i\right) \Big). \quad \text{(F.19)}
\end{aligned}$$

Proof of Lemma F.3: To prove Lemma F.3, we need to show that

$$\tilde{\gamma}_i^2(\tilde{l}_i(l_i)) \tilde{W}_i^2\left(\kappa_i, l_i, y_i, \bar{e}_i, r_i\right) \geqslant \gamma_{\tilde{l}_i(l_i), i}^2 W^2(\kappa_i, \bar{e}_i).$$

Recalling (7.44), we obtain for $\tilde{l}_i(l_i) = 0$ (and thus $l_i = \mathbf{0}_N$) that

$$\tilde{\gamma}_i^2(0)\tilde{W}_i^2\left(\kappa_i, \mathbf{0}_N, y_i, \bar{e}_i, r_i\right) = \gamma_{0,i}\tilde{W}_i^2\left(\kappa_i, \mathbf{0}_N, y_i, \bar{e}_i, r_i\right) \overset{(F.3)}{\geqslant} \gamma_{\tilde{l}_i(l_i),i}^2 W^2(\kappa_i, \bar{e}_i) \tag{F.20}$$

and for $\tilde{l}_i(l_i) = 1$, $l_i \in \{0,1\}^N$ that

$$\tilde{\gamma}_i^2(1)\tilde{W}_i^2\left(\kappa_i, l_i, y_i, \bar{e}_i, r_i\right) = \gamma_{1,i}^2\zeta_i^{-2}\tilde{W}_i^2\left(\kappa_i, l_i, y_i, \bar{e}_i, r_i\right) \overset{(F.3)}{\geqslant} \gamma_{\tilde{l}_i(l_i),i}^2 W^2(\kappa_i, \bar{e}_i) \tag{F.21}$$

for all $\bar{e}_i \in \mathbb{R}^{Nn_y}$, $r_i \in \mathbb{R}^{n_y}$ and all $\kappa_i \in \mathbb{N}$. □

Step IV. *Properties of η*

As described in (7.9), the dynamics of η are governed by the functions Ψ_i and η_i^0 which are given in (7.45) and (7.46), respectively. These functions are specified such that the following lemma holds.

Lemma F.4. *For all $y, \hat{y}^i, \bar{\tilde{y}}_i \in \mathbb{R}^{Nn_y}$, $e \in \mathbb{R}^{N^2n_y}$, $\kappa_i \in \mathbb{N}$, $l_i \in \{0,1\}$, $x \in \mathbb{R}^{n_x}$ and all $\tau_i \in \mathbb{R}_{\geqslant 0}$, $i \in \mathcal{V}$, it holds that*

$$\begin{aligned}\Psi_i(y_i, \hat{y}^i, \bar{\tilde{y}}_i, \bar{e}_i, \tau_i, \eta_i) \leqslant\ & \varrho_i(y_i, \hat{y}^i) \\ & - (1-\omega_i(\tau_i))\gamma_{\tilde{l}_i(l_i),i}\tilde{W}_i^2(\kappa_i, l_i, y_i, \bar{e}_i, r_i)\Big(2\tilde{L}_i(\tilde{l}_i(l_i))\tilde{\phi}_{\tilde{l}_i,i}(\tau_i) \\ & + (\gamma_{\tilde{l}_i(l_i),i}(\tilde{\phi}_{\tilde{l}_i(l_i),i}^2(\tau_i)+1))\Big).\end{aligned} \tag{F.22}$$

Moreover, for all $y, \hat{y}^i, \bar{\tilde{y}}_i \in \mathbb{R}^{Nn_y}$, $e \in \mathbb{R}^{N^2n_y}$, $\kappa_i \in \mathbb{N}$, $x \in \mathbb{R}^{n_x}$ and $\tau_i \geqslant \tau_{miet}^i$, $i \in \mathcal{V}$, it holds that

$$\begin{aligned}\eta_i^0(y_i, \hat{y}^i, \bar{\tilde{y}}_i, \bar{e}_i, \tau_i, \eta_i) \leqslant\ & \gamma_{0,i}\tilde{\phi}_{0,i}(\tau_i)\tilde{W}_i^2(\kappa_i, \mathbf{0}_N, y_i, \bar{e}_i, r_i) \\ & - \bar{\gamma}_i(1)\tilde{\phi}_{1,i}(0)\tilde{W}_i^2(\kappa_i+1, Z_i(\kappa_i, \bar{e}_i)\mathbf{1}_N, y_i, \bar{e}_i, g_{y,i}(x)).\end{aligned} \tag{F.23}$$

Proof of Lemma F.4: By combining the fact that $\max_{\tau\in[0,\tau_{mad}^i]} |\tilde{y}_i^j(t-\tau, j) - y_i(t,j)|^2 \geqslant |\bar{e}_i|^2 \overset{(7.30a),(F.3)}{\geqslant} \overline{\alpha}_{W,i}^{-1}\tilde{W}_i^2(\kappa_i, l_i, y_i, \bar{e}_i, r_i)$ with (7.45), we obtain that

$$\Psi_i(y_i, \hat{y}^i, \bar{e}_i, \tau_i, \eta_i) \leqslant \varrho_i(y_i, \hat{y}^i) - (1-\omega_i(\tau_i))\overline{\alpha}_{W,i}^{-1}\bar{\gamma}_i\tilde{W}_i^2(\kappa_i, l_i, y_i, \bar{e}_i, r_i). \tag{F.24}$$

Due to Assumption 7.1, we have that $l_i = \mathbf{0}_N$ when $\tau_i \geqslant \tau_{miet}^i$. By combining that latter fact with (7.47), (7.48) and (F.2), we obtain that for all $\tau_i \in \mathbb{R}_{\geqslant 0}$

$$\begin{aligned}(1-\omega_i(\tau_i))\bar{\gamma} = (1-\omega_i(\tau_i))\overline{\alpha}_{W,i}\tilde{\gamma}_i(\tilde{l}_i(l_i))\Big(2\tilde{L}_i(\tilde{l}_i(l_i))\tilde{\phi}_{\tilde{l}_i(l_i),i}(\tau_i) + \\ \tilde{\gamma}_i(\tilde{l}_i(l_i))(1+\tilde{\phi}_{\tilde{l}_i(l_i),i}^2(\tau_i))\Big).\end{aligned} \tag{F.25}$$

Consequently, (F.22) follows from (F.24) and (F.25). By combining the fact that $\min_{\tau\in[0,\tau^i_{mad}]} |\tilde{y}^j_i(t-\tau,j) - y_i(t,j)|^2 \leqslant |\bar{e}_i|^2 \overset{(7.30a),(F.3)}{\leqslant} \underline{\alpha}^{-1}\tilde{W}_i^2(\kappa_i, \mathbf{0}_N, y_i, \bar{e}_i, r_i)$ with (7.46) and (F.2), we obtain that

$$\eta_i^0(o_i) \quad \leqslant \quad \left(\tilde{\gamma}_i(0)\tilde{\phi}_{0,i}(\tau^i_{miet}) - \tilde{\gamma}_i(1)\tilde{\phi}_{1,i}(0)\lambda_i^2\right)\tilde{W}_i^2(\kappa_i, \mathbf{0}_N, y_i, \bar{e}_i, r_i). \quad \text{(F.26)}$$

By means of (F.6), we can conclude that (F.23) indeed holds, which completes the proof of Lemma F.4. □

Step V. *Validate conditions storage function*

In this step, we verify that the function U as given in (F.1) is indeed a valid storage function for the supply rate $s(x,e,w)$ as described in Definition 7.3.

Flow Dynamics of $U(\xi)$: By combining (7.9), (7.42), Lemma F.2 and Lemma F.3, we obtain that for almost all $(\xi, w) \in \mathbb{X} \times \mathbb{R}^{n_w}$

$$\begin{aligned}\langle \nabla U(\xi), F(\xi,w)\rangle \leqslant s(x,e,w) + \sum_{i=1}^{N}\Big[&-\varrho_i - N_i H_i^2 + \gamma^2_{\tilde{l}_i(l_i),i}\tilde{W}_i^2 \\ &+ 2\sqrt{N_i}\gamma_{\tilde{l}_i(l_i),i}\tilde{\phi}_{\tilde{l}_i(l_i),i}\tilde{W}_i(H_i + \tilde{L}_i(\tilde{l}_i(l_i))\tilde{W}_i) \\ &- \omega(\tau_i)\gamma_{\tilde{l}_i(l_i),i}\tilde{W}_i^2\left(2\tilde{L}_i(\tilde{l}_i(l_i))\tilde{\phi}_{\tilde{l}_i,i} + (\gamma_{\tilde{l}_i(l_i),i}\tilde{\phi}^2_{\tilde{l}_i(l_i),i} + 1)\right) + \Psi_i - \sigma_i(\eta_i)\Big],\end{aligned} \quad \text{(F.27)}$$

where we omitted the arguments of $\tilde{W}_i(\kappa_i, l_i, y_i, \bar{e}_i, r_i)$, $\varrho_i(y_i, \hat{y}^i)$, $\Psi(o_i)$ with $o_i = (y_i, \hat{y}^i, \bar{\tilde{y}}_i, \bar{e}_i, \tau_i, \eta_i)$. By using the fact that $2\gamma_{\tilde{l}_i,i}\tilde{\phi}_{\tilde{l}_i,i}\tilde{W}_i H_i \leqslant \gamma^2_{\tilde{l}_i,i}\tilde{\phi}^2_{\tilde{l}_i,i}\tilde{W}_i^2 + H_i^2$ and by substituting (7.45), we obtain

$$\langle \nabla U(\xi), F(\xi,w)\rangle \leqslant \tilde{s}(\xi,w). \quad \text{(F.28)}$$

Hence, U satisfies (7.26a).

Jump Dynamics of $U(\xi)$: For the jump dynamics, we need to consider the following three cases.

- Case 1: $\xi \in \mathcal{D}_{i,j} \wedge \sum_{j\in\mathcal{V}_i^{\text{out}}} l_i^j = 0$ for some $i \in \mathcal{V}$ and $j \in \mathcal{V}_i^{\text{out}}$

$$\begin{aligned}U(\xi^+) - U(\xi) = \tilde{\gamma}_i(1)\tilde{\phi}_{1,i}(0)\tilde{W}_i^2(\kappa_i + 1, Z_i(\kappa_i, \bar{e}_i)\mathbf{1}_N, y_i, \bar{e}_i, y_i) \\ - \gamma_{0,i}\tilde{\phi}_{0,i}(\tau_i)\tilde{W}_i^2(\kappa_i, \mathbf{0}_N, y_i, \bar{e}_i, r_i) + \eta_i^0(o_i).\end{aligned} \quad \text{(F.29)}$$

  By combining (7.40), (7.46) and (F.5), we obtain that $U(\xi^+) - U(\xi) \leqslant 0$ for all $\xi \in \bigcup_{j\in\mathcal{V}} \mathcal{D}_{i,j}$ with $\sum_{j\in\mathcal{V}_i^{\text{out}}} l_i^j = 0$, for some $i \in \mathcal{V}$.

- Case 2: $\xi \in \mathcal{D}_{i,j} \wedge \sum_{j\in\mathcal{V}_i^{\text{out}}} l_i^j > 1$ for some $i \in \mathcal{V}$ and $j \in \mathcal{V}_i^{\text{out}}$

$$U(\xi^+)-U(\xi)=\gamma_{1,i}\tilde{\phi}_{1,i}(\tau_i)\tilde{W}_i^2(\kappa_i,l_i-\Gamma_j\mathbf{1}_N,y_i,\bar{e}_i+Y_j\bar{s}_i(l_i,y_i,\bar{e}_i,r_i),r_i)\\ -\gamma_{1,i}\tilde{\phi}_{1,i}(\tau_i)\tilde{W}_i^2(\kappa_i,\mathbf{0}_N,y_i,\bar{e}_i,r_i). \quad \text{(F.30)}$$

Based on (F.5), we can conclude that $U(\xi^+)-U(\xi)\leqslant 0$ for all $\xi\in\bigcup_{j\in\mathcal{V}}\mathcal{D}_{i,j}$ with $\sum_{j\in\mathcal{V}_i^{\text{out}}}l_i^j>1$, for some $i\in\mathcal{V}$.

- Case 3: $\xi\in\mathcal{D}_{i,j}$ and $\sum_{j\in\mathcal{V}_i^{\text{out}}}l_i^j=1$ for some $i\in\mathcal{V}$ and $j\in\mathcal{V}_i^{\text{out}}$

$$U(\xi^+)-U(\xi)=\gamma_{0,i}\tilde{\phi}_{0,i}(0)\tilde{W}_i^2(\kappa_i,\mathbf{0}_N,y_i,\bar{e}_i+Y_j\bar{s}_i(\Gamma_j\mathbf{1}_N,y_i,\bar{e}_i,r_i),r_i)\\ -\gamma_{1,i}\tilde{\phi}_{1,i}(\tau_i)\tilde{W}_i^2(\kappa_i,\Gamma_j\mathbf{1}_N,y_i,\bar{e}_i,r_i). \quad \text{(F.31)}$$

Observe that according to (7.22), when $\xi\in\mathcal{D}_{i,j}$ and $\sum_{j\in\mathcal{V}_i^{\text{out}}}l_i^j=1$, $l_i^j=1$, $l_i=\Gamma_j\mathbf{1}_N$. Recalling (7.41) and (F.7), we obtain that $U(\xi^+)-U(\xi)\leqslant 0$ for all $\xi\in\bigcup_{j\in\mathcal{V}}\mathcal{D}_{i,j}$ with $\sum_{j\in\mathcal{V}_i^{\text{out}}}l_i^j=1$, $i\in\mathcal{V}$.

Based on these three cases, we can conclude that U satisfies (7.26b).

Persistently flowing property:

To verify the persistently flowing property, we first follow similar conditions as provided in [98, Proposition 6.10] to show that each maximal solution is complete. First of all, observe from (7.22) that $G(\mathcal{D})\subset\mathcal{C}\cup\mathcal{D}$ since for all $\xi\in G(\mathcal{D})$, it holds that $\tau_i^+\geqslant 0$, $\eta_i^+\geqslant 0$ since $\eta_i^0(o_i)\geqslant 0$ for all $o_i\in\mathbb{O}_i$. Next, we show that for any $\varphi\in\mathcal{C}\backslash\mathcal{D}$ there exists a neighborhood S of ξ such that, it holds for every $\varphi\in S\cap\mathcal{C}$ that $F(\varphi,w)\cap T_{\mathcal{C}}(\varphi)\neq\emptyset$, where $T_{\mathcal{C}}(\varphi)$ is the tangent cone[1] to $\mathcal{C}$ at φ. Observe that for each $\xi\in\mathcal{C}$ for which $l_i^j=0$ for all $i,j\in\mathcal{V}$ (recall that $\xi=(x,e,\tau,\kappa,r,\tilde{y},l,\eta)$), $T_{\mathcal{C}}(\xi)=\mathbb{R}^{n_x}\times\mathbb{R}^{N^2n_y}\times(T_{\mathbb{R}_{\geqslant 0}}(\tau_1)\times\ldots\times T_{\mathbb{R}_{\geqslant 0}}(\tau_N))\times\{0\}^N\times\{0\}^N\times\mathbb{R}^{N^2n_y}\times\{0\}^{N^2}\times(T_{\mathbb{R}_{\geqslant 0}}(\eta_1)\times\ldots\times T_{\mathbb{R}_{\geqslant 0}}(\eta_N))$. Observe also from (7.21) and (7.25) that $\mathcal{C}/\mathcal{D}=\bigcap_{i,j\in\mathcal{V}}\{\xi\in\mathbb{X}:l_i^j=0\text{ and }(\tau_i<\tau_{miet}^i\text{ or }\eta_i>0)\}$. Given the facts that, according to (7.12a) and (7.17), for all $i\in\mathcal{V}$, $\dot{\tau}_i=1$ and that $\dot{\eta}_i>0$ when $\tau_i<\tau_{miet}^i$ and $\eta_i=0$ due to (7.45), it indeed follows that for any $\xi\in\mathcal{C}\backslash\mathcal{D}$ there exists a neighborhood S of ξ such that, it holds for every $\varphi\in S\cap\mathcal{C}$ that $F(\varphi,w)\cap T_{\mathcal{C}}(\varphi)\neq\emptyset$.

Secondly, we show that the system $\mathcal{H}$ does not exhibit finite-escape times when $\tilde{s}(\xi,w)\leqslant c_V V(x)+c_W\sum_{i\in\mathcal{V}}|\bar{e}_i|^2+\sigma_w(|w|)$. Observe from (7.26a) and (7.26b) that in this case, we have that

1. for almost all $\xi\in\mathcal{C}$,

$$\langle\nabla U,F(\xi,w)\rangle\leqslant c_V V(x)+c_W\sum_{i\in\mathcal{V}}|\bar{e}_i|^2+\sigma_w(|w|) \quad \text{(F.32)}$$

[1] The tangent cone to a set $S\subset\mathbb{R}^n$ at a point $x\in\mathbb{R}^n$, denoted $T_S(x)$, is the set of all vectors $\omega\in\mathbb{R}^n$ for which there exist $x_i\in S,\tau_i>0$ with $x_i\to x,\tau\to 0$ as $i\to\infty$ such that $\omega=\lim_{i\to\infty}(x_i-x)/\tau_i$ (see Definition 5.12 in [99]).

2. for all $\xi \in \mathcal{D}$,

$$U(G(\xi)) - U(\xi) \leqslant 0. \tag{F.33}$$

Based on (7.30a), (F.1) and (F.32), we can conclude that the storage storage function grows at most exponentially when $w(t, j) = 0$ for all $(t, j) \in \operatorname{dom} \xi$. Given the fact that the function V as in Condition 7.3 and the function W as in Condition 7.1 and Condition 7.2 are proper, we can conclude from F.1 that the system $\mathcal{H}$ does not exhibit finite-escape times. Due to the latter fact, the fact that each maximal solution of $\mathcal{H}$ is complete and due to the time-regularization, the system $\mathcal{H}(\mathcal{C}, F, \mathcal{D}, G)$ with data F, G, $\mathcal{C}$ and $\mathcal{D}$ as described in (7.17)-(7.25), is indeed persistently flowing when $\tilde{s}(\xi, w) \leqslant c_V V(x) + c_W \sum_{i \in \mathcal{V}} |\bar{e}_i|^2 + \sigma_w(|w|)$, which completes the proof of Theorem 7.1. □

Appendix G

Proofs of Chapter 8

Proof of Theorem 8.1: To analyze the $\mathcal{L}_2$-gain property of the hybrid system $\mathcal{H}_i$, $i \in \bar{N} \setminus \{1\}$, we aim to find a positive semidefinite storage function S_i that satisfies

$$\dot{S}_i \leqslant (1+\epsilon)|\chi_{i-1}|^2 - |\chi_i|^2, \tag{G.1}$$

when $\xi_i \in \mathcal{C}_i$ and

$$S_i(\xi_i^+) - S_i(\xi_i) \leqslant 0, \tag{G.2}$$

when $\xi_i \in \mathcal{D}_i$, $i \in \bar{N} \setminus \{1\}$. We consider the following candidate storage function for the hybrid system $\mathcal{H}_i$

$$U_i(\xi_i) = V_i(\tilde{x}_i) + \eta_{i-1} + \gamma_{l_{i-1}} \tilde{\phi}_{l_{i-1}}(\tau_{i-1}) W_i^2(e_{u_{i-1}}, s_{i-1}, l_{i-1}), \tag{G.3}$$

where

$$V_i(\tilde{x}_i) = \tilde{x}_i^\top P \tilde{x}_i \tag{G.4}$$

with P as in (8.35) and where $\tilde{\phi}_{l_{i-1}}$ is given by

$$\tilde{\phi}_{l_{i-1}}(\tau) := \begin{cases} \phi_{l_{i-1}}(\tau) & \text{when } \tau \leqslant \tau_{miet} \\ \phi_0(\tau_{miet}) & \text{when } \tau > \tau_{miet} \end{cases} \tag{G.5}$$

for $l_{i-1} \in \{0,1\}$ and $\tau \in \mathbb{R}_{\geqslant 0}$ with $\phi_{l_{i-1}}$ satisfying (8.38). The function W_i is defined as

$$W_i(e_{u_{i-1}}, s_{i-1}, l_{i-1}) := \max\{\lambda^{l_{i-1}} |e_{u_{i-1}}|, |e_{u_{i-1}} + s_{i-1}|\}, \tag{G.6}$$

Observe that the functions V_i, W_i are semi-positive definite. Moreover, observe that $\tilde{\phi}_{l_{i-1}}(\tau) > 0$, $l_{i-1} \in \{0,1\}$, for all $\tau \in \mathbb{R}_{\geqslant 0}$ due to (8.36)-(8.38). Since, per definition of $\mathbb{X}_i$, $\eta_i(t,j) \geqslant 0$ for all $(t,j) \in \operatorname{dom} \xi_i$, the candidate storage

function U_i is positive semidefinite. Hence, indeed, the function U_i constitutes a valid candidate storage function.

Before we evaluate the behavior of U_i, we first consider the flow dynamics of the functions $\tilde{\phi}_{l_{i-1}}$, $l_{i-1} \in \{0,1\}$, W_i, V_i and η_i.

Consider the following lemma.

Lemma G.1. *For each solution ξ_i to $\mathcal{H}_i$, $i \in \bar{N} \setminus \{1\}$, with $\xi_i(0,0) \in \mathbb{X}_{0,i}$ and $\chi_{i-1} \in \mathcal{L}_2$, $\tau_{i-1}(t,j) \geqslant \tau_{miet}$, for some $(t,j) \in \operatorname{dom} \xi_i$ implies that $l_{i-1}(t,j) = 0$.*

Proof of Lemma G.1: Per definition of $\mathbb{X}_{0,i}$, $i \in \bar{N} \setminus \{1\}$, we have that $l_{i-1}(0,0) = 0$. Hence, $\tau_{i-1}(0,0) = \tau_{miet}$ implies that $l_{i-1}(0,0) = 0$. Observe from (8.25) that when $l_{i-1}(t,j) = 1$, for some $(t,j) \in \operatorname{dom} \xi_i$, the system is only allowed to flow if $\tau_{i-1}(t,j) \leqslant \tau_{mad}$. Given the latter and the fact that $\tau_{mad} \leqslant \tau_{miet}$, due to Assumption 8.2, it follows from (8.27) and (8.31) that $l_{i-1}(t,j) = 0$, $i \in \bar{N} \setminus \{1\}$, $(t,j) \in \operatorname{dom} \xi_i$, when $\tau_{i-1}(t,j) = \tau_{miet}$. □

Given Lemma G.1, we have that $\tilde{\phi}_{l_{i-1}}(\tau_{miet}) = \phi_0(\tau_{miet})$. By combining the latter fact with (8.38) and (G.5), we obtain that

$$\dot{\tilde{\phi}}_{l_{i-1}} = -(1-\omega(\tau_{i-1}))\gamma_{l_{i-1}}(\tilde{\phi}_{l_{i-1}}(\tau_{i-1})^2 + 1). \tag{G.7}$$

By recalling (8.30), we obtain from (G.6) that for $\xi_i \in \mathcal{C}_i$

$$\dot{W}_i \leqslant |\dot{e}_{u_{i-1}}| \leqslant \frac{1}{h}|\chi_{i-1} - u_{i-1}|. \tag{G.8}$$

From (8.27), we obtain that for $\xi_i \in \mathcal{C}_i$

$$\begin{aligned}
\dot{V}_i &= \tilde{x}_i^\top \left(A_{11}^\top P + P A_{11}\right) \tilde{x}_i + 2e_{u_{i-1}}^\top A_{12}\tilde{x}_i + 2\chi_{i-1}^\top A_{13}\tilde{x}_i \\
&\overset{(8.35)}{\leqslant} -\varrho u_{i-1}^2 - \frac{1}{h^2}(\chi_{i-1} - u_{i-1})^2 + \mu((1+\epsilon)|\chi_{i-1}|^2 - |\chi_i|^2) + \gamma^2|e_{u_{i-1}}|^2 \\
&\overset{(G.6)}{\leqslant} -\varrho u_{i-1}^2 - \frac{1}{h^2}(\chi_{i-1} - u_{i-1})^2 + \mu((1+\epsilon)|\chi_{i-1}|^2 - |\chi_i|^2) + \gamma_{l_{i-1}}^2 W_i^2,
\end{aligned} \tag{G.9}$$

where, for the sake of compactness, we omitted the arguments of W_i. By recalling Assumption 8.2 and using the fact that $\tau_{mad} \leqslant \tau_{miet}$, we can deduce from (G.6) that

$$\omega(\tau_{i-1})\gamma_{l_{i-1}}^2 \left(1 + \frac{1}{\varepsilon}\tilde{\phi}_{l_{i-1}}^2(\tau_{i-1})\right) W_i^2 = \omega(\tau_{i-1})\bar{\gamma}^2|e_{u_{i-1}}|^2. \tag{G.10}$$

By means of the latter, we can deduce from (8.15) and (8.39) that for $\xi_i \in \mathcal{C}_i$

$$\dot{\eta}_{i-1} = \varrho u_{i-1}^2 + \omega(\tau_{i-1})\Big(\frac{1-\varepsilon}{h^2}(\chi_{i-1} - u_{i-1})^2 - \gamma_{l_{i-1}}^2 \left(1 + \frac{1}{\varepsilon}\tilde{\phi}_{l_{i-1}}^2(\tau_{i-1})\right) W_i^2\Big). \tag{G.11}$$

By means of (G.7)-(G.11), we can now obtain that

$$\dot{U}_i \leqslant \dot{V}_i + 2\gamma_{l_{i-1}}\tilde{\phi}_{l_{i-1}} W_i \dot{W}_i - (1-\omega(\tau_{i-1}))\gamma_{l_{i-1}}\dot{\tilde{\phi}}_{l_{i-1}} W_i^2 + \dot{\eta}_{i-1}$$

$$\begin{aligned}
&\leqslant -\varrho u_{i-1}^2 - \frac{1}{h^2}(\chi_{i-1}-u_{i-1})^2 + \mu((1+\epsilon)|\chi_{i-1}|^2 - |\chi_i|^2) + \gamma_{l_{i-1}}^2 W_i^2 \\
&\quad + 2\gamma_{l_{i-1}}\tilde{\phi}_{l_{i-1}} W_i \frac{1}{h}|\chi_{i-1}-u_{i-1}| - (1-\omega(\tau_{i-1}))\gamma_{l_{i-1}}^2(\tilde{\phi}_{l_{i-1}}^2+1)W_i^2 \\
&\quad + \varrho u_{i-1}^2 + \omega(\tau_{i-1})\Big(\frac{1-\varepsilon}{h^2}(\chi_{i-1}-u_{i-1})^2 - \gamma_{l_{i-1}}^2\left(1+\frac{1}{\varepsilon}\tilde{\phi}_{l_{i-1}}^2\right)W_i^2\Big) \\
&\leqslant -\frac{1}{h^2}(\chi_{i-1}-u_{i-1})^2 + 2\gamma_{l_{i-1}}\tilde{\phi}_{l_{i-1}} W_i \frac{1}{h}|\chi_{i-1}-u_{i-1}| \\
&\quad - \gamma_{l_{i-1}}^2\tilde{\phi}_{l_{i-1}}^2 W_i^2 + \mu((1+\epsilon)|\chi_{i-1}|^2 - |\chi_i|^2) \\
&\quad + \omega(\tau_{i-1})\left(\frac{1-\varepsilon}{h^2}(\chi_{i-1}-u_{i-1})^2 + \gamma_{l_{i-1}}^2(1-\frac{1}{\varepsilon})\tilde{\phi}_{l_{i-1}}^2 W_i^2\right) \qquad \text{(G.12)}
\end{aligned}$$

for $\xi_i \in \mathcal{C}_i$. Now by using completion of the squares and the fact that for some constants $a, b \in \mathbb{R}$ and $\varepsilon > 0$, it holds that $2ab \leqslant (1/\varepsilon)\, a^2 + \varepsilon b^2$, we obtain that

$$\begin{aligned}
\dot{U}_i &\leqslant (\omega(\tau_{i-1})-1)(|\chi_{i-1}-u_{i-1}| - \gamma_{l_{i-1}}\tilde{\phi}_{l_{i-1}} W_i)^2 + \mu((1+\epsilon)|\chi_{i-1}|^2 - |\chi_i|^2) \\
&\leqslant \mu((1+\epsilon)|\chi_{i-1}|^2 - |\chi_i|^2). \qquad \text{(G.13)}
\end{aligned}$$

At transmissions events, *i.e.*, when $\xi_i \in \mathcal{D}_i$ with $l_{i-1} = 0$, $\tau_{i-1} \geqslant \tau_{miet}$ and the system jumps according to $\xi_i^+ = G(\xi_i)$, we have that

$$\begin{aligned}
U_i(\xi_i^+) - U_i(\xi_i) &= \gamma_1\tilde{\phi}_1(0) W_i^2(e_{u_{i-1}}, -e_{u_{i-1}}, 1) - \gamma_0\tilde{\phi}_0(\tau_{i-1}) W_i^2(e_{u_{i-1}}, s_{i-1}, 0) \\
&\overset{(8.38)}{\leqslant} (\gamma_1\phi_1(0)\lambda^2 - \gamma_0\phi_0(\tau_{miet}))|e_{u_{i-1}}|^2. \qquad \text{(G.14)}
\end{aligned}$$

At update events, *i.e.*, when $\xi_i \in \mathcal{D}_i$ with $l_{i-1} = 1$ (and thus $0 \leqslant \tau_{i-1} \leqslant \tau_{mad}$) and the system jumps according to $\xi_i^+ = G(\xi_i)$, we have that

$$\begin{aligned}
&U_i(\xi_i^+) - U_i(\xi_i) = \gamma_0\tilde{\phi}_0(\tau_{i-1}) W_i^2(s_{i-1} + e_{u_{i-1}}, 0, 0) \\
&- \gamma_1\tilde{\phi}_1(\tau_{i-1}) W_i^2(e_{u_{i-1}}, s_{i-1}, 1) \overset{(8.38)}{\leqslant} (\gamma_0\phi_0(\tau_{i-1}) - \gamma_1\phi_1(\tau_{i-1}))|e_{u_{i-1}} + s_{i-1}|^2. \qquad \text{(G.15)}
\end{aligned}$$

By recalling (8.36) and (G.5), we obtain that

$$U_i(\xi_i^+) - U_i(\xi_i) \leqslant 0, \qquad \text{(G.16)}$$

for all $\xi_i \in \mathcal{D}_i$. From (G.13)-(G.16), we can conclude that the storage function $S_i = U_i/\mu$ satisfies (G.1) and (G.2).

At last, we need to show that all maximal solutions of the hybrid system $\mathcal{H}_i$, $i \in \bar{N} \setminus \{1\}$, are t-complete. To do so, we verify the conditions provided in [98, Proposition 6.10]. First of all, observe from (8.31) that $G_i(\mathcal{D}_i) \subset \mathcal{C}_i \cup \mathcal{D}_i$, $i \in \bar{N} \setminus \{1\}$, since for all $\xi_i \in G_i(\mathcal{D}_i)$, it holds that $\tau_{i-1}^+ \geqslant 0$, $\eta_{i-1}^+ \geqslant 0$. Next, we show that for any point $p \in \mathcal{C}_i \setminus \mathcal{D}_i$, $i \in \bar{N} \setminus \{1\}$, there exists a neighborhood U of p such that, it holds for every $q \in U \cap \mathcal{C}_i$ and every $w \in \mathbb{R}$ that $F_i(q, w) \in T_{\mathcal{C}_i}(q)$, where $T_{\mathcal{C}_i}(q)$ denotes the tangent cone[1] to $\mathcal{C}_i$ at q. Observe that for each point $p \in \mathcal{C}_i$ (recall that $p = (\tilde{x}_i, e_{u_{i-1}}, \tau_{i-1}, l_{i-1}, s_{i-1}, \eta_{i-1})$), $T_{\mathcal{C}_i}(p) = \mathbb{R}^7 \times \mathbb{R} \times T_{\mathbb{R}_{\geqslant 0}}(\tau_{i-1}) \times \{0\} \times \{0\} \times T_{\mathbb{R}_{\geqslant 0}}(\eta_{i-1})$. From (8.25) and (8.31), we obtain that $\mathcal{C}_i/\mathcal{D}_i = \{\xi_i \in \mathbb{X}_i : (l_{i-1} = 0 \wedge \tau_{i-1} < \tau_{miet}) \vee \eta_{i-1} > 0)\}$. Given the facts that according to (8.27) and (8.39), $\dot{\tau}_{i-1} = 1$ and that $\dot{\eta}_{i-1} > 0$ when $\tau_{i-1} < \tau_{miet}$ and $\eta_{i-1} = 0$, for all $i \in \bar{N} \setminus \{1\}$, it indeed follows that for any $p \in \mathcal{C}_i \setminus \mathcal{D}_i$ there exists a neighborhood S of ξ such that, it holds for every $q \in S \cap \mathcal{C}_i$ and every $w \in \mathbb{R}$ that $F_i(q, w) \in T_{\mathcal{C}_i}(q)$. Since finite escape times are excluded due to (G.13), we can conclude that all maximal solutions of the hybrid system $\mathcal{H}_i$, $i \in \bar{N} \setminus \{1\}$, with $\xi_i(0, 0) \in \mathbb{X}_{0,i}$ and $\chi_{i-1} \in \mathcal{L}_2$, are t-complete, which completes the proof.

[1] The tangent cone to a set $S \subset \mathbb{R}^n$ at a point $x \in \mathbb{R}^n$, denoted $T_S(x)$, is the set of all vectors $\omega \in \mathbb{R}^n$ for which there exist $x_i \in S, y_i > 0$ with $x_i \to x, y \to 0$ as $i \to \infty$ such that $\omega = \lim_{i \to \infty}(x_i - x)/y_i$ (see Definition 5.12 in [98]).

Bibliography

[1] [Online]. Available: http://www.sonyenergy-devices.co.jp/en/keyword/

[2] M. Abdelrahim, V. S. Dolk, and W. P. M. H. Heemels, "Input-to-state stabilizing event-triggered control for linear systems with distributed and quantized output measurements," *IEEE Transactions on Automatic Control*.

[3] ——, "Input-to-state stabilizing event-triggered control for linear systems with output quantization," in *Proceedings of the 55th IEEE Conference on Decision and Control*, 2016, pp. 483–488.

[4] M. Abdelrahim, R. Postoyan, and J. Daafouz, "Event-triggered control of nonlinear singularly perturbed systems based only on the slow dynamics," *Automatica*, vol. 52, pp. 15–22, 2015.

[5] M. Abdelrahim, R. Postoyan, J. Daafouz, and D. Nešić, "Stabilization of nonlinear systems using event-triggered output feedback laws," in *Proceedings of the 21st International Symposium on Mathematical Theory of Networks and Systems*, 2014.

[6] ——, "Event-triggered dynamic feedback controllers for nonlinear systems with asynchronous transmissions," in *Proceedings of the 54th IEEE Conference on Decision and Control*, Dec 2015, pp. 5494–5499.

[7] ——, "Stabilization of nonlinear systems using event-triggered output feedback controllers," *IEEE Transactions on Automatic Control,*, vol. 61, no. 9, pp. 2682–2687, Sept 2016.

[8] M. Abdelrahim, R. Postoyan, J. Daafouz, and D. Nešić, "Co-design of output feedback laws and event-triggering conditions for linear systems," in *Proceedings of the 53rd IEEE Conference on Decision and Control, Los Angeles, U.S.A.*, 2014, pp. 3560–3565.

[9] M. Abdelrahim, R. Postoyan, J. Daafouz, and D. Nei, "Robust event-triggered output feedback controllers for nonlinear systems," *Automatica*, vol. 75, pp. 96 – 108, 2017.

[10] A. Adaldo, D. Liuzza, D. V. Dimarogonas, and K. H. Johansson, "Control of multi-agent systems with event-triggered cloud access," in *Proceedings of the 2015 European Control Conference (ECC)*, July 2015, pp. 954–961.

[11] ——, "Multi-agent trajectory tracking with self-triggered cloud access," in *2016 IEEE 55th Conference on Decision and Control (CDC)*, Dec 2016, pp. 2207–2214.

[12] A. Alam, B. Besselink, V. Turri, J. Martensson, and K. H. Johansson, "Heavy-duty vehicle platooning for sustainable freight transportation: A cooperative method to enhance safety and efficiency," *IEEE Control Systems*, vol. 35, no. 6, pp. 34–56, Dec 2015.

[13] A. A. Alam, A. Gattami, and K. H. Johansson, "An experimental study on the fuel reduction potential of heavy duty vehicle platooning," in *13th International IEEE Conference on Intelligent Transportation Systems*, Sept 2010, pp. 306–311.

[14] M. Andreasson, D. V. Dimarogonas, K. H. Johansson, and H. Sandberg, "Distributed vs. centralized power systems frequency control," in *Proceedings of the 12th European Control Conference*, July 2013, pp. 3524–3529.

[15] A. Anta and P. Tabuada, "To sample or not to sample: Self-triggered control for nonlinear systems," *IEEE Transactions Automatic Control*, vol. 55, no. 9, pp. 2030–2042, Sept 2010.

[16] P. Antsaklis, "Goals and challenges in cyber-physical systems research editorial of the editor in chief," *IEEE Transactions on Automatic Control*, vol. 59, no. 12, pp. 3117–3119, Dec 2014.

[17] D. Antunes and W. Heemels, "Rollout event-triggered control: Beyond periodic control performance," *IEEE Transactions on Automatic Control*, vol. 59, pp. 3296–3311, August 2014.

[18] K. E. Årzén, "A simple event-based PID controller," in *Proceedings of the 14th IFAC World congress*, Beijing, P.R. China, Jan. 1999.

[19] B. Asadi Khashooei, D. Antunes, and W. Heemels, "Output-based event-triggered control with performance guarantees," *IEEE Transactions on Automatic Control*, February 2018.

[20] K. J. Åström and B. Bernhardsson, "Comparison of periodic and event based sampling for first-order stochastic systems," in *Proceedings of the 14th IFAC World congress*, vol. 11, 1999, pp. 301–306.

[21] K. J. Åström and P. R. Kumar, "Control: A perspective," *Automatica*, vol. 50, no. 1, pp. 3 – 43, 2014.

[22] T. Başar and P. Bernhard, *H^∞-Optimal Control and Relaxed Minimax Design Problems: A Dynamic Game Approach*, 2nd ed. Boston, MA, USA: Birkhäuser, 1995.

[23] J. Baillieul and P. J. Antsaklis, "Control and communication challenges in networked real-time systems," *Proceedings of the IEEE*, vol. 95, no. 1, pp. 9–28, 2007.

[24] B. A. Bamieh and J. B. Pearson, "A general framework for linear periodic systems with applications to H^∞ / sampled-data control," *IEEE Transactions on Automatic Control*, vol. 37, no. 4, pp. 418–435, 1992.

[25] G. Bansal, J. B. Kenney, and C. E. Rohrs, "Limeric: A linear adaptive message rate algorithm for dsrc congestion control," *IEEE Transactions on Vehicular Technology*, vol. 62, no. 9, pp. 4182–4197, Nov 2013.

[26] P. Baran, "On distributed communications networks," *IEEE Transactions on Communications Systems*, vol. 12, no. 1, pp. 1–9, 1964.

[27] L. D. Baskar, B. De Schutter, J. Hellendoorn, and Z. Papp, "Traffic control and intelligent vehicle highway systems: A survey," *IET Intelligent Transport Systems*, vol. 5, no. 1, pp. 38–52, Mar. 2011.

[28] T. Batsuuri, R. J. Bril, and J. J. Lukkien, *Model, Analysis, and Improvements for Inter-Vehicle Communication Using One-Hop Periodic Broadcasting Based on the 802.11p Protocol*, D. Benhaddou and A. Al-Fuqaha, Eds. New York, NY: Springer New York, 2015.

[29] N. W. Bauer, P. J. H. Maas, and W. P. M. H. Heemels, "Stability analysis of networked control systems: A sum of squares approach," *Automatica*, vol. 48, no. 8, pp. 1514 – 1524, 2012.

[30] N. W. Bauer, S. J. L. M. van Loon, N. V. de Wouw, and W. P. M. H. Heemels, "Exploring the boundaries of robust stability under uncertain communication: An ncs toolbox applied to a wireless control setup," *IEEE Control Systems Magazine*, vol. 34, pp. 65–86, August 2014.

[31] N. Bekiaris-Liberis, C. Roncoli, and M. Papageorgiou, "Predictor-based adaptive cruise control design," in *Proceedings of the 2016 IEEE Conference on Control Applications*, Sept 2016, pp. 97–102.

[32] A. Bemporad, M. Heemels, and M. Vejdemo-Johansson, *Networked Control Systems*, ser. Lecture Notes in Control and Information Sciences. Springer London, 2010.

[33] A. Bemporad and M. Morari, *Robust model predictive control: A survey*. London: Springer London, 1999, pp. 207–226.

[34] B. Besselink and K. H. Johansson, "String stability and a delay-based spacing policy for vehicle platoons subject to disturbances," *IEEE Transactions on Automatic Control*, 2017, to Appear.

[35] H. Bevrani, *Robust Power System Frequency Control*, ser. Power Electronics and Power Systems. Springer US, 2008.

[36] B. Bollobas, *Modern Graph Theory*. Springer, 1998.

[37] P. Bommannavar and T. Basar, "Optimal control with limited control actions and lossy transmissions," in *Proceedings of the 47th IEEE Conference on Decision and Control*, Dec 2008, pp. 2032–2037.

[38] C. Bonnet and H. Fritz, "Fuel consumption reduction in a platoon: Experimental results with two electronically coupled trucks at close spacing," in *SAE Technical Paper*. SAE International, Aug 2000.

[39] D. P. Borgers, "Event-triggered control with robust communication and guaranteed performance," 2017.

[40] D. P. Borgers, V. S. Dolk, and W. P. M. H. Heemels, "Riccati-based design of event-triggered controllers for linear systems with delays," *IEEE Transactions on Automatic Control*, 2017.

[41] D. P. Borgers and W. P. M. H. Heemels, "Event-separation properties of event-triggered control systems," *IEEE Transactions Automatic Control*, vol. 59, no. 10, pp. 2644–2656, Oct 2014.

[42] ——, "Stability analysis of large-scale networked control systems with local networks: A hybrid small-gain approach," in *Proceedings of the 17th Hybrid Systems: Computation and Control Conference*, 2014.

[43] D. P. Borgers, R. Postoyan, A. Anta, P. Tabuada, D. Nešić, and W. P. M. H. Heemels, "Periodic event-triggered control of nonlinear systems using overapproximation techniques," submitted.

[44] D. Borgers, V. Dolk, and W. Heemels, "Dynamic event-triggered control with time regularization for linear systems (invited paper)," in *IEEE Conference on Decision and Control (CDC), Las Vegas, NV, USA, 2016*, 2016, pp. 1352–1357.

[45] ——, "Dynamic periodic event-triggered control for linear systems," in *Proceedings of the 20th Hybrid Systems: Computation and Control Conference*, Apr 2017.

[46] D. Borgers, R. Geiselhart, and W. Heemels, "Tradeoffs between quality-of-control and quality-of-service in large-scale nonlinear networked control systems," *Nonlinear Analysis: Hybrid Systems*, vol. 23, p. 142165, 2017.

[47] S. L. Bowman, C. Nowzari, and G. J. Pappas, "Coordination of multi-agent systems via asynchronous cloud communication," in *Proceedings of the 55th IEEE Conference on Decision and Control (CDC)*, Dec 2016, pp. 2215–2220.

[48] R. W. Brockett and D. Liberzon, "Quantized feedback stabilization of linear systems," *IEEE Transactions on Automatic Control*, vol. 45, no. 7, pp. 1279–1289, 2000.

[49] C. Cai and A. R. Teel, "Characterizations of input-to-state stability for hybrid systems," *Systems & Control Letters*, vol. 58, no. 1, pp. 47–53, 2009.

[50] ——, "Characterizations of input-to-state stability for hybrid systems," *Systems & Control Letters*, vol. 58, no. 1, pp. 47 – 53, 2009.

[51] D. Carnevale, A. R. Teel, and D. Nešić, "A Lyapunov proof of an improved maximum allowable transfer interval for networked control systems," *IEEE Transactions Automatic Control*, vol. 52, no. 5, pp. 892–897, 2007.

[52] C. G. Cassandras, "The event-driven paradigm for control, communication and optimization," *Journal of Control and Decision*, vol. 1, no. 1, pp. 3–17, 2014.

[53] V. G. Cerf and R. E. Khan, "A protocol for packet network intercommunication," *IEEE TRANSACTIONS ON COMMUNICATIONS*, vol. 22, pp. 637–648, 1974.

[54] A. Cervin and T. Henningsson, "Scheduling of event-triggered controllers on a shared network," in *Proceedings of the 47th IEEE Conference Decision and Control*, 2008, pp. 3601–3606.

[55] X. Chen and F. Hao, "Periodic event-triggered state-feedback and output-feedback control for linear systems," *International Journal on Control, Automation and Systems*, vol. 13, no. 4, pp. 779–787, 2015.

[56] T. M. Cheng, "Robust stabilisation of nonlinear systems using output measurements via finite data-rate communication channels," in *Proceedings of the 44th IEEE Conference on Decision and Control*, 2005, pp. 866–871.

[57] C. Y. Chong and S. P. Kumar, "Sensor networks: evolution, opportunities, and challenges," *Proceedings of the IEEE*, vol. 91, no. 8, pp. 1247–1256, Aug 2003.

[58] M. B. G. Cloosterman, N. van de Wouw, W. P. M. H. Heemels, and H. Nijmeijer, "Stability of networked control systems with uncertain time-varying delays," *IEEE Transactions on Automatic Control*, vol. 54, no. 7, pp. 1575–1580, July 2009.

[59] R. D'Andrea and G. E. Dullerud, "Distributed control design for spatially interconnected systems," *IEEE Transactions on automatic control*, vol. 48, no. 9, pp. 1478–1495, 2003.

[60] S. Dashkovskiy and R. Promkam, "Alternative stability conditions for hybrid systems," in *Proceedings of the 52nd IEEE Conference on Decision and Control*, Dec 2013, pp. 3332–3337.

[61] D. W. Davies, "The principles of a data communication network for computers and remote peripherals," in *IFIP Congress (2)*, 1968, pp. 709–715.

[62] ——, "An historical study of the beginnings of packet switching," *The Computer Journal*, vol. 44, no. 3, pp. 152–162, 2001.

[63] C. De Persis and P. Tesi, "On resilient control of nonlinear systems under denial-of-service," in *Proceedings of the 53rd IEEE Conference Decision and Control*, Dec 2014, pp. 5254–5259.

[64] ——, "Input-to-state stabilizing control under denial-of-service," *IEEE Transactions Automatic Control*, vol. 60, no. 11, pp. 2930–2944, 2015.

[65] B. DeBruhl and P. Tague, "Digital filter design for jamming mitigation in 802.15.4 communication," in *Proceedings of 20th International Conference on Computer Communications and Networks*, July 2011, pp. 1–6.

[66] M. A. Demetriou, "Design of consensus and adaptive consensus filters for distributed parameter systems," *Automatica*, vol. 46, no. 2, pp. 300 – 311, 2010.

[67] M. di Bernardo, A. Salvi, and S. Santini, "Distributed consensus strategy for platooning of vehicles in the presence of time-varying heterogeneous communication delays," *IEEE Transactions on Intelligent Transportation Systems*, vol. 16, no. 1, pp. 102–112, Feb 2015.

[68] R. Diestel, *Graph Theory*, ser. Electronic library of mathematics. Springer, 2006.

[69] D. V. Dimarogonas, E. Frazzoli, and K. H. Johansson, "Distributed event-triggered control for multi-agent systems," *IEEE Transactions on Automatic Control*, vol. 57, no. 5, pp. 1291–1297, May 2012.

[70] V. S. Dolk, M. Abdelrahim, and W. P. M. H. Heemels, "Event-triggered consensus seeking under non-uniform time-varying delays," in *Proceedings of the 20th IFAC World Congress*, 2017.

[71] V. S. Dolk, D. P. Borgers, and W. P. M. H. Heemels, "Dynamic event-triggered control: Tradeoffs between transmission intervals and performance," in *Proceedings of the 53rd IEEE Conference Decision and Control*, Dec 2014, pp. 2764–2769.

[72] ——, "Output-based and decentralized dynamic event-triggered control with guaranteed $\mathcal{L}_p$-gain performance and zeno-freeness," *IEEE Transactions on Automatic Control*, vol. 62, no. 1, pp. 34–49, 2017.

[73] V. S. Dolk and W. P. M. H. Heemels, "Dynamic event-triggered control under packet losses: The case with acknowledgements," in *Proceedings of the International Conference on Event-based Control, Communication, and Signal Processing*, June 2015, pp. 1–7.

[74] ——, "Event-triggered control under packet losses," *Automatica*, vol. 80, pp. 143–155, June 2017.

[75] V. S. Dolk, J. Ploeg, and W. P. M. H. Heemels, "Event-triggered control for string-stable vehicle platooning," *IEEE Transactions on Intelligent Transport Systems*, 2017, accepted for publication.

[76] V. S. Dolk, P. Tesi, C. De Persis, and W. P. M. H. Heemels, "Output-based event-triggered control systems under denial-of-service attacks," in *Proceedings of the 54th IEEE Conference on Decision and Control*, Dec 2015, pp. 4824–4829.

[77] ——, "Event-triggered control systems under denial-of-service attacks," *IEEE Transactions on Control of Network Systems*, vol. 4, pp. 93 – 105, March 2017.

[78] M. C. F. Donkers and W. P. M. H. Heemels, "Output-based event-triggered control with guaranteed $\mathcal{L}_\infty$-gain and improved and decentralized event-triggering," *IEEE Transactions Automatic Control*, vol. 57, no. 6, pp. 1362–1376, 2012.

[79] D. M. Doolin and N. Sitar, "Wireless sensors for wildfire monitoring," pp. 477–484, 2005.

[80] C. Ebenbauer, T. Raff, and F. Allgöwer, "Dissipation inequalities in systems theory: An introduction and recent results," in *Proceedings of the 6th International Congress on Industrial and Applied Mathematics*, Jul 2007.

[81] "Intelligent transport systems (its); vehicular communications; geonetworking," European Telecommunications Standards Institute, Tech. Rep., 2014.

[82] "Intelligent transport systems (its); decentralized congestion control mechanisms for intelligent transport systems operating in the 5 ghz range; access layer part," European Telecommunications Standards Institute, Tech. Rep., 2011.

[83] J. A. Fax and R. M. Murray, "Information flow and cooperative control of vehicle formations," *IEEE Transactions on Automatic Control*, vol. 49, no. 9, pp. 1465–1476, Sept 2004.

[84] S. Feng and P. Tesi, "Resilient control under denial-of-service: Robust design," *Automatica*, vol. 79, pp. 42 – 51, 2017.

[85] P. Fernandes and U. Nunes, "Platooning with ivc-enabled autonomous vehicles: Strategies to mitigate communication delays, improve safety and traffic flow," *IEEE Transactions on Intelligent Transportation Systems*, vol. 13, no. 1, pp. 91–106, March 2012.

[86] A. Festag, "Cooperative intelligent transport systems standards in europe," *IEEE Communications Magazine*, vol. 52, no. 12, pp. 166–172, December 2014.

[87] F. Forni, S. Galeani, D. Nešić, and L. Zaccarian, "Event-triggered transmission for linear control over communication channels," *Automatica*, vol. 50, no. 2, pp. 490–498, 2014.

[88] H. S. Foroush and S. Martínez, "On triggering control of single-input linear systems under pulse-width modulated DoS jamming attacks," *SIAM Journal on Control and Optimization*, 2013, submitted, Revised 2016.

[89] H. Fujioka, "Stability analysis for a class of networked/embedded control systems: Output feedback case," in *Proceedings of the 17th IFAC World Congress*, vol. 41, no. 2, 2008, pp. 4210–4215.

[90] F. Gao, S. Eben Li, Y. Zheng, and D. Kum, "Robust control of heterogeneous vehicular platoon with uncertain dynamics and communication delay," *IET Intelligent Transport Systems*, vol. 10, pp. 503–513(10), September 2016.

[91] C. E. Garca, D. M. Prett, and M. Morari, "Model predictive control: Theory and practicea survey," *Automatica*, vol. 25, no. 3, pp. 335 – 348, 1989.

[92] E. Garcia and P. J. Antsaklis, "Model-based event-triggered control for systems with quantization and time-varying network delays," *IEEE Transactions on Automatic Control*, vol. 58, no. 2, pp. 422–434, Feb 2013.

[93] E. Garcia, P. J. Antsaklis, and L. A. Montestruque, *Model-Based Control of Networked Systems*, ser. Systems & Control: Foundations & Applications. Springer International Publishing, 2014.

[94] E. Garcia, Y. Cao, and D. W. Casbeer, "Periodic event-triggered synchronization of linear multi-agent systems with communication delays," *IEEE Transactions on Automatic Control*, vol. 62, no. 1, pp. 366–371, Jan 2017.

[95] O. Gehring and H. Fritz, "Practical results of a longitudinal control concept for truck platooning with vehicle to vehicle communication," in *Proceedings of the Conference on Intelligent Transportation Systems*, Nov 1997, pp. 117–122.

[96] A. Girard, "Dynamic triggering mechanisms for event-triggered control," *IEEE Transactions on Automatic Control*, vol. 60, no. 7, pp. 1992–1997, July 2015.

[97] D. N. Godbole and J. Lygeros, "Longitudinal control of the lead car of a platoon," *IEEE Transactions on Vehicular Technology*, vol. 43, no. 4, pp. 1125–1135, Nov 1994.

[98] R. Goebel, R. G. Sanfelice, and A. R. Teel, *Hybrid Dynamical Systems: Modeling, Stability, and Robustness*. Princeton University Press, 2012.

[99] ——, *Hybrid Dynamical Systems: Modeling, Stability, and Robustness*. Princeton University Press, 2012.

[100] R. Goebel and A. R. Teel, "Solutions to hybrid inclusions via set and graphical convergence with stability theory applications," *Automatica*, vol. 42, no. 4, pp. 573–587, 2006.

[101] T. M. P. Gommans, D. Antunes, M. C. F. Donkers, P. Tabuada, and W. P. M. H. Heemels, "Self-triggered linear quadratic control," *Automatica*, vol. 50, pp. 1279–1287, 2014.

[102] L. Grüne, E. D. Sontag, and F. R. Wirth, "Asymptotic stability equals exponential stability, and ISS equals finite energy gain – if you twist your eyes," *Syst. Control Lett.*, vol. 38, no. 2, pp. 127–134, 1999.

[103] M. Guinaldo, D. Lehmann, J. Sánchez, S. Dormido, and K. H. Johansson, "Distributed event-triggered control with network delays and packet losses," in *Proceedings of the 51st IEEE Conference on Decision and Control*, Dec 2012, pp. 1–6.

[104] ——, "Distributed event-triggered control for non-reliable networks," *Journal of the Franklin Institute*, vol. 351, no. 12, pp. 5250 – 5273, 2014.

[105] G. Guo, L. Ding, and Q. L. Han, "A distributed event-triggered transmission strategy for sampled-data consensus of multi-agent systems," *Automatica*, vol. 50, no. 5, pp. 1489 – 1496, 2014.

[106] W. M. Haddad, V. Chellaboina, and S. G. Nersesov, *Impulsive and Hybrid Dynamical Systems: Stability, Dissipativity, and Control*. Princeton University Press, 2006.

[107] M. Hammache, M. Michaelian, and F. Browand, "Aerodynamic Forces on Truck Models, Including Two Trucks in Tandem," Institute of Transportation Studies, UC Berkeley, Institute of Transportation Studies, Research Reports, Working Papers, Proceedings, Oct. 2001.

[108] J. Hedrick, M. Tomizuka, and P. Varaiya, "Control issues in automated highway systems," *IEEE Control Systems*, vol. 14, no. 6, pp. 21–32, Dec 1994.

[109] W. P. M. H. Heemels, D. P. Borgers, V. S. Dolk, R. Geiselhart, and S. H. J. Heijmans, "Constructions of lyapunov functions for large-scale networked control systems with packet-based communication (invited paper)," in *Proceedings of the 2016 European Control Conference (ECC)*, 2016, pp. 936–938.

[110] W. P. M. H. Heemels, D. P. Borgers, N. van de Wouw, D. Nešić, and A. R. Teel, "Stability analysis of nonlinear networked control systems with asynchronous communication: A small-gain approach," in *Proceedings of the IEEE 52nd Annual Conference on Decision and Control*, 2013, pp. 4631–4637.

[111] W. P. M. H. Heemels and M. C. F. Donkers, "Model-based periodic event-triggered control for linear systems," *Automatica*, vol. 49, no. 3, pp. 698–711, 2013.

[112] W. P. M. H. Heemels, M. C. F. Donkers, and A. R. Teel, "Periodic event-triggered control for linear systems," *IEEE Transactions Automatic Control*, vol. 58, no. 4, pp. 847–861, 2013.

[113] W. P. M. H. Heemels, G. E. Dullerud, and A. R. Teel, "L2-gain analysis for a class of hybrid systems with applications to reset and event-triggered control: A lifting approach," *IEEE Transactions on Automatic Control*, vol. 61, pp. 2766–2781, October 2016.

[114] W. P. M. H. Heemels, K. H. Johansson, and P. Tabuada, "An introduction to event-triggered and self-triggered control," in *Proceedings of the 51th IEEE Conference Decision and Control*, Dec 2012, pp. 3270–3285.

[115] ——, *Event-Triggered and Self-Triggered Control*. London: Springer London, 2013.

[116] W. P. M. H. Heemels, D. Nešić, and A. R. Teel, "Networked and quantized control systems with communication delays," in *Proceedings of the joint 48th IEEE Conference on Decision and Control and 28th Chinese Control Conference*, 2009, pp. 7929–7935.

[117] W. P. M. H. Heemels, J. H. Sandee, and P. P. J. Van Den Bosch, "Analysis of event-driven controllers for linear systems," *International Journal of Control*, vol. 81, no. 4, pp. 571–590, 2008.

[118] W. P. M. H. Heemels and B. D. Schutter, "Special issue on analysis and design of hybrid and networked control systems," *Nonlinear Analysis: Hybrid Systems*, vol. 10, pp. 1–3, November 2013.

[119] W. P. M. H. Heemels, B. D. Schutter, J. Lunze, and M. Lazar, "Stability analysis and controller synthesis for hybrid dynamical systems," *Philosophical Transactions of the Royal Society A*, vol. 368, pp. 4937–4960, October 2010.

[120] W. P. M. H. Heemels, A. R. Teel, N. van de Wouw, and D. Nešić, "Networked control systems with communication constraints: Tradeoffs between transmission intervals, delays and performance." *IEEE Transactions Automatic Control*, pp. 1781–1796, 2010.

[121] W. P. M. H. Heemels and S. Weiland, "Input-to-state stability and interconnections of discontinuous dynamical systems," *Automatica*, vol. 44, pp. 3079–3086, December 2008.

[122] S. H. J. Heijmans, D. P. Borgers, and W. P. M. H. Heemels, "Stability and performance analysis of spatially invariant systems with networked communication," *IEEE Transactions on Automatic Control*, October 2017.

[123] S. H. J. Heijmans, V. S. Dolk, D. Borgers, and W. P. M. H. Heemels, "Stability analysis of spatially invariant systems with event-triggered communication," in *Conference on Event-Based Control, Communication and Signal Processing (EBCCSP) 2016*, 2016.

[124] J. P. Hespanha and A. S. Morse, "Stability of switched systems with average dwell-time," in *Proceedings of the 38th IEEE Conference Decision and Control*, vol. 3, 1999, pp. 2655–2660 vol.3.

[125] J. P. Hespanha, P. Naghshtabrizi, and Y. Xu, "A survey of recent results in networked control systems," *Proceedings of the IEEE*, vol. 95, no. 1, pp. 138–162, 2007.

[126] S. Hu and D. Yue, "$\mathcal{L}_2$-gain analysis of event-triggered networked control systems: a discontinuous lyapunov functional approach," *International Journal of Robust and Nonlinear Control*, vol. 23, no. 11, pp. 1277–1300, 2013.

[127] Ibraheem, P. Kumar, and D. P. Kothari, "Recent philosophies of automatic generation control strategies in power systems," *IEEE Transactions on Power Systems*, vol. 20, no. 1, pp. 346–357, Feb 2005.

[128] I. Karafyllis and C. Kravaris, "Global stability results for systems under sampled-data control," *International Journal of Robust and Nonlinear Control*, vol. 19, no. 10, pp. 1105–1128, 2009.

[129] S. Kato, S. Tsugawa, K. Tokuda, T. Matsui, and H. Fujii, "Vehicle control algorithms for cooperative driving with automated vehicles and intervehicle communications," *IEEE Transactions on Intelligent Transportation Systems*, vol. 3, no. 3, pp. 155–161, Sep 2002.

[130] L. Kester, W. van Willigen, and J. de Jongh, "Critical headway estimation under uncertainty and non-ideal communication conditions," in *Proceedings of the 17th International IEEE Conference on Intelligent Transportation Systems*, Oct 2014, pp. 320–327.

[131] H. K. Khalil, *Nonlinear Systems, 3rd Edition.* Upper Saddle River, NJ: Prentice-Hall, 2002.

[132] B. A. Khashooei, B. van Eekelen, D. J. Antunes, and W. P. M. H. Heemels, "Suboptimal event-triggered control over unreliable communication links with experimental validation," in *3rd International Conference on Event-based Control, Communication and Signal Processing 2017*, May 2017.

[133] S. Kia, J. Cortés, and S. Martínez, "Distributed event-triggered communication for dynamic average consensus in networked systems," *Automatica*, vol. 59, pp. 112 – 119, 2015.

[134] S. Kühlmorgen, I. Llatser, A. Festag, and G. Fettweis, "Performance evaluation of etsi geonetworking for vehicular ad hoc networks," in *Proceedings of the 81st IEEE Vehicular Technology Conference*, May 2015, pp. 1–6.

[135] F. Laermer and A. Urban, "Milestones in deep reactive ion etching," in *Proceedings of the 13th International Conference on Solid-State Sensors, Actuators and Microsystems.*, vol. 2, June 2005, pp. 1118–1121.

[136] F. Lamnabhi-Lagarrigue, A. Annaswamy, S. Engell, A. Isaksson, P. Khargonekar, R. M. Murray, H. Nijmeijer, T. Samad, D. Tilbury, and P. v. Hof, "Systems & control for the future of humanity, research agenda: Current and future roles, impact and grand challenges," *Annual Reviews in Control*, vol. 43, pp. 1 – 64, 2017.

[137] E. Lee, "Cyber physical systems: Design challenges," EECS Department, University of California, Berkeley, Tech. Rep. UCB/EECS-2008-8, Jan 2008.

[138] D. Lehmann and J. Lunze, "Event-based control with communication delays and packet losses," *International Journal of Control*, vol. 85, no. 5, pp. 563–577, 2012.

[139] W. Levine and M. Athans, "On the optimal error regulation of a string of moving vehicles," *IEEE Transactions on Automatic Control*, vol. 11, no. 3, pp. 355–361, Jul 1966.

[140] H. Li, X. Liao, T. Huang, and W. Zhu, "Event-triggering sampling based leader-following consensus in second-order multi-agent systems," *IEEE Transactions on Automatic Control*, vol. 60, no. 7, pp. 1998–2003, July 2015.

[141] L. Li, X. Wang, and M. Lemmon, "Stabilizing bit-rate of perturbed event triggered control systems," in *Proceedings of the 4th IFAC Conference on Analysis and Design of Hybrid Systems*, 2012, pp. 70–75.

[142] G. Liang, S. R. Weller, J. Zhao, F. Luo, and Z. Y. Dong, "The 2015 ukraine blackout: Implications for false data injection attacks," *IEEE Transactions on Power Systems*, 2017.

[143] D. Liberzon, "Hybrid feedback stabilization of systems with quantized signals," *Automatica*, vol. 39, no. 9, pp. 1543–1554, 2003.

[144] ——, "Quantization, time delays, and nonlinear stabilization," *IEEE Transactions on Automatic Control*, vol. 51, no. 7, pp. 1190–1195, 2006.

[145] D. Liberzon and D. Nešić, "Input-to-state stabilization of linear systems with quantized state measurements," *IEEE Transactions on Automatic Control*, vol. 52, no. 5, pp. 767–781, 2007.

[146] P. Lin and Y. Jia, "Consensus of second-order discrete-time multi-agent systems with nonuniform time-delays and dynamically changing topologies," *Automatica*, vol. 45, no. 9, pp. 2154 – 2158, 2009.

[147] S. Linsenmayer, D. V. Dimarogonas, and F. Allgöwer, "Nonlinear event-triggered platooning control with exponential convergence," *IFAC-PapersOnLine*, vol. 48, no. 22, pp. 138 – 143, 2015.

[148] T. Liu, M. Cao, C. De Persis, and J. M. Hendrickx, "Distributed event-triggered control for synchronization of dynamical networks with estimators," in *Proceedings of The 4th IFAC Workshop on Distributed Estimation and Control in Networked Systems*, vol. 46, no. 27, 2013, pp. 116 – 121.

[149] ——, "Distributed event-triggered control for asymptotic synchronization of dynamical networks," *CoRR*, vol. abs/1508.04606, 2015.

[150] T. Liu and Z. Jiang, "Quantized event-based control of nonlinear systems," in *Proceedings of the 54th IEEE Conference on Decision and Control*, 2015, pp. 4806–4811.

[151] X. Liu, A. Goldsmith, S. S. Mahal, and J. K. Hedrick, "Effects of communication delay on string stability in vehicle platoons," in *Proceedings of the 2001 IEEE Intelligent Transportation Systems*, 2001, pp. 625–630.

[152] I. Llatser, A. Festag, and G. Fettweis, "Vehicular communication performance in convoys of automated vehicles," in *Proceedings of the 2016 IEEE International Conference on Communications*, May 2016, pp. 1–6.

[153] J. Lofberg, "Yalmip : a toolbox for modeling and optimization in matlab," in *Proceedings of the 2014 IEEE Computer Aided Control System Design Conference*, Sept 2004, pp. 284–289.

[154] J. Lunze and F. Lamnabhi-Lagarrigue, *Handbook of Hybrid Systems Control Theory, Tools, Applications*. Cambridge University Press, 2009.

[155] J. Lunze and D. Lehmann, "A state-feedback approach to event-based control," *Automatica*, vol. 46, no. 1, pp. 211–215, 2010.

[156] M. H. Mamduhi, D. Tolic, A. Molin, and S. Hirche, "Event-triggered scheduling for stochastic multi-loop networked control systems with packet dropouts," in *Proceedings of the IEEE 53rd Annual Conference on Decision and Control*, Dec 2014, pp. 2776–2782.

[157] J. Marescaux, J. Leroy, M. Gagner, F. Rubino, D. Mutter, M. Vix, S. E. Butner, and M. K. Smith, "Transatlantic robot-assisted telesurgery," *Nature*, vol. 413, pp. 379–380, Sep. 2001.

[158] M. Mazo Jr., A. Anta, and P. Tabuada, "An ISS self-triggered implementation of linear controllers," *Automatica*, vol. 46, no. 8, pp. 1310–1314, 2010.

[159] A. Medina, N. v. d. Wouw, and H. Nijmeijer, "Automation of a t-intersection using virtual platoons of cooperative autonomous vehicles," in *Proceedings of the IEEE 18th International Conference on Intelligent Transportation Systems*, Sept 2015, pp. 1696–1701.

[160] X. Meng and T. Chen, "Event based agreement protocols for multi-agent networks," *Automatica*, vol. 49, no. 7, pp. 2125 – 2132, 2013.

[161] P. Millán, L. Orihuela, I. Jurado, C. Vivas, and F. Rubio, "Distributed estimation in networked systems under periodic and event-based communication policies," *International Journal of Systems Science*, vol. 46, no. 1, pp. 139–151, 2015.

[162] P. Millán, L. Orihuela, C. Vivas, and F. R. Rubio, "Distributed consensus-based estimation considering network induced delays and dropouts," *Automatica*, vol. 48, no. 10, pp. 2726 – 2729, 2012.

[163] M. Miskowicz, "Send-on-delta concept: An event-based data reporting strategy," *Sensors*, vol. 6, no. 1, pp. 49–63, 2006.

[164] A. Molin and S. Hirche, "On the optimality of certainty equivalence for event-triggered control systems," *IEEE Transactions on Automatic Control*, vol. 2, no. 58, pp. 470–474, 2013.

[165] ——, "Suboptimal event-triggered control for networked control systems," *ZAMM - Journal of Applied Mathematics and Mechanics / Zeitschrift für Angewandte Mathematik und Mechanik*, vol. 94, no. 4, pp. 277–289, 2014.

[166] L. A. Montestruque and P. J. Antsaklis, "State and output feedback control in model-based networked control systems," in *Proceedings of the 41st IEEE Conference on Decision and Control*, vol. 2, Dec 2002, pp. 1620–1625 vol.2.

[167] ——, "Static and dynamic quantization in model-based networked control systems," *International Journal of Control*, vol. 80, no. 1, pp. 87–101, 2007.

[168] S. H. Mousavi, M. Ghodrat, and H. J. Marquez, "Integral-based event-triggered control scheme for a general class of non-linear systems," *IET Control Theory Applications*, vol. 9, no. 13, pp. 1982–1988, 2015.

[169] R. M. Murray, K. J. Astrom, S. P. Boyd, R. W. Brockett, and G. Stein, "Future directions in control in an information-rich world," *IEEE Control Systems*, vol. 23, no. 2, pp. 20–33, Apr 2003.

[170] R. Naldi and R. G. Sanfelice, "Passivity-based control for hybrid systems with applications to mechanical systems exhibiting impacts," *Automatica*, vol. 49, no. 5, pp. 1104–1116, May 2013.

[171] G. J. L. Naus, R. P. A. Vugts, J. Ploeg, M. J. G. van de Molengraft, and M. Steinbuch, "String-stable cacc design and experimental validation, a frequency-domain approach," *IEEE Transactions on Vehicular Technology*, vol. 59, no. 9, pp. 4268–4279, 2010.

[172] R. R. Negenborn, P. J. van Overloop, T. Keviczky, and B. De Schutter, "Distributed model predictive control of irrigation canals," *Networks and Heterogeneous Media*, vol. 4, no. 2, pp. 359–380, Jun. 2009.

[173] D. Nešić and A. R. Teel, "Input-output stability properties of networked control systems," *IEEE Transactions Automatic Control*, vol. 49, no. 10, pp. 1650–1667, 2004.

[174] D. Nešić, A. R. Teel, and D. Carnevale, "Explicit computation of the sampling period in emulation of controllers for nonlinear sampled-data systems," *IEEE Transactions on Automatic Control*, vol. 54, no. 3, pp. 619–624, March 2009.

[175] D. Nešić and D. Liberzon, "A unified framework for design and analysis of networked and quantized control systems," *IEEE Transactions on Automatic Control*, vol. 54, no. 4, pp. 732–747, 2009.

[176] D. Nešić, A. R. Teel, G. Valmorbida, and L. Zaccarian, "Finite-gain $\mathcal{L}_p$ stability for hybrid dynamical systems," *Automatica*, vol. 49, no. 8, pp. 2384–2396, 2013.

[177] A. Nordrum, "Popular internet of things forecast of 50 billion devices by 2020 is outdated," Aug 2016.

[178] C. Nowzari and G. J. Pappas, "Multi-agent coordination with asynchronous cloud access," in *Proceedings of the 2016 American Control Conference (ACC)*, July 2016, pp. 4649–4654.

[179] R. Olfati-Saber, J. A. Fax, and R. M. Murray, "Consensus and cooperation in networked multi-agent systems," *Proceedings of the IEEE*, vol. 95, no. 1, pp. 215–233, Jan 2007.

[180] S. Öncü, J. Ploeg, N. van de Wouw, and H. Nijmeijer, "Cooperative adaptive cruise control: Network-aware analysis of string stability," *IEEE Transactions on Intelligent Transportation Systems*, vol. 15, no. 4, pp. 1527–1537, Aug 2014.

[181] S. Öncü, N. van de Wouw, W. P. M. H. Heemels, and H. Nijmeijer, "String stability of interconnected vehicles under communication constraints," in *Proceedings of the 51st IEEE Conference on Decision and Control*, Dec 2012, pp. 2459–2464.

[182] I. C. Paschalidis and M. Egerstedt, "The inaugural issue of the ieee transactions on control of network systems," *IEEE Transactions on Control of Network Systems*, vol. 1, no. 1, pp. 1–3, Mar 2014.

[183] F. Pasqualetti, F. Dorfler, and F. Bullo, "Attack detection and identification in cyber-physical systems," *IEEE Transactions on Automatic Control*, vol. 58, no. 11, pp. 2715–2729, Nov 2013.

[184] C. Peng and T. C. Yang, "Event-triggered communication and control co-design for networked control systems," *Automatica*, vol. 49, no. 5, pp. 1326 – 1332, 2013.

[185] C. D. Persis and R. Postoyan, "A lyapunov redesign of coordination algorithms for cyber-physical systems," *IEEE Transactions on Automatic Control*, vol. 62, no. 2, pp. 808–823, Feb 2017.

[186] J. Ploeg, D. P. Shukla, N. van de Wouw, and H. Nijmeijer, "Controller synthesis for string stability of vehicle platoons," *IEEE Transactions on Intelligent Transportation Systems*, vol. 15, no. 2, pp. 854–865, April 2014.

[187] J. Ploeg, N. van de Wouw, and H. Nijmeijer, "$\mathcal{L}_p$ string stability of cascaded systems: Application to vehicle platooning," *IEEE Transactions Automatic Control*, vol. 22, no. 2, pp. 768–793, 2013.

[188] R. Postoyan, A. Anta, W. P. M. H. Heemels, P. Tabuada, and D. Nešić, "Periodic event-triggered control for nonlinear systems," in *Proceedings of the 52nd IEEE Conference Decision and Control*, Dec 2013, pp. 7397–7402.

[189] R. Postoyan, A. Anta, D. Nešić, and P. Tabuada, "A unifying Lyapunov-based framework for the event-triggered control of nonlinear systems," in *Proceedings of the 50th IEEE Conference Decision and Control and European Control Conference*, 2011, pp. 2559–2564.

[190] R. Postoyan, P. Tabuada, D. Nešić, and A. Anta, "Event-triggered and self-triggered stabilization of networked control systems," in *Proceedings of the 50th IEEE Conference Decision and Control and European Control Conference*, 2011, pp. 2565–2570.

[191] ——, "A framework for the event-triggered stabilization of nonlinear systems," *IEEE Transactions on Automatic Control*, vol. 60, no. 4, pp. 982–996, April 2015.

[192] C. Prieur, A. R. Teel, and L. Zaccarian, "Relaxed persistent flow/jump conditions for uniform global asymptotic stability," *IEEE Transactions on Automatic Control*, vol. 59, no. 10, pp. 2766–2771, Oct 2014.

[193] ——, "Relaxed persistent flow/jump conditions for uniform global asymptotic stability," *IEEE Transactions on Automatic Control*, vol. 59, no. 10, pp. 2766–2771, 2014.

[194] F. Qu, Z. Guan, D. He, and M. Chi, "Event-triggered control for networked control systems with quantization and packet losses," *Journal of the Franklin Institute*, vol. 352, pp. 974–986, 2015.

[195] C. Ramesh, H. Sandberg, and K. H. Johansson, "Performance analysis of a network of event-based systems," *IEEE Transactions on Automatic Control*, vol. 61, no. 11, pp. 3568–3573, Nov 2016.

[196] W. Ren, "On consensus algorithms for double-integrator dynamics," *IEEE Transactions on Automatic Control*, vol. 53, no. 6, pp. 1503–1509, July 2008.

[197] L. G. Roberts and B. D. Wessler, "Computer network development to achieve resource sharing," in *Proceedings of the May 5-7, 1970, Spring Joint Computer Conference*, ser. AFIPS '70 (Spring). New York, NY, USA: ACM, 1970, pp. 543–549.

[198] H. Sandberg, S. Amin, and K. Johansson, "Cyberphysical security in networked control systems: An introduction to the issue," *IEEE Control Systems Magazine*, vol. 35, no. 1, pp. 20–23, Feb 2015.

[199] R. G. Sanfelice, "Input-output-to-state stability tools for hybrid systems and their interconnections," *IEEE Transactions on Automatic Control*, vol. 59, no. 5, pp. 1360–1366, May 2014.

[200] R. G. Sanfelice, D. A. Copp, and P. Nanez, "A toolbox for simulation of hybrid systems in Matlab/Simulink: Hybrid Equations (HyEQ) Toolbox," in *Proceedings of the 16th Hybrid Systems: Computation and Control Conference*, 2013, pp. 101–106.

[201] J. Schiffer, F. Drfler, and E. Fridman, "Robustness of distributed averaging control in power systems: Time delays & dynamic communication topology," *Automatica*, vol. 80, pp. 261 – 271, 2017.

[202] P. Seiler, A. Pant, and K. Hedrick, "Disturbance propagation in vehicle strings," *IEEE Transactions on Automatic Control*, vol. 49, no. 10, pp. 1835–1842, Oct 2004.

[203] P. Seiler and R. Sengupta, "Analysis of communication losses in vehicle control problems," in *Proceedings of the 2001 American Control Conference*, vol. 2, 2001, pp. 1491–1496 vol.2.

[204] ——, "An $\mathcal{H}_\infty$ approach to networked control," *IEEE Transactions on Automatic Control*, vol. 50, no. 3, pp. 356–364, March 2005.

[205] A. Selivanov and E. Fridman, "Event-triggered h_∞ control: A switching approach," *IEEE Transactions on Automatic Control*, vol. 61, no. 10, pp. 3221–3226, Oct 2016.

[206] G. S. Seyboth, D. V. Dimarogonas, and K. H. Johansson, "Event-based broadcasting for multi-agent average consensus," *Automatica*, vol. 49, no. 1, pp. 245 – 252, 2013.

[207] Y. Sharon and D. Liberzon, "Input to state stabilizing controller for systems with coarse quantization," *IEEE Transactions on Automatic Control*, vol. 57, no. 4, pp. 830–844, 2012.

[208] S. Sheikholeslam and C. A. Desoer, "Longitudinal control of a platoon of vehicles with no communication of lead vehicle information: a system level study," *IEEE Transactions on Vehicular Technology*, vol. 42, no. 4, pp. 546–554, Nov 1993.

[209] P. Shi, H. Wang, and C. Lim, "Network-based event-triggered control for singular systems with quantizations," *IEEE Transactions on Industrial Electronics*, vol. 63, no. 2, pp. 1230–1238, 2016.

[210] S. Shladover, Partners for Advanced Transit, Highways (California) and Cambridge Systematics, United States Federal Highway Administration Office of Operations R&D, United States Federal Highway Administration Office of Corporate Research, and Exploratory Advanced Research Program and Turner-Fairbank Highway Research Center, *Recent international activity in cooperative vehicle-highway automation systems.* McLean, VA : U.S. Department of Transportation, Federal Highway Administration, Office of Operations Research and Development, Turner-Fairbank Highway Research Center, 2012.

[211] S. E. Shladover, "Research updates in intelligent transportation systems," *Intellimotion* AHS Demo '97 Issue, vol. 6, no. 3, 1997.

[212] S. E. Shladover, C. A. Desoer, J. K. Hedrick, M. Tomizuka, J. Walrand, W. B. Zhang, D. H. McMahon, H. Peng, S. Sheikholeslam, and N. McKeown, "Automated vehicle control developments in the path program," *IEEE Transactions on Vehicular Technology*, vol. 40, no. 1, pp. 114–130, Feb 1991.

[213] S. Shladover, D. Su, and X. Lu, "Impacts of cooperative adaptive cruise control on freeway traffic flow," *Transportation Research Record: Journal of the Transportation Research Board*, vol. 2324, pp. 63–70, 2012.

[214] D. Siljak, *Decentralized control of complex systems*, ser. Mathematics in Science and Engineering. Elsevier Science, 1991.

[215] J. Song, S. Han, A. Mok, D. Chen, M. Lucas, M. Nixon, and W. Pratt, "Wirelesshart: Applying wireless technology in real-time industrial process control," in *2008 IEEE Real-Time and Embedded Technology and Applications Symposium*, April 2008, pp. 377–386.

[216] J. Song, A. K. Mok, D. Chen, M. Nixon, T. Blevins, and W. K. Wojsznis, "Improving PID control with unreliable communications," in *Proceedings of the Instrument Society of America Conference*, Oct 2006.

[217] Y. F. Steinbuch, "Sequential optimal and predictive control for cascaded systems with applications to a quadcopters," 2017.

[218] C. Stöcker and J. Lunze, "Event-based feedback control of disturbed input-affine systems," *Journal of Applied Mathematics and Mechanics*, vol. 94, no. 4, pp. 290–302, 2014.

[219] C. Stöcker, D. Vey, and J. Lunze, "Decentralized event-based control: Stability analysis and experimental evaluation," *Nonlinear Analysis: Hybrid Systems*, vol. 10, pp. 141–155, 2013.

[220] J. F. Sturm, "Using SeDuMi 1.02, A Matlab toolbox for optimization over symmetric cones," *Optimization Methods and Software*, vol. 11, no. 1-4, pp. 625–653, 1999.

[221] Y. Sun and X. Wang, "Stabilizing bit-rates in networked control systems with decentralized event-triggered communication," *Discrete Event Dynamic Systems*, pp. 219–245, 2014.

[222] Y. G. Sun and L. Wang, "Consensus of multi-agent systems in directed networks with nonuniform time-varying delays," *IEEE Transactions on Automatic Control*, vol. 54, no. 7, pp. 1607–1613, July 2009.

[223] D. Swaroop and J. K. Hedrick, "String stability of interconnected systems," *IEEE Transactions on Automatic Control*, vol. 41, no. 3, pp. 349–357, Mar 1996.

[224] P. Tabuada, "Event-triggered real-time scheduling of stabilizing control tasks," *IEEE Transactions Automatic Control*, vol. 52, no. 9, pp. 1680–1685, 2007.

[225] P. Tallapragada and N. Chopra, "Event-triggered dynamic output feedback control for LTI systems," in *Proceedings of the 51st IEEE Conference Decision and Control*, 2012, pp. 6597–6602.

[226] ——, "Decentralized event-triggering for control of LTI systems," in *Proceedings of the IEEE International Conference on Control Applications, 2013*, 2013, pp. 698–703.

[227] ——, "Event-triggered dynamic output feedback control of LTI systems over sensor-controller-actuator networks," in *Proceedings of the 52nd IEEE Conference on Decision and Control*, 2013, pp. 4625–4630.

[228] ——, "Decentralized event-triggering for control of nonlinear systems," *IEEE Transactions on Automatic Control*, vol. 59, no. 12, pp. 3312–3324, Dec 2014.

[229] P. Tallapragada and J. Cortés, "Event-triggered stabilization of linear systems under bounded bit rates," *IEEE Transactions on Automatic Control*, vol. 61, no. 6, pp. 1575–1589, June 2016.

[230] Z.-J. Tang, T.-Z. Huang, J.-L. Shao, and J.-P. Hu, "Consensus of second-order multi-agent systems with nonuniform time-varying delays," *Neurocomputing*, vol. 97, pp. 410 – 414, 2012.

[231] A. Tanwani, C. Prieur, and M. Fiacchini, "Observer-based feedback stabilization of linear systems with event-triggered sampling and dynamic quantization," *Systems & Control Letters*, vol. 94, pp. 46–56, 2016.

[232] A. R. Teel and D. Nešić, "Lyapunov functions for $\mathcal{L}_2$ and input-to-state stability in a class of quantized control systems," *Proceedings of the 50th IEEE Conference on Decision and Control and European Control Conference*, pp. 4542–4547, 2011.

[233] S. C. N. Thissen, "Co-design of dynamic event-triggering mechanisms and output-feedback laws for networked linear control systems," 2017.

[234] T. Tielert, D. Jiang, Q. Chen, L. Delgrossi, and H. Hartenstein, "Design methodology and evaluation of rate adaptation based congestion control for vehicle safety communications," in *Proceedings of the 2011 IEEE Vehicular Networking Conference (VNC)*, Nov 2011, pp. 116–123.

[235] S. Trimpe and M. C. Campi, "On the choice of the event trigger in event-based estimation," in *Event-based Control, Communication, and Signal Processing (EBCCSP), 2015 International Conference on*, June 2015, pp. 1–8.

[236] S. Trimpe and R. D'Andrea, "Event-based state estimation with variance-based triggering," *IEEE Transactions on Automatic Control*, vol. 59, no. 12, pp. 3266–3281, Dec 2014.

[237] S. Trip, M. Brger, and C. De Persis, "An internal model approach to (optimal) frequency regulation in power grids with time-varying voltages," *Automatica*, vol. 64, pp. 240 – 253, 2016.

[238] V. Turri, B. Besselink, and K. H. Johansson, "Cooperative look-ahead control for fuel-efficient and safe heavy-duty vehicle platooning," *IEEE Transactions on Control Systems Technology*, vol. 25, no. 1, pp. 12–28, Jan 2017.

[239] R. P. V. S. Dolk, M. M. O. Abdelrahim and W. P. M. H. Heemels, "Event-triggered multi-agent systems under non-uniform time-varying delays," 2017, under review.

[240] B. van Arem, C. J. G. van Driel, and R. Visser, "The impact of cooperative adaptive cruise control on traffic-flow characteristics," *IEEE Transactions on Intelligent Transportation Systems*, vol. 7, no. 4, pp. 429–436, Dec 2006.

[241] A. J. Van der Schaft, *$\mathcal{L}_2$-Gain and Passivity Techniques in Nonlinear Control, 3rd Edition*, ser. Lecture Notes in Control and Information Sciences. Springer International Publishing, 2017.

[242] S. J. L. M. van Loon, M. C. F. Donkers, N. van de Wouw, and W. P. M. H. Heemels, "Stability analysis of networked and quantized linear control systems," *Nonlinear Analysis: Hybrid Systems*, vol. 10, pp. 111–125, 2013.

[243] S. J. L. M. van Loon, W. P. M. H. Heemels, and A. R. Teel, "Improved $\mathcal{L}_2$-gain analysis for a class of hybrid systems with applications to reset and event-triggered control," in *Proceeding of the 53rd IEEE Conference Decision and Control*, 2014, pp. 1221–1226.

[244] M. Velasco, J. M. Fuertes, and P. Marti, "The self triggered task model for real-time control systems," in *24th IEEE Real-Time Systems Symposium (work in progress)*, 2003, pp. 67–70.

[245] G. C. Walsh, H. Ye, and L. G. Bushnell, "Stability analysis of networked control systems," *IEEE Transactions Control Systems Technology*, vol. 10, no. 3, pp. 438–446, 2002.

[246] W. Wang and Z. Lu, "Cyber security in the smart grid: Survey and challenges," *Computer Networks*, vol. 57, no. 5, pp. 1344 – 1371, 2013.

[247] W. Wang, R. Postoyan, D. Nei, and W. P. M. H. Heemels, "Stabilization of nonlinear systems using state-feedback periodic event-triggered controllers," in *2016 IEEE 55th Conference on Decision and Control (CDC)*, Dec 2016, pp. 6808–6813.

[248] X. Wang and M. D. Lemmon, "Event design in event-triggered feedback control systems," in *Proceedings of the 47th IEEE Conference on Decision and Control*, Dec 2008, pp. 2105–2110.

[249] ——, "Self-triggered feedback control systems with finite-gain $\mathcal{L}_2$ stability," *IEEE Transactions Automatic Control*, vol. 54, no. 3, pp. 452–467, 2009.

[250] ——, "Self-triggered feedback systems with state-independent disturbances," in *Proceedings of the 2009 American Control Conference*, 2009, pp. 3842–3847.

[251] ——, "Event-triggering in distributed networked control systems," *IEEE Transactions Automatic Control*, vol. 56, no. 3, pp. 586–601, 2011.

[252] M. Webb, *SMART 2020: enabling the low carbon economy in the information age*, 2008.

[253] X. Wenyuan, W. Trappe, and Y. Zhang, "Jamming sensor networks: Attack and defense strategies," *IEEE Network*, vol. 20, no. 3, pp. 41–47, May 2006.

[254] J. C. Willems, "Dissipative dynamical systems part i: General theory," *Archive for Rational Mechanics and Analysis*, vol. 45, no. 5, pp. 321–351, 1972.

[255] W. K. Wojsznis, T. Blevins, and M. J. Nixon, "Model predictive control with event driven operation," in *Proceedings of the International Conference on Event-based Control, Communication, and Signal Processing*, June 2015, pp. 1–6.

[256] N. Xu, S. Rangwala, K. K. Chintalapudi, D. Ganesan, A. Broad, R. Govindan, and D. Estrin, "A wireless sensor network for structural monitoring," in *Proceedings of the 2nd International Conference on Embedded Networked Sensor Systems*, ser. SenSys '04. New York, NY, USA: ACM, 2004, pp. 13–24.

[257] W. Y. Yi, K. M. Lo, T. Mak, K. S. Leung, Y. Leung, and M. L. Meng, "A survey of wireless sensor network based air pollution monitoring systems," *Sensors*, vol. 15, no. 12, pp. 31 392–31 427, 2015.

[258] J. K. Yook, D. M. Tilbury, and N. R. Soparkar, "Trading computation for bandwidth: reducing communication in distributed control systems using state estimators," *IEEE Transactions on Control Systems Technology*, vol. 10, no. 4, pp. 503–518, Jul 2002.

[259] H. Yu, E. Garcia, and P. Antsaklis, "Model-based scheduling for networked control systems," in *Proceedings of the 2013 American Control Conference*, June 2013, pp. 2350–2355.

[260] D. Yue, E. Tian, and Q. L. Han, "A delay system method for designing event-triggered controllers of networked control systems," *IEEE Transactions on Automatic Control*, vol. 58, no. 2, pp. 475–481, 2013.

[261] X. M. Zhang, Q. L. Han, and X. Yu, "Survey on recent advances in networked control systems," *IEEE Transactions on Industrial Informatics*, vol. 12, no. 5, pp. 1740–1752, Oct 2016.

[262] W. Zhu and Z. P. Jiang, "Event-based leader-following consensus of multi-agent systems with input time delay," *IEEE Transactions on Automatic Control*, vol. 60, no. 5, pp. 1362–1367, May 2015.

[263] I. H. Zohdy, R. K. Kamalanathsharma, and H. Rakha, "Intersection management for autonomous vehicles using icacc," in *Proceedings of the 15th International IEEE Conference on Intelligent Transportation Systems*, Sept 2012, pp. 1109–1114.

Dankwoord

Het schrijven van dit proefschrift zou voor mij onmogelijk zijn geweest zonder de steun van fantastische mensen om me heen. Dankzij jullie was mijn promotietraject een enorm waardevolle en leuke ervaring waarin ik niet alleen veel geleerd heb op wetenschappelijk vlak maar vooral ook op persoonlijk vlak. Graag wil ik jullie bedanken met de onderstaande woorden.

Maurice, de afgelopen jaren heb ik ontzettend veel van je geleerd. Jouw enthousiasme, perfectionisme en jouw geduld om ieder bewijs grondig door te ploegen en eerste versies van mijn artikelen van uitgebreid commentaar te voorzien hebben er tot geleid dat ik het maximale uit mezelf heb kunnen halen. Ik ben ook heel dankbaar voor de vrijheid en het vertrouwen dat je me hebt gegeven. Ontzettend bedankt voor de goede begeleiding en het zijn van een goede coach.

Jeroen, dankzij jou heb ik kunnen laten zien dat wiskundige bewijzen met storage functions niet alleen leuk staan op papier maar daadwerkelijk iets kunnen betekenen voor een enorm gave en relevante applicatie. Ik heb enorm veel respect voor je brede deskundigheid op zowel praktisch als theoretisch gebied. Ik wil je daarom graag bedanken voor het mogelijk maken van de korte stage bij TNO en voor alle kennis die jij mij hebt bijgebracht. In addition, I would also like to thank Jeroen, Jeroen, Joep, Ellen, Elham, Jacco, Jan and Jan for the great experience I had at TNO.

Pietro, thank you for inviting me to Groningen and for the fruitful discussions. I am really glad I had the opportunity to work with you which led my research into a very interesting and relevant direction. I would also like to thank Claudio for his hospitality.

Romain, I would like to thank you for the time and effort to provide comments on Chapter 7. I really appreciate your willingness and expertise.

I would like to thank Siep Weiland, Nathan van de Wouw, Bart De Schutter and Karl Johansson for taking part in my defense committee that approved this thesis.

I would also like to thank my colleagues for creating a great work atmosphere and many memorable moments of outings and conferences. In particular, I would like to thank my (former) office mates Behnam, Xi, Robert, Emanuel, Guo, Matthijs and Hugo. I always enjoyed our discussions, especially the ones not related to work. I would also like to thank Mahmoud for the collaboration on quantization which resulted in Chapter 4. It took us a while to let all puzzle pieces fall together, but because that, I am extra proud of the result we attained. I promise I will take good care of Boeffie. Special thanks to Behnam and Niek for all the support whenever I was feeling stressed or concerned. It is great pleasure to have you as colleagues but even a bigger pleasure to have you as friends. Ik wil ook graag Petra, Thea en Geertje bedanken voor alle hulp die ervoor gezorgd heeft dat ik me maximaal heb kunnen focussen op mijn onderzoek.

Menno and Duarte, as my MSc supervisors, you played an important role in my decision to pursue a PhD. Therefore, I would like to thank you for convincing me to do so.

During my PhD, I had the opportunity to work with enthusiastic and talented students. Hence, I would like to thank Eric, Stijn, Yuri, Laura, Tim, Alessandro, Monica, Peter, Sebas, Dave and Jerrel for all the hard work of which you can all be proud. In addition, I would like to thank Duarte, Michel and Asia for involving me in the supervision of students which led to many interesting, informative and enjoyable discussions. Due to you, I also learned a lot about topics not related to my research.

I would like to thank Jos, Bas, Adityen, Irfan, Jason, Kirsten, Debayan, Debargha, Paul, Esref, Archita, Chao, Sander and all other (former) ATeam members. Being part of the team is an invaluable experience for me and I am really proud of our work on cooperative and automated driving, and the public attention it gained. The team helped me to get familiar with the many practical issues involved in translating an idea into a real-life demonstration.

Music is a crucial part of my life and I especially like to make music with others. Therefore, I would like to thank the people that make this possible. Daniel, Altug, Vojta, Manon, Polina, Alessandro, Tim, Matteo and Thomas, thanks for letting me be part of Chaloyna. Our rehearsals and performances are always epic. I would also like thank all the members of Bigband Groove Connexxion. I always look forward to our rehearsals on Tuesday evening and it is really a delight to be part of the band. In het bijzonder wil ik ook graag onze dirigent Danny Cuypers bedanken, ik heb over de jaren veel van je geleerd. Marjolein en Jurgen, ook jullie wil ik graag bedanken voor alle leuke repetities en optredens met het hoornensemble.

Sam, Robin en Bart, bedankt voor de hechte vriendschap en alle mooie avonturen die we beleefd hebben. Vooral onze Woodstock der Blasmusik avonturen zijn om niet te vergeten en ik hoop dat er in de toekomst nog meer bijkomen! Sam

en Robin, ook bedankt dat jullie mijn paranimfen willen zijn. Mijn vrienden uit Breda, Sander en Vivienne, wil ik ook graag bedanken voor de langdurige vriendschap die we hebben welke veel voor mij betekent.

Naast mijn collega's en vrienden wil ik uiteraard ook graag mijn familie bedanken en in het bijzonder mijn ouders en mijn broers. Papa, mama, Christiaan, Rutger en Olivier, bedankt dat ik altijd bij jullie terecht kan voor steun en advies.

Tenslotte wil ik graag mijn grootste dank betuigen aan Jessica. Bedankt voor de enorme steun die jij me hebt gegeven gedurende mijn promotie en het geluk dat je me brengt. Jij bent mijn topper!

Curriculum vitae

Victor Dolk was born on July 5, 1988 in Breda, the Netherlands. He received the Bachelor of Science (cum laude) and Master of Science degree (with great appreciation) in Mechanical Engineering from the Eindhoven University of Technology (TU/e), Eindhoven, the Netherlands, in 2010 and 2013, respectively. His master's thesis focused on feedback design for mixing of fluids using a switched system approach, and was carried out within the Control Systems Technology group under the supervision of Maurice Heemels.

Since November 2013, he started his Ph.D. project within the Control Systems Technology group at the department of Mechanical Engineering at the TU/e, under the supervision of Maurice Heemels. His research project was part of the project "Integrated design approach for safety-critical real-time automotive systems", which is (partly) financed by the Netherlands Organisation for Scientific Research (NWO) and was focused on the analysis and design of robust and resilient event-triggered control systems with performance guarantees. The results of his research are printed in this dissertation.